Access to new heterocyclic structures using organometallic and visible-light catalysis

Maxime De Abreu

Université de Paris

École doctorale MTCI (n°563)

Laboratoire Cibles Thérapeutiques et Conception de Médicaments

(CiTCoM UMR CNRS 8038)

Access to New Heterocyclic Structures using Organometallic and Visible-Light Catalysis

Par Maxime De Abreu

Thèse de doctorat de Chimie Organique

Dirigée par le Pr. Philippe Belmont

Co-encadrée par le Dr. Etienne Brachet

Présentée et soutenue publiquement le 27 Novembre 2020

Devant un jury composé de :

Pr. Mélanie Ethève-Quelquejeu, Professeur des Universités, Université de Paris	Présidente du Jury
Pr. Daniele Leonori, Professor, University of Manchester	Rapporteur
Dr. Amandine Guérinot, Maître de Conférences HDR, ESPCI	Rapporteur
Dr. Julie Broggi, Maître de Conférences, Aix-Marseille Université	Examinatrice
Dr. Etienne Brachet, Maître de Conférences HDR, Université de Paris	Examinateur
Pr. Philippe Belmont, Professeur des Universités, Université de Paris	Directeur de thèse

Acknowledgements

To begin, I would like to warmly thank Pr. Mélanie Ethève-Quelquejeu, Pr. Daniele Leonori, Dr. Amandine Guérinot, Dr. Julie Broggi, member of the Jury, for taking the time to read and review my PhD work but also for coming from far away (if possible) to my defense.

Normalement on dit qu'on garde le meilleur pour la fin mais j'ai envie de commencer par toi Etienne. Je ne sais pas si je pourrais trouver tous les mots pour décrire à quel point je suis reconnaissant de tout ce que tu m'as appris depuis maintenant 4 ans (oui ça fait longtemps depuis le stage de M2). Merci d'avoir su faire preuve de patience, surtout avec ma mémoire défaillante au début, de m'avoir expliqué les choses quand je ne comprenais rien, de m'avoir fait confiance pour continuer en thèse dans ton milieu de recherche et surtout de ne m'avoir jamais abandonné quand j'avais besoin de ton aide, surtout pendant ces derniers mois de rédaction. Avec du recul, ces 4 années sont passées très (trop !) vite grâce à la bonne ambiance que l'on a instauré dans le bureau et au labo. Nos discussions scientifiques mais aussi personnelles vont me manquer et aussi les sorties benne. Je te souhaite le meilleur pour l'ère post-Maxime, ça va être dur pour toi, comme pour moi !

A ton tour Philippe maintenant. Je tenais à te remercier d'avoir cru en moi en M2 et de m'avoir proposé le sujet de thèse qui a tracé ma vie pendant ces 3 ans. Merci pour ton soutien durant la thèse et d'avoir toujours apporté ta bonne humeur lors de tes passages au labo, au bureau mais aussi et surtout chaque midi au restaurant universitaire !

Je souhaiterai également remercier le Pr. Michel Vidal, le Pr. Sylviane Giorgi-Renault, le Dr. Philippe Helissey et le Dr. Stéphanie Desbène-Finck, membres de l'équipe « Chimie médicinale et recherche translationnelle » de l'UMR 8038 (ex-équipe « Hétérocycles et peptides » de l'UMR 8638) de m'avoir accueilli lors de la première moitié de ma thèse au sein de leur équipe et de leur laboratoire.

Je souhaiterai aussi remercier tous les membres de l'équipe Produits Naturels Analyse et Synthèse (PNAS) de l'UMR 8038, mon équipe d'adoption, dans laquelle j'ai poursuivi la deuxième moitié de ma thèse. Merci pour votre bienveillance et votre accueil et je tenais tout particulièrement à remercier le Dr. Florence Souquet pour avoir pris le temps de me montrer comment utiliser le potentiostat afin de réaliser mes mesures de voltamétrie cyclique, Chouaha Bouzidi pour avoir géré mes analyses HRMS mais surtout d'avoir réalisé des injections LC-MS qui m'ont bien aidées, Pascale Leproux pour avoir réalisé mes analyses HRMS au début de ma thèse malgré les difficultés rencontrées avec le matériel, Thomas Gaslonde pour avoir effectué une HPLC prép avec moi et enfin Karim Hammad pour m'avoir enseigné énormément de choses en rapport (ou non) à la RMN et de m'avoir formé à l'utilisation du spectromètre 600 MHz.

Mes remerciements s'adressent également envers l'équipe des TP de Voies d'Accès aux Médicaments, et notamment vers le Dr. Sylvain Broussy, le Dr. Sylvie Robin ainsi que le Dr. Wang Qing Liu ainsi qu'une pensée pour le Dr. Jean-Michel Delacotte, qui ont su me montrer l'art et la manière d'encadrer un TP avec des étudiants novices.

Je souhaite remercier le Dr. Joanna Wencel-Delord de m'avoir accordé sa confiance et de m'offrir l'opportunité de poursuivre mon parcours de recherche avec un contrat post-doctoral au sein de son équipe. Merci également au Dr. Angélique Ferry de m'avoir fait parvenir des produits nécessaires à ma thèse plus rapidement que Sigma !

Je remercie également mes camarades du « bureau labo terrasse » : Camille, Alice, Alexandros, Dang et Youssef pour la bonne ambiance de travail au quotidien, mais également le Pr. Marie-Christine Lallemand pour son entièreté mais surtout pour sa franchise et ses « bonjour » qui m'ont fait peur plus d'une fois.

Je tiens également à remercier le Pr. Luc Demange pour animer avec passion les conversations du midi (le truc des méduses) mais aussi le Dr. Antoine Franche et Stéphane Duflocq pour les mêmes raisons (sauf le truc des méduses).

Merci également à Doriane, je pense sincèrement que sans toi, ma relation avec Etienne aurait été différente (moins sympa). Je te souhaite le meilleur dans les projets que tu entreprendras à l'avenir.

Un grand merci à Claire qui m'a aidé avec la mise en forme du manuscrit.

Je souhaite le meilleur à William, mon successeur. J'espère que la chimie sera gentille avec toi. Amuse-toi bien avec Etienne et Philippe ! Je souhaite aussi remercier tous les stagiaires qui ont eu l'honneur de me côtoyer au laboratoire pendant ces 3 ans : Joe, Hanane, Marie, and the last but not least, my dearest canadian pharmacist Jennifer.

Mes pupiti d'amour Maria Concetta (la mia farfallina preferita) et Davide (pupito), je garde un excellent souvenir de votre passage au laboratoire, merci de m'avoir appris des choses utiles et moins utiles (mais toujours très intéressantes 😊) en italien, d'avoir partagé BEAUCOUP de choses à manger d'Italie mais surtout d'avoir partagé avec vous de très très bons moments (au labo tard le soir, dans la cuisine, à la terrasse…). Vous me manquez beaucoup.

Merci à Maximiliene d'être un vrai rayon de soleil chaque jour quand on se croise en RMN ou au labo. T'inquiètes pas, c'est bientôt fini !!! Je te souhaite pleins de bonnes choses pour l'après thèse !

Je remercie ma famille et mes amis pour leur amour et le soutien qu'ils m'apportent, chaque jour, depuis des années. Notamment ma cousine/sœur Jennifer, d'avoir toujours été présente pour moi,

dans les bons comme les pires moments. Merci d'avoir été mon phare quand j'étais perdu, j'espère être le tien également.

Je tiens également à remercier Elodie, ma coréenne, jadis voisine de SVT il y a plus de 10 ans, tu es devenue très importante pour moi aujourd'hui. Je remercie aussi Julie d'avoir éclairé mes années de lycée notamment les cours d'histoire-géo, en apportant une bonne aMosphère de travail. J'espère vous garder à mes côtés encore longtemps et que vous serez encore mes partenaires de voyage.

Merci à Cyndel d'être toujours aussi kokultobwant, mais aussi pour le soutien psychologique que tu m'as apporté (surtout à la fin).

Je remercie Léa d'avoir apporté sa bonne humeur et sa soif insatiable de sensations fortes dans ma vie il y a maintenant 4 ans (même si on dirait que ça fait beaucoup plus longtemps).

Je tiens à remercier Sarah, qui me comprend parfois plus que je ne me comprends moi-même, d'être toujours présente malgré la distance qui nous sépare. Merci à Saïd de m'avoir supporté (dans le bon comme le mauvais sens) depuis le début en 2012 quand on avait encore 17 ans, jusqu'à la fin de ce périple, 8 ans plus tard, mais aussi Fatima, 3ème membre de la triade catalytique, je vous souhaite plein de bonheur pour la suite (mariage tout ça tout ça). Merci à Phoulinh également d'être un très bon catalyseur à conneries, merci de nous faire rire même si parfois c'est une accumulation.

Merci à toi Sergio pour ton aide à mon adaptation lors de mon arrivée au labo terrasse. Merci d'avoir pris le temps de me montrer comment fonctionne la HPLC et certains trucs en RMN et par-dessus tout, merci pour le soutien que tu m'as apporté pendant les moments difficiles de la rédaction. Gracias por hablar en español conmigo y ser un buen compañero para embriagarse.

Merci à mes frères, à mes parents et mes grands-mères et Mathilde qui m'ont soutenu durant la thèse.

Je souhaite le meilleur à mes sœurs et frères d'armes en dernière année de thèse également : Maximiliene, Stéphane, Sarah, Saïd et Phoulinh. Apparemment je vais être le premier à passer à la casserole, je vous souhaite bonne chance pour votre soutenance.

Enfin, je souhaiterai remercier la chimie, qui a été plutôt clémente avec moi pendant 3 ans, sans trop me mettre de bâtons dans les roues, ni trop me traumatiser.

Abbreviations and chemical formula

A	
A	Electron acceptor
Å	Angstrom (= 10^{-10} m)
Ac	Acetate
AcOH	Acetic acid
B	
Bn	Benzyl group
C	
Cat.	Catalytic amount
C_6D_6	Deuterated benzene
$CDCl_3$	Deuterated chloroform
D	
D	Electron donor
DCE	Dichloroethane
DCM	Dichloromethane
DMA	Dimethylacetamide
DMF	Dimethylformamide
DMSO	Dimethylsulfoxide
E	
EA	Ethyl acetate
Eq.	Equivalent
Et	Ethyl
EtOH	Ethanol
H	
h	hour
HAT	Hydrogen Atom Transfer
HRMS	High Resolution Mass Spectrometry
I	
iPr	Isopropyle
IR	Infrared
L	
LED	Light-emitting diode
λ	Wavelength

M	
M	Molar concentration (mol.L^{-1})
min	minute
mmol	millimole
Mp	Melting point
N	
NCR	Nitrogen-Centered Radical
NMR	Nuclear Magnetic Resonance
Nu	Nucleophile
P	
pdt	Product
Ph	Phenyl
Py	Pyridine
Q	
Quant.	Quantitative
R	
R_f	Retardation factor
RT	Room temperature
S	
SCE	Saturate Calomel Electrode
SET	Single Electron Transfer
$S_{RN}1$	Substitution Radical-Nucleophilic Unimolecular
T	
*t*Bu	*tert*-butyle
TEMPO	(2,2,6,6-Tetramethylpiperidin-1-yl)oxyl
Tf	Triflate
THF	Tetrahydrofurane
TMS	Trimethylsilyl
U	
UV	Ultraviolet
V	
vs	versus

Résumé en Français

Les hétérocycles sont des composés organiques cycliques distribués largement au sein du monde vivant. Ces molécules sont essentielles à toute vie complexe sur Terre puisqu'elles sont retrouvées dans les briques élémentaires (A, T, G, C) constituant par exemple l'ADN et l'ARN mais aussi dans d'autres molécules omniprésentes telles que l'hème qui transporte le dioxygène, la chlorophylle et la cellulose présentes dans les plantes (Schéma 1).

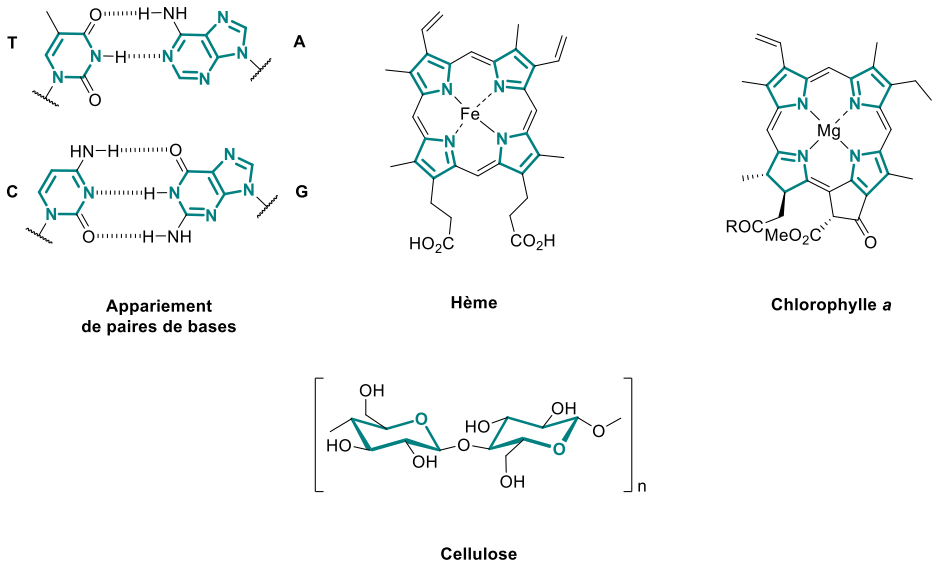

Schéma 1 - Exemples d'hétérocycles d'origine naturelle

Dans ce travail de thèse nous nous intéresserons aux hétérocycles azotés qui présentent un intérêt synthétique majeur. En effet, ces derniers sont retrouvés dans d'innombrables produits naturels et notamment dans de nombreux médicaments puisque 59% des médicaments approuvés aux Etats-Unis par la FDA, et qui sont basés sur des petites molécules uniques, contiennent un hétérocycle azoté.

Cette thèse est divisée en deux axes : un axe mettant l'accent sur la synthèse de dérivés d'isoquinoléines par catalyse à l'argent et un second axe plus développé et novateur basé sur la synthèse de dérivés de phtalazines par photocatalyse visible. Ces deux familles d'hétérocycles sont connues pour posséder de nombreuses propriétés biologiques intéressantes et sont même présentes dans plusieurs médicaments commercialisés. Nous allons donc nous intéresser à leur synthèse en utilisant de nouvelles approches synthétiques pour leur obtention.

Les sels d'argent, en tant que catalyseur ou acide de Lewis, ont été utilisés depuis des décennies dans des différentes réactions. En effet, ils peuvent être utilisés dans des réactions de cycloaddition, de cycloisomérisation, de couplage, d'allylation, d'activation C-H mais aussi en chimie radicalaire. Leurs capacités à catalyser des réactions de cycloisomérisation sont bien connues et ont été notamment

appliquées au sein de notre laboratoire sur des substrats de type *ortho*-alcynyl(hetero)arylaldéhyde engagés dans des réaction tandem, notamment d'hydroarylation/cycloisomérisation (Schéma 2).

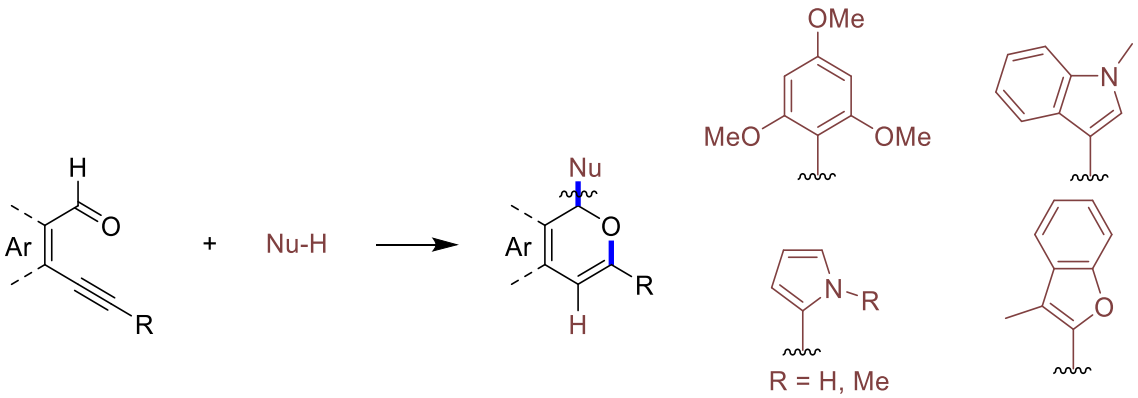

Schéma 2 - Exemples de réaction tandem catalysée à l'argent développées dans l'équipe du Pr. Belmont

Nous nous sommes penchés par la suite sur une variation de ces méthodologies en utilisant des substrats de départ de type *ortho*-alcynyl(hetero)arylaldéhyde dont la fonction carbonylée a été transformée en fonction imine. Des exemples d'utilisation de ces dérivés de type *ortho*-alcynylarylimine existaient déjà dans la littérature depuis la fin des années 1990 avec des catalyseurs au palladium par exemple. Cependant, ce n'est qu'en 2003 que le groupe du Pr. Larock a publié pour la première fois un exemple d'utilisation de complexe d'argent pour réaliser une réaction de cycloisomérisation et en a démocratisé l'usage par la suite avec de nombreuses applications publiées (Schéma 3).

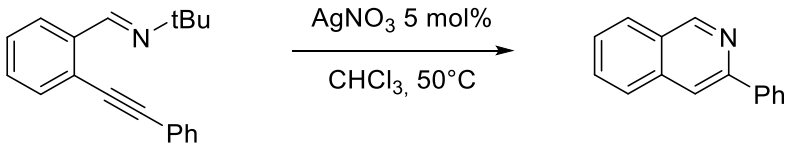

Schéma 3 - Premier exemple d'une réaction tandem d'hydroarylation suivie par une cycloismérisation catalysée à l'argent publiée par le groupe du Pr. Larock

Par la suite, l'équipe du Pr. Wu a développé de nombreuses variations de ces réactions à l'argent en insistant particulièrement sur les réactions tandem de cycloisomérisation suivie par l'incorporation d'une très grande variété de nucléophiles (cétones *α,β*-insaturées, phosphonates, imidazoles, cétones, indoles et trifluorométhyle) en position 1 de l'isoquinoléine obtenue.

Malgré toutes les méthodologies disponibles, nous devons continuer de développer de nouvelles réactions, compatibles avec la plus grande variété de substitutions sur le substrat de départ tout en étant également compatible avec plus de nucléophiles hétérocycliques afin de former efficacement une liaison C-C et C-N en une seule étape.

Après une optimisation rigoureuse des conditions réactionnelles, nous avons réussi à développer des nouvelles conditions, compatible avec une grande variété de substitutions sur l'alcyne, l'imine et le cycle principal du substrat de départ, tout en étant compatible avec différent nucléophiles hétérocycliques azotés.

Tableau 1 - Exemples d'isoquinoléines finales obtenues avec les conditions réactionnelles optimisées

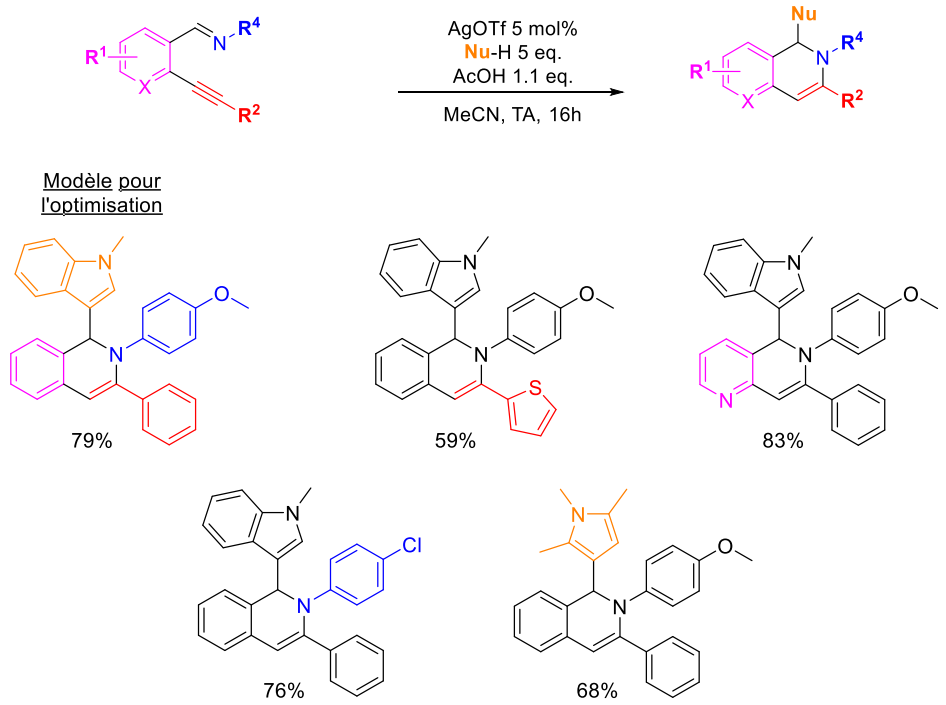

17 exemples (rendements de 16% à quant.)

Malheureusement, les nucléophiles hétérocycliques oxygénés et soufrés testés n'ont pas permis la formation des produits de type isoquinoléine désirés. Le manque de réactivité de ces nucléophiles peut être expliqué par la différence de nucléophilie relative observée entre les hétérocycles azotés (plus nucléophiles) et ceux oxygénés et soufrés (moins nucléophiles) utilisés, ce qui est confirmé par les travaux de l'équipe du Pr. Mayr qui ont mis au point une échelle permettant le classement relatif de la nucléophilie d'une grande variété de molécules dont divers hétérocycles.

Différentes expériences supplémentaires ont par la suite été réalisées afin d'aider à élucider le mécanisme réactionnel. Ce dernier commence par l'activation de l'alcyne par le sel d'argent. Cette étape permet d'augmenter l'électrophilie de l'alcyne et permettre l'attaque 6-*endo-dig* de l'imine. L'intermédiaire isoquinoléinium ainsi formé est attaqué par le nucléophile hétérocyclique présent dans le milieu, puis une étape de protodémétallation et réaromatisation du nucléophile a lieu afin de former le produit désiré (Schéma 4).

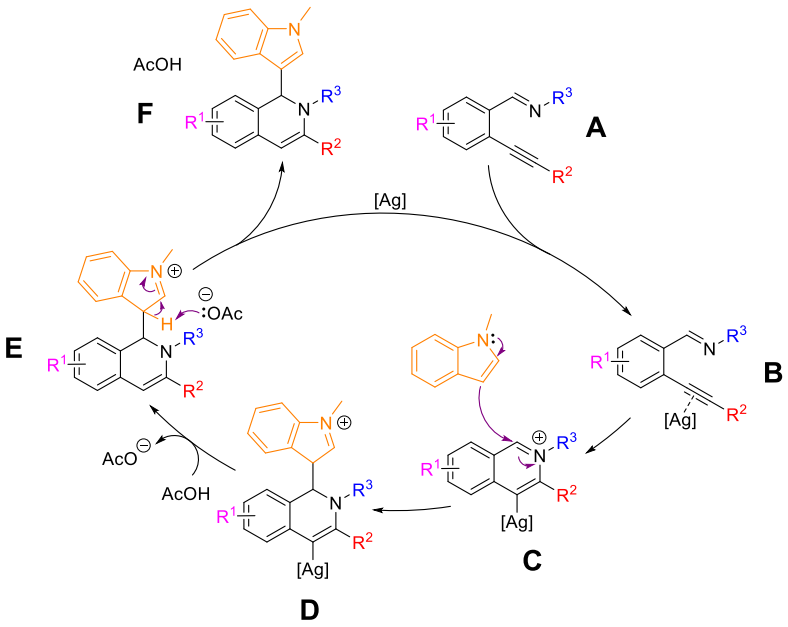

Schéma 4 - Méchanisme réactionnel proposé

La plus grande partie de cette thèse s'est ensuite portée sur le développement de nouvelles méthodologies photocatalysées afin de former des liaisons C-N. Pour ce faire, nous nous sommes intéressés à la génération de radicaux centrés sur l'azote afin de former la liaison C-N. Différentes méthodes existent déjà dans la littérature afin de générer ces radicaux et sont basées sur la rupture de liaisons N-Hétéroatome, N-Halogène ou bien tout simplement sur l'oxydation de liaisons N-H. Cependant, ces méthodes restent particulièrement rares dans la littérature et c'est pourquoi le développement de nouvelles méthodes d'obtention de radicaux centrés sur l'azote reste nécessaire.

Notre intérêt s'est porté sur les phosphonohydrazines, un dérivé de phosphoramidate, que nous avons fait réagir sur des substrats *ortho*-alcynylarylaldéhyde et *ortho*-alcynylarylcétone afin de former des phosphonohydrazones. Nous avons envisagé que la base conjuguée de ces dernières pouvait être oxydée par un photocatalyseur excité adéquat afin de générer le radical désiré et mener ensuite à une réaction intramoléculaire 6-*exo*-*dig* (Schéma 5). Après quelques tests nous nous sommes aperçus que la formation d'un produit d'addition du radical centré sur l'azote pouvait être obtenu. Cependant, nous avons été surpris par le fait que la particule phosphorée était coupée durant la réaction, menant à la formation de dérivés de type benzylphtalazine. Cette coupure rend la réaction d'autant plus attractive puisqu'elle évite d'avoir besoin d'une étape supplémentaire afin de retirer la particule phosphorée pré-activatrice qui permet la génération du radical centré sur l'azote.

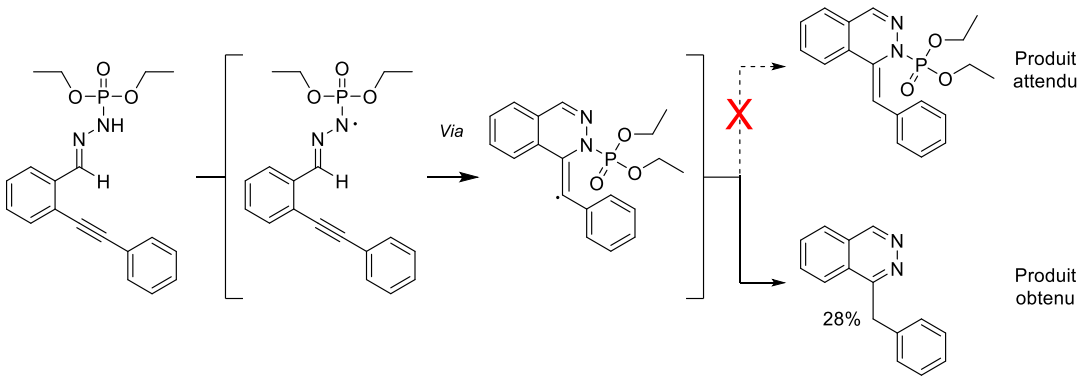

Schéma 5 - Produit attendu et produit obtenu à l'issue de la réaction photocatalysée

Une optimisation poussée de la réaction a permis l'obtention de conditions réactionnelles capables de mener à la formation d'une grande bibliothèque de phtalazines comprenant 22 exemples avec des rendements compris entre 17 et 95% (Tableau 2).

Tableau 2 - Exemples de phtalazines finales obtenues avec les conditions réactionnelles optimisées

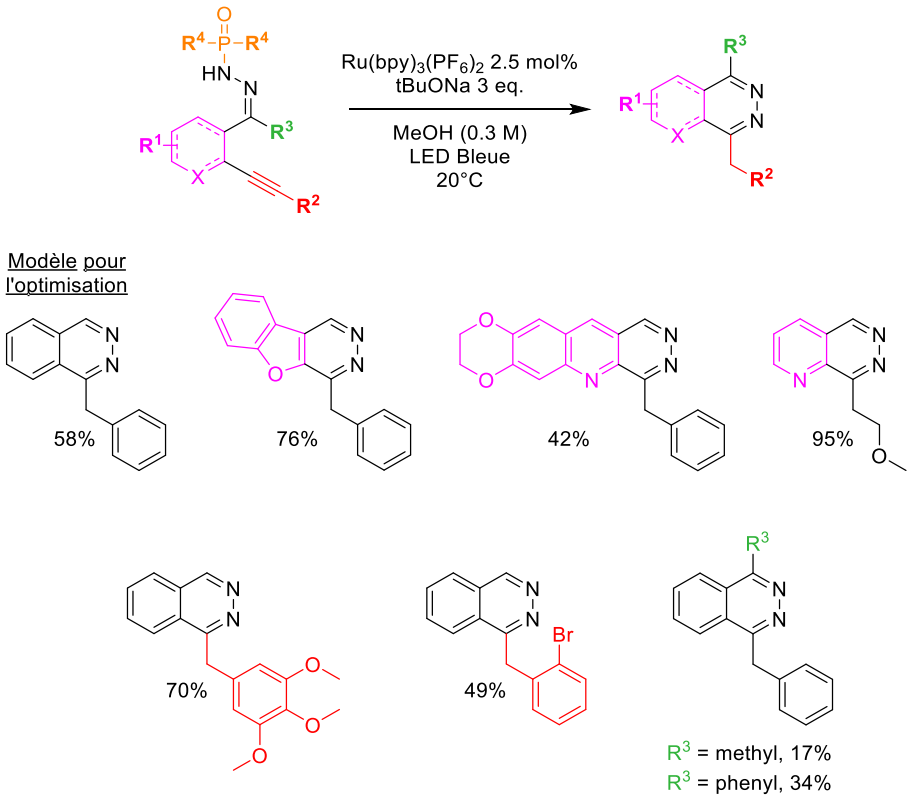

22 exemples (rendements de 17% à 95%)

Durant l'étude de la compatibilité fonctionnelle de cette réaction, nous avons obtenu un résultat inattendu avec l'une de nos phosphonohydrazones. En effet, celle portant un atome de fluor en position *para* de l'alcyne, sur le cycle principal, a bien mené à la formation d'un produit de type phtalazine (56%, Schéma 6). Cependant, ce dernier ne présente plus d'atome de fluor, un groupement méthoxy le remplace. Ce groupement méthoxy provient du solvant de la réaction (méthanol), de façon

intéressante, en effectuant la réaction avec la même phosphonohydrazone mais dans l'éthanol, on obtient un résultat similaire, avec l'incorporation d'une chaîne éthoxy à la place de l'atome de fluor. Ce phénomène de substitution de l'atome de fluor par le solvant de type alcool n'a pas été observé lorsque l'atome de fluor se trouvait en *para* de l'alcyne (Schéma 6). Malheureusement, aucune réactivité similaire n'a été observée sur des substrats fluorés plus simples comme le fluorobenzène, dans les mêmes conditions.

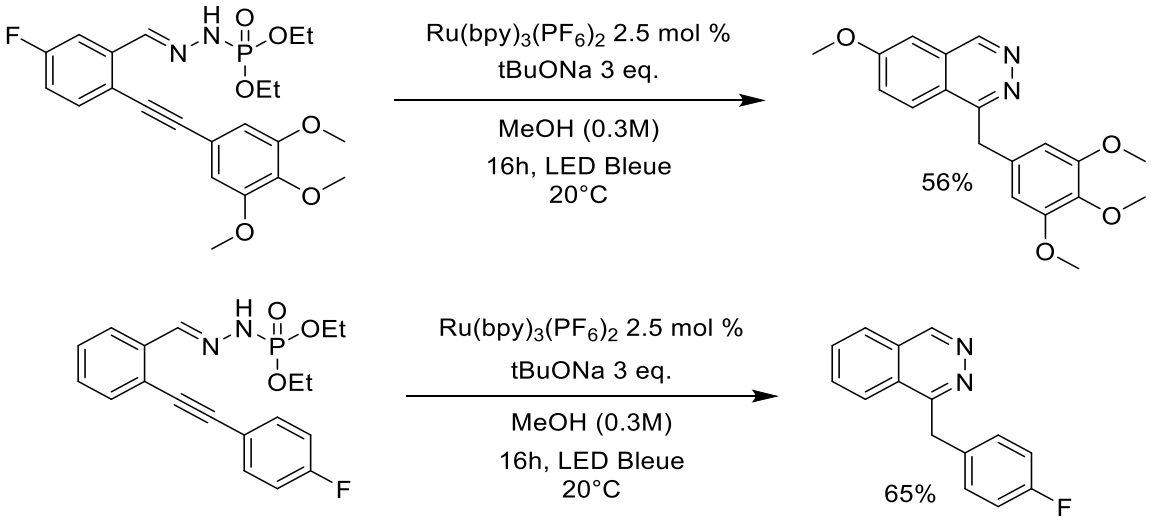

Schéma 6 - Expériences menant ou non à un échange de l'atome de fluor par le solvent

Une variation de notre méthodologie a été faite sur des phosphonohydrazones portant un alcène en lieu et place de l'alcyne utilisé jusqu'alors. Cette modification donne lieu à une réactivité différente puisque la particule pré-activatrice phosphorée n'est pas coupée à l'issue de la réaction, contrairement à ce qui est observé avec les dérivés portant une fonction alcyne. Nous pensons que cette différence vient du fait que la coupure de la particule phosphorée s'associe avec la réaromatisation de la phtalazine dans le cas où un alcyne est présent dans le réactif de départ. Avec un alcène, cette réaromatisation n'est pas possible et donc ne permet pas la coupure de la liaison N-P.

Quelques expériences de piégeage radicalaire furent effectuées afin d'obtenir plus d'indices sur le mécanisme réactionnel. La réaction, effectuée en présence de TEMPO, ne mène à aucune formation de produit. Cependant, en présence de disulfure de diphényle, un adduit entre la phtalazine finale et une molécule de thiophénol a été isolé (Schéma 7). Ce produit permet de conclure de la présence transitoire d'un radical sur le carbone qui sera piégé par le groupe thiophényle. D'autres expériences de réaction d'un intermédiaire radicalaire avec des électrophiles/accepteurs de Michael se sont toutes soldées par des échecs.

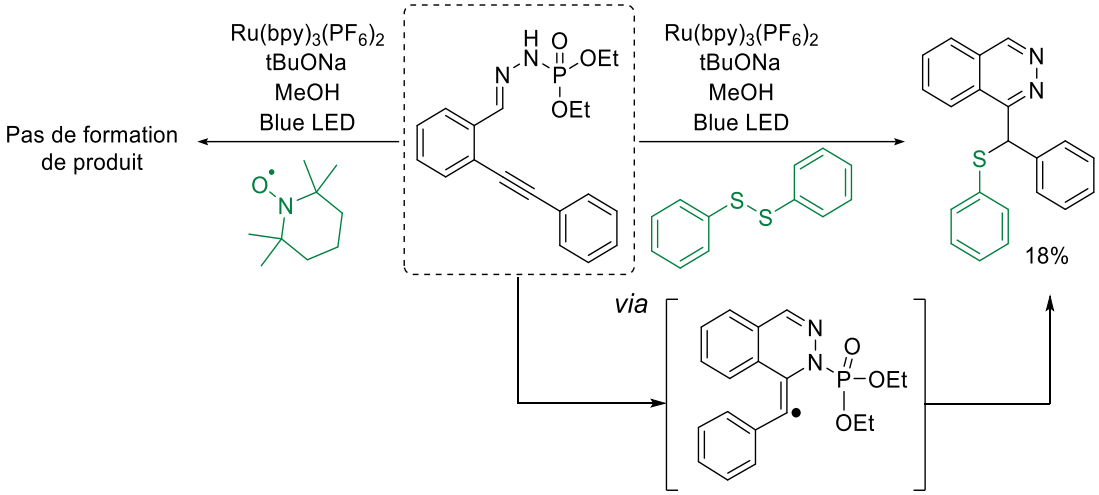

Schéma 7 - Expériences de piégeage radicalaire

Une expérience de deutériation a permis de confirmer l'origine du proton incorporé à la fin de la réaction en réalisant la réaction dans du méthanol deutérié. Une deutériation à hauteur de 86% a été observée pour la fonction CH_2 de la phthalazine. Enfin, notre méthodologie a été soumise à une expérience de type « on-off » dans laquelle le milieu réactionnel est soumis consécutivement à des périodes d'exposition à la lumière et des périodes d'obscurité totale (Schéma 8). Cela se traduit concrètement par une consommation du substrat phosphonohydrazone lorsque la réaction est soumise à la lumière et aucune variation en absence de lumière.

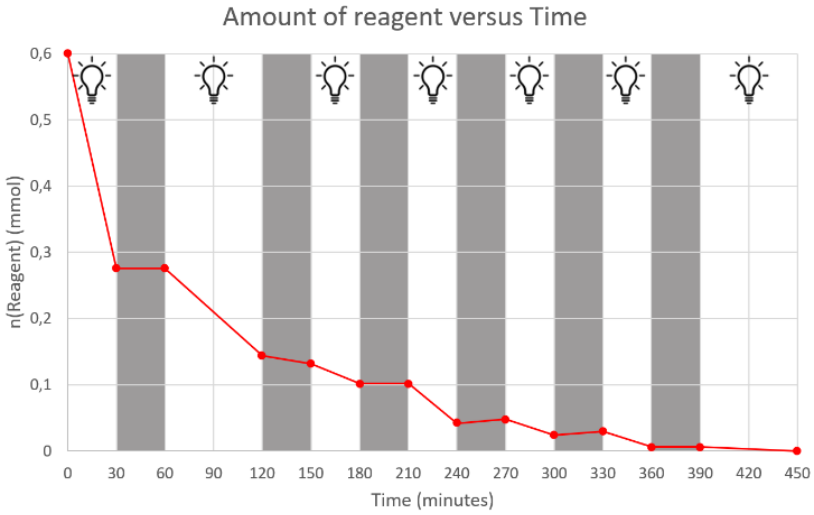

Schéma 8 - Expérience dite de "on-off"

L'isolement d'un composé phosphoré à l'issue de la réaction a permis de comprendre comment la particule phosphorée était coupée. Toutes ces données expérimentales ont permis la proposition d'un mécanisme réactionnel plausible pour cette réaction. Dans un premier temps, la phosphonohydrazone A est déprotonée dans le milieu réactionnel basique. L'anion B est ensuite oxydé par le photocatalyseur dans un état excité, menant à la formation du radical centré sur l'azote, intermédiaire clé de cette

réaction. Ce dernier réalise ensuite une réaction intramoléculaire 6-*exo-dig* avec l'alcyne. Le résultat de cette étape est l'intermédiaire radicalaire D qui est réduit par le photocatalyseur. Cette étape permet la fermeture du cycle catalytique et l'obtention d'un intermédiaire anionique E qui réagit très rapidement avec le solvant protique de la réaction. Finalement, la liaison azote-phosphore est coupée suite à l'attaque du méthanolate de sodium formé *in situ*. La phtalazine I est ainsi formée ainsi que le sous-produit phosphoré G (Schéma 9).

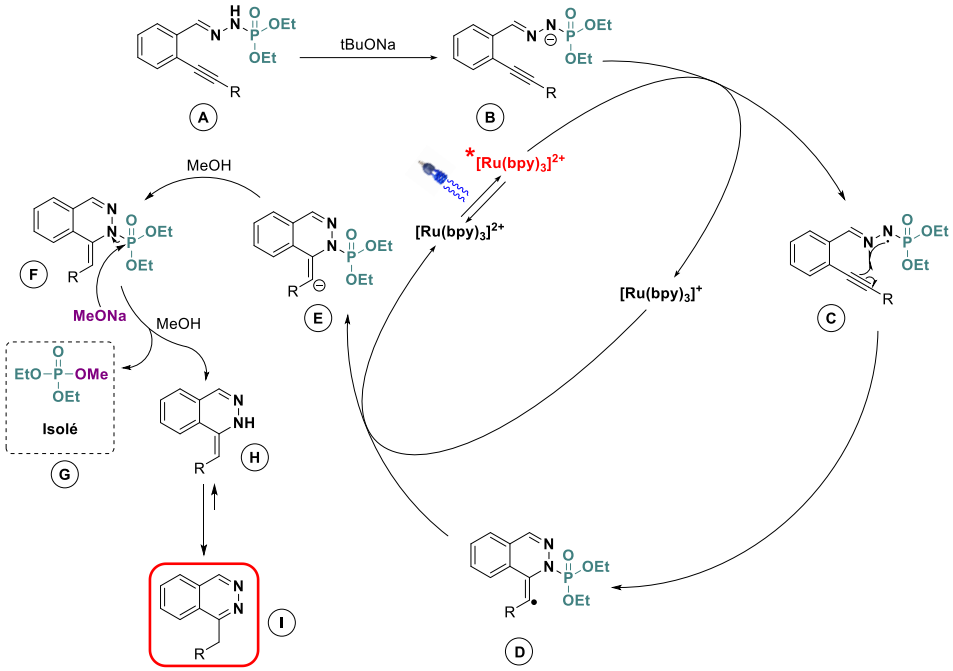

Schéma 9 - Mécanisme réactionnel proposé

Au cours de l'optimisation de la réaction présentée ci-dessus, nous avons fait varier les substituants au niveau de l'atome de phosphore par diverses chaînes (méthoxy, éthoxy, benzyloxy) mais aussi par des groupements phényles (Schéma 10). Ces derniers ont mis en exergue une réactivité tout à fait inédite puisqu'un nouveau type de phtalazine a été isolé. Cette nouvelle réactivité passe par un intermédiaire de type spiro bicyclique (Schéma 11) qui donne lieu à une migration d'aryle 1,4 radicalaire.

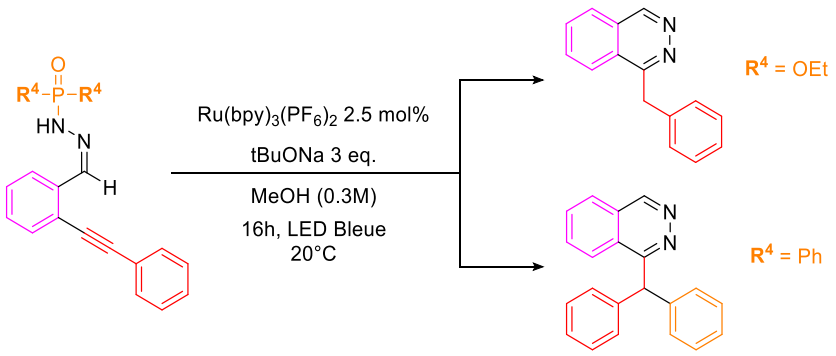

Schéma 10 - Différence de réactivité observée lorsque l'atome de phosphore est substitué différemment

Après optimisation de la voie de synthèse des phosphonohydrazones substituées par divers groupements aryles, et l'optimisation de la réaction en elle-même, nous avons obtenu une large famille de phtalazines portant une substitution supplémentaire comparée à la méthodologie précédemment décrite. Une grande variété de groupements aryle ont été en mesure d'effectuer la migration radicalaire et nous avons été en mesure d'obtenir 18 exemples avec des rendements compris entre 11 et 65% (Tableau 3).

Tableau 3 - Exemples de phtalazines finales obtenues après migration du groupement aryle avec les conditions réactionnelles optimisées

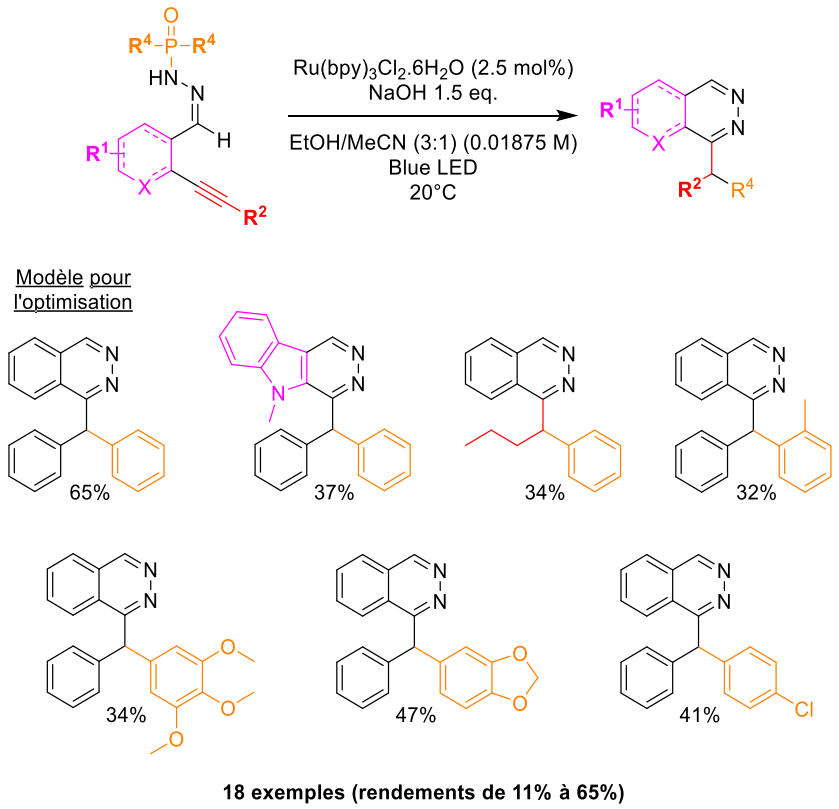

Dans ces 2 méthodologies photocatalysées, nous avons réalisé des expériences de voltammétrie cyclique afin de déterminer le potentiel d'oxydation de nos phosphonohydrazones en milieu basique (*t*BuONa ou NaOH en fonction de la méthodologie). Ces mesures nous ont permis de confirmer le fait que les potentiels d'oxydation de ces phosphonohydrazones sont bel et bien accessibles par le photocatalyseur utilisé $(Ru(bpy)_3)^{2+}$ dans son état excité (tous les potentiels mesurés sont inférieurs à 0.77V, ce qui signifie que le photocatalyseur est plus oxydant que les molécules utilisées dans nos travaux).

Dans certains cas, des phosphonohydrazones n'ont pas permis la migration du groupement aryle et ont mené à la formation du même type de phtalazines obtenues dans la précédente méthodologie. Toutes ces informations ont permis la proposition d'un mécanisme pour cette réaction comprenant le cas où une migration d'aryle a lieu et le cas où elle n'a pas lieu. En effet, la formation de l'intermédiaire

IV s'opère de la même manière que dans la méthodologue précédente et peut s'engager dans deux voies différentes. Dans la voie A, le radical peut réagir avec l'un des substituant aryle présent sur l'atome de phosphore et former l'intermédiaire spiro bicyclique V, aussi appelé complexe de Meisenheimer. Ce dernier mène, après un réarrangement de type 1,4, au radical centré sur le phosphore qui, après réduction et protonation, donne l'intermédiaire VII. Une ultime étape de coupure de la liaison azote-phosphore par l'éthanoate de sodium donne la phtalazine finale ainsi que le sous-produit VIII. L'intermédiaire IV peut aussi s'engager dans une autre voie réactionnelle (voie B), similaire à celle décrite dans la méthodologie précédente et mener à la formation d'un autre type de phtalazine. (Schéma 11).

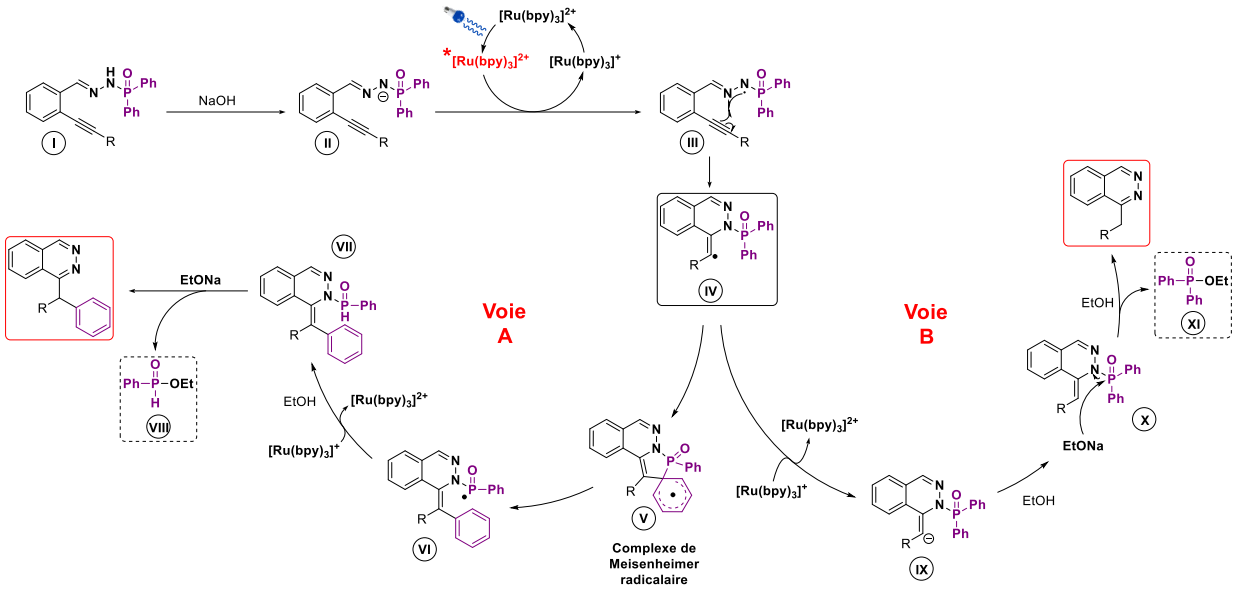

Schéma 11 - Mécanisme réactionnel proposé

Table of contents

General Introduction

I) General introduction

Nitrogen-containing heterocycles are probably one of the most significant chemical scaffolds in medicinal chemistry. As of 2014, 59% of the FDA approved unique small-molecule drugs comprise a nitrogen-containing heterocycle.[1] Their synthesis has been studied and perfectioned along with the development of organic synthesis throughout the centuries and even nowadays, with modern catalytic systems.[2]

We propose here to study the synthesis of two relevant nitrogen-containing heterocycles using attractive methodologies.

In **chapter I**, we will tackle the relevance of the isoquinoline scaffold in medicinal chemistry before presenting the use and synthetic attractiveness of silver in catalysis. We will apply this type of mild catalysis to a well-mastered synthon in our laboratory: *ortho*-alkynylbenzaldehyde. The latter will be transformed into the corresponding imine in order to be the precursor for the synthesis of isoquinoline derivatives under silver catalysis (Scheme 1).

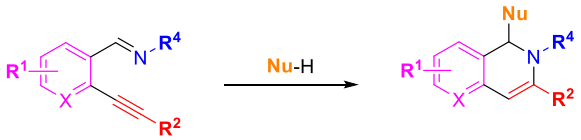

Scheme 1 - Access to isoquinoline derivatives under silver-catalysis

The second part of this thesis will focus on visible-light catalysis and will be divided in three chapters. In **chapter II**, we will introduce the basics of visible-light catalysis and the main reaction pathways accessible using this method. **Chapters III** and **IV** will be dedicated to the development of new photoredox methodologies, empowered by the development and application of a new family of nitrogen-centered radical precursors: phosphonohydrazones. These innovations will be applied to the synthesis of phthalazine derivatives, diversely substituted, upon an hydroamination reaction (**chapter III**) or a tandem hydroamination/"phospho-Smiles" reaction (**chapter IV**) (Scheme 2).

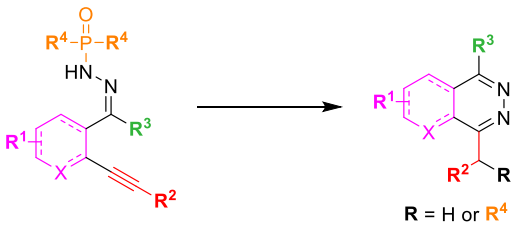

Scheme 2 - Access to phthalazine derivatives under visible-light catalysis

[1] E. Vitaku, D. T. Smith, J. T. Njardarson, *J. Med. Chem.* **2014**, *57*, 10257–10274.
[2] J. F. Campos, S. Berteina-Raboin, *Catalysts* **2020**, *10*, 429.

Chapter I:
Access to the isoquinoline scaffold via a silver-catalyzed tandem cycloisomerization/ hydroarylation reaction

Chapter I: Access to the isoquinoline scaffold via a silver-catalyzed tandem cycloisomerization/hydroarylation reaction

A) Ubiquity of nitrogen-containing heterocycles, focus on isoquinolines

1. Introduction

Heterocycles are organic cyclic compounds widely distributed in nature that contain at least two different elements, usually, several atoms of carbon and at least one heteroatom such as oxygen, nitrogen or sulfur.[3] They are essential for life such as in nucleic acids (see DNA base pairing, Figure 1), which store the genetic information of every living cell, in amino acids present in proteins, and also in the heme derivatives present in the red blood cells or in the chlorophyll derivatives, essential for plants' photosynthesis (haem and chlorophyll a, Figure 1).[4] Heterocycles are also found in a majority of drugs' pharmacophores (β-lactam, piperidine, furan, thiophene derivatives…), in most of the biomass (cellulose, hemicellulose, lignin…), and in many synthetic and natural dyes (indigo, eosin…), see Figure 1 (penicillin core, cellulose, indigo).[5]

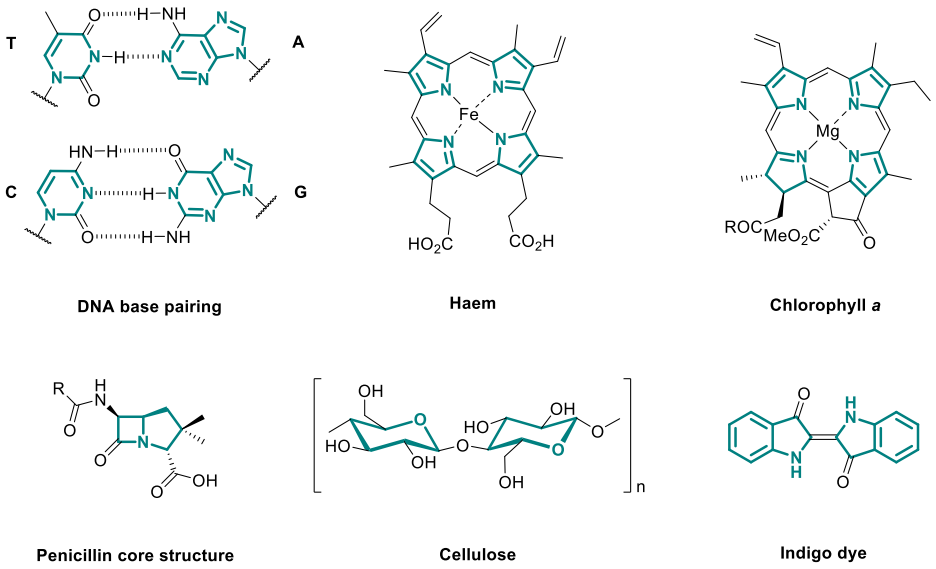

Figure 1 - Examples of naturally occurring heterocyclic compounds

The history of heterocyclic chemistry began almost two centuries ago, in parallel with the development of organic chemistry when Brugnatelli oxidized uric acid into alloxan back in 1818.[6] The synthesis of nitrogen-containing heterocycles constantly attracted the interest of the chemist

[3] A. D. McNaught, A. Wilkinson, **1997**, DOI https://doi.org/10.1351/goldbook.H02798.
[4] A. F. Pozharskii, A. T. Soldatenkov, A. R. Katritzky, *Heterocycles in Life and Society: An Introduction to Heterocyclic Chemistry, Biochemistry and Applications*, John Wiley & Sons, Ltd, Chichester, UK, **2011**.
[5] M. Sainsbury, *Heterocyclic Chemistry*, Royal Society Of Chemistry, Cambridge, UK, **2001**.
[6] E. Campaigne, *J. Chem. Educ.* **1986**, *63*, 860.

community due to their ubiquitous presence in natural products and because of their interesting properties such as in drugs, for instance.[1] Some example of these drugs are given in Figure 2 (Ledipasvir, lenalidomide, rivaroxaban, sitagliptin and sofosbuvir).

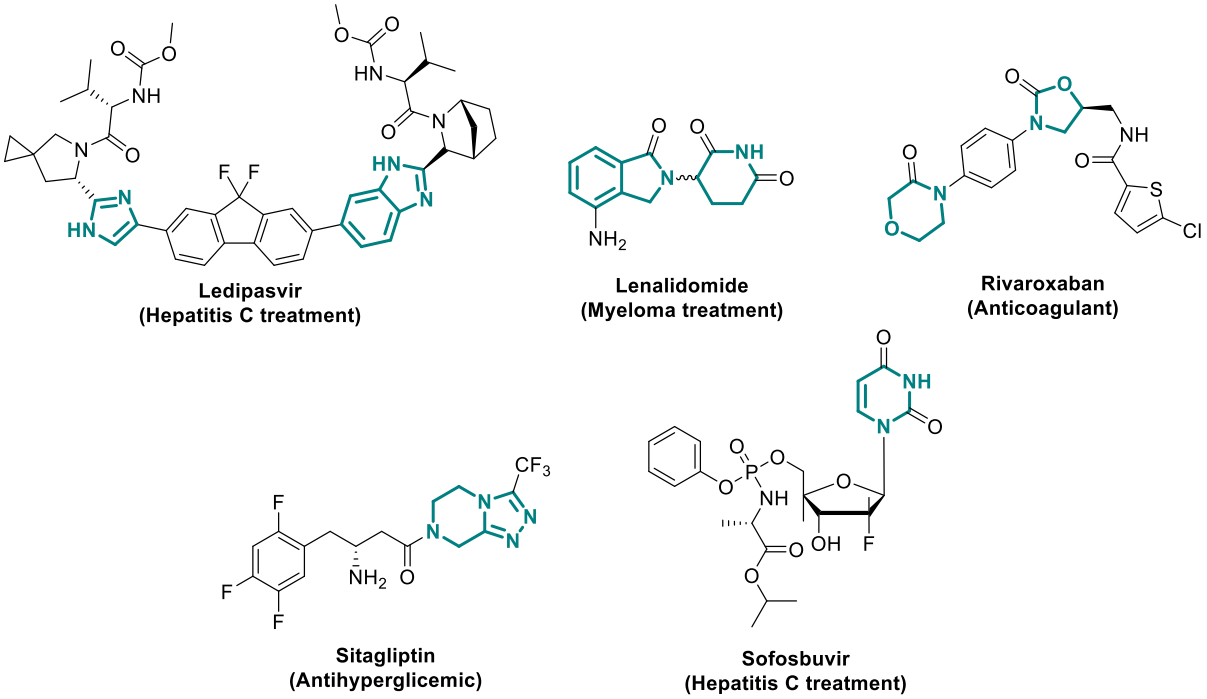

Figure 2 - Examples of top selling drugs exhibiting a nitrogen-containing heterocycle

One of the most interesting subclasses of heterocycles is certainly the quinoline core and its derivatives due to their prevalence in many useful compounds. For example, quinine extracted from the bark of cinchona trees has been used for centuries to treat malaria in South America and Europe.[7] New treatment also based on the quinoline core such as chloroquine and mefloquine, appeared in the first half of the 20th century to circumvent antimalarial-drug resistance.[8] Moreover, quinine is also used as a cheap chiral auxiliary.[9] Light was recently shed on chloroquine and hydroxychloroquine after their use to treat COVID-19 during the global pandemic.[10] As of August 2020, there is still no strong scientific consensus to support its use for either preventing or treating the disease.[11] Therefore, the

[7] H. M. Staines, S. Krishna, Eds. , *Treatment and Prevention of Malaria*, Springer Basel, Basel, **2012**.
[8] P. B. Bloland, "Drug resistance in malaria," can be found under https://www.who.int/csr/resources/publications/drugresist/malaria.pdf, **n.d.**
[9] Y. Zhang, S. Chitale, N. Goyal, G. Li, Z. S. Han, S. Shen, S. Ma, N. Grinberg, H. Lee, B. Z. Lu, C. H. Senanayake, *J. Org. Chem.* **2012**, *77*, 690–695.
[10] D. N. Juurlink, **2020**, *192*, 4.
[11] T. Fiolet, A. Guihur, M. E. Rebeaud, M. Mulot, N. Peiffer-Smadja, Y. Mahamat-Saleh, *Clinical Microbiology and Infection* **2020**, *0*, DOI 10.1016/j.cmi.2020.08.022.

emergency use authorizations for its use was revoked in the USA on June 15th and many other countries stopped using it in hospitals.[12]

2. Isoquinoline scaffold

We propose to focus our attention on one of its isomers: the isoquinoline core. This scaffold exists also in several reduced forms as shown in Figure 3:

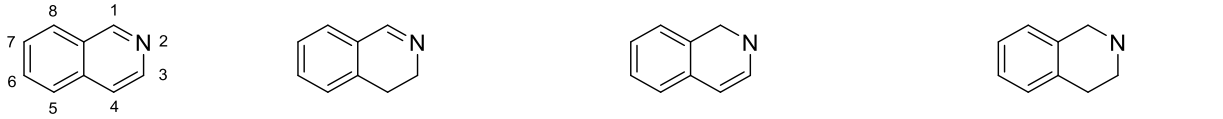

Figure 3 – Isoquinoline scaffold and its different reduced states

2.1. Biological interest

Isoquinoline derivatives are found in many alkaloids and possess several interesting attributes. Indeed, it has been reported that derivatives of this scaffold have antidepressant,[13] antimicrobial,[14] antiviral,[15] antiparasitic,[16] and antitumor properties.[17] Therefore, this is not surprising to find it in many marketed drugs, as represented in the Figure 4:

[12] D. N. Juurlink, **2020**, *192*, 4E. A. Meyerowitz, A. G. L. Vannier, M. G. N. Friesen, S. Schoenfeld, J. A. Gelfand, M. V. Callahan, A. Y. Kim, P. M. Reeves, M. C. Poznansky, *FASEB j.* **2020**, *34*, 6027–6037M. S. Cohen, *N Engl J Med* **2020**, NEJMe2020388D. R. Boulware, M. F. Pullen, A. S. Bangdiwala, K. A. Pastick, S. M. Lofgren, E. C. Okafor, C. P. Skipper, A. A. Nascene, M. R. Nicol, M. Abassi, N. W. Engen, M. P. Cheng, D. LaBar, S. A. Lother, L. J. MacKenzie, G. Drobot, N. Marten, R. Zarychanski, L. E. Kelly, I. S. Schwartz, E. G. McDonald, R. Rajasingham, T. C. Lee, K. H. Hullsiek, *N Engl J Med* **2020**, NEJMoa2016638.

[13] P. Zajdel, K. Marciniec, A. Maślankiewicz, G. Satała, B. Duszyńska, A. J. Bojarski, A. Partyka, M. Jastrzębska-Więsek, D. Wróbel, A. Wesołowska, M. Pawłowski, *Bioorganic & Medicinal Chemistry* **2012**, *20*, 1545–1556.

[14] A. Kubo, S. Nakahara, K. Inaba, Y. Kitahara, *Chem. Pharm. Bull.* **1986**, *34*, 4056–4068.

[15] J. Bedard, S. May, L. L'Heureux, T. Stamminger, A. Copsey, J. Drach, J. Huffman, L. Chan, H. Jin, R. F. Rando, *Antimicrob. Agents Chemother.* **2000**, *44*, 929–937.

[16] *Approaches to Design and Synthesis of Antiparasitic Drugs*, Elsevier, **1997**.

[17] M. M. Ghorab, M. S. Alsaid, M. S. Al-Dosari, F. A. Ragab, A. A. Al-Mishari, A. N. Almoqbil, *Acta Pharmaceutica* **2016**, *66*, 155–171.

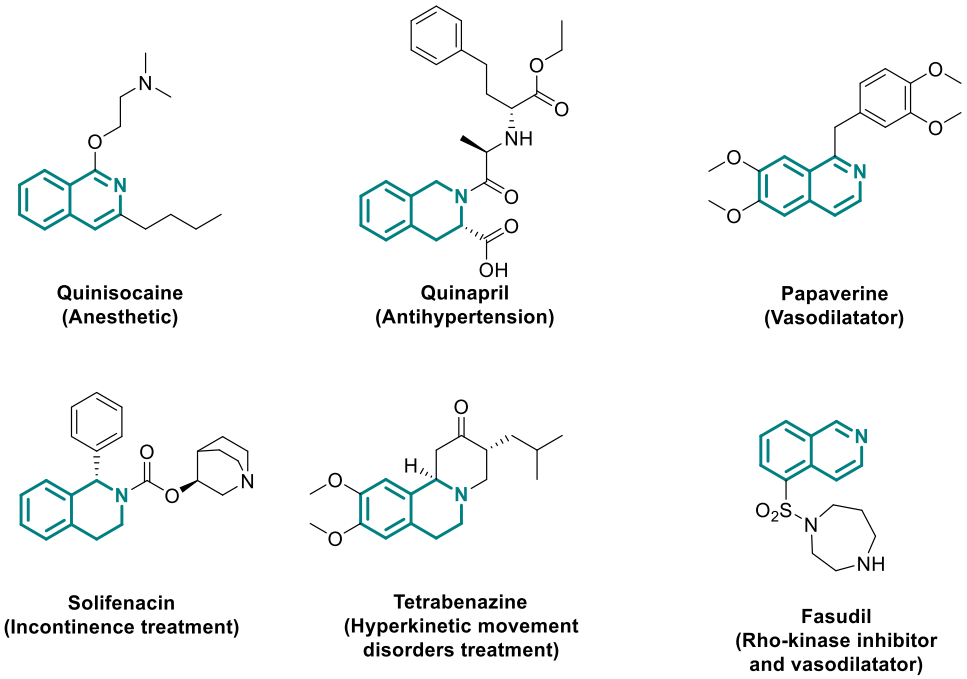

Figure 4 - Examples of drugs containing the isoquinoline scaffold

It is thus important to keep on developing efficient, fast and eco-compatible methods in order to access this scaffold of interest.

2.2. History of their synthesis

Isoquinolines' synthesis started a century ago and required harsh conditions leading to reduced functional group compatibility. Using side-products of the coal industry, it has been possible to isolate isoquinoline from coal tar in 1885.[18] Later, in 1893, the progress in the field of organic chemistry led to the first synthesis of the isoquinoline scaffold by the Bischler-Napieralski[19] and Pomeranz-Fritsch[20] processes, both reported the same year (Scheme 3). However, limitations of the methods reside in either the use of toxic reagents (PCl_5/$POCl_3$) or high operating temperatures. Two mechanisms are proposed for the Bischler-Napieralski reaction. Starting from a phenethylamide derivative **1** (eq. 1, Scheme 3) in the presence of a coupling reagent ($POCl_3$ or PCl_5), the reaction can be carried out in two different ways: *via* an imine-ester intermediate **2** or *via* a nitrilium intermediate **3**, both followed by an intramolecular electrophilic aromatic substitution, yielding **4**. On the other hand, the Pomeranz-Fritsch reaction (eq. 2, Scheme 3) requires high operating temperatures (e.g. 150 °C) and starts with the formation of an imine **7** with a benzaldehyde unit **5** and a 2,2-alkoxyethanolamine reagent **6**. Then, under acidic conditions, an intramolecular electrophilic aromatic substitution leads to the formation

[18] S. Hoogewerff, W. A. van Dorp, *Recl. Trav. Chim. Pays-Bas* **1885**, *4*, 125–129.
[19] Aug. Bischler, B. Napieralski, *Ber. Dtsch. Chem. Ges.* **1893**, *26*, 1903–1908.
[20] C. Pomeranz, *Monatshefte für Chemie und verwandte Teile anderer Wissenschaften* **1893**, *14*, 116–119P. Fritsch, *Ber. Dtsch. Chem. Ges.* **1893**, *26*, 419–422.

of the isoquinoline scaffold **8**, after release of two equivalents of alcohol units. The Pictet-Spengler process (eq. 3, Scheme 3) [21] was developed later, in 1911, and requires slightly milder operating temperature (100 °C). Its mechanism is similar to the Pomeranz-Fritsch mechanism: formation of an iminium **10** and then ring closure *via* an electrophilic aromatic substitution. Variations of these name reactions exists. A variation of the Bischler-Napieralski process allows the direct synthesis of the aromatic isoquinoline scaffold in one step. This process was developed by Pictet and Gams in 1909,[22] using a β-hydroxylated starting material. To finish, a variation of the Pomeranz-Fritsch process called the Schlitter-Müller variation allow the synthesis of 1-substituted isoquinolines using slightly different starting materials.[23]

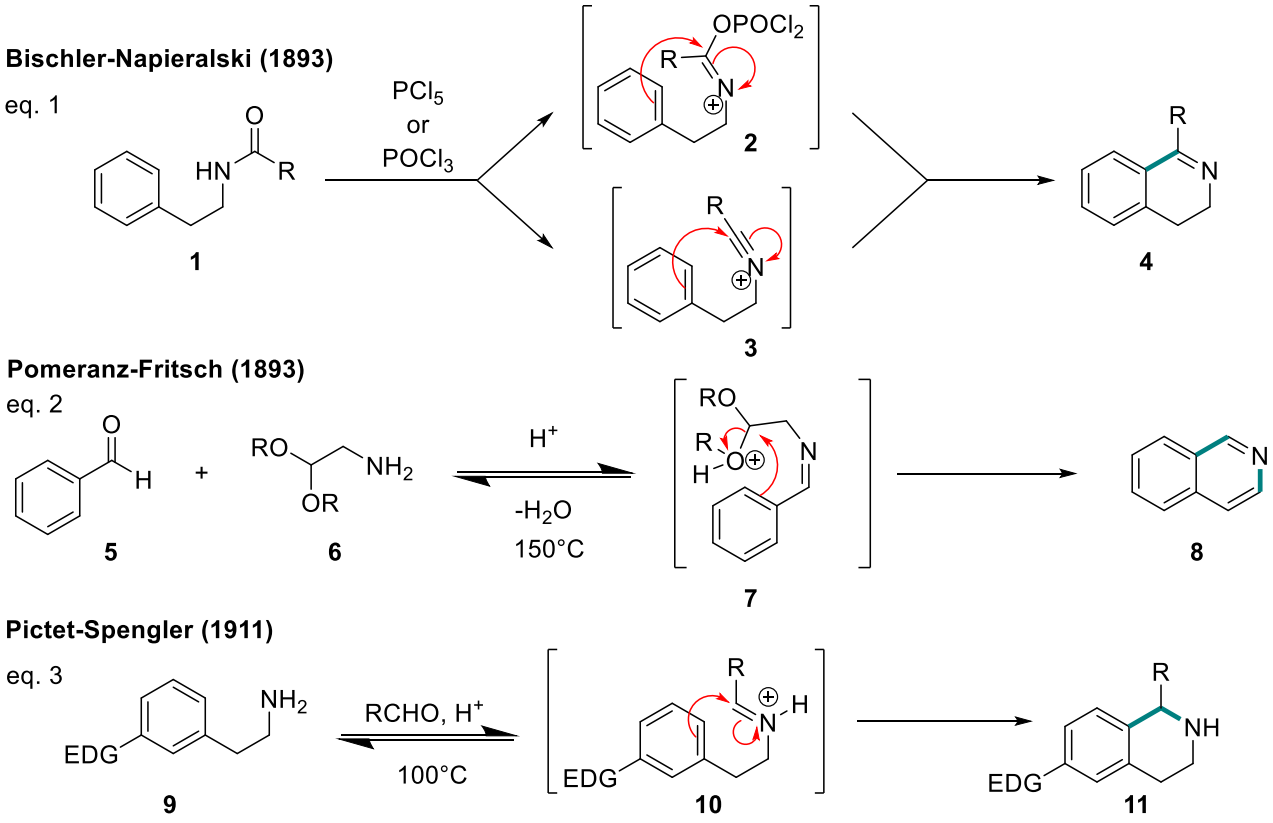

Scheme 3 - Traditional synthesis of isoquinoline derivatives

2.3. Modern synthesis

Palladium appeared to be an ally of choice for the synthesis of isoquinoline derivatives since the beginning of the 80's, about a century after the first synthesis of this scaffold was reported. Indeed, in 1982, Widdowson and his coworker reported a novel reaction to access the desired scaffold starting

[21] A. Pictet, T. Spengler, *Ber. Dtsch. Chem. Ges.* **1911**, *44*, 2030–2036.
[22] A. Pictet, A. Gams, *Ber. Dtsch. Chem. Ges.* **1909**, *42*, 2943–2952.
[23] E. Schlittler, J. Müller, *Helvetica Chimica Acta* **1948**, *31*, 914–924.

from a cyclopalladated arylimine.[24] Five years later, Pfeffer and coworkers reported the use of similar cyclopalladated compounds for the synthesis of isoquinolines.[25] Then, Heck reported the use of cyclopalladated benzylamine and benzaldimine derivatives for the same purpose.[26] Despite their novelty at that time, all these reactions suffer from the same common drawbacks from a modern standpoint. Indeed, cyclopalladated starting materials must be synthesized using stoichiometric amounts of palladium (Figure *5*) and in order to be efficient, these reactions require heating from 100°C to 200°C. The cost associated with the use of stoichiometric amounts of Pd simply makes those reactions not applicable on bigger scales.

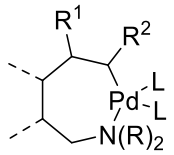

Figure 5 - Example of a cyclopalladated compound

Nowadays, progress in catalysis led to the development of new methodologies in order to access this scaffold of interest. As a matter of facts, in 1998, Larock's group played an important role in the development of methodologies as they reported for the first time the synthesis of isoquinolines **14** using only a catalytic amount of Pd catalyst via an iminoannulation reaction (Scheme 4).[27] The mechanism is thought to proceed via the oxidative addition of the Pd catalyst within the aryl-iodide bond of **12**. Then, a migratory insertion of the alkyne **13** yields a vinylic Pd intermediate **16**. The latter reacts with the nitrogen of the imine, forming a seven-membered palladacycle **17** followed by a reductive elimination which regenerates the catalyst and yields the isoquinoline ring **14**.

[24] D. A. Widdowson, **n.d.**, 4.
[25] F. Maassarani, M. Pfeffer, G. Le Borgne, *J. Chem. Soc., Chem. Commun.* **1987**, 565.
[26] Guangzhong. Wu, A. L. Rheingold, S. J. Geib, R. F. Heck, *Organometallics* **1987**, *6*, 1941–1946G. Wu, S. J. Geib, A. L. Rheingold, R. F. Heck, *J. Org. Chem.* **1988**, *53*, 3238–3241.
[27] K. R. Roesch, R. C. Larock, *J. Org. Chem.* **1998**, *63*, 5306–5307.

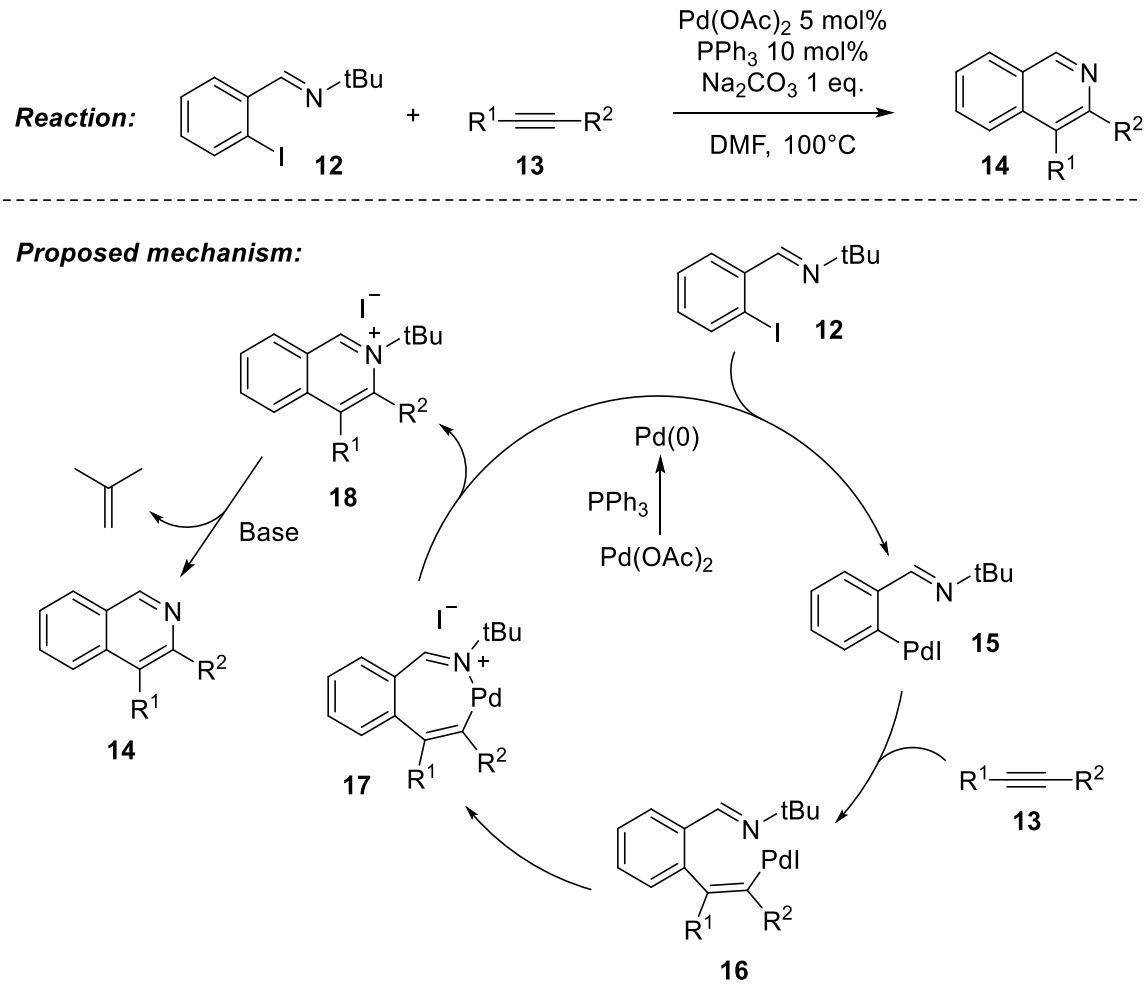

Scheme 4 - First example of isoquinoline synthesis using a catalytic amount of Pd, reported by Larock and Roesch

Later, the same team developed variations of this reaction while adding in the same time various substitutions on position 4 of the isoquinoline (Scheme 5). This time, they used *ortho*-alkynylbenzaldimine derivatives **19** with halogenated derivatives (aryl, allylic and alkynyl halides),[28] aryl halides under a carbon monoxide atmosphere[29] or an alkene[30] in order to substitute the desired position. The position 4 of the isoquinoline core is the easiest to substitute during the reaction mechanism since an alkenyl-palladium intermediate is formed at this position. The latter can react with a halogenated derivative (as listed above) or with an alkene which, after a reductive elimination or β-H elimination, lead to the incorporation of a substitution at this position. On the other hand, the aroylation of isoquinoline is afforded via the reaction of the palladium catalyst with CO and the aryl halide derivative prior to the reaction with the starting material.

[28] G. Dai, R. C. Larock, *Org. Lett.* **2001**, *3*, 4035–4038.
[29] G. Dai, R. C. Larock, *Org. Lett.* **2002**, *4*, 193–196.
[30] Q. Huang, R. C. Larock, *Tetrahedron Letters* **2002**, *43*, 3557–3560.

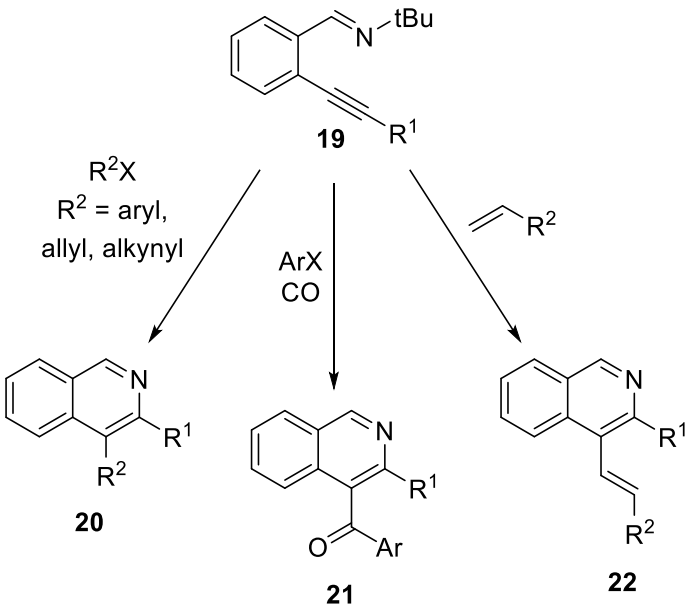

Scheme 5 - Various possible substitutions on the 4 position of the isoquinoline scaffold reported by Larock's team

Xu's team reported in 2013 a Rh-catalyzed oxidative coupling of hydrazone derivatives in order to synthesize multisubstituted isoquinolines.[31] They first screened the reactivity of various *N*-substituted benzophenone-derived hydrazones and selected the diethoxyphosphoryl group as the most suitable leaving group (Scheme 6). The proposed mechanism starts with the *ortho* C-H activation of the starting material **23**, helped by the nitrogen atom of the hydrazone, yielding the five-membered rhodacycle **26**. Then, an alkyne can insert within the Rh-C bond, affording the vinyl rhodium intermediate **27** which can lead to the formation of an iminium within the seven-membered rhodacycle **28**. Then, a reductive elimination followed by the elimination of the phosphoramidate moiety affords the desired isoquinoline scaffold **25**.

[31] W. Liu, X. Hong, B. Xu, *New York* **2013**, 13.

Reaction:

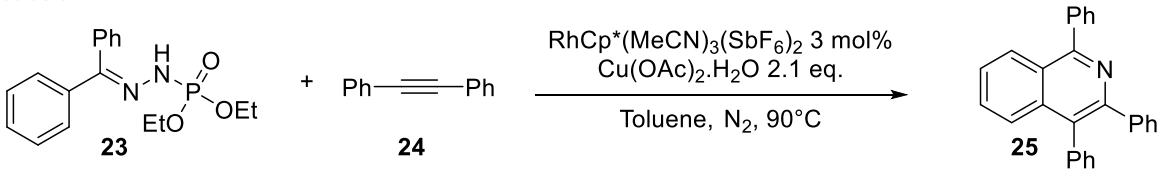

Proposed mechanism:

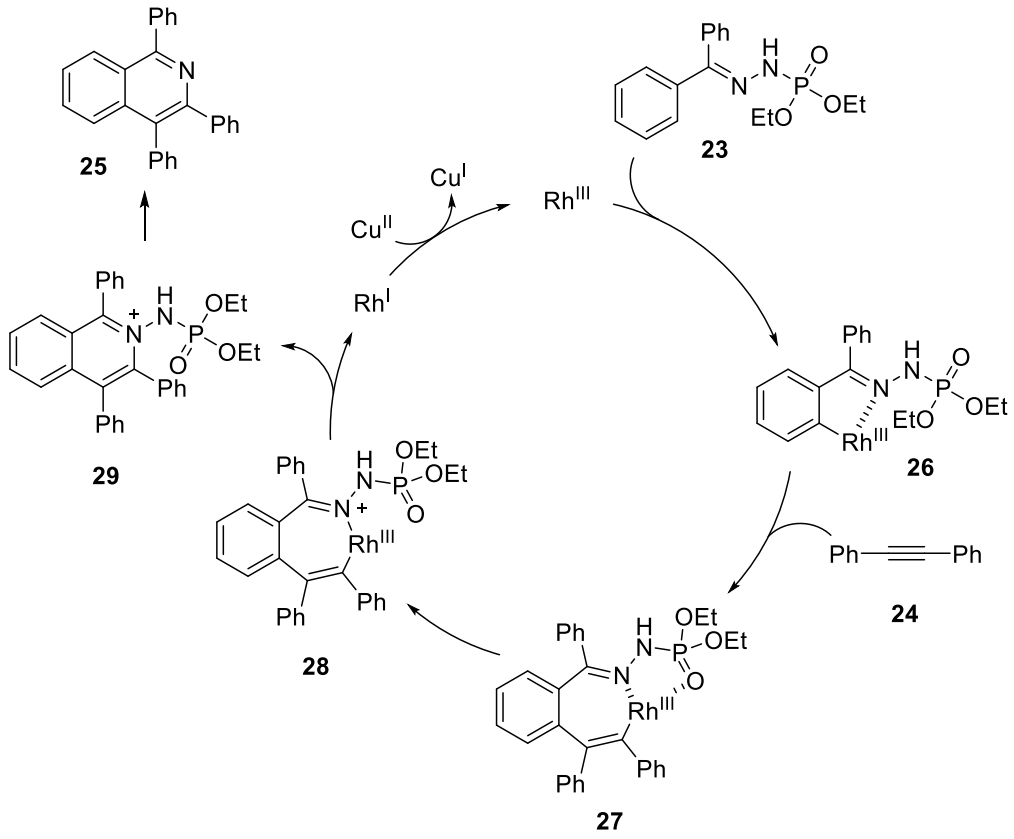

Scheme 6 - Rh-catalyzed oxidative coupling of aryl hydrazones with internal alkynes, reported by Xu's team

Many other reactions were later reported under transition metal catalysis and we will not tackle all of them in this chapter. However, it is worth noting that, recently, visible-light catalyzed methodologies were reported in the literature, opening a whole new way to access the isoquinoline scaffold. In 2015, Yu's team reported the synthesis of the phenanthridine core **31** which can be regarded as a benzoisoquinoline nucleus (Scheme 7).[32] This work relies on the synthesis of acyl oxime derivatives **30** which can lead, under photoredox catalysis, to the formation of an iminyl radical **32**. The latter can then react with the intramolecular aryl group via a homolytic aromatic substitution (HAS). Then, the formed radical intermediate **33** can be oxidized by the photocatalyst and close the catalytic cycle. They reported a few months later a one-pot variation of this methodology.[33]

[32] H. Jiang, X. An, K. Tong, T. Zheng, Y. Zhang, S. Yu, *Angew. Chem. Int. Ed.* **2015**, *54*, 4055–4059.
[33] X.-D. An, S. Yu, *Org. Lett.* **2015**, *17*, 2692–2695.

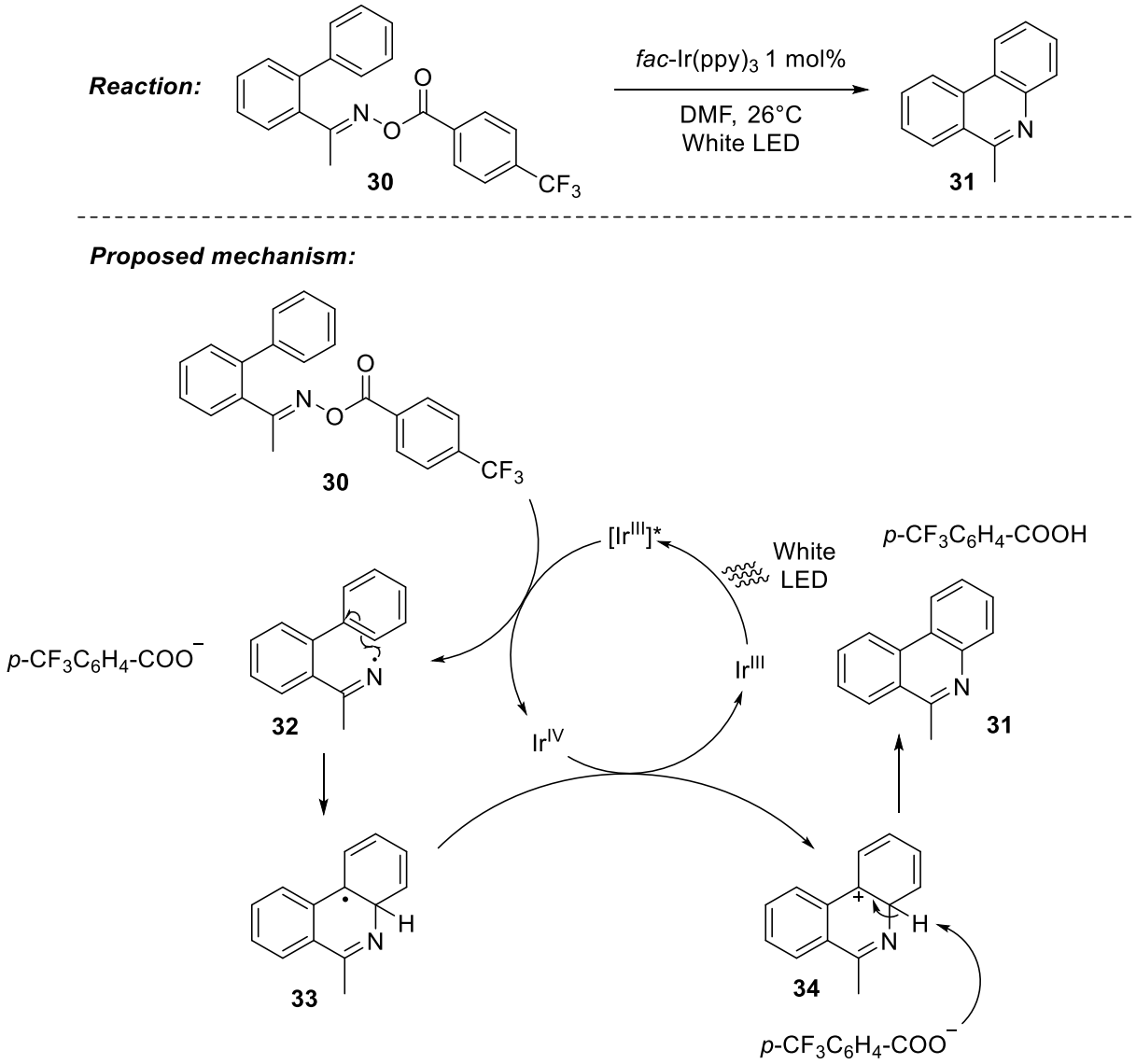

Scheme 7 - Synthesis of substituted isoquinolines under photoredox catalysis reported by Yu's team

During the past decades, transition-metal catalysis has taken a significant place in the landscape of modern chemistry. Pd, Ru, Rh and Ir no longer have to prove their usefulness and effectiveness in catalysis.[34] However, they bear common inherent disadvantages such as their very low Earth abundance within the crust and their high price (closely linked to their scarcity). Indeed, when we compare their abundance in mg/kg (*i.e.* ppm), they are all comprised in the range of 0.001 to 0.015 mg/kg. Their prices range between about 270$ per Troy ounce (about 31.1 g) for Ru, up to about 8500$ per Troy ounce for Rh.[35] This is why nowadays chemists explore the reactivity and the successful application of Earth abundant metals in catalysis such as Fe, Ni, Cu, Co and even Ag in a very broad

[34] *Homogeneous Catalysis: Mechanisms and Industrial Applications*, John Wiley & Sons, Inc, Hoboken, NJ, **2014**.
[35] "Daily Metal Price: Free Metal Price Tables and Charts," can be found under https://www.dailymetalprice.com/, **n.d.**

variety of reactions as evidenced by the increased number of publications in this field just during the last decade (see the following graph, Figure 6).

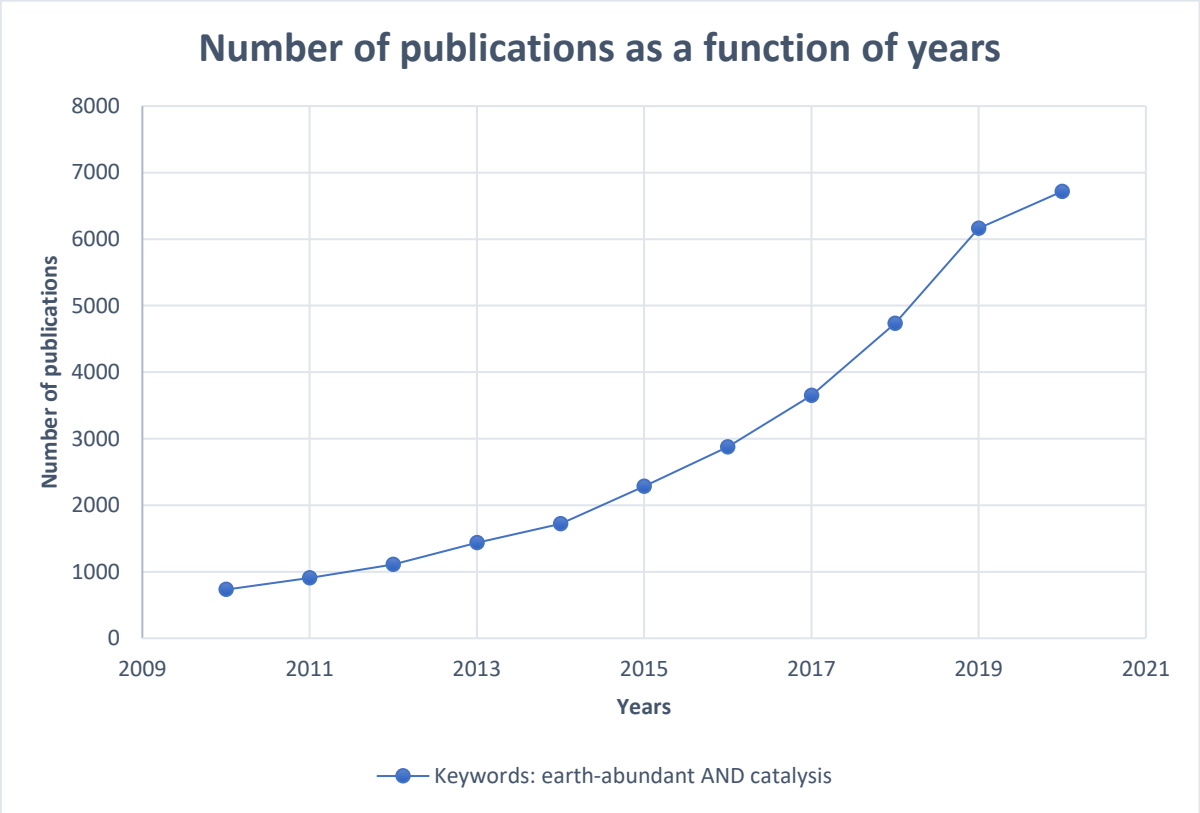

Figure 6 - Number of publications per year (Data retrieved on dimensions.ai on September 13th 2020)

These last metals are sold at a much cheaper prices of as low as 0.003$ per Troy ounce for Fe and up to 19$ per Troy ounce for Ag, which is the most expensive of the Earth-abundant metals cited above. We will now focus on Ag and its applications in catalysis for the synthesis of isoquinolines.

B) Silver

1. Silver in history

Silver is located in group 11, period 5 of the periodic table. It is located, within group 11, between Copper (period 4) and Gold (period 6). This metal is found as a mixture of two isotopes in an almost equal proportion of ^{107}Ag and ^{109}Ag and its most common oxidation state is either 0 or +I, although oxidation states of +II and +III have been witnessed.[36] Cu, Ag and Au are also called coinage metals for their use, centuries ago and even until now, in coin minting. Indeed, the very good wear resistance and

[36] Z. Mazej, D. Kurzydłowski, W. Grochala, in *Photonic and Electronic Properties of Fluoride Materials* (Eds.: A. Tressaud, K. Poeppelmeier), Elsevier, Boston, **2016**, pp. 231–260S. Riedel, M. Kaupp, *Coordination Chemistry Reviews* **2009**, *253*, 606–624.

anti-corrosive properties of alloys containing these metals pushed for their use. The earliest known use of silver in coins was found in the Kingdom of Lydia (eastern Turkey) around 600 BC and were made out of electrum, a naturally occurring alloy of silver and gold (**A**, Figure 7).[37]

Silver is known to be used since Human prehistory, all over the world because of its natural occurrence in pure ores but even naturally occurring alloys. However, its softness prevented its application in fields others than ornament and decoration. Its use gained a lot more interest after the development of sterling silver (an alloy of 92.5% of silver and 7.5% of another metal, generally copper) which is much more resistant and harder. It was therefore used more commonly to mint coins, create silverware and jewelry (**B**, Figure 7).[38] Another prominent use of silver is in medicine. Indeed, Hippocrates reported as early as the 5th century BC the use of silver to treat wounds (**C**, Figure 7). It is only later, around the end of the 18th and beginning of the 19th century that surgeon started using silver sutures to prevent inflammations and infections. It later fell into disuse around World War II with the development of antibiotics but is still used nowadays in topical creams and solutions for its antibacterial properties against a broad spectrum of gram-positive and gram-negative bacterias.[39] Moreover, silver has the highest electrical conductivity, thermal conductivity and optical reflectivity of any other metal making it a key element for the production of semiconductors, circuits and other associated elements.[40] Lastly, silver salts were used in the early development of photography. Nicéphore Niépce developed in 1816 what was called a heliographic process in which a paper coated with silver chloride was exposed to light through a camera (**D**, Figure 7). This process created negative photographs. He left his notes to Louis Daguerre before his death, in 1833. Daguerre perfected the technique and disclosed it in front of the French academy of sciences in 1839. The development of other processes continued such as the collodion process which dominated the latter half of the 19th century and still required silver salts as its key photoreactive component.[41]

---

[37] R. Seaford, *Money and the Early Greek Mind: Homer, Philosophy, Tragedy*, Cambridge University Press, **2009**.
[38] A. C. Reardon, *Metallurgy for the Non-Metallurgist*, ASM International, Materials Park, Ohio, **2011**.
[39] T. Dai, Y.-Y. Huang, S. K. Sharma, J. T. Hashmi, D. B. Kurup, M. R. Hamblin, *PRI* **2010**, *5*, 124–151.
[40] C.-J. Li, X. Bi, "Silver Catalysis in Organic Synthesis, 2 Volume Set | Wiley," can be found under https://www.wiley.com/en-us/Silver+Catalysis+in+Organic+Synthesis%2C+2+Volume+Set-p-9783527342815, **n.d.**
[41] R. Hirsch, *Seizing the Light: A Social & Aesthetic History of Photography*, Routledge, Taylor & Francis Group, New York, **2017**.

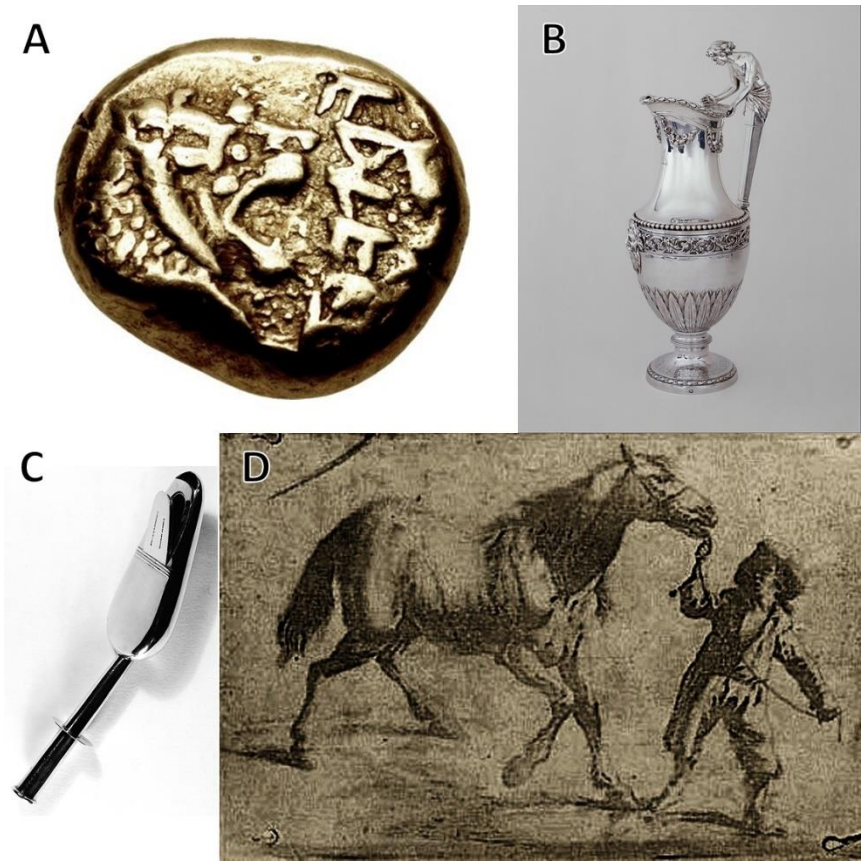

Figure 7 -A) Electrum coin, Kingdom of Lydia (circa 620 BC) B) French neoclassical ewer (1784-1785) C) Silver medicine spoon (1828) D) Earliest known heliographic engraving made by Niépce (1825)

2. State of the art

Our goal is not to depict an exhaustive presentation of the versatility and wide use of silver in chemistry. However, we need to keep in mind that silver catalysis was applied to a range of reactions almost as wide as its more common metal counterparts. Indeed, silver catalysis can be applied to various types of reactions such as cycloadditions, cycloisomerizations, radical reactions, coupling reactions, allylations, aldol reactions, and C-H bond activation.[42] Asymmetric reaction has also been developed under silver catalysis. [43]

[42] J.-M. Weibel, A. Blanc, P. Pale, *Chem. Rev.* **2008**, *108*, 3149–3173M. Álvarez-Corral, M. Muñoz-Dorado, I. Rodríguez-García, *Chem. Rev.* **2008**, *108*, 3174–3198Y. Yamamoto, *Chem. Rev.* **2008**, *108*, 3199–3222H. V. R. Dias, C. J. Lovely, *Chem. Rev.* **2008**, *108*, 3223–3238M. M. Díaz-Requejo, P. J. Pérez, *Chem. Rev.* **2008**, *108*, 3379–3394N. T. Patil, Y. Yamamoto, *Chemical Reviews* **2008**, *108*, 3395–3442.

[43] M. Naodovic, H. Yamamoto, *Chem. Rev.* **2008**, *108*, 3132–3148H. Pellissier, *Chem. Rev.* **2016**, *116*, 14868–14917.

C) Ag-catalyzed tandem cycloisomerization/hydroarylation reactions: state of the art

1. Hydroarylation and cycloisomerization reactions

As showcased earlier, Ag-catalysis can be applied for a wide variety of reactions. We will focus in this chapter on silver-catalyzed tandem cycloisomerization/hydroarylation reactions.

To begin, hydroarylation reactions encompass all addition of an aromatic or heteroaromatic C-H bond across an alkene or an alkyne group, thus creating, in a single step, a C-C and a C-H bond.[44] A general representation of such reaction is represented in Scheme 8:

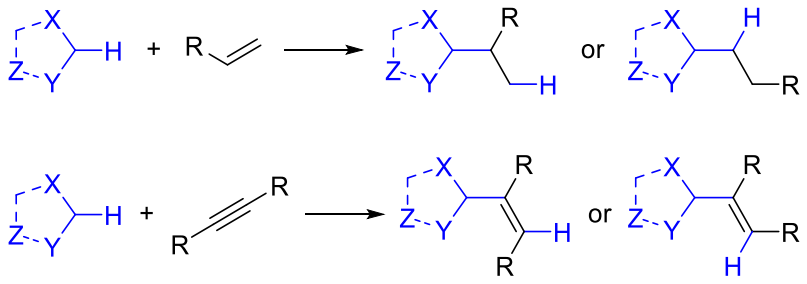

Scheme 8 - General scheme of a hydroarylation reaction

Cycloisomerization reactions are, on the other hand, a transformation of polyunsaturated substrates by which C-C bonds are formed while at least one degree of unsaturation is consumed in order to make a cyclic isomer (without losing or gaining any atom).[45] A representation of such general reaction is made in Scheme 9, where many combinations are presented:

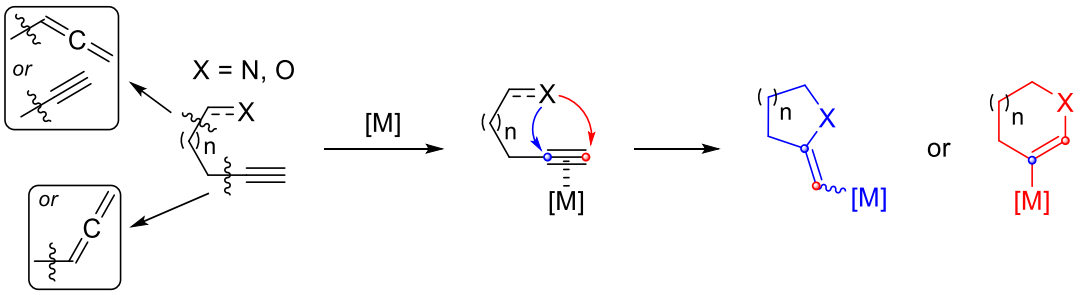

Scheme 9 - General scheme of a cycloisomerization reaction

These two reactions have in common their extreme atom economical nature which is a pinnacle in organic chemistry. Therefore, merging them in a tandem reaction catalyzed by Ag provides a very desirable approach to access complex and exotic scaffolds in one step. Our group already reported

---

[44] L. Ackermann, *Catalytic Hydroarylation of Carbon-Carbon Multiple Bonds*, Wiley-VCH Verlag GmbH & Co. KGaA, Weinheim, Germany, **2017**.

[45] A. Marinetti, H. Jullien, A. Voituriez, *Chem. Soc. Rev.* **2012**, *41*, 4884.

various examples of such tandem reactions which includes an oxygen-containing starting material.[46,47,48,49]

2. Previous work in Oxygen-containing series

2.1. In our group

Our group started working on silver-catalyzed tandem reactions in 2007. They reported the versatile synthesis of either furoquinolines **36** or pyranoquinolines **37** depending on the intramolecular attack of the oxygen on an alkynyl group of **35**, in a 5-*exo*-dig or 6-*endo*-dig fashion (Scheme 10).[46] This selectivity was possible by using different types of silver salts. Indeed, two groups were identified in order to promote the preferential formation of one product or another. $AgSbF_6$, $AgPF_6$, AgOTf, and $AgNO_3$ led to the exclusive formation of the 6-*endo*-dig product. These catalysts are known to form π-complexes with alkynes,[50] thus acting like transition-metal catalysts.[51] On the contrary, Ag_2CO_3, Ag_2O, and AgO exhibits oxidizing properties of oxygenated functions[52] and can activate aldehyde/ketone function (Lewis acid properties), therefore creating σ-complexes.

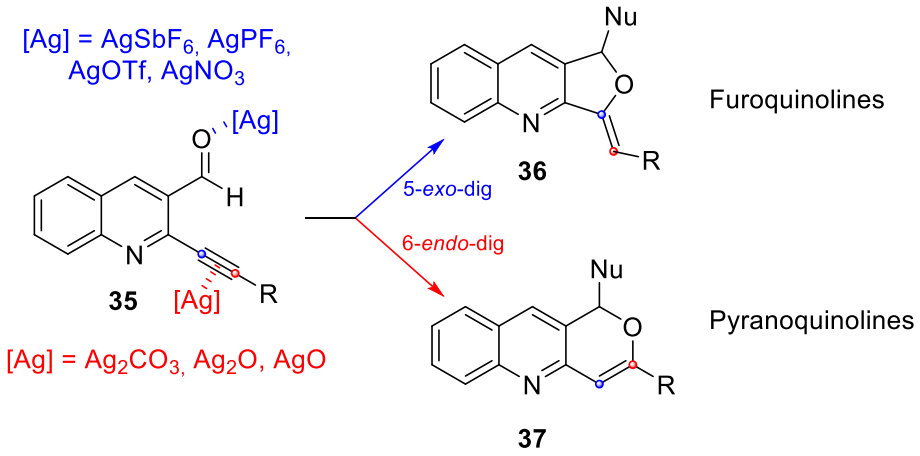

Scheme 10 - Control of regiochemistry via the use of different Silver salts

Later, the addition of (hetero)aromatic nucleophiles onto the starting material via a hydroarylation reaction, concomitant with the cycloisomerization, was developed leading to the synthesis of

[46] T. Godet, C. Vaxelaire, C. Michel, A. Milet, P. Belmont, *Chemistry - A European Journal* **2007**, *13*, 5632–5641.
[47] E. Parker, N. Leconte, T. Godet, P. Belmont, *Chem. Commun.* **2011**, *47*, 343–345.
[48] G. Mariaule, G. Newsome, P. Y. Toullec, P. Belmont, V. Michelet, *Organic Letters* **2014**, *16*, 4570–4573.
[49] A. Bontemps, G. Mariaule, S. Desbène-Finck, P. Helissey, S. Giorgi-Renault, V. Michelet, P. Belmont, *Synthesis* **2016**, *48*, 2178–2190.
[50] G. S. Lewandos, D. K. Gregston, F. R. Nelson, *Journal of Organometallic Chemistry* **1976**, *118*, 363–374.
[51] X. Yao, C.-J. Li, *J. Org. Chem.* **2005**, *70*, 5752–5755.
[52] M. Fétizon, K. A. Parker, D.-S. Su, pp. 361-372, *Handbook of Reagents for Organic Synthesis, Oxidizing and Reducing Agents*, Wiley, Chichester, West Sussex, UK ; New York, **1999**.

elaborated scaffolds (Scheme 11). Indeed, our group reported the synthesis of (hetero)aryl functionalized isochromenes[48] and pyranoquinolines[49] using AgOTf as the catalyst.

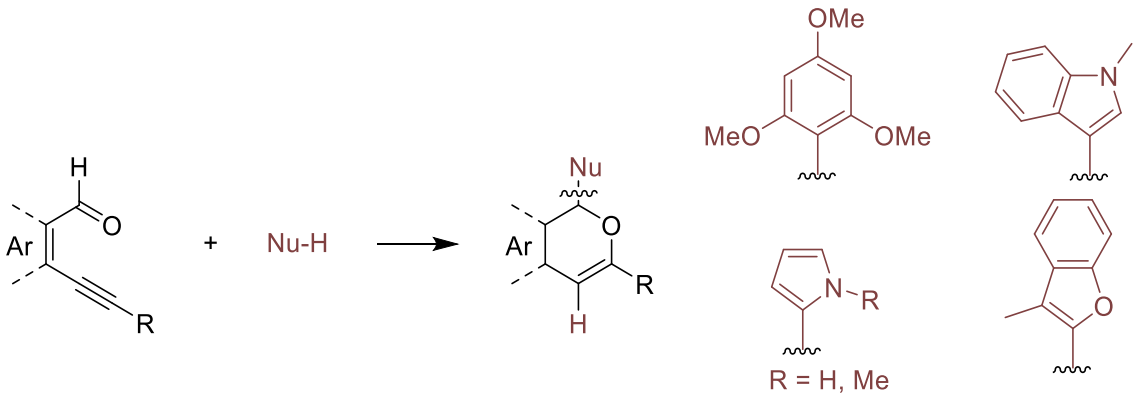

Scheme 11 - Silver catalyzed tandem cycloisomerization/hydroarylation reported by Belmont and coworkers

With all these developments on aldehyde/ketone-containing starting material, we envisioned that a variation of it was possible by transforming these functions into imine derivatives. Reports were already made in the last two decades about such reaction.

3. Previous work in Nitrogen-containing series

As previously shown, Larock's group was the first to report the synthesis of isoquinoline derivatives **39** under Pd catalysis, back in 1998.[27] They later reported a dual Pd/Cu-catalyzed variation of their methodology with terminal alkynes **38** (Scheme 12).[53]

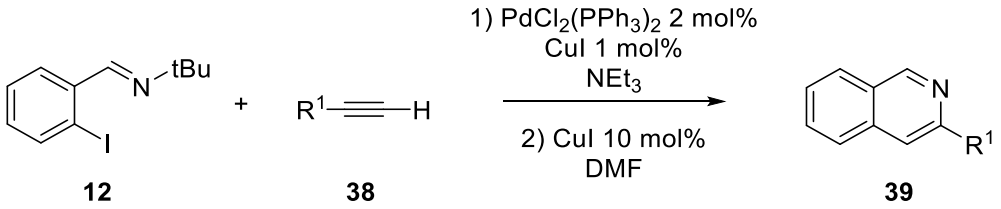

Scheme 12 -Synthesis of isoquinolines using terminal alkynes, reported by Larock's group

Then, in 2003, they reported the first Ag-catalyzed cycloisomerization reaction of an *o*-(1-alkynyl)benzaldimine **40**, among other electrophiles that could activate the alkynyl unit.[54] Indeed, I_2, ICl, CuI, PhSeCl as well as $AgNO_3$ (among others) could promote the cycloisomerization reaction (Scheme 13). The mechanism is believed to proceed via an activation of the alkynyl group by the silver salt, therefore increasing its electrophilicity. Then, the nitrogen of the imine function can attack in 6-*endo*-dig fashion, yielding the isoquinolinium intermediate **43**. The *tert*-butyl function on the nitrogen

[53] K. R. Roesch, R. C. Larock, *Org. Lett.* **1999**, *1*, 553–556*J. Org. Chem.* **2002**, *67*, 86–94.
[54] Q. Huang, J. A. Hunter, R. C. Larock, *The Journal of Organic Chemistry* **2002**, *67*, 3437–3444.

is then lost, giving a *tert*-butyl cation **45** which leads to isobutene **46**. The final scaffold **41** is obtained after a protodeargentation step.

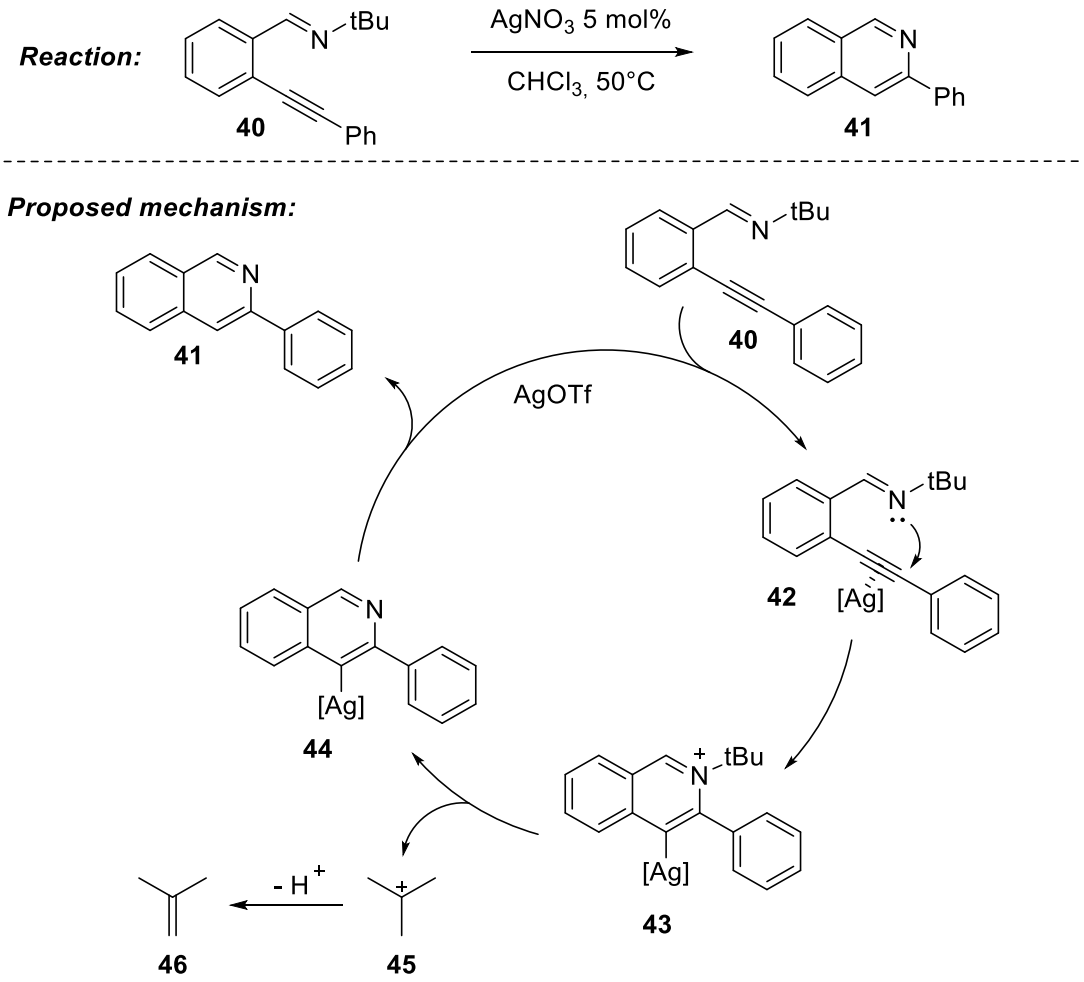

Scheme 13 – First example of a Ag-catalyzed cycloisomerization of an o-(1-alkynyl)benzaldimine reported by Larock's group

Asao's group later investigated the addition of various pronucleophiles during the reaction in order to functionalize the position 1 of the isoquinoline scaffold.[55] Using AgOTf as the catalyst, they were able to incorporate on the final scaffold nitromethane, nitroethane, acetylacetone, malonate, malonitrile, acetone, and even terminal alkynes. The proposed mechanism is similar to the one reported by Larock's group. However, they did not use *tert*-butylimine in their methodology but instead they used imine derivatives, formed using aniline and aliphatic imine derivatives. Moreover, the presence of a pronucleophile in the reaction medium results in its nucleophilic addition onto the iminium of the isoquinolinium intermediate and also the substitution at position 1.

[55] N. Asao, S. Yudha S., T. Nogami, Y. Yamamoto, *Angewandte Chemie International Edition* **2005**, *44*, 5526–5528.

Later, Porco Jr. and Su reported a new synthetis of pyrroloisoquinolines **48** under silver catalysis via a cycloisomerization/dipolar cycloaddition (Scheme 14).[56] Pyrroloisoquinolines **48** are present in the core of lamellarins, a family of alkaloids, and some lamellarin derivatives exhibit *in vitro* activity towards the inhibition of HIV-1 integrase. The reaction proceeds first via the coordination the alkynyl group with a silver salt, followed by its attack by an imino group, yielding **50**. The starting materials employed in the methodology bears an *N*-benzylidene glycinate moiety which leads to the formation of an azomethine ylide **51** after the attack of the imine. This intermediate is then capable of reacting with an external alkynyl group **52** leading to the final pyrroloisoquinoline scaffold **48** upon oxidation.

[56] S. Su, J. A. Porco, *Journal of the American Chemical Society* **2007**, *129*, 7744–7745.

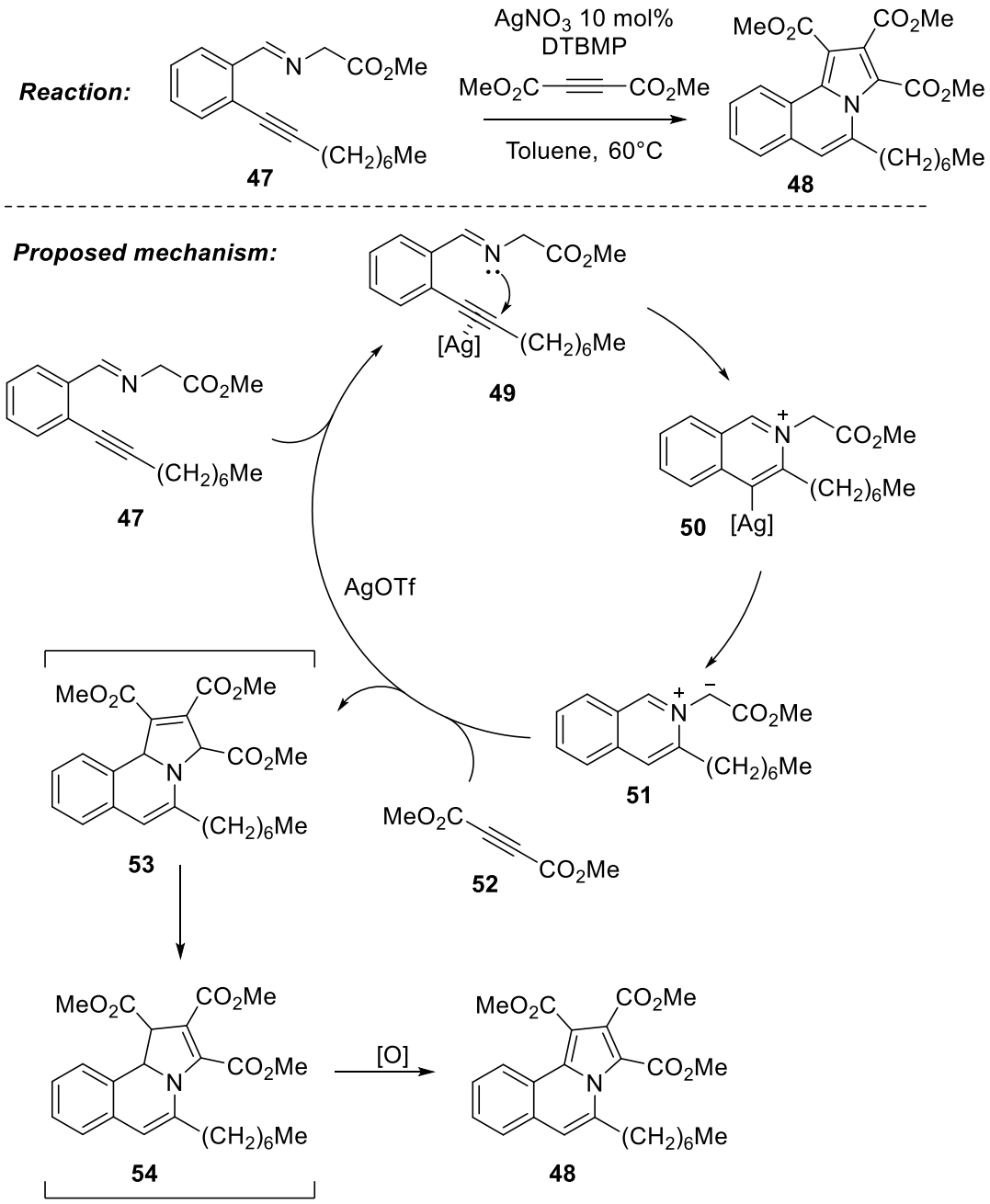

Scheme 14 - Ag-catalyzed formation of pyrrolo-isoquinoline derivates reported by Porco Jr and Su

Jie Wu's group played an important role in the development of new silver-catalyzed methodologies for the formation of isoquinolines, with a focus on varying the nature of the nucleophile. They were able to incorporate a wide variety of substitutions in the final scaffold such as α,β-unsaturated ketones **55**,[57] phosphonates **56**,[58] imidazoles **57**,[59] ketones **58**,[60] indoles **59**,[61] and even trifluoromethyl groups

[57] S. Ye, J. Wu, *Tetrahedron Letters* **2009**, *50*, 6273–6275.
[58] W. Sun, Q. Ding, X. Sun, R. Fan, J. Wu, *J. Comb. Chem.* **2007**, *9*, 690–694.
[59] H. Lou, S. Ye, J. Zhang, J. Wu, *Tetrahedron* **2011**, *67*, 2060–2065.
[60] Q. Ding, J. Wu, *Org. Lett.* **2007**, *9*, 4959–4962.
[61] X. Yu, J. Wu, *J. Comb. Chem.* **2010**, *12*, 238–244.

61[62] at position 1 (Scheme 15). The latter being the only one made straightforwardly from the reaction of an imino derivative **60** and a nucleophile, all the other transformations being set up as a three-component reaction *i.e.* from the reaction of an aldehyde-containing aromatic bearing an alkynyl unit, an amino derivative (often anilines) and the nucleophile.

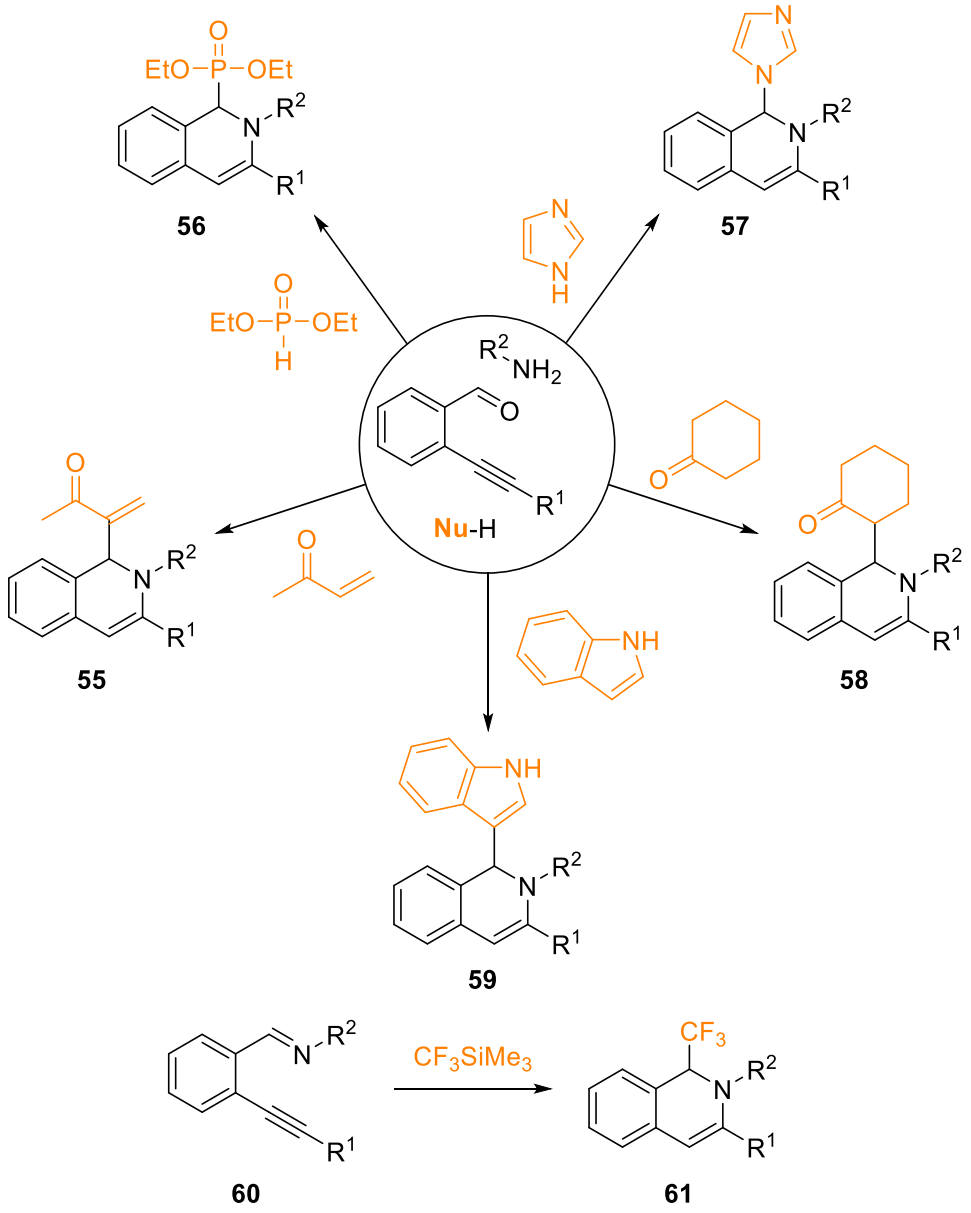

Scheme 15 - Various examples of Wu's team for the two/three-components silver-catalyzed formation of isoquinolines

In 2011, Abbiati et coll.[63] reported a silver-catalyzed microwave-assisted domino addition/annulation reaction leading to the formation of isoquinolines **63** and naphthalen-1-amine **64** structures in the presence of ammonia (Scheme 16). The reaction begins with the nucleophilic attack of ammonia onto the activated carbonyl function **65**. Then, the formation of the two different products

[62] X. Wang, G. Qiu, L. Zhang, J. Wu, *Tetrahedron Letters* **2014**, *55*, 962–964.
[63] M. Dell'Acqua, G. Abbiati, A. Arcadi, E. Rossi, *Organic & Biomolecular Chemistry* **2011**, *9*, 7836.

originates from the tautomeric equilibrium between the imine **66** and enamine **67**, resulting in a C- or N-addition onto the alkynyl unit.

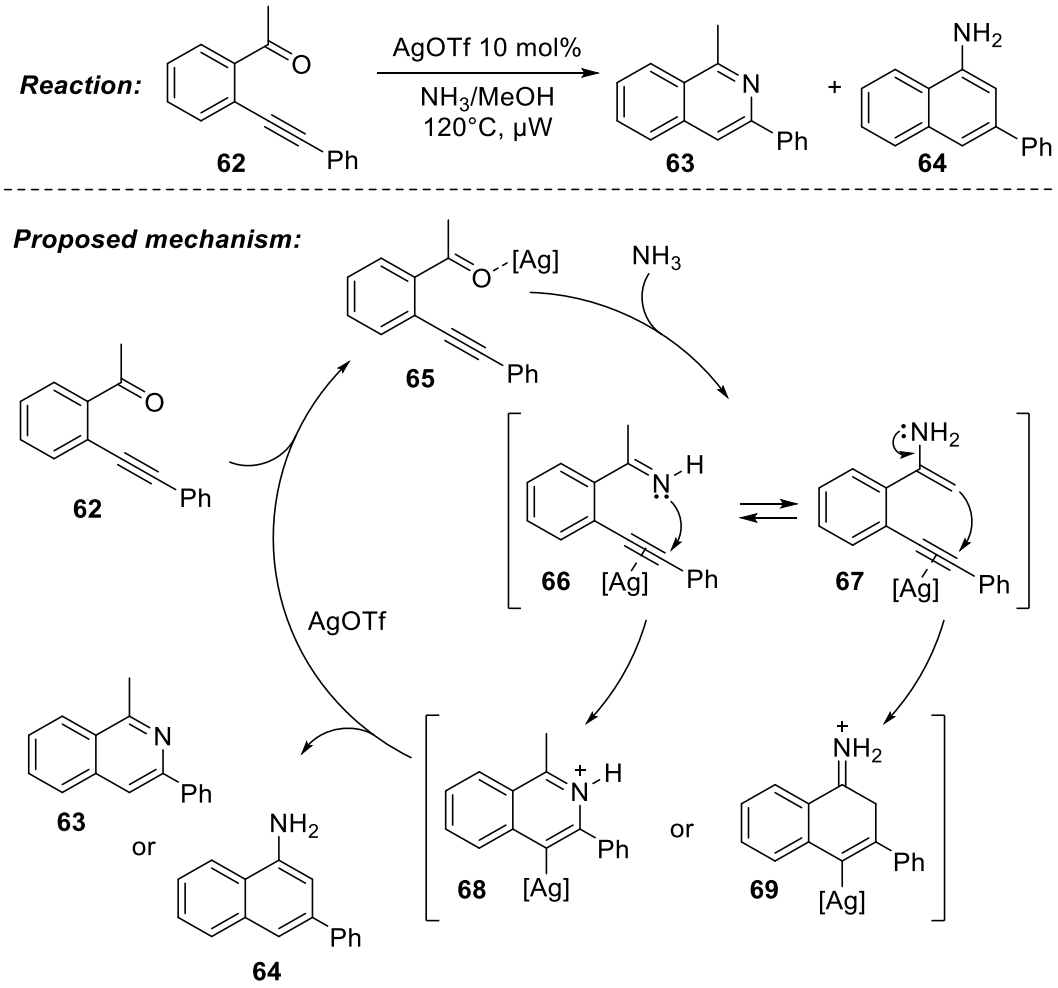

Scheme 16 - Silver-catalyzed microwave-assisted domino addition/annulation for the synthesis of isoquinoline, reported by Abbiati et coll.

Despite all those available methodologies, we still need to develop new reactions that are compatible with the broadest types of substitutions on the starting material while also being compatible with more heterocyclic nucleophiles for the efficient formation of C-C bonds through the hydroarylation step.

With that aim in mind, we intended to develop a new Ag-catalyzed tandem reaction which comprises all together the hydroarylation of an aryl nucleophile onto a C-N double-bond and the cycloisomerization reaction between an amino function and an alkynyl group (Scheme 17).

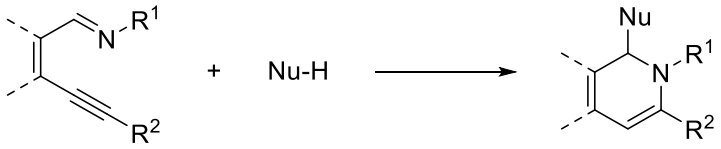

Scheme 17 - General representation of a tandem cycloisomerization/hydroarylation reaction on ortho-alkynylbenzaldimine derivatives

D) Silver-catalyzed tandem cycloisomerization/hydroarylation reactions applied to the synthesis of isoquinolines (*via* the use of imino derivatives).

1. Synthesis of the starting materials

1.1. Synthesis of carbonyl/alkynyl derivatives

Aldehyde and ketone derivates, bearing alkynyl substituents, were synthesized using the classical Sonogashira cross-coupling reaction. The synthesis of *ortho*-alkynylbenzaldehyde/*ortho*-alkynylarylketone derivatives was made using commercially available or synthesized *ortho*-haloarylaldehyde/*ortho*-haloarylketone with an alkyne derivative, itself being commercially available or synthesized. Alkynes were synthesized using halogenated derivatives cross-coupled with trimethylsilylacetylene and subsequently deprotected.[64] The Sonogashira cross-coupling reactions were performed in triethylamine as a solvent as reported in 2014 by Mariaule *et al*[48] which is suitable with a majority of molecules. We chose 2-(phenylethynyl)benzaldehyde as our model substrate and investigated the influence of various substitutions on its scaffold. Table 1 contains the list of all the Sonogashira cross-coupling products.

[64] C. Ye, Y. Li, H. Bao, *Advanced Synthesis & Catalysis* **2017**, *359*, 3720–3724.

Table 1 - Sonogashira cross-coupling products

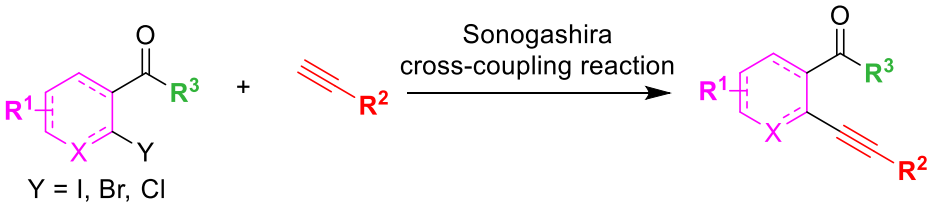

Model substrate

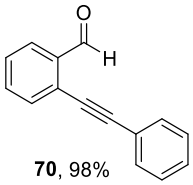

70, 98%

Main ring modifications

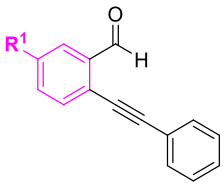

71, R^1 = fluorine, 72%
72, R^1 = chlorine, 78%
73, R^1 = methoxy, quant.

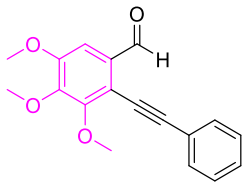

74, quant.

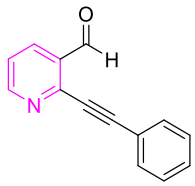

75, 60%

Alkynyl modifications

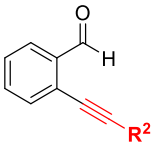

76, R^2 = 4-methoxyphenyl, 88%
77, R^2 = 2,5-dimethylphenyl, quant.
78, R^2 = 4-trifluoromethylphenyl, 74%
79, R^2 = 3-nitrophenyl, 66%
80, R^2 = 2-thiophenyl, 69%
81, R^2 = 1-cyclohexenyl, 99%
82, R^2 = *n*-hexyl, 69%
83, R^2 = $C(CH_3)_2OH$, 89%
84, R^2 = TMS, 78%

The model substrate (**70**) for this reaction was isolated in a very high 98% yield. The cross-coupling reaction was also compatible with a wide variety of substitutions on the main ring. Halogen groups such as a fluorine (**71**) or a chlorine (**72**) led to a high yield of 72% and 78%, respectively. Electron-donating group were even better tolerated since a methoxy (**73**) or a trimethoxy (**74**) substitution gave the desired Sonogashira products in quantitative yields. The presence of a pyridine on the main ring instead of a phenyl was a bit detrimental for the reaction, yielding the desired product (**75**) in a medium 60% yield.

Finally, alkynyl modifications were very well tolerated for the cross-coupling, with yields ranging between 66% and 99%. Various alkynes were coupled, including EWG/EDG aromatics (**76**-**79**), a thiophene (**80**), aliphatic chains (**81**, **82**), an alcohol (**83**) and even a TMS group (**84**).

1.2. Synthesis of imine derivatives

Once the Sonogashira cross-coupling products are obtained, the synthesis of the imine is very straightforward. Indeed, following the protocol reported by Obika *et al.* in 2007[65] on the same type of substrates, they can be obtained after the reaction of an aldehyde or ketone derivative with an amine or aniline in dichloromethane in the presence of 3 Å molecular sieves. The latter is required to remove

[65] S. Obika, H. Kono, Y. Yasui, R. Yanada, Y. Takemoto, *The Journal of Organic Chemistry* **2007**, *72*, 4462–4468.

all the water molecules released after the formation of the imine derivatives and prevent the hydrolysis of the imine. In some cases, a slightly different protocol was used in order to access greater yields. Indeed, using an excess of imine, in the presence again of molecular sieves and a catalytic amount of acetic acid helped to afford greater yields for some substrates (see experimental part).

We were able to synthesize a wide variety of aromatic imines with few aliphatic ones. They are represented in Table 2:

Table 2 - Imine starting material

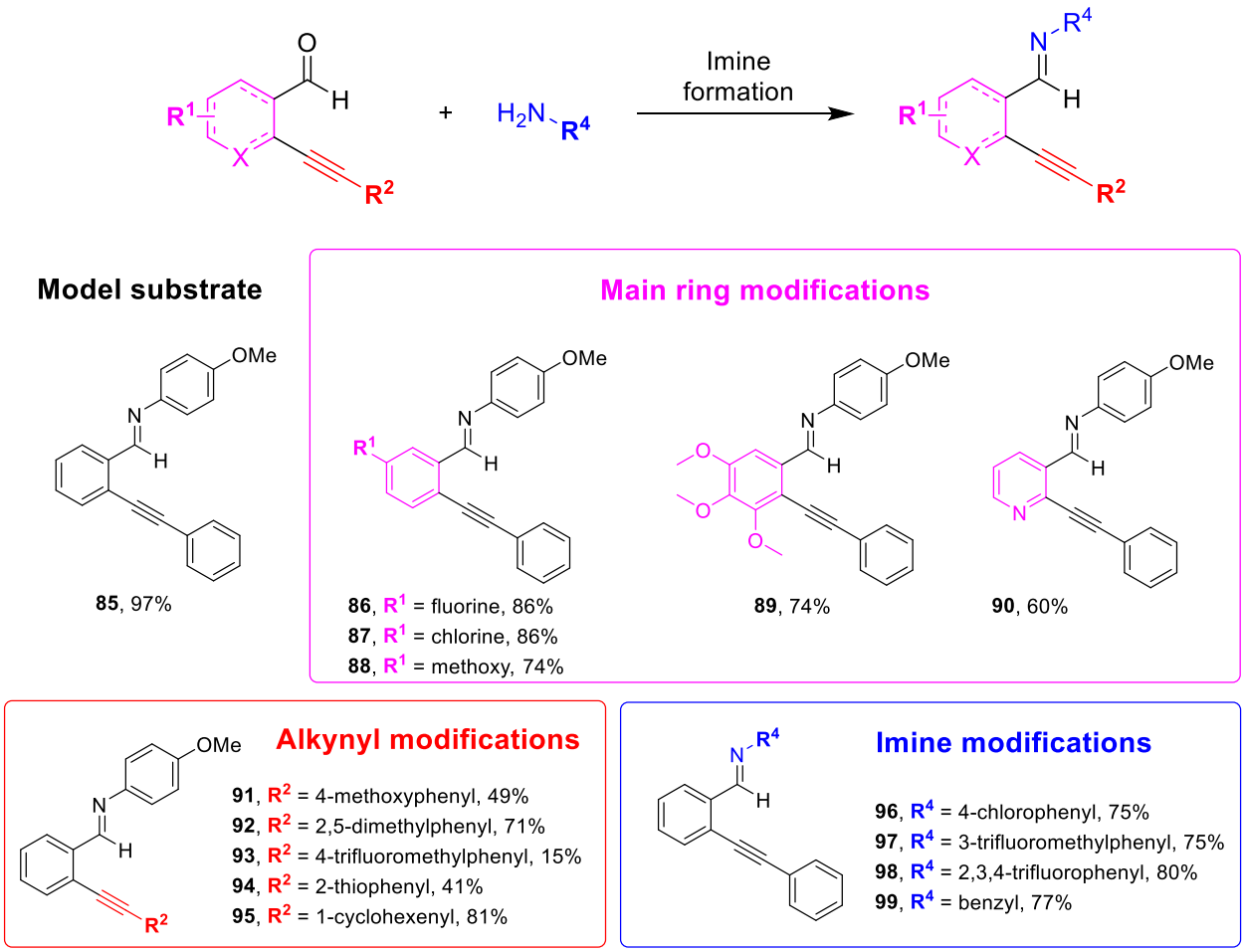

Our model starting material (**85**) was isolated in a very high 97% yield, and, overall, the formation of the imines was a high-yielding process. When modifying the main ring with halogen derivatives, we were pleased to obtain an 86% yield with both fluorine (**86**) and chlorine (**87**) substitution. Electron-donating groups such as a methoxy or three methoxy groups both led to 74% yields (**88**, **89**). Finally, a pyridine instead of a phenyl led to the formation of **90** in a good 60% yield.

However, modifying the alkynyl group with a 4-methoxyphenyl substitution led to a medium 49% yield (**91**). A dimethyl substituted aromatic (**92**) was isolated in a better 71% yield. It is important to note that a 4-trifluoromethylphenyl substitution (**93**) led to a very low 15% yield which might be due

to the strong electron-deficiency caused by this substituent. An heteroaromatic such as a thiophene (**94**) was tolerated in a medium 41% yield. An aliphatic cyclohexenyl substitution (**95**) led to the formation of the corresponding imine derivative in a high 81% yield.

Imino group substitutions led to high yields with differently substituted halogenated anilines. 4-chlorophenyl, 3-trifluoromethylphenyl and 2,3,4-trifluorophenyl substitutions led to 75% (**96**), 75% (**97**) and 80% (**98**) yields, respectively. Finally, a benzylamine could lead to the formation of the desired product **99** in a high 77% yield.

The low yields obtained could be imputed to the relatively difficult isolation of imine derivatives on silica gel. Indeed, the slight acidity of the silica led to the hydrolysis of imines during the purification process. To overcome this problem, neutralization of the silica using a 1% solution of triethylamine in cyclohexane was performed (see experimental part).

2. Methodology

We optimized the cycloisomerization/hydroarylation reaction by tuning the silver catalyst, the solvent, the operating temperature and adding or not an additive (Table 3).

Table 3 - Optimization of the reaction conditions

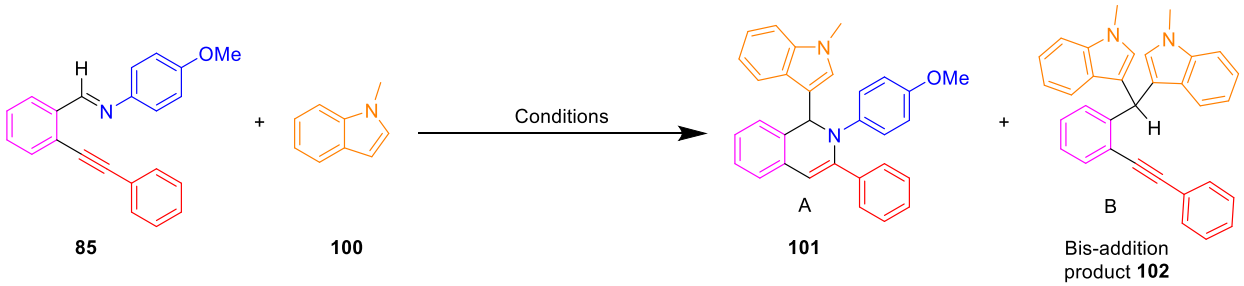

Entry	Catalyst	Solvent	Additive	T (°C)	Time	Yield[a] A/B
1	AgOTf (10 mol%)	DMF (0.5 M)	-	80	overnight	-
2	AgOTf (10 mol%)	DCE (0.2 M)	-	80	overnight	-
3	AgOTf (10 mol%)	DCE (0.2 M)	3 Å M.S.	80	2 days	-
4	AgOTf (5 mol%)	Toluene (0.1 M)	3 Å M.S.	50	overnight	-
5	AgOTf (5 mol%)	CH_3CN (0.08 M)	AcOH (1.1 eq)	RT	overnight	79/0[b]
6	AgOTf (5 mol%)	CH3CN (0.08 M)	-	RT	overnight	-
7	$AgSbF_6$ (5 mol%)	CH_3CN (0.08 M)	AcOH (1.1 eq)	RT	overnight	53/0
8	-	CH_3CN (0.08 M)	AcOH (1.1 eq)	RT	overnight	-
9	AgOTf (5 mol%)	DCE (0.08 M)	AcOH (1.1 eq)	RT	overnight	78/0
10	AgOTf (5 mol%)	DMF (0.08 M)	AcOH (1.1 eq)	RT	overnight	traces
11	AgOTf (5 mol%)	CH_3CN (0.08 M)	AcOH (0.1 eq)	RT	2.5 days	57/0
12	AgOTf (5 mol%)	CH_3CN (0.08 M)	APTS (1.1 eq)	RT	overnight	0/43
13	AgOTf (5 mol%)	CH_3CN (0.08 M)	CSA (1.1 eq)	RT	overnight	0/46
14	AgOTf (5 mol%)	CH_3CN (0.08 M)	TFA (1.1 eq)	RT	overnight	0/56
15	AgOTf 1 eq.	CH_3CN (0.08 M)	-	RT	overnight	-
16	AgOTf (5 mol%)	CH_3CN (0.08 M)	NaOAc (1.1 eq)	RT	overnight	19/0
17	AgOAc 1 eq.	CH_3CN (0.08 M)	-	RT	overnight	34/0

[a] Isolated yields. [b] Standard condition: reactions were performed with **85** (0.16 mmol), AgOTf (5 mol %), *N*-methylindole (5 eq.) and acetic acid (1.1 eq.) in 2 mL of solvent and was agitated at room temperature for 16 h.

We began our investigation by using AgOTf as the catalyst. Indeed, we focused our attention on this catalyst since it already proved to be suitable for 6-*endo*-dig cyclization with *ortho*-alkynylbenzaldehyde derivatives.[46] Our aim being the synthesis of isoquinoline derivatives, we decided to start using this silver salt. We first tried our previous optimized reaction conditions developed for the tandem cycloisomerization/hydroarylation of aldehyde derivatives. Using the conditions reported by Mariaule *et al.*,[48] or by Bontemps *et al.*,[49] only led to degradation of the starting material and did not lead to the formation of the desired product (entries 1 and 2, respectively, Table 3). We then wondered if traces of water could lead to the hydrolysis of our starting material, or even act as a nucleophile instead of *N*-methylindole, so we decided to add 3 Å M.S. to circumvent this hypothetical problem. Once again, no product formation was observed, even after two days (entry 3). Switching the solvent to toluene did not lead to any product formation as well (entry 4).

A report from Zhang, Wu et coll.[62] in 2014 allowed us to successfully form the desired product. Indeed, when using the same type of tert-butylimine as Larock, they were able to incorporate a trifluoromethyl group on the final scaffold with the help of acetic acid. Without the latter, they could not attain yields superior to 50% and postulated that it could act as a Brønsted acid for the activation of the imino group. Having a similar starting material, we decided to add 1.1 eq. of acetic acid in the reaction medium as well as using the same solvent they used (MeCN) and were pleased to obtain the desired product in a good 79% yield (entry 5). We then performed a control experiment without acid in order to confirm that the reaction can proceed thanks to the presence of acetic acid and not only because of the solvent change. We observed no product formation, confirming the crucial role of acetic acid for the formation of the desired product (entry 6). We also changed our catalyst and employed $AgSbF_6$ as reported in their work, but this led to a yield drop to 53% (entry 7). Another control experiment was run without silver catalyst in order to know whether the reaction was purely acid-catalyzed or if the silver salt really played a role and again, no product was obtained (entry 8).

A solvent change to DCE led to the formation of the desired product in a good 78% yield (entry 9) while changing the solvent to DMF afforded only traces of the isoquinoline (entry 10). Moreover, Mariaule *et al.* confirmed the origin of the proton in the position 4 of the isoquinoline scaffold by using a deuterated nucleophile.[48] With that in mind, we wondered if using a catalytic amount of acetic acid would result in a similar result since it is not supposed to be the proton source of the reaction. After using only 0.1 eq. of acetic acid, we were surprised to obtain a medium 57% yield after 2.5 days (entry 11), indicating that the acid present in a slight excess help achieving a faster formation of the desired isoquinoline.

We then investigated the influence of the nature of the acid additive on the reaction by using other common acids. *p*-Toluenesulfonic acid, camphorsulfonic acid and trifluoroacetic acid did not allow the formation of the desired product, however, when using these acids, we were able to isolate the product **102** of a double addition of the nucleophile onto the starting material, in yields of 43%, 46% and 56%, respectively (entries 12, 13 and 14). Our hypothesis is that the tested acids have a pKa value much lower than acetic acid. Indeed, acetic acid is the weakest acid among the 4 tested with a pKa of 4.76. APTS has a pKa value of -6.5, CSA has a pKa value of 1.2 and TFA has a pKa value of 0.52 (in aqueous medium).[66] On the other hand, we ran a pKa prediction of our starting material and found a predicted pKa value of 2.57. With these data in hand, the formation of the double nucleophilic addition product becomes logical since when using APTS, TFA or CSA, the protonation of the starting material

[66] W. M. Haynes, *CRC Handbook of Chemistry and Physics, 96th Edition*, CRC Press, **2015**.

is possible, leading to a great increase of its electrophilicity and therefore its attack by two nucleophiles, and the departure of the aniline derivative (Scheme 18).

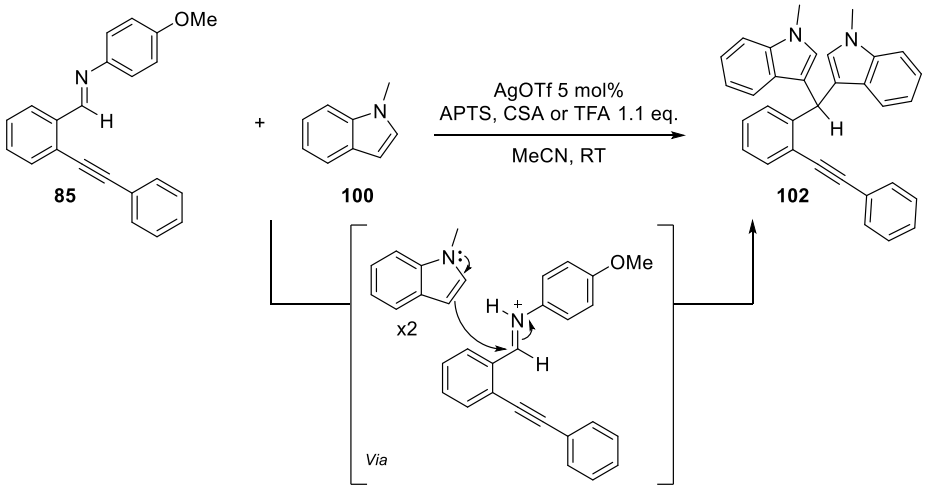

Scheme 18 - Formation of the undesired product via a double addition of the nucleophile onto the activated imine

In entry 15, we ran the reaction using 1 equivalent of AgOTf in order to study if the reaction could proceed in the absence of acid. Unfortunately, no product was formed. We then decided to run the reaction with 1.1 eq. of the conjugate base of acetic acid, NaOAc and were surprised to observe the formation of 19% of isoquinoline (entry 16). Following this result, we performed the reaction using this time 1 equivalent of AgOAc without any additive and once again, we could obtain the desired product in a low 34% yield (entry 17). These last two results are interesting, and we believe that the reaction can proceed, even without any acid additive, because acetic acid can be formed *in situ*. In fact, after the attack of the nucleophile, a proton is released in the reaction medium and can be readily captured by the conjugate base of acetic acid.

We decided to settle our reaction conditions with the one described in entry 5: AgOTf 5 mol%, imine derivative (0.16 mmol) nucleophile (5 eq.), acetic acid (1.1 eq.) in MeCN (0.08 M) at RT for 16h.

3. Scope of the reaction

3.1. Functional groups compatibility on the starting material

Using the optimized reaction conditions, we investigated the functional compatibility of the reaction with the substitutions present on various part of the imine derivatives (Table 4).

Table 4 – Products of the tandem cycloisomerization/hydroarylation reaction

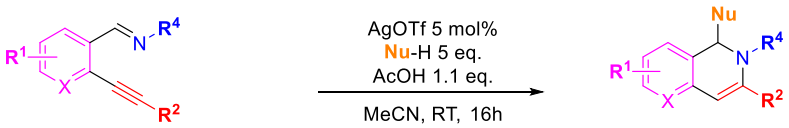

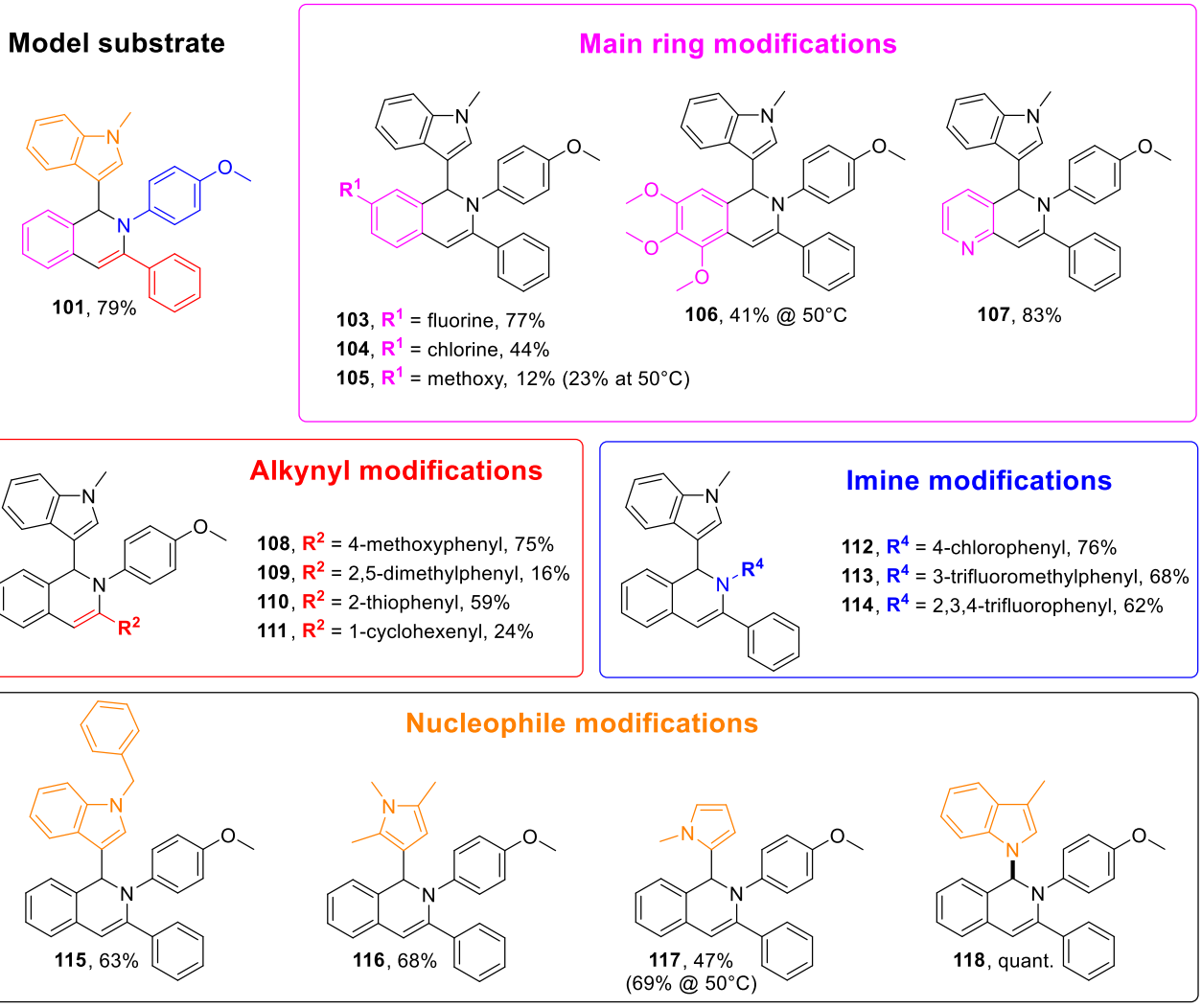

As presented above in Table 4, the model starting material led to the formation of 79% of the corresponding isoquinoline (**101**). We then modified the nature of the substitutions of the main ring, the alkynyl part, the imine substitution and finally the nucleophile.

A fluorine substitution on the main ring was not detrimental for the reaction, as the product was isolated in a good 77% yield (**103**). However, when another halogen substitution was present such as a chlorine (**104**), the yield dropped to 44%. It dropped much further when a methoxy substitution was present on the same carbon (**105**), leading to a low 12% isolated yield that could be slightly increased to 23% when heating the reaction at 50°C. The trimethoxy substitution afforded the desired isoquinoline (**106**) in a higher 41% yield upon heating at 50°C again. It is important to note that the reaction is compatible with the presence of a heterocycle on the main ring such as a pyridine (**107**), leading to a high 83% yield. It appears that electron-donating groups on the main ring are detrimental for the reaction, while electron-withdrawing groups lead to better isolated yields.

A 4-methoxyphenyl substitution on the alkyne of the starting material was well tolerated and led to a good 75% yield (**108**) whereas a 2,5-dimethylphenyl led to a low 16% yield (**109**). This can be

explained by the steric hindrance on the *ortho* position of the alkyne that can interfere with the attack of the imino group on the alkynyl unit. A heterocycle, 2-thiophenyl substitution could lead to a good 59% yield (**110**). Finally, an alkenyl substituted alkyne could also afford the desired isoquinoline (**111**) with a low 24% yield when using a 1-cyclohexenyl substitution.

We then changed the nature of the substituents on the aniline that lead to the formation of the imine starting material. The reaction could proceed normally when electron-withdrawing substituents were present on the imine such as a 4-chlorophenyl substitution (**112**), a 3-trifluoromethylphenyl substitution (**113**) and a 2,3,4-trifluorophenyl substitution (**114**) that all led to satisfactory yields of 76%, 68%, 62%, respectively.

Finally, we investigated the reactivity of various nucleophiles towards our starting material and their ability to perform a hydroarylation reaction. We used various nitrogen-containing heterocyles such as a *N*-methylindole and *N*-benzylindole that gave the desired product in nice 79% (**101**) and 63% (**115**) yields, respectively. We also used differently substituted pyrroles such as 1,2,5-trimethylpyrrole that led to a good 68% yield (**116**) and a *N*-methylpyrrole that afforded the desired product **117** in a medium 47% yield but up to 69% upon heating at 50°C. 3-Methylindole, led to the quantitative formation of a product **118**. However, we purposely used this indole derivative to prevent any attack of its position 3 and instead to favor the attack of the indole's position 2. We did not obtain any attack from the position 2, maybe because of the steric hindrance of the methyl substitution in the position 3 and the only attack observed was from the nitrogen atom.

Unfortunately, our reaction conditions were incompatible with a range of starting materials bearing various substitutions (Table 5).

Table 5 - Imines that did not lead to the formation of a product

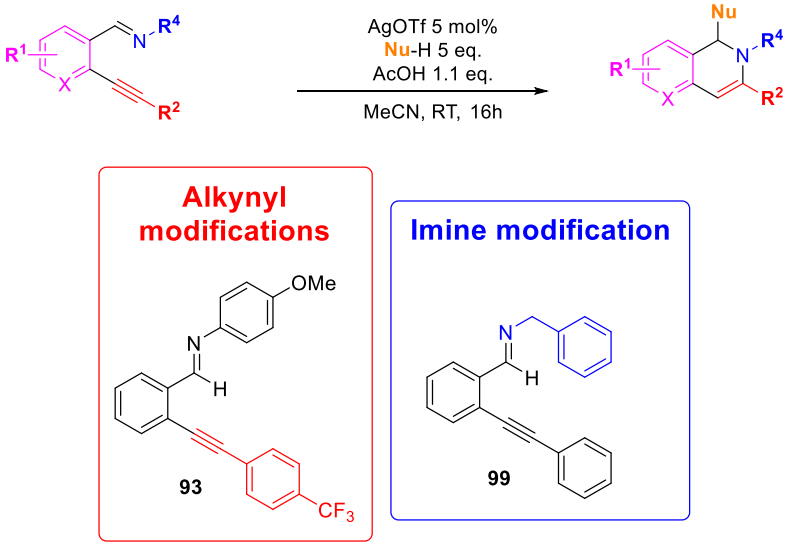

To begin with the alkyne substitution, an electron-withdrawing substitution such as 4-trifluoromethylphenyl (**93**) was detrimental for the reaction. A benzylated imine (**99**) did not lead to any product formation.

3.2. Nucleophiles' compatibility

We also employed a wide variety of nucleophiles, and not only nitrogen-containing ones. Unfortunately, as presented above, our reaction was only compatible with some nitrogen-containing heterocycles and not compatible with aryls, thiophene derivatives or a furan derivative (Figure 8).

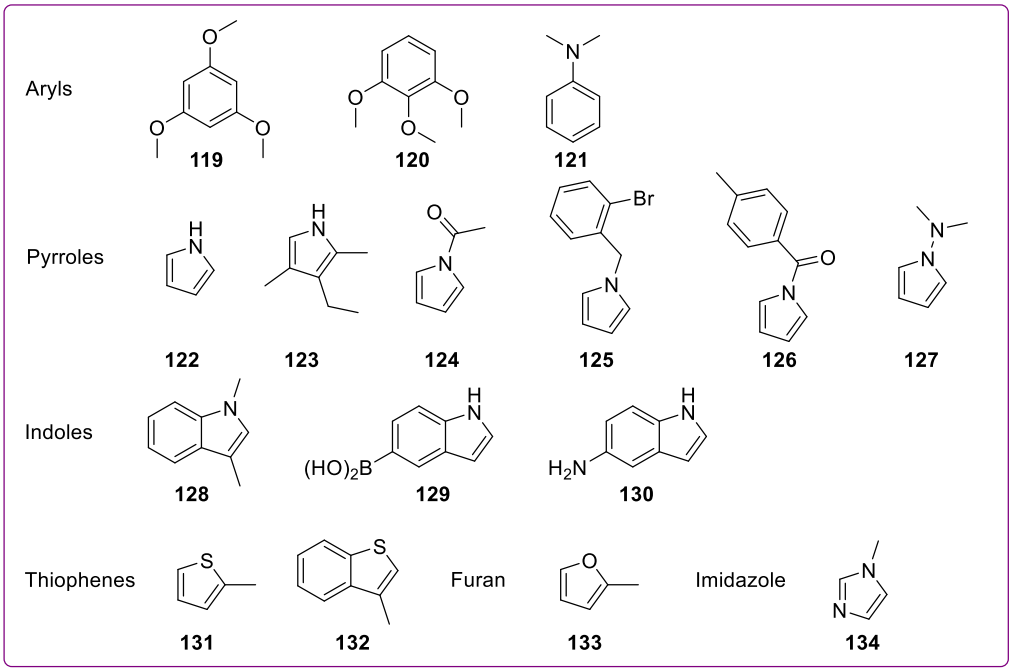

Figure 8 - Nucleophiles that did not lead to any product formation

Carbon nucleophiles such as 1,3,5-trimethoxybenzene **119** or 1,2,3-trimethoxybenzene **120** (Aryls, Figure 8) could not perform a hydroarylation reaction on imine derivatives unlike the previous reports of our group made on aldehyde derivatives.[48] The same observation is made for dimethylaniline **121**.

Interestingly, we reported the addition of two pyrrole derivatives on our imines but some nucleophiles with the same core could not perform the hydroarylation. Indeed, pyrrole **122** and its alkylated derivative **123** (Pyrroles, Figure 8) were not suitable for the hydroarylation reaction, maybe due to their free unprotected N-H bond. On the other hand, *N*-substituted derivatives with an acetyl **124**, benzyl **125** or benzoyl group **126** did not lead to the desired products as well as for 1-(dimethylamino)pyrrole **127**.

An indole derivative bearing methyl groups on the nitrogen and in position 3 **128** (Indoles, Figure 8) was not suitable for an attack in the position 2 since this position is not the most reactive one and it may be too hindered between the two methyl groups. Substitutions on the position 5 of the scaffold with a boronic acid **129** or an amino group **130** did not afford the desired product as well, and it might be due to the unprotected N-H bond which could chelate the silver catalyst and quench the reaction.

To finish, thiophene derivatives (**131**, **132**) (Thiophenes, Figure 8) and 2-methylfuran **133** (Furan, Figure 8) could not be added on the scaffold, showing the incompatibility of our methodology with such heterocycle. Moreover, an imidazole derivative **134** (Imidazole, Figure 8) was also incompatible for this reaction.

3.3. Mayr's nucleophilicity scale

It is rather surprising that some of these nucleophiles could not afford a product. Indeed, Mayr's group studied for years the relative reactivity of various families of molecules (both their electrophilicity and nucleophilicity) and established a scale of these two parameters for a facile visualization. We used their work to compare the nucleophilic strength of the different nucleophiles used in our study.[67] We were surprised to see that some of the nucleophiles we employed and which didn't afford the desired product had a higher nucleophilicity parameter than others that led to the desired compound. Here is represented the relative nucleophilicity of some nucleophiles we used in our work and that were studied by Mayr's group (Figure 9):

[67] J. Ammer, C. Nolte, H. Mayr, *J. Am. Chem. Soc.* **2012**, *134*, 13902–13911H. Mayr, T. Bug, M. F. Gotta, N. Hering, B. Irrgang, B. Janker, B. Kempf, R. Loos, A. R. Ofial, G. Remennikov, H. Schimmel, *J. Am. Chem. Soc.* **2001**, *123*, 9500–9512T. A. Nigst, M. Westermaier, A. R. Ofial, H. Mayr, *European Journal of Organic Chemistry* **2008**, *2008*, 2369–2374S. Lakhdar, M. Westermaier, F. Terrier, R. Goumont, T. Boubaker, A. R. Ofial, H. Mayr, *The Journal of Organic Chemistry* **2006**, *71*, 9088–9095H. Mayr, A. R. Ofial, *Tetrahedron Letters* **1997**, *38*, 3503–3506M. Baidya, F. Brotzel, H. Mayr, *Org. Biomol. Chem.* **2010**, *8*, 1929.

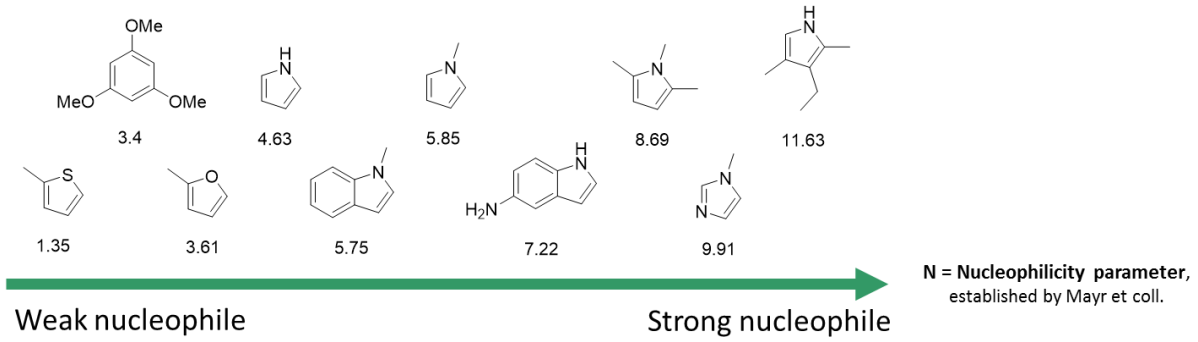

Figure 9 - Nucleophilicity scale showing the relative strength of some nucleophiles employed in this work and studied by Mayr's group

As represented in Figure 9, some strong nucleophiles did not lead to the desired product formation. For instance, 3-Ethyl-2,4-dimethylpyrrole **123** or 1-methylimidazole **134** present nucleophilicity parameters N of 11.63 and 9.91, respectively. Nevertheless, no product formation was witnessed when using them as nucleophiles. Such result might be due to the impossibility to perform a reaction with the carbon atom (C-nucleophile), steric hindrance around the nucleophilic atom or even the presence of an unprotected N-H bond.

4. Mechanistic investigations

4.1. Deuteration experiments

We wanted to confirm the source of the proton in the position 4 of the final isoquinoline scaffold. As reported earlier in our group, when using aldehyde derivatives to perform a similar tandem reaction and a deuterated 1,3,5-trimethoxybenzene as the nucleophile, they were able to isolate the final isochromene derivative with 84% of deuteration at position 4.[48] In our case, the proton source can either be the nucleophile or the acetic acid. In order to decipher which of these two is the proton source, we ran our optimized reaction in four conditions:

- with AcOD (1.1 eq.)
- with *N*-methylindole bearing a deuterium atom at position 3 (5 eq.)
- with both of these two deuterated molecules
- with AcOD (1.1 eq.), deuterated *N*-methylindole (in position 3) (5 eq.) and CD_3CN as the solvent

No reaction condition led to any deuteration of the position 4. We believe that the absence of deuteration is due to the very reactive position in which the deuterium should be incorporated. As represented in Scheme 19, the position 4 of the isoquinoline is part of the equilibrium between an enamine and an imine (iminium here) thus increasing the probability of an exchange of the deuterium with a proton during the work-up of the reaction or its purification on silica gel.

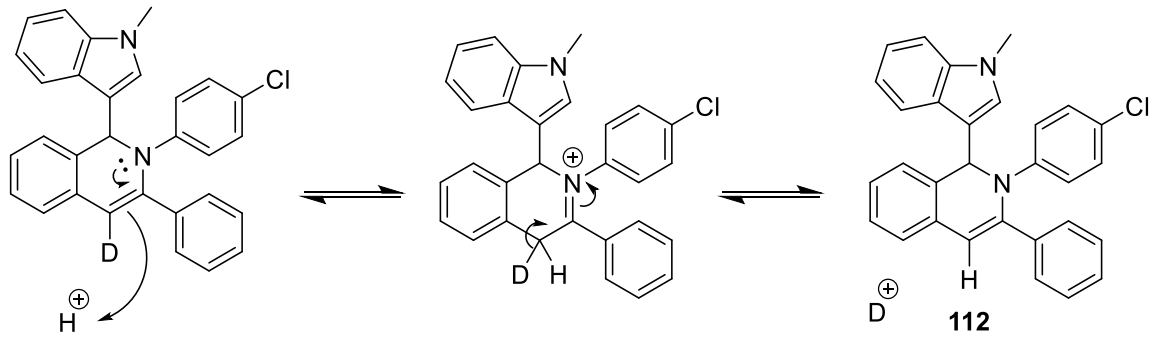

*Scheme 19 - Deuterium exchange in the final isoquinoline **112***

We wondered if we could force this proton to a deuterium exchange by putting the isolated purified isoquinoline in an NMR tube with AcOD and $CDCl_3$. As a result, the proton at position 4 (H_A in Figure 10) neatly disappeared on the ^1H NMR spectrum and was identified with a 2D experiment, as represented in the following NMR spectra (Figure 10):

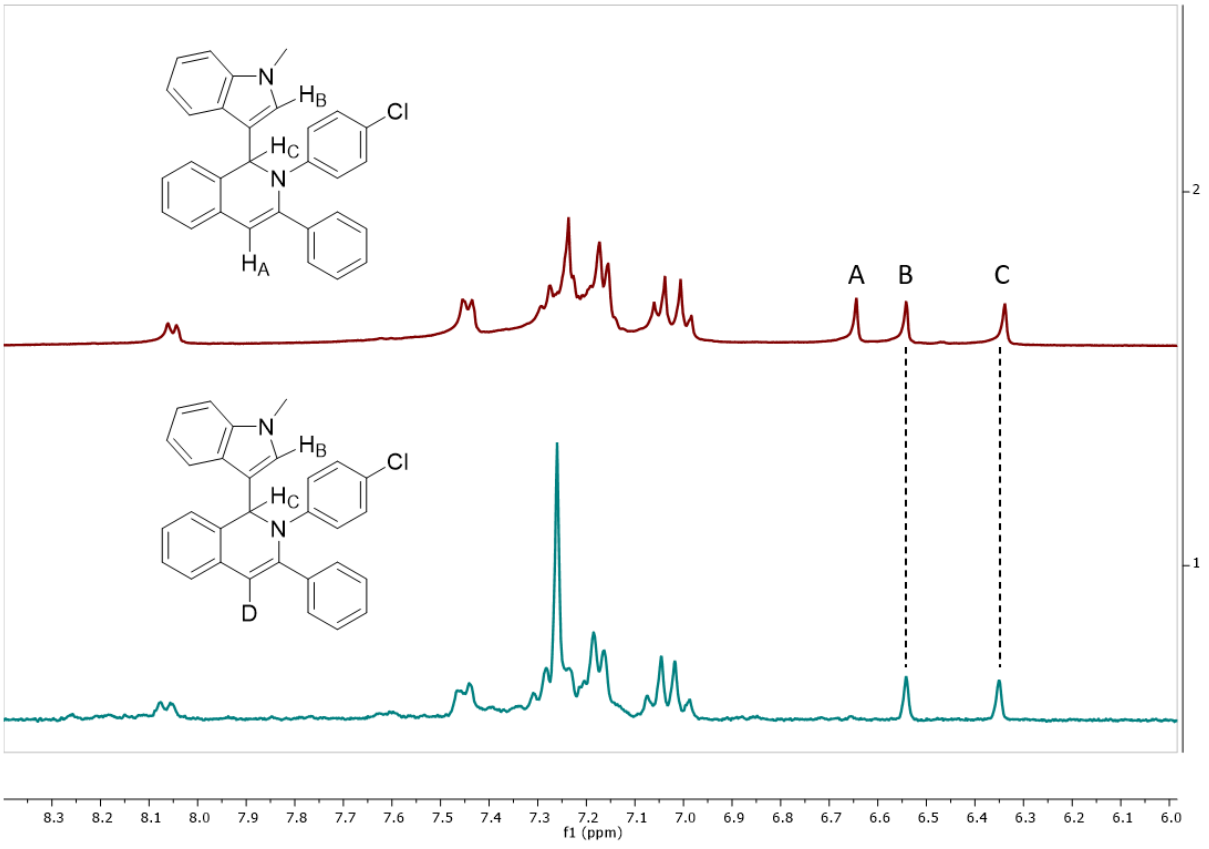

Figure 10 - Deuteration experiment in the presence of AcOD

4.2. Precipitation of supposed reaction intermediate

In order to deepen our understanding of the reaction mechanism, we tried to isolate a reaction intermediate, following a methodology reported by Asao *et coll.* in 2005.[68] They reported that the

[68] N. Asao, S. Yudha S., T. Nogami, Y. Yamamoto, *Angewandte Chemie International Edition* **2005**, *44*, 5526–5528.

precipitation and recrystallization of an isoquinolinium intermediate was possible by running the reaction in dichloromethane with 1 eq. of AgOTf, followed by the addition of triflic acid. Moreover, we were able to obtain a single crystal suitable for an X-Ray diffraction (Scheme 20 and Figure 11)

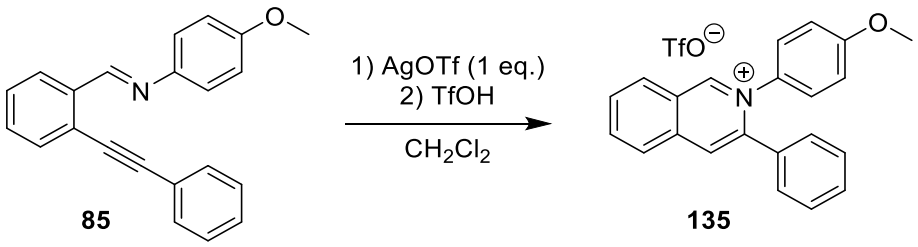

*Scheme 20 - Precipitation of a supposed reaction intermediate **135***

This precipitate was successfully recrystallized in a mixture of hexane and EtOH and the crystal were suitable for an X-Ray Diffraction, as represented in Figure 11:

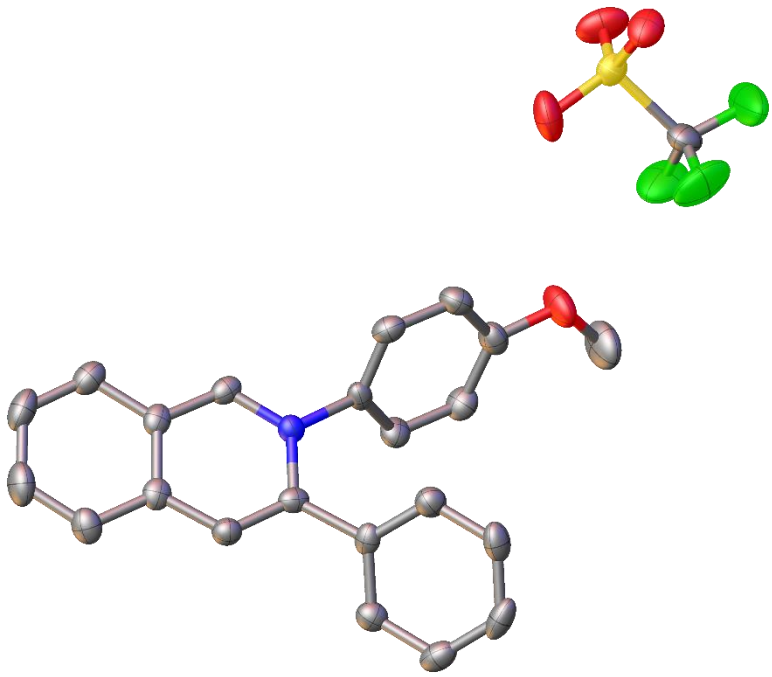

*Figure 11 - Crystal structure of the precipitated isoquinolinium **135***

This result indicates that the first step of the reaction is a coordination between the silver salt and the alkynyl group, leading to an electron-deficient alkyne. The latter is then attacked by the imino group to form an isoquinolinium intermediate presenting an alkenylsilver. The subsequent addition of triflic acid leads to the protodeargentation and the formation and precipitation of the isoquinolinium salt **135**.

4.3. Reactivity of the isoquinolinium ion

In an attempt to further understand the reaction mechanism, we used this isoquinolinium salt in the presence of *N*-methylindole, with and without AcOH, in acetonitrile (Scheme 21). To our surprise, no product formation was observed.

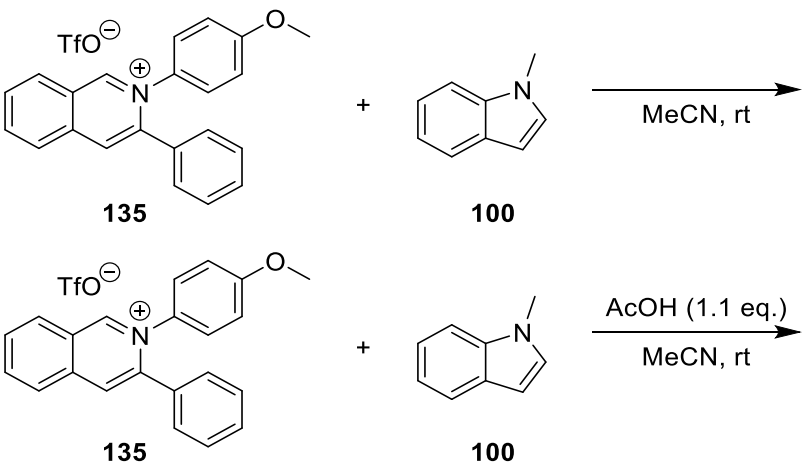

Scheme 21 - Reactivity of the isoquinolinium ion towards N-methylindole

These results questioned our understanding of this reaction's mechanism since we were expecting a straightforward reaction between the nucleophile and the isoquinolinium ion. We therefore concluded that this isolated salt **135** is probably not a reaction intermediate and the addition of the nucleophile might occur onto the isoquinolinium which still bear the alkenylsilver, as indicated by several reports of Asao and Wu.[69]

To test this hypothesis, we performed new experiments, in a one-pot two-steps fashion (Scheme 22). The first step was the reaction of the imine derivative **96** with 1 eq. of AgOTf in order to form the hypothetical isoquinolinium alkenylsilver specie **136** and then the second step was the addition of 1.1 eq. of AcOH with 5 eq. of *N*-methylindole. After 10 days of reaction, we were able to isolate the desired isoquinoline **112** in a low 21% yield. We have no clue as to why the desired product was formed in such low yield, but the product was indeed formed.

[69] N. Asao, S. Yudha S., T. Nogami, Y. Yamamoto, *Angewandte Chemie International Edition* **2005**, *44*, 5526–5528S. Ye, J. Wu, *Tetrahedron Letters* **2009**, *50*, 6273–6275X. Yu, J. Wu, *J. Comb. Chem.* **2010**, *12*, 238–244.

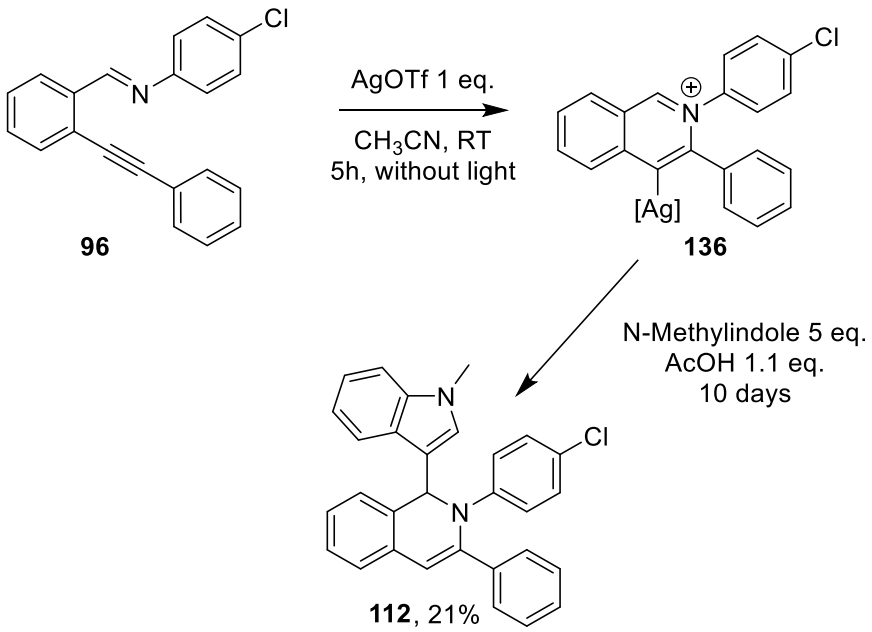

*Scheme 22 - One-pot two-steps synthesis of isoquinoline **112***

4.4. Silver NMR

The reaction is believed to proceed via an alkenylsilver intermediate. We therefore intended to witness its formation using ^{109}Ag NMR. This spectroscopic method being rather uncommon, we had to parameter our 400MHz spectrometer in order to be able to perform such acquisition. Silver has two naturally occurring isotopes: ^{107}Ag and ^{109}Ag. Their abundance is almost equal with about 52% of ^{107}Ag and about 48% of ^{109}Ag.[70] The most important property for NMR spectroscopy is that these two isotopes have a very low sensitivity but ^{109}Ag is preferred since it has a slightly better sensitivity. The relaxation time of Ag is rather long with a magnitude of up to hundreds of seconds. In order to calibrate our spectrometer with the literature's chemical shift, we used a solution of $AgNO_3$ 1M in D_2O in order to set the 0 ppm, as it is commonly described in the literature.[71]

Prior to investigate the chemical shift of the alkenylsilver intermediate, we wanted to determine the chemical shift of AgOTf alone, in deuterated acetonitrile and, after a night-long experiment, we obtained one peak at around 441 ppm, as represented in the following spectrum (Figure 12):

[70] W. M. Haynes, *CRC Handbook of Chemistry and Physics, 96th Edition*, CRC Press, **2015**.
[71] G. Kidd, R. J. Goodfellow, *NMR and the Periodic Table*, Academic Press: London, **1978**.

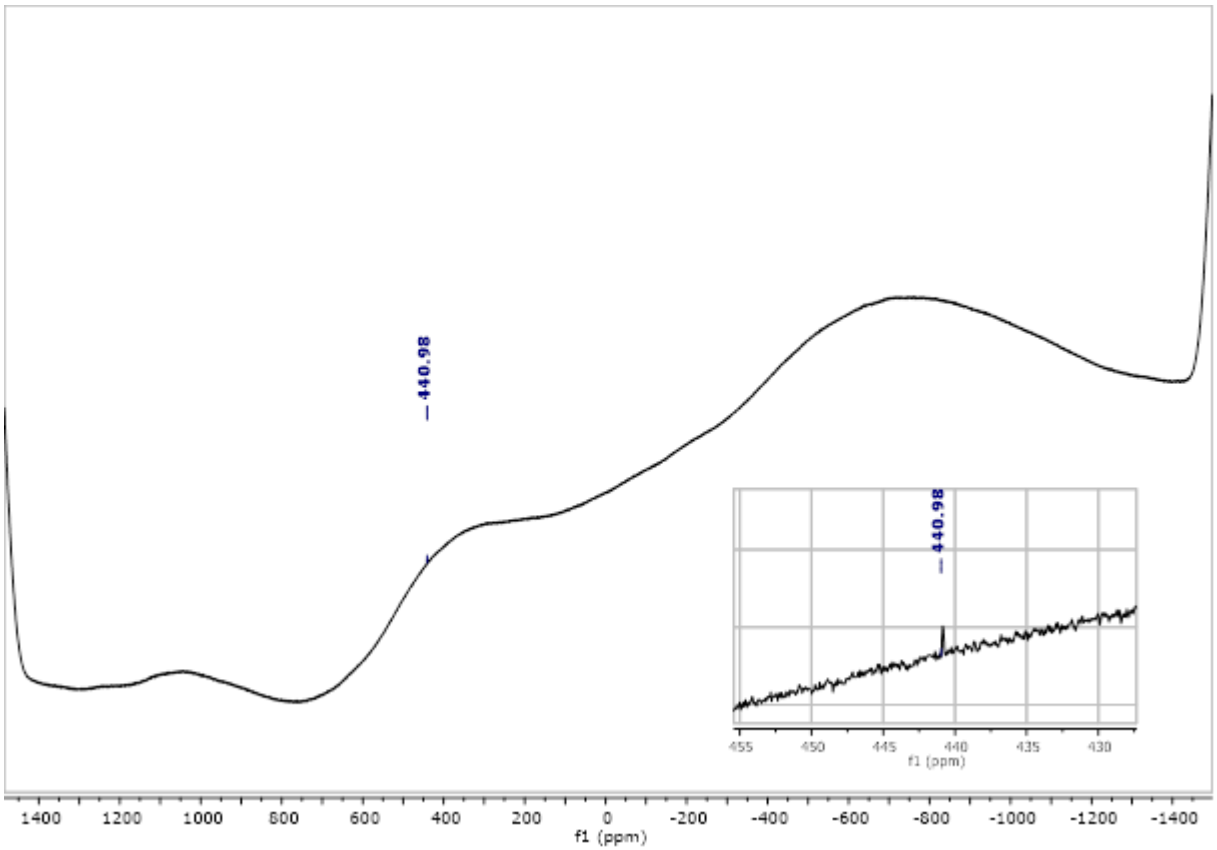

Figure 12 - ^{109}Ag NMR spectrum of AgOTf in CD_3CN

It is worth noting that reports of ^{109}Ag chemical shifts are very scarce in the literature. Thereby, we were not able to find the chemical shift of AgOTf in deuterated acetonitrile. However, we were able to find its chemical shift value in other solvents, such as water (43 ppm),[72] benzene (294 ppm),[73] DMF (80 ppm).[73] These values vary greatly from one another and this is why we are not surprised by our 441 ppm chemical shift in acetonitrile. Another important point is that Létinois-Halbes *et al.* studied the influence of silver complexation for the formation of π-alkyne complexes and alkynyl silver species (in the presence of a base). Indeed, they recorded the ^{1}H NMR spectra of: hexyne in deuterated benzene alone, after addition of AgOTf and after addition of AgOTf + DIPEA. By doing so, they were able to witness the signal shifts after complexation of the silver with the alkyne and after the formation of hexynyl silver. In the meantime, they also recorded the ^{109}Ag spectra in deuterated benzene. As mentioned above, they reported a chemical shift of 294 ppm of AgOTf in solution. When they added hexyne, the peak shifted to 416 ppm (shift from 80 to 750 ppm in DMF when adding hexyne). This unshielding is the result of the *in-situ* formation of π-complexes which leads to an electron density partially transferred to the silver cation. As a result, the signals of the terminal C-H (alkyne) and the silver ion are shifted towards greater values in ppm.

[72] L. Lumata, M. E. Merritt, Z. Hashami, S. J. Ratnakar, Z. Kovacs, *Angew. Chem. Int. Ed.* **2012**, *51*, 525–527.
[73] U. Létinois-Halbes, P. Pale, S. Berger, *The Journal of Organic Chemistry* **2005**, *70*, 9185–9190.

We then ran our experiment using an imine derivative **96** in the presence of 1 eq. of AgOTf in order to form the isoquinolinium alkenylsilver intermediate **136** in deuterated acetonitrile, in an NMR tube. Unfortunately, after a night long experiment, we obtained only one peak at around 437 ppm (Figure 13).

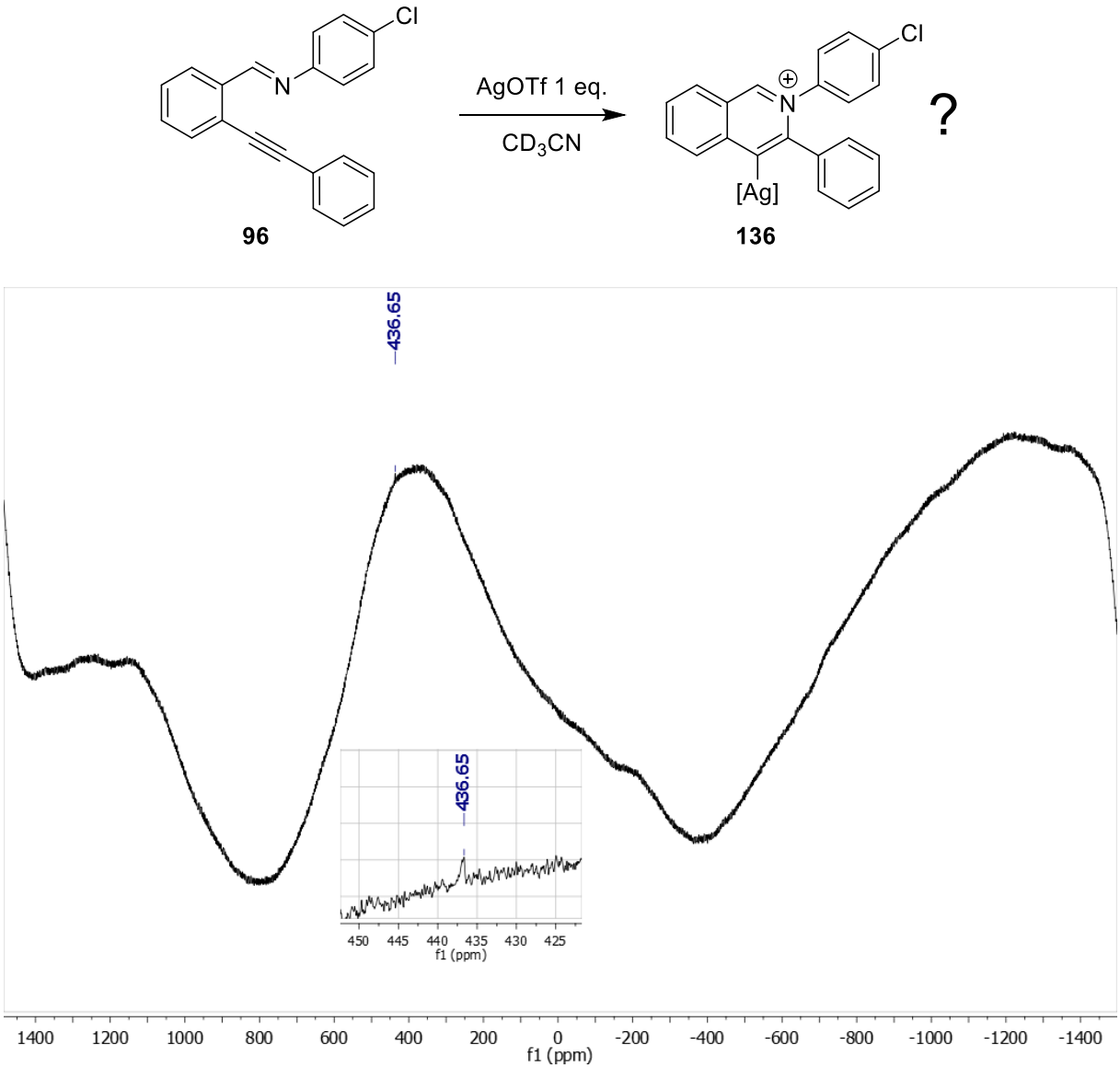

Figure 13 - Attempt to witness the formation of the alkenylsilver intermediate using ^{109}Ag NMR

As no new peak was observed during this experiment, we assumed that the peak at 437 ppm could be the same as the one in Figure 12 *i.e.* the peak of the free AgOTf catalyst, since we were expecting a shift of at least 50 to 100ppm upon formation of the π-complex. Therefore, we could not conclude on whether the isoquinolinium alkenylsilver specie **136** is formed or not due to the possibility that this specie is even less sensitive for this type of NMR acquisition.

4.5. Attempt to react a Michael acceptor/electrophile with the alkenylsilver intermediate

Since we couldn't evidence the formation of the alkenylsilver intermediate, we intended to make it react with various molecules such as Michael acceptors or electrophiles. Such reaction was already described in the literature, both on arylsilver[74] **137** and alkenylsilver[75] **141** species, as represented in Scheme 23:

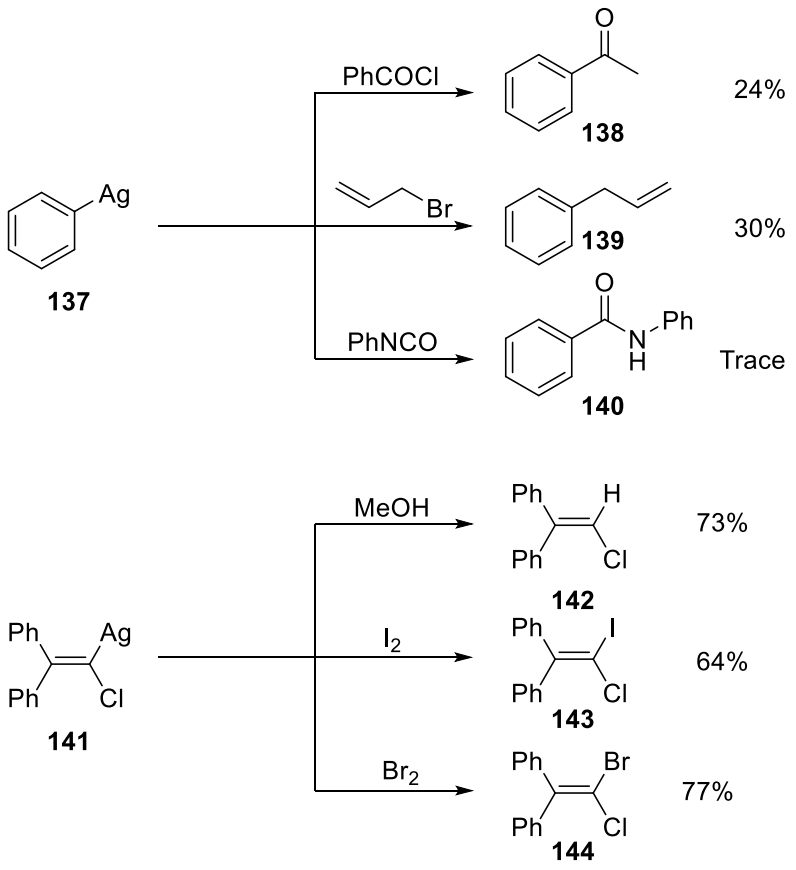

Scheme 23 - Reported examples of reactions using arylsilver and alkenylsilver species as nucleophile

Our operative conditions were the same as the one we employed for the formation of the isoquinolinium alkenylsilver (as mentioned above). After a few hours of agitation of the imine **85** and AgOTf in acetonitrile, we added methyl vinyl ketone **146**, I_2 **147** and several acyl chlorides (**148**-**150**) (Scheme 24).

[74] H. Gilman, J. M. Straley, *Recl. Trav. Chim. Pays-Bas* **1936**, *55*, 821–834.
[75] G. Koebrich, H. Froehlich, W. Drischel, *J. Organomet. Chem.* **1965**, *6*, 194–201.

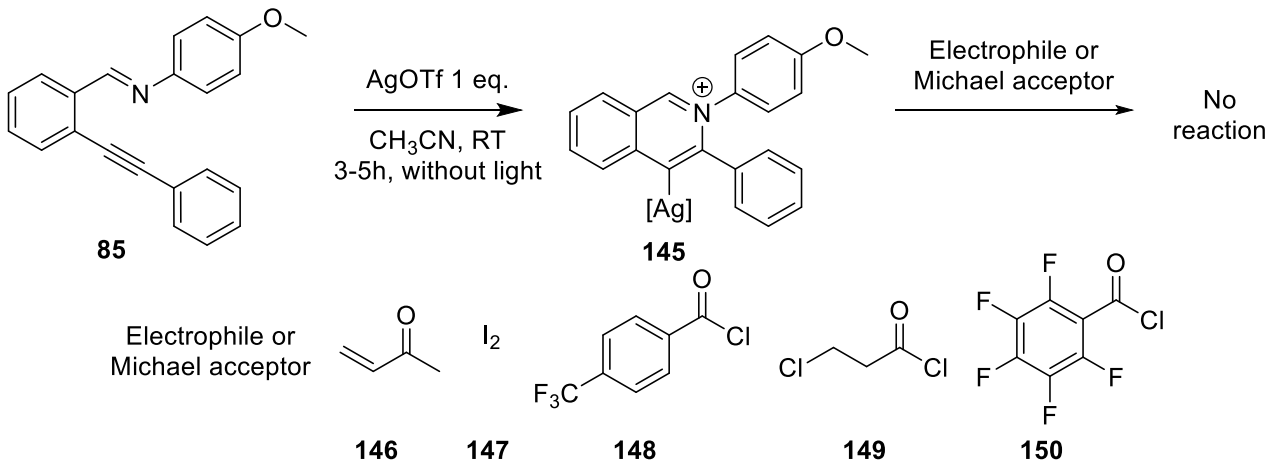

Scheme 24 - Attempt to react a Michael acceptor or electrophile with an alkenylsilver intermediate

Unfortunately, no reaction between the hypothetical alkenylsilver intermediate **145** and an electrophile or Michael acceptor occurred. We then decided to run a variation of these experiments by adding at the same time the electrophile/Michael acceptor and *N*-methylindole in order to yield an isoquinoline that is both substituted in the position 1 by the nucleophile and 4 by the electrophile or Michael acceptor but, once again, no reaction was witnessed. In a last attempt, we added 1.1 eq. of AcOH to these previous experiments, both with and without nucleophile but this led to no product formation.

4.6. NMR experiments (with different equivalents of acid/Ag)

We ran more NMR experiments with a variable amount of acid and AgOTf. These experiments' goal was to know if we could see the formation of the reaction intermediate right in the NMR tube in order to bring us some insight on the reaction mechanism.

We began by acquiring NMR spectra of the imine derivative **85**, in deuterated acetonitrile with less than 1 equivalent of AgOTf. In this case, when comparing the NMR spectra of the imine and the imine + AgOTf, we noticed that when AgOTf is added, most of the peaks are split in two (Figure 14). Our hypothesis is that one set of peaks belong to the imine derivative **85** alone and the other set belongs to the imine derivative upon coordination **151**, through its alkynyl part, to the silver salt. When integrating the two sets of peaks separately, we find a perfect correlation (in the number of protons), based on the amount of silver salt added.

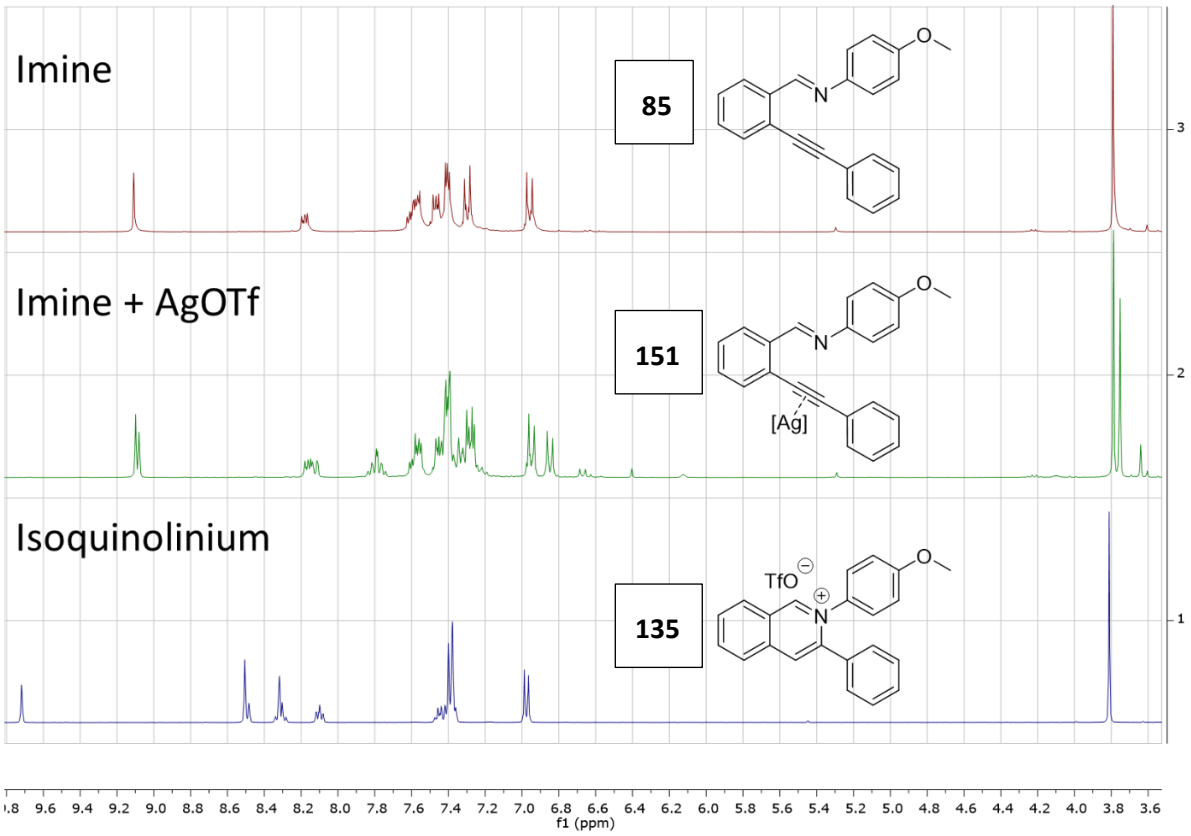

Figure 14 - ^{1}H NMR spectra of the imine before and after addition of less than 1 eq. of AgOTf

We can clearly see on the spectra that no isoquinolinium **135** is formed since we don't see the formation of any peaks around 8.5 and 9.7 ppm. However, it is clear that a new "roof effect" is visible in the spectra "imine+AgOTf" at 6.85 ppm, attributed to the *para*-methoxyphenyl moiety of the imine coordinated with Ag **151**, as well as a new singlet around 3.8 ppm, corresponding to the methoxy group and a new singlet at 9.1 ppm, attributed to the imine proton. The one peak that really stands out is the one formed at 7.8 ppm. It has an integration of two protons compared to the newly formed set of peaks and might originate either from the peak at 8.1 ppm or the aromatic multiplet between 7.35 and 7.65 ppm, although it would be surprising since all the newly formed peaks are shielded, not unshielded.

When we add a slight excess of AgOTf in the NMR tube and we took NMR spectra: 1/ right after the addition of this excess of AgOTf, 2/ after 2h and 3/ after 22h (Figure 15). We began to see the formation of the characteristic peaks of the isoquinolinium ion **135**, in addition to other minor peaks between 6 and 6.8 ppm. We believe that upon adding an excess of AgOTf, all the alkynyl groups of the imine derivatives were coordinated to silver which resulted in the formation of the isoquinolinium intermediate **135** after attack of the imino group onto the electron-deficient alkynyl unit. However, we do not have an explanation for the formation of small peaks at 6.12, 6.41, 6.6, 6.66 and 6.77 ppm. It is

interesting to remark that after 22h in the NMR tube, the peaks at 6.12, 6.41 and 6.66 ppm all neatly disappeared while the ones at 6.6 and 6.77 pm remained.

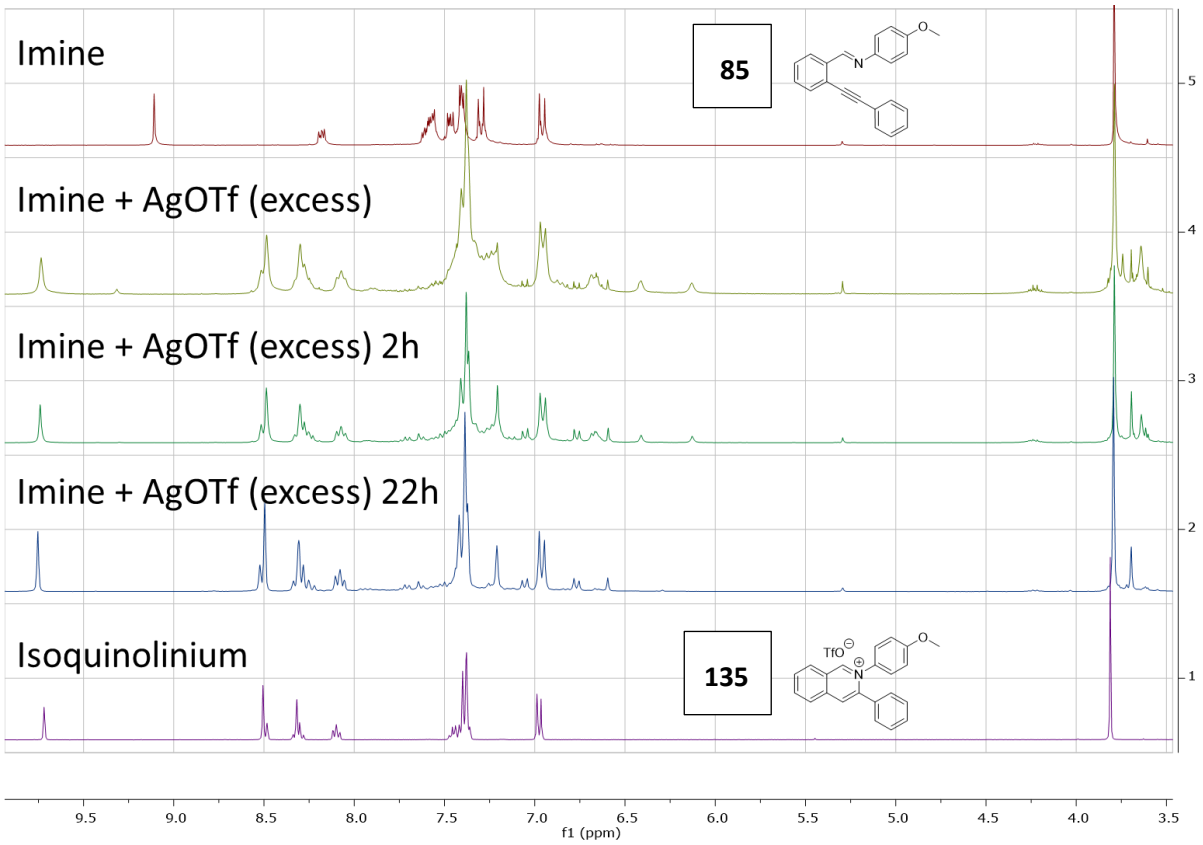

Figure 15 - ^{1}H NMR spectra of the imine before and after addition of a slight excess of AgOTf

4.7. Proposed mechanisms

Thanks to all the data acquired, we were able to propose a reaction mechanism (Scheme 25). As discussed above, the first step of the reaction is expected to be the coordination between the silver catalyst and the alkynyl group of the starting material **A** leading to the activated alkyne **B**. The imine group of **B** attacks intramolecularly the electron-deficient alkyne, leading to the formation of an alkenylsilver intermediate **C**. We believe that this intermediate is the one being attacked by the external nucleophile (*N*-methylindole here), yielding the intermediate **D**. Then, after a protodeargentation step, the intermediate **E** is obtained and yields the final desired product **F** upon rearomatization of the indole core.

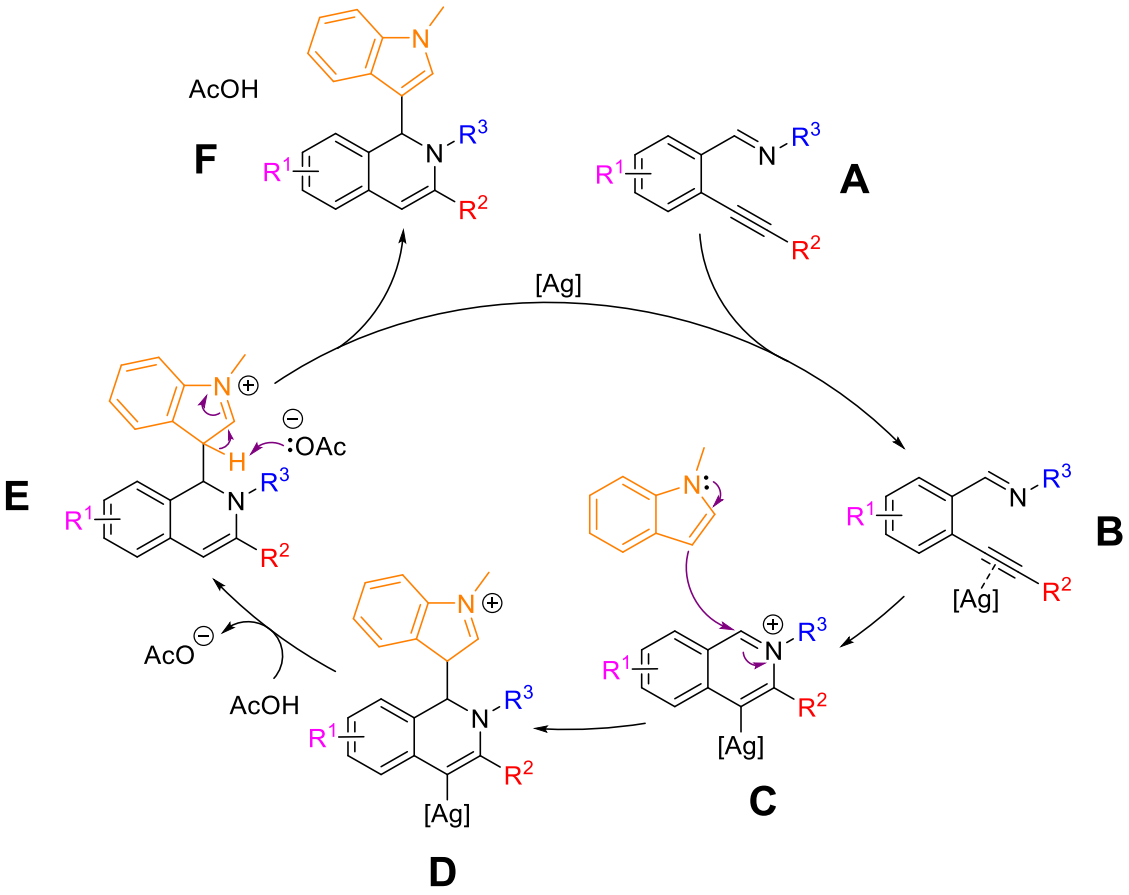

Scheme 25 - Proposed mechanism for the silver catalyzed tandem cycloisomerization/hydroarylation reaction

E) Conclusion & perspectives

Although silver-catalyzed tandem reactions have been widely studied during the last two decades, we were able to report a convenient synthesis of 1,2-dihydroisoquinolines under very mild conditions, using easily synthesizable starting materials and cheap catalyst and additive.

Further studies should be focused on the control of the stereochemistry of this reaction since we used an achiral catalyst. However, the distance between the reactive site where the asymmetric carbon is created is rather far from the coordination site of the catalyst and might lead to a difficult control over the stereochemistry.

As an introduction and transition to the major part of this manuscript, it would be interesting to develop a visible-light catalyzed synthesis of isoquinolines, using iminyl radicals, as reported by Leonori's team in 2015.[76] They reported the synthesis of *O*-aryl oximes as nitrogen-centered radical precursor which are generated upon single electron transfer. Once obtained, the nitrogen-centered

[76] J. Davies, S. G. Booth, S. Essafi, R. A. W. Dryfe, D. Leonori, *Angew. Chem.* **2015**, *127*, 14223–14227.

radical can react with an intramolecular alkenyl unit, yielding their desired product. We propose here (Scheme 26) the formation of isoquinolines **41** via the same type of nitrogen-centered radical generation but with an intramolecular reaction on an alkynyl unit.

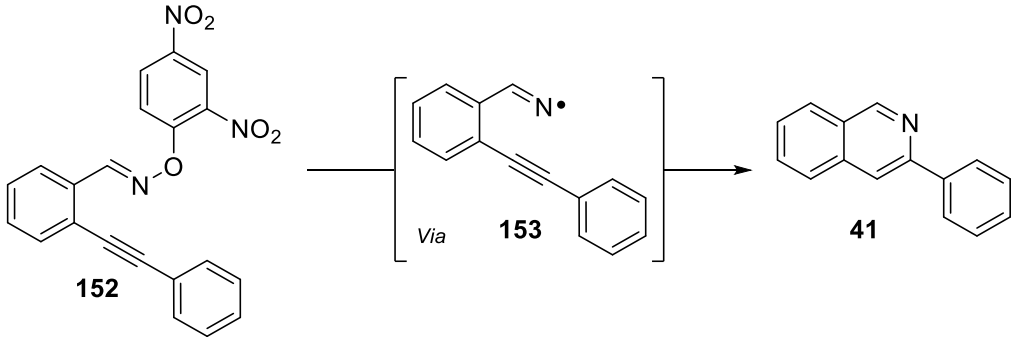

Scheme 26 - Proposed formation of isoquinolines under visible-light catalysis

Chapter II:
Visible-Light Catalysis

Chapter II: Visible-Light Catalysis

A) Introduction

The decay of "classical" radical chemistry often using high temperatures, harsh and radical initiators such as Bu_3SnH and AIBN[77] led chemists to develop new enticing alternatives. In this aim, visible-light catalysis has gained an important growing interest during the last decade with a fast-increasing number of publications in this field. It is not surprising that such a technique became so popular among organic chemists considering its attractiveness for the development of efficient and selective chemical transformations. This can be clearly highlighted by the following graph with the keywords "visible-light", "photoredox" with "catalysis" (Figure 16).

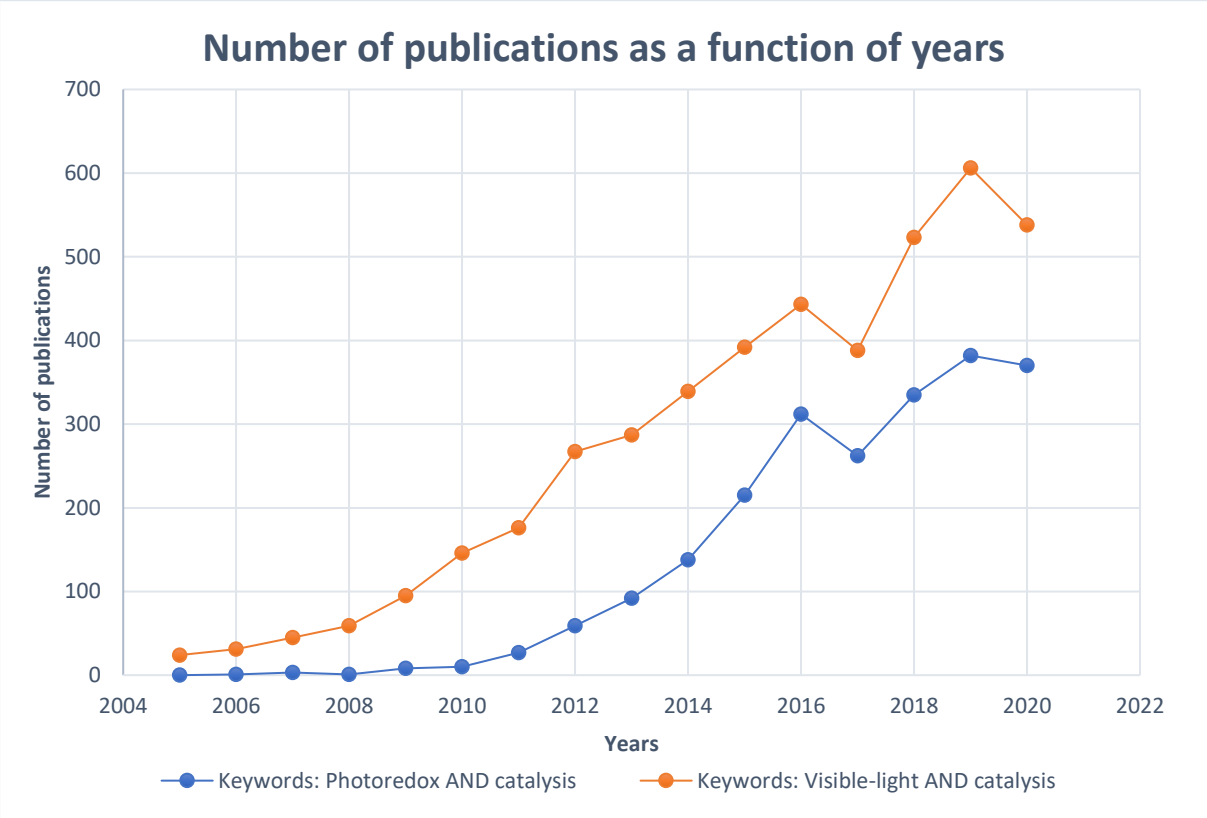

Figure 16 - Number of publications per year (Data retrieved on dimensions.ai on September 13th 2020)

Before diving into the different modes of action of visible-light catalysis, it is important to define what visible-light is and what is the purpose of a photocatalyst.

[77] W. R. Bowman, S. L. Krintel, M. B. Schilling, *Org. Biomol. Chem.* **2004**, *2*, 585–592.

Visible-light is a region of the electromagnetic spectrum that is visible to our human eye. It is comprised in a relatively small area (when comparing to the whole spectrum), between 380 nm and 780 nm (Figure 17).[78]

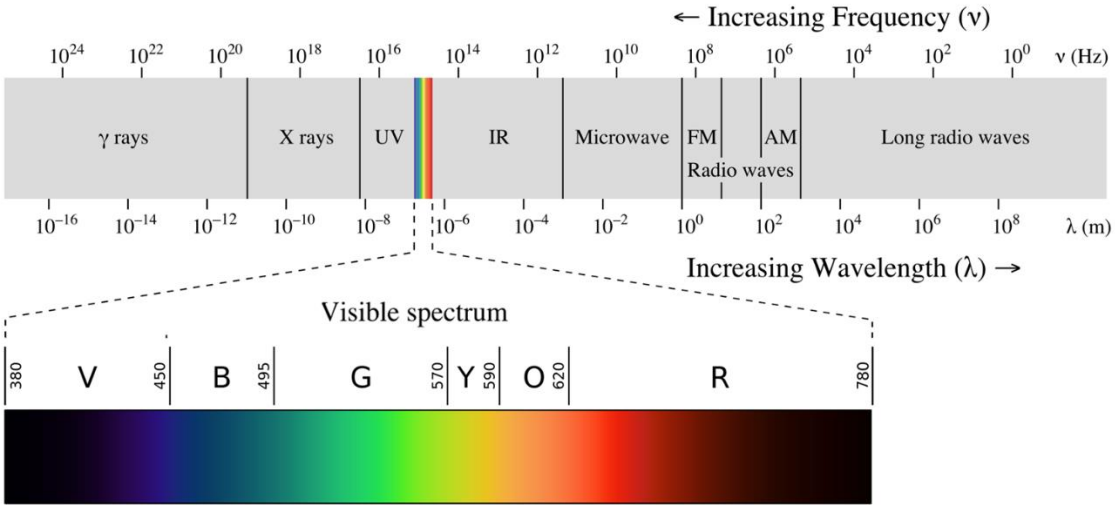

Figure 17 - Full electromagnetic spectrum with the area of visible-light highlighted

The energy carried by the light inversely proportional to its wavelength, following this formula:

$$E = \frac{hc}{\lambda}$$

With E being the photon energy, h being the Planck constant, c being the speed of light and λ being the photon's wavelength. Visible-light is therefore less energetic than UV light (which has shorter wavelength) and can promote reactions with a greater functional group compatibility than UV light.

Another point to highlight is the need for a photocatalyst in a majority of visible-light induced reactions. Most organic molecules do not absorb in visible-light and that is therefore why we usually need to reveal them under a UV lamp (particularly for conjugated molecules and aromatic cycles). In order to transfer the energy brought by visible-light, we need to use a "shuttle" that will have the ability to be excited by visible-light and transmit the energy absorbed during this excitation to the molecule we want to transform. These "shuttles" are called photocatalysts and they can be of different types such as organometallic complexes or organic molecules (dyes that are highly conjugated).[79] They have many different properties such as different excitation wavelength (λ_{max}), different excited state lifetime (τ) but most importantly, different redox potentials whether they are in an excited state or not

[78] D. H. Sliney, *Eye* **2016**, *30*, 222–229.
[79] C. Stephenson, T. Yoon, D. W. MacMillan, *Visible Light Photocatalysis in Organic Chemistry*, Wiley-VCH Verlag GmbH & Co. KGaA, **2018**.

(Figure 18).[80] One last point, the term photocatalysis is a bit misused since light is never used in a catalytic amount in such reactions. In fact, light is even used in a large excess and should therefore be considered more as a reagent. The photocatalyst is the one used in catalytic amount.

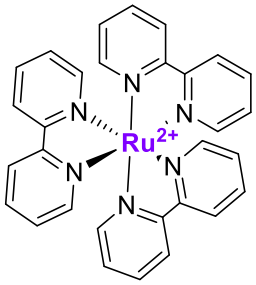

[Ru(bpy)$_3$]$^{2+}$

$E_{1/2}$(Ru(III)/**Ru(II)**) = +1.29 V
$E_{1/2}$(**Ru(II)**/Ru(I)) = -1.37 V
$E^*_{1/2}$(Ru(III)/**Ru(II)***) = -0.81 V
$E^*_{1/2}$(**Ru(II)***/Ru(I)) = + 0.77V
λ_{max} = 452 nm; τ = 1100 ns

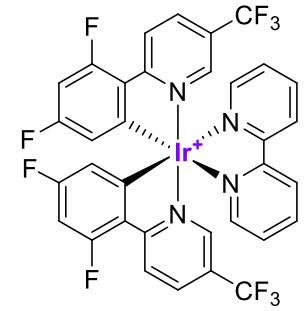

[Ir(dF(CF$_3$)ppy)$_2$(bpy)]$^+$

$E_{1/2}$(Ir(IV)/**Ir(III)**) = +1.69 V
$E_{1/2}$(**Ir(III)**/Ir(II)) = -1.37 V
$E^*_{1/2}$(Ir(IV)/**Ir(III)***) = -0.89 V
$E^*_{1/2}$(**Ir(III)***/Ir(II)) = + 1.21 V
λ_{max} = 380 nm; τ = 2300 ns

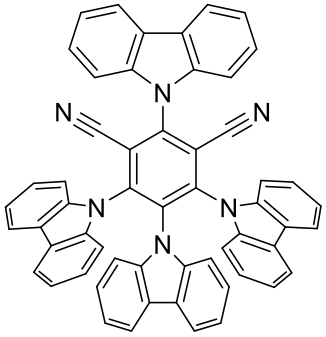

4CzIPN

$E_{1/2}$(**PC**/PC$^{\cdot-}$) = -1.21 V
$E_{1/2}$(PC$^{\cdot+}$/**PC**) = n.d.
$E^*_{1/2}$(**PC***/PC$^{\cdot-}$) = +1.35 V
$E^*_{1/2}$(PC$^{\cdot+}$/**PC***) = n.d.
λ_{max} = 435 nm; τ = 5100 ns

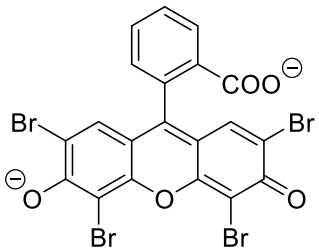

Eosin Y

$E_{1/2}$(**PC**/PC$^{\cdot-}$) = -1.14 V
$E_{1/2}$(PC$^{\cdot+}$/**PC**) = +0.72 V
$E^*_{1/2}$(**PC***/PC$^{\cdot-}$) = +1.18 V
$E^*_{1/2}$(PC$^{\cdot+}$/**PC***) = -1.6 V
λ_{max} = 539 nm; τ = 2.1 ns

Figure 18 - Examples of commonly used photocatalysts and their respective properties

Visible-light catalyzed reactions can be divided in different categories and will be presented in the following section.

[80] K. Teegardin, J. I. Day, J. Chan, J. Weaver, *Org. Process Res. Dev.* **2016**, *20*, 1156–1163L. Marzo, S. K. Pagire, O. Reiser, B. König, *Angew. Chem. Int. Ed.* **2018**, *57*, 10034–10072.

B) History of photochemistry

1. Early beginnings

Sunlight has had an influence on Earth and its atmosphere since its formation, billions of years ago.[81] However, more complex processes using sunlight only appeared much later, with the formation of the first photosynthetic systems, about 3.4 billion years ago.[82] Evolution perfectioned the photosynthetic system to a flawless photochemical system, capable of converting efficiently carbon dioxide and water into carbohydrates and oxygen. This is only much later that our ancestors began to use sunlight, but only for its heating properties, for a wide variety of applications.

The first photochemical reaction studied in a laboratory could be attributed to Priestley who discovered that nitric acid solutions, when exposed to sunlight, took a reddish color, indicating the formation of nitrogen dioxide gas that was solubilized in the liquid phase.[83] More developments in the use of sunlight were made later, notably on solid-state photochemistry with the study of santonin crystals by Trommsdorff, in 1834.[84]

2. Father of photochemistry

It is commonly established that the Italian chemist Giacomo Ciamician is considered as the father of photochemistry.[85] He reported, as early as in 1886, the conversion of quinone into quinol and the conversion of *o*-nitrobenzaldehyde **154** into *o*-nitrosobenzoic acid **156** under sunlight irradiation among many other light-induced chemical transformations through 40 notes and 9 memoirs published between 1900 and 1914 (Scheme 27).[86]

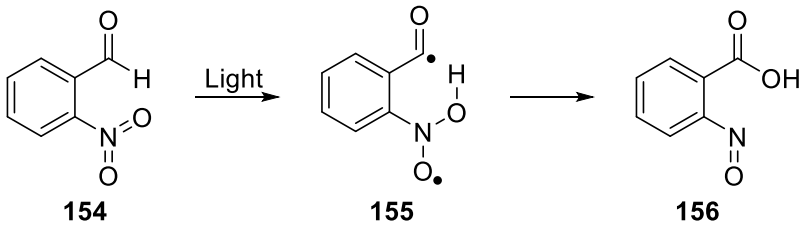

154 **155** **156**

Scheme 27 - Photoconversion of o-nitrobenzaldehyde into o-nitrobenzoic acid

His aim at that time was clear: find alternatives to aggressive reagents and high temperatures to carry out chemical reactions, mimicking what nature had been doing for millions of years using

[81] R. J. Rapf, V. Vaida, *Phys. Chem. Chem. Phys.* **2016**, *18*, 20067–20084J. D. Haigh, *Living Rev. Sol. Phys.* **2007**, *4*, 2.
[82] T. Cardona, *Heliyon* **2018**, *4*, e00548.
[83] J. Priestley, **1790**, *3*, 126–128.
[84] H. Trommsdorff, *Annalen der Pharmacie* **1834**, *11*, 190–207.
[85] J. Šima, *Acta Chimica Slovaca* **2017**, *10*, 84–90.
[86] T. E. Thorpe, *Nature* **1922**, *109*, 245–246.

sunlight. This is why he started to study photochemical processes along with biochemistry (Figure 19).[87] He even postulated in 1912: "If our black and nervous civilization, based on coal, shall be followed by a quieter civilization based on the utilization of solar energy, that will not be harmful to progress and to human happiness" and "When all of the coal will have been burnt, it may become necessary to resort to exploiting light energy for the progress of society" which is still relevant nowadays, as our fossil fuel resources are disappearing.[88] All of his work in photochemistry was made with green chemistry in mind, even though this concept did not exist at that time.[89]

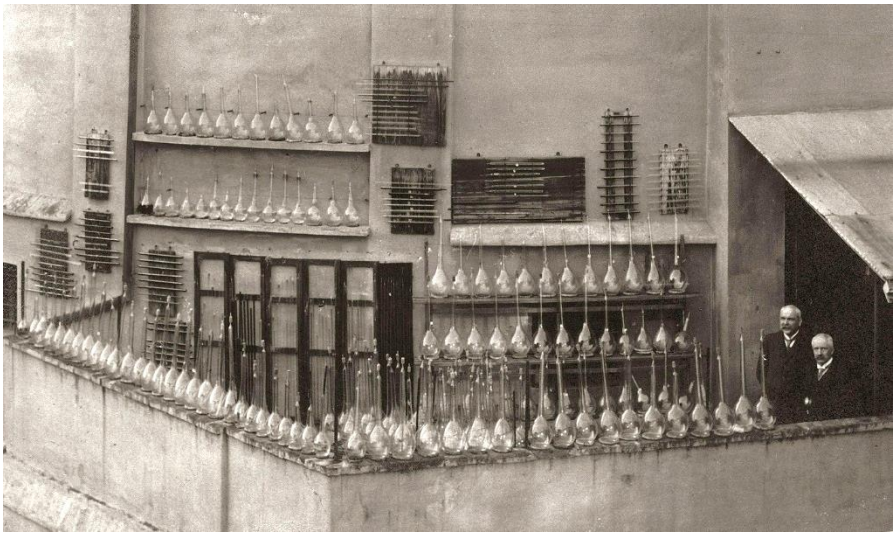

Figure 19 – Ciamician and coworker on the roof of the chemistry building in Bologna

C) Photophysical properties of Ru-based polypyridine complex

Ruthenium polypyridine complexes have been known for decades, with the discovery of $Ru(bpy)_3Cl_2$ in 1936 by Burstall.[90] This complex gained a great interest in the recent years along with the booming of photoredox catalysis due to its unique photophysical properties. In order to understand why it became a photocatalyst of choice, we need to take a closer look at the UV/Vis absorption spectrum[91] of $[Ru(bpy)_3]^{2+}$ which is represented in the Figure 20:

[87] A. Albini, M. Fagnoni, *ChemSusChem* **2008**, *1*, 63–66.
[88] G. Ciamician, *Science* **1912**, *36*, 385–394.
[89] A. Albini, M. Fagnoni, *Green Chem.* **2004**, *6*, 1.
[90] F. H. Burstall, *J. Chem. Soc.* **1936**, 173–175.
[91] S. Campagna, F. Puntoriero, F. Nastasi, G. Bergamini, V. Balzani, in *Photochemistry and Photophysics of Coordination Compounds I* (Eds.: V. Balzani, S. Campagna), Springer, Berlin, Heidelberg, **2007**, pp. 117–214.

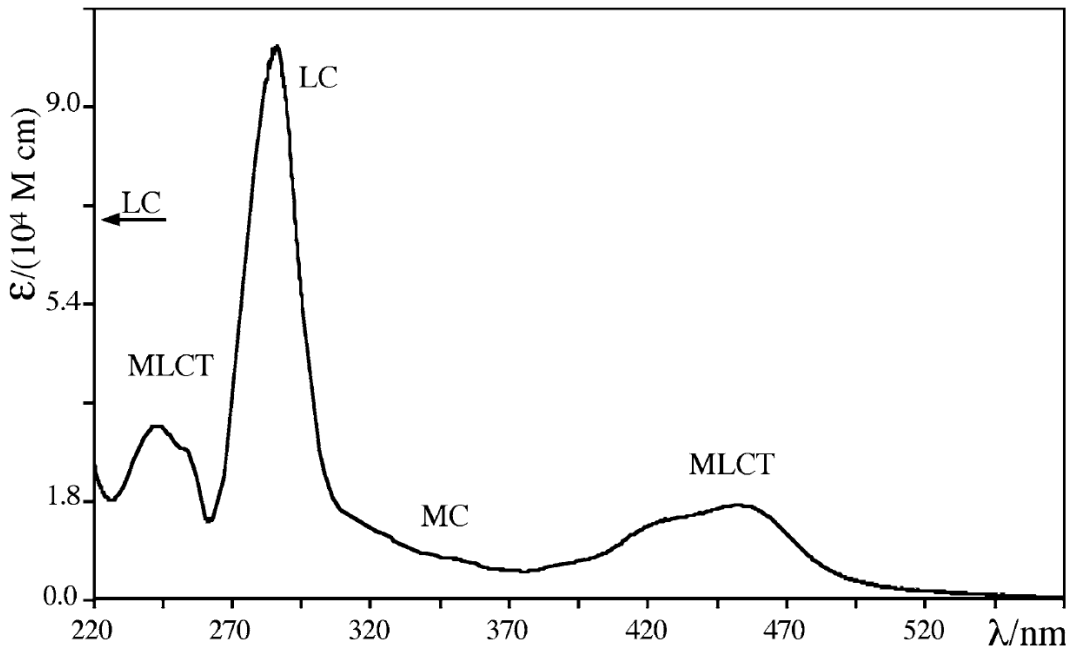

Figure 20 - Electronic absorption spectrum of $[Ru(bpy)_3]^{2+}$ in alcoholic solution

Indeed, three distinct regions are noticeable on this spectrum: Ligand Centered transfers (LC), Metal Centered (MC), the electrons stay in the same spatial region before and after excitation, and the most important one, Metal-to-Ligand Charge Transfer (MLCT), capable of absorbing visible-light at 452 nm (Scheme 28). MLCT can be considered as simultaneous oxidation of the metal center and reduction of one of the ligands. This results in a separation of charges within the excited-state complex and the oxidized Ru^{III} can act as an oxidant while the reduced bpy ligand can act as a reductant (both being stronger oxidant and reductant than in their ground state). The simultaneous presence within the same molecule of these two reactive species accounts for the great versatility of such class of molecules as photocatalysts in photoredox catalysis.[92]

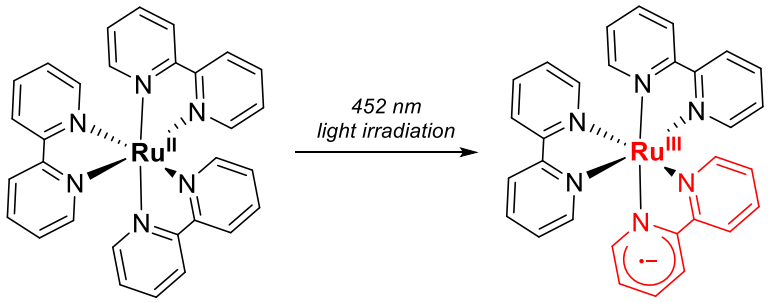

Scheme 28 - Representation of a Metal-to-Ligand Charge Transfer

[92] C. Stephenson, T. Yoon, D. W. MacMillan, *Visible Light Photocatalysis in Organic Chemistry*, Wiley-VCH Verlag GmbH & Co. KGaA, **2018**.

The photophysical properties of the complex can be further tuned by changing the ligands around the metal center in order to change its redox potentials, λ_{max} of absorption or its excited-state lifetime.[93]

When irradiated by visible-light, the complex can absorb a photon (Figure 21). This absorption leads to a conversion of the complex in an excited singlet state $\mathbf{S_1}$ of higher energy. The latter quickly goes back to a more stable level within the same electronic level $\mathbf{S_1}$, *via* an intersystem crossing, leading rapidly to the corresponding triplet state that is lower in energy. This triplet state has a rather long lifetime (hundreds to thousands of ns depending on the complex) which allows it to perform single electron transfer. Fluorescence and phosphorescence properties are highlighted on Figure 21.

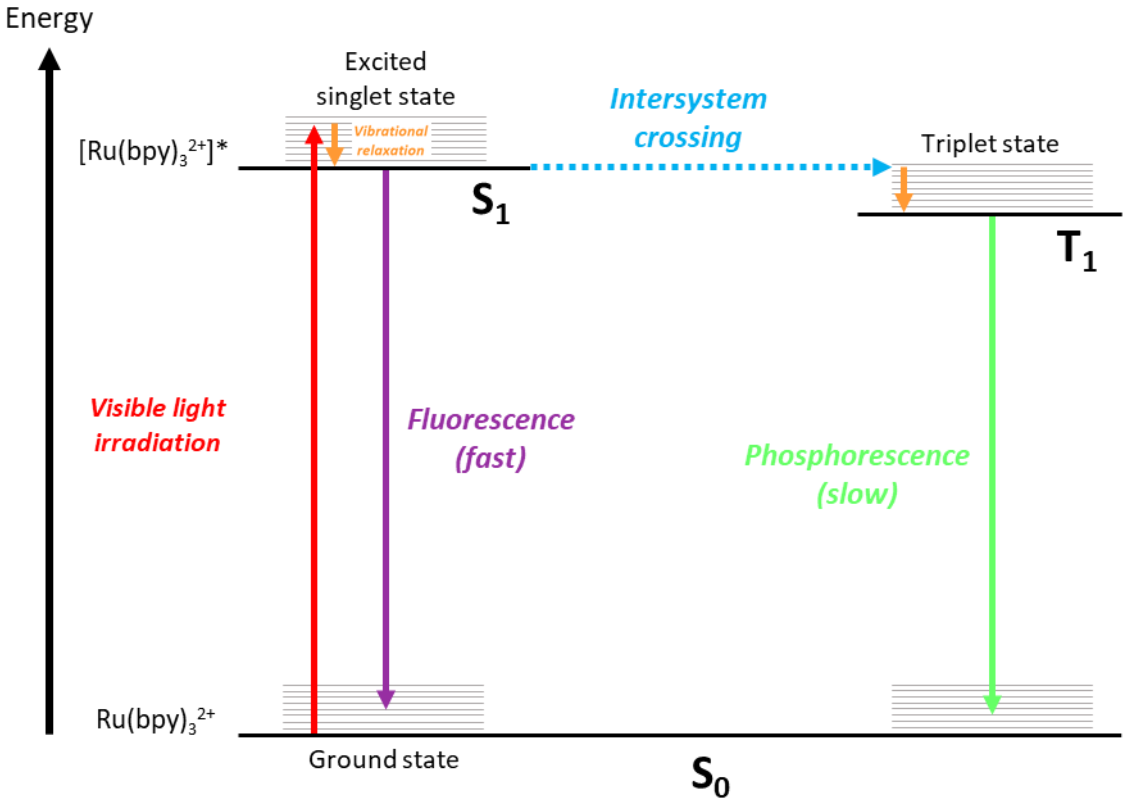

Figure 21 - Simplified representation of the energy diagram associated with the photoinduced excitation of $Ru(bpy)_3^{2+}$

D) Different modes of action

1. Photoredox catalysis

Electron transfer processes concentrate most of the reports in visible-light catalysis due to their wide applicability. They all start by the excitation of the photocatalyst (**PC**) which then enters an excited state, **PC*** (Scheme 29). Then a single electron transfer becomes possible with a reaction

[93] C. Stephenson, T. Yoon, D. W. MacMillan, *Visible Light Photocatalysis in Organic Chemistry*, Wiley-VCH Verlag GmbH & Co. KGaA, **2018**.

partner which has a compatible redox potential. However, the electron transfer does not always occur between the excited state catalyst and a reaction partner. Sometimes, an extra step called a reductive or oxidative quenching (requiring the use of a sacrificial reductant or oxidant) is necessary in order to obtain a reduced or oxidized photocatalyst that is no longer in an excited state but has a much stronger reduction or oxidation potential. To finish, a photocatalytic cycle comprising both an oxidation and a reduction step, and that do not require any sacrificial oxidant or reductant, is named redox-neutral. These four pathways are represented in the following scheme:

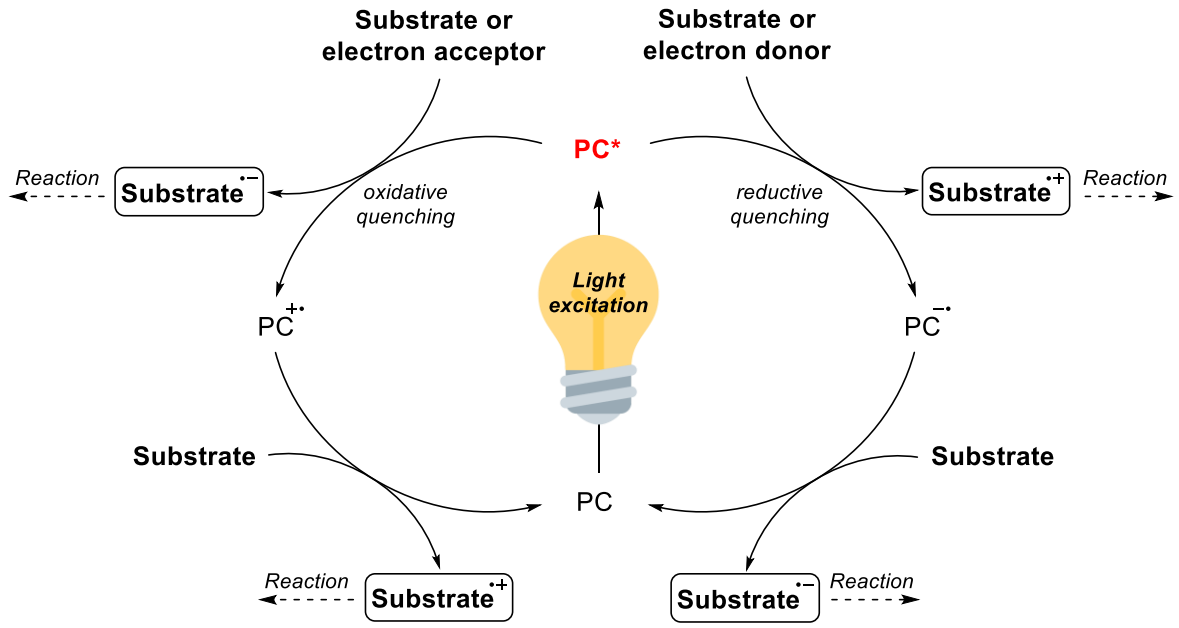

Scheme 29 - Different mechanistic pathways in photoredox catalysis

Another simplified version of such processes could be represented as following (with **A** being an electron acceptor and **D** being an electron donor, Scheme 30):

Single-electron oxidation:

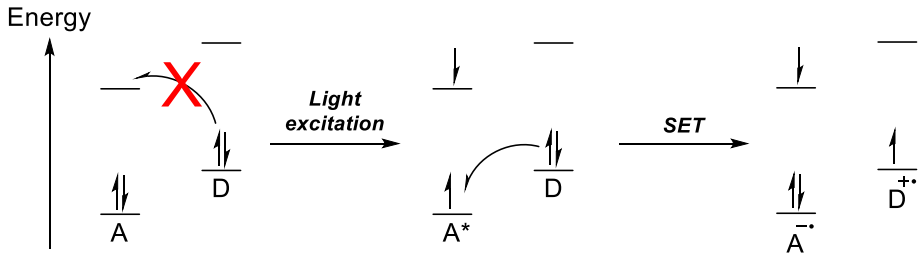

Single-electron reduction:

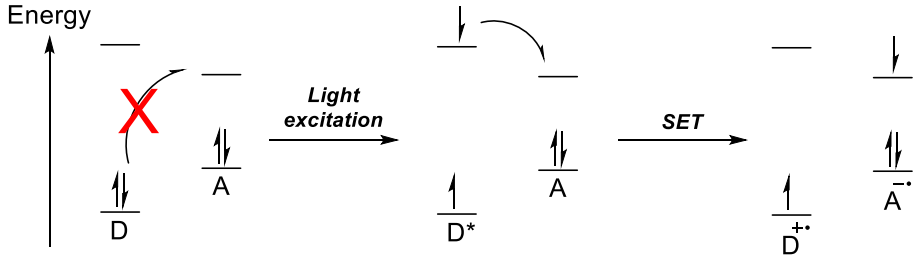

Scheme 30 - Photoinduced electron transfer promoting single-electron oxidation and reduction

Indeed, when considering only the HOMO and LUMO orbitals of the molecules in this simplified scheme, a light irradiation can induce an electron to switch from the HOMO to the higher energy LUMO orbital, yielding an excited-state (Scheme 30). In this excited-state, the HOMO orbital of **A** presents a hole that can be filled, in other word a strong single-electron oxidant property, which is then able to oxidize the donor molecule **D**. The same behavior is applicable the other way around, when a donor molecule **D** enters an excited state and has enough energy to reduce an acceptor molecule **A**.

We will tackle this first point about single electron transfer induced under photoredox catalysis later in the manuscript (**chapter III** and **IV**) since our methods only uses SET processes.

2. Proton-coupled electron transfer

Proton-coupled electron transfer (PCET) processes can be described as reactions in which both electrons and protons are transferred without regard to the mechanism and sites where they are being transferred to.[94] This process allows an access to a wider range of substrates *via* an oxidation or a reduction reaction, as represented in Scheme 31:

[94] N. Hoffmann, *Eur. J. Org. Chem.* **2017**, *2017*, 1982–1992.

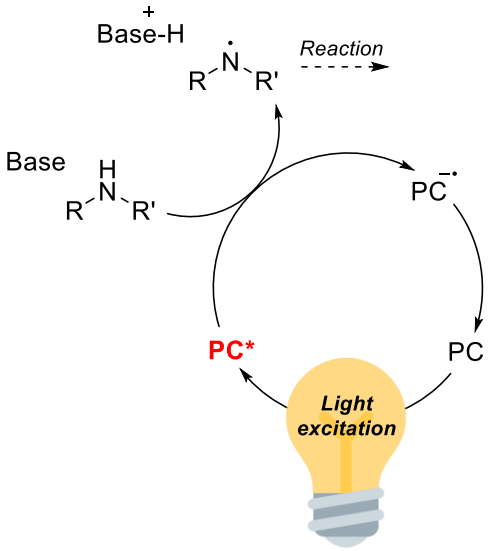

Scheme 31 – Example of a proton-coupled electron transfer for the generation of nitrogen-centered radicals

Knowles's team reported the visible-light catalyzed hydroamination of olefins using simple anilines.[95] This example proceeds via a PCET mechanism and is presented in the following section about the different types of NCR precursors.

3. Synergistic catalysis

Synergistic catalysis comprises two types of mechanisms depending on the nature of the coupling partner of photogenerated radical species. The latter can be coupled with transition-metals catalysts in order to access further synthetic possibilities. This type of dual photoredox/transition-metal catalysis has been studied in our laboratory in the form of a review.[96] Moreover, coupling with an organic partner which can be chiral can allow the control of stereoselectivity through a dual photoredox/organocatalysis pathway (Scheme 32).[97]

[95] A. J. Musacchio, L. Q. Nguyen, G. H. Beard, R. R. Knowles, *J. Am. Chem. Soc.* **2014**, *136*, 12217–12220.
[96] M. De Abreu, P. Belmont, E. Brachet, *European Journal of Organic Chemistry* **2020**, *2020*, 1327–1378.
[97] C. K. Prier, D. W. C. MacMillan, in *Visible Light Photocatalysis in Organic Chemistry*, John Wiley & Sons, Ltd, **2018**, pp. 299–333.

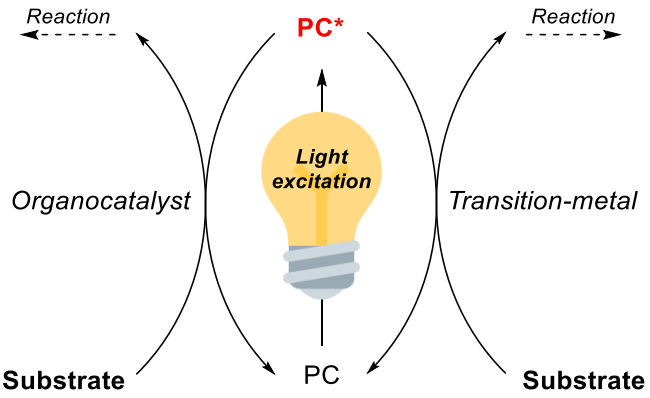

Scheme 32 - General scheme of a synergistic photoredox reaction

4. Photosensitization

This mode of action does not involve electron transfer. A photocatalyst **PC** (named photosensitizer as well) enters an excited state (**PC***) upon light irradiation and can transfer this energy to a substrate that is unable to absorb visible-light. The energy received by the substrate allows it to perform a reaction (Scheme 33).[98]

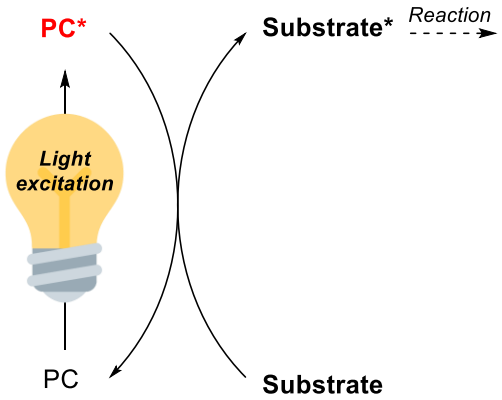

Scheme 33 – Energy transfer through sensitization

Brachet *et al.* disclosed an example of reaction that proceeds via an energy transfer induced by a Ru-based photocatalyst.[99] Their reported methodology relies on the energy transfer between the Ru photocatalyst and benzoyl azide derivatives **157**, triggering a loss of N_2 while affording a reactive benzoyl nitrene intermediate **159** (Scheme 34). The latter is attacked by a heterocycle **158** present in the reaction medium and yields the desired C-H amidation product **160**.

[98] F. Strieth-Kalthoff, M. J. James, M. Teders, L. Pitzer, F. Glorius, *Chem. Soc. Rev.* **2018**, *47*, 7190–7202.
[99] E. Brachet, T. Ghosh, I. Ghosh, B. König, *Chem. Sci.* **2015**, *6*, 987–992.

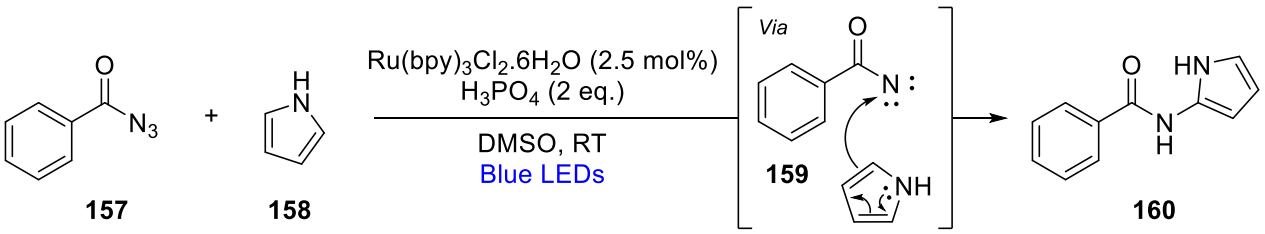

Scheme 34 - Visible-light C-H amidation of heteroarenes reportes by Brachet et al.

5. Electron-donor-acceptor complexes

This last mode of action relies on the association of two or more molecules into a complex that has the ability to absorb visible-light whereas, taken apart, its individual constituents cannot. An electron transfer can occur between the constituents upon light excitation, yielding an oxidized and a reduced molecule that can engage in a reaction (Scheme 35).[100] Such electron-donor-acceptor is tackled in **chapter III** (Scheme 72).[101]

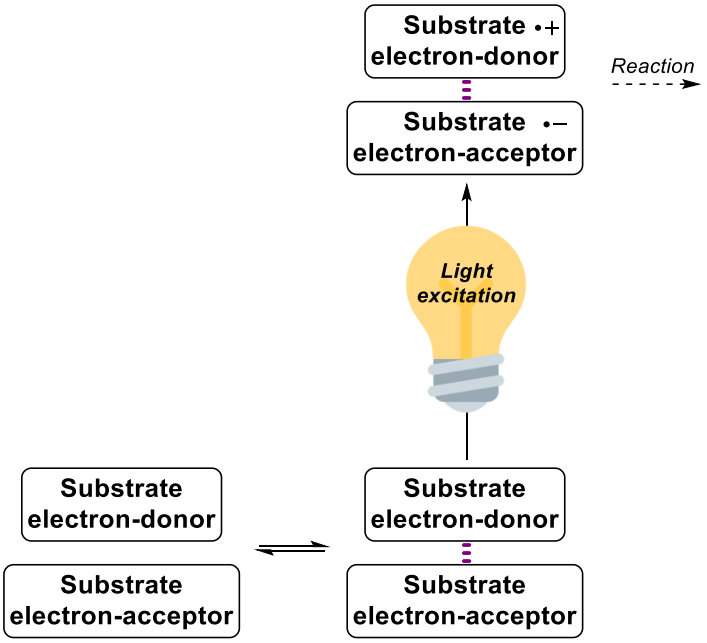

Scheme 35 - Excitation of a donor-acceptor complex

[100] G. E. M. Crisenza, D. Mazzarella, P. Melchiorre, *J. Am. Chem. Soc.* **2020**, *142*, 5461–5476.
[101] G. Nocera, A. Young, F. Palumbo, K. J. Emery, G. Coulthard, T. McGuire, T. Tuttle, J. A. Murphy, *J. Am. Chem. Soc.* **2018**, *140*, 9751–9757.

E) Formation of Carbon-Nitrogen bonds via Nitrogen-Centered Radicals (NCR)

1. History

When putting into perspective the amount of reports that includes the generation of carbon-centered radicals, it clearly appears that nitrogen-centered radicals have been underexplored for synthetic purposes.[102] For a long time, the Hofmann-Löffler-Freytag reaction and its multiple variations remained the main strategy to generate such radicals (Scheme 36). This reaction consists in a thermal or photochemical homolysis of nitrogen-halogen bond (**161**) in a highly acidic medium, leading to the formation of the desired nitrogen-centered radical **164**. The latter can then perform an intramolecular 1,5-Hydrogen Atom Transfer (HAT), leading to a carbon-centered radical **165** that can react with a halogen atom to form a *γ*-halogenated amine **166**. Finally, an ionic cyclization allows the formation of the desired cyclic compound **162** upon treatment with the adequate base.

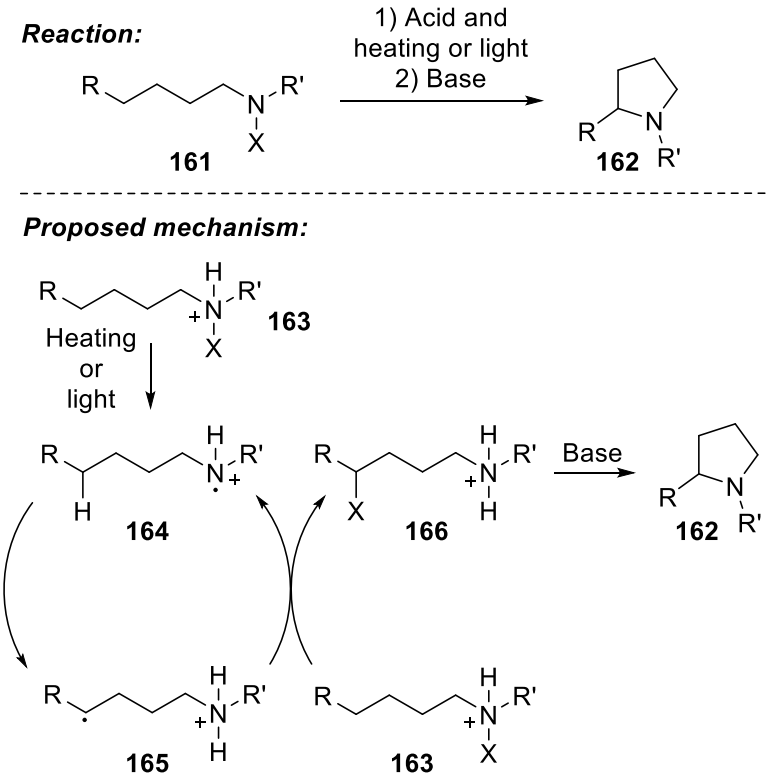

Scheme 36 - Hofmann-Löffler-Freytag reaction

New methods to generate nitrogen-centered radicals in a milder and more selective way were developed along with the development of visible-light catalysis.[103]

[102] M. D. Kärkäs, *ACS Catalysis* **2017**, *7*, 4999–5022.
[103] M. D. Kärkäs, *ACS Catalysis* **2017**, *7*, 4999–5022X.-Y. Yu, Q.-Q. Zhao, J. Chen, W.-J. Xiao, J.-R. Chen, *Acc. Chem. Res.* **2020**, *53*, 1066–1083.

2. Different types of NCR precursors

These new methodologies to generate nitrogen-centered radicals under photoredox catalysis are based on the cleavage of N-X, N-O and N-N, N-H bonds.

Phthalimide derivatives were already studied in the 80s for the generation of nitrogen-centered radical via the homolysis cleavage of a N-Br bond under UV light.[104] In an effort to develop a similar reactivity under visible-light catalysis, Lee and coworkers reported a visible-light induced imidation using *N*-chlorophthalimide derivatives **167** as the NCR precursor (Scheme 37).[105] The generation of the NCR is straightforward with only a single electron reduction necessary to cleave the N-Cl bond. Other variations revolving around phthalimide derivatives for the generation of NCR were also reported such as an example of Sanford and coworkers using *N*-trifluoromethylacyloxyphthalimides **168** as NCR precursors[106] or the example of Studer and coworkers in which *N*-aminopyridinium salts **169** are employed as such precursors.[107]

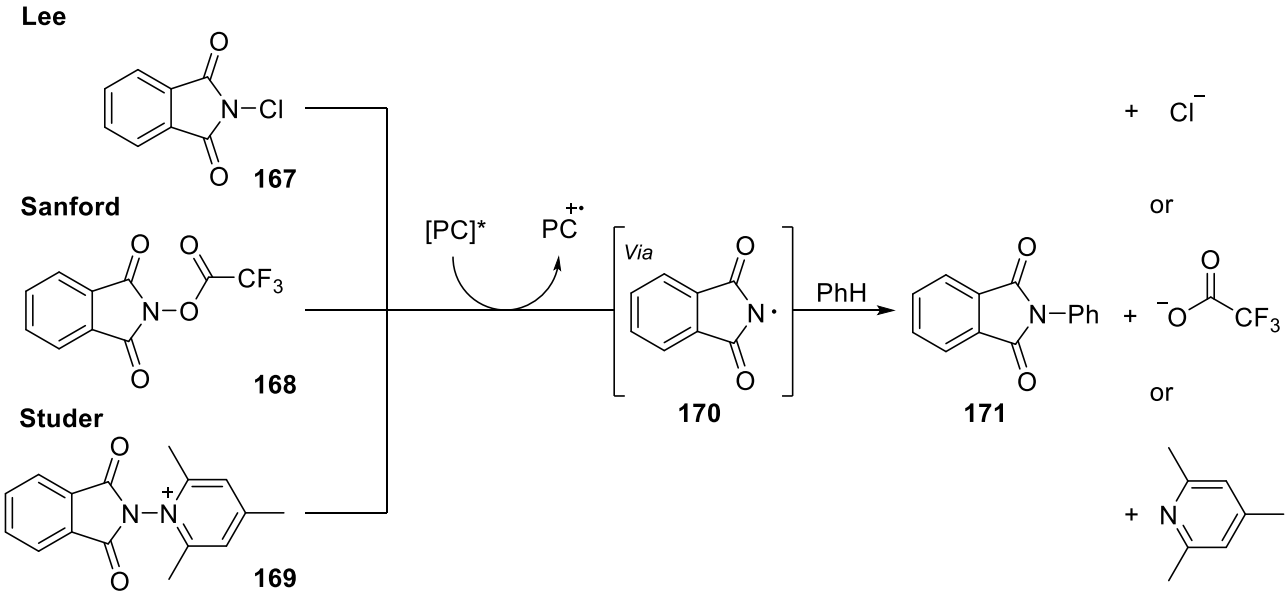

Scheme 37 - NCR generation reported by Lee, Sanford and Studer

The Leonori group reported the generation of iminyl radical **173** using *O*-aryl oximes **172** as NCR precursors (Scheme 38). These precursors can be readily reduced thanks to the low reduction potentials of 2,4-dinitro-substituted aryl oximes **172**. The reaction proceeds *via* a single electron reduction of the 2,4-dinitro-substituted aryl group, leading to the cleavage of the N-O bond and the obtention of the NCR.

[104] U. Lüning, P. S. Skell, *Tetrahedron* **1985**, *41*, 4289–4302.
[105] H. Kim, T. Kim, D. G. Lee, S. W. Roh, C. Lee, *Chem. Commun.* **2014**, *50*, 9273–9276.
[106] L. J. Allen, P. J. Cabrera, M. Lee, M. S. Sanford, *J. Am. Chem. Soc.* **2014**, *136*, 5607–5610.
[107] T. W. Greulich, C. G. Daniliuc, A. Studer, *Org. Lett.* **2015**, *17*, 254–257.

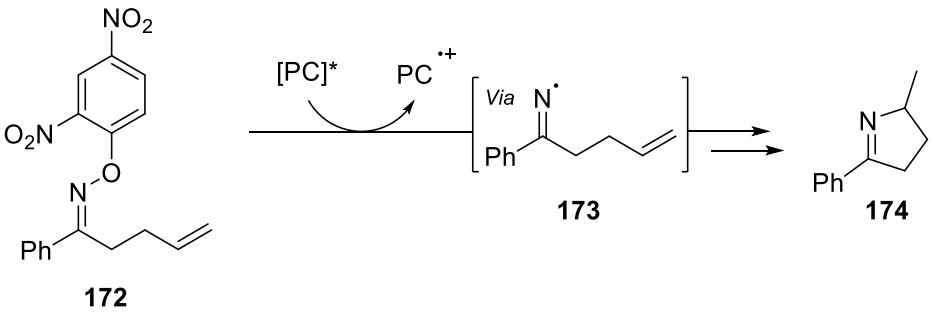

Scheme 38 - NCR generation reported by Leonori's team

Other examples were also reported and based on the cleavage of N-O bonds[108] **175** or N-Cl bonds[109] **178** by Yu and coworkers (Scheme 39). Their methodology is based on the single-electron reduction of the precursor to generate a NCR. The same group developed later a direct oxidative C-H amidation of heteroarenes using sulfonamides **181** as NCR precursors. The latter is oxidized, in the presence of a base, in order to yield the desired radical.[110]

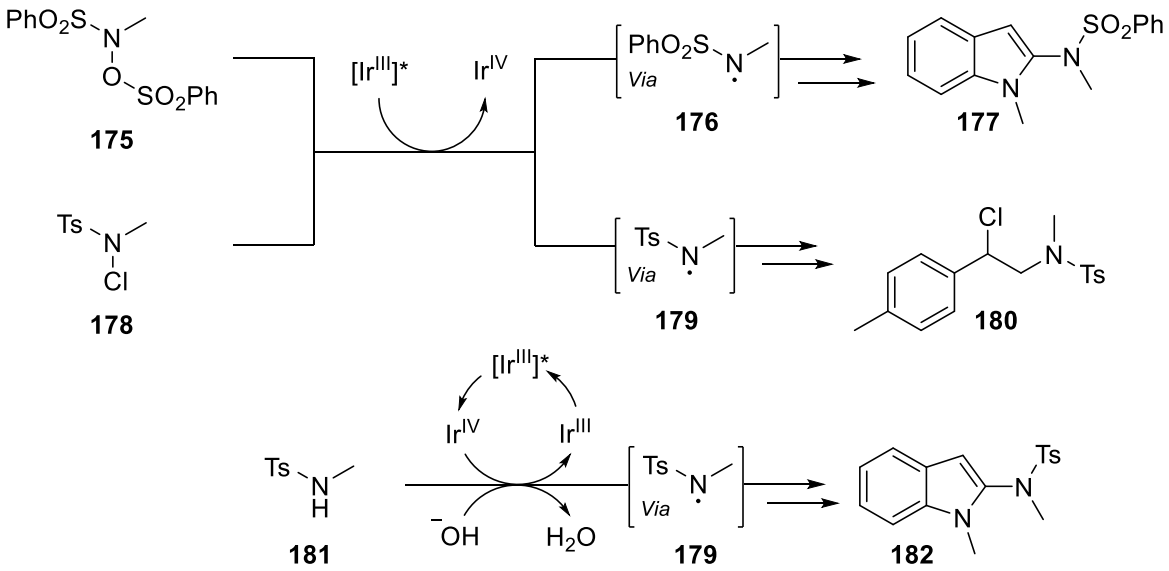

Scheme 39 – Different approaches for NCR generation reported by Yu and coworkers

This strategy for the generation of a NCR was also applied in our laboratory[111] and also by the groups of Xiao and Chen,[112] both on sulfonohydrazone derivatives. This type of NCR generation is called an Oxidative Deprotonation Electron Transfer (ODET) and requires the presence of a base for the deprotonation step which is followed by an oxidation of the formed anion to yield the NCR.

---

[108] Q. Qin, S. Yu, *Org. Lett.* **2014**, *16*, 3504–3507.
[109] Q. Qin, D. Ren, S. Yu, *Org. Biomol. Chem.* **2015**, *13*, 10295–10298.
[110] K. Tong, X. Liu, Y. Zhang, S. Yu, *Chemistry - A European Journal* **2016**, *22*, 15669–15673.
[111] E. Brachet, L. Marzo, M. Selkti, B. König, P. Belmont, *Chem. Sci.* **2016**, *7*, 5002–5006.
[112] X.-Q. Hu, J.-R. Chen, Q. Wei, F.-L. Liu, Q.-H. Deng, A. M. Beauchemin, W.-J. Xiao, *Angewandte Chemie International Edition* **2014**, *53*, 12163–12167.

Our laboratory reported in 2016 a cascade reaction involving a hydroamination reaction followed by a Smiles rearrangement (Scheme 40).[111] Indeed, they were able to generate a NCR starting from a *N*-tosylhydrazone **183**. The generated NCR was then able to react intramolecularly with the alkynyl unit, yielding a hydroaminated radical intermediate **184**. Then, a radical 1,4-aryl migration was able to occur and yield the phthalazine scaffold **185**.

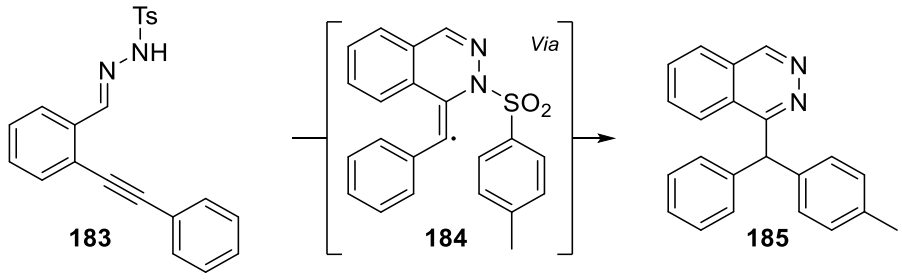

Scheme 40 - Hydroamination of N-tosylhydrazones under visible-light catalysis reported by Brachet, Belmont and coworkers

The same year, Xiao, Chen and coworkers[112] reported a hydroamination reaction on a terminal alkene **186**, yielding the Markovnikov product **188** as the only product of the reaction, as represented in Scheme 41:

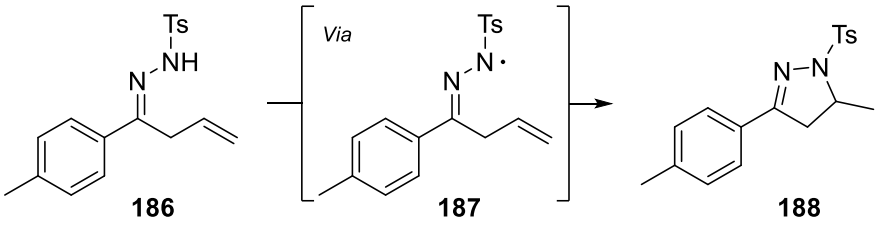

Scheme 41 - Hydroamination of N-tosylhydrazones under visible-light catalysis reported by Xiao, Chen and coworkers

They later developed variations of their methodologies and achieved to switch the regioselectivity of their reaction by wisely adding an aryl group at position 2 of the alkene and adding TEMPO in the reaction medium to mediate a HAT (Scheme 42).[113] They also adapted their reaction to different starting material, bearing N-O bonds. By doing so, they were able to successfully convert *N*-tosylhydrazones **189** (eq. 1, Scheme 42), *N*-sulfonyl-*O*-butenyl hydroxylamines **192** (eq. 2) and benzamides **195** (eq. 3) derivatives into the corresponding dihydropyridazines **191**, isoxazolidines **194** and 3,4-dihydroisoquinolinones **197**.[114] These different variations are represented in Scheme 42:

[113] X.-Q. Hu, X. Qi, J.-R. Chen, Q.-Q. Zhao, Q. Wei, Y. Lan, W.-J. Xiao, *Nat Commun* **2016**, *7*, 11188.
[114] J. Chen, H.-M. Guo, Q.-Q. Zhao, J.-R. Chen, W.-J. Xiao, *Chem. Commun.* **2018**, *54*, 6780–6783.

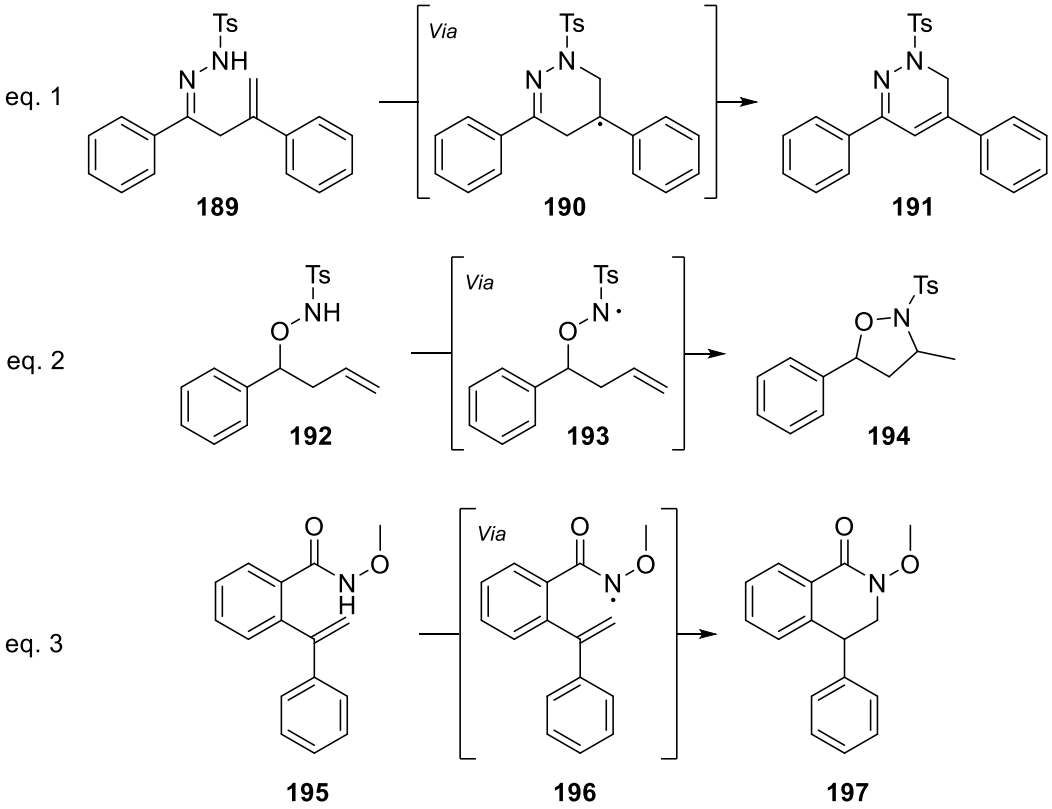

Scheme 42 - Various work reported by Xiao, Chen and coworkers

When looking at the examples for the generation of NCR, it appears that all the precursors present a very specific environment for the obtention of the desired radical (phthalimides, sulfonamides…). The milestone would be the possibility to develop such radical on simple amines, without any required specific neighboring bonds. This is where the work of Knowles and coworkers stands out since they were able to generate a NCR straightforwardly, starting from aniline derivatives **198**. Indeed, the NCR is obtained *via* the direct oxidation of an arylamine **198** into an aminium radical **199**, thus preventing the need to use labile NCR precursors or specific starting materials (Scheme 43). This reaction has the particularity to yield an anti-Markovnikov product **200** and to proceed via a Proton-Coupled Electron Transfer (PCET).

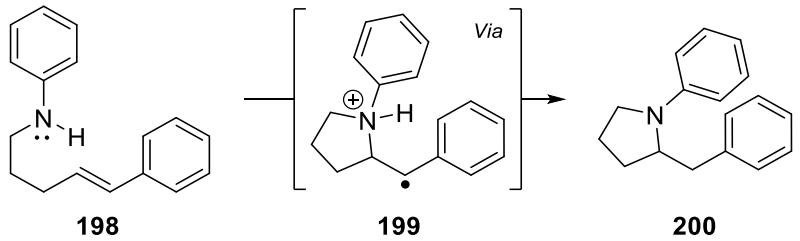

Scheme 43 - Anti-Markovnikov hydroamination of aryl olefins under visible-light catalysis reported by Knowles and coworkers

F) Conclusion & perspectives

Although being very attractive, the example reported by Knowles's team is still rather rare in the literature since the majority of reports employs cleavable moiety for the generation of a NCR. This is why the development of new NCR precursors is still a relevant topic in order to broaden the possibilities to access such useful radical intermediates.

Chapter III:

Visible-Light catalyzed hydroamination using phosphonohydrazones as novel NCR precursors

Chapter III: Visible-Light catalyzed hydroamination reactions using phosphonohydrazones as novel NCR precursors

Nitrogen-centered radicals are a very attractive alternative for the formation of carbon-nitrogen bonds. During the last decade, along with the booming of visible-light catalysis, the development of new nitrogen-centered radical precursors took-off, as attested by the synthesis of a range of precursors by many research groups.[115] In order to bring our contribution to this field, we investigated the reactivity of phosphorus-containing starting materials, and more specifically, phosphoramidates (Scheme 44).

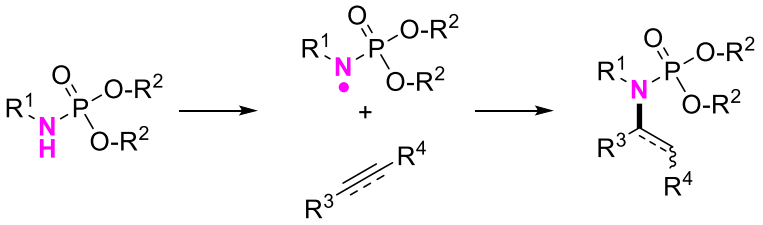

Scheme 44 – Investigation of phosphoramidates as novel NCR precursors

A) Hydroamination reactions

1. Introduction

A hydroamination reaction is, by definition, the addition of a N-H bond of a nucleophilic primary, secondary amine or even ammonia onto an unsaturated C-C multiple bond (alkene, alkyne, diene or allene) with a cleavage of the N-H bond and the concomitant formation of a C-N bond and a C-H bond.[116] The general scheme for such a reaction could be represented as follows (Scheme 45), on various partners such as alkenes (eq. 1), alkynes (eq. 2), allenes (eq. 3) with two regioisomers formed and dienes (eq. 4) leading to 3 different products:

[115] M. D. Kärkäs, *ACS Catalysis* **2017**, *7*, 4999–5022X.-Y. Yu, Q.-Q. Zhao, J. Chen, W.-J. Xiao, J.-R. Chen, *Acc. Chem. Res.* **2020**, *53*, 1066–1083.
[116] L. Huang, M. Arndt, K. Gooßen, H. Heydt, L. J. Gooßen, *Chem. Rev.* **2015**, *115*, 2596–2697.

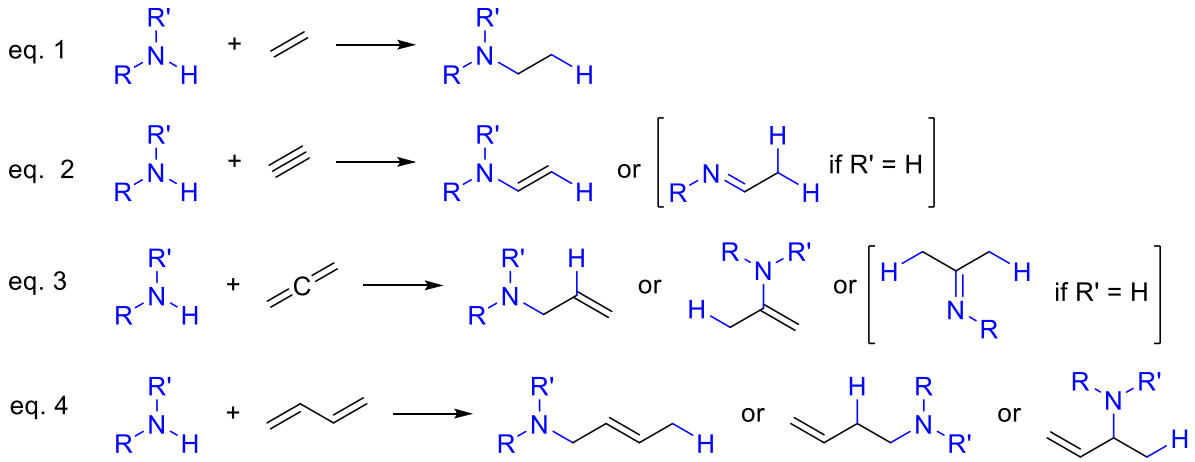

Scheme 45 - General representation of a hydroamination reaction on diverse substrates

This reaction has the particularity of being one of the most atom-economical process for the formation of amines, imines and enamines (Scheme 45) and this is why it is of great interest, both for industrial applications and fundamental research.[117] These functional groups are present in a plethora of fine chemicals, pharmaceuticals and, more broadly, building blocks in organic synthesis.[118] Hydroaminations have been both described in an intramolecular and intermolecular fashion and they present a high activation barrier, preventing it from happening under unactivated reaction conditions except if the olefin is structurally activated (*i.e.* electron-deficient) and therefore does not require a catalyst.[119] Another point to take into account is that this kind of reaction possesses a highly negative entropy which, associated with a temperature increase in the reaction medium, leads to a shift of the reaction towards the starting materials and not the desired product. This is why a catalyst is used, to lower this high activation barrier and reverse the reactivity.[120] Hydroamination reactions can yield Markovnikov and anti-Markovnikov products (Scheme 46).

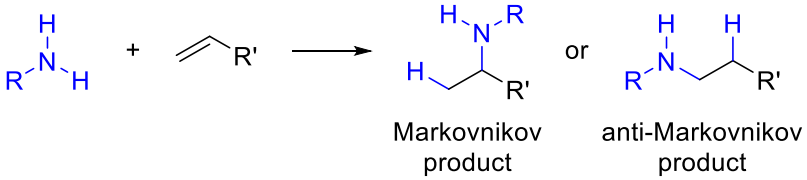

Scheme 46 - Representation of the Markovnikov and anti-Markovnikov products that can be obtained after a hydroamination reaction

[117] J. Seayad, A. Tillack, C. G. Hartung, M. Beller, *Advanced Synthesis & Catalysis* **2002**, *344*, 795–813.
[118] "Ullmann's Encyclopedia of Industrial Chemistry, 40 Volume Set, 7th Edition | Wiley," can be found under https://www.wiley.com/en-us/Ullmann%27s+Encyclopedia+of+Industrial+Chemistry%2C+40+Volume+Set%2C+7th+Edition-p-9783527329434, **n.d.**
[119] M. F. Semmelhack, B. M. Trost, I. Fleming, Eds. , *Comprehensive Organic Synthesis: Selectivity, Strategy & Efficiency in Modern Organic Chemistry. Vol. 4: Additions to and Substitutions at C - C π-Bonds*, Pergamon Press, Oxford, **1993**.
[120] D. Steinborn, R. Taube, *Z. Chem.* **2010**, *26*, 349–359.

Only the hydroamination reaction performed under homogeneous catalysis will be tackled in this introduction. Moreover, after discussing the early work reported in this field, we will mainly focus on recent advances which are still reported nowadays even if this reaction was initially reported almost a century ago, and more importantly we will focus on the visible-light catalyzed reactions which arose in the literature during the last decade.[121]

2. State of the art

The first hydroamination reaction reported in a homogeneous medium could be attributed to Hickinbottom, back in 1932 (Scheme 47).[122] He discovered that when cyclohexene **201** was heated in a sealed tube with an aniline derivative **202**, the addition of the nitrogen to the double-bond could occur, yielding the corresponding cyclohexylaniline derivative **203**, among other products.

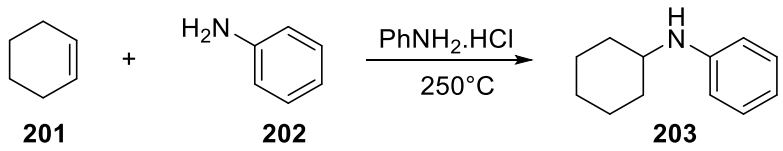

Scheme 47 - First example of a hydroamination reaction reported by Hickinbottom

It is only about 40 years later that the first transition-metal catalyzed (in a catalytic amount) hydroamination reaction was reported, by Coulson.[123] He reported the use of Rhodium (Scheme 48) or Iridium catalysts for the hydroamination reaction of ethylene **204** with piperidine **205**.

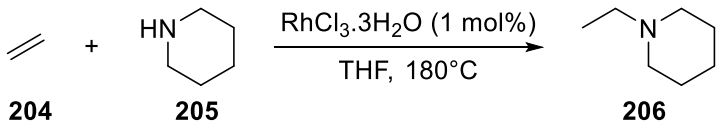

Scheme 48 - First example of a catalytic transition-metal catalyzed hydroamination reaction reported by Coulson

Narasaka's team worked at the beginning of the 2000's on a near-UV light (above 320 nm) catalyzed synthesis of reduced pyrroles derivatives **174**, starting from oximes derivatives **172** (Scheme 49).[124]

[121] J. Huo, G. He, W. Chen, X. Hu, Q. Deng, D. Chen, *BMC Chemistry* **2019**, *13*, 89.
[122] W. Hickinbottom, *J. Chem. Soc.* **1932**, 2646–2654.
[123] D. R. Coulson, *Tetrahedron Letters* **1971**, *12*, 429–430.
[124] T. Mikami, K. Narasaka, *Chemistry Letters* **2000**, 338–339.

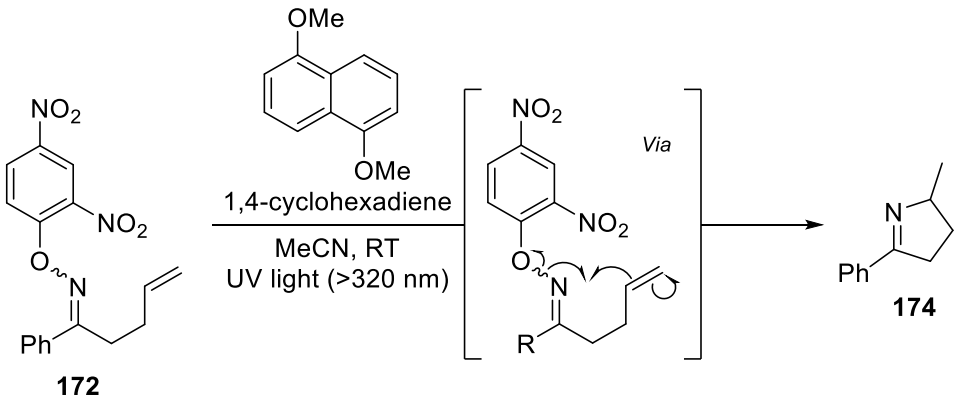

Scheme 49 - UV-light induced hydroamination of oximes into pyrrole derivatives reported by Narasaka and coworkers

The development of visible-light catalyzed methodologies for hydroamination reactions is still relevant, especially as attractive alternatives to the existing methodologies reported using higher energy UV-light

We will focus now on the visible-light catalyzed hydroamination reactions reported in the literature. To the best of our knowledge, Nicewicz and Nguyen were the first to report such reaction under visible-light catalysis, in 2013 (Scheme 50). They developed a methodology using a different approach from the ones that will be reported later in the literature.[125] Indeed, they used a highly oxidant organic photocatalyst, 9-mesityl-10-methylacridinium tetrafluoroborate, also known as Fukuzumi acridinium salt,[126] which is capable of the direct oxidation of non-activated alkenes **207** into the corresponding radical cation alkenes **209** that can be readily attacked by an intramolecular sulfonylamine. This reaction can either yield 5-*exo*-trig **210** or 6-*exo*-trig (not shown) products which are both anti-Markovnikov products. Moreover, it is important to note that the presence of a hydrogen atom donor (thiophenol here) is crucial in this reaction in order to obtain the desired product **208** with good yield and prevents the dimerization of the last radical intermediate. They also developed an intermolecular variation of their reaction. [127]

[125] T. M. Nguyen, D. A. Nicewicz, *J. Am. Chem. Soc.* **2013**, *135*, 9588–9591.
[126] S. Fukuzumi, K. Ohkubo, *Chem. Sci.* **2013**, *4*, 561–574.
[127] T. M. Nguyen, N. Manohar, D. A. Nicewicz, *Angew. Chem. Int. Ed.* **2014**, *53*, 6198–6201.

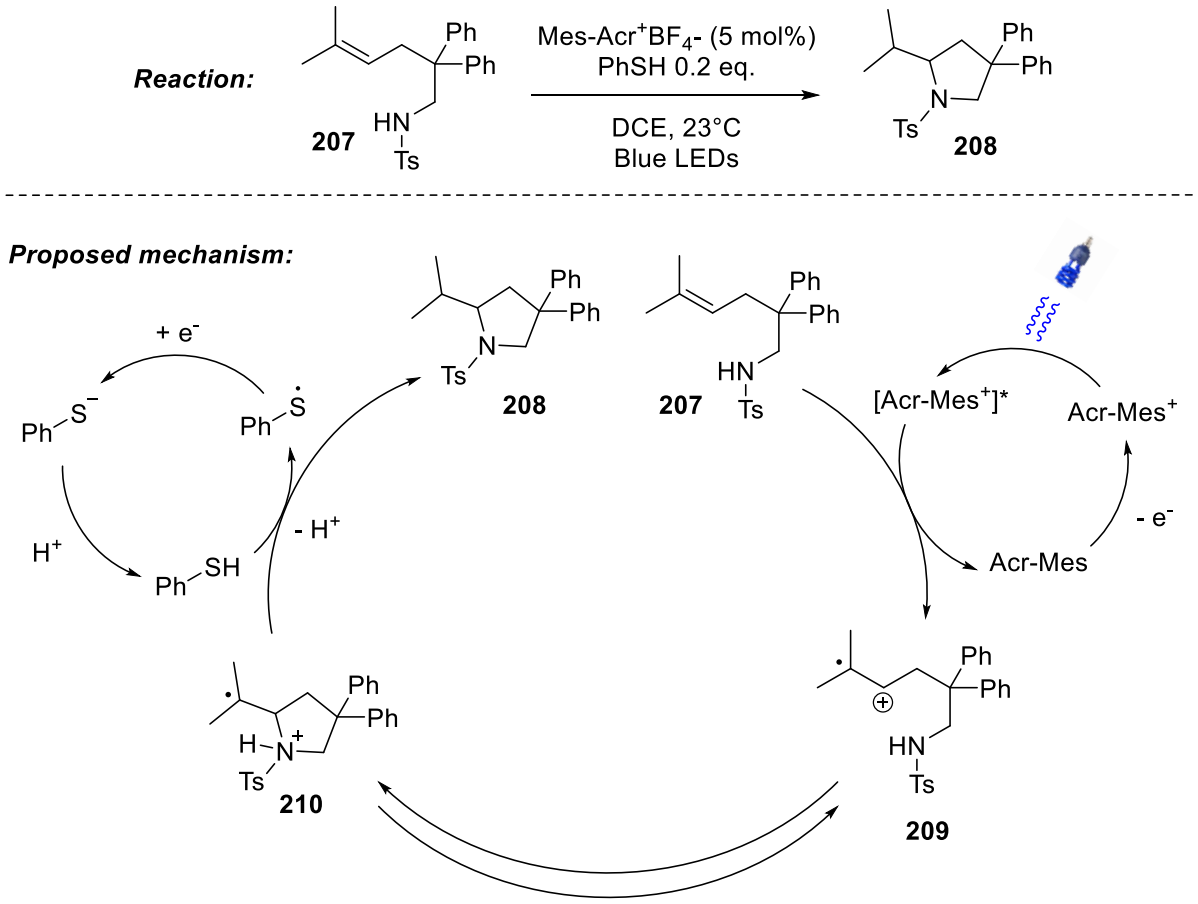

Scheme 50 – Mechanism of the anti-Markovnikov hydraomination reported by Nicewicz and Nguyen

The reports of Xiao/Chen, Brachet and Knowles that were tackled in the previous chapter are also examples of hydroamination reactions.

B) Phosphonohydrazones: a new family of pre-activated NCR precursor

1. Why them?

1.1. Existing sulfonohydrazones and exploration of their reactivity as NCR precursors

As presented above, in 2016, our group successfully developed a novel cascade reaction of hydroamination followed by a Smiles rearrangement (Scheme 51). This reaction was very important on three counts: *i)* the radical addition onto alkynes was totally unknown and therefore not reported in the field of visible-light catalysis, *ii)* it was the first cascade reaction of a hydroamination followed by a Smiles rearrangement, and finally, *iii)* it was the first example of phthalazine synthesis under visible-light catalysis.

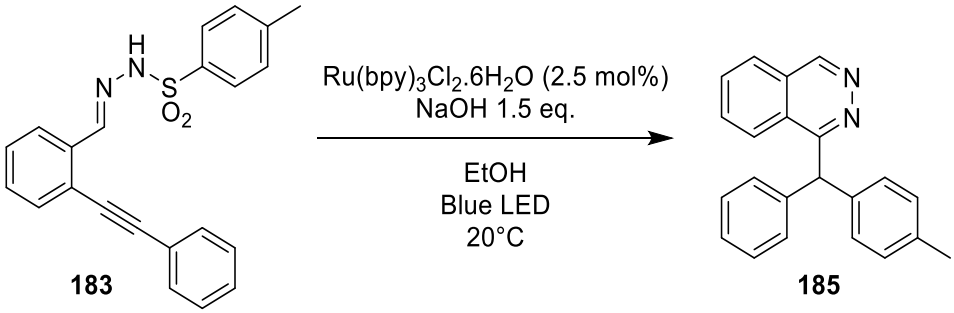

Scheme 51 - Visible light catalyzed amination/Smiles rearrangement cascade reported by Brachet et al. in 2016

Despite its originality, this reaction was not conclusive with alkene derivatives and the synthesis of the starting material required the highly corrosive chlorosulfuric acid, among other reagents, in order to obtain aryls bearing a chlorosulfonyl group. A remaining question after developing this methodology was: how else can we access nitrogen-centered radicals? Therefore, in 2018, we started looking for new structures able to generate these radicals.

With this statement in mind, we focused our attention on phosphorus containing starting materials. Indeed, we were inspired by a report in the literature, reported by Taniguchi *et al.* in 2011,[128] where diethylphosphonohydrazine **212** was used as a phosphorus-centered radical precursor under iron catalysis (Scheme 52). The reported reaction proceeds via an oxidation of the hydrazine moiety into a diazene **216** using an iron phthalocyanine complex as the catalyst. Then, after the release of dinitrogen gas, the phosphorus-centered radical **218** is generated and can react with an alkene moiety **211** to yield β-hydroxyphosphonates **213**.

[128] T. Taniguchi, A. Idota, S. Yokoyama, H. Ishibashi, *Tetrahedron Letters* **2011**, *52*, 4768–4770.

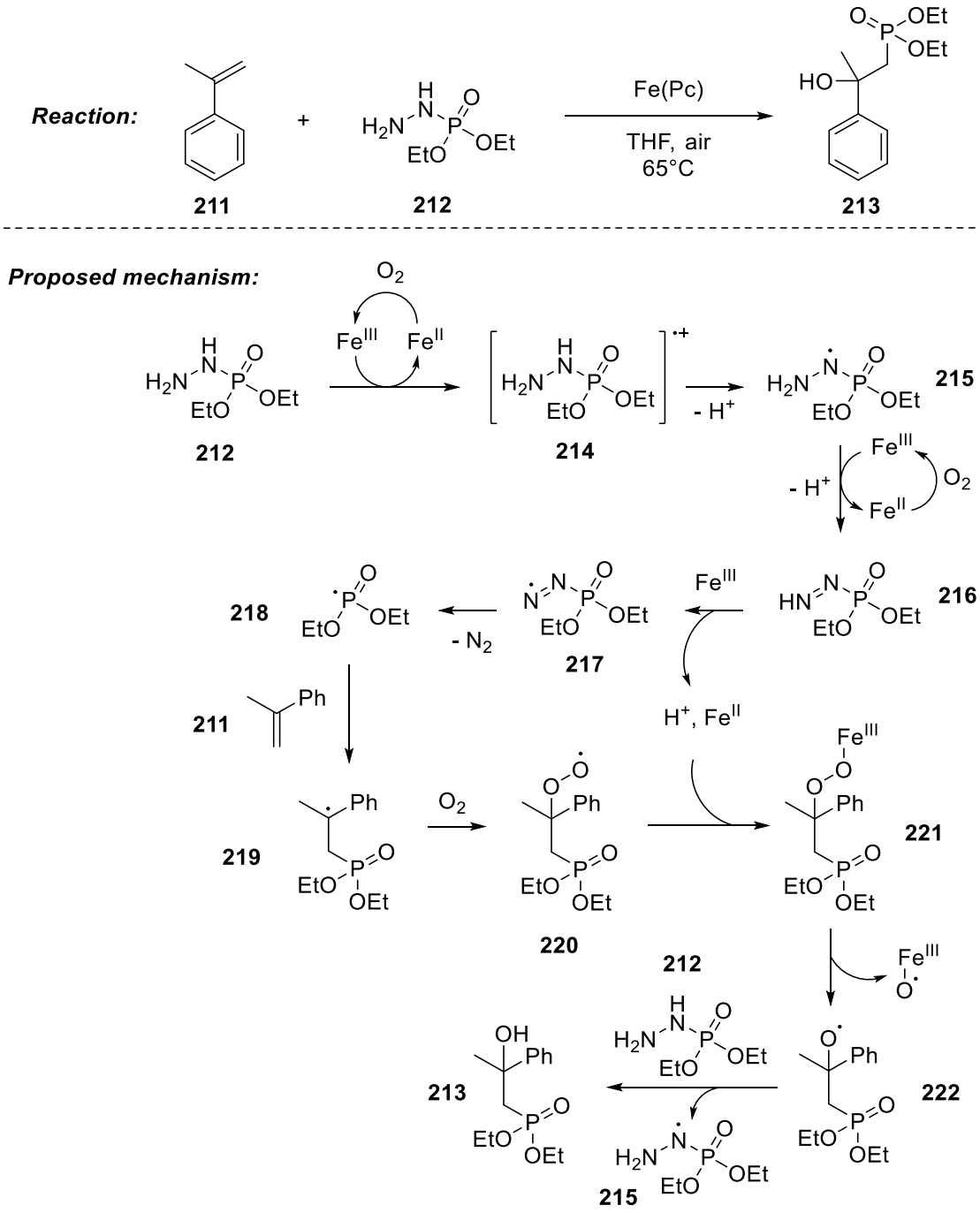

Scheme 52 - Synthesis of β-hydroxyphosphonates reported by Tanigushi et al. in 2011

Our first goal was to evaluate if this transformation could also be possible under visible-light catalyzed conditions, in order to generate a radical using light instead of conventional conditions. Unfortunately, after screening several reaction parameters, we did not succeed in generating a phosphorus-centered radical capable of performing additions onto alkenes. Nevertheless, this failure allowed us to bounce back and investigate another path, using the synthesized phosphonohydrazines, engaging them with aldehyde or ketone derivatives in order to form phosphonohydrazones

(Figure 22). The latter present a totally unknown reactivity with alkenes and alkynes that is going to be investigated in this chapter.

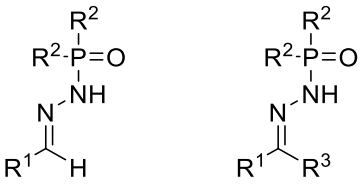

Figure 22 - General representation of phosphonohydrazones

Some reports exist on such phosphonohydrazones, like in the reaction reported by Xu's team, in 2013,[129] in 2015[130] and 2017.[131] They described the use of phosphonohydrazones (**223**, **226** and **229**) as nitrogen-centered radical precursors under copper catalysis in order to synthesize isoquinolines **225**, pyrazolines **228** and cinnolines **231** (Scheme 53). It appears that the generation of a nitrogen-centered radical seems possible from such phosphorus moiety, but no information exists under visible-light catalysis.

[129] W. Liu, X. Hong, B. Xu, *New York* **2013**, 13.
[130] Z. Ding, Q. Tan, M. Gao, B. Xu, *Org. Biomol. Chem.* **2015**, *13*, 4642–4646.
[131] C. Lan, Z. Tian, X. Liang, M. Gao, W. Liu, Y. An, W. Fu, G. Jiao, J. Xiao, B. Xu, *Advanced Synthesis & Catalysis* **2017**, *359*, 3735–3740.

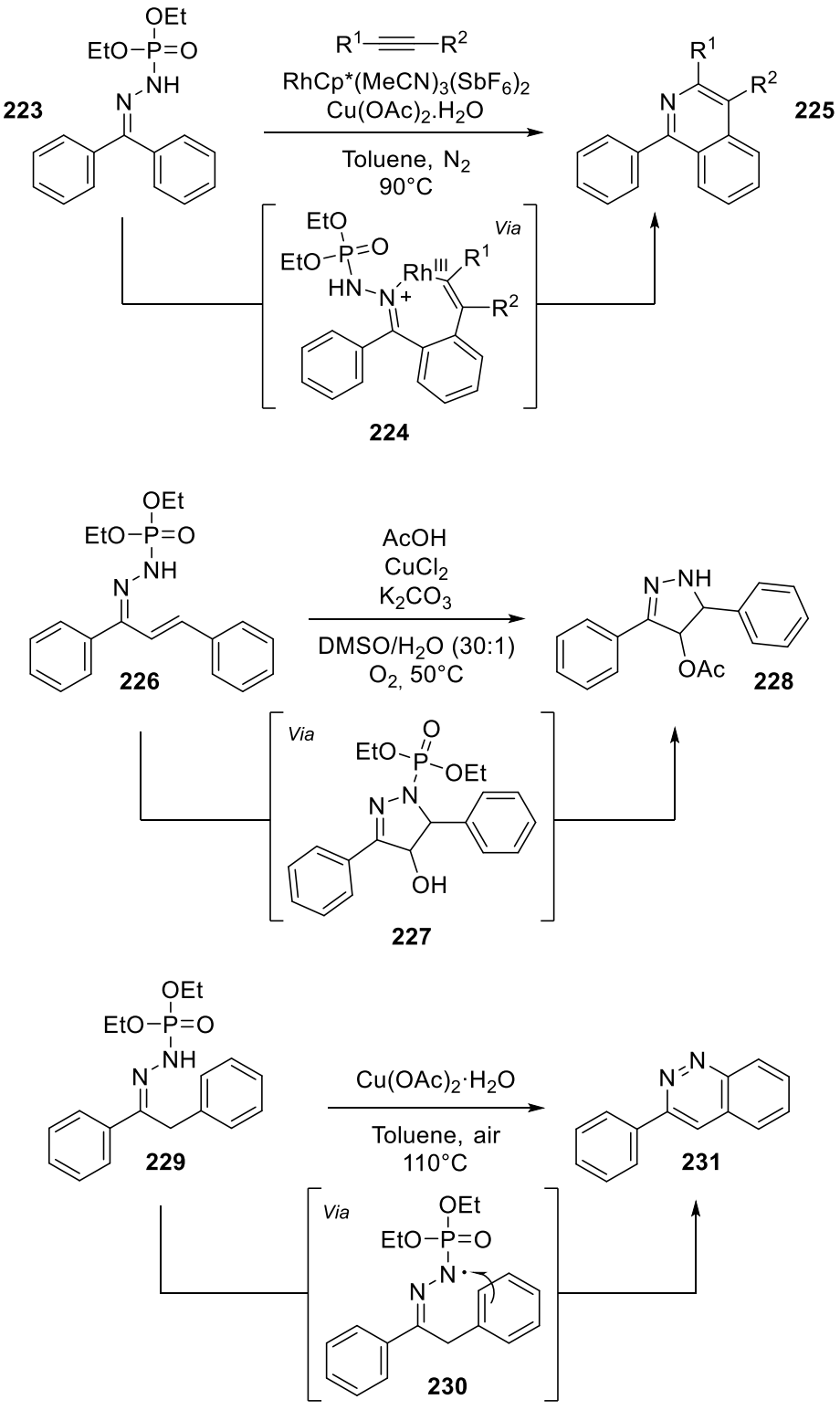

Scheme 53 - Synthesis of isoquinoline, pyrazoline and cinnoline derivatives via a NCR generated on phosphonohydrazones reported by Xu's team

Therefore, we propose to investigate phosphonohydrazones as nitrogen-centered radical precursors in order to better understand if such radicals could be generated thanks to visible-light catalysis and be stable enough to participate in a subsequent radical reaction.

1.2. History

To the best of our knowledge, the earliest report of the use of a phosphonohydrazone could be attributed to Scott and Lalor, in 1969.[132] They demonstrated that oxime derivatives bearing a phosphonydrazone on an *ortho* position **232** can lead to the formation of triazoles **237** under basic conditions. Different plausible mechanisms were postulated and two of them are represented in Scheme 54. Path *a* is the result of an initial degradation of the hydrazone to an unsubstituted hydrazide anion **233** followed by a nucleophilic displacement of a hydroxide anion from the neighboring oxime **234**. Path *b*, on the other hand, would start with the nucleophilic attack of the phosphorus moiety in **235**, which lead to its migration from the hydrazone to the oxime. Then, a nucleophilic displacement of a diphenyl phosphate **236** would lead to the desired compound **237**.

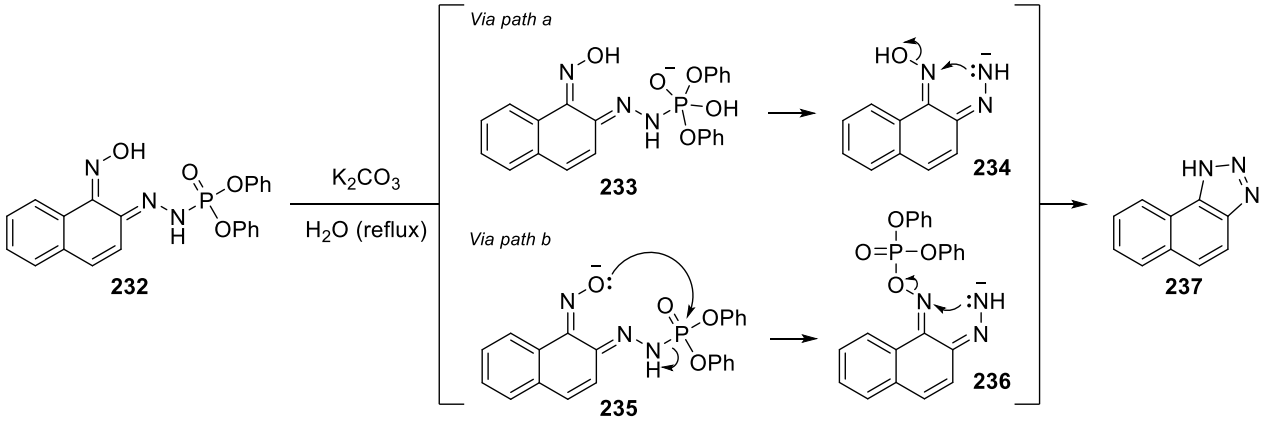

Scheme 54 - Synthesis of triazole derivatives reported by Scott and Lalor in 1969

A decade later, another reaction was reported by El-Deek et al.[133] in which they react 1,3-dicarbonyls why phosphonohydrazines in order to form the corresponding hydrazones **238** (Scheme 55). Then, upon heating to their melting point, the hydrazones were converted in the corresponding pyrazoline-5-ones **239** (predominantly under the OH tautomeric form).

Scheme 55 - Synthesis of pyrazoline-5-one derivatives reported by El-Deek et al. in 1981

In 1986, Zwierzak *et al.* reported the synthesis of unsymmetrical azines **243** in a sequential fashion (Scheme 56).[134] Indeed, the first step is the formation of the hydrazone via a reaction of the

[132] J. F. Lalor, F. L. Scott, *J. Chem. Soc.* **1969**, 1034–1043.
[133] M. El-Deek, E. El-Sawi, M. Mohamed, *J. Chem. Eng. Data* **1981**, *26*, 340–342.
[134] A. Koziara, K. Turski, A. Zwierzak, *Synthesis* **1986**, *4*, 298–301.

phosphonohydrazone **240** on an aldehyde **241** or a ketone. Then, a reaction with NaH yields an anionic nitrogen intermediate **242** which reacts in a similar fashion to the Horner-Wadsworth-Emmons olefination with the phosphorus atom, leading to the formation of an azine and the departure of the phosphorus moiety.[135]

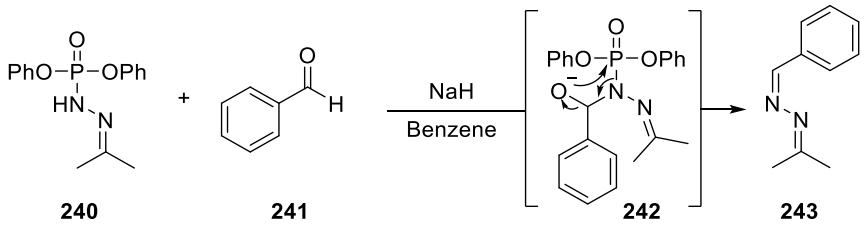

Scheme 56 - Synthesis of unsymmetrical azine derivatives reported by Zwierzak et al. in 1981

Later, other teams reported the study of this type of functional group such as Marek *et al.* in 1997[136] or Potacek *et al.* in 2004.[137]

In 2010, Loiseau *et al.* reported an improved Cope-type hydroamination reaction using phosphonohydrazine derivatives **244** (Scheme 57).[138] The reaction only requires high heating in trifluorotoluene in order to afford the desired product **245**. Unfortunately, using phosphonohydrazones led to the formation of side-products, especially at high temperature. Indeed, the authors reported that an aza-Cope elimination of an ammonium ylide formed via a proton transfer could occur at high temperature with a reactivity similar to the work reported by Morris *et al.* in 1968.[139] The optimization of the reaction was therefore done without the phosphorous group but instead with benzoic hydrazide derivatives.

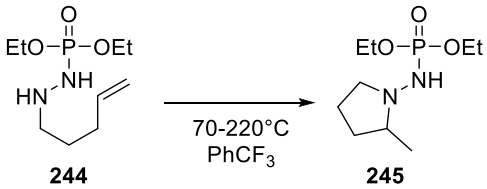

Scheme 57 - Cope-type hydroamination reported by Loiseau et al. in 2010

Finally, the latest example of the use of such phosphonohydrazone derivatives was reported by Zhang *et al.* in 2019 (Scheme 58).[140] They were able to attain 1*H*-indazole derivatives **247** using phosphonohydrazones **246** as a directing group for the copper-promoted oxidative intramolecular C-

[135] W. S. Wadsworth, W. D. Emmons, *J. Org. Chem.* **1964**, *29*, 2816–2820.
[136] R. Marek, I. St'astna-Sedlackova, J. Tousek, J. Marek, M. Potacek, *Bulletin des Societes Chimiques Belges* **1997**, *106*, 645.
[137] S. Man, J.-P. Bouillon, M. Nečas, M. Potáček, *Tetrahedron Letters* **2004**, *45*, 9419–9421.
[138] F. Loiseau, C. Clavette, M. Raymond, J.-G. Roveda, A. Burrell, A. M. Beauchemin, *Chem. Commun.* **2011**, *47*, 562–564.
[139] D. G. Morris, B. W. Smith, R. J. Wood, **n.d.**, 2.
[140] G. Zhang, Q. Fan, Y. Zhao, C. Ding, *Eur. J. Org. Chem.* **2019**, *2019*, 5801–5806.

H amination reaction. Once again, phosphonohydrazones were not employed in the final optimized reaction since phosphorus contamination was observed post-treatment.

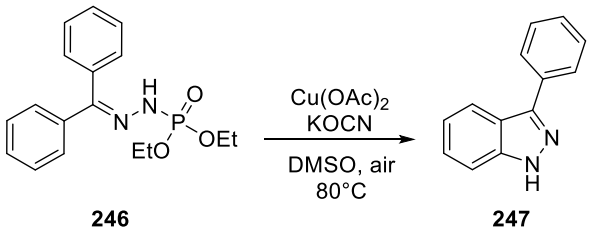

Scheme 58 - Synthesis of 1H-indazole derivatives reported by Zhang et al.

Phosphonohydrazones can be synthesized *via* the condensation of an aldehyde or ketone derivative with a phosphonohydrazine. The latter can be accessed via different starting material, as presented in the following section.

At this point, my thesis personal work will be presented.

2. Synthesis of phosphonohydrazines

Three different starting materials are used in order to access differently substituted phosphonohydrazines: dialkykphosphites, trialkylphosphites and diarylchlorophosphates. We will shortly review these three paths.

2.1. Starting from dialkylphosphites

The synthesis of phosphonohydrazines is possible starting from dialkylphosphites *via* an Atherton-Todd reaction followed by a nucleophilic substitution. This reaction was first reported in 1945 by Atherton, Openshaw and Todd as a method to convert dialkylphosphites into dialkyl chlorophosphates (Scheme 59).[141] The highly reactive dialkylchlorophosphate that is formed is too reactive to be isolated and is therefore directly engaged in a following step (with hydrazine in this case).

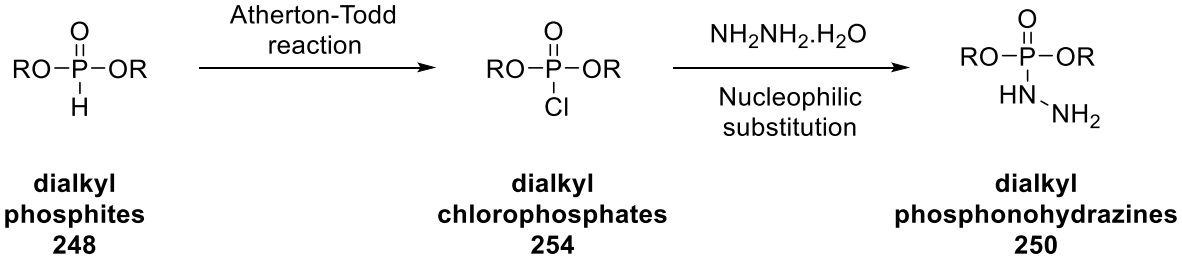

Scheme 59 - Synthesis of dialkylphosphonohydrazines starting from dialkylphosphites

Classically, the Atherton-Todd reaction requires the use of carbon tetrachloride in the presence of an amine (which can be a primary, secondary or tertiary amine) but here, we used a slightly different

[141] F. R. Atherton, H. T. Openshaw, A. R. Todd, *J. Chem. Soc.* **1945**, 660–663.

methodology. Indeed, we followed the protocol described by Jabli *et al*.[142] in which they report the use of potassium carbonate as a base in the presence of CCl_4 **252**. In our case, using potassium carbonate, we believe that the traces of water present in the base are enough to initiate the reaction through a hydrolysis step, yielding a RO-HP(=O)-OH intermediate **250** as proposed in the following reaction mechanism (Scheme 60):

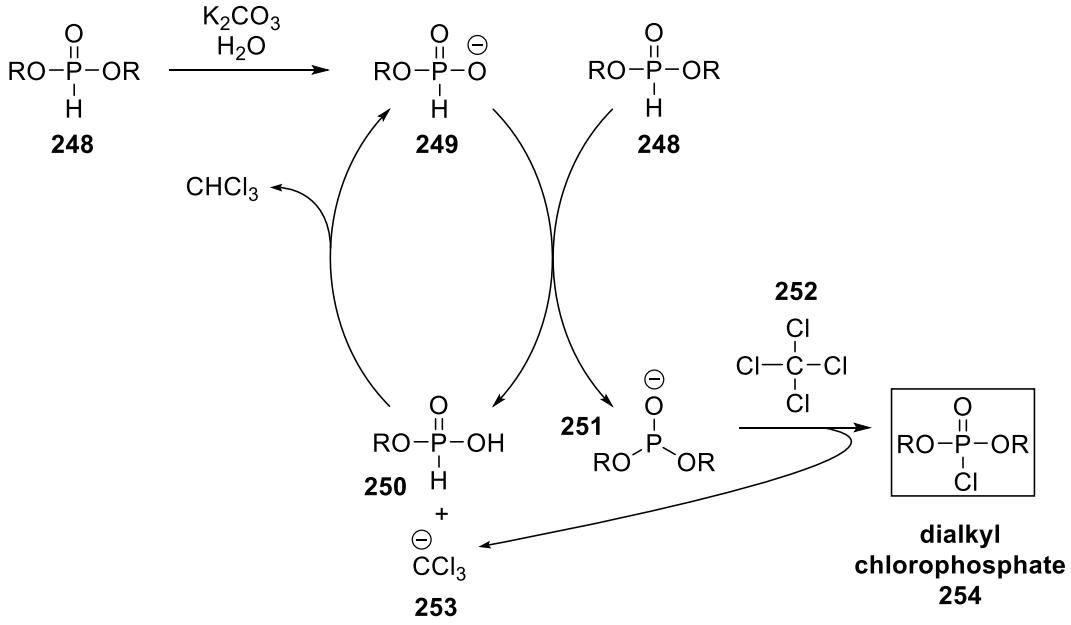

Scheme 60 - Atherton-Todd-like mechanism using potassium carbonate as a base

This RO-HP(=O)-OH intermediate **250** is then deprotonated and able to deprotonate the P-H bond of another equivalent of starting material **248**, yielding another anionic dialkyl intermediate **251**. The latter can react with carbon tetrachloride **252** in order to give the desired dialkylchlorophosphate intermediate **254** which is directly engaged in the reaction with hydrazine without any purification. A last reaction occurs with the trichloromethanide ion **253** and the monoalkyl phosphate **250** previously generated. This step completes the catalytic cycle by yielding the key anionic monoalkyl intermediate **249**. This methodology has been used for compound **212** and **262** (Table 6).

2.2. Starting from trialkylphosphite

Dialkylphosphites can also be accessed starting from trialkylphosphites (Scheme 61).[143] In the presence of water, trimethylphosphites lead to the formation of the desired dimethylphosphites which were isolated by distillation. The isolated dialkylphosphites are then engaged in an Atherton-Todd reaction. This methodology has been used for compound **263** (Table 6).

[142] D. Jabli, K. Dridi, M. L. Efrit, *Phosphorus, Sulfur, and Silicon and the Related Elements* **2016**, *191*, 759–764.
[143] R. Boobalan, C. Chen, *Advanced Synthesis & Catalysis* **2013**, *355*, 3443–3450.

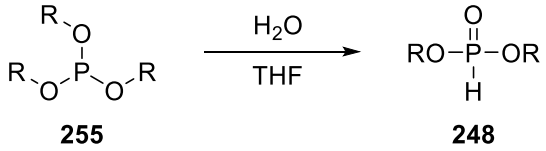

255 **248**

Scheme 61 - Synthesis of dialkylphosphite starting from trialkylphosphite

2.3. Starting from diarylchlorophosphate

Commercially available diarylchlorophosphates **256** can also be transformed into diarylphosphonohydrazines **257**. We decided first to follow a protocol reported by Steininger in 1966.[144] The protocol is straightforward and only requires mixing hydrazine monohydrate and diphenylchlorophosphate, in this case (Scheme 62). However, we faced some complications. Instead of having the nucleophilic substitution of hydrazine onto the phosphorus atom and displacement of the chlorine atom, we ended up having the solvent, ethanol, being added onto the phosphorus atom. To overcome this problem, we decided to change the solvent to THF, as reported for the synthesis of sulfonylhydrazines.[145] The reaction, in this case, is proceeding as described above for dialkylchlorophosphate, and therefore diarylphosphonohydrazines are generated. This methodology has been used for compound **264** (Table 6).

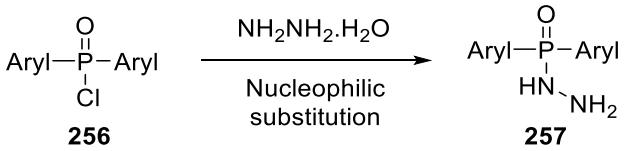

256 **257**

Scheme 62 - Synthesis of diarylphosphonohydrazines starting from diarylchlorophosphates

Using these three methodologies, we were able to synthesize the following phosphonohydrazines (Table 6):

Table 6 - Synthesis of differently substituted phosphonohydrazines

Starting material	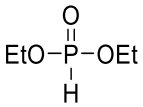	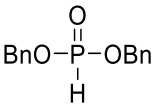	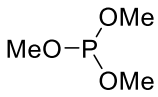	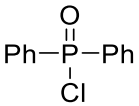
	258	**259**	**260**	**261**

[144] E. Steininger, *Monatshefte für Chemie* **1966**, *97*, 383–390.
[145] G. Chen, X. Zhang, Z. Zeng, W. Peng, Q. Liang, J. Liu, *ChemistrySelect* **2017**, *2*, 1979–1982.

Product	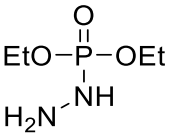 **212**, Quant.	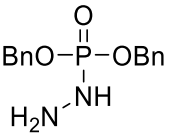 **262**, Quant.	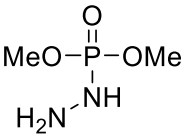 **263**, 84%	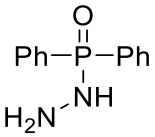 **264**, 88%

Overall, the yields were good, regardless of the employed methodology, with varying yields between 84% and quantitative.

3. Synthesis of phosphonohydrazones

3.1. Synthesis of ketones and aldehydes functionalized derivatives via Sonogashira cross-coupling reaction

We used the same strategy as reported in chapter I in order to access Sonogashira cross-coupling products. We decided to choose 2-(phenylethynyl)benzaldehyde as our model substrate and investigate the reactivity of electron-withdrawing groups as well as electron-donating groups, either on the principal aromatic core or on the alkyne. Moreover, we wanted to probe the compatibility of our methodology with aromatic alkynes and aliphatic ones along with ketones derived from acetophenone and benzophenone. Moreover, we wanted to probe the compatibility of our methodology with aromatic-substituted alkynes and aliphatic-substituted ones (R^2 group, Table 7) along with ketones derived from acetophenone or benzophenone (R^3 group, Table 7). Here is the list of all the Sonogashira cross-coupling products:

Table 7 - Sonogashira cross-coupling products

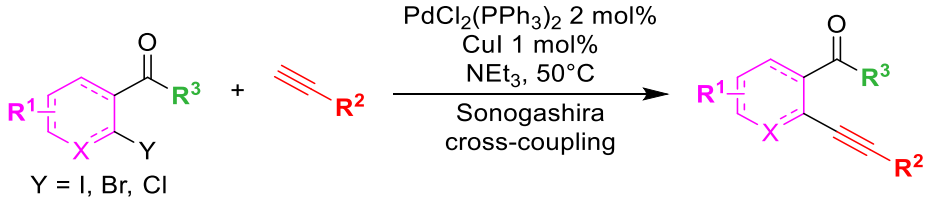

Model substrate

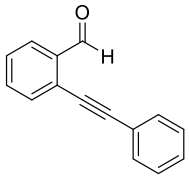

70, 98%

Main ring modifications

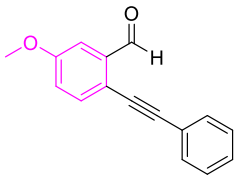

73, quant.

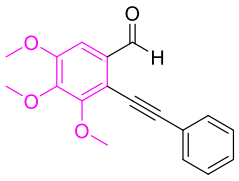

74, quant.

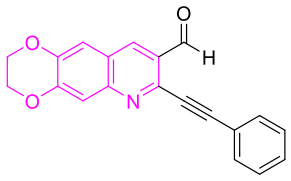

265, 53%

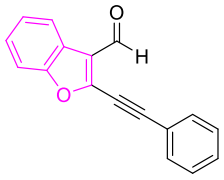

266, 51%

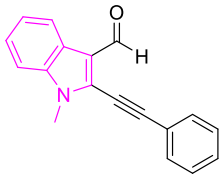

267, 95%

Alkynyl modifications

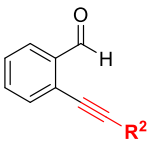

76, R^2 = 4-methoxyphenyl, 88%
268, R^2 = 3,4,5-trimethoxyphenyl, 60%
269, R^2 = 4-tolyl, 81%
270, R^2 = 4-fluorophenyl, 90%
271, R^2 = 4-cyanophenyl, quant.
272, R^2 = 2-bromophenyl, 77%
80, R^2 = 2-thiophenyl, 69%
84, R^2 = TMS, 78%
81, R^2 = 1-cyclohexenyl, 99%
273, R^2 = cyclopropyl, 67% (done by GM)
82, R^2 = *n*-hexyl, 69%
83, R^2 = $C(CH_3)_2OH$, 89%

Main ring and alkynyl modifications

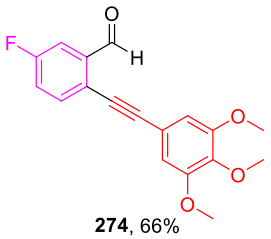

274, 66%

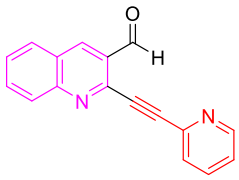

275, 78%

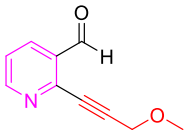

276, 80%
(done by GM)

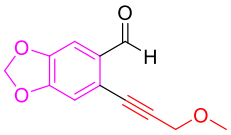

277, 85%
(done by GM)

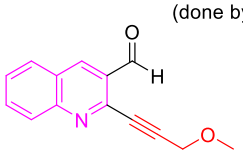

278, quant.

Ketone substrates

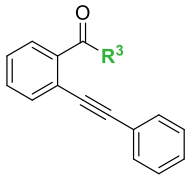

279, R^3 = methyl, 38%
280, R^3 = phenyl, 38%

The model substrate **70** of this methodology was obtained in a high 98% yield. When considering modifications on the main ring, high yields were observed globally (above 85%) except for the benzofuran **266** and quinoline **265** derivatives which were obtained in 51% and 53% yield, respectively. This may be due to the fact that the cross-coupling was performed using chlorinated starting material instead of brominated/iodinated starting material as for the other molecules of this table, without changing the reaction conditions. It may also be possible that a deleterious coordination effect with the catalyst occurs with the oxygen or nitrogen atom of these two molecules.

With the modified alkynes, again, the yields were good.

The Sonogashira cross-coupling products bearing a modified main ring and a modified alkynyl substituent were formed in good yields: 66% for the fluorophenyl ring **274** and 78%-quant for the quinoline one (**275**, **278**). The two other substrates (**276** and **277**) were from the lab collection and synthesized by Dr. Gaëlle Mariaule (GM) during her PhD.

To finish, ketone derivatives led to poor Sonogashira cross-coupling product yields of 38% in both cases with acetophenone **279** or benzophenone **280** derivatives. Anew, steric hindrance may be to blame for the yield drop, preventing the palladium catalyst from getting close to the reactive site. Moreover, an electronegativity difference between a ketone and an aldehyde function in the *ortho*-position of the halogen could also be the source of the yield difference.

3.2. Synthesis of benzaldehyde functionalized derivatives via Heck cross-coupling reaction

A benzaldehyde derivatives bearing an alkenyl group instead of an alkynyl group was synthesized using the Heck cross-coupling reaction. We synthesized a molecule **281** using ligand-free conditions[146] which led to a high 88% yield (Table 8).

[146] S. K. Pawar, C.-D. Wang, S. Bhunia, A. M. Jadhav, R.-S. Liu, *Angew. Chem. Int. Ed.* **2013**, *52*, 7559–7563.

Table 8 - Heck cross-coupling products

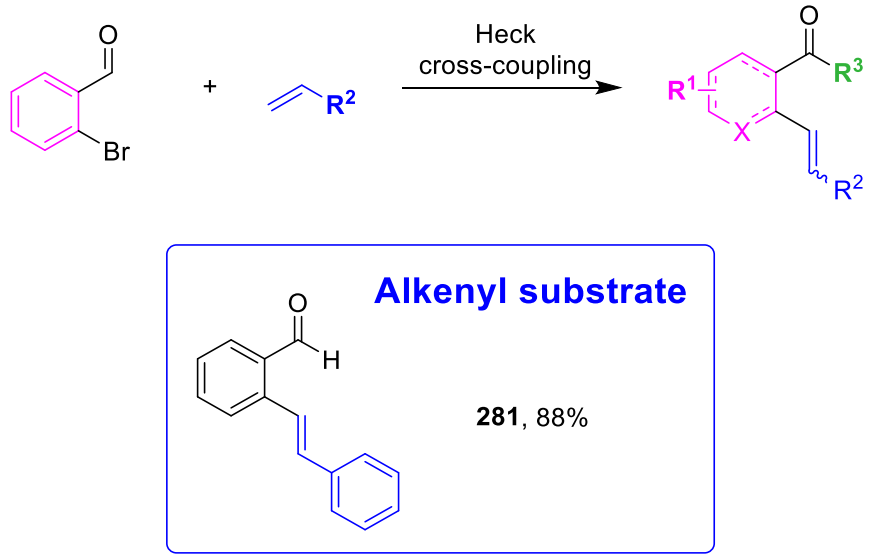

3.3. Reaction of phosphonohydrazine derivatives with arylketone and arylaldehyde derivatives

When both the phosphonohydrazines and the arylaldehyde/arylketone derivatives were synthesized, the formation of phosphonohydrazones has been undertaken. Their synthesis with arylaldehyde derivatives only requires mixing with the phosphonohydrazones in methanol, at room temperature. Then, in most cases, a precipitation occurs within a few minutes, and the phosphonohydrazone is finally isolated upon filtration. When a precipitation does not occur, a chromatography on silica gel becomes necessary.

On another side, arylketone derivatives are less electrophilic than their arylaldehyde counterparts and therefore heating at 60°C is required to form the desired phosphonohydrazones. Here is the list of all the phosphonohydrazone products (Table 9):

Table 9 - Phosphonohydrazones starting material

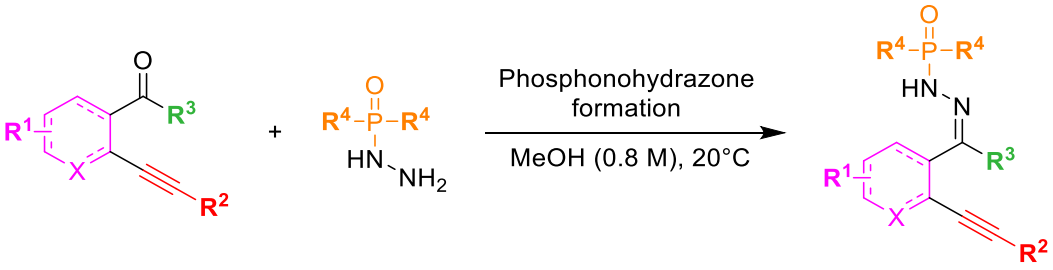

Model substrate

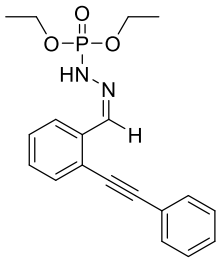

282, 70%

Main ring modifications

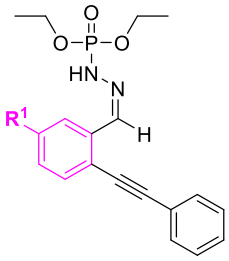

283, R^1 = methoxy, 55%
284, R^1 = chlorine, 84%
285, R^1 = bromine, 88%

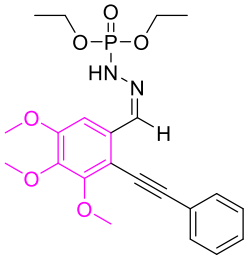

286, 89%

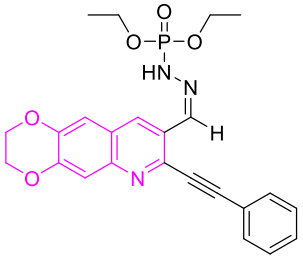

287, 34%

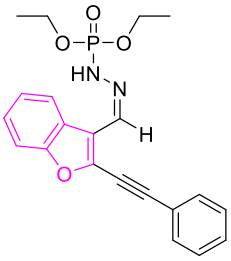

288, 49%

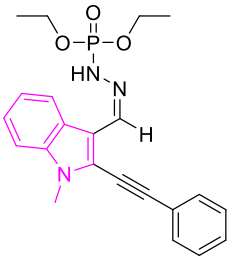

289, 38%

Alkynyl modifications

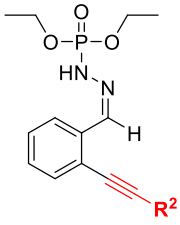

290, R^2 = 4-methoxyphenyl, 73%
291, R^2 = 3,4,5-trimethoxyphenyl, 83%
292, R^2 = 4-tolyl, 51%
293, R^2 = 4-fluorophenyl, 57%
294, R^2 = 4-cyanophenyl, 66%
295, R^2 = 2-bromophenyl, 73%
296, R^2 = 2-thiophenyl, 44%
297, R^2 = TMS, 96%
298, R^2 = 1-cyclohexenyl,69%
299, R^2 = cyclopropyl, 83%
300, R^2 = *n*-hexyl, 61%

Main ring and alkynyl modifications

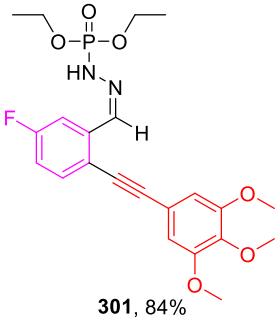

301, 84%

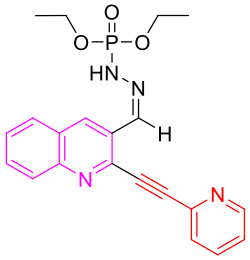

302, 72%

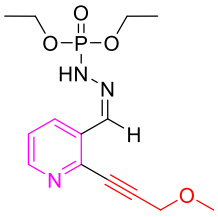

303, 75%

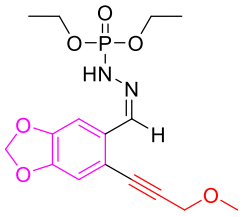

304, 83%

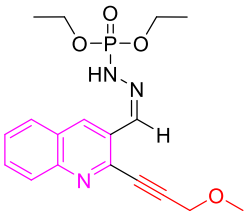

305, 69%

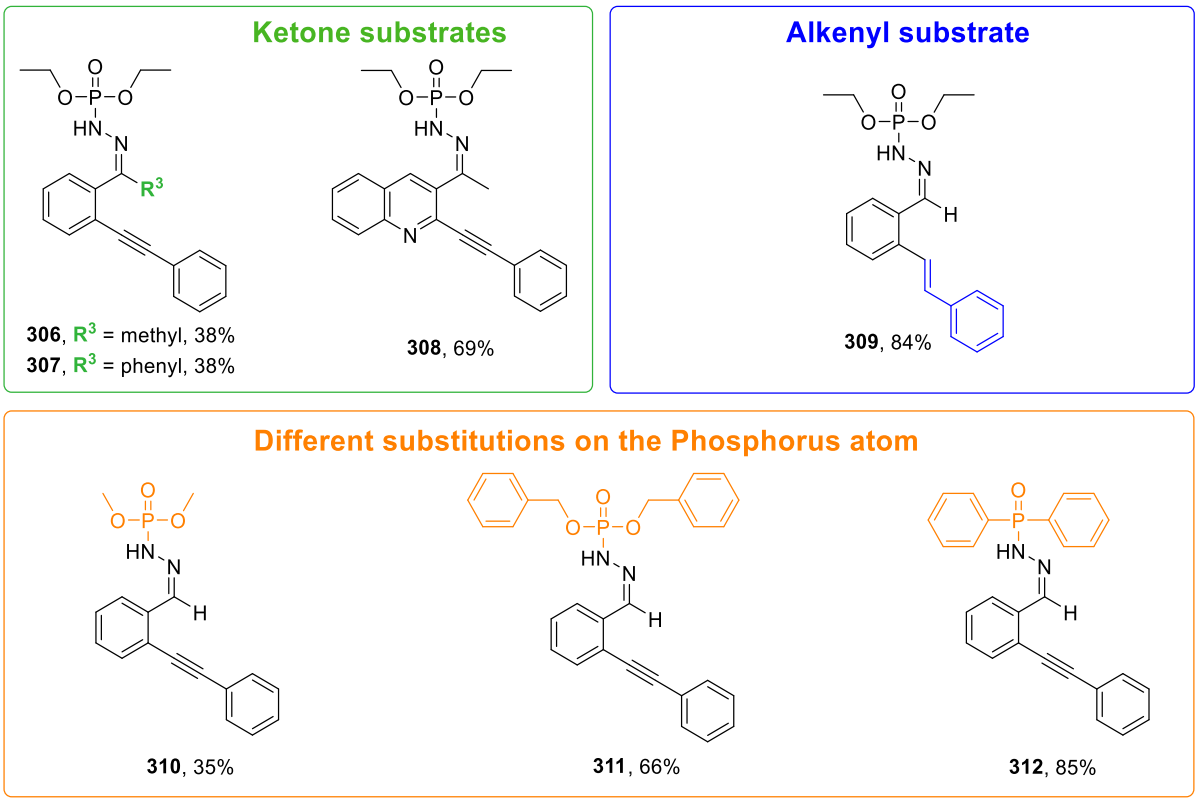

EDG on the main ring, such as with one methoxy **283** or three methoxy groups **286** led to the formation of the corresponding phosphonohydrazones in medium to good yield with 55% and 89% yield respectively. Good yields were also obtained with halogen substituted phosphonohydrazones with a chlorine **284** or a bromine **285** (84% and 88%). Heterocycles, on the other hand, led to poorer yields. Indeed, the presence of a quinoline core **287**, a benzofuran core **288** or a N-methylindole core **289** led to medium or moderate yields of 34%, 49% and 38%, respectively.

Overall, all substitutions on the alkynyl unit were well tolerated, with EDG such as 4-methoxyphenyl **290**, 3,4,5-trimethoxyphenyl **291** and 4-tolyl **292** giving good yields of 73%, 83% and 51%, respectively. EWG also led to good yields of 57% for the 4-fluorophenyl **293**, 66% for the 4-cyanophenyl **294** and 73% with the 2-bromophenyl substitution **295**. A thiophenol was also tolerated, although giving the lowest yield of 44% (**296**). Moreover, a TMS group gave an almost quantitative yield of 96% (**297**) and aliphatic alkynes gave also good yields of 69% for the 1-cyclohexenyl substitution **298**, 83% for the cyclopropyl **299** and 61% for the *n*-hexyl chain **300**.

Substrates bearing modifications both on the main ring and the alkynyl part all gave good yields, regardless of the presence of a heteroatom on the main ring or the nature of the alkynyl part, thus the presence of a pyridine or a quinoline core was well tolerated.

It is not surprising to note that phosphonohydrazones formed with an arylketone as a starting material led to lower yields compared to their arylaldehyde counterparts, because of their lower

electrophilicity. Moreover, heating was required for their formation. A phosphonohydrazone formed from an acetophenone **306** or from a benzophenone derivative **307** was obtained in both cases in a moderate 38% yield. Moreover, an acetylquinoline derivative led to the formation of the corresponding phosphonohydrazone **308** in a good 69% yield.

An alkene-containing derivative **309** was obtained in a good 84% yield.

Finally, the formation of phosphonohydrazones bearing differently substituted phosphorus atoms resulted in good yields of 66% and 85% for the -OBn (**311**) and -Ph (**312**) substitutions, respectively. On the contrary, a -OMe substitution (**310**) led to a low 35% yield.

A single crystal of the model starting material allowed us to confirm its structure after X-Ray diffraction (Figure 23, see experimental part).

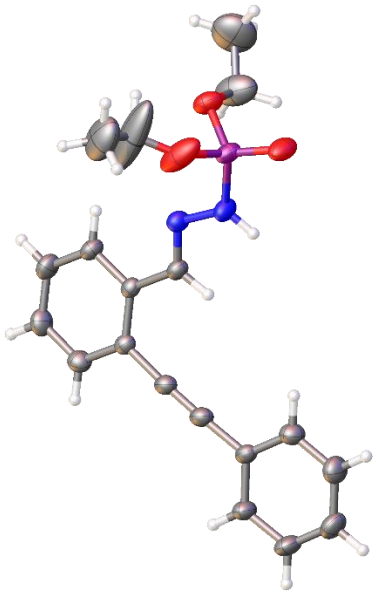

Figure 23 - Crystal structure of the model starting material

4. Use of phosphonohydrazones as a novel family of NCR precursor

4.1. Expectations: hydroamination product

With these new molecules in hand, we started our investigations towards NCR generation *via* visible-light catalysis by discovering and optimizing a new family of pre-activated NCR precursors. The first problematic was the fact that there was no previous report on this family of molecules in the field of photoredox catalysis. Moreover, if the nitrogen-centered radical could be generated, we could expect several reactivities, the radical could stay on the nitrogen atom or delocalize on the oxygen linked to the phosphorus atom. To finish, if the radical could be generated, we would have to verify if it could be engaged in a radical reaction with an insaturation, such as an alkyne.

We also thought that, after generating the NCR on our phosphonohydrazones, we would finally get a 1,2-dihydrophthalazine still carrying the phosphorus moiety **313**. Thus, we first started our investigation by employing the conditions previously reported in our group to generate a NCR on sulfonohydrazones: $Ru(bpy)_3Cl_2.6H_2O$ (2.5 mol%) with 1.5 equiv. of NaOH in EtOH.[111] We were pleased to obtain a product **314** (28%) under these conditions (Scheme 63).

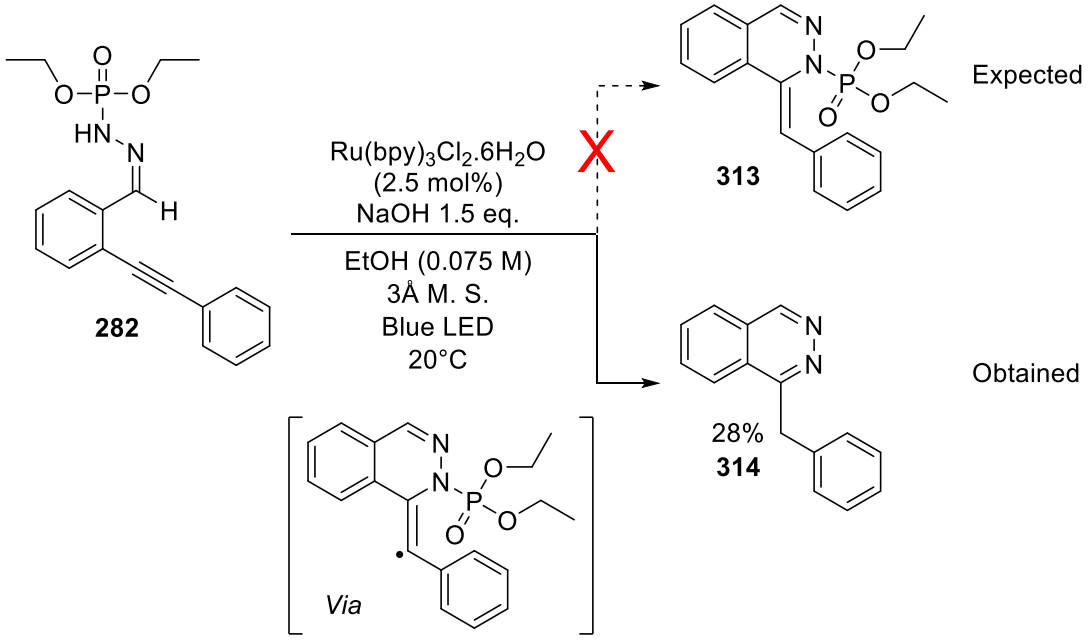

Scheme 63 - Expected and obtained product after visible-light catalyzed reaction

Surprisingly, the isolated major product of this reaction did not bear any phosphorus atom, contrary to what was expected. Its absence was confirmed with the ^{1}H, ^{31}P NMR spectra and HR-MS analysis.

4.2. Reality: an interesting reactivity

The structure was confirmed by NMR studies which clearly indicate the presence of a CH_2 group. The reaction led to the formation of a 1-benzylphthalazine, and it appeared that the phosphorus moiety was cleaved in the process and result as a by-product in the reaction medium.

As a matter of facts, the phosphorus moiety that was originally designed with the sole purpose of being a pre-activated NCR precursor, turned out to also be a self-immolative moiety, thus enhancing its attractiveness and preventing a tedious additional step to cleave the N-P bond. It is also important to point out that the reaction reported by Xu's team[131] (presented earlier in the manuscript) requires an extra hydrolysis step followed by an extraction in order to cleave the N-P bond.

Then, further investigations were conducted in order to probe the versatility of this new reaction, understand its mechanism and explore its functional compatibility.

C) Application in visible-light catalyzed reactions as a NCR precursor

1. Methodology

As seen above, we were pleased to achieve with these conditions a 28% yield for the desired phthalazine product **314** (entry 1, Table 10). Then we changed the other parameters, starting with the nature of the photocatalyst.

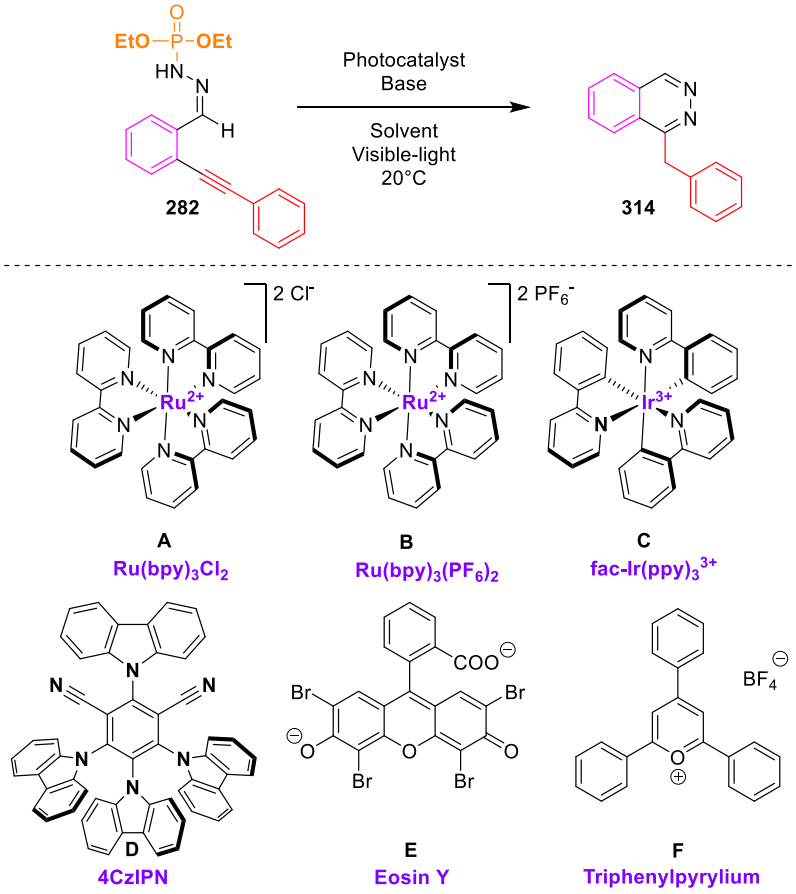

Table 10 - Optimization of the reaction conditions

Entry	Catalyst	Base (3 equiv)	Solvent (M)	Yield[a]
1	**A** (2,5 mol%)	NaOH[b]	EtOH (0.075 M)	28%
2	**B (2,5 mol%)**	NaOH	EtOH (0.075 M)	43%
3	**C** (2,5 mol%)	NaOH	EtOH (0.075 M)	35%
4	**D** (5 mol%)	NaOH	EtOH (0.075 M)	24%
5	**E** (5 mol%)	NaOH	EtOH (0.075 M)	21%
6	**F** (5 mol%)	NaOH	EtOH (0.075 M)	0%
7	B (2,5 mol%)	Triton B	EtOH (0.075 M)	23%
8	B (2,5 mol%)	KOH	EtOH (0.075 M)	41%
9	B (2,5 mol%)	K_2CO_3	EtOH (0.075 M)	0%
10	B (2,5 mol%)	K_3PO_4	EtOH (0.075 M)	0%
11	B (2,5 mol%)	**tBuONa**	EtOH (0.075 M)	51%
12	B (2,5 mol%)	tBuONa	MeOH (0.075 M)	38%
13	B (2,5 mol%)	tBuONa	EtOH (0.0375 M)	0%
14	B (2,5 mol%)	tBuONa	EtOH (0.300 M)	52%
15	B (2,5 mol%)	tBuONa	PEG300 (0.300 M)	49%
16	B (2,5 mol%)	tBuONa	1,3-butanediol (0.300 M)	50%
17	B (2,5 mol%)	tBuONa	2-methoxyethanol (0.300 M)	34%
18	**B (2,5 mol%)**	**tBuONa**	**MeOH (0.300 M)**	**58%**[c]
19	B (2,5 mol%)	tBuONa	MeOH (0.300 M)	0%[d]
20	B (2,5 mol%)	-	MeOH (0.300 M)	0%[e]

[a)] Isolated yields. [b)] 1.5 eq. of NaOH. [c)] Standard condition: reactions were performed with **1a** (0.30 mmol), Ru photocatalyst (2.5 mol %), and base (3 equiv,) in 1 mL of solvent and was irradiated with 3W blue LED for 16 h at 20°C. [d)] Reaction performed without light. [e)] Reaction performed without base.

The structure of the desired compound **314** was finally confirmed with XRD analysis after we successfully crystallized it as its hydrochloride salt. (Figure 24)

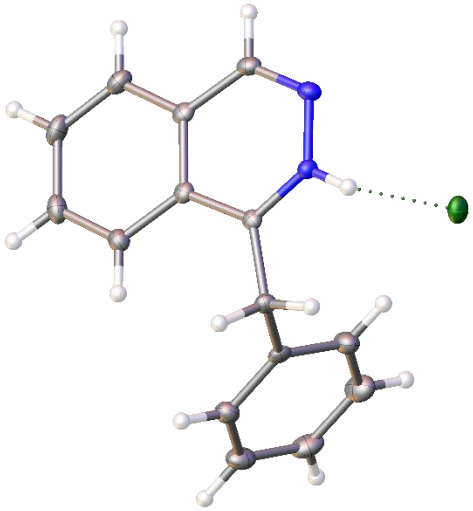

Figure 24 - Crystal structure of the hydrochloride salt of the desired product

1.1. Photocatalysts

To increase the isolated yield of the phthalazine, we first decided to change the nature of the photocatalyst by using Ir/Ru based organometallic complexes as well as organic molecules (Table 10). $Ru(bpy)_3(PF_6)_2$ (entry 2), $Ir(ppy)_3$ (entry 3), 4-CzIPN (entry 4), eosin Y (entry 5) and triphenylpyrylium (entry 6) were tested and gave respectively yields of 43%, 35%, 24%, 21% and 0%. It is surprising to note that photocatalyst **C** with the lowest oxidation potential among the ones tested was able to yield 35% of the desired compound whereas the most oxidizing one (**F**) gave absolutely no conversion. $Ru(bpy)_3(PF_6)_2$ was hence the best photocatalyst for this specific reaction and was selected to pursue the optimization with different bases.

1.2. Bases

In order to have an insight of the pKa of our starting materials, we ran a pKa prediction of our model phosphonohydrazone and we found a pKa value of 9.98 for the deprotonation of the N-H bond. Different types of bases were studied for the optimization of the reaction conditions. Hydroxide (entry 7 and 8, Table 10), carbonate (entry 9), phosphate (entry 10) and alkoxide (entry 11) bases gave disproportionate results and only hydroxide and alkoxide bases stood out. Indeed, no desired product was obtained with potassium carbonate (entry 9) and tripotassium phosphate (entry 10). This is not surprising for the first one because its pKa is around 10, like the pKa of the targeted N-H bond. For the second one, surprisingly, despite a pKa value of 12 no reaction occurred. The problem may come from a poor solubility in methanol.[147] Potassium hydroxide gave similar result as with sodium hydroxide with a 41% yield (entry 8), both bases having pKa close to 14. Finally, sodium *tert*-butoxide gave the best result with a 51% yield (entry 11) with a pKa value around 17. Other organic bases were tested as well such as pyridine but gave no results.

1.3. Solvents

To finish with the optimization step, different solvents were tested, at various concentrations. Indeed, decreasing the concentration from 0.075 M to 0.0375 M led to an impressive yield drop from 51% to 0% (entries 11 and 13, Table 10). On the contrary, increasing greatly the concentration to 0.3 M did not affect the reaction as much with a similar yield of 52% (entry 14). We also probed several hydroxyl containing solvents such as PEG300 (entry 15), 1,3-butanediol (entry 16) or 2-methoxyethanol (entry 17) but the results were similar or worse. In the end, MeOH with a concentration of 0.3 M led to the best yield for this optimization, giving 58% of the desired product (entry 18), although it was only at 38% with a concentration of 0.075 M (entry 12).

---

[147] PubChem, "Potassium phosphate," can be found under https://pubchem.ncbi.nlm.nih.gov/compound/62657, **n.d.**

Control experiments were made without light (entry 19) or without base (entry 20), hinting the fact that the reaction should be catalyzed by visible light solely.

After this extensive search for the best reaction parameter, we selected as the best condition the entry 18, using phosphonohydrazone (0.3 mmol), $Ru(bpy)_3(PF_6)_2$ (2.5 mol %, 7.5 µmol), *t*BuONa (3 eq.) in MeOH (0.3 M) and irradiated with 3W blue LED for 16 h.

2. Scope

2.1. Functional group compatibility

In Table 11 is displayed the scope for all the molecules that were obtained *via* our methodology from various starting materials:

Table 11 - Final phthalazine products: scope

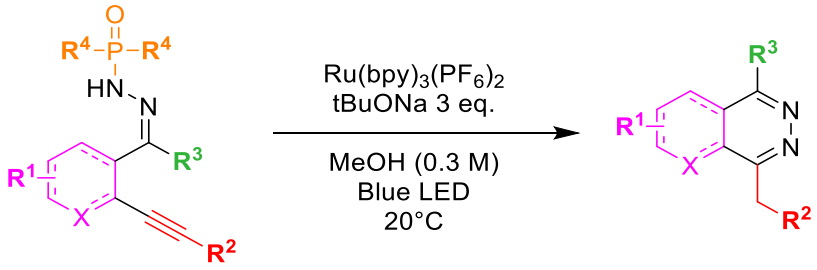

Model product

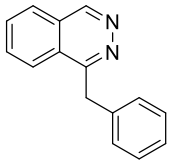

314, 58%
(15% using **312** as SM)

SM with main ring modifications

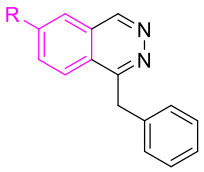

315, R = methoxy, 77%
316, R = chlorine, 51%
317, R = bromine, 41%

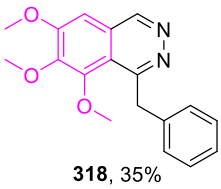

318, 35%

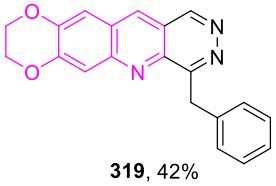

319, 42%

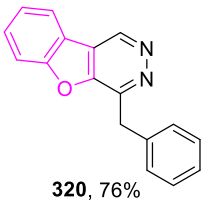

320, 76%

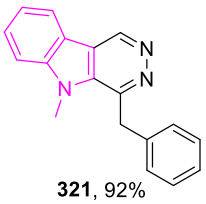

321, 92%

SM with alkynyl modifications

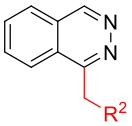

322, R^2 = 4-methoxyphenyl, 62%
323, R^2 = 3,4,5-trimethoxyphenyl, 70%
324, R^2 = 4-tolyl, 47%
325, R^2 = 4-fluorophenyl, 65%
326, R^2 = 4-cyanophenyl, 44%
327, R^2 = 2-bromophenyl, 49%
328, R^2 = 2-thiophenyl, 23%
329, R^2 = H, 70% (from TMS SM)
330, R^2 = 1-cyclohexenyl, 26%

SM with main ring and alkynyl modifications

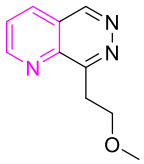

331, 95%

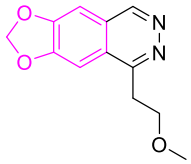

332, 72%

SM with a ketone

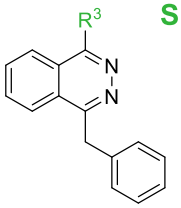

333, R^3 = methyl, 17%
334, R^3 = phenyl, 34%

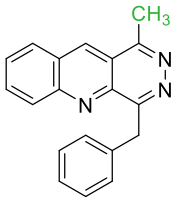

335, 50%

To begin, an EDG (OMe) on the *para* position of the alkyne led to 1-benzyl-6-methoxyphthalazine **315** with a high 77% yield. On the contrary, having additional methoxy substitutions led to a yield drop to 35% (**318**), the excess in electron density on the aromatic core seems to be detrimental. Moreover, there is a slight steric hindrance due to the methoxy group close to the alkynyl group on the starting material. Halogen derivatives were also well tolerated and remained after the reaction's completion, leading to further possible substitutions on the scaffold. Indeed, a chlorine and a bromine led to the

corresponding phthalazine in medium 51% (**316**) and 41% (**317**) yield, respectively. Moreover, a starting material bearing a quinoline with an ethylenedioxy substitution (**319**) led to a medium 42% yield, confirming the compatibility of the reaction with heterocycles on the main ring. Substitutions on the main ring such as a benzofuran or an indole derivative led to high product yields of 76% (**320**) and 92% (**321**) respectively.

Final products bearing a 4-methoxyphenyl group (**322**) or 3,4,5-trimethoxyphenyl EDG group (**323**) gave a similar yield as the final product bearing a 4-fluorophenyl EWG (**325**) (62%/70% vs 65% respectively). On the other hand, a strong EWG such as 4-cyanophenyl led to a decrease in the yield (44%, **326**) and a 4-tolyl substitution led to a medium 47% yield (**324**). An alkenyl substituent such as a 1-cyclohexenyl gave a modest 26% yield (**330**) probably because of the less stabilizing nature of an alkene *vs.* an aromatic ring. Our reaction conditions were also compatible with heterocycles such as thiophene with a modest 23% yield (**328**) and also substitution on the *ortho*-position on the aromatic ring (-Br with 49% yield, **327**) which could be further functionalized with classical cross-coupling reactions. Using a starting material bearing a trimethylsilylacetylene group led to 1-methylphthalazine (**329**) with the TMS being cleaved in the process, which is not surprising since the reaction conditions (basic methanolic solution) are the one usually used for TMS cleavage.

The products formed from SMs bearing a modified main ring and a modified alkynyl group showed the compatibility of the reaction with aliphatic ether chains as well as the presence of a pyridine (**331**) or a methylenedioxyphenyl (**332**) with high yields of 95% and 72%, respectively.

Finally, starting materials derived from arylketones instead of arylaldehydes could also be converted using our reported conditions, although in modest yields unfortunately. A methyl substitution and a phenyl substitution led to 17% (**333**) and 34% (**334**) product yield respectively. Furthermore, a phosphonohydrazone containing a quinoline ring bearing a methylketone could be transformed into quinolinopyridazine (**335**) with a 50% yield.

These results were published in a special issue about radical chemistry of Advanced Synthesis and Catalysis[148] and the article "Phosphoramidates as Transient Precursors of Nitrogen-Centered Radical Under Visible-Light Irradiation: Application to the Synthesis of Phthalazine Derivatives" has been selected by the editorial team as a Very Important Publication, highlighted on the cover picture of the issue (Figure 25).[149]

[148] M. De Abreu, M. Selkti, P. Belmont, E. Brachet, *Advanced Synthesis & Catalysis* **2020**, *362*, 2216–2222.
[149] M. De Abreu, M. Selkti, P. Belmont, E. Brachet, *Adv. Synth. Catal.* **2020**, DOI 10.1002/adsc.202000382.

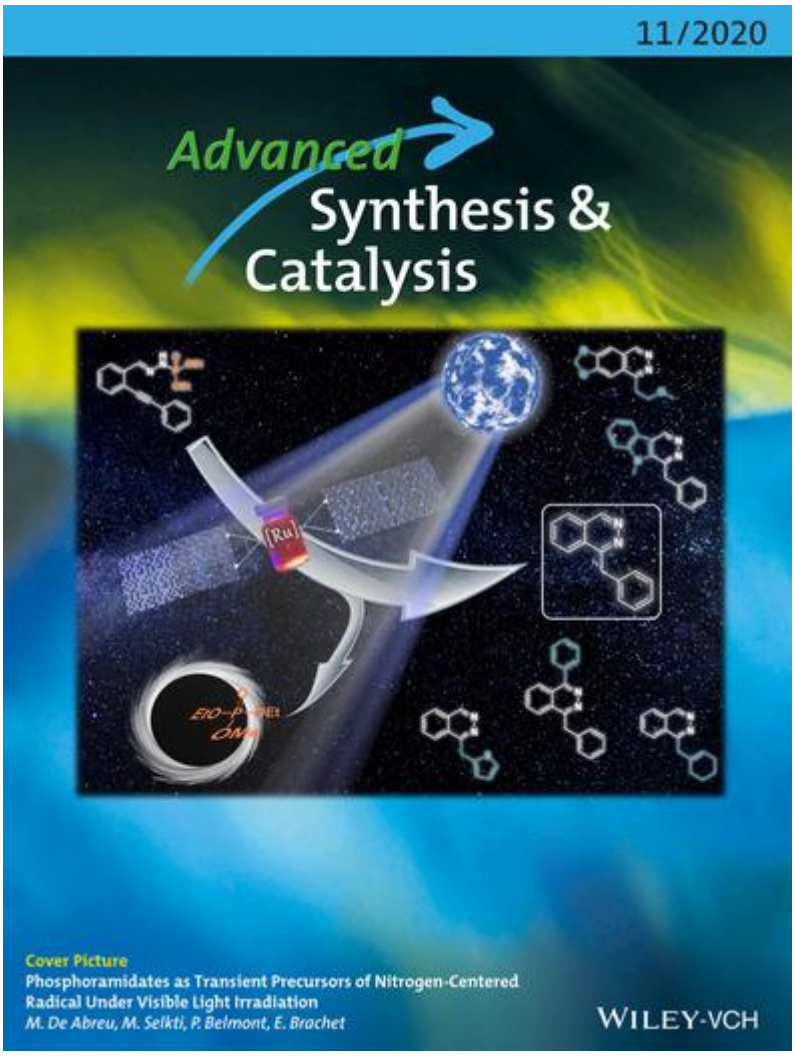

Figure 25 - Cover picture of the special issue on radical chemistry

Some starting materials (Table 12) bearing diverse aliphatic chains such as a cyclopropane (**299**) or a hexyl chain (**300**) did not lead to the phthalazine formation. A quinoline ring bearing a pyridine ring on the alkynyl part (**302**) or an ether alkyl chain (**305**) did not allow either the formation of the desired product, maybe because of a possible chelation of the Ru metal center with a ligand exchange.

Table 12 - Phosphonohydrazones that did not lead to the desired phthalazine

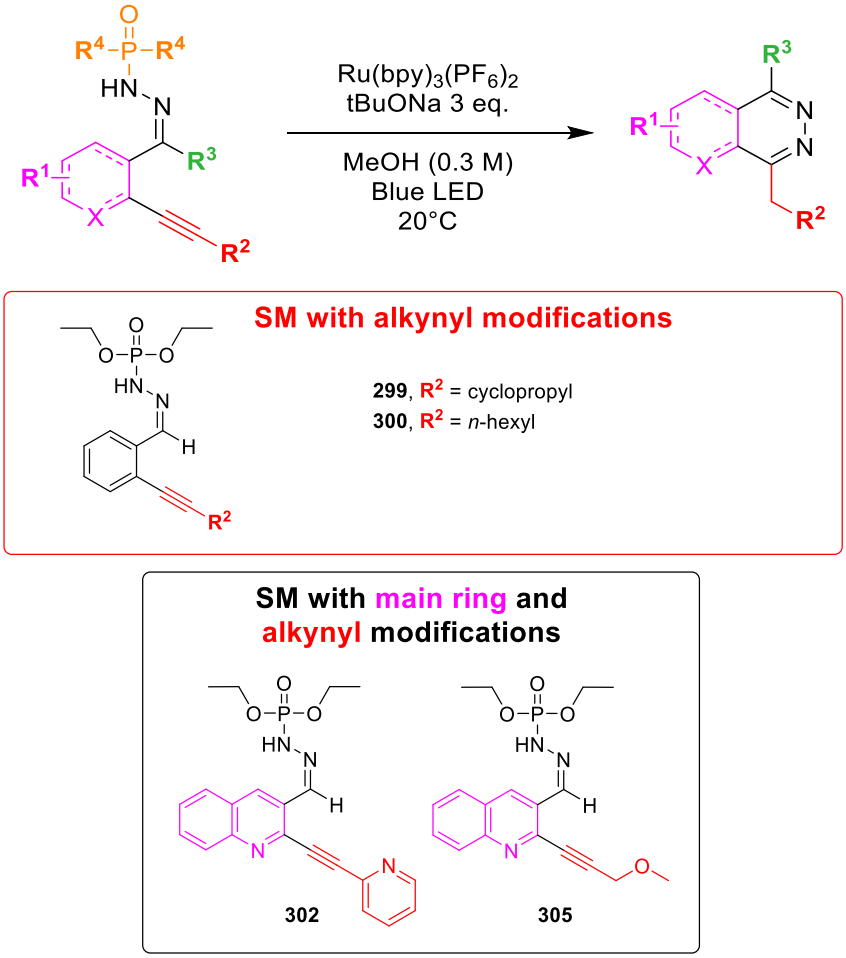

We also synthesized substrate molecules bearing diverse modifications, in which the alkynyl part is replaced either by a nitrile (**336**) or a phenol group (**337**) and they were obtained with high 81% and 68% yield, respectively (Table 13). These substitutions were made in order to probe the reactivity of substrates bearing groups other than alkynes.

Table 13 - Phosphonohydrazones starting material bearing diver modifications

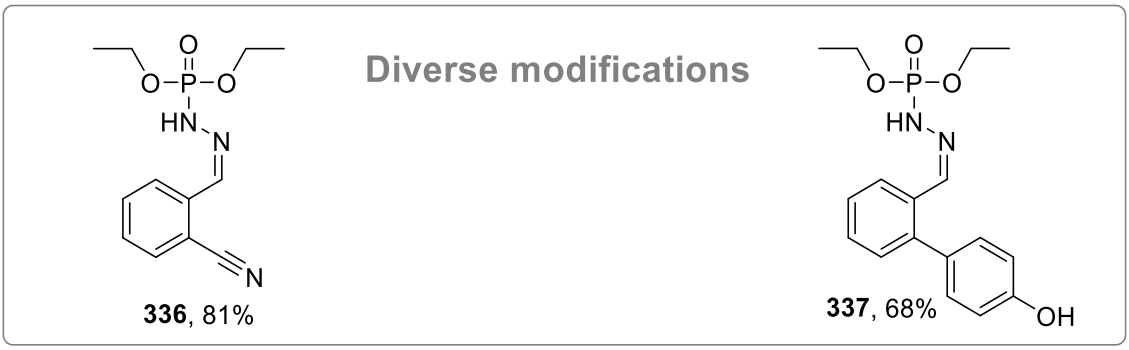

Indeed, we assumed that, when using the phenol-containing starting material **337**, we could obtain a spiro compound, as presented in the following schemes. It is unsure whether the phosphorus moiety

would be kept or not at the end of the reaction but in the end this starting material did not lead to any product. We know that the formation of spiro compounds is possible under visible-light catalysis with for instance the early report of the Reiser group[150] back in 2013. Moreover, such spiro compounds can also be formed from the intramolecular reaction of a phenol and a secondary radical as reported in 2015 by Gao *et al.*[151] in which N-(4-hydroxyphenyl)-N-methylcinnamamide and its derivatives can yield spiro compounds under visible-light catalysis (Scheme 64). Indeed, in this report, a trifluoromethyl radical is generated *in situ* and reacts with the double bond of the cinnamamide derivative, giving another radical intermediate that reacts intramolecularly with the phenol group in order to yield the final spiro-quinone compound.

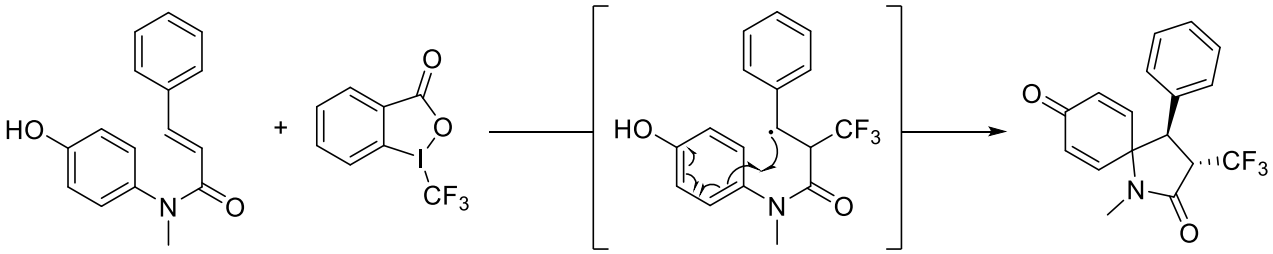

Scheme 64 - Synthesis of 1-Azaspiro[4.5]decanes reported by Gao et al. in 2015

In our case, with the *N*-centered radical generated in our reaction conditions, we propose that it could react with the phenol on the *para* position to yield a spiro-quinone derivative (Scheme 65). Unfortunately, no targeted product was obtained under our reaction conditions as no conversion was observed.

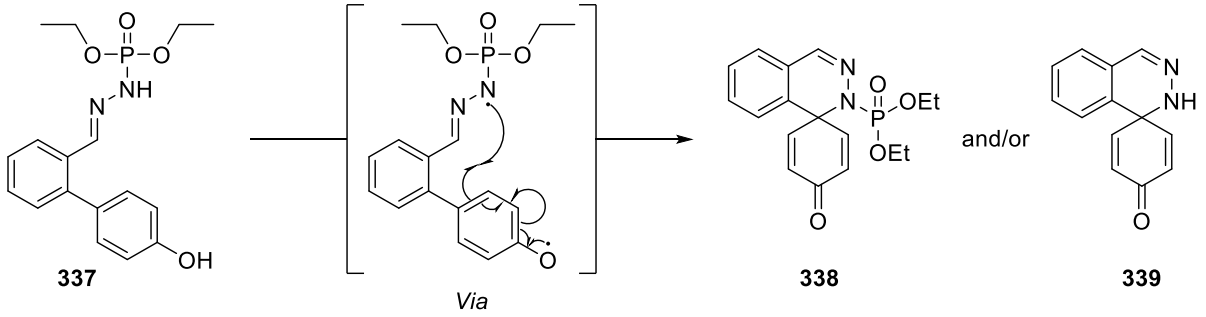

Scheme 65 - Expected products when using a phenol-containing starting material

On the other hand, we synthesized a starting material bearing a nitrile group instead of the alkynyl part **336** (Scheme 66). We wanted to investigate the reactivity of this nitrile group with a nitrogen-centered radical and see if a 6-*exo*-*dig* cyclization could occur, yielding an extracyclic imine **340** or carbonyl if the former is hydrolyzed. Furthermore, we did not exclude a possible 1,3-migration of the phosphorus moiety onto the nitrogen or oxygen atom in its close vicinity *via* a concerted mechanism,

[150] G. Kachkovskyi, C. Faderl, O. Reiser, *Adv. Synth. Catal.* **2013**, *355*, 2240–2248.
[151] F. Gao, C. Yang, G.-L. Gao, L. Zheng, W. Xia, *Org. Lett.* **2015**, *17*, 3478–3481.

yielding **341**, as well as a possible cleavage of the N-P bond, like in the previously presented methodology.

^{1}H NMR studies confirmed the presence of two ethoxy chains as well as 5 aromatic protons and the presence of a mobile proton above 12 ppm. These informations were confirmed in ^{13}C NMR experiments as well as the presence of a unique phosphorus atom in ^{31}P NMR. To finish, mass spectrometry indicated that 3 nitrogen were present. All these data are helping us to propose the structure of two products (Scheme 66):

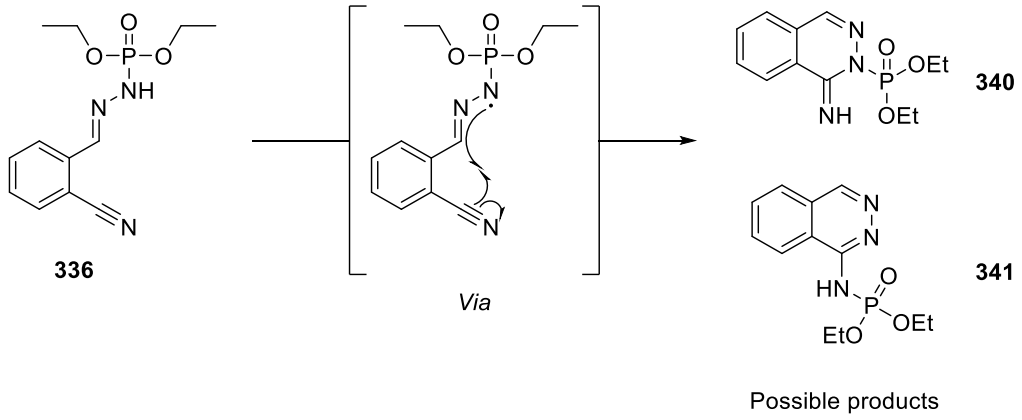

Scheme 66 - Expected products when using a nitrile-containing starting material

2.2. Phosphorus substitution variation

With these results in hand, we wanted to explore the influence of the substituents on the phosphorus atom for the generation of NCRs and phthalazine products. We synthesized 3 additional starting materials, bearing -OMe, -OBn, or -Ph substituents on the phosphorus atom. The results are presented in Table 14:

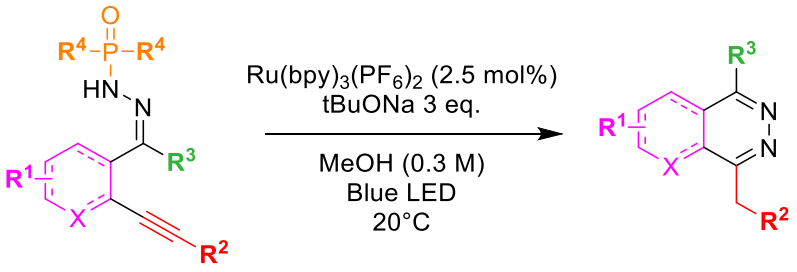

Table 14 - Influence of the substituents on the phosphorus atom

Starting materials	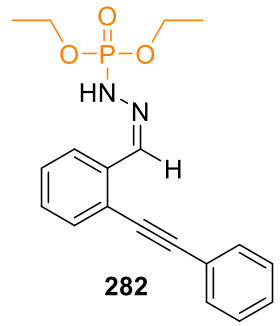 **282**	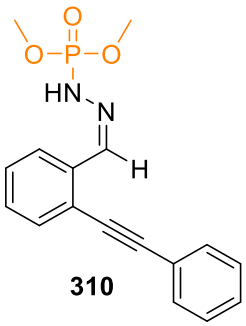 **310**	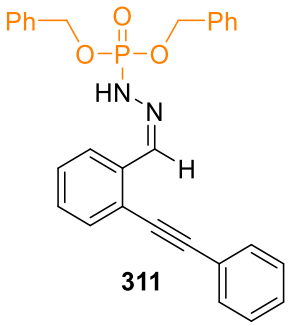 **311**	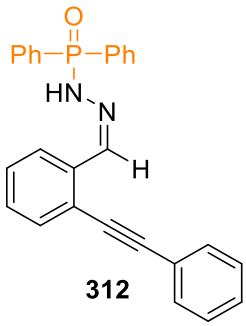 **312**
Yield of phthalazine	58%	52%	43%	15%

We were pleased to observe that none of them exhibited a better reactivity than the -OEt derivative (58%) and that's why we kept it for the entire scope. The -OMe substitution exhibited a similar reactivity but with a slightly lower 52% yield. It is important to note that the yield drop is more important when using -OBn substitutions on the phosphorus atom (43%). This drop could be the result of a greater hindrance around the phosphorus as well as the nitrogen-centered radical due to the benzyl groups. Finally, our reaction is less efficient with phenyl groups directly present on the phosphorus atom (15% yield). This could be explained by the direct vicinity of the bulky phenyl with the nitrogen on which the radical is generated. Moreover, we ran a pKa prediction of this starting material and we found a much higher value (16.38 instead of ~10 for the P-OR substitutions) which may explain its lower conversion into the desired product.

2.3. Discovery of an intriguing reactivity

Among all the negative results emerged an unexpected reactivity. One of the starting materials bearing a fluorine atom on the main ring and a trimethoxy group on its alkynyl part led to a surprising result since its fluorine atom was not present on the product. Moreover, we noticed on the ^{1}H and ^{13}C NMR spectra the presence of an additional -OMe group. We first thought about the presence of residual traces of the reaction's solvent which is methanol but its chemical shift did not clearly match the reported ones in the literature.[152] Thanks to a High-Resolution Mass-Spectrometry (HR-MS) analysis, we had the confirmation that the fluorine atom had been replaced by the solvent of the reaction, methanol here, in a nice 56% unoptimized yield (Scheme 67).

[152] G. R. Fulmer, A. J. M. Miller, N. H. Sherden, H. E. Gottlieb, A. Nudelman, B. M. Stoltz, J. E. Bercaw, K. I. Goldberg, *Organometallics* **2010**, *29*, 2176–2179.

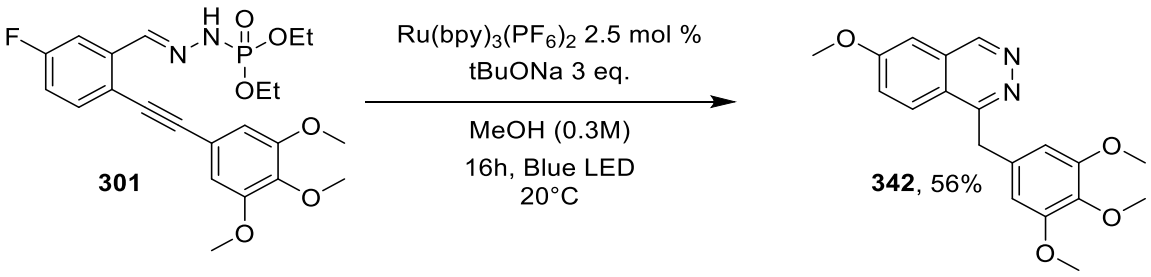

Scheme 67 - First fluorine exchange experiment

To investigate this unprecedented reactivity, we performed the same reaction but on a different starting material bearing a fluorine atom on the para-position of the alkyne **293** (Scheme 68). It is interesting to note that this position is not reactive for the reaction and no exchange between the fluorine atom and the solvent was witnessed. The final 1-(4-fluorobenzyl)phthalazine **325** was obtained instead in a good 65% yield. We decided to run more experiments on substrates bearing a fluorine atom on various positions as well as changing the nature of the incorporated alcohol. New attempts to reproduce the same intriguing reactivity ended in failures. Indeed, we first tried using fluorobenzene **343** as a simple block to recreate the exchange reaction, under the same conditions as our methodology, without any result. Then we tried on another small molecule such as 1-fluoro-3-nitrobenzene **345** and ended up with a complex mixture of products. To finish, hexafluorobenzene **344** did not give any interesting result.

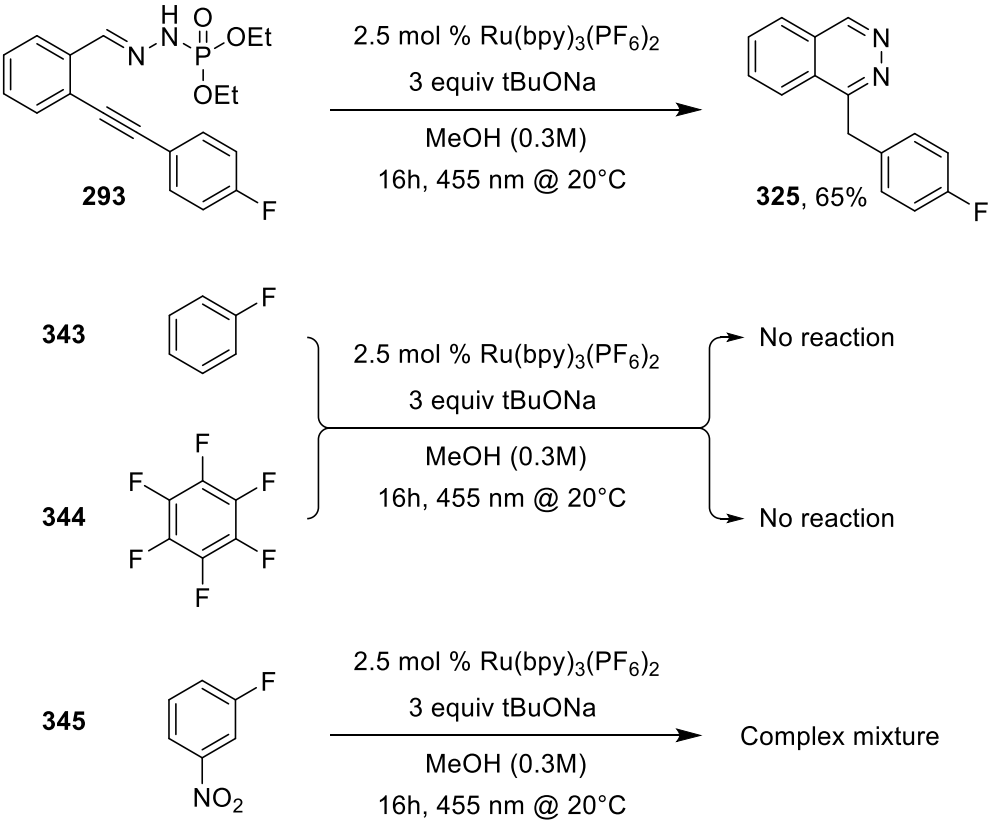

Scheme 68 - Diverse unsuccessful attempts to replace the fluorine atom

To confirm that the result of the fluorine exchange was not just an isolated event, we decided to run a similar experiment on a slightly different starting material **346**, in ethanol. We were pleased to obtain a similar exchange product with an ethoxy group successfully incorporated in the final scaffold. This product **347** was obtained with a low 22% yield (Scheme 69).

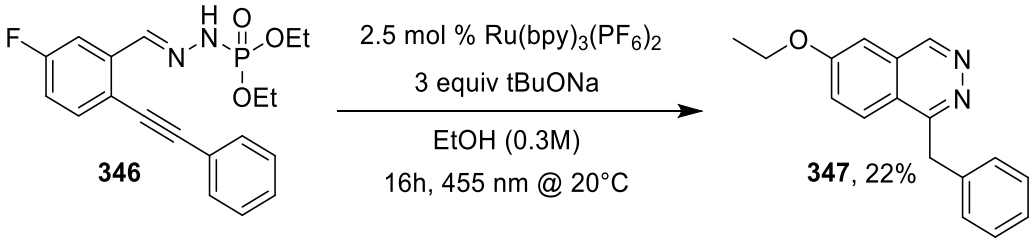

Scheme 69 - Fluorine exchange experiment in ethanol

This singular substitution resembles the net result of a nucleophilic aromatic substitution. However, in our case, we don't have any EWG in the *ortho* or *para*-position of the fluorine atom.

It is interesting to note that a base-promoted nucleophilic fluoroarenes substitution of C-F bonds was reported by Su *et al.* in 2018.[153] In their work, they describe the use of a mixture of KOH in DMSO in order to generate a superbase medium. They were able to incorporate many nucleophiles in lieu of a fluorine, such as methanol **349**, like in our case, regardless of the presence of an EWG or EDG on the aromatic cycle **348** (Scheme 70).

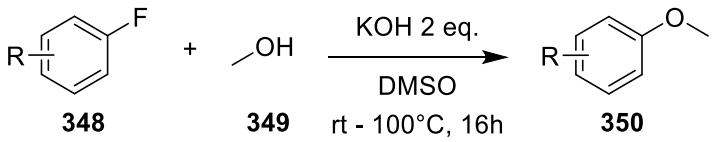

Scheme 70 - Base-promoted nucleophilic aromatic substitution reported by Su et al.

Moreover, tBuOK **353** is cited in several reports as an electron-transfer promoter. Indeed, Tuttle, Murphy et coll.[154] studied the use of tBuOK as such for the reduction of CBr_4 **354** (Scheme 71). The same team reported two years later the use of tBuOK, under visible-light, as an electron-donor in order to reduce benzophenone.[155] In these two examples, the oxidation potential of tBuOK (+0.10 V vs SCE) is not low enough to reduce their partner CBr_4 partner (reduction potential: -0.31 V vs SCE) or benzophenone (first reduction potential: -1.31 V vs SCE). However, they reported that the electron-transfer was indeed possible to CBr_4 as they calculated an achievable barrier of 23.3 kcal.mol^{-1}.

[153] J. Su, Q. Chen, L. Lu, Y. Ma, G. H. L. Auyoung, R. Hua, *Tetrahedron* **2018**, *74*, 303–307.
[154] J. P. Barham, G. Coulthard, K. J. Emery, E. Doni, F. Cumine, G. Nocera, M. P. John, L. E. A. Berlouis, T. McGuire, T. Tuttle, J. A. Murphy, *J. Am. Chem. Soc.* **2016**, *138*, 7402–7410.
[155] G. Nocera, A. Young, F. Palumbo, K. J. Emery, G. Coulthard, T. McGuire, T. Tuttle, J. A. Murphy, *J. Am. Chem. Soc.* **2018**, *140*, 9751–9757.

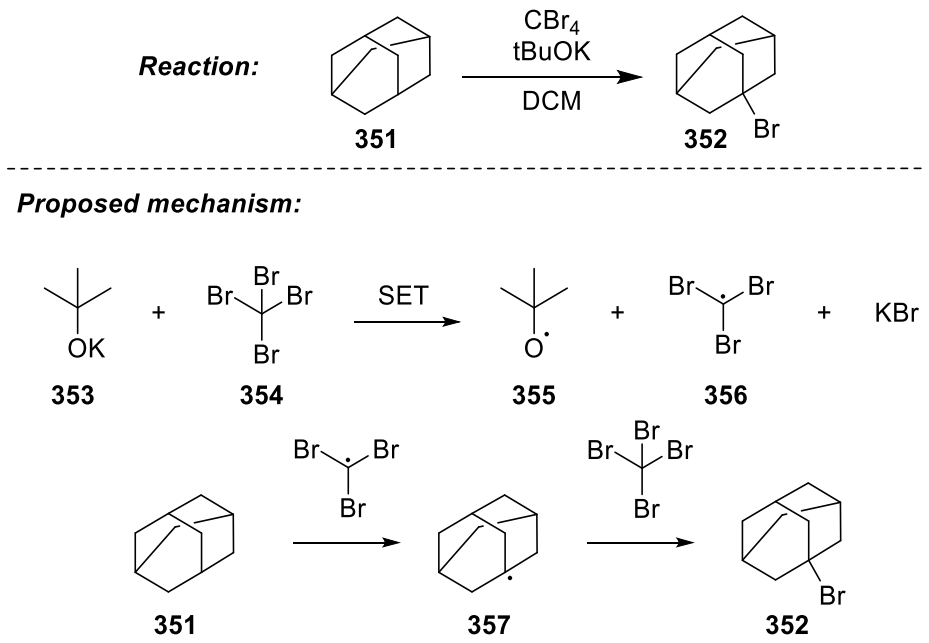

Scheme 71 - Use of tBuOK as an electron donor to CBr_4, reported by Tuttle, Murphy et coll.

On the other hand, they reported that an electron-donor-acceptor complex **359** is formed between benzophenone **358** and *t*BuOK **353**, with the potassium ion being the link between the two (Scheme 72). This complex leads to an absorption shift in the visible-light area, therefore enabling the electron-transfer. It is interesting to note that no reaction was observed using *t*BuONa, showing the importance of the alkali metal ion for this process.

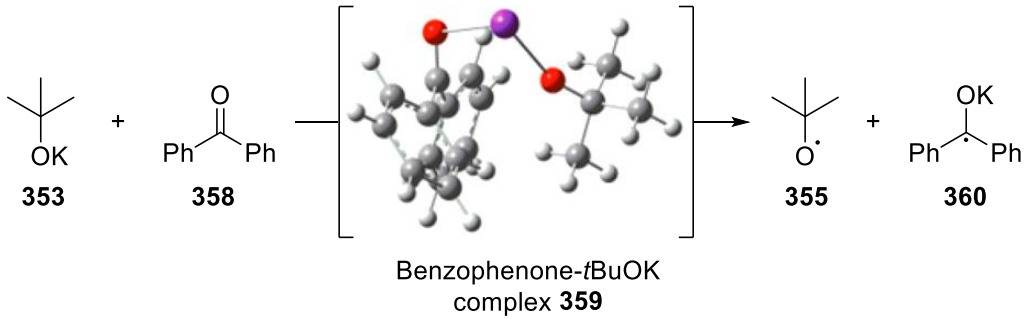

Scheme 72 - Reduction of benzophenone using tBuOK and visible-light, reported by Tuttle, Murphy et coll.

Lastly, Pichette Drapeau *et al.* reported in 2015 the use of *t*BuOK **353**, in the presence of DMF **364**, to perform a $S_{RN}1$ reaction. $S_{RN}1$ stands for substitution radical-nucleophilic unimolecular and was first discovered by Bunnett and Kim in 1970.[156] This type of reaction is a chain process, with the first step being the initiation *i. e.* formation of the intermediate $ArX^{\bullet -}$. Then a fragmentation leads to the generation of the aromatic radical **367** which can react with the nucleophile and form the radical anion $ArNu^{\bullet -}$ **369** which, after an electron transfer with the starting material **362**, lead to the desired

[156] J. F. Bunnett, J. Kook. Kim, *J. Am. Chem. Soc.* **1970**, *92*, 7463–7464.

substituted product **363** and regenerate the $ArX^{\bullet -}$ radical necessary to continue the propagation cycle.[157] Again, *t*BuONa was not suitable for the reaction because of its poor solubility in DMF, according to the authors. This is represented in Scheme 73, applied to the example of Pichette Drapeau *et al.*:

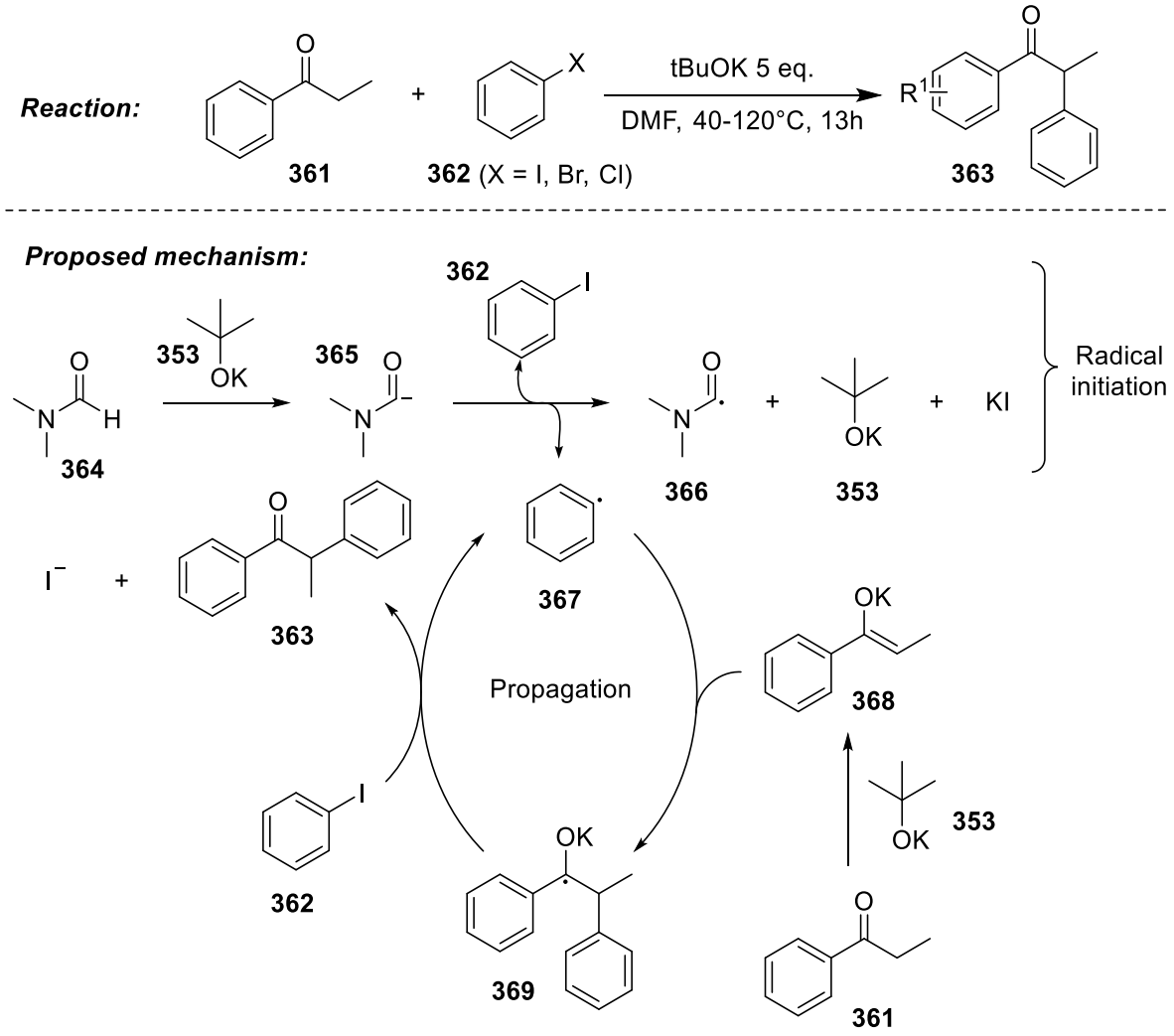

Scheme 73 - Transition-metal-free α-arylation of enolizable aryl ketones reported by Pichette Drapeau et al.

A very recent report of Ding et al.[158] demonstrated as well the use of tBuOK **353**, in the presence of DMF **364**, but this time under visible-light, to perform the dehalogenation of various aryl halides **362**, including aryl fluorine derivatives (Scheme 74). In this report, tBuOK only acts as a base, as in the previous example, in order to yield the deprotonated DMF which can perform an electron-transfer under visible-light to the aryl halide, therefore reducing it.

[157] R. A. Rossi, J. F. Guastavino, M. E. Budén, in *Arene Chemistry* (Ed.: J. Mortier), John Wiley & Sons, Inc, Hoboken, NJ, **2015**, pp. 243–268.
[158] T.-H. Ding, J.-P. Qu, Y.-B. Kang, *Org. Lett.* **2020**, DOI 10.1021/acs.orglett.0c00827.

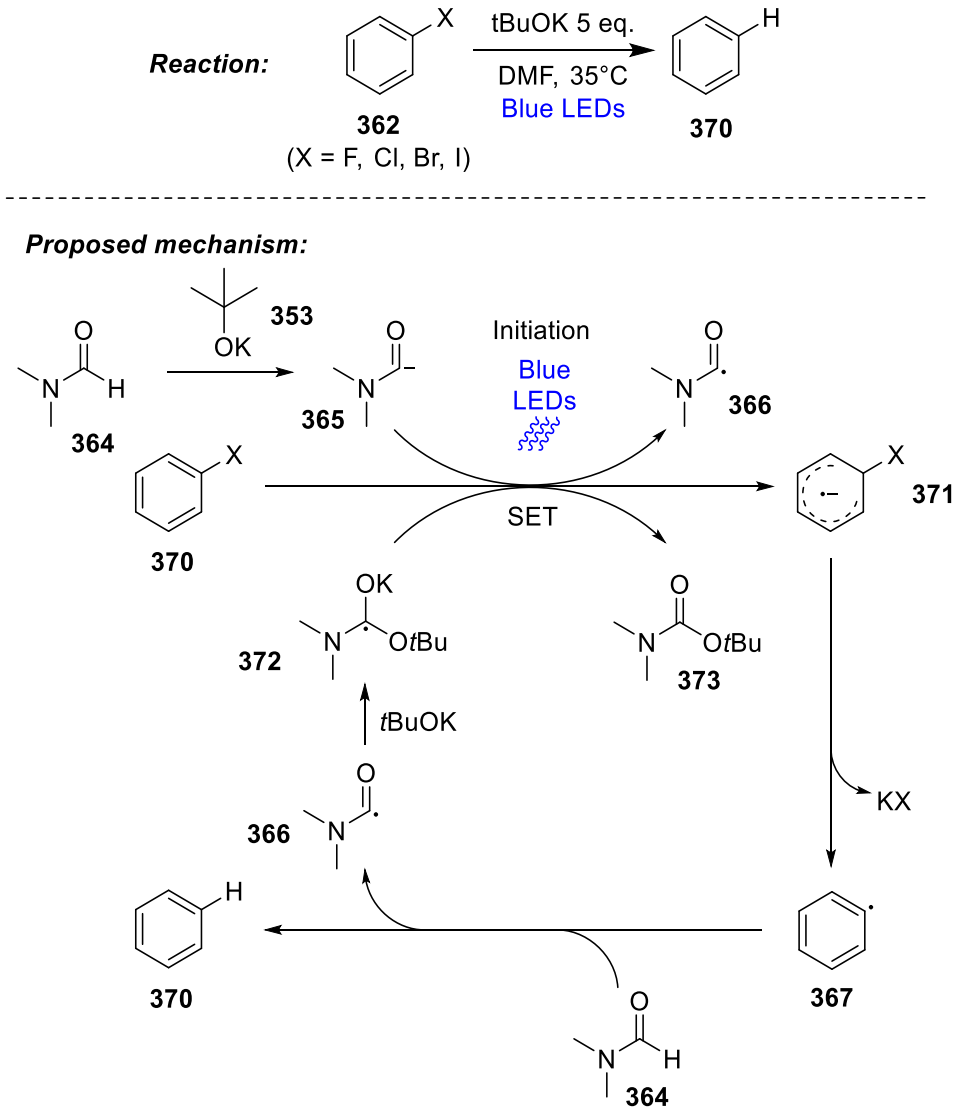

Scheme 74 - Visible-Light induced, base-promoted dehalogenation of aryl halides reported by Ding et al.

According to the reported examples in the literature, we can exclude, in our case, some hypothetical reaction pathways. Indeed, a straightforward base-promoted nucleophilic substitution as reported by Su *et al.* can be ruled-out since the combination of tBuONa and MeOH does not lead to the formation of a superbase like the mix of tBuOK and DMSO. The hypothesis of the formation of a complex between our molecule and the base as reported by Tuttle, Murphy *et coll.* can be ruled out as well because we performed our reaction without photocatalyst but in the presence of visible-light and did not observe the formation of any product. To date, the reaction mechanism of this fluorine atom exchange is still unclear.

2.4. Reactivity difference between alkynyl and alkenyl derivatives

We also synthesized starting material bearing an alkenyl unit instead of an alkynyl one. Interestingly, they displayed a similar reactivity. It is quite exciting that a reaction occurs here since

attempts to perform such a reaction on alkenyl derivatives during of previous work, using sulfonohydrazones as starting materials, led to multiple failure (Brachet *et al*.[111]). On top of this result, no N-P bond cleavage was witnessed this time and the resulting major products were the following (Table 15):

Table 15 - Reactivity of a phosphonohydrazone bearing a pendant alkene

Starting material	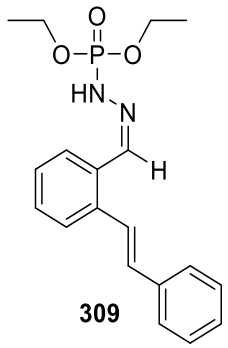 **309**
Final product	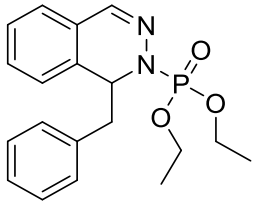 **374**, 40%

We observed on product **374** that some signals were not spectroscopically equivalent, and we could see 2 signals for the CH_2, two signals for the CH_3 of the ethoxy chains and 3 signals for the CH_2 of the ethoxy chains. The latter signal was split in 2H:1H:1H integration (Figure 26). We believe that this effect is due to the position of the ethyl chains compared with the plane of the only aromatic ring present in the structure. The molecule being not completely planar, the two ethoxy chains are not equivalent in NMR spectroscopy due to a different environment.

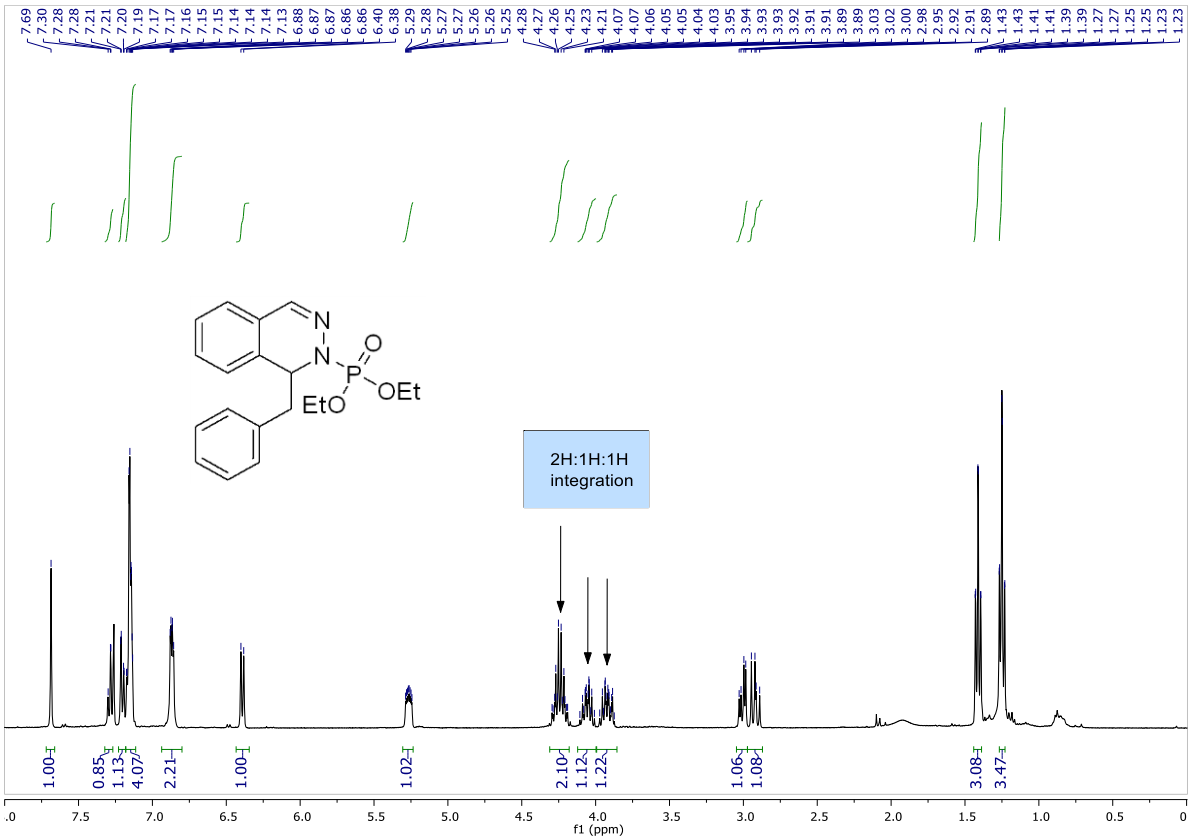

*Figure 26 - Proton NMR spectrum of product **374***

Our hypothesis is that the cleavage of the N-P bond, with alkynyl starting materials, is concomitant with the rearomatization of the heterocycle. We believe that the rearomatization drives the reaction towards the cleavage of this bond (eq. 1, Scheme 75). On the other hand, with alkenyl starting materials, the reactivity is slightly different since the N-P bond cleavage cannot lead to a rearomatization as for alkynyl derivatives (eq. 2, Scheme 75). This deprives the molecule from the needed driving force necessary for the cleavage and that is why the phosphorous moiety is still present at the end.

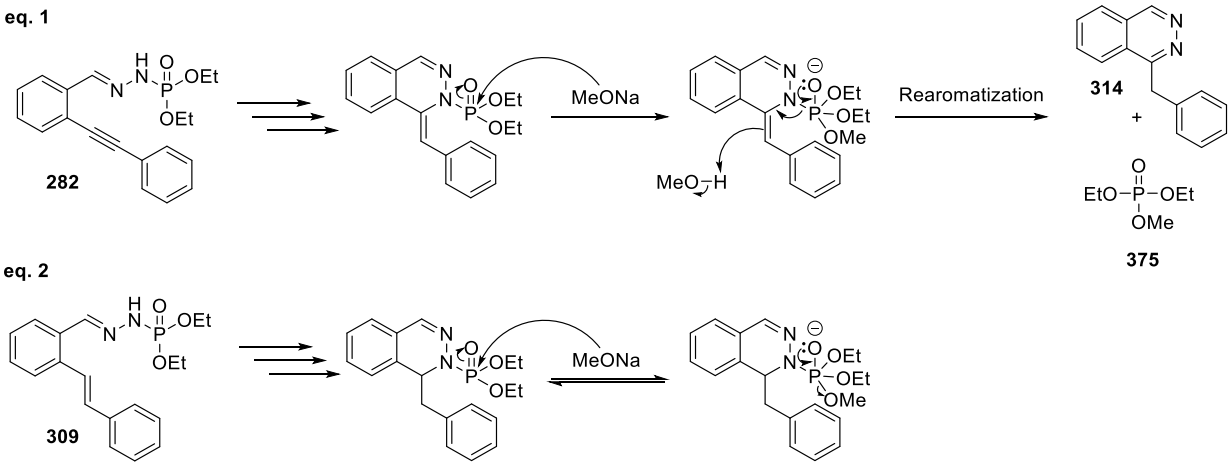

Scheme 75 - Reactivity difference in the N-P bond cleavage when alkyne vs. alkene starting material are employed

3. Mechanistic investigations

To gain a deeper insight into the reaction mechanism, we performed some extra experiments.

3.1. N-P bond cleavage

To understand the reaction mechanism and how the nitrogen-phosphorus bond was cleaved, we decided to seek out the phosphorus-containing by-product, since it was isolated during a purification step. The by-product appeared to be the phosphorus atom bearing two ethoxy chains and, interestingly, a methoxy chain, consistently with the literature.[159] Ultimately, a part of the reaction mechanism seems to be clearer thanks to the identified structure and we hypothesized that, in order to cleave the phosphorus-nitrogen bond, a methoxide anion must attack the phosphorus atom, resulting in the cleavage of the N-P bond and the release of the by-product **375** (Figure 27).

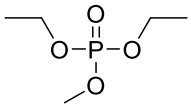

375

*Figure 27 - Structure of the isolated phosphorus-containing by-product **375***

Another attempt was made using sodium phenoxide as a base with the idea in mind that the cleaved phosphorus moiety would bear a -OPh that would be UV active and therefore easily identifiable and isolable. This attempt did not bear any fruit and no product was obtained nor a phosphorus by-product, probably for the same reason as potassium carbonate: a pKa value identical to the N-H bond, around 10. We then slightly changed our approach by synthesizing sodium benzyloxide which has a higher pKa value (around 15). When using sodium benzyloxide, the desired phthalazine is obtained in a mediocre 13% yield and again, no phosphorus-containing by-product could be isolated, probably because of its very low yield.

3.2. Cyclic voltammetry

We already knew that it was possible to generate a nitrogen-centered radical on the phosphonohydrazone moiety present on the starting materials reported by Xu's team[130,131] (detailed in Scheme 53) under copper catalysis but no information was available on our starting material. In this aim, study of the oxidation potential of our phosphonohydrazones in a basic medium could be interesting, to know if it is an attainable potential for our excited state photocatalyst.

We first started by running the CV experiments without a supportive electrolyte in order to mimic our reaction conditions and we believed that our base, sodium *tert*-butoxide, would act as one. We

[159] J. Dhineshkumar, K. R. Prabhu, *Org. Lett.* **2013**, *15*, 6062–6065.

ran these experiments in methanol, with 3 equivalents of base regarding to the phosphonohydrazone (see appendix for the experimental protocols). We obtained the following voltammograms (Figure 28):

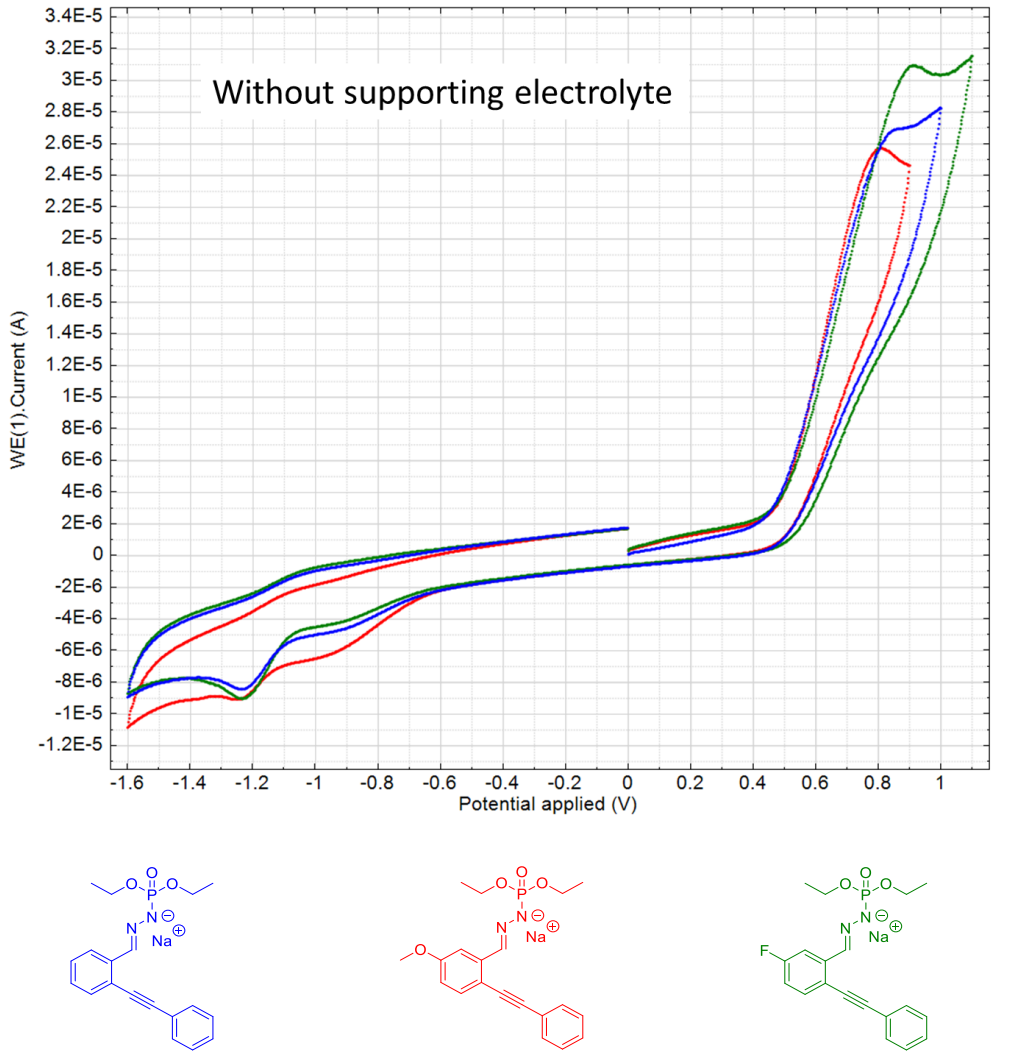

E_{Ox}(MeOH) = +0,86 V vs. SCE E_{Ox}(MeOH) = +0,81 V vs. SCE E_{Ox}(MeOH) = +0,91 V vs. SCE

Figure 28 - Cyclic voltammetry performed on selected phosphonohydrazines without a supportive electrolyte

We were thrilled to obtain such defined oxidation peaks and we could also see what seems to be reduction peaks in the negative currents and potentials. A relation between the electron density and the oxidation potential can be observed with the diminution of the oxidation potential when an electron-donating substitution was present on the main ring such as a methoxy (E_{ox} = +0.81 V vs. SCE). On the contrary, an electron-withdrawing fluorine atom on the same position led to an increase of this oxidation potential (E_{ox} = +0.91 V vs. SCE). These observations are made in comparison to the model starting material (E_{ox} = +0.86 V vs. SCE).[160]

[160] K. M. Pelzer, L. Cheng, L. A. Curtiss, *J. Phys. Chem. C* **2017**, *121*, 237–245.

These results were a bit surprising since they are not are compatible with the known oxidation potential of the excited state $Ru(bpy)_3^{2+}$ photocatalyst in solution which is E_{ox} (Ru(II)*/Ru(I)) = +0.77 V (vs. SCE in acetonitrile) and E_{ox}(Ru(II)*/Ru(I)) = +0.84V (vs. NHE in water).[161] We assume that the oxidation potential of the excited state $Ru(bpy)_3^{2+}$ in methanol is within the same window as the potentials in water and acetonitrile.

We ran again the cyclic voltammetry experiments but with a supportive electrolyte this time. We chose lithium perchlorate because of its good solubility in methanol and its compatible potential window with our substrates. We obtained the following voltammograms (Figure 29):

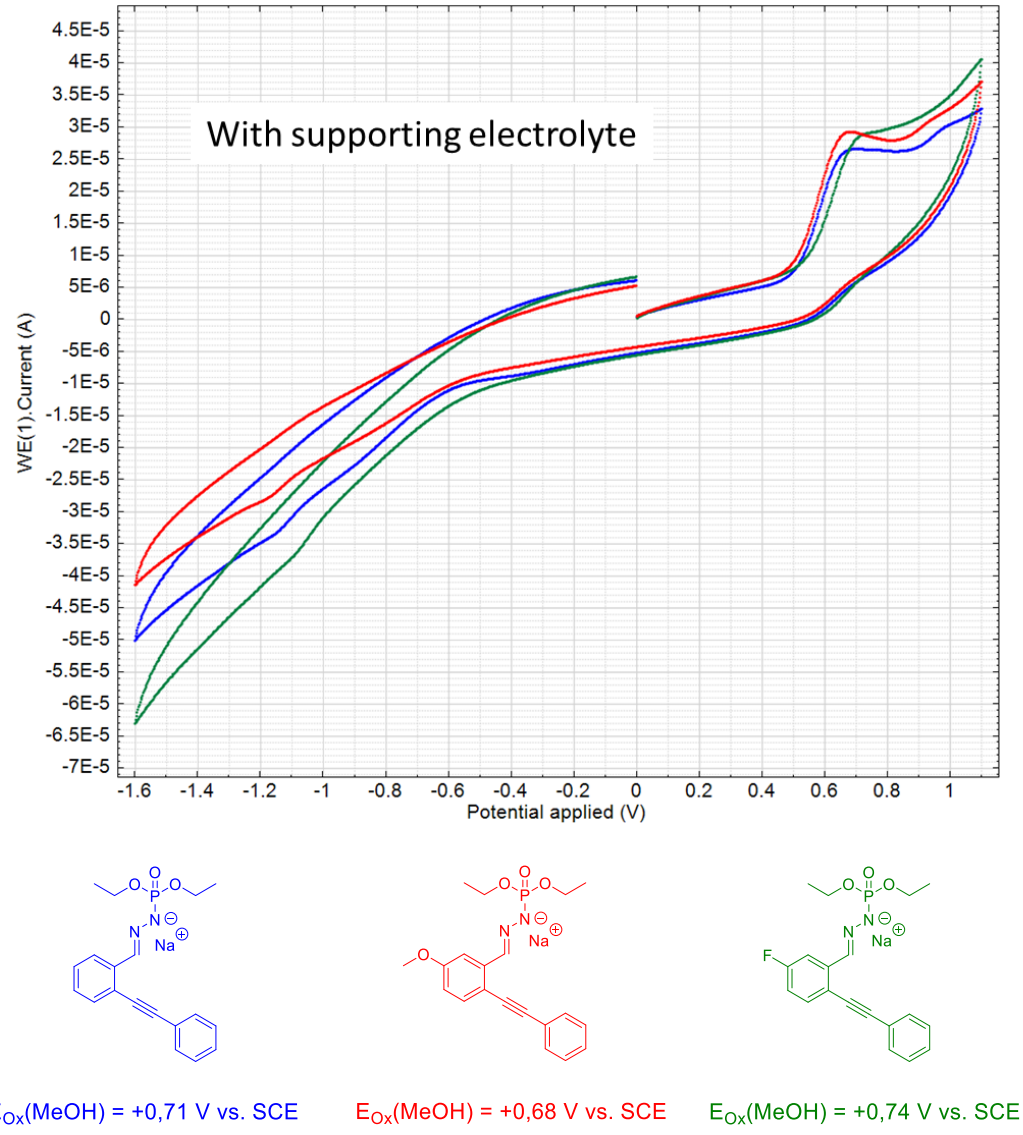

Figure 29 - Cyclic voltammetry performed on selected phosphonohydrazines with a supportive electrolyte

Again, the substitution on the principal aromatic ring have an influence on the oxidation potential measured. Our model substrate has a measured E_{ox} = +0.71 V vs. SCE. When adding an electron

[161] K. Kalyanasundaram, *Coordination Chemistry Reviews* **1982**, *46*, 159–244.

donating substituent such as a methoxy, it results in a lower oxidation potential *id est* an easier oxidation with an E_{ox} = +0.68 V vs. SCE. On the contrary, an electron withdrawing substituent such as a fluorine atom lead to a higher oxidation potential E_{ox} = +0.74 V vs. SCE. The oxidation potential of $Ru(bpy)_3^{2+}$ is higher than our measured oxidation potential of phosphonohydrazones, so this time our photocatalyst seems compatible to perform an electron transfer.

3.3. Radical trapping experiments

Another type of reaction was performed to gain insight into the radical intermediates that are transitorily formed during this visible-light catalyzed reaction. To begin with radical trapping experiments, we decided to use TEMPO **376**, a classical radical marker (Scheme 76). In this first attempt, no product formation was observed but also no adduct of the TEMPO with the starting material nor a reaction with an intermediate was found. We only witnessed a slight degradation of the starting material. Moreover, TEMPO is known to react easily with photocatalysts under visible-light catalysis conditions.[162] This may explain why no product was formed because of TEMPO interaction with the excited state Ru photocatalyst.

Thus, we decided to use diphenyl disulfide **377** in the reaction mixture. A thiophenol radical was successfully incorporated in the final scaffold **378** with an 18% yield and suggested the presence of a radical intermediate **379** on a specific position as shown in the Scheme 76:

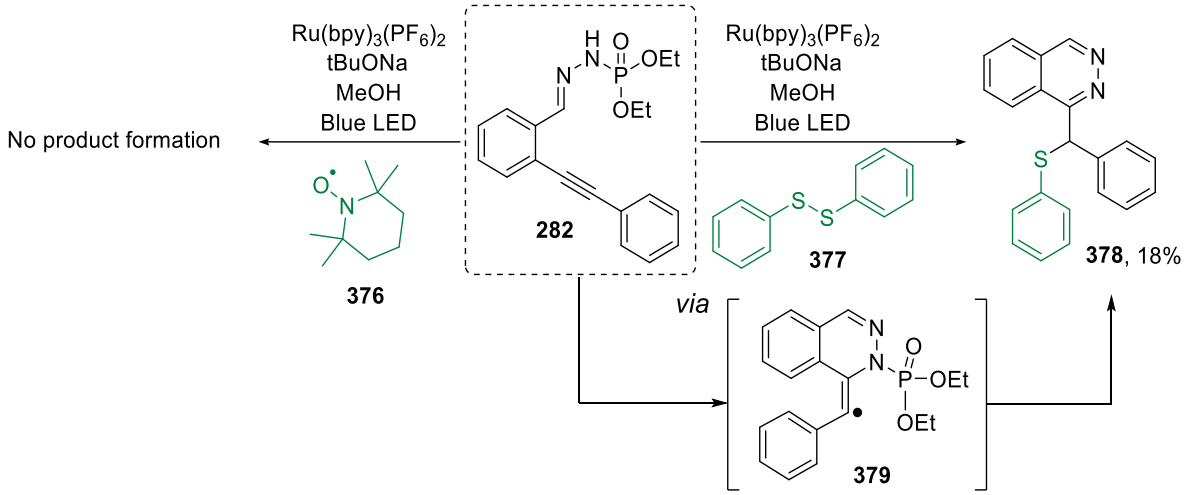

Scheme 76 - Radical trapping experiments

Once we confirmed the existence of the radical intermediate, we intended to make it react with a Michael acceptor such as the methyl vinyl ketone (MVK) **146** or the α-methylstyrene **211** (Scheme 77).

[162] X. Lang, J. Zhao, *Chemistry – An Asian Journal* **2018**, *13*, 599–613.

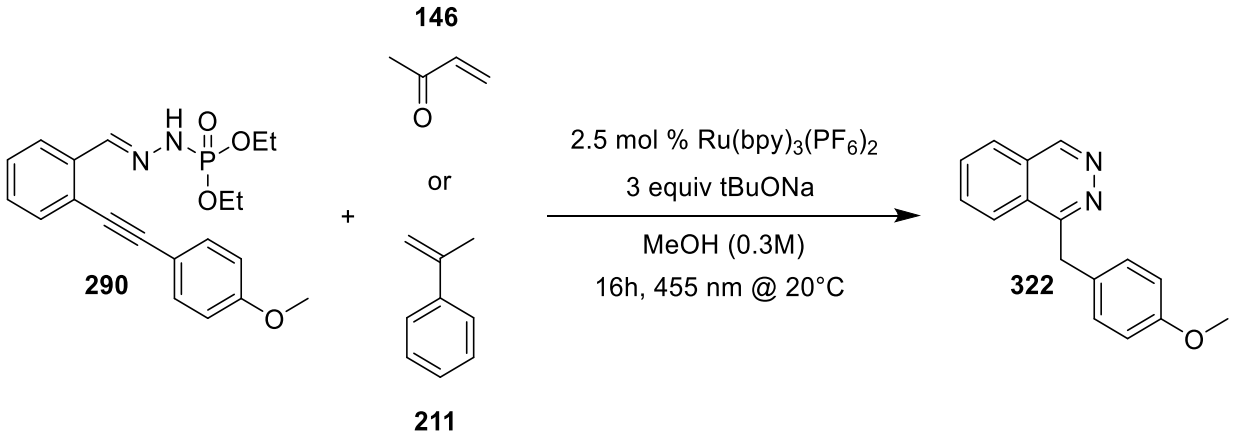

Scheme 77 - Attempt to make react the radical intermediate with an alkenyl derivative

When using 5 equivalents of an alkene derivative in the reaction medium, no addition product was obtained. Instead, the regular expected benzylated phthalazine **322** was formed.

3.4. Deuteration experiment

The reaction was performed in deuterated MeOH (MeOD) instead of MeOH in order to confirm the origin of the incorporated proton in the final phthalazine scaffold (on the CH_2 position). As expected, the incorporated proton comes from the solvent as we obtained 86% of deuterium incorporation with a 63% yield for the phthalazine **380** (Scheme 78). This allow us to confirm that the solvent is assuredly the proton source in the final step of the reaction.

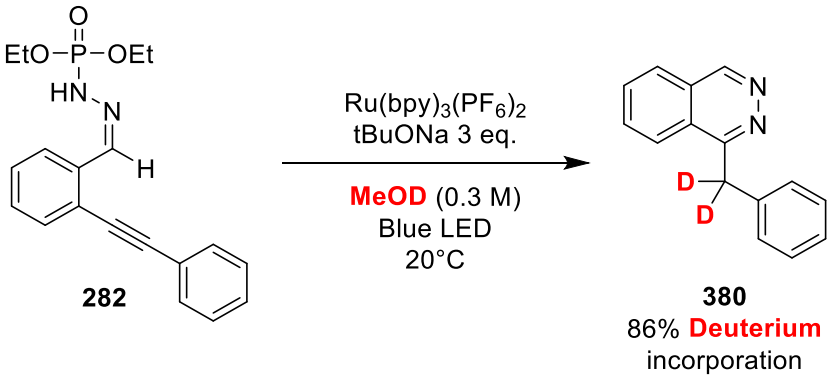

Scheme 78 - Deuteration experiment

3.5. NMR follow-up of the reaction and on-off diagram

We ran an NMR follow-up of the model reaction after periods of light irradiation or not, using deuterated methanol as the solvent of the reaction and withdrawing 50 µL aliquot every 30 to 60 minutes to take the ^{1}H NMR spectra (see appendix for more details about the protocol).

With all these ^{1}H NMR spectra in hand, we followed a characteristic chemical shift of the starting material (8.55 ppm) and, thanks to the internal standard (1,3,5-trimethoxybenzene), we calculated the

amount of starting material left at each time. We then proceeded to plot the amount of reagent as a function of time with the following values (Table 16, Figure 30):

Table 16 - Amount of reagent as a function of time during the On-Off experiment

	Time (min)	Reagent integration (8.55 ppm)	mmole reagent
Light	0	1	0,6
/	30	0,46	0,276
Light	60	0,46	0,276
/	120	0,24	0,144
Light	150	0,22	0,132
/	180	0,17	0,102
Light	210	0,17	0,102
/	240	0,07	0,042
Light	270	0,08	0,048
/	300	0,04	0,024
Light	330	0,05	0,03
/	360	0,01	0,006
Light	390	0,01	0,006
Light	450	0	0

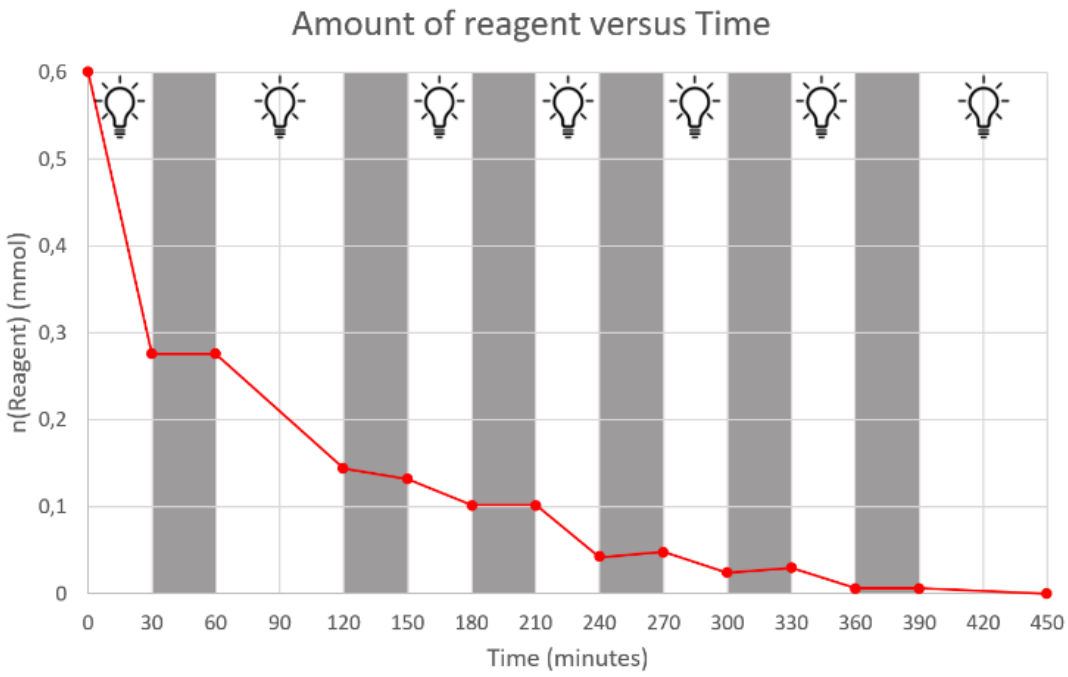

Figure 30 - Amount of reagent as a function of time during the On-Off experiment

We can clearly see a large diminution of the amount of starting material within the first minutes with a 54% drop. Then when no light was shed onto the reaction medium, no change in the amount of reagent was witnessed. This pattern remains quite constant as the reaction progresses until a plateau

is reached, roughly 360 minutes after the beginning of the experiment, when no more reagent is available.

By superposing the ^{1}H NMR spectra, we also noticed that a transitory peak was observed around 7.73 ppm, appearing and disappearing as the reaction proceeds (Figure 31). It is interesting to note that the highest peak corresponds to the aliquot of the reaction taken at 30 minutes. We could hypothesize that this transitory peak that is greatly formed and visible at 30 minutes could be linked to the big drop in the amount of starting material that is observed at 30 minutes as well. This transitory peak could then be associated with a reaction intermediate **381**, such as the hydroamination product, prior to the N-P bond cleavage (Figure 32).

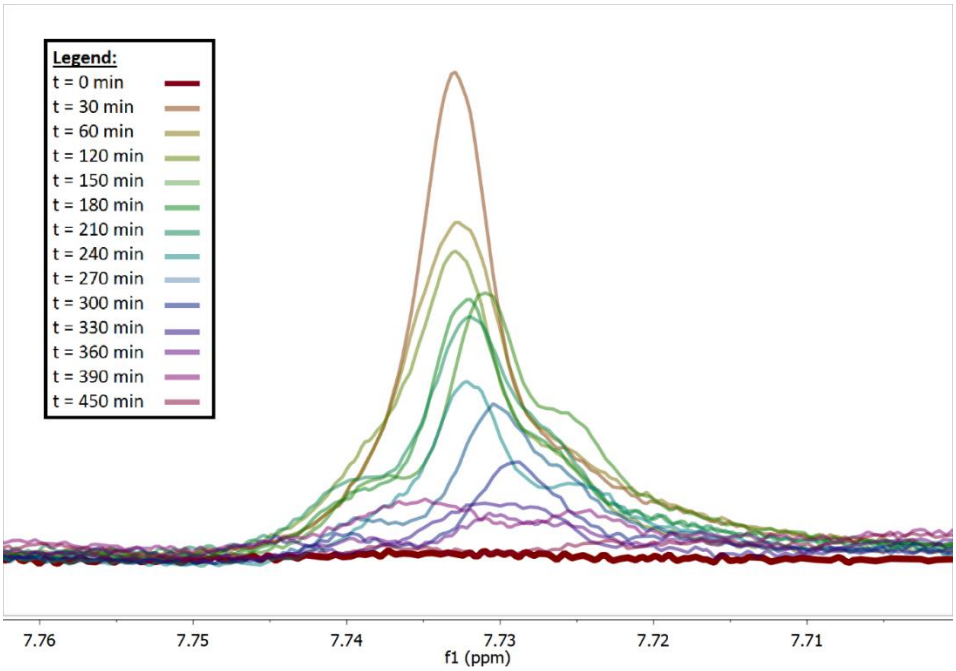

Figure 31 - Transitory peak observed during the "on/off" experiment, at 7.73 ppm

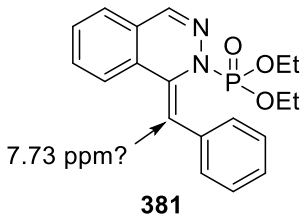

381

*Figure 32 - Hypothetical reaction intermediate **381** associated with the transitory peak at 7.73 ppm*

These data indicate that the reaction can only proceed during periods of light irradiation, giving us an indication that a visible-light catalyzed process happens in this reaction. We acknowledge the fact that we cannot definitely conclude on the termination of the reaction without the quantum yield

information in hand, as demonstrated by the Yoon group in 2015.[163] Indeed, when performing an "on/off" experiment as we did, turning the light off does not necessarily means that all catalyzed processes will stop. Some reactions can continue in the dark if radical chain processes happen and allows the reaction to be self-sustained for a few turnovers. This would mean that 1 absorbed photon can lead to more than 1 molecule of product. This relation between the number of absorbed photon and the number of molecules of products formed is what defines the quantum yield:

$$\Phi = \frac{number\ of\ molecules\ of\ product\ formed}{number\ of\ photons\ absorbed}$$

If the quantum yield was superior to 1, we would expect the catalytic cycle to be maintained by a radical intermediate within the reaction medium. If it was inferior to 1 on the other hand, we would expect the reaction to end with the closure of the catalytic cycle by the photocatalyst itself. Unfortunately, we do not have the required apparatus to measure the quantum yield of our reaction but here, we assume that it would not be peculiar to envision a quantum yield similar to the one reported by Brachet *et al*,[111] therefore below 1.

3.6. Proposed mechanism

All the acquired data allowed us to propose the following mechanism, on Scheme 79, in which the first reaction to occur is an acid-base reaction with the deprotonation of the phosphonohydrazone **A** leading to the formation of the anionic intermediate **B**. In the meantime, the Ru^{II} photocatalyst enters an excited state after light irradiation and yields the Ru^{II}* photocatalyst. The latter being an oxidant, it oxidizes with 1 electron the anionic intermediate **B** to generate the NCR **C**. This is followed by an intramolecular reaction with the alkynyl unit, giving a radical intermediate **D**. The previously reduced Ru^{I} photocatalyst reduces the radical intermediate **D** into an anionic intermediate **E** and this closes the catalytic cycle by giving the Ru in its original oxidation state. The anionic intermediate **E** gets protonated with the protic solvent (MeOH here) to give the intermediate **F**. We believe that the N-P bond cleavage is happening at this moment during the reaction since we were able to isolate and characterize the phosphorus containing by-product coming from the attack of the phosphorus moiety by sodium methoxide. This step provides the by-product **G** and the intermediate **H** which is in a very balanced equilibrium toward the formation of the final phthalazine **I**.

[163] M. A. Cismesia, T. P. Yoon, *Chem. Sci.* **2015**, *6*, 5426–5434.

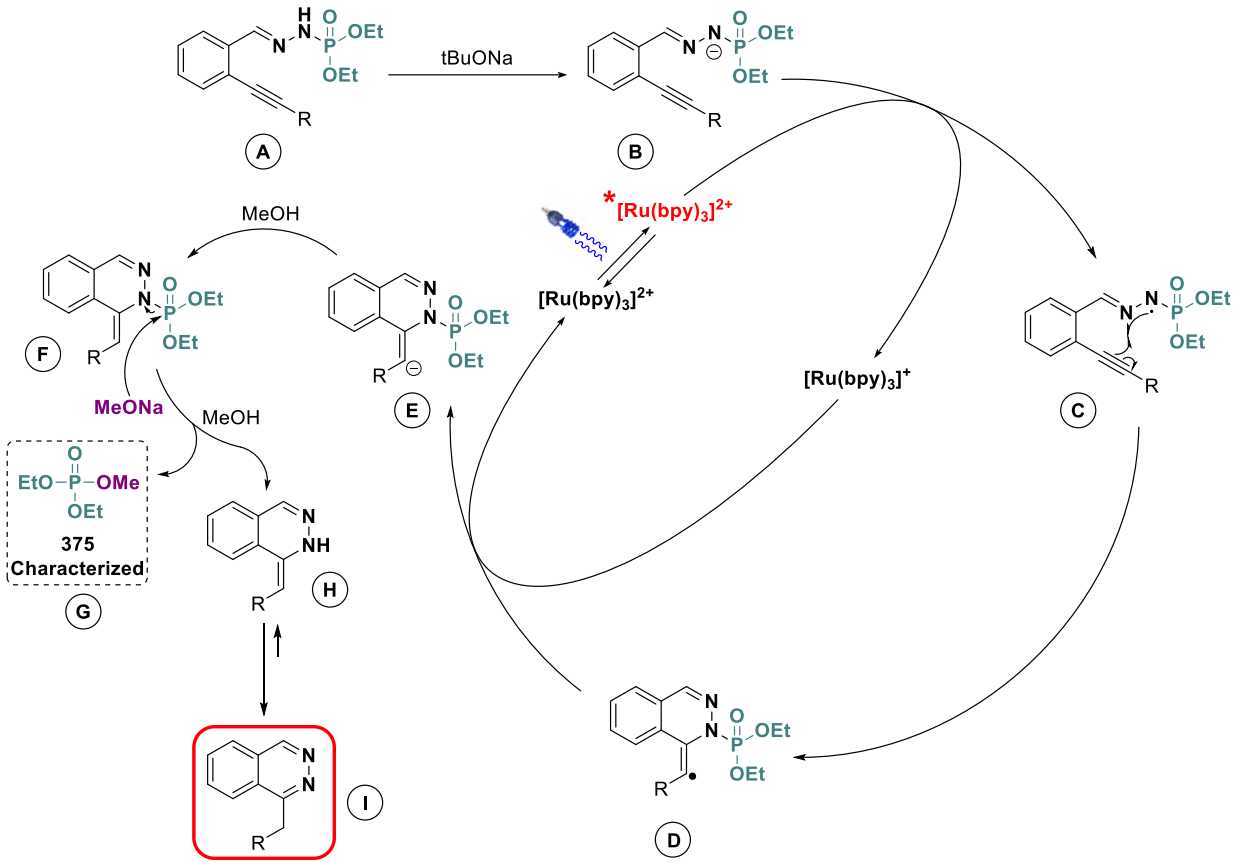

Scheme 79 - Mechanistic proposal

Compared to the above mechanistic proposal, we cannot exclude another pathway. Indeed, compound **D** in the presence of MeOH may produce a HAT leading to a MeO• residue (Scheme 80). This last derivative could be able to reoxidize the Ru^{I} to complete the catalytic cycle. Sodium methylate generated from this process is then able to cleave the phosphoramidate group, to provide, at the end, the desired compound **I**.

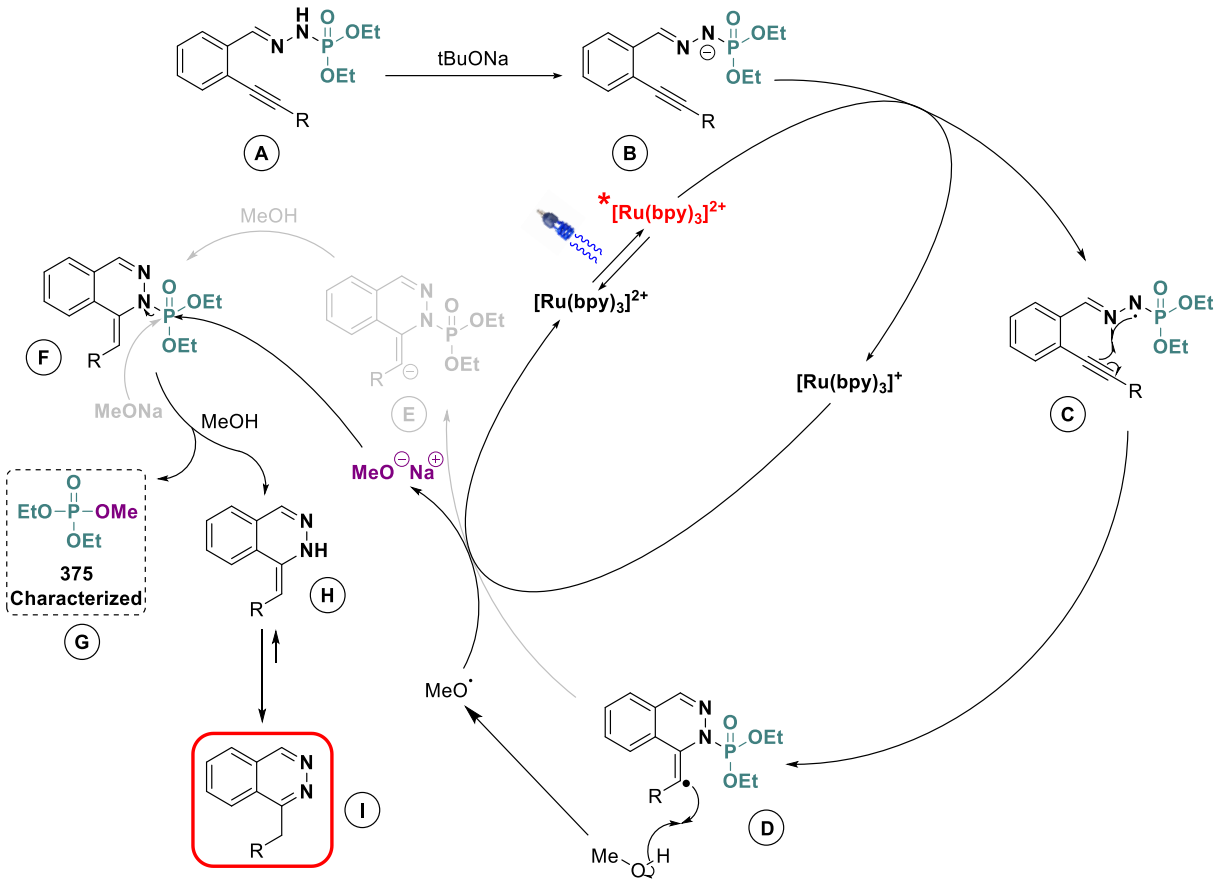

Scheme 80 - Alternative mechanistic proposal

D) Conclusion & perspectives

In this chapter, we presented a new family of pre-activated NCR precursors called phosphonohydrazones. These molecules bear ethoxy chains on the phosphorus atom and we also developed several molecules with differently substituted phosphorus atom in order to investigate the reactivity of such starting material.

This methodology proved that phosphonohydrazones can successfully be employed as a new family of transient nitrogen-centered radical precursor. Furthermore, their synthesis is readily applicable in a few steps with well-known and mastered synthetic steps such as the Sonogashira cross-coupling reaction, a varied access to the phosphonohydrazine molecules and finally, a very convenient reaction to form phosphonohydrazones. The latter can be engaged in our optimized reaction conditions to yield a broad variety of molecules bearing various modifications playing on the electron density, the steric hindrance and even the reactivity when alkenyl derivatives are employed.

Alkenyl derivatives lead to the formation of an interesting phthalazine core which still bears the phosphorus moiety. The ^{1}H NMR spectroscopy data confirmed that these molecules are not planar and the ethoxy chains on the phosphorus atoms are therefore not spectroscopically equivalent. In other

word, these molecules are chiral, and this property could be used, after some structure tweaking, to create atropoisomeric ligands or catalysts (if we increase their light-harvesting properties). Many chiral ligands have been described in the literature and they bear, as well as our molecules, nitrogen and phosphorus atoms.[164] Consequently, there might be some possible future developments in this direction.

It would be very interesting and exciting to modulate the reactivity of phosphonohydrazones and direct them toward migratory reactions of the substituents on the phosphorus atom. During our investigation, a phosphonohydrazone carrying two phenyl substituents was made and led to poor yields of the desired phthalazine, unfortunately. However, a new reactivity appeared with this starting material and a migration of a phenyl group was for the first time witnessed on this kind of molecule under visible-light catalysis, which is the playground for **chapter IV**.

[164] P. J. Guiry, C. P. Saunders, *Advanced Synthesis & Catalysis* **2004**, *346*, 497–537A. Pfaltz, I. Drury, William J., *ChemInform* **2004**, *35*, DOI 10.1002/chin.200436268P. Nareddy, L. Mantilli, L. Guénée, C. Mazet, *Angew. Chem. Int. Ed.* **2012**, *51*, 3826–3831M. P. Carroll, P. J. Guiry, *Chem. Soc. Rev.* **2014**, *43*, 819–833B. V. Rokade, P. J. Guiry, *ACS Catal.* **2018**, *8*, 624–643.

Chapter IV:

Visible-Light catalyzed cascade of hydroamination reaction and Smiles rearrangement using phosphonohydrazones as novel NCR precursors

Chapter IV: Visible-Light catalyzed cascade of hydroamination reaction and Smiles rearrangement using phosphonohydrazones as novel NCR precursors

In this chapter, we will tackle the development and optimization of a novel methodology which comprises a cascade of a hydroamination reaction followed by an aryl migration (related to a Smiles rearrangement). The type of final product obtained in this methodology could be technically regarded as coming from a carboamination reaction.

A) Carboamination reactions

1. Introduction

A carboamination is defined as a reaction that leads to the formation of one C-N bond and one C-C bond, in either order, across an alkene or an alkyne.[165] We chose to separate the two distinct events taking place in this reaction as 1) hydroamination reaction and 2) Smiles rearrangement and we acknowledge that the product of this reaction could also be named a carboamination product.

Carboamination reactions are very attractive as they allow to avoid the inherent drawbacks of a hydroamination reaction followed by a Heck-type reaction for functionalizing one end of an alkenyl group. Stereoselective carboamination reactions can be divided in five categories (Scheme 81):

- Annulation reactions which lead to a cyclic product,
- Intramolecular reactions with substrates bearing an amine tethered to the alkene,
- Intermolecular reactions (two-components) with a molecule bearing both the nitrogen and carbon that will be added onto the alkenyl moiety,
- Intermolecular reactions (three-components) with a molecule that contains a carbon and another one that contains a nitrogen that will both be added onto the alkenyl partner,
- Radical reactions via either a *C*- or *N*-centered radical.

[165] J. P. Wolfe, Ed. , *Synthesis of Heterocycles via Metal-Catalyzed Reactions That Generate One or More Carbon-Heteroatom Bonds*, Springer Berlin Heidelberg, Berlin, Heidelberg, **2013**.

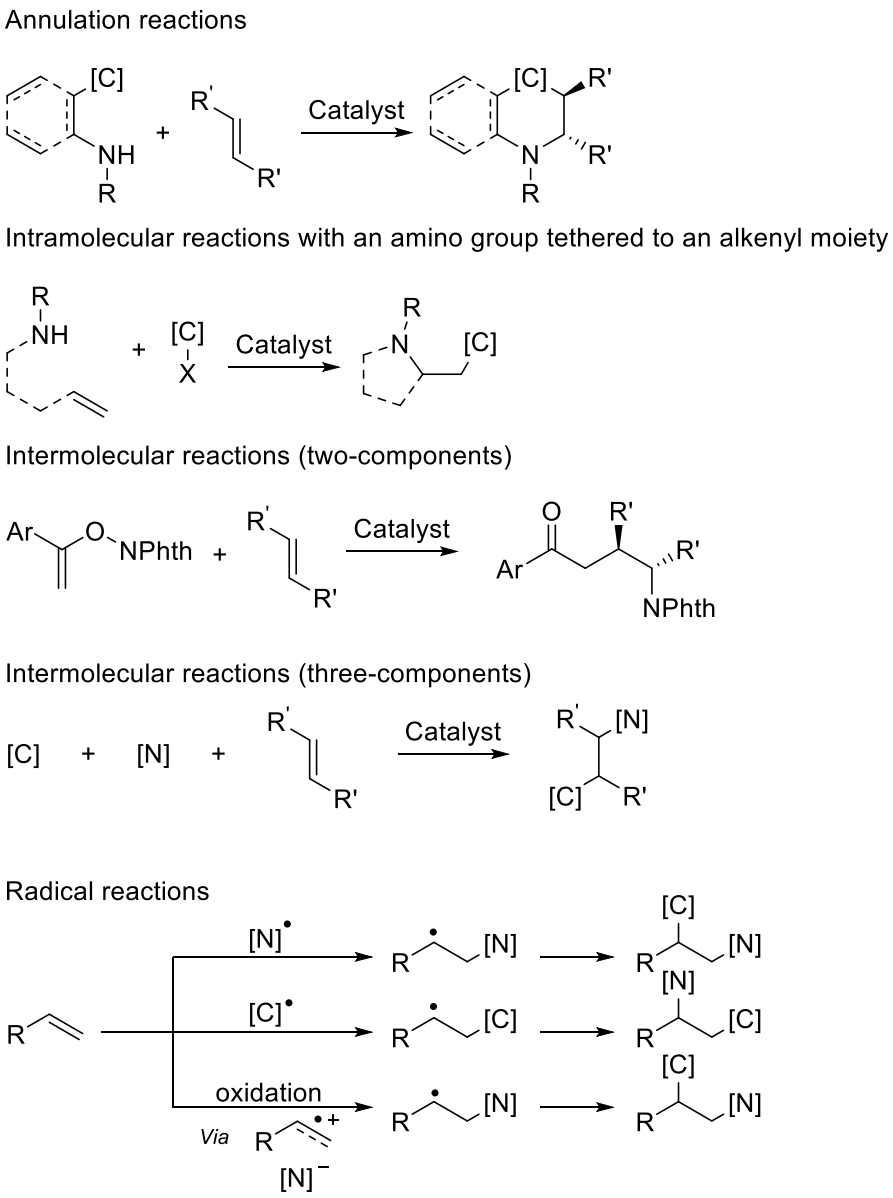

Scheme 81 - General representation of the different types of carboamination reactions

Since a carboamination product is obtained with this novel cascade reaction, we will present the classical synthetic pathways to perform such a reaction.

2. State of the art

Wolfe's group played an important role in the development of diverse types of carboamination reactions. Indeed, his team developed for instance a tandem N-arylation/cyclization/C-arylation under Pd-catalysis for the formation of indoline derivatives **386** (Scheme 82).[166] The reaction takes place between an *ortho*-allylaniline **382** and an aryl bromide **383** and proceeds via the arylation of the nitrogen atom in the first step. Then, an oxidative addition occurs between the Pd catalyst and the aryl

[166] R. Lira, J. P. Wolfe, *J. Am. Chem. Soc.* **2004**, *126*, 13906–13907.

bromide derivative. After action of *t*BuONa a palladium amido complex **389** is obtained. A migration of the alkene into the Pd-N bond affords a new palladium intermediate **390** which leads to the desired product **386** while forming the final C-Ar bond upon reductive elimination.

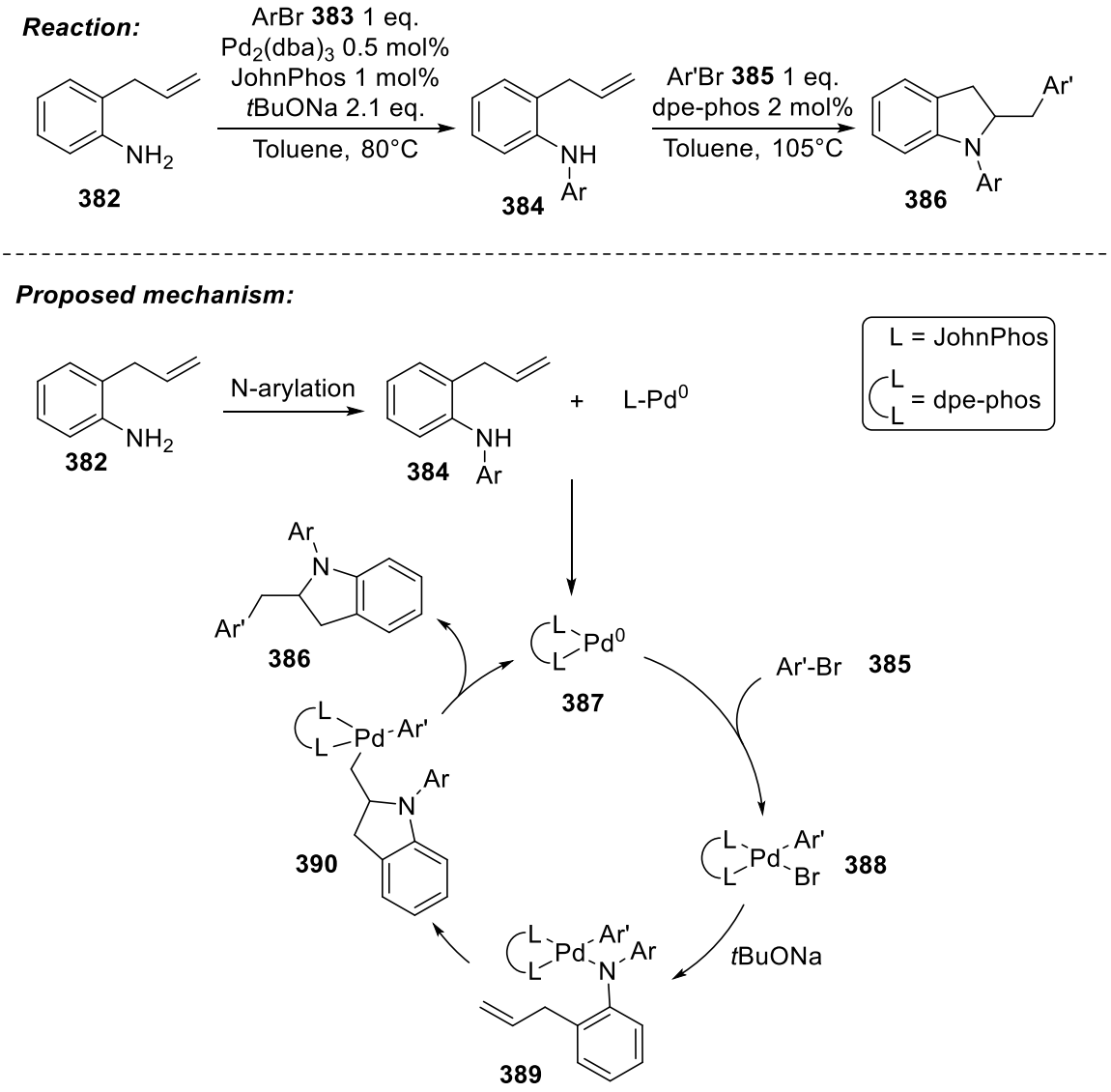

Scheme 82 – Intramolecular carboamination reaction with an alkene derivative reported by Wolfe's group

Yamamoto *et coll.* also reported an intramolecular carboamination reaction, with alkynyl derivatives **391** this time.[167] They disclosed a Pt-catalyzed intramolecular addition of an amido group onto an alkynyl moiety using ortho-alkynyl amide derivatives **391** (Scheme 83). First, a coordination of the platinum catalyst to the alkynyl group leads to the formation of a π-complex **393**, increasing the electrophilicity of the alkyne. Then, a nucleophilic attack of the *ortho*-nitrogen atom leads to a zwitterionic intermediate **394**. The C-C bond is formed after an intramolecular [1,3]-migration of the acyl moiety, followed by the obtention of the desired product **392** and regeneration of the catalyst.

[167] T. Shimada, I. Nakamura, Y. Yamamoto, *J. Am. Chem. Soc.* **2004**, *126*, 10546–10547.

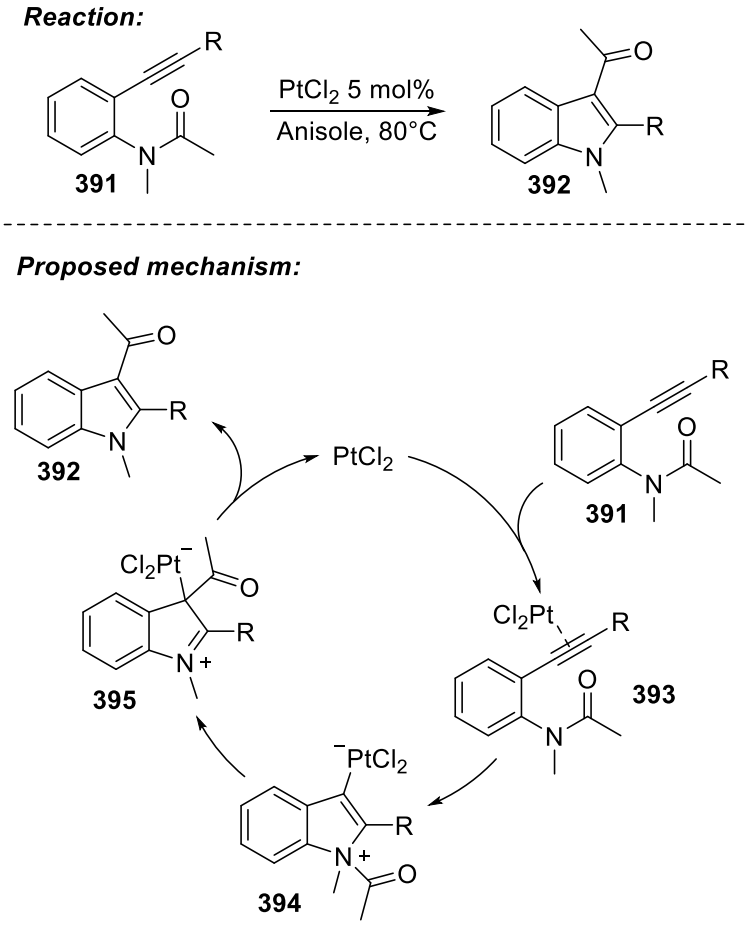

Scheme 83 - Intramolecular carboamination reaction with an alkyne derivative, reported by Yamamoto et coll.

Later, Rovis and Piou[168] disclosed a two-component Rh-catalyzed stereoselective intermolecular carboamination of alkene groups, using enoxyphthalimides **396** as the source of both the carbon and the nitrogen atoms (Scheme 84). The reaction can proceed following two paths at the beginning since the Rh catalyst can undergo an irreversible C-H bond activation prior or after the opening of the phthalimide in the presence of methanol (**Path A** or **B** respectively). An alkene **397** can then be inserted in the intermediate **401** and a C-N bond is formed after a reductive elimination step, also reducing Rh(III) to Rh(I). The latter inserts into the N-O bond and, after a protonolysis, yields an intermediate **405** that subsequently undergoes a cyclization to form back the phthalimide moiety of **398**.

[168] T. Piou, T. Rovis, *Nature* **2015**, *527*, 86–90.

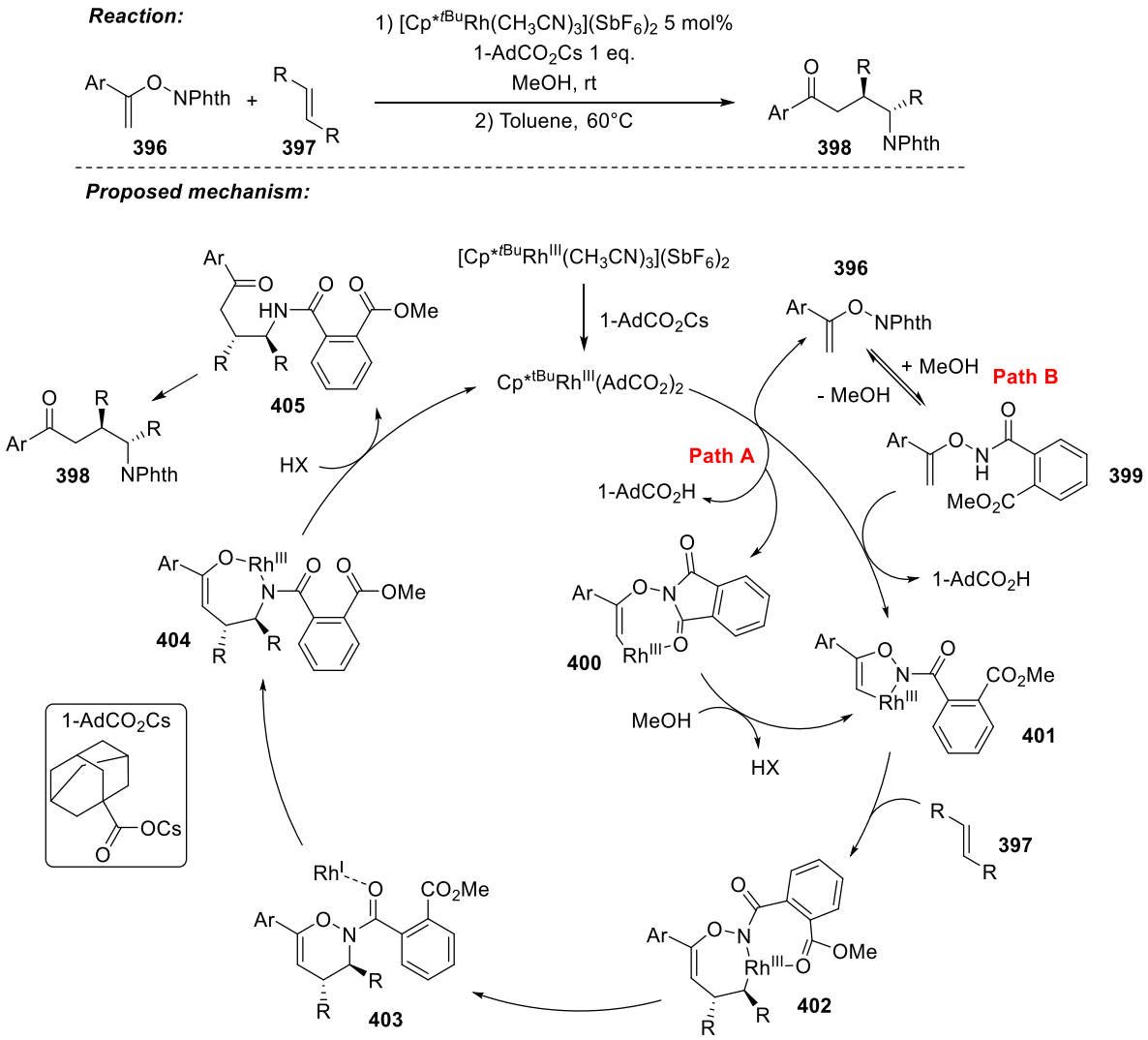

Scheme 84 - Two-component intermolecular carboamination reaction reported by Rovis and Piou.

Also, Glorius' team reported a three-components intermolecular 1,4-carboamination of dienes via a Rh-catalysis (Scheme 85). To do so, they were able to develop a methodology for the coupling of Weinreb amides **406** with 1,3-dienes **407** and dioxazolones **408**. In a first step, the active cationic catalyst is generated after halogen abstraction by $AgBF_4$ and AgOAc. The Weinreb amide coordinates to the catalyst's metal center and gives the rhodacyclic intermediate **410** upon C-H activation. Then, a migratory insertion of the 1,3-diene gives the Rh(III)-allyl intermediate **411** which undergoes an oxidative addition into the N-O bond of the dioxazolone followed by a CO_2 extrusion, affording a Rh(V) intermediate **412**. A final reductive elimination and protodemetallation yield the final product **409** and closes the catalytic cycle.

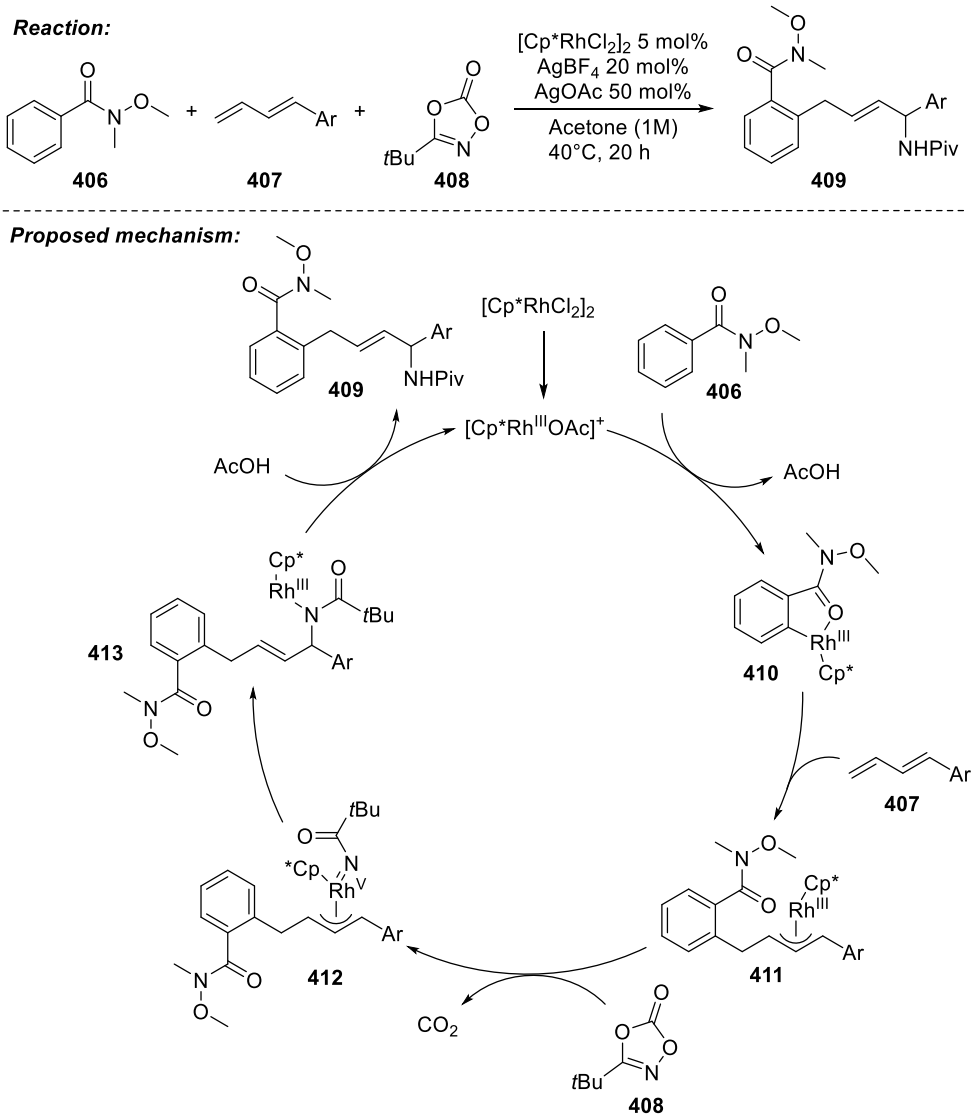

Scheme 85 - Three-component intermolecular 1,4-carboamination reaction reported by Glorius' team

In order to highlight the broad possibilities offered to perform a carboamination reaction, we will tackle the report of Feng's team. They described an intermolecular carboamination reaction of unactivated alkenes under photoredox catalysis (Scheme 86). The reaction proceeds via a radical mechanism, initiated by visible-light catalysis, and is proposed to proceed between an *O*-vinylhydroxylamine **414** derivative and an alkene moiety (enolether) **415** as following: the Ir photocatalyst enters an excited state upon excitation by visible-light irradiation. An energy transfer between the excited photocatalyst $[Ir^{III}]^*$ and the *O*-vinylhydroxylamine **414** leads to an homolytic cleavage of the N-O bond, affording an oxygen **418** and a nitrogen-centered radical **419**. The latter reacts with the alkene moiety **415** and gives rise to a secondary alkyl radical **420** which reacts with another equivalent of *O*-vinylhydroxylamine. Then, a cleavage of the N-O bond regenerates the nitrogen-centered radical and yields the desired product.

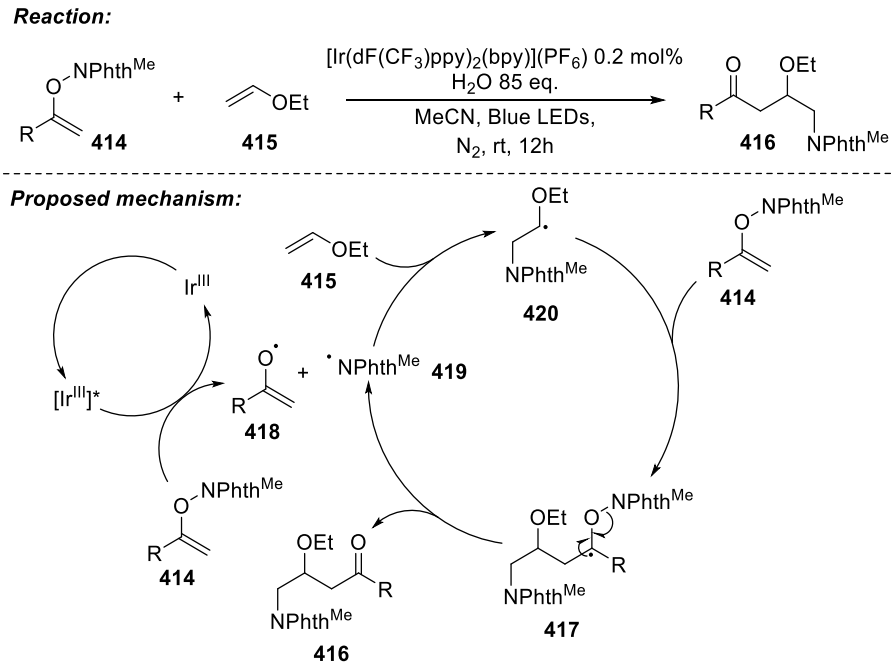

Scheme 86 - Visible-light catalyzed intermolecular carboamination reported by Feng's team

B) Aryl rearrangement reactions

1. Introduction

1.1. First examples

The history of aryl migration reactions stretches all the way back to 1838, almost 200 years ago, when Justus Von Liebig described the first example of this unprecedented reaction.[169] The benzilic acid rearrangement was named after the first example reported which leads to the formation of benzilic acid **426** starting from benzil **421** (Scheme 87). The reaction consists in a nucleophilic attack of a hydroxide ion on one of the carbonyl group of the benzil. After a rotation of the central C-C bond, one of the phenyl group can perform a 1,2-migration within the molecule and lead to another alkoxide **424**, originating from the other carbonyl. The final benzylic acid is obtained after an acid treatment.

[169] J. Liebig, *Ann. Pharm.* **1838**, *25*, 1–31.

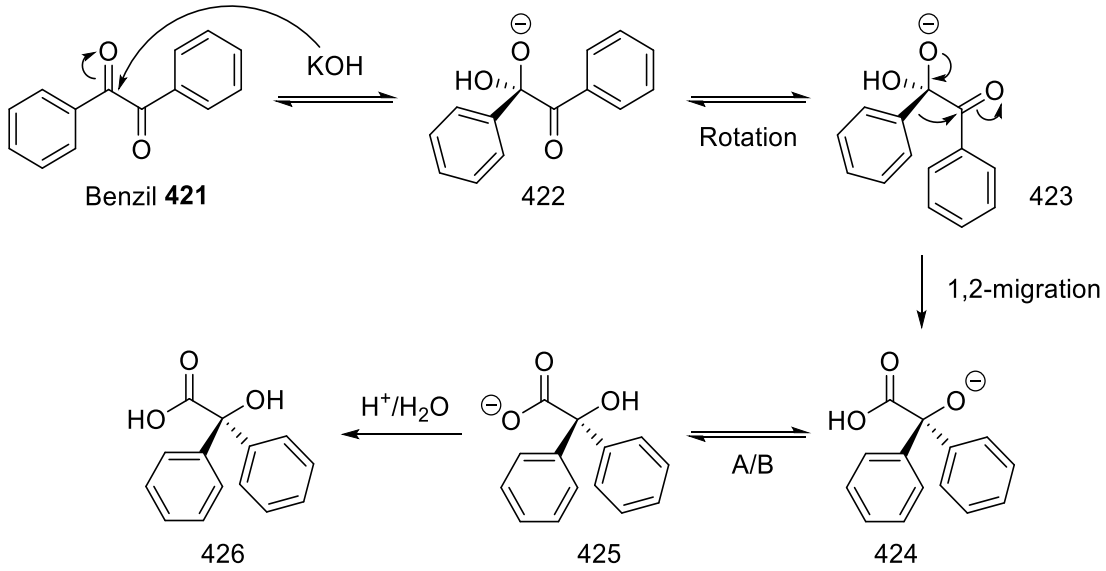

Scheme 87 – First example of an ionic 1,2-aryl migration reported by Liebig in 1838 – Mechanism of the benzylic acid rearrangement

Radical-type aryl migration were only reported about 70 years later, in 1911, by Heinrich Otto Wieland. He was the first to report a radical migration of an aryl group (Scheme 88).[170] This 1,2 radical rearrangement took place on a bis(triphenylmethyl)peroxide molecule **427**, after formation of an alkoxide radical **428**, to yield a tetraphenylethane derivative **431** by conjugation of C-radicals.

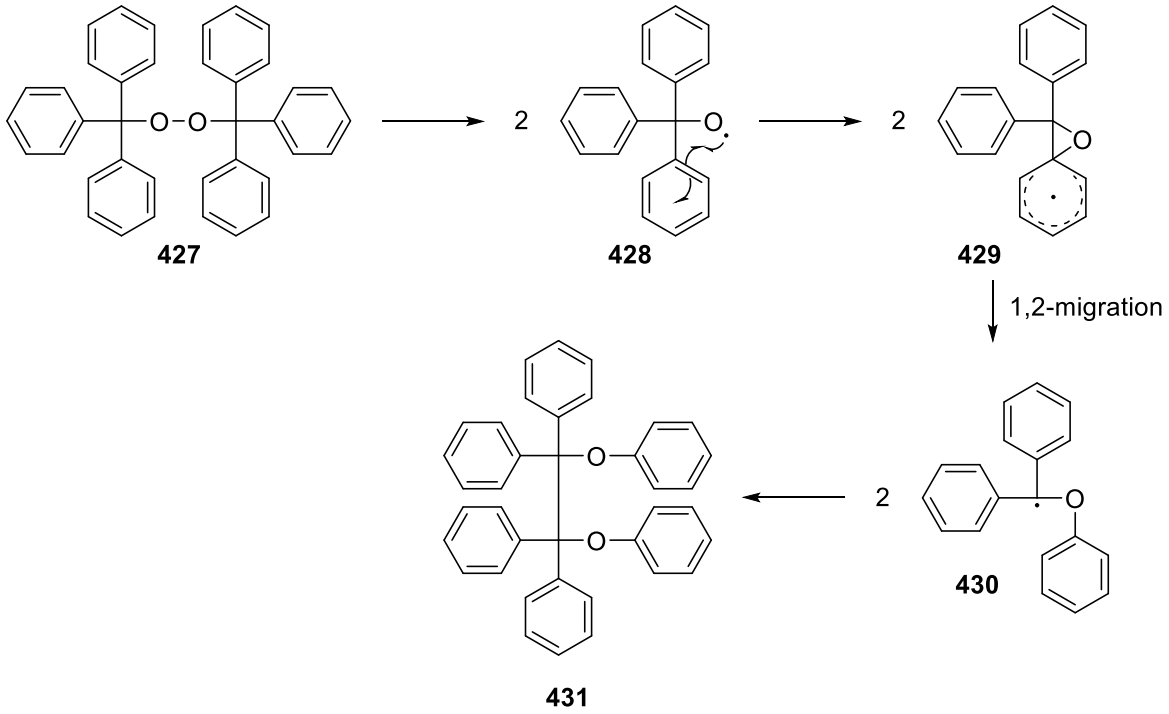

Scheme 88 - First example of a radical 1,2-aryl migration reported by Wieland in 1911

[170] H. Wieland, *Ber. Dtsch. Chem. Ges.* **1911**, *44*, 2550–2556.

1.2. Nomenclature

The nomenclature of rearrangement reactions relies on two numbers, separated by a coma which, to put it simply, represents the number of bonds between the group about to migrate and the atom where it will migrate. It also relies on the nature of the atom carrying the migrating group and the nature of the one receiving it (Scheme 89).

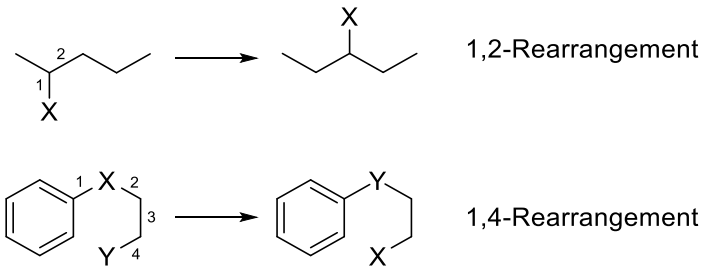

Scheme 89 - Examples of different types of rearrangement reactions

C) State of the art

As shown above, reactions involving an intramolecular aryl migration have been known for more than a century and they have been studied ever since. In this section, we are not going to make an exhaustive presentation of all the existing reports in the field of intramolecular aryl rearrangements, but we are going to present some of the most notable ones. They can be organized into two families: the ionic-type rearrangement and the radical-type rearrangement. To reach another level of detail, the ionic-type rearrangements can be further divided into different subfamilies: the rearrangements induced by anionic/basic/electron-rich sites and the rearrangements induced by cationic/electron-poor sites. The neutral rearrangements will not be tackled in this manuscript because of the vastness of notions associated with the electrocyclic and sigmatropic reactions.[171]

1. Anionic-type aryl rearrangement

Justus Von Liebig was the first chemist to report an actual aryl migration, almost two centuries ago.[172] The benzylic acid rearrangement that he described is an anionic-type rearrangement. Another notable rearrangement is a reaction derived from the Favorskii rearrangement and called the Quasi-Favorskii rearrangement, a type of semipinacol rearrangements.[173] The standard Favorskii rearrangement (Scheme 90) implies an enolate intermediate **433** formed after a deprotonation step,

[171] S. Thompson, A. G. Coyne, P. C. Knipe, M. D. Smith, *Chem. Soc. Rev.* **2011**, *40*, 4217–4231C. W. Spangler, *Chem. Rev.* **1976**, *76*, 187–217E. A. Ilardi, C. E. Stivala, A. Zakarian, *Chem. Soc. Rev.* **2009**, *38*, 3133–3148.
[172] J. Liebig, *Ann. Pharm.* **1838**, *25*, 1–31.
[173] Z.-L. Song, C.-A. Fan, Y.-Q. Tu, *Chem. Rev.* **2011**, *111*, 7523–7556.

followed by the formation of a cyclopropane **434** concomitant with the nucleophilic substitution of a halide. This reaction was reported in 1894 and named after the Russian chemist who discovered it.[174]

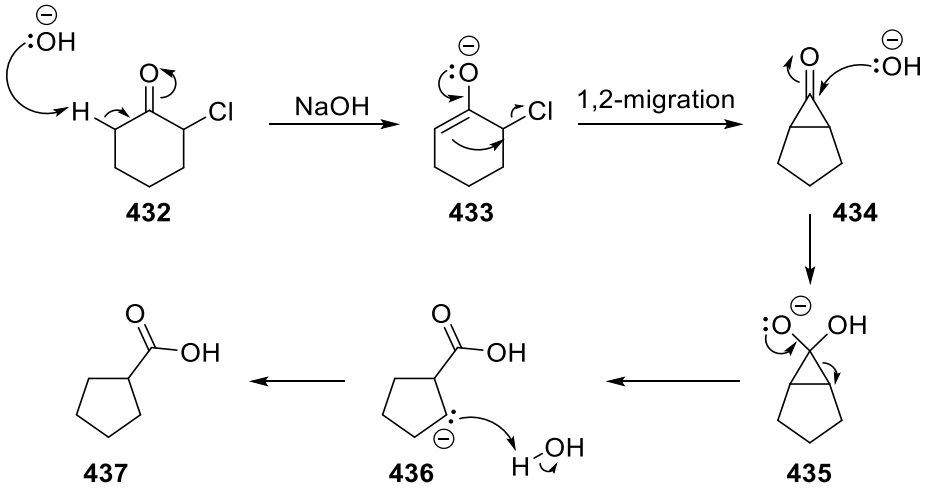

Scheme 90 - Mechanism of the Favorskii rearrangement

For starting materials lacking the α-proton (enolization not possible), or suffering from steric hindrance or simply when the formation of the enolate is not favored, the Quasi-Favorskii rearrangement is preferred, leading to a 1,2-migration of an aryl after a nucleophilic attack onto the carbonyl function. Although it was not recognized as such back in 1903, Tiffeneau was the first chemist to report this rearrangement, using 1-chloropropan-2-one **438** and phenyl magnesium bromide, as a nucleophile, to form 1-phenylpropan-2-one **440** (Scheme 91).[175]

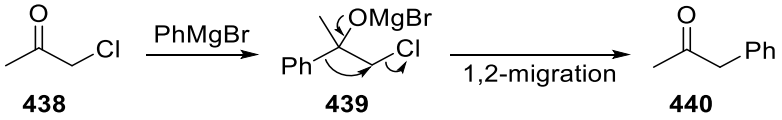

Scheme 91 – Mechanism of the Quasi-Favorskii rearrangement

2. Cationic-type aryl rearrangement

Contrary to the anionic-type rearrangement, there is a greater number of reports of cationic-type rearrangement. These reports started in the 19th century with, for instance, the description of a pinacol (**441**)-pinacolone (**443**) rearrangement in 1860 by Fittig (Scheme 92).[176] Unfortunately, at that time, the concept of intramolecular migration in organic chemistry was still unknown and Fittig was unable to find the correct structure of the pinacolone. It took 13 years to finally elucidate the correct structure after that Aleksandr Butlerov understood that carbon atoms could migrate within an intramolecular

[174] A. Y. Favorskii, *Journal of the Russian Physical and Chemical Society* **1894**, *26*, 590.
[175] M. Tiffeneau, *Comptes rendus hebdomadaires des séances de l'Académie des sciences* **1903**, *137*, 989–991.
[176] R. Fittig, *Ann. Chem. Pharm.* **1860**, *114*, 54–63.

scaffold.[177] Although this example does not include an aryl migration step, it is worth noting that it is part of a larger family of carbocationic 1,2-rearrangement reactions called Wagner-Meerwein reactions. These reactions include a 1,2-migration of hydrogen atom, alkyl or aryl groups from a carbon to a neighbor carbocation (Scheme 93).

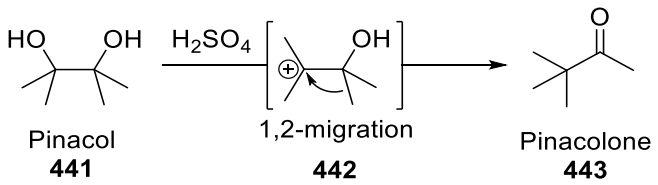

Scheme 92 - Pinacol rearrangement

In 1925, Tiffeneau reported a Wagner-Meerwein rearrangement including an aryl-migration (Scheme 93).[178] This reaction is possible in an acidic medium, leading to a dehydration of an alcohol **445** and the obtention of a carbocation **446**, followed by a 1,2-aryl migration on this carbocation.

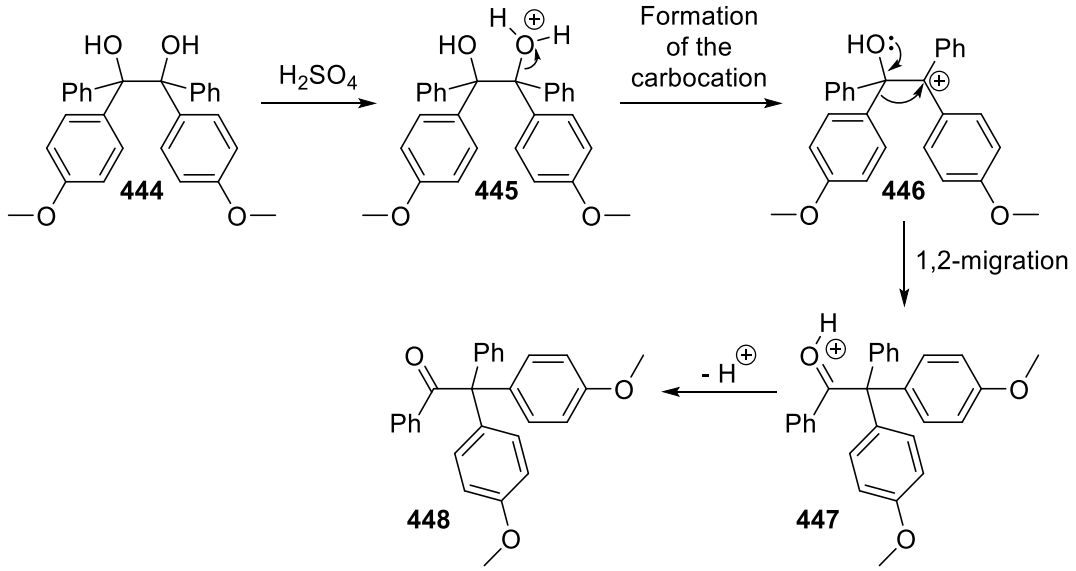

Scheme 93 – Mechanism of the Wagner-Meerwein rearrangement reported by Tiffeneau

In addition to rearrangements onto electron-deficient carbons, rearrangement onto electron-deficient nitrogens and oxygens are also possible with the Beckmann rearrangement and the Baeyer-Villiger rearrangement, respectively.

Indeed, Ernst Otto Beckmann reported a cationic-type migration in 1886 (Scheme 94).[179] His work led to the establishment of a single-step transformation of oximes **449** into functionalized amides **456**

[177] A. Butlerow, *Justus Liebigs Ann. Chem. Pharm.* **1873**, *170*, 151–162.
[178] M. Tiffeneau, *Bull. Soc. Chim. Fr.* **1925**, *4*, 437.
[179] E. Beckmann, *Ber. Dtsch. Chem. Ges.* **1886**, *19*, 988–993.

and is still employed notably on an industrial scale to synthesize caprolactam and laurolactam, respectively used as precursors for the synthesis of Nylon 6 and Nylon 12, on a 5 million tons scale each year.[180] Moreover, a year later, he reported in a second communication the migration of an aryl group under acidic conditions.

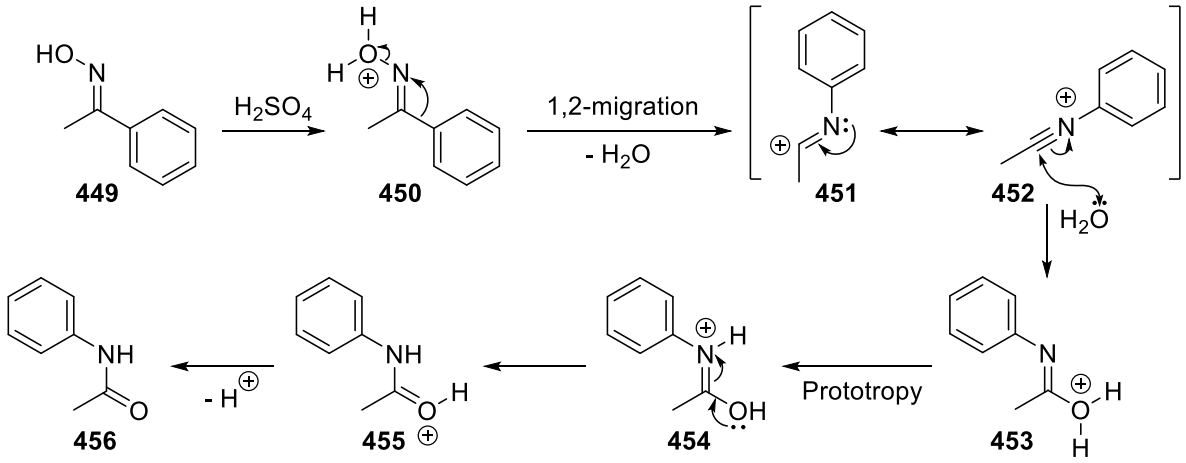

Scheme 94 - Mechanism of the Beckmann rearrangement

The last example that will be tackled in this part is the Baeyer-Villiger rearrangement or oxidation. It is named after the two chemists who first described it in 1899 (Scheme 95).[181] During this reaction, a peracid **458** is used to perform a nucleophilic attack on a carbonyl group **459**, yielding the Criegee intermediate **460**. Then, following a concerted mechanism, one of the substituents of the carbonyl group migrates onto the oxygen of the peroxyacid with a concomitant loss of a carboxylic acid. An aryl group can migrate through this process such as a phenyl group in the example.[182]

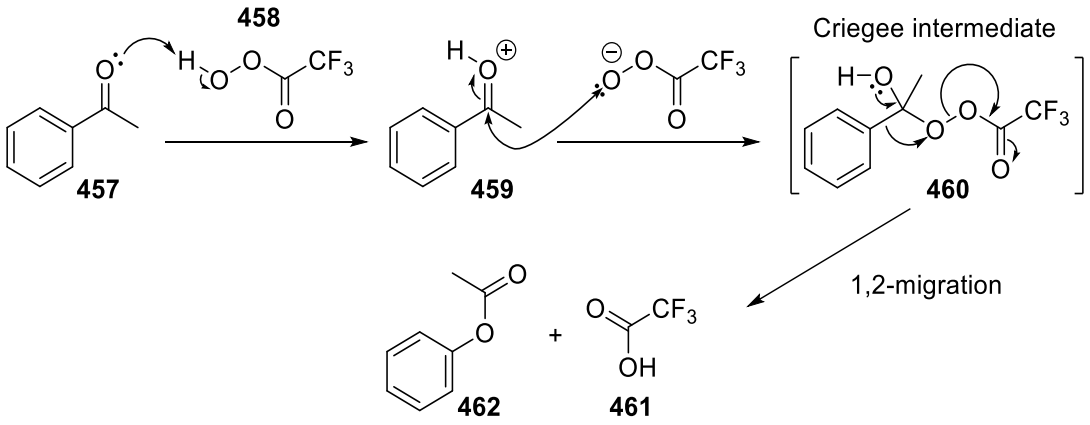

Scheme 95 - Mechanism of the Baeyer-Villiger rearrangement

[180] J. Tinge, M. Groothaert, H. op het Veld, J. Ritz, H. Fuchs, H. Kieczka, W. C. Moran, in *Ullmann's Encyclopedia of Industrial Chemistry*, Wiley-VCH Verlag GmbH & Co. KGaA, Weinheim, Germany, **2018**, pp. 1–31.
[181] A. Baeyer, V. Villiger, *Ber. Dtsch. Chem. Ges.* **1899**, *32*, 3625–3633.
[182] E. E. Smissman, J. P. Li, Z. H. Israili, *J. Org. Chem.* **1968**, *33*, 4231–4236.

3. Radical-type aryl rearrangement

To continue, it is important to note that we will only tackle here radical 1,2-; 1,3-; 1,4- and 1,5-aryl migration reactions. We will start this part by some notable examples of radical 1,2-aryl migrations (Scheme 96).

3.1. Radical 1,2-aryl migrations

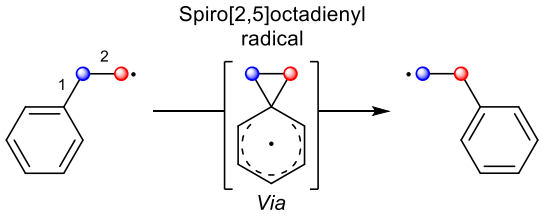

Scheme 96 - General scheme of a radical 1,2-aryl migration

As presented above, Heinrich Otto Wieland was the first chemist to report a radical-type rearrangement that also appeared to be an aryl-migration (Scheme 88). To date, it remains one of the few examples of radical 1,2-aryl migration from a carbon to an oxygen atom. Another important example of a radical-type aryl rearrangement is the neophyl rearrangement (Scheme 97). It is named after the reagent used to first report this reaction (neophyl chloride **463**) and was reported in 1944 by Urry and Kharasch.[183] Although being the most famous radical aryl migration reaction, mechanistic studies to understand its mechanism lasted for decades.

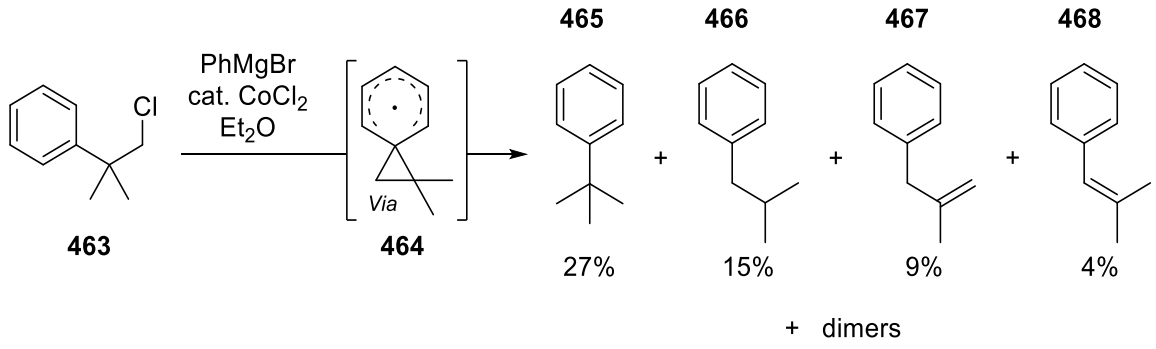

Scheme 97 - Neophyl rearrangement as first reported by Urry and Kharasch

Indeed, there is a controversy around the spiro[2,5]octadienyl radical **464** and whether it is an intermediate or a transition state in this reaction. After being first detected *via* fluorescence

[183] W. H. Urry, M. S. Kharasch, *J. Am. Chem. Soc.* **1944**, *66*, 1438–1440.

spectroscopy on a similar reaction,[184] finally this radical existence was proven after it self-combined into an isolable dimer **471** (Scheme 98).[185]

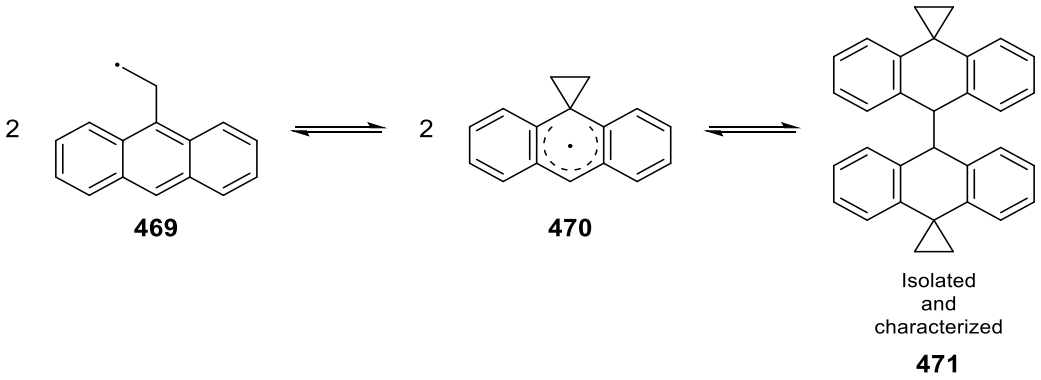

Scheme 98 - Evidence of the existence of the spiro[2,5]octadienyl radical

Moreover, quantitative DFT calculations were performed in 2001 and supported the hypothesis that the spiro[2,5]octadienyl radical **464** is a short-lived intermediate rather than a transition state.[186] It is worth noting that this rearrangement is a 1,2-aryl migration reaction and some variations of this reaction have been reported, like the thia-neophyl-type rearrangement described by Franz *et al.* in 1992 (Scheme 99).[187]

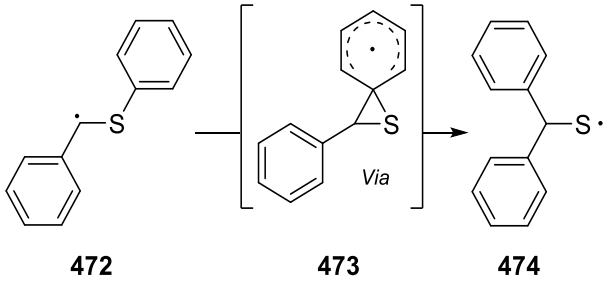

Scheme 99 - Thia-neophyl-type rearrangement reported by Franz and coworker

The study of the neophyl rearrangement led to the measure of its rate constant *k* and is now used as a radical clock. This designation has been first employed by Griller and Ingold when they first published their seminal work in the establishment of this new method.[188] Radical clocks are used to determine the kinetics of free-radical reactions by employing a molecule (the radical clock itself) that reacts at a known rate and is used as a calibration for determining the unknown rate of another reaction.

---

[184] A. Effio, D. Griller, K. U. Ingold, J. C. Scaiano, S. J. Sheng, *Journal of the American Chemical Society* **1980**, *102*, 6063–6068.
[185] R. Leardini, G. Zanardi, E. Foresti, P. Palmieri, **1989**, *111*, 7723–7732.
[186] A. Asensio, J. J. Dannenberg, *J. Org. Chem.* **2001**, *66*, 5996–5999.
[187] M. S. Alnajjar, J. A. Franz, *J. Am. Chem. Soc.* **1992**, *114*, 1052–1058.
[188] D. Griller, K. U. Ingold, *Acc. Chem. Res.* **1980**, *13*, 317–323.

The first example of a radical 1,2-aryl migration from a carbon to a nitrogen atom was described by Kim *et al.* in 1995 (Scheme 100).[189] They reported the migration of aryl, furanyl and thiophenyl groups onto an azide moiety with the use of classical radical initiators (Bu_3SnH, AIBN).

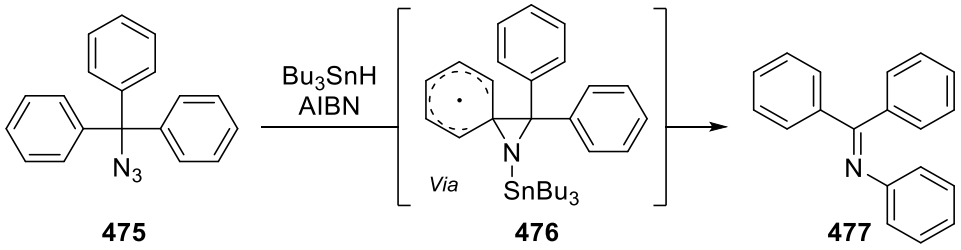

Scheme 100 - Radical 1,2-aryl migration reaction reported by Kim et al.

3.2. Radical 1,3-aryl migrations

We are now going to tackle the radical 1,3-aryl migrations (Scheme 101).

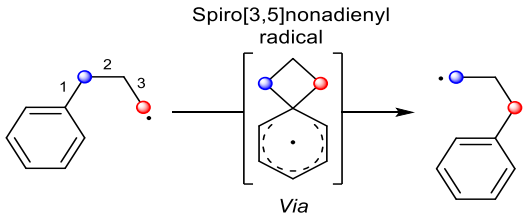

Scheme 101 - General scheme of a radical 1,3-aryl migration

To the best of our knowledge, only two examples of radical 1,3-aryl migration are known. This few number of reports is due to the difficulty to form a strained four-membered spiro-radical intermediate or even as a transition state. The first one was reported by Zard and coworkers in 2005 (Scheme 102).[190] They described the use of xanthate derivatives as radical precursor for this reaction,[191] employing *N*-(α-xanthyl)-acetylaminopyridines **478** under the presence of peroxides. Once the carbon-centered radical is formed, it can react with the aryl group and lead to the four-membered spiro-radical intermediate **479**. It is important to note that the formation of such strained intermediate is only possible thanks to the presence of a chlorine substitution on *ortho* to the amide bond and a *tert*-butyl substitution on the nitrogen atom of the amide. These substitutions result in a steric repulsion that forces the carbon-centered radical to move closer to the pyridine ring.

[189] S. Kim, J. Y. Do, *J. Chem. Soc., Chem. Commun.* **1995**, 1607–16082.
[190] E. Bacqué, M. El Qacemi, S. Z. Zard, *Org. Lett.* **2005**, *7*, 3817–3820.
[191] B. Quiclet-Sire, S. Z. Zard, *Pure and Applied Chemistry* **2010**, *83*, 519–551.

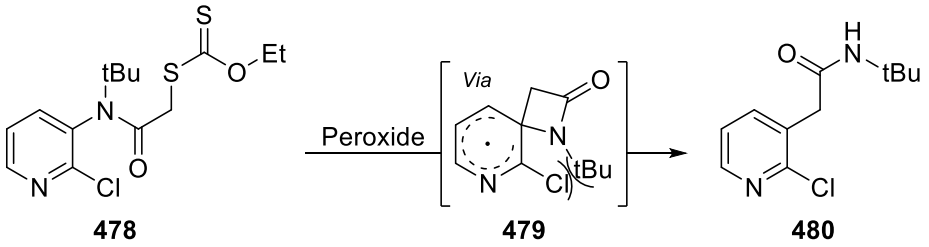

Scheme 102 - First example of a radical 1,3-aryl migration by Zard and coworkers.

The other example was reported in 2013 by Chen and Duan (Scheme 103).[192] In their work, they synthesized benzo[*b*]phosphole oxide derivatives **485** starting from diphenylphosphine oxide **481** and diphenylacetylene **24** under silver catalysis. This methodology yields two different products and one of them is proposed to be the result of a radical 1,3-aryl migration from a phosphorus to a carbon atom.

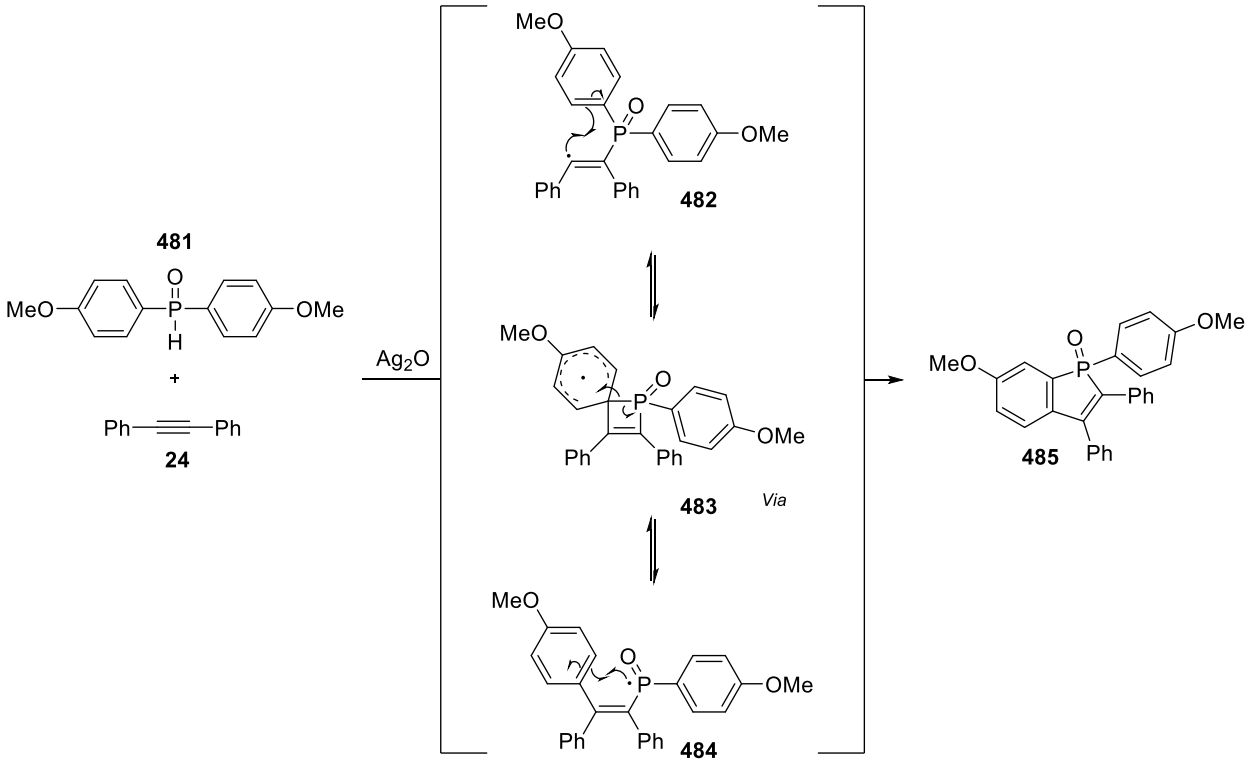

Scheme 103 - Second example of radical 1,3 aryl-migration reported by Chen and Duan

3.3. Radical 1,4-aryl migrations

Radical 1,4-aryl migrations are, with radical 1,2-aryl migrations, the most described rearrangement in the literature. We are now going to broach radical 1,4-aryl migration reactions (Scheme 104).

[192] Y.-R. Chen, W.-L. Duan, *J. Am. Chem. Soc.* **2013**, *135*, 16754–16757.

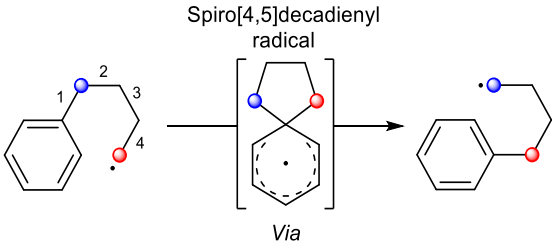

Scheme 104 - General scheme of a radical 1,4-aryl migration

The first example of a radical 1,4-aryl migration was reported in 1956 by Winstein *et al.* (Scheme 105).[193] Indeed, they described the radical decarbonylation of 5-methyl-5-phenylhexanal **486** that led to (4-methylpentyl)benzene **489** *via* a 1,4-aryl migration of the phenyl group. Here, the highly unstable primary radical **487** is immediately isomerized into the more stable tertiary radical through the formation of the spiro[4,5]decadienyl radical **488**.

The reaction is favored thanks to an anchimerically assisted ionization process, helping the formation of the unstable primary radical thanks to the assistance of the phenyl group which reacts with it.

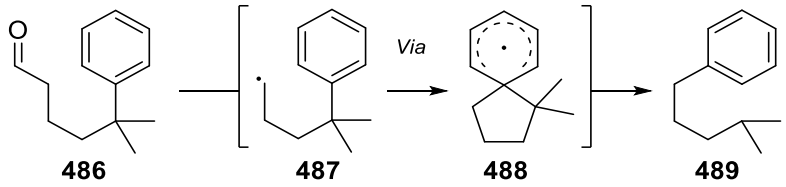

Scheme 105 – Radical 1,4-aryl migration reaction reported by Winstein et al.

This publication was shortly followed by the first example of a radical aryl-migration from a nitrogen to a carbon atom, reported by Hey *et al.* in 1959 (Scheme 106).[194] They described the generation of a carbon-centered radical after decomposition of a diazonium salt. This radical was then capable to react with an aryl present on the molecule, to form a spiro radical intermediate **491**, and yield a 1,4-aryl migration product **492**.

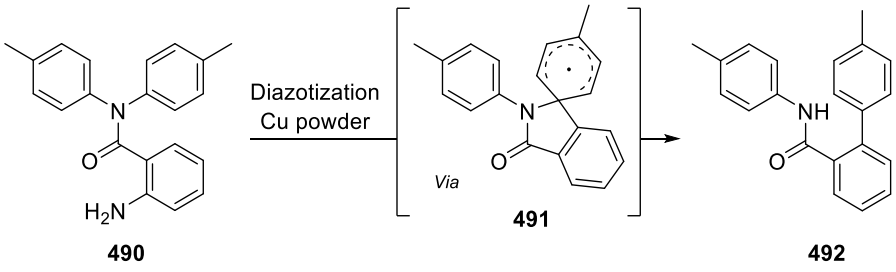

Scheme 106 - Radical 1,4-aryl migration reaction reported by Hey et al.

[193] S. Winstein, R. Heck, S. Lapporte, R. Baird, *Experientia* **1956**, *12*, 138–141.
[194] D. H. Hey, T. M. Moynehan, *J. Chem. Soc.* **1959**, 1563–1572.

Another example including a heteroatom was reported by Bachi *et al.* in 1992 with the radical 1,4-aryl migration from an oxygen to a carbon atom (Scheme 107).[195] After the generation of the stannyl radical (from Bu_3SnH and AIBN), it can add onto the sulfur atom of the carbonothioate derivative **493**. Then a 5-*exo*-trig cyclization occurs and yields a carbon-centered intermediate which reacts with the neighbor aryl in order to yield a lactone **495**, the 1,4-aryl migration product.

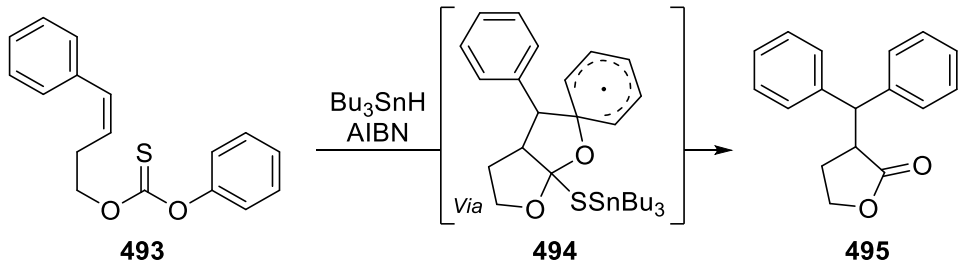

Scheme 107 - Radical 1,4-aryl migration reaction reported by Bachi et al.

Less common heteroatoms like silicon can be involved in radical aryl migrations as well, as in the report of Wilt and coworker in 1970 (Scheme 108).[196] After the generation of the primary carbon-centered radical using di-*tert*-butyl peroxide (DTBP), the formation of a spiro[4,5]decadienyl radical **497** is possible and leads to the 1,4-phenyl migration from the silicon to the carbon atom. Interestingly, this reaction is versatile and can lead to a 1,5-aryl migration as well when the alkyl chain separating the silicon and the carbon radical is one carbon longer.

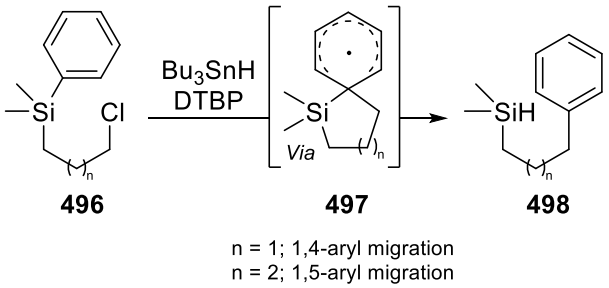

Scheme 108 - Radical 1,4- and 1,5-aryl migration reaction reported by Wilt and coworkers

3.4. Radical 1,5-aryl migrations

To finish, we will tackle the radical 1,5-aryl migration reactions (Scheme 109).

[195] M. D. Bachi, E. Bosch, D. Denenmark, D. Girsh, *J. Org. Chem.* **1992**, *57*, 6803–6810.
[196] J. W. Wilt, C. F. Dockus, *J. Am. Chem. Soc.* **1970**, *92*, 5813–5814.

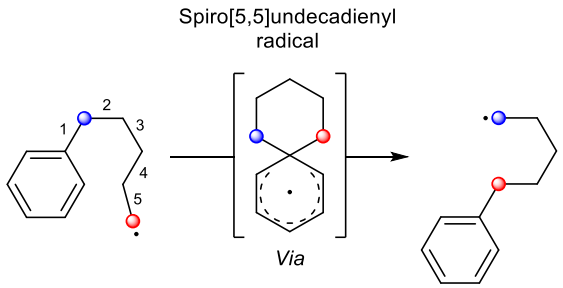

Scheme 109 - General scheme of a radical 1,5-aryl migration

Examples of radical 1,5-aryl migration have been reported between two carbon atoms or from an oxygen to a carbon atom. Giraud *et al.* reported in 1997 a method to prepare biaryls **501** starting from aryl bromide derivatives **499** (Scheme 110).[197] The carbon-centered radical is formed, after the action of Bu_3SnH and AIBN on Ar-Br, and it then undergoes an *ipso*-substitution to yield the 1,5-aryl migration product.

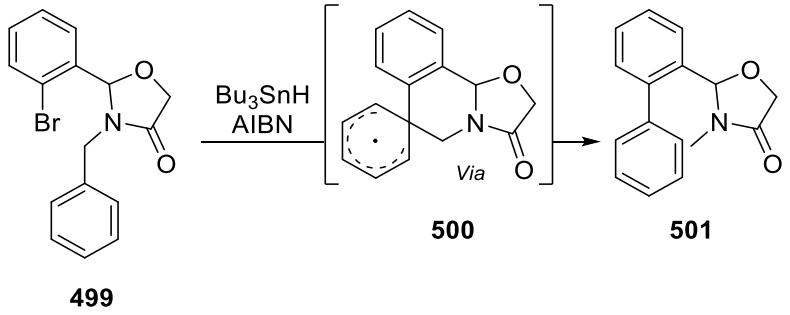

Scheme 110 - Radical 1,5-aryl migration reaction reported by Giraud et al.

The first example of a radical 1,5-aryl migration from an oxygen to a carbon was described by Guidotti *et al.* in 1995[198] and allowed the preparation of benzophenone derivatives **358** (Scheme 111). Under the action of diisopropyl peroxydicarbonate (DPDC), an imidoyl radical can be obtain and can perform an intramolecular *ipso*-substitution and yield a phenoxyl radical. The latter can further be reduced and after a hydrolysis of **504**, the desired benzophenone **358** is obtained.

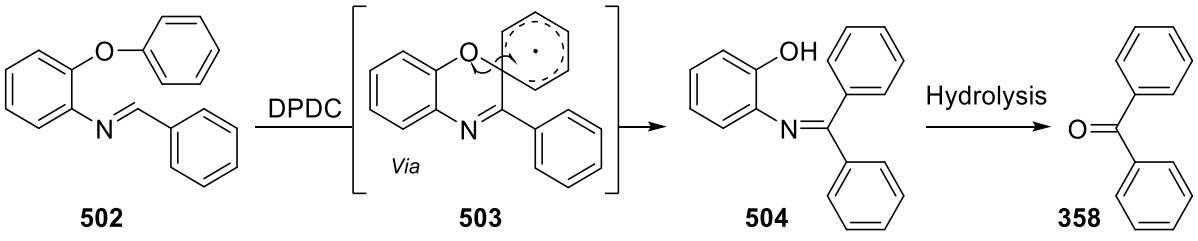

Scheme 111 - Radical 1,5-aryl migration reaction reported by Guidotti et al.

[197] L. Giraud, E. Lacôte, P. Renaud, *HCA* **1997**, *80*, 2148–2156.
[198] S. Guidotti, R. Leardini, D. Nanni, P. Pareschi, G. Zanardi, *Tetrahedron Letters* **1995**, *36*, 451–454.

To finish, 1,5-aryl migrations from a phosphorus atom to a carbon nucleus were reported for the first time by Clive and Kang in 2000,[199] and extended in 2001 (Scheme 112).[200] They remain, to the best of our knowledge, the only examples of such radical rearrangement in the literature. They reported the use of the classic chemical radical initiator couple Bu_3SnH and AIBN in their seminal work in order to obtain a 1,5-aryl migration. Indeed, when using phosphinate derivatives **505** presenting an aryl-bromine bond, they discovered that after the reduction of the C-Br bond and the obtention of a phenyl radical, a reaction was possible with one of the phenyl atoms present on the phosphinate moiety.

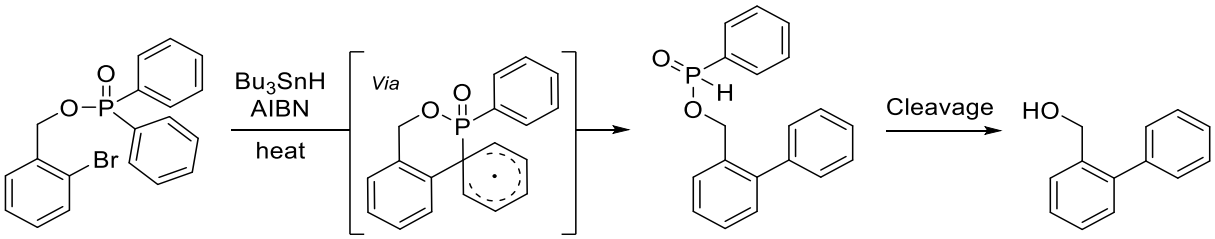

Scheme 112 - Radical 1,5-aryl migration reaction reported by Clive and Kang

This work will also be discussed later in the development of this chapter.

When looking at all these examples, we can clearly see a trend. Indeed, the radicals are, in general, obtained using conventional reagents such as Bu_3SnH/AIBN. Starting from the 2010s, a new tendency appeared alongside the booming of visible-light catalysis, a technique relying on single electron transfers induced by excited-state photocatalysts. In other words, the method to generate the reactive radical intermediates changed but the concept remains the same. Thus, reports in the field of radical aryl migration continued with the development of new innovative methodologies.

3.5. Visible-light catalyzed radical 1,2-aryl migration

We will start with the visible-light catalyzed radical 1,2-aryl migration reactions. The first example of such reaction was reported by Huang *et al.* in 2015 (Scheme 113).[201] Indeed, they reported the first example of visible-light photocatalyzed arylation of alkenes *via* a radical addition followed by the 1,2-aryl migration. This reaction relies on the use of an *α*,*α*-diphenyl allylic alcohol molecule **509** which undergoes an addition from a radical $R^{3\bullet}$ formed *in situ*. In the reaction reported by Huang et al. the added radical is a malonate one **511**. It is worth noting that the few other examples of a 1,2-aryl migration induced under visible-light photocatalysis all relies on the same scaffold (*α*,*α*-diphenyl allylic alcohol **509**) and the parameters that differs is the type of radical being added on the alkene and the reactions conditions (different photocatalyst, solvent etc.). Other examples include the addition of an

[199] D. L. J. Clive, S. Kang, *Tetrahedron Letters* **2000**, *41*, 1315–1319.
[200] D. L. J. Clive, S. Kang, *J. Org. Chem.* **2001**, *66*, 6083–6091.
[201] H.-L. Huang, H. Yan, C. Yang, W. Xia, *Chem. Commun.* **2015**, *51*, 4910–4913.

acetophenone radical **512** (Li *et al.*[202]), a trifluoromethyl radical **513** (Cai et *al*.[203]), an *α*-sulfinyl radical **514** (Lu *et al*.[204]) or a cyanomethyl radical **515** (Wang *et al*.[205]) as represented in the general Scheme 113:

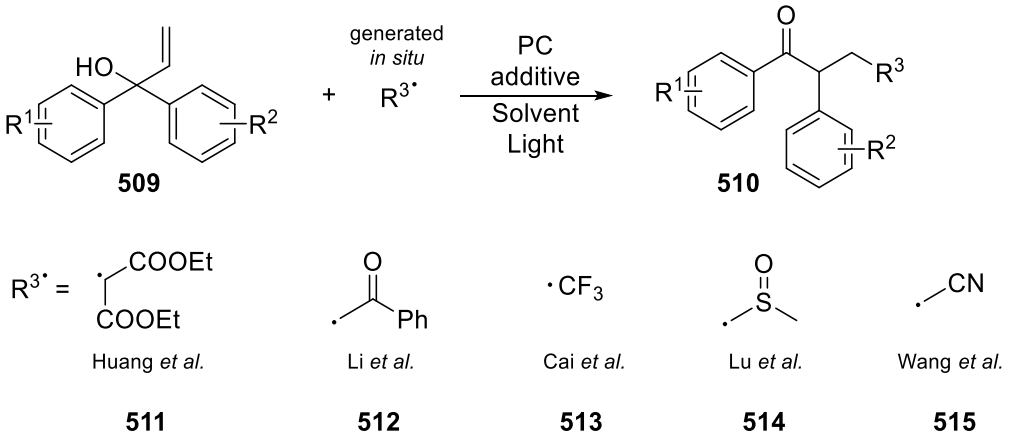

Scheme 113 - General scheme of visible-light catalyzed radical 1,2-aryl migration reported by various groups

The mechanism of the reaction reported by Huang *et al.* is represented in Scheme 114. It is worth pointing out that all the other examples based on the same scaffold follow a similar mechanism after the radical addition. The reaction proceeds via a single electron transfer from the excited state of an Ir photocatalyst to diethyl bromomalonate **516**, leading to a reduction and concomitant generation of the carbon-centered malonate radical **511**. Then, the latter reacts with the *α*,*α*-diphenyl allylic alcohol **509**. A radical *ipso*-addition of one of the aryl group with the newly generated radical occurs, yielding a spiro[2,5]octadienyl radical intermediate **518** which leads to the formation of a benzyl radical **519**. The latter is oxidized by the photocatalyst, thus closing the catalytic cycle and leading to the desired product **520** along with the loss of a proton.

[202] Y. Li, B. Liu, X.-H. Ouyang, R.-J. Song, J.-H. Li, *Org. Chem. Front.* **2015**, *11*, 1457–1467.
[203] S. Cai, Y. Tian, J. Zhang, Z. Liu, M. Lu, W. Weng, M. Huang, *Adv. Synth. Catal.* **2018**, *360*, 4084–4088.
[204] M. Lu, H. Qin, Z. Lin, M. Huang, W. Weng, S. Cai, *Org. Lett.* **2018**, *20*, 7611–7615.
[205] Q.-L. Wang, Z. Chen, C.-S. Zhou, B.-Q. Xiong, P.-L. Zhang, C.-A. Yang, Y. Liu, Q. Zhou, *Tetrahedron Letters* **2018**, *59*, 4551–4556.

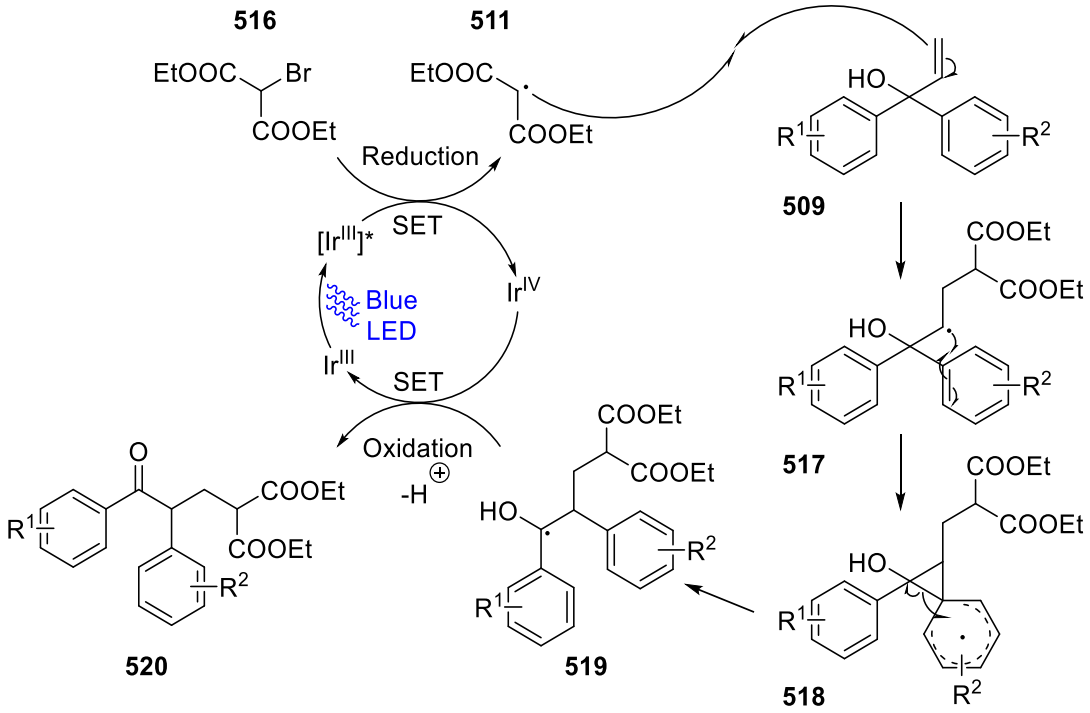

Scheme 114 - Mechanism of the visible-light photocatalyzed arylalkylation of alkenes reported by Huang et al.

As said previously, there are only very few examples of radical 1,3-aryl migration. In fact, only few groups published their results (Zard, Chen and Duan). It is therefore not surprising to notice that, to the best of our knowledge, there is absolutely no example of such rearrangement induced by visible-light catalysis.

3.6. Visible-light catalyzed radical 1,4-aryl migration

1,4-aryl migration is also the most common type of reported rearrangement under visible-light catalyzed conditions. Most of the examples recently reported in the literature carry a sulfonamide or a sulfonyl group due to the facility of sulfur dioxide to be extruded during the reaction mechanism (similar to a decarboxylation). Its extrusion often happens after the formation of the spiro intermediate, leading to very interesting structural modification, in one step. One of the first example of such reaction under visible-light catalysis was reported by Zheng *et al.* in 2015 (Scheme 115).[206] Indeed, they reported a cascade of a trifluoromethylation reaction followed by a 1,4-aryl migration and a desulfonylation process. This elegant cascade allowed the preparation of various products such as oxindoles **528**, but also isoquinolinediones **529** (with CO instead of SO_2) and *α*-aryl-*β*-trifluoromethyl amides **530** (with *N*-aryl substitution). The reaction proceeds via the reduction of trifluoromethanesulfonyl chloride **521** into the corresponding trifluoromethyl radical **513**. The latter can perform a radical addition onto the alkene substrate and, after another radical addition and

[206] L. Zheng, C. Yang, Z. Xu, F. Gao, W. Xia, *J. Org. Chem.* **2015**, *80*, 5730–5736.

formation of a spiro intermediate **524**, lead to the obtention of a nitrogen-centered radical **525** with a concomitant release of SO_2 gas. This nitrogen-centered radical reacts in the *ortho* position of the aryl and, after an oxidation step and subsequent rearomatization, the desired product **528** is obtained. It is worth mentioning that this reaction is also compatible with a carbonyl group instead of the sulfonyl group leading to the formation of an imido derivative. When aryl-substituted nitrogen atoms are employed, the nitrogen radical does not engage in a radical addition onto the aryl and a HAT is favored, yielding an amido derivative.

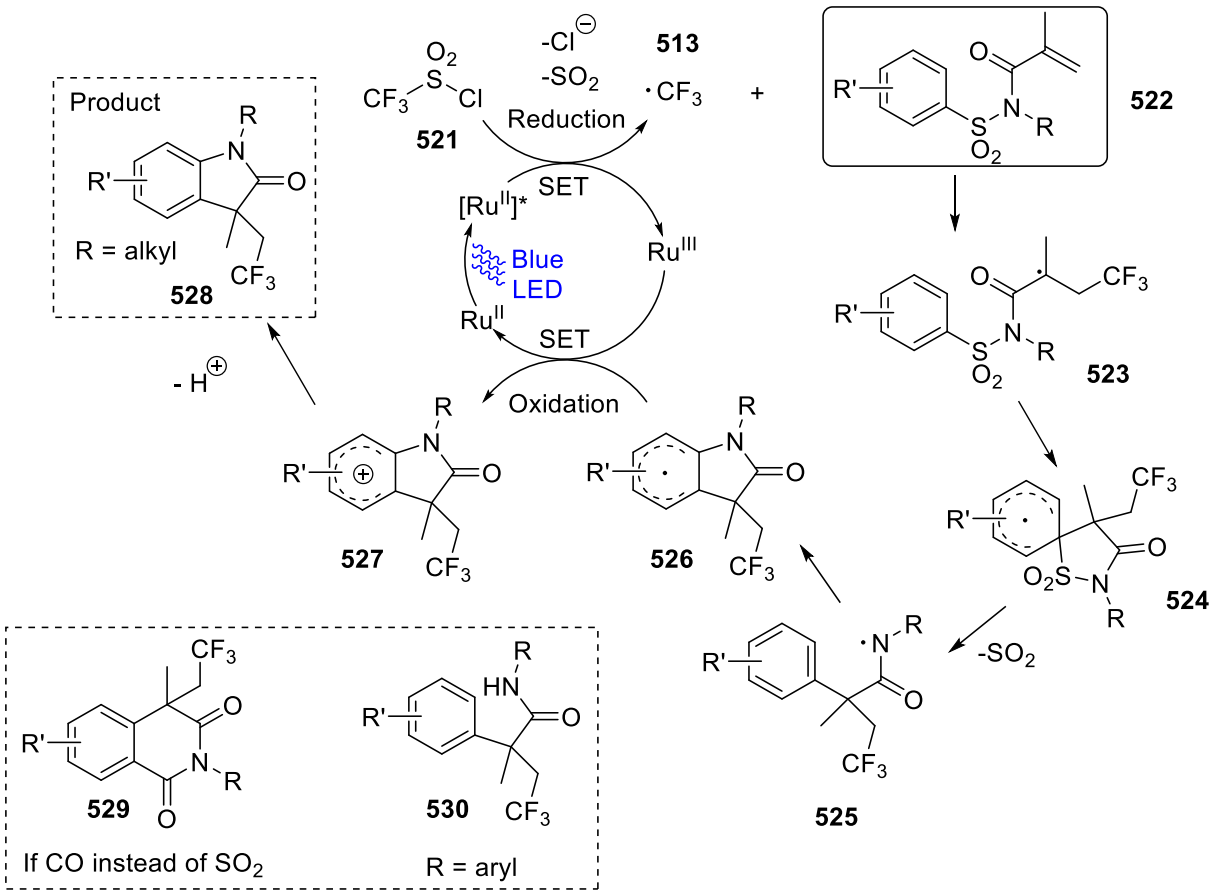

Scheme 115 - Mechanism of a cascade of a trifluoromethylation/1,4-aryl migration/desulfonylation reported by Zheng et al.

Other examples were also reported based on this approach. Zhang and coworkers[207] reported a reaction with the radical being generated from the reduction of a C-Br bond (Scheme 116).

[207] Y. Li, B. Hu, W. Dong, X. Xie, J. Wan, Z. Zhang, *J. Org. Chem.* **2016**, *81*, 7036–7041.

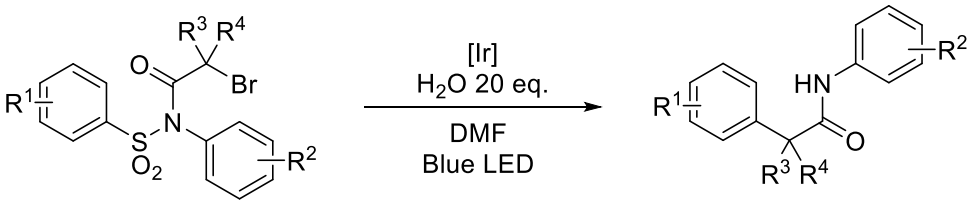

531 **532**

Scheme 116 - Visible-light catalyzed radical aryl-migration reported by Zhang and coworkers

Some variations on the starting material were also reported such as the presence of an alkynyl group, in the *ortho* position of the sulfonamide. The alkyne adds an extra level of complexity on the final scaffold, allowing the formation of elaborated structures in a cascade reaction. Close to the work of Zhang *et al.*, Huang *et al.*[208] reported the cascade reaction of 1,8-enynes **534** leading to a highly functionalized tetracyclic N-fused indolo[2,1-*a*]isoquinolin-6(5H)-one scaffold **536** (Scheme 117). Following their previous work, Zhang's team added an alkynyl group on their scaffold.[209] Their work is represented in Scheme 117 and Scheme 118 and the reaction mechanism also applies to the reaction reported by Huang *et al.* The reaction starts with a single electron transfer from the excited state of the Ir photocatalyst, leading to the reduction of the C-Br bond of **533** and the generation of a carbon-centered radical **537**. The latter can perform a radical addition in the *ortho* position of the alkyne, yielding a spiro intermediate **538**. After a rearrangement and release of SO_2 gas, a nitrogen centered radical **539** is obtained and can readily react with the alkyne present in the molecule in a 6-*exo*-dig fashion. The carbon-centered radical **540** obtained after this step can perform an ortho radical addition with the aromatic ring present on the nitrogen atom and yield the desired product **543** after an oxidation from the photocatalyst that also closes the catalytic cycle. The reaction reported by Huang *et al.* only differs from the fact that the first radical is generated from the reduction of ethyl bromodifluoroacetate **535** which leads to a carbon-centered radical that reacts with the alkene group present on the starting material **534**.

[208] H. Huang, Y. Li, *J. Org. Chem.* **2017**, *82*, 4449–4457.
[209] X. Gao, C. Li, Y. Yuan, X. Xie, Z. Zhang, *Org. Biomol. Chem.* **2020**, *18*, 263–271.

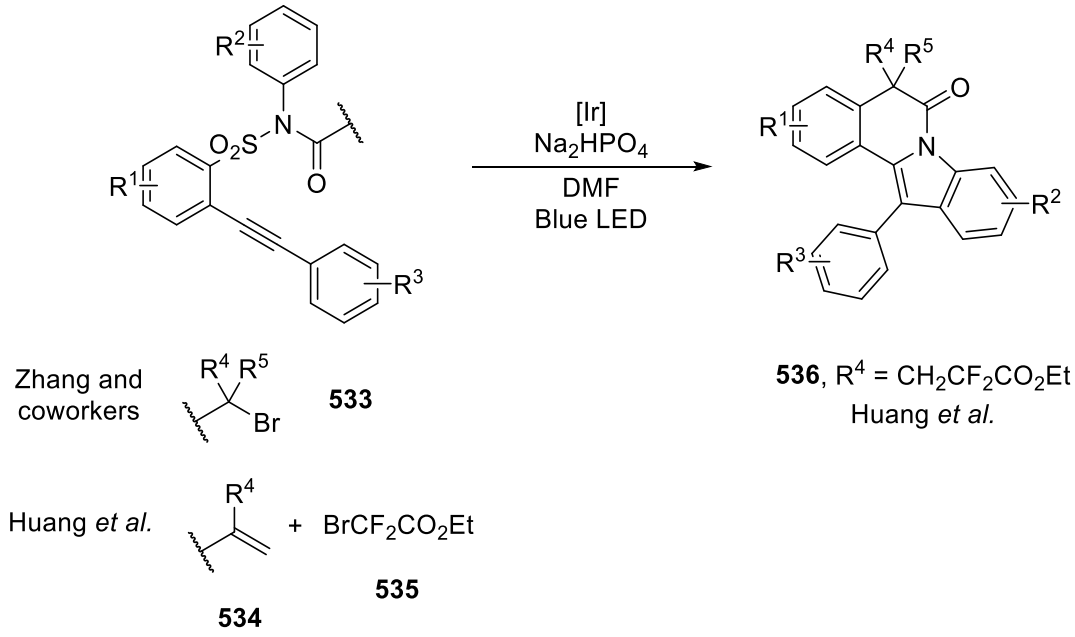

Scheme 117 - Visible-light catalyzed radical aryl-migration reported by Zhang and coworkers and Huang et al.

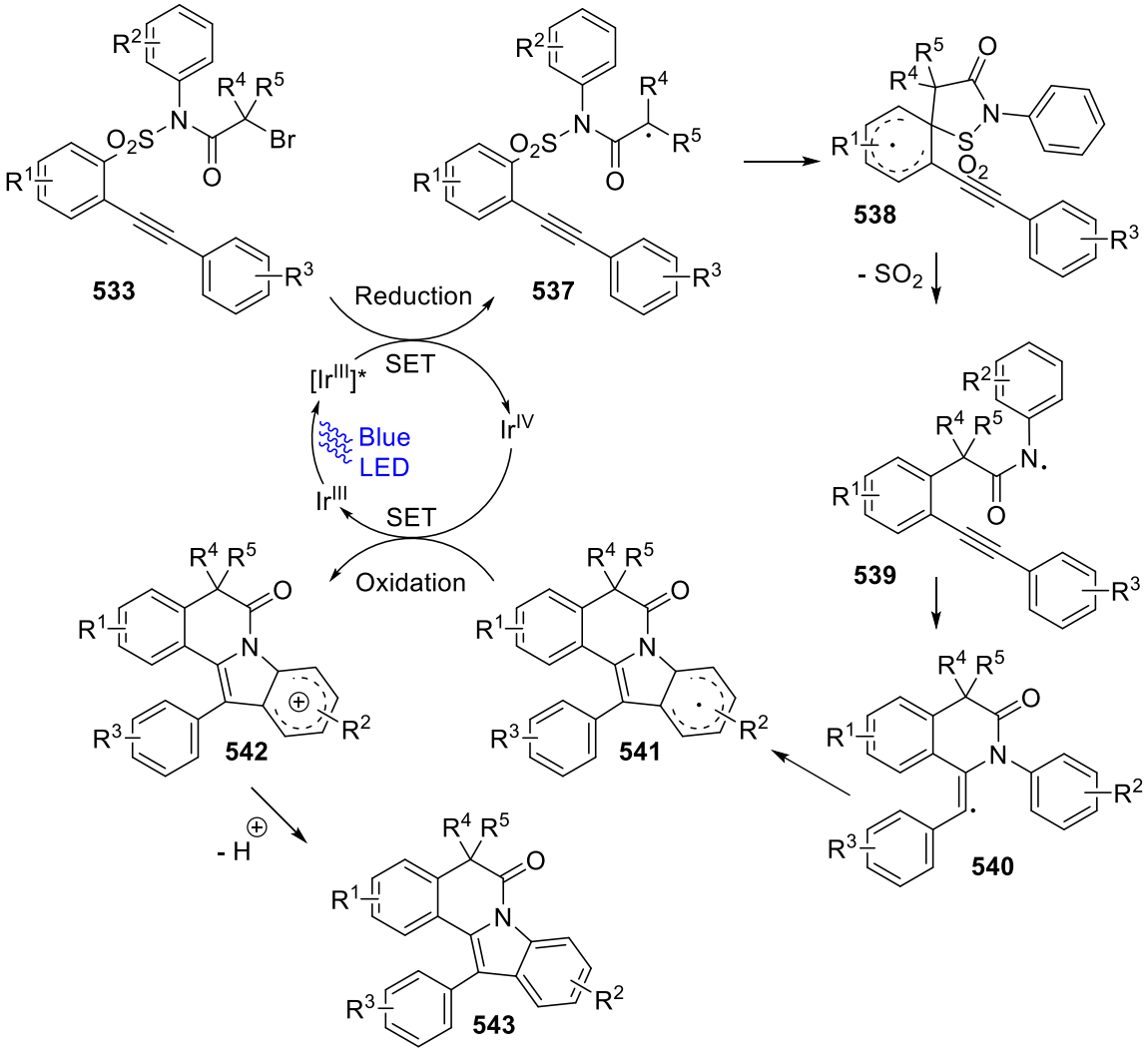

Scheme 118 - Mechanism of the reaction reported by reported by Zhang and coworkers

Stephenson and coworkers reported in 2015 the visible-light catalyzed radical 1,4-aryl migration of 2-bromo-2,2-difluoroethyl arylsulfonate **544** into the corresponding 2,2-difluoro-2-arylethanol **545** (Scheme 119).[210] The reactions proceed in a similar fashion to the reaction reported by Zhang *et al.* a few months earlier with, at first, the generation of the radical intermediate, via a reduction, followed by the radical 1,4-aryl migration concomitant with the loss of sulfur dioxide. This reaction is of particular interest because Stephenson's team showed that it was possible to access 2,2-difluoro-2-(thiophen-2-yl)ethanol **546** on a gram-scale, with extremely low catalytic loading (up to 0.01% of ruthenium photocatalyst) and in very short reaction times. This molecule could be then further modified in order to form the desired difluoro-substituted spirocyclic thiophene derivative **547** that can be used to treat depression and/or obesity.

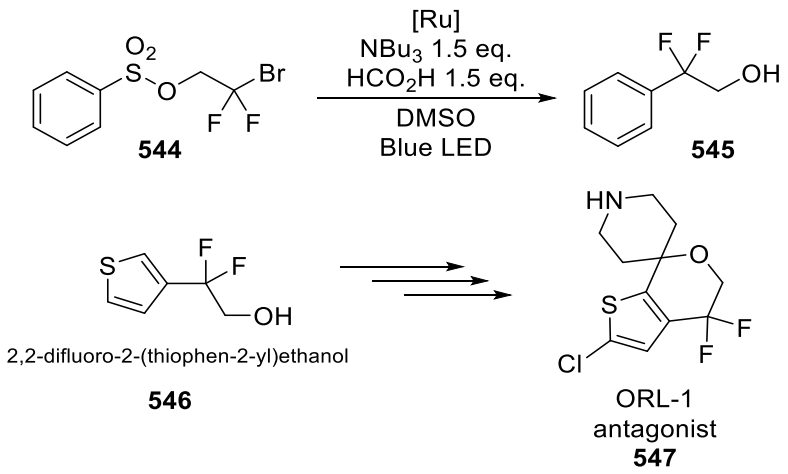

Scheme 119 – Visible-light catalyzed radical aryl-migration reported by Stephenson and coworkers and synthesis of a scaffold of interest using their methodology

Later, Stephenson's team reported a diastereoselective alkene aminoarylation based on the intermolecular reaction of an alkene group and an arylsulfonylacetamide derivative (Scheme 120).[211] After the one-electron oxidation of the alkene derivative **548**, an addition of the arylsulfonylacetamide **549** allow the formation of the key radical intermediate **550**, responsible for 1,4-aryl migration with a concomitant loss of sulfur dioxide.

[210] J. J. Douglas, H. Albright, M. J. Sevrin, K. P. Cole, C. R. J. Stephenson, *Angewandte Chemie International Edition* **2015**, *54*, 14898–14902.
[211] T. M. Monos, R. C. McAtee, C. R. J. Stephenson, *Science* **2018**, *361*, 1369–1373.

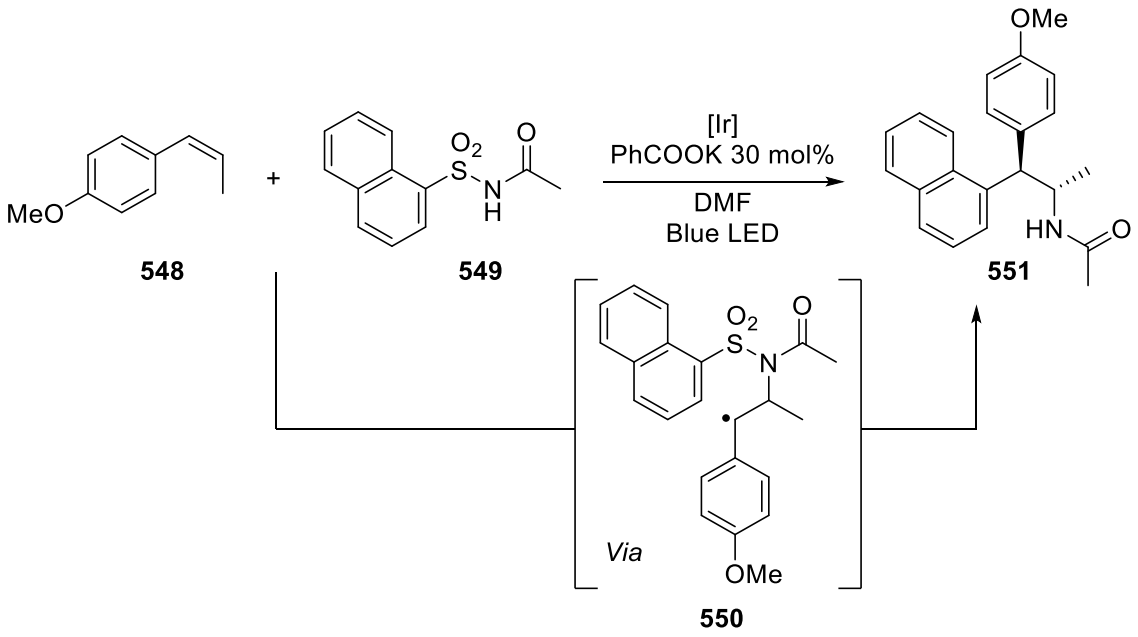

Scheme 120 - Visible-light catalyzed radical aryl-migration reported by Stephenson and coworkers

Other teams developed methodologies without using a sulfonyl group as a key functional group. Indeed, Nevado's group reported in 2016 a work allowing the γ-functionalization of amines via a C(sp^3)-C(sp^2) bond cleavage and the formation of a C(sp^3)-C(sp^3) bond (Scheme 121).[212] The reactions at first proceeds via a single-electron oxidation of the anionic amine **553** in order to yield the key *N*-centered radical **554**. Then, a 1,4-aryl migration leads to another radical intermediate **556**, on a carbon this time. The latter can react with an alkene **557**, leading to the desired compound **559** after the loss of a benzenesulfonyl radical **560**.

[212] W. Shu, A. Genoux, Z. Li, C. Nevado, *Angew. Chem. Int. Ed.* **2017**, *56*, 10521–10524.

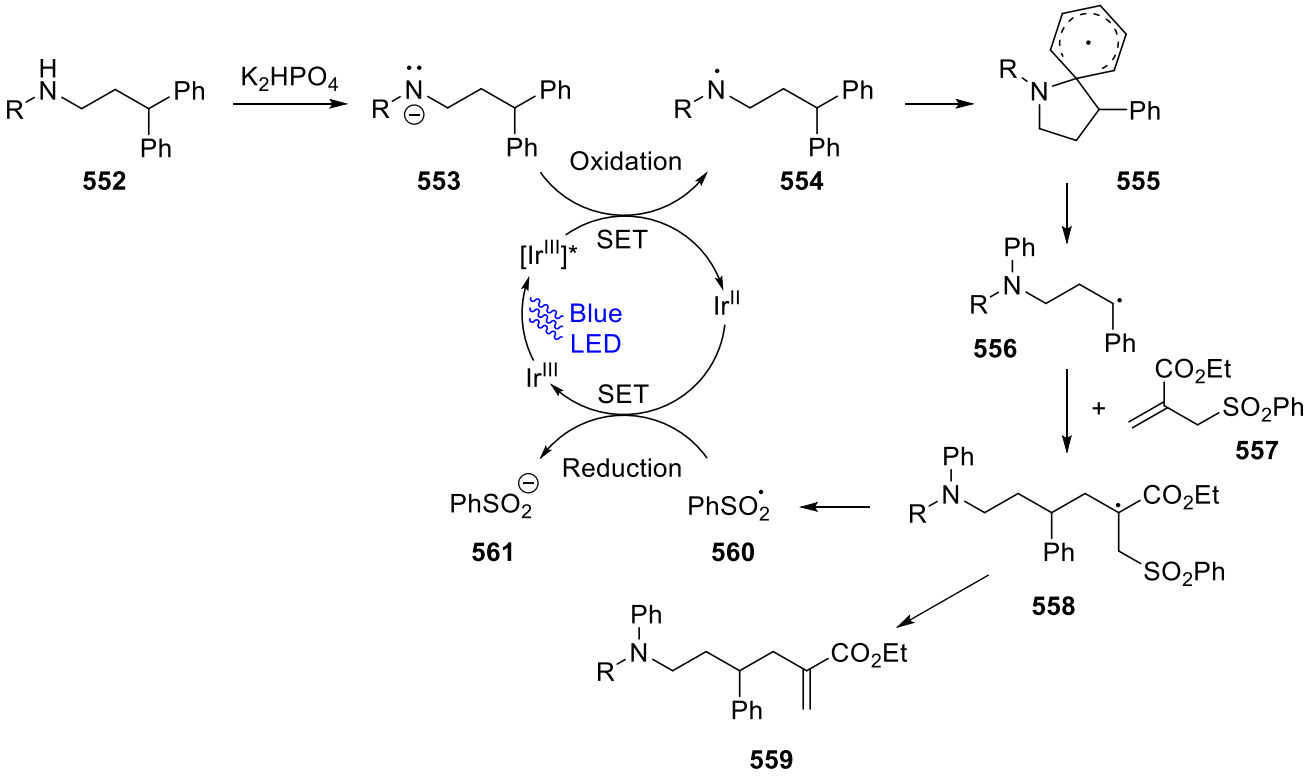

Scheme 121 - Visible-light catalyzed radical aryl-migration reported by Nevado and coworkers

Later, Stephenson's group and Reiser's group reported a 1,4-aryl migration reactions on different substrates *via* the visible-light catalyzed reduction of a carbon-iodine bond in **563**[213] or a phthalimide group **565**,[214] respectively (Scheme 122). These reactions follow different mechanisms. The methodology reported by Stephenson and coworkers relies on the reduction of a carbon-iodine bond of **563** in order to obtain the desired radical while the strategy reported by Reiser and coworkers is based on an energy transfer from the iridium photocatalyst to the starting material **565** without any oxidation state change. This is further supported by the fact that the reaction proceeds also without any photocatalyst but under UV-light irradiation. The energy transfer leads to an intramolecular electron transfer which results in a radical intermediate **566** that can lose its phthalimide moiety as well as CO_2 via a decarboxylation reaction. This yields the desired radical intermediate **567** for the 1,4-aryl migration sequence.

[213] D. Alpers, K. P. Cole, C. R. J. Stephenson, *Angew. Chem. Int. Ed.* **2018**, *57*, 12167–12170.
[214] C. Faderl, S. Budde, G. Kachkovskyi, D. Rackl, O. Reiser, *J. Org. Chem.* **2018**, *83*, 12192–12206.

Stephenson:

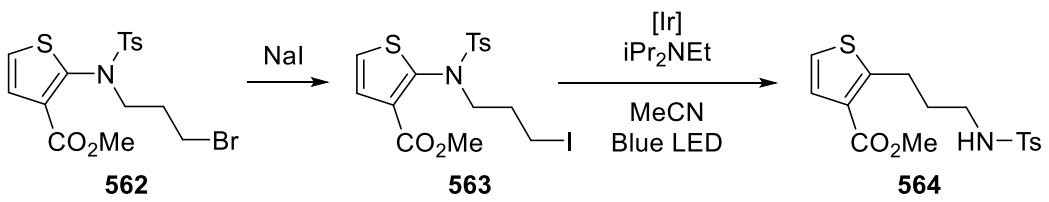

Reiser:

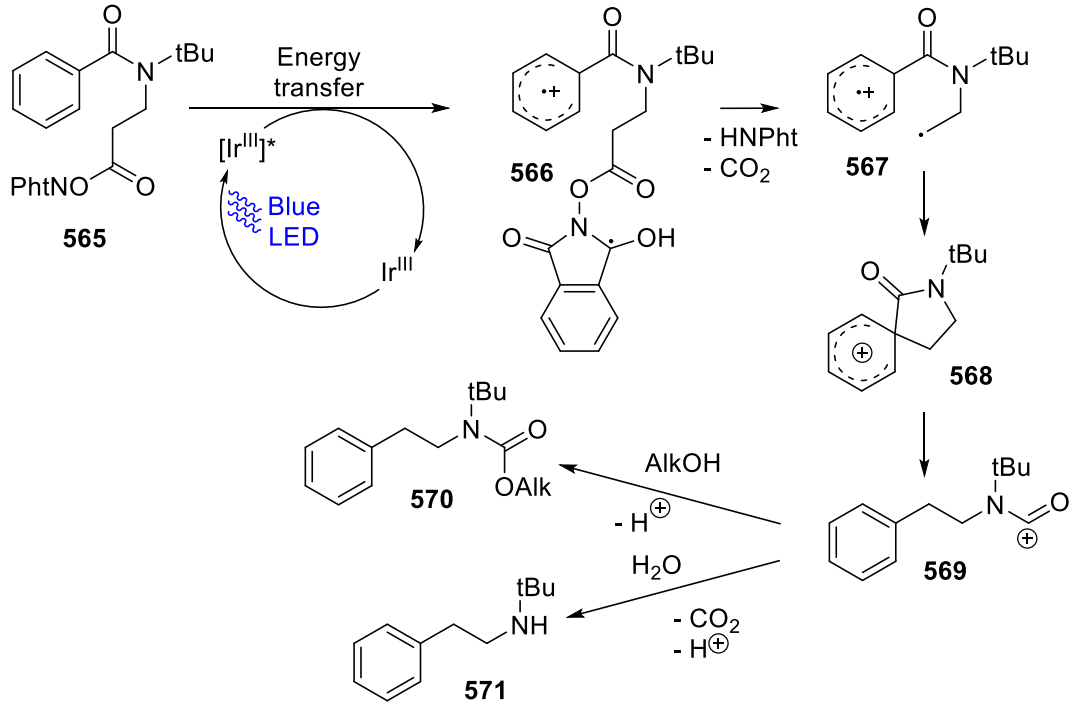

Scheme 122 - Visible-light catalyzed radical aryl-migration reported by Stephenson's and Reiser's groups

In 2019, Li *et al.* reported another type of visible-light catalyzed radical 1,4-aryl migration in order to synthesize hydroxybenzophenone derivatives **577** in one step.[215] This reaction was the first visible-light induced acyl radical rearrangement. The creation of this radical is possible after the formation of a benziodoxole-ketoacid complex **574**, thanks to BI-OAc reagent **573**, which can be readily oxidized by the excited-state photocatalyst. Once the radical is generated, a 1,4-aryl migration leads to the formation of the rearranged product **578**, as presented in Scheme 123:

[215] J. Li, Z. Liu, S. Wu, Y. Chen, *Org. Lett.* **2019**, *21*, 2077–2080.

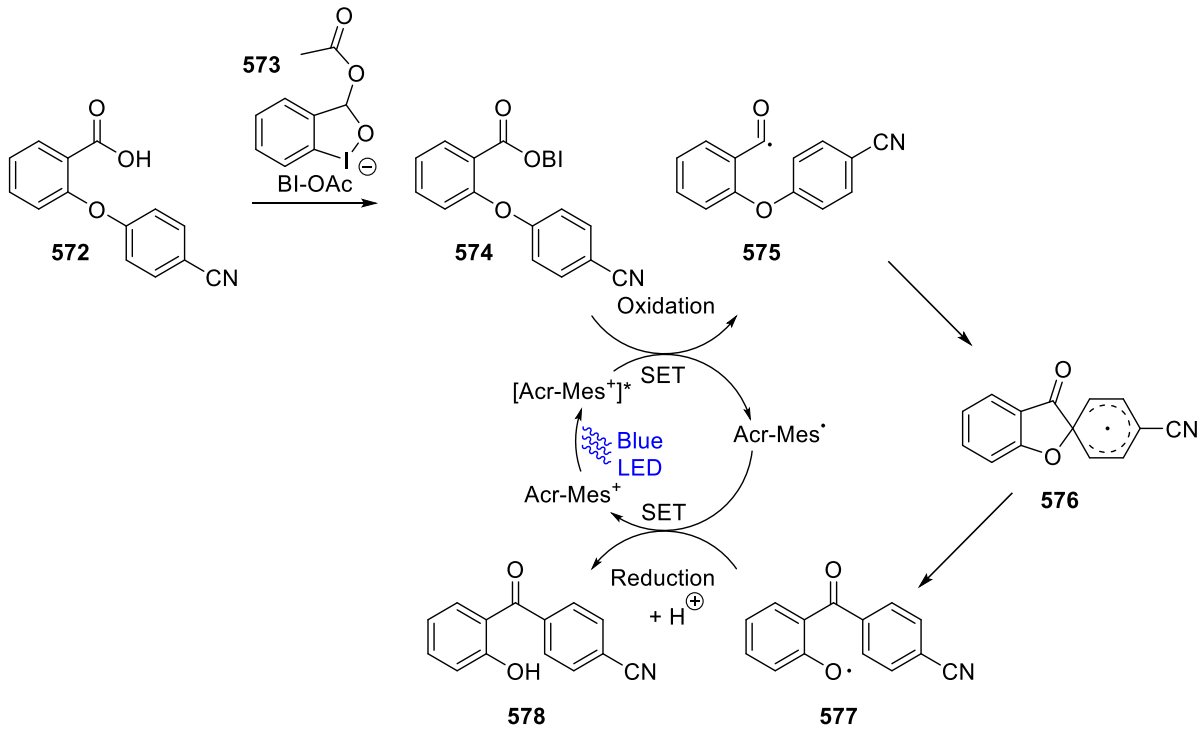

Scheme 123 - Visible-light catalyzed radical aryl-migration reported by Li et al.

Finally, Wu's team reported very recently a visible-light catalyzed diastereoselective radical Smiles rearrangement, using eosin Y as a direct hydrogen atom transfer photocatalyst (Scheme 124). This reaction is different from most of the radical Smiles rearrangement since there is no extrusion of SO_2 as it is being kept within the final scaffold. Eosin Y has a versatile role in the reaction mechanism since it abstracts the hydrogen of an aldehyde **579** or a diarylphosphite substrate during a HAT and gives it back later in the reaction to close the catalytic cycle during a RHAT (reverse HAT).

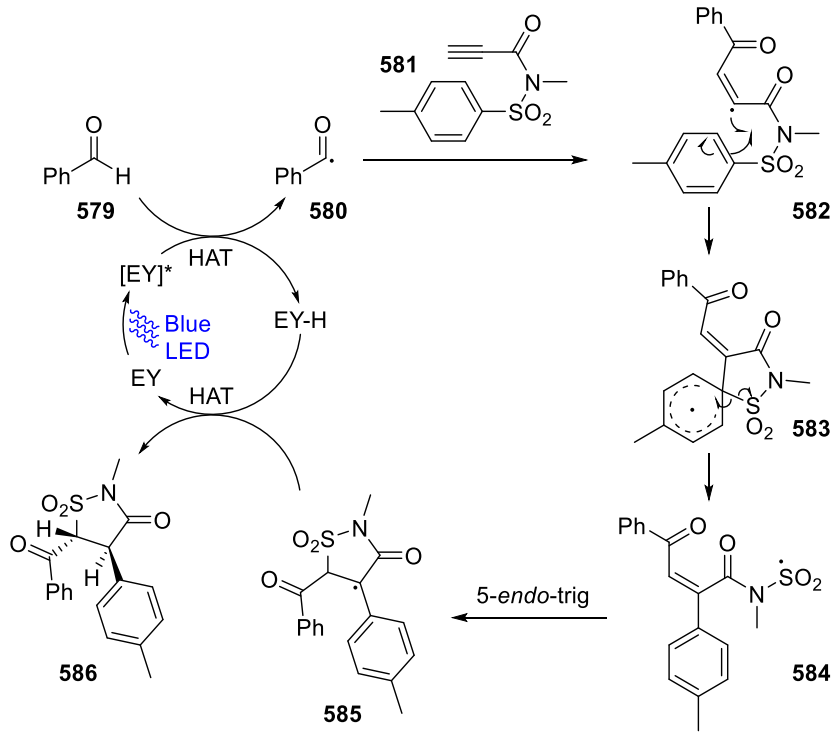

Scheme 124 - Visible-light catalyzed radical aryl-migration reported by Wu's team

3.7. Visible-light catalyzed radical 1,5-aryl migration

A synthetic methodology reported in 2017 by Wang *et al.* allows us to make the transition with the last bibliographical part which will be about visible-light catalyzed radical 1,5-aryl migrations.[216] Although being anterior to the work reported by Li *et al.* that was tackled above (Scheme 123), the example reported by Wang *et al.* implies one more atom separating the aryl group to the radical (Scheme 125). The radical is obtained in a straightforward way, simply by oxidizing a carboxylate intermediate.

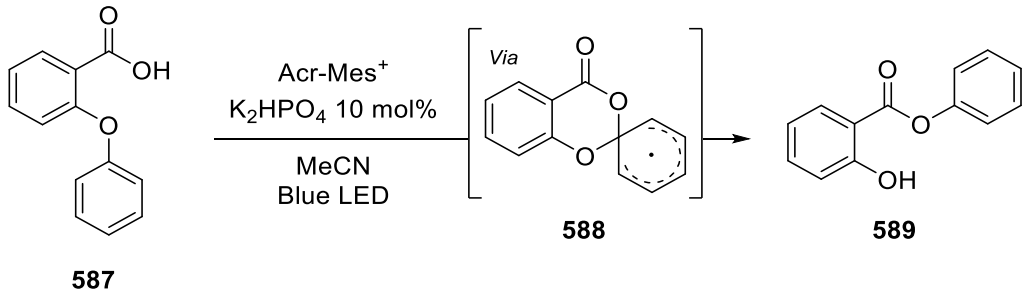

Scheme 125 - Visible-light catalyzed radical aryl-migration reported by Wang et al.

In 2019, Ruzi *et al.* reported a methodology based on a scaffold including a sulfonyl group this time (Scheme 126).[217] An acyl radical is obtained after the reductive quenching of the photocatalyst, leading

[216] S.-F. Wang, X.-P. Cao, Y. Li, *Angew. Chem. Int. Ed.* **2017**, *56*, 13809–13813.
[217] R. Ruzi, J. Ma, X. Yuan, W. Wang, S. Wang, M. Zhang, J. Dai, J. Xie, C. Zhu, *Chem. Eur. J.* **2019**, *25*, 12724–12729.

to the formation of a triphenylphosphine radical which reacts with a carboxylate intermediate. The cleavage of the carbon-oxygen bond leads to the formation of triphenylphosphine oxide and the desired radical. The reaction proceeds then in a similar fashion as the reactions reported above when sulfur dioxide is extruded. It is interesting to note that the reaction uses as starting materials both *ortho*-hydroxybenzoic acid derivatives as well as *ortho*-aminobenzoic acid derivatives **590**. They can readily react with sulfonyl chloride derivatives **591** in order to form the desired starting material **592** that is engaged into the visible-light catalyzed step of the reaction without further purification.

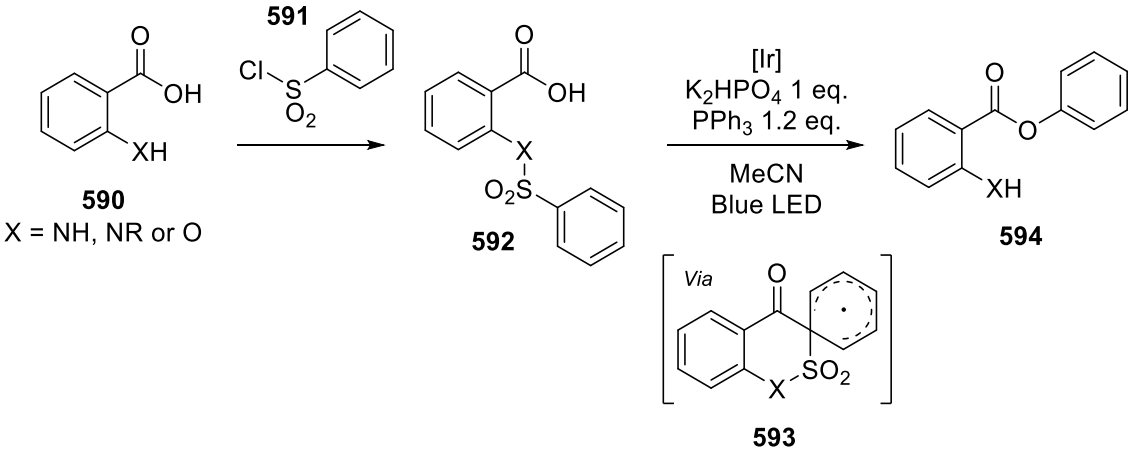

Scheme 126 - Visible-light catalyzed radical aryl-migration reported by Ruzi et al.

Gonzalez-Gomez *et al.* reported a reaction related to the one reported by Wang *et al.*[218] The interesting thing about their methodology is that they were able to adapt it under flow chemistry conditions. This adaptation allows them to shorten drastically the reaction times from up to 36 hours to just 1 hour.

Recently, in 2020, Xia *et al.* reported a new variation of this reaction, starting from aldehyde derivatives **595** this time (Scheme 127).[219] Indeed, they reported a reaction using a *N*-heterocyclic carbene in order to oxidize the aldehyde substrates into the corresponding carboxylic acid **597** using oxygen as the terminal oxidant. The carboxylic acid intermediate proceeds like the reaction described above to form the desired rearrangement product.

[218] Jose. C. Gonzalez-Gomez, N. P. Ramirez, T. Lana-Villarreal, P. Bonete, *Org. Biomol. Chem.* **2017**, *15*, 9680–9684.
[219] Z.-H. Xia, L. Dai, Z.-H. Gao, S. Ye, *Chem. Commun.* **2020**, *56*, 1525–1528.

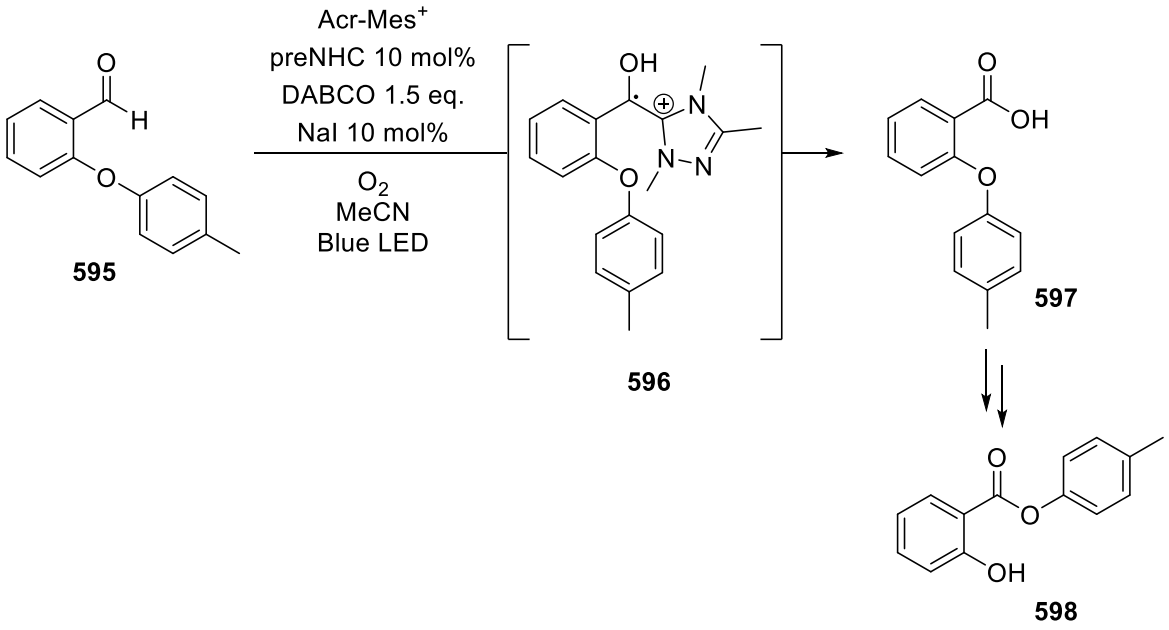

Scheme 127 - Visible-light catalyzed radical aryl-migration reported by Xia et al.

UV-light induced intramolecular aryl migration reactions were also reported prior to the examples under visible-light. Indeed, Cossy and Pete reported in 1981 the photochemical transformation of alkylarenesulfonamido-2-cyclohexene-2-one derivatives **599** through a radical 1,4-aryl migration pathway (Scheme 128).[220]

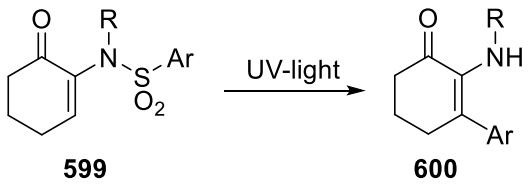

Scheme 128 - UV-light induced radical 1,4-aryl migration reported by Cossy and Pete

These examples, among others, were disclosed in a review named "Spotlight on Photo-Induced Aryl Migration Reactions" published in Chemistry – A European Journal.[221]

All the reactions presented above including an ionic or radical-type 1,4-aryl migration can be considered as Smiles-type rearrangements.

[220] J. Cossy, J.-P. Pete, *Tetrahedron* **1981**, *37*, 2287–2296.
[221] M. Huynh, M. D. Abreu, P. Belmont, E. Brachet, *Chemistry – A European Journal* **2020**, DOI 10.1002/chem.202003507.

4. Focus on the Smiles rearrangement

4.1. Introduction and first example

Although bearing the name of the chemist who actually understood its mechanism, the Smiles rearrangement was, in fact, reported decades prior to its understanding. The first example of such rearrangement was reported back in 1894 by Henriques using bis-(2-hydroxy-1-naphthyl) sulfide **601** in an alkaline ferricyanide solution (Scheme 129).[222] He obtained an isomeric dibasic mixture after reduction of the obtained intermediate. Later, in 1914, Hinsberg, reported a reaction with a sulfonyl group **604** instead of a sulfur atom linking the two naphthalene units.[223]

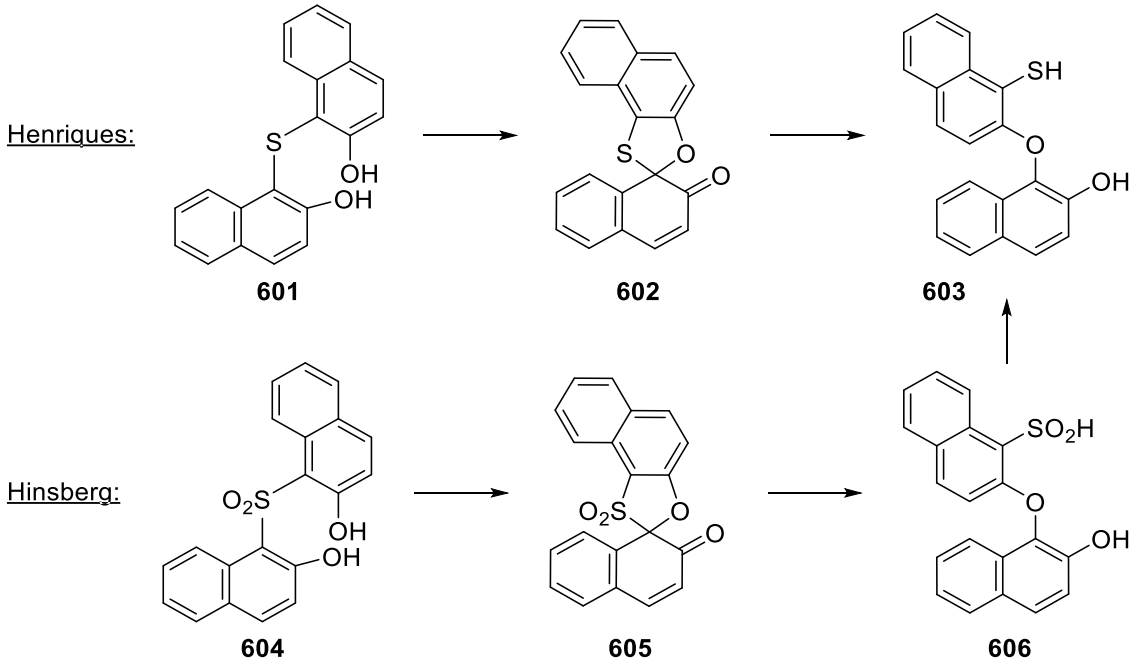

Scheme 129 - Seminal work of Henriques and Hinsberg, later understood by Smiles

Smiles finally understood the occurrence of a new type of intramolecular nucleophilic rearrangement. His findings were reported in two publications in 1930 and 1931.[224] Later, in 1970, Truce, Kreider and Brand described the Smiles rearrangement as follows[225] (Scheme 130):

[222] R. Henriques, *Ber. Dtsch. Chem. Ges.* **1894**, *27*, 2993–3005.
[223] O. Hinsberg, *J. Prakt. Chem.* **1914**, *90*, 345–353*J. Prakt. Chem.* **1915**, *91*, 307–324*J. Prakt. Chem.* **1916**, *93*, 277–301.
[224] L. A. Warren, S. Smiles, *J. Chem. Soc.* **1930**, 1327–1331Arthur. A. Levy, Harry. C. Rains, S. Smiles, *Journal of the Chemical Society (Resumed)* **1931**, 3264–3269.
[225] W. E. Truce, E. M. Kreider, W. W. Brand, *Organic Reactions* **1970**, 99–215.

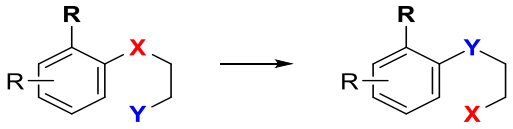

Scheme 130 - General representation of the Smiles rearrangement

The two carbon atoms joining **X** and **Y** can be either part of an aromatic ring or an aliphatic chain, in some cases they can be replaced by a heteroatom. The reaction is, in fact, an intramolecular nucleophilic aromatic substitution. More importantly, Smiles determined four different factors that plays a big role in the eponym rearrangement:

- Activation in the aromatic ring: the **R** group is of great importance since the migrating aromatic ring needs to be activated by electron-withdrawing groups, either on the *ortho* or *para* position. This group is usually a nitro or sulfonyl substituent but sometimes, a more moderate electron-withdrawing group such as a chloro-substitution can also activate enough the migrating ring for the reaction to happen.
- Replaceability of the leaving group: the **X** group is the leaving group and usually consists in an oxygen or a sulfur atom but can also be a sulfoxide, a sulfonyl or a carboxyl group. The two latter being synthetically interesting since they can be extruded during the reaction mechanism as sulfur dioxide or carbon dioxide gas.
- Nucleophilicity of the entering group: the **Y** group, on the other hand, is the entering group *i.e.* the nucleophile of the reaction. It is usually an alcohol, a primary or secondary amine, a thiol, an amide or even a sulfonamide group. It is also important to note that the nucleophilic **Y** group can react either as its acid form **Y**H or its conjugated base form $\mathbf{Y}^-$.
- Acidity of the nucleophilic function: It is important to note that substituents which may increase the acidity of the **Y**H group (*i.e.* facilitate its deprotonation and use as a nucleophile) may also decrease the nucleophilicity of its conjugated base. The sum of these two effects must be taken into account.

Therefore, the reaction proceeds even more readily when either the leaving group **X** is a good leaving group or when the nucleophile **Y** is a strong one. On the contrary, the rearrangement becomes more difficult when **X** is a less good leaving group or **Y** a weak nucleophile. The fact that these two parameters are entangled means that, when using a strong nucleophile **Y** it allows the use of a poorer leaving group **X**.[226] It is worth noting that the substituents on the two carbon atoms separating **X** and **Y** can also exert an influence on the reaction and promote the rearrangement when well manipulated, through Thorpe-Ingold effects for instance (Steric repulsion effect).

[226] A. Levi, L. A. Warren, S. Smiles, *Journal of the Chemical Society* **1933**, 1490–1493.

As said previously the Smiles rearrangement is an intramolecular nucleophilic aromatic substitution. Its mechanism is thought to proceeds *via* a Meisenheimer complex, also called a sigma complex. Due to the intramolecularity of the reaction, this complex takes the form of a spirobicyclic intermediate.

In 1958, Truce developed a variation of the Smiles rearrangement that does not require an activated (electron-poor) aromatic ring (Scheme 131).[227] This reaction was called the Truce-Smiles rearrangement and requires very strong bases since the **Y** group that is deprotonated here (**607**) is a carbon atom. The general scheme of the reaction is related to the Smiles rearrangement. The first example of this reaction is based on the conversion of an aryl sulfone **607** into a sulfinic acid derivative **611** under the action of *n*-BuLi, *via* a Meisenheimer complex **609** as well as the original Smiles rearrangement.

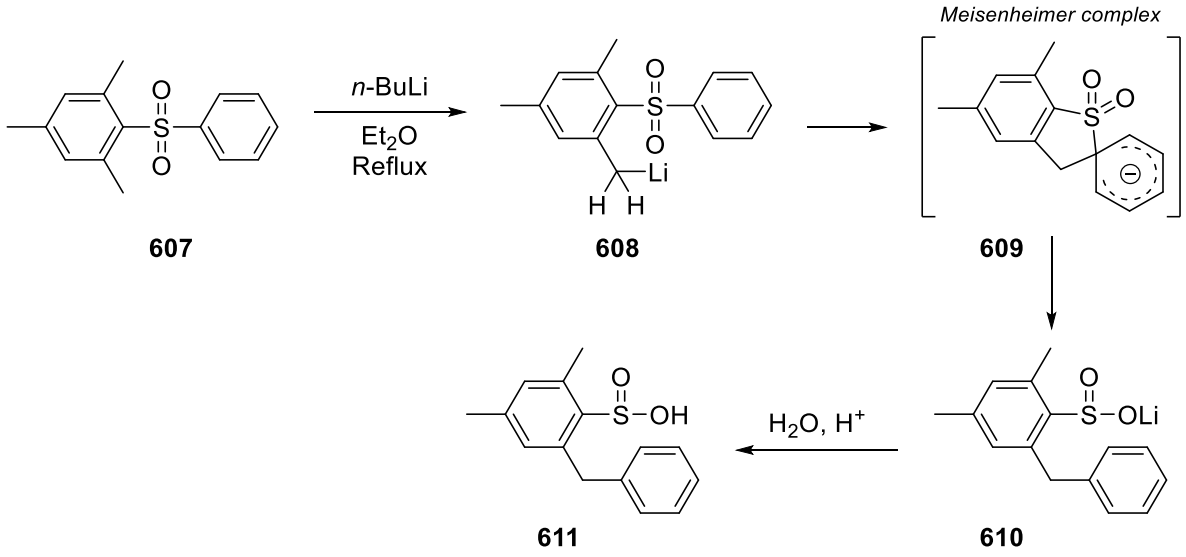

Scheme 131 - First example of the Truce-Smiles rearrangement, reported by Truce and coworkers

With all this information in hand, we kept wondering if a reaction similar to a Smiles rearrangement could occur on substrates bearing a phosphorus moiety that could be extruded, as for SO_2 during the reaction mechanism. We therefore faced several barriers:

- the absence of examples of visible-light catalyzed reactions including an extrudable phosphorus moiety,
- the fact that no example of such radical 1,4-aryl migration was reported, to the best of our knowledge, with such substrates.

[227] W. E. Truce, W. J. Ray, O. L. Norman, D. B. Eickemeyer, *J. Am. Chem. Soc.* **1958**, *80*, 3625–3629.

D) Modification of reactivity via a substitution change on phosphonohydrazones

1. An unexpected reactivity of aryl-substituted phosphonohydrazones

1.1. 1st example

In our previous work, the phenyl-substituted phosphonohydrazone units only led to a very small 15% yield of the expected 1-benzylphthalazine, giving us room for improvements (Scheme 132).

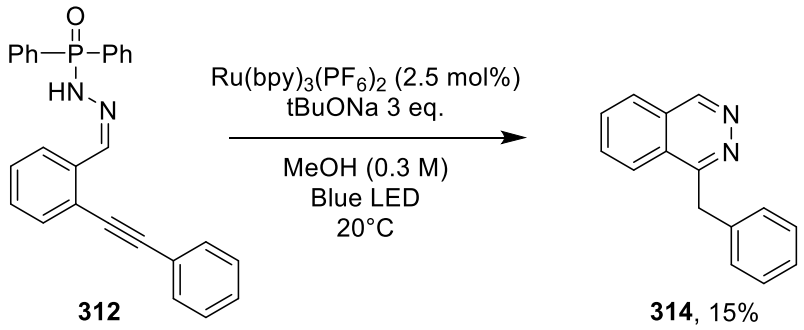

Scheme 132 - Use of phenyl-substituted phosphonohydrazone for the synthesis of 1-benzylphthalazine

As discussed earlier in this chapter, Clive and Kang reported a radical 1,5-aryl migration from a phosphorus atom to a carbon atom, back in 2000 (Scheme 133).[200]

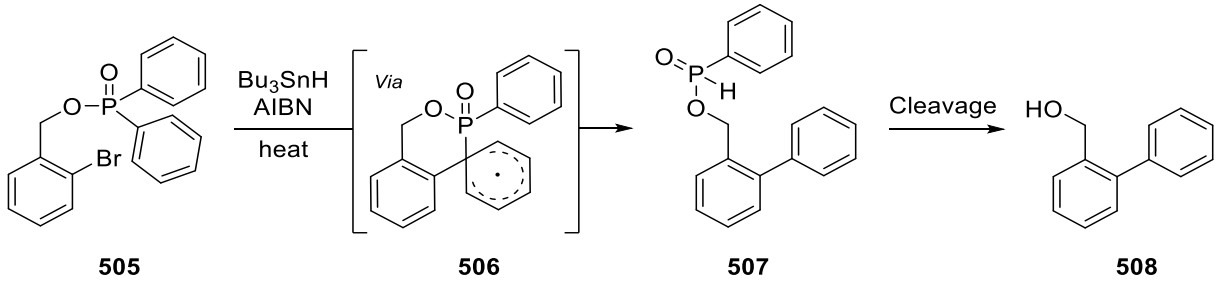

Scheme 133 - Radical 1,5-aryl migration from a phosphorus to a carbon atom

Today, it is still very important to note that neither in their 2000 work nor in their 2001 work,[200] they were able to isolate nor characterize the phosphorus by-product being cleaved during the reaction. However, they were able to isolate an intermediate bearing a P-H bond after the aryl migration has taken place. Moreover, this reaction suffers from harsh operating conditions such as reflux of either benzene, toluene or xylene with an excess of tin species (tributyl- or triphenyltin hydride). To finish, their reaction only works on their specific scaffold, with no other examples described, which limits its applications.

In an attempt to reproduce the work of Clive and Kang, we synthesized a starting material **612** with a slight structural difference from their work (Scheme 134). Instead of having 5 bonds separating the phenyl prone to migrate and its final migration position, we synthesized substrates having 4 bonds

between the phenyl and the migration spot in order to reproduce the same atom distance as in our phosphonohydrazones and "force" a 1,4-migration, if possible.

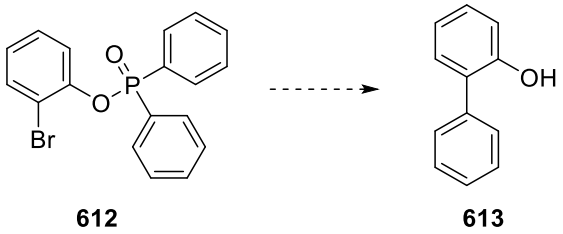

612 **613**

Scheme 134 - Attempt to reproduce the work of Clive and Kang under visible-light catalysis

We also decided to employ $Ir(ppy)_3$ as our photocatalyst since it is a strong reductant, largely enough to reduce aryl-halides.[228,229] Unfortunately, after a few experiments, we did not obtain the same reactivity and no aryl-migration happened. Instead, a molecule **616** resulting of the ortho radical addition, happening between one of the aryl group on the phosphorus atom and the aryl group were the C-Br bond has been reduced, is formed. This reaction is represented in Scheme 135:

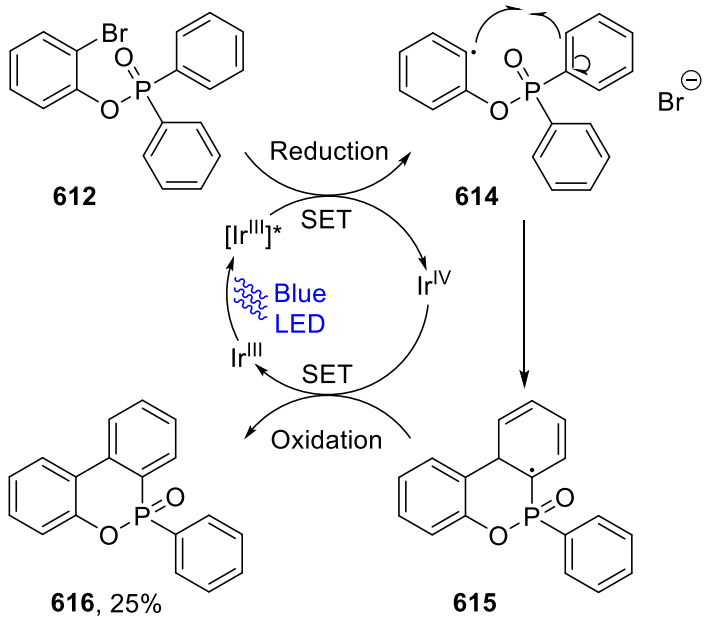

Scheme 135 - Mechanism of the ortho radical addition obtained when trying to induce a 1,4-aryl migration

This product **616** had already been reported in the literature by Revol *et al.* in 2013.[230] In their work, they reported the reductive radical reaction of unactivated alkyl/aryl bromides using dimeric gold complexes as photocatalysts under UVA or sunlight irradiation.

[228] Y. Cheng, X. Gu, P. Li, *Org. Lett.* **2013**, *15*, 2664–2667.
[229] J. D. Nguyen, E. M. D'Amato, J. M. R. Narayanam, C. R. J. Stephenson, *Nature Chem* **2012**, *4*, 854–859.
[230] G. Revol, T. McCallum, M. Morin, F. Gagosz, L. Barriault, *Angew. Chem. Int. Ed.* **2013**, *52*, 13342–13345.

We thus continued our investigation by using our optimized conditions developed during our previous methodology (see **chapter III**, R^4 = OEt, Scheme 136), but this time with aryl-substituted phosphonohydrazones. We witnessed the formation of the hydroamination product **314** along with another product in small quantities when using the diphenylphosphonohydrazone unit (R^4 = Ph, Scheme 136). This product appeared to be the result of a hydroamination reaction/Smiles rearrangement cascade in a 16% yield. This first promising result demonstrates the versatility of our newly described family of NCR precursors in different reactions. Indeed, depending on the substitution on the phosphorus atom, a different reactivity can be attained and therefore diversely substituted scaffolds can be synthesized.

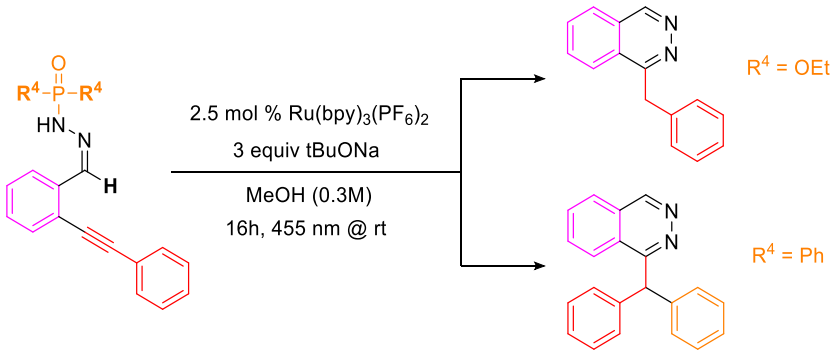

Scheme 136 - Versatility of phosphonohydrazones, depending on their substitution

1.2. Competition between the Smiles rearrangement and the formation of the classical phthalazine

The only downside to this exciting versatile reactivity is that, with arylphosphonohydrazones, a competition occurs between the formation of the cascade product and the formation of the regular benzylated phthalazine (when using the model core). To prevent the formation of the latter, an optimization of the reaction conditions is necessary and will be detailed in the following sections.

2. Synthesis of phosphonohydrazines

2.1. Substitution of the phosphorus atom

Before diving into the optimization of the reaction, we needed to synthesize new phosphonohydrazines, bearing different aryl substituents on the phosphorus atom, in order to probe their reactivity. There are several synthesis routes to make them. A route we took is based on the attack of aryl Grignard reagent on diethylphosphite **258** to replace the ethoxy chains with the desired aryl groups (Scheme 137). This method allows the synthesis of symmetric diarylphosphine oxides **617** which are then engaged in an Atherton-Todd reaction followed by a nucleophilic attack of hydrazine, as described in **chapter III**. Another route, also described in **chapter III**, is based on the direct attack of hydrazine onto commercially available diarylphosphinic chloride **256**.

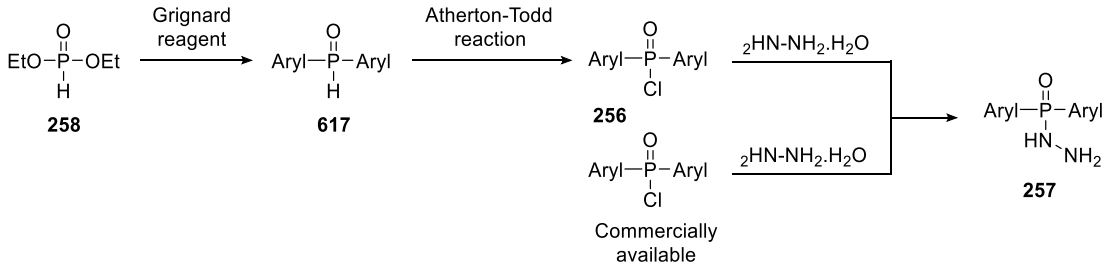

Scheme 137 - Synthetic routes to form diarylphosphonohydrazines

2.2. Synthesis of dissymmetric phosphonohydrazines

Another class of phosphonohydrazine was also synthesized and is based on dissymmetrically substituted phosphonohydrazones. Their synthesis differs from the one described in the previous section. A first attempt was made following the protocol reported by Volle *et al*.[231] in which they use triethylphosphite **618** which is treated with an arylmagnesium bromide prepared beforehand and followed by an acidic treatment (eq. 1, Scheme 138). Unfortunately, after several attempts, using a commercial solution of Grignard reagent, adding it slowly with a syringe pump, only a mixture of differently substituted phosphorus-containing derivatives was obtained. We decided to change our approach and use a modification of the methodology reported by Rahil and Haake (eq. 2, Scheme 138).[232] We slightly adapted it by using THF instead of Et_2O for solubility reasons. We started with dichlorophenylphosphine oxide **621** and, in the presence of 1 eq. of EtOH and 1.5 eq. of NEt_3 in THF at 0°C, we obtained the dissymmetric phosphinic chloride **620**. This intermediate is subsequently used without any separation and reacted with hydrazine monohydrate to yield the final dissymmetric phosphonohydrazine **622**.

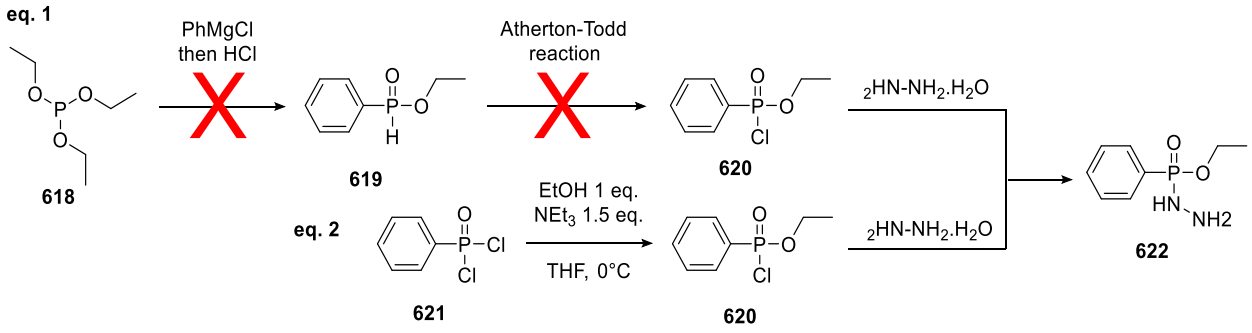

Scheme 138 - Synthetic routes to form dissymmetric phosphonohydrazines

2.3. Scope

We synthesized 8 different phosphonohydrazines using the techniques aforementioned (Table 17).

[231] J.-N. Volle, D. Filippini, C. Midrier, M. Sobecki, M. Drag, D. Virieux, J.-L. Pirat, *Synthesis* **2011**, *2011*, 2490–2494.
[232] J. Rahil, P. Haake, *J. Am. Chem. Soc.* **1981**, *103*, 1723–1734.

Table 17 - Synthesis of differently substituted phosphonohydrazines

Starting material	Product
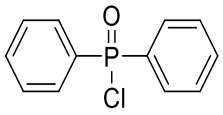 **261** Commercially available	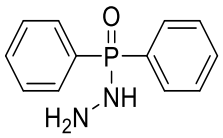 **264**, 88%
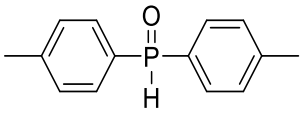 **623**	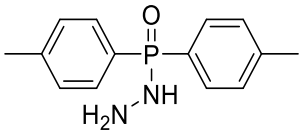 **629**, Quant.
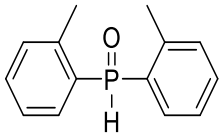 **624**	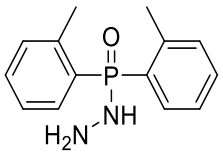 **630**, 64%
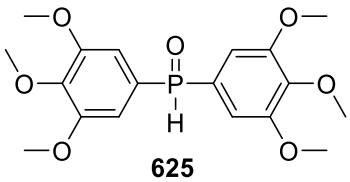 **625**	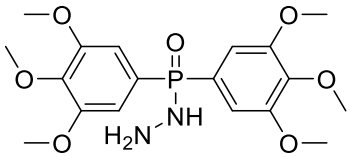 **631**, 86%
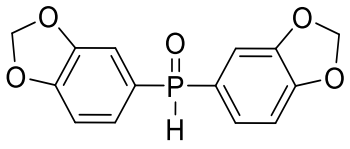 **626**	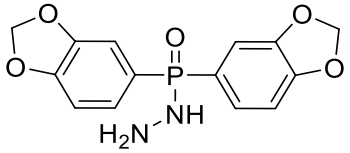 **632**, Quant.
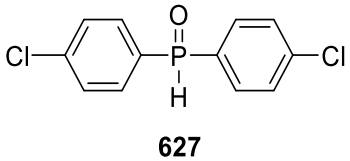 **627**	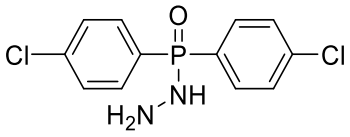 **633**, 91%

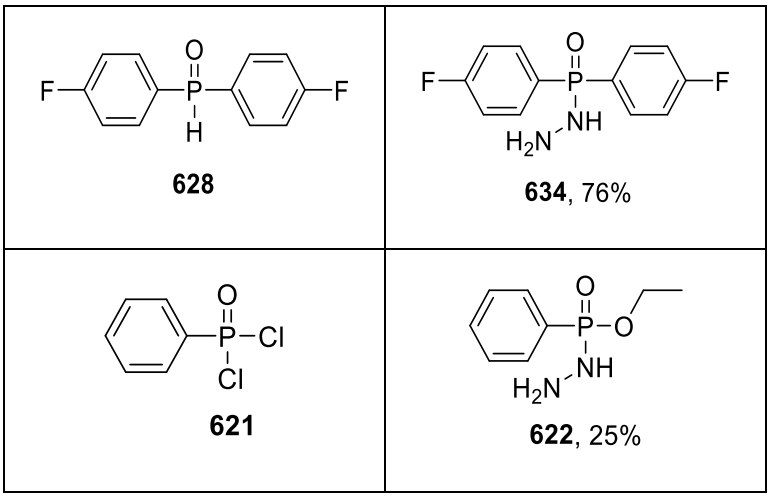

The yields are globally good with the protocols we employed, our model phosphonohydrazine was obtained from the commercially available diphenylphosphinic chloride in a good 88% yield (**XX**). Then, when synthesizing phosphonohydrazines with substitutions on the aryl moiety, we were pleased to obtain also very good yields. The 4-tolyl substitution gave a quantitative yield (**629**), while the 2-tolyl substitution gave a lower 64% yield (**630**), which could be imputed to the steric hindrance resulting from the *ortho*-substitution. More electron-rich aryls such as 3,4,5-trimethoxyphenyl or 3,4-methylenedioxyphenyl led to a high 86% yield (**631**) and a quantitative yield (**632**), respectively. Moreover, an electron-deficient aryl such as 4-chlorophenyl or 4-fluorophenyl were not detrimental for the synthesis of their corresponding phosphonohydrazines which were obtained in a 91% (633) and 76% (634) yield, respectively. Finally, the dissymmetric phosphonohydrazine **622** was synthesized, in order to see the impact of such modification on the reactivity of the aryl-migration event, in a poor 25% yield.

3. Synthesis of phosphonohydrazones

3.1. Synthesis of ketone and aldehyde functionalized derivatives via Sonogashira cross-coupling reactions

The synthesis of ketone and aldehyde derivatives was made following the same conditions described in **chapter I** and are represented in Table 18.[48]

Table 18 - Sonogashira cross-coupling products

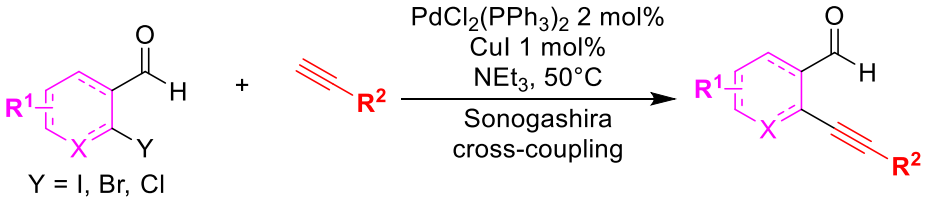

Model substrate

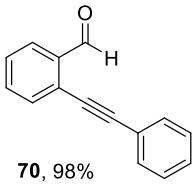

70, 98%

Main ring modifications

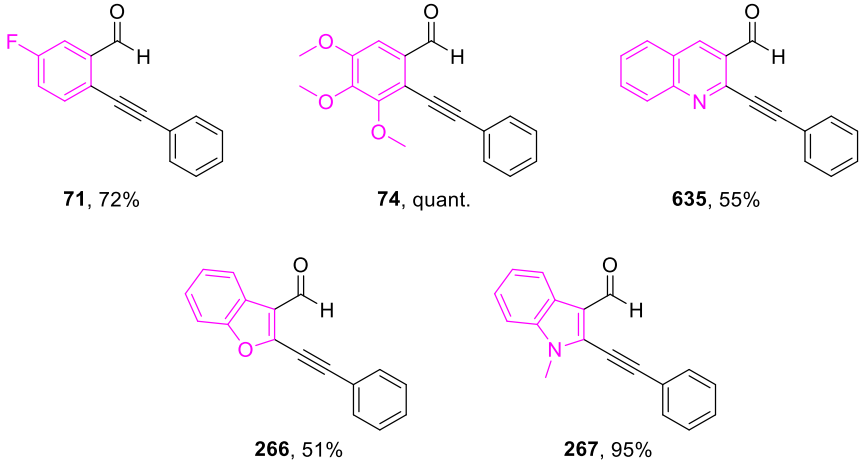

71, 72%

74, quant.

635, 55%

266, 51%

267, 95%

Alkynyl modifications

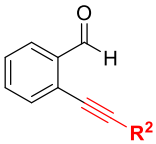

269, R^2 = 4-tolyl, 81%
270, R^2 = 4-fluorophenyl, 90%
271, R^2 = 4-cyanophenyl, quant.
84, R^2 = TMS, 69%
636, R^2 = *tert*-Butyl, 93%
79, R^2 = 3-nitrophenyl, quant.
637, R^2 = 2-(6-methoxynaphthyl), quant.
638, R^2 = 2-(dibenzothiophene), 81%

Main ring and alkynyl modifications

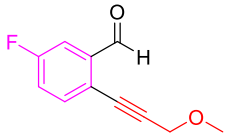

639, 84%

Yields are overall good to excellent and it should be pointed out that many of the Sonogashira cross-coupling products were took from the methodology developed in **chapter III**.

The fluoro substituted main ring led to formation of 72% of product **71**. Moreover, a quinoline ring in place of the main ring led to a lower yield of 55% (**635**).

Moreover, some new alkynyl substitutions were synthesized here with for instance a *tert*-butyl (**636**) in a 93% yield, a 2-(6-methoxynaphthyl) substitution (**637**) in quantitative yield. A heterocycle was also successfully cross-coupled with a 2-dibenzothiophene derivative obtained in a good 81% yield (**638**).

Finally, a substrate bearing both a fluoro substitution on the main ring and an ether alkynyl chain was formed in a high 84% yield (**639**).

3.2. Reaction of phosphonohydrazine units with ketones/aldehydes derivatives

The formation of the phosphonohydrazone derivative is the result of the addition of phosphonohydrazine units onto aldehyde or ketone derivatives, performed in methanol (Table 19). Many of them do precipitate which greatly facilitates their isolation. If not, a classic column chromatography on silica gel is needed to retrieve the desired product (see experimental part).

Table 19 - Phosphonohydrazones starting materials

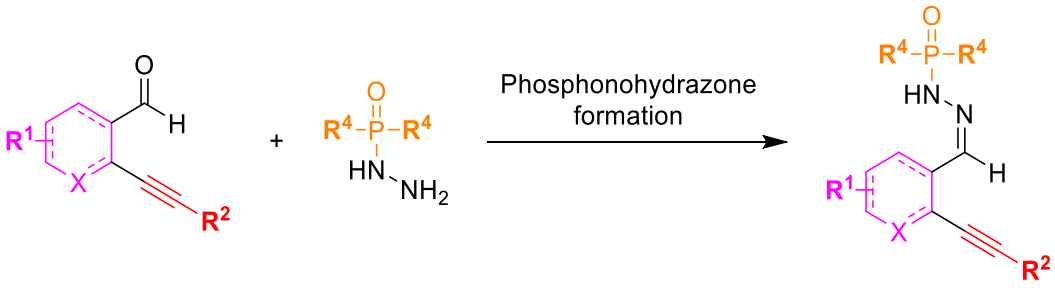

Model substrate

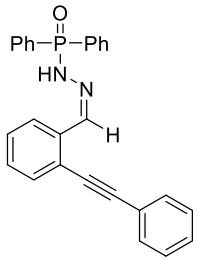

312, 85%

Main ring modifications

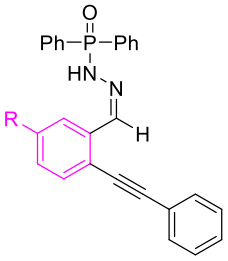

640, R^1 = fluorine, 87%
641, R^1 = chlorine, 91%
642, R^1 = bromine, 74%

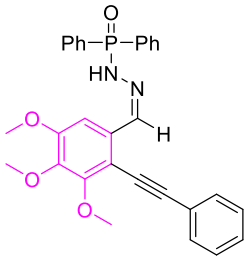

643, 96%

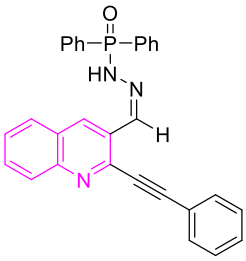

644, 76%

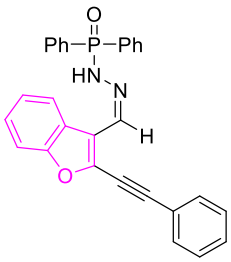

645, 71%

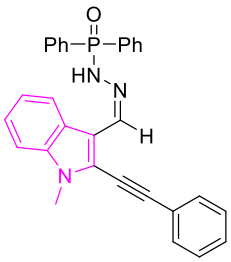

646, 92%

Alkynyl modifications

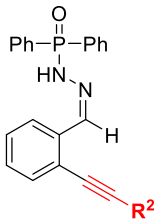

647, R^2 = 4-tolyl, 93%
648, R^2 = 4-fluorophenyl, Quant.
649, R^2 = 4-cyanophenyl, 76%
650, R^2 = TMS, 44%
651, R^2 = *tert*-Butyl, 70%
652, R^2 = 3-nitrophenyl, 85%
653, R^2 = 2-(6-methoxynaphthyl), 53%
654, R^2 = 2-(dibenzothiophene), 96%
655, R^2 = *n*-propyl, 52%

Main ring and alkynyl modifications

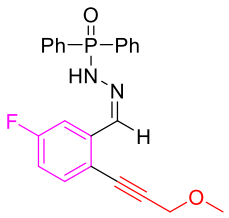

656, 91%

Different substitutions on the Phosphorus atom

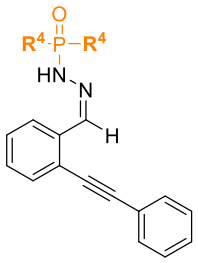

657, R^4 = 4-tolyl, 58%
658, R^4 = 2-tolyl, 83%
659, R^4 = 3,4,5-trimethoxyphenyl, 73%
660, R^4 = 3,4-methylenedioxyphenyl, 67%
661, R^4 = 4-chlorophenyl, 80%
662, R^4 = 4-fluorophenyl, 67%

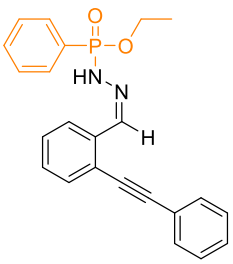

663, 44%

The overall yields of formation of phosphonohydrazones bearing aryl substituted phosphorus atom is very good. Indeed, the model substrate **312** was obtained in a good 85% yield. Moreover, all the modifications on the main ring were well tolerated to form phosphonohydrazones. A fluoro substitution led to an 87% yield (**640**) while a chlorine and a bromine led to the formation of the desired phosphonohydrazone in a high 91% (**641**) and 74% yield (**642**), respectively. A trimethoxy substitution led to an almost quantitative 96% yield (**643**). Heterocycles-containing aldehydes such as quinoline, benzofuran and a *N*-methyl indole led to the products in 76% (**644**), 71% (**645**) and 92% (**646**) yield, respectively.

Aldehyde derivatives bearing modified alkynes also led to high yields for phosphonohydrazones formation with a good tolerance of EWG such as 4-fluorophenyl (**648**), 4-cyanophenyl (**649**) and 3-nitrophenyl (**652**) with quantitative, 76% and 85% yields, respectively. Other modifications such as a 4-tolyl (**647**), a 2-(6-methoxynaphthyl) (**653**) and a 2-dibenzothiophene (**654**) gave varying yields of 93%, 53% and 96%, respectively. A TMS substitution allowed the formation of the phosphonohydrazone **650** in a medium 44% yield. To finish, aliphatic alkynes bearing a *tert*-butyl, or *n*-propyl chain provided the desired phosphonohydrazone in a 70% (**651**) and 52% (**655**) yield, respectively.

A phosphonohydrazones formed from a substrate bearing a fluoro substitution on its main ring and an ether chain on its alkynyl chain was obtained in a 91% yield (**656**).

Finally, as we wanted to investigate the migratory reactivity of different aryl on the phosphorus atom, we synthesized phosphonohydrazones bearing various substitutions like a 4-tolyl (**657**) and 2-tolyl (**658**) substitution with 58% and 83% yield. We also made phosphonohydrazones that bear electron-rich substitutions such as a 3,4,5-trimethoxyphenyl (**659**) and a 3,4-methylenedioxyphenyl (**660**) with respectively, 73% and 67% yield. Lastly, a 4-chlorophenyl and 4-fluorophenyl substitutions led to high yields of the phosphonohydrazone formation (**661**, 80% and **662**, 67%). The nonsymmetric phosphonohydrazine that we synthesized led to a medium 44% yield for the phosphonohydrazone **663** formation.

E) Application in visible-light catalyzed reactions as a new precursor of NCR and Smiles rearrangement

1. Methodology

1.1. Tuning the balance toward the formation of the Smiles product

As previously said, a competition occurs between the formation of the Smiles rearrangement product and the benzylated phthalazine (hydroamination reaction). To address this problem, we

optimized the reaction conditions to favor the formation of the Smiles rearrangement product while limiting the formation of the undesired product. The first result we had for the formation of the Smiles rearrangement product was a 16% yield, using the previously reported optimized conditions for the formation of the regular phthalazine (Table 20).

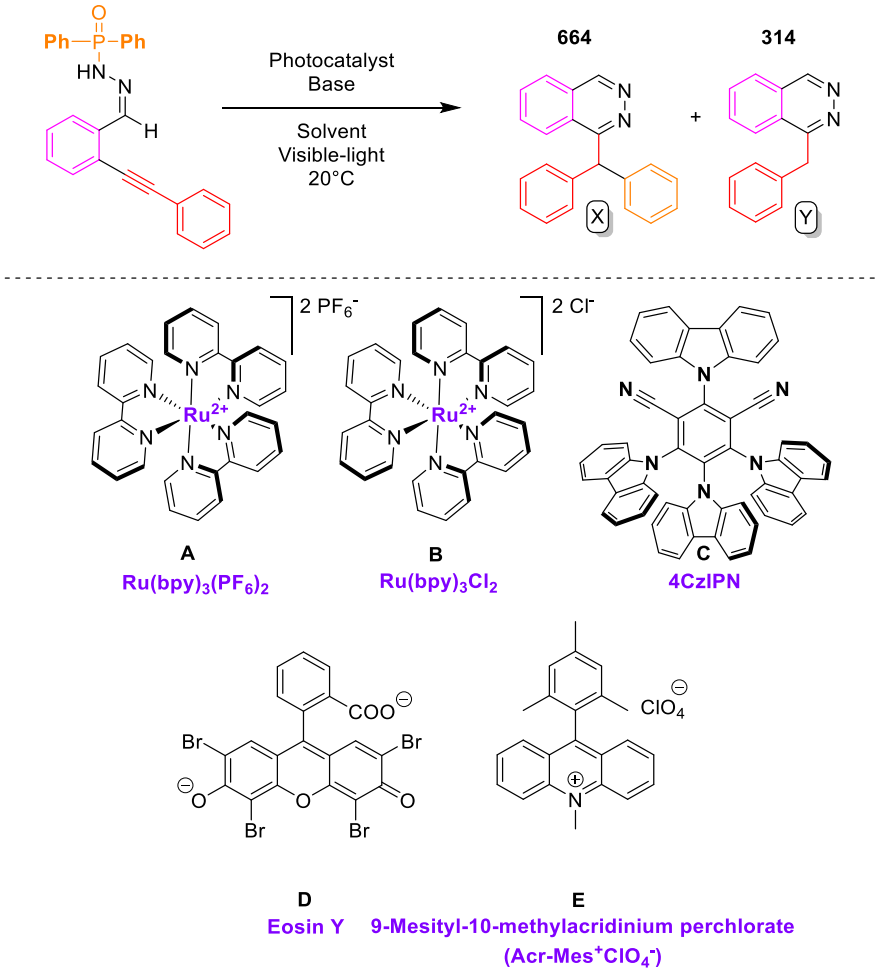

Table 20 - Optimization of the reaction conditions

Entry	Catalyst	Base	Solvent (M)	Yield[a] X	Yield[a] Y
1	**A** (2,5 mol%)	tBuONa 3 eq.	MeOH (0,3 M)	16%	15%
2	**A** (2,5 mol%)	tBuONa 3 eq.	EtOH (0,3 M)	15%	27%
3	**B** (2,5 mol%)	tBuONa 3 eq.	EtOH (0,3 M)	18%	39%
4	**C** (5 mol%)	tBuONa 3 eq.	EtOH (0,3 M)	0%	Traces
5	**D** (5 mol%)	tBuONa 3 eq.	EtOH (0,3 M)	0%	Traces
6	**E** (5 mol%)	tBuONa 3 eq.	EtOH (0,3 M)	0%	Traces
7	B (2,5 mol%)	**NaOH 3 eq.**	EtOH (0,3 M)	21%	31%
8	B (2,5 mol%)	**NaOH 1.5 eq.**	EtOH (0,3 M)	21%	39%
9	B (2,5 mol%)	NaOH 1.5 eq.	**EtOH (0,075 M)**	25%	64%
10	B (2,5 mol%)	NaOH 3 eq.	**EtOH (0,075 M)**	22%	28%
11	B (2,5 mol%)	NaOH 1.5 eq.	**EtOH (0.01875 M)**	45%	25%
12	B (2,5 mol%)	NaOH 1.5 eq.	**EtOH (0.01875 M)**	20%[b]	57%[b]
13	B (2,5 mol%)	NaOH 1.5 eq.	**Propan-1-ol (0.01875 M)**	36%	62%
14	B (2,5 mol%)	NaOH 1.5 eq.	**Butan-1-ol (0.01875 M)**	42%	52%
15	B (2,5 mol%)	NaOH 1.5 eq.	**EtOH/DMSO 15:1 (0.01875 M)**	48%	28%
16	B (2,5 mol%)	NaOH 1.5 eq.	**EtOH/DMSO 15:1 (0.01875 M)**	46%[c]	Traces
17	B (2,5 mol%)	NaOH 1.5 eq.	**EtOH/Acetone 15:1 (0.01875 M)**	38%[c]	Traces
18	B (2,5 mol%)	NaOH 1.5 eq.	**EtOH/MeCN 15:1 (0.01875 M)**	58%[c]	Traces
19	**B (2,5 mol%)**	**NaOH 1.5 eq.**	**EtOH/MeCN 3:1 (0.01875 M)**	**65%**[c/d]	**Traces**
20	B (2,5 mol%)	NaOH 1.5 eq.	EtOH/MeCN 3:1 (0.01875 M)	38%[e]	Traces
21	A (2,5 mol%)	NaOH 1.5 eq.	EtOH/MeCN 3:1 (0.01875 M)	0%[f]	0%
22	A (2,5 mol%)	/	EtOH/MeCN 3:1 (0.01875 M)	0%	0%[g]
23	/	NaOH 1.5 eq.	EtOH/MeCN 3:1 (0.01875 M)	0%	0%[h]

[a)] Isolated yields. [b)] Heated at 40°C. [c)] Reaction performed using an 18W blue LED (when not specified, a 3W blue LED was used). [d)] Standard condition: reactions were performed with **1a** (0.15 mmol), Ru photocatalyst (2.5 mol %), base (1.5 eq.) and 3 Å M. S. in 6 mL of EtOH and 2 mL of MeCN and was irradiated with 18W blue LED for 16 h at 20°C. [e)] Reaction performed under sunlight. [f)] Reaction performed without light. [g)] Reaction performed without base. [h)] Reaction performed without photocatalyst.

1.2. Variations of photocatalysts, solvents and bases

To begin, we started by using the reaction condition developed in our previous methodology. We were pleased to obtain the desired cascade product in a 16% yield along with 15% yield of the undesired phthalazine (entry 1, Table 20).

We witnessed that by only changing the solvent to ethanol, a similar 15% yield of the desired product was obtained but the most notable result was an overall higher conversion of the starting material with the formation of 27% of the undesired product (entry 2). We then decided to test other photocatalysts, having in mind that the first step of the reaction is an oxidation of an anionic intermediate. We thus focused our attention on photocatalysts capable of performing reductive quenching (*i.e.* capable of oxidizing the *N*-anion, see C. V.). $Ru(bpy)_3Cl_2.6H_2O$ (**B**) appeared to be a better choice since it led to a slight increase of the desired 1-benzhydrylphthalazine to 18% yield while also increasing the formation of the undesired 1-benzylphthalazine to 39% yield (entry 3). We then

faced some limitations since no organic photocatalyst was able to yield more than traces of the undesired phthalazine and no Smiles rearrangement product was obtained in each case (entries 4, 5 and 6). We decided to keep the photocatalyst **B** for the rest of the optimization since it led to the best yield of the desired product at that moment and also the best overall conversion of the starting material into a phthalazine scaffold. Moreover, the photocatalyst **B** ($Ru(bpy)_3Cl_2.6H_2O$) is much more common than $Ru(bpy)_3(PF_6)_2$ in visible-light catalyzed methodologies.

We then switched the base to sodium hydroxide (compared to entry 1) in the entry 7 and this resulted in the formation of the desired compound in a 21% yield. In entry 8, we halved the amount of the base and we noticed that it did not change the yield of the formed product, so we decided to keep 1.5 eq. of base for the following experiments. After this result, we decided to try the reaction conditions previously established in our laboratory[111] (entry 9) and we were pleased to achieve a slightly better Smiles rearrangement product yield but, in the meantime, the regular phthalazine product was formed in a 64% yield. To address this, we tried one more time to modify the amount of base by doubling it, while no big yield increase was observed for the desired product, we were pleased to see that the undesired product yield was lowered to 28% (entry 10). A big change appeared when we started decreasing greatly the reaction's concentration from 0.075 M to 0.01875 M (four-fold decrease). This time, the major product formed was the desired Smiles rearrangement product in a 45% yield whereas the undesired phthalazine was obtained in a 25% yield (entry 11). We were also interested in the influence of the reaction's temperature as we always set our visible-light catalysis apparatus at 20°C to prevent a temperature increase caused by the LED lights. Thus, we set for one experiment the temperature at 40°C. Interestingly, the reactivity is reversed with a majority of the undesired phthalazine formed and only 20% of the Smiles rearrangement product obtained, even if the reaction had the same concentration as the entry 11 (entry 12). We believe that the phenomenon is due to the increased reaction rate associated with an increased temperature and this increases the cleavage of the phosphorus moiety before an aryl migration can occur (see later in this chapter).

The solvent was then changed to other alcohols or some solvent mixes. Only a few of them are displayed in this table for clarity and consistency. No interesting result was obtained with solvents such as DMSO, chloroform, HFIP, TFE, DME, toluene etc. Propan-1-ol and butan-1-ol (entries 13 and 14, respectively) did not give better yields than the conditions of entry 11. Moreover, when using a mixture of solvents like EtOH and DMSO in a 15:1 ratio (DMSO help solubilizing the starting material) we obtain good yields again with 48% of the Smiles rearrangement product and 28% of undesired phthalazine (entry 15). The entries 16 to 19 benefited new LED lights with a power jump from 3W to 18W. This change was immediately visible in the reactions yields with almost no formation of the regular phthalazine (only traces) and 46% of the desired product (entry 16). This is not surprising since when

increasing the power of the LED lights, we also irradiate our reaction medium with much more photons and therefore increase the number of possible light-catalyzed reactions. When the co-solvent was changed while maintaining EtOH as the main solvent and the same diluted concentration, 38% and 58% of the desired product was formed using acetone and acetonitrile respectively (entries 17 and 18). Acetonitrile proved to be a good candidate as a co-solvent used with ethanol and, finally, changing the ratio between the two solvents from 15:1 to 3:1 led to the best yield obtained which is 65% of the desired product and only traces of the undesired product (entry 19). Our hypothesis for the increase of the yield of the cascade product when the reaction is more diluted is that while diminishing the concentration, we also decrease the probability that the radical intermediate (Figure 33) meets and reacts with the photocatalyst in order to be reduced. This also means that the radical intermediate has therefore more time to react intramolecularly with the aryls on the phosphorus moiety and induce the aryl-migration.

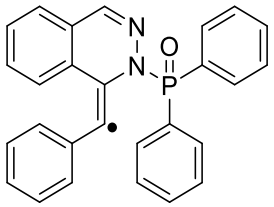

665

Figure 33 - Key radical intermediate in the cascade of hydroamination and Smiles rearrangement

We did not obtain any better yield than the conditions in entry 19 and decided to keep them for the scope investigation. The parameters are $Ru(bpy)_3Cl_2.6H_2O$ (2.5 mol %), NaOH (1.5 equiv) in a mixture of EtOH/MeCN (3:1) (0.01875 M) and irradiated with 18W blue LED for 16 h.

We also decided to perform the reaction under direct sunlight during a sunny day (entry 20). The yield of the Smiles rearrangement product was poor (38%) and the reaction was much faster (6h), almost half of the yield obtained using the optimized conditions. Only traces of the undesired by-product were formed during the process. An explanation of such poor yield could be the fact that absolutely no control over the temperature of the reaction could be done in this case and the reaction could attain temperatures as high as 40 to 50°C. Moreover, we did not filter the incoming light reaching the reaction, all wavelengths between about 100 nm and 1 mm (from UVC to infrared-C) were thus involved in the reaction which may promote other types of reactions.

Another attempt was made on preparing ahead of the reaction, a solution of solvent (EtOH/MeCN 3:1) in which is dissolved the sodium hydroxide base (1 eq. regarding the starting material at a concentration of 0.01875 M). We were pleased to observe a much faster conversion of our starting material into the desired product with reaction time shortened to less than 3 hours and a 58% yield.

We also reduced the amount of base in that solution to just 0.5 eq. but, after 24 hours, the reaction was still not complete. Although facilitating the set-up of the reaction, we did not choose the solution of solvents and base prepared beforehand for our optimized conditions since it led to lower yields.

Finally, we ran the usual control experiments in order to verify and confirm that our optimized reaction is not only due to the sole visible-light catalysis or the action of the base alone. We performed three experiments: in absence of visible-light (Blue LEDs) (entry 21), in absence of the base (entry 22) and in absence of the photocatalyst (entry 23). We were pleased to witness absolutely no product formation in these three conditions and only degradation of the starting material was observed in all three cases. It is important to note that the control reaction without base (entry 22) led to the formation of a new compound. After purification on silica-gel chromatography, we obtained what appeared to be the isomerized starting material (hydrazone part). We were surprised to obtain such result since it has a very distinct retention factor (Rf) compared to the starting material of the reaction and we were able to isolate it easily on a classic column chromatography and confirmed by HR-MS analysis.

We selected as the best condition the entry 19, using phosphonohydrazone (0.15 mmol), $Ru(bpy)_3Cl_2.6H_2O$ (2.5 mol %), NaOH (1.5 eq.) in a mixture of EtOH and MeCN (3:1, 0.01875 M) and irradiated with 18W blue LED for 16 h.

2. Scope

After setting the optimal reaction conditions for our methodology, we wanted to see the field of application of such conditions. Hence, we changed different parts of the molecule, using our model starting material as a reference to all the modifications that took place on the main ring, on the alkynyl chain and the aryl groups on the phosphorus atom.

2.1. Functional compatibility

Here are displayed the molecules we obtained using our methodology (Table 21):

Table 21 - Final phthalazine products of the methodology

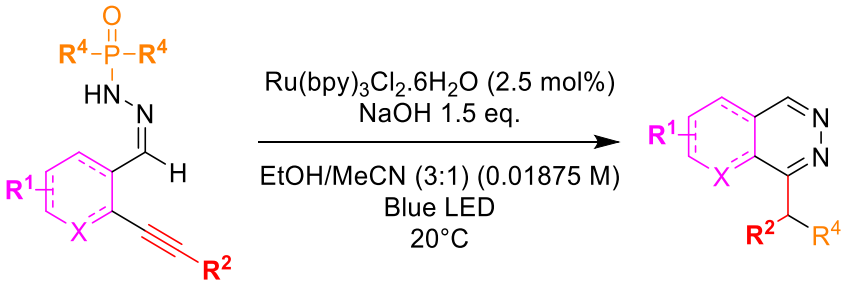

Model product

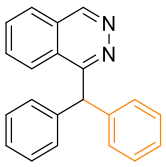

664, 65%

SM with main ring modifications

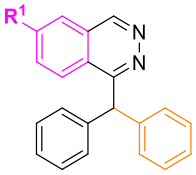

666, R^1 = fluorine, 50%
667, R^1 = chlorine, 50%
668, R^1 = bromine, 11%

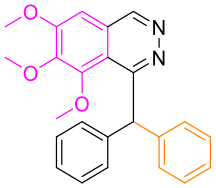

669, 26%

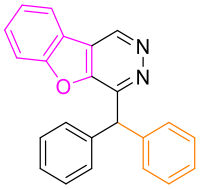

670, 31%

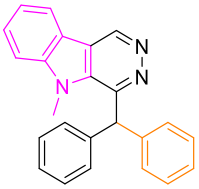

671, 37%

SM with alkynyl modifications

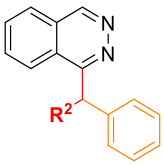

672, R^2 = 4-tolyl, 62%
673, R^2 = 4-fluorophenyl, 49%
674, R^2 = *n*-propyl, 34%
675, R^2 = 2-(6-methoxynaphthyl), 12%
676, R^2 = 2-(dibenzothiophene), 44%

SM with different substitutions on the Phosphorus atom

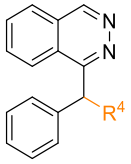

672', R^4 = 4-tolyl, 52%
677, R^4 = 2-tolyl, 32%
678, R^4 = 3,4,5-trimethoxyphenyl, 34%
679, R^4 = 3,4-methylenedioxyphenyl, 47%
680, R^4 = 4-chlorophenyl, 41%
673', R^4 = 4-fluorophenyl, 42%

A phenyl migration was possible on various phosphonohydrazones with differently substituted main ring. A migration was possible on a starting material bearing a fluoro, chloro or bromo substitution led to, respectively, 50% (**666**), 50% (**667**) and 11% (**668**) yield. It is interesting to note that during the reaction with the bromo derivative, the major product of the reaction was the dehalogenated final Smiles rearrangement scaffold, in a low yet higher, 25% yield. A trimethoxy substitution led to a 26% yield (**669**). The low 26% yield could be explained by the steric hindrance of one of the methoxy group next to the migration position. Moreover, an electron-rich substituent such as a methoxy on the *para*-position of the alkynyl chain could also be detrimental to the reaction.

Heterocycles are also tolerated on the main ring with 31% and 37% yield for the benzofurane (**670**) and *N*-methylindole (**671**) derivatives, respectively.

To continue, modifications on the alkynyl chain of the starting material were also compatible with this reaction, with the 4-tolyl and 4-fluorophenyl substitutions yielding 62% and 49% of the corresponding final product **672** and **673**, respectively. The 4-tolyl substituted alkyne gave a yield almost as good as the model starting material and this can be explained by their very similar structure. It is important to note that the reaction was possible with an alkyne bearing a short alkyl chain (*n*-propyl). Indeed, we were able to isolate the final product in an encouraging 34% yield (**674**), thus proving that a migration is possible on non-aromatic alkynyl derivatives.

Bulkier alkynyl substitutions such as a 2-(6-methoxynaphthyl) led to a poor 12% yield of the final product (**675**) but, on the other hand, a 2-(dibenzothiophene) gave the final phthalazine **676** in a medium 44% yield. We cannot conclude on a relation between the yield and the bulkiness on the alkyne.

Finally, we were pleased to observe that various aryls could indeed migrate using our conditions. A 4-tolyl and a 2-tolyl group could migrate and lead to 52% and 32% of the corresponding final phthalazine **672'** and **677**, respectively. It is not surprising to witness a yield drop with the 2-tolyl substitution when compared to the 4-tolyl one since it is much more hindered right next to the migration position. Electron-rich aryls such as 3,4,5-trimethoxyphenyl and 3,4-methylenedioxyphenyl successfully migrated with poor 34% (**678**) and medium 47% (**679**) yield, respectively. Moreover, electron-deficient substitutions such as 4-chlorophenyl or a 4-fluorophenyl group gave the final product **680** and **673'** in a medium 41% and 42% yield, respectively.

Surprisingly, the Smiles rearrangement did not occur on some starting materials represented in the following Table 22. Instead, the regular phthalazine, product of an hydroamination reaction followed by the cleavage of the N-P bond present in the pre-activation moiety was obtained (similar to the reaction described in **chapter III**).

Table 22 - Final products that did not undergo a Smiles rearrangement

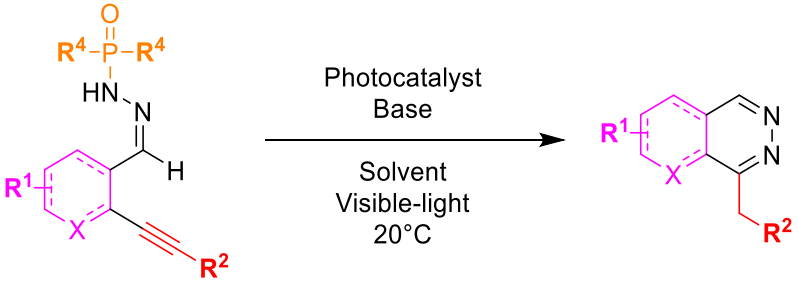

SM with alkynyl modifications

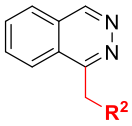

326, R^2 = 4-cyanophenyl, 51%
329, R^2 = H, 77% (from TMS SM)
681, R^2 = 3-nitrophenyl, 79%

SM with main ring and alkynyl modification

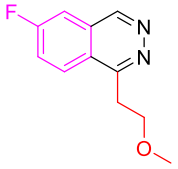

682, 72%

It seems that more electron-withdrawing groups like a 4-cyanophenyl or a 3-nitrophenyl substitution on the alkynyl chain of the starting material prevent the Smiles rearrangement from occurring. These two substitutions led to the corresponding phthalazines **326** and **681** in a 51% and a 79% yield, respectively. This may be because these electron-withdrawing groups could destabilize one of the radical intermediates playing a role in the aryl migration. The same result is observed with the TMS alkyne on the starting material (yielding 1-methylphthalazine **329** in a 77% yield), although here, the electron density is not to blame. The fact that the reaction is taking place in a basic ethanolic medium explains why the TMS is not present on the final scaffold because it is cleaved in the process (like the classical cleavage of TMS groups occurring in methanol with potassium carbonate). When it is cleaved, no group is present to stabilize a hypothetic transitory intermediate where the Smiles rearrangement could occur and therefore, we obtain a similar 1-methylphthalazine like in the previous methodology (see **chapter III**). Finally, the same reactivity was observed on the only starting material bearing modifications on both the main ring and the alkynyl chain with a fluoro substitution and an ether chain, leading to the phthalazine **682** in a good 72% yield. This is surprising since we observed a migration with an alkyne bearing an alkyl chain (see above). However, this example remains different since the alkyne bears an ether chain (although being of a same length) which has a totally different electron density compared to the propyl chain. The presence of the oxygen might destabilize the radical intermediate due to its inductive effect.

When the alkyne TMS derivative was engaged in our methodology, we noticed the formation of another non negligible side-product. Indeed, this product was formed in a 36% yield regarding its molar mass and is the result of the cleavage of the N-P bond by what seems to be an ethoxide ion. The

structure obtained (Figure 34) bears 2 phenyl groups on the phosphorus atom, as well as one ethoxy chain. This product gives us an indication on how the reaction proceeds when no Smiles rearrangement occurs.

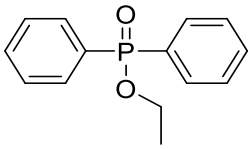

683

Figure 34 - Side-product obtained when using a starting material bearing an alkyne TMS substitution

To finish, some starting materials did not lead to any product formation (Table 23).

Table 23 - Starting material that did not lead to any product

Main ring modification	Alkynyl modifications
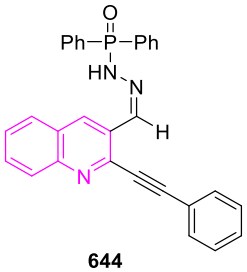 **644**	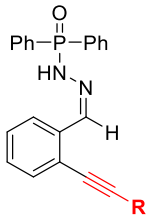 **651**, R = *tert*-Butyl

The reaction is compatible with various heterocycles present on the main ring, such as benzofuran or *N*-methylindole but it's not compatible with a quinoline (**644**). To finish, a *tert*-butyl substituted alkyne (**651**) did not lead to any product as well, because of a possible steric hindrance.

2.2. One-pot two steps

Our reaction was also attempted in a one-pot sequential strategy (Scheme 139). The first step being the formation of the phosphonohydrazone with only EtOH as the solvent and, after 1 hour, addition of the rest of the reagents (photocatalyst, solvent, base and molecular sieves). Unfortunately, the reaction yielded the desired phthalazine **664** in a lower 42% yield.

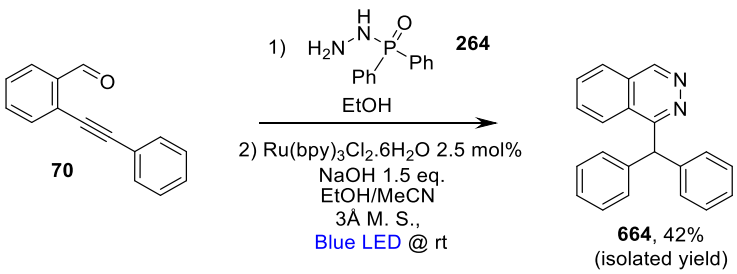

Scheme 139 - One-pot two-steps synthesis of phthalazine derivatives

3. Mechanistic investigations

3.1. Cyclic voltammetry

In order to determine the oxidation potentials of this new family of molecules, we used cyclic voltammetry in the same solvent mixture and base as our reaction and with lithium perchlorate as the supporting electrolyte.

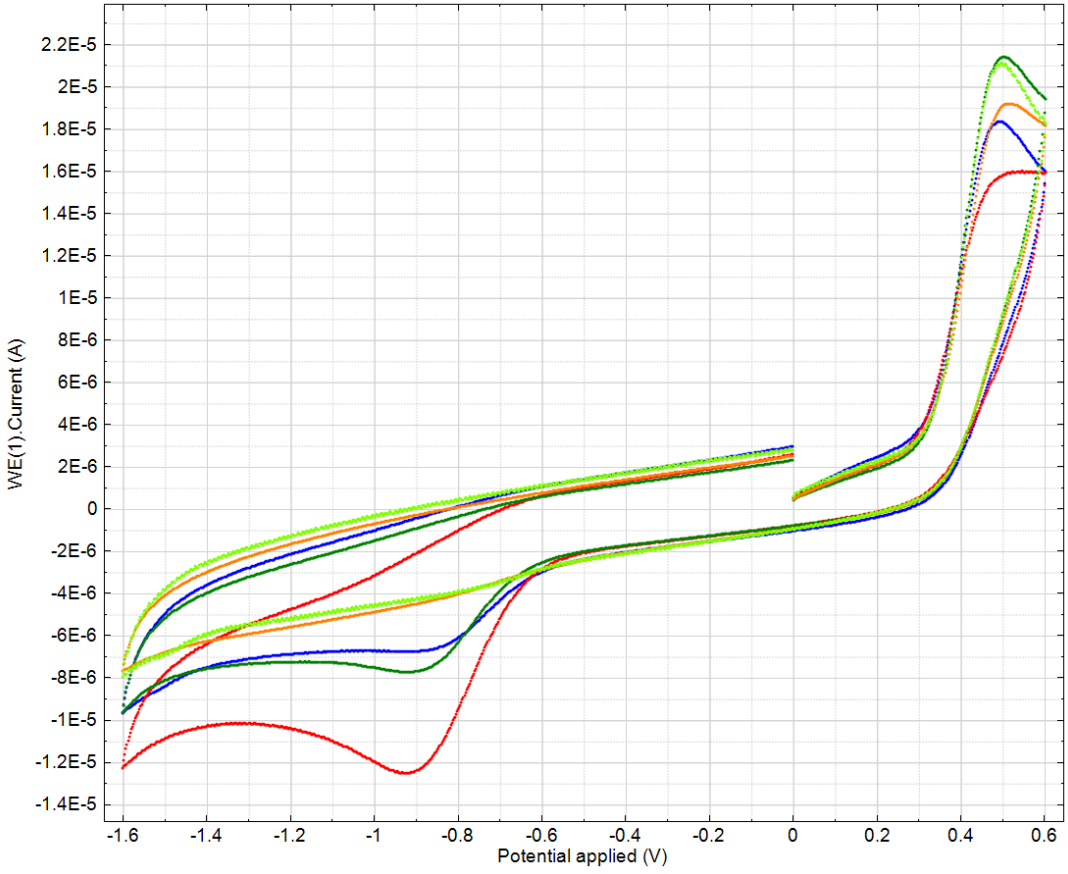

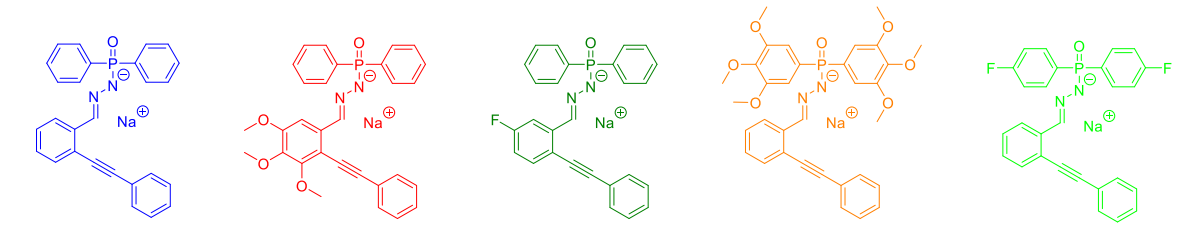

E_{Ox} = +0,5 V vs. SCE E_{Ox} = +0,54 V vs. SCE E_{Ox} = +0,5 V vs. SCE E_{Ox} = +0,52 V vs. SCE E_{Ox} = +0,5 V vs. SCE

We chose differently substituted phosphonohydrazones, bearing a fluorine or a methoxy substitutions either on the main ring or on the aryl groups on the phosphorus atom to see the influence of such groups' position on the oxidation potentials. Our model starting material present an oxidation potential of E_{ox} = +0.5 V vs. SCE. Three methoxy substitutions on the main ring slightly affected the

oxidation potential to a higher value of E_{ox} = +0.54 V vs. SCE while a fluorine substitution did not affect the potential compared to the model starting material. Once again, three methoxy substitutions present on the aryls on the phosphorus atom led to a slightly increased potential (E_{ox} = +0.52 V vs. SCE) while fluorine substitutions did not change it compared to the model. We observe with these molecules a reverse effect when comparing with our other type of phosphonohydrazone bearing ethoxy chains. Indeed, this time, electron-donating substitutions lead to a higher redox potential whereas electron withdrawing groups did not change the redox potential.

3.2. Proposed mechanism

We assume that the mechanism proceeds through a similar process as our previous methodology, at the beginning at least. Indeed, the starting phosphonohydrazone **A** is deprotonated by the hydroxide ions present in the reaction medium. Then, this anionic intermediate **B** is oxidized by the excited-state $[Ru(bpy)_3^{2+}]$* photocatalyst, yielding the desired nitrogen-centered radical **C** which is subsequently engaged in an intramolecular addition onto the alkyne, giving a carbon-centered radical **D**. The latter is a key intermediate since it can give rise to two products. Indeed, in **path A** (Scheme 140), it can react with the aryl group in its close vicinity in order to form a spiro intermediate **E** which yields the phosphorus radical-centered intermediate **F**. We believe that a HAT or a reduction of this intermediate by the photocatalyst followed by a protonation yield the intermediate **G** as described by Clive and Kang in their study.[200] **G** then undergoes an ethanolysis, yielding the desired product and the phosphorus by-product **H**. In **path B** (Scheme 141), the intermediate **D** can be reduced by the photocatalyst which closes the catalytic cycle and yields the anionic intermediate **I**. Then a protonation of the anion gives **J** and an ethanolysis yields the undesired product (*i.e.* when no aryl migration occurs) and the phosphorus by-product **K** containing two aryl groups. Unfortunately, we were not able to isolate the by-product **H** but we could witness its presence in the reaction medium with an LC-MS experiment. **K** was isolated and characterized.

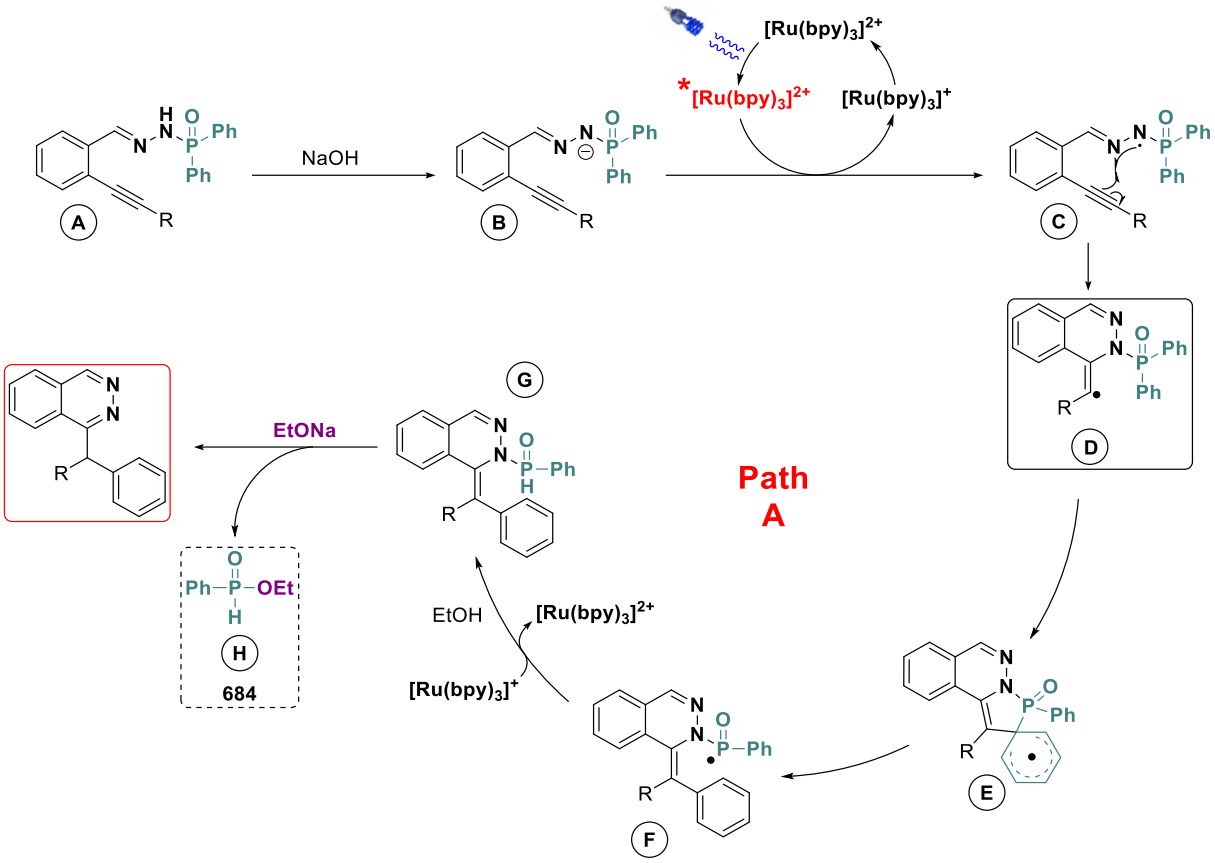

Scheme 140 - Proposed mechanism (Path A)

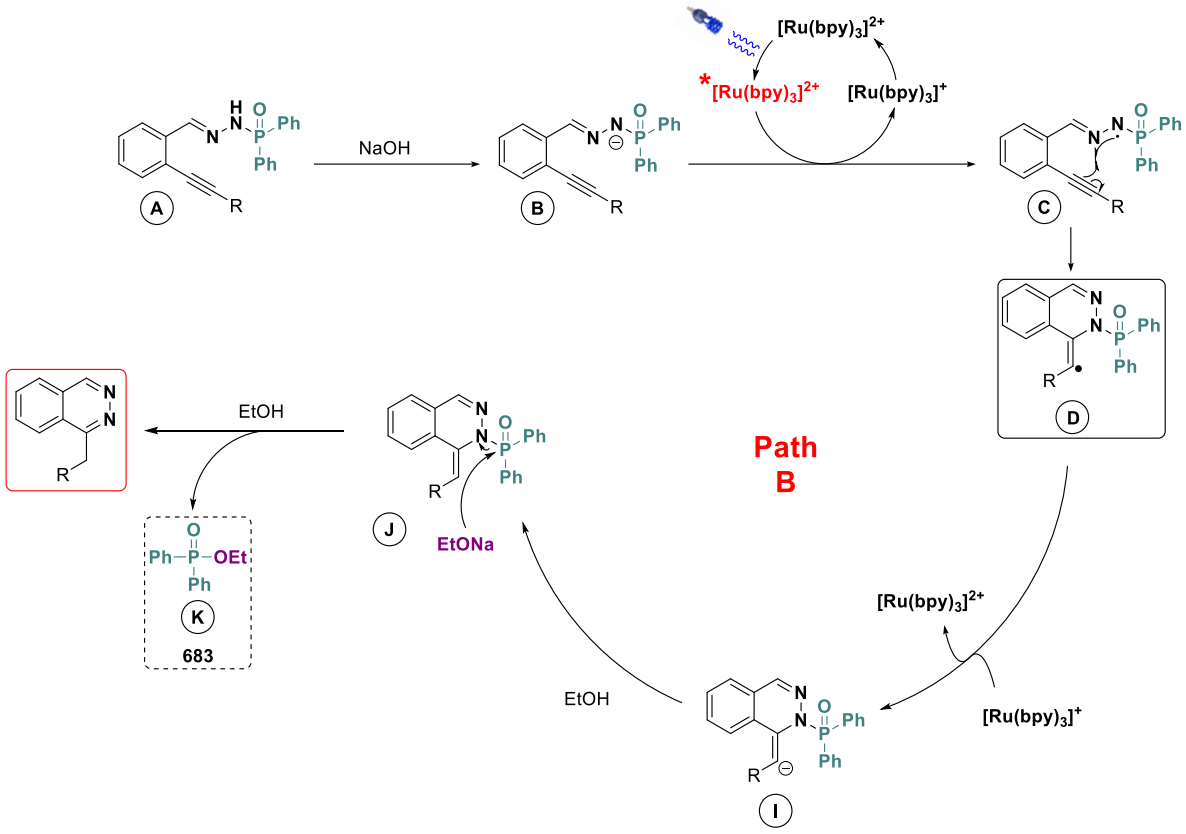

Scheme 141 - Proposed mechanism (Path B)

F) Conclusion & perspectives

We reported herein a new reactivity associated with phosphonohydrazones. Changing the substitution on the phosphorus atom with aryl groups allow the obtention of a new type of reactivity with a radical 1,4-aryl migration occurring within the scaffold, while keeping the attractiveness of the self-immolative phosphorus moiety.

Although presenting moderate yields overall, this methodology brings a new addition in the world of photoinduced radical aryl migration reactions by being one of the very few examples of such migration of an aryl from a phosphorus to a carbon atom

It would be interesting to extend the applicability of such precursor to 1,3 or 1,5 aryl migration reactions, as well as new scaffolds.

General Conclusion

II) General conclusion & perspectives

This thesis was divided in two axes, both aiming toward the synthesis of nitrogen-containing heterocycles.

In one hand, we were able to develop an attractive synthetic methodology for the efficient formation of 1,2-dihydroisoquinoline derivatives. This methodology comprises a tandem cycloisomerization/hydroarylation reaction, allowing the rapid access to an elaborate scaffold in just one step (Scheme 142).

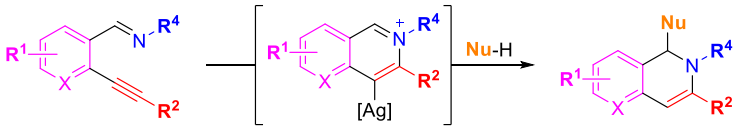

Scheme 142 - Silver-catalyzed tandem cycloisomerization/hydroarylation reaction to access 1,2-dihydroisoquinolines

On the other hand, visible-light was used as an energy source for photoredox catalyzed reactions. We successfully developed a new family of nitrogen-centered radical precursors called phosphonohydrazones which contain a phosphoramidate moiety. The latter proved to be an efficient radical precursor under the right conditions and even exhibited unexpected, yet desirable, properties such as being a self-immolative moiety. Mechanistic investigations allowed to gain a deeper insight in the reaction mechanism and therefore to propose a plausible mechanism for the formation of phthalazine derivatives.

It is only after a further modification of the phosphoramidate moiety that we witnessed a new reactivity. Indeed, when substituting the phosphorus atom with aryls instead of ethoxy chains, we were pleased to observe a novel radical 1,4 aryl migration occurring within the scaffold.

These methodologies are novel since they prove for the first time that phosphoramidates can serve as nitrogen-centered radical precursors under photoredox conditions, paving the way for further application of this moiety in other methodologies for the efficient formation of C-N bonds. Moreover, it is also the first time that a radical 1,4-aryl migration was reported from a phosphoramidate moiety, or more broadly, from a phosphorus atom to a carbon atom, under photoredox conditions (Scheme 143).

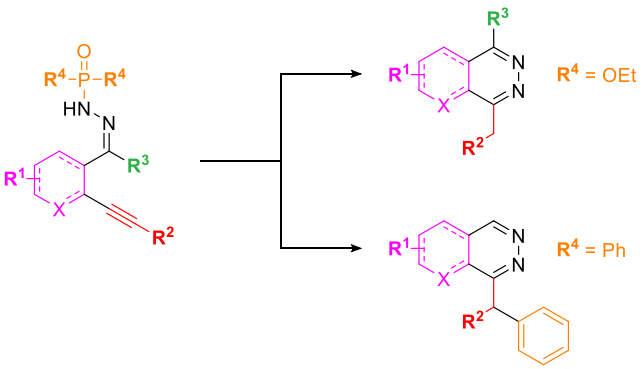

Scheme 143 - Visible-light catalyzed hydroamination reaction, followed or not by a radical aryl migration reaction

In the future, further investigations should be undertaken in two directions. The first one should focus on the understanding of the fluorine exchange (highlighted in **chapter III**) and its extension to other types of substrates (Scheme 144).

The second one should take advantage of the unusual property that exhibits alkene substituted phosphonohydrazones which keep their phosphorus-containing moiety up to the end of the reaction. After a fine tuning of their structure and substitutions on the phosphorus atom, these substrates could present a P-chirogenic center that could be useful in order to induce chirality within the products themselves or be used as a ligand for further experiments (Scheme 144).

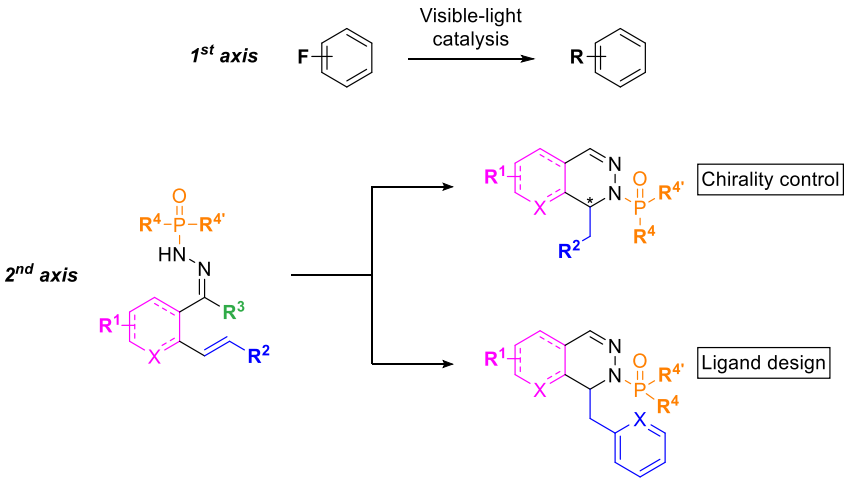

Scheme 144 - Perspectives of this thesis

Experimental part

III) Experimental part

General considerations

1) Solvents and reagents

Methanol and ethanol used for photoredox catalysis were stored under inert atmosphere with molecular sieves, prior to use. THF and DCM were taken from a solvent purification system (Innovative Technology®). All other commercial solvents and reagents were used as received without further distillation/purification.

2) Analysis

All reactions were monitored by thin-layer chromatography using Merck silica gel plates 60 F254. Visualization was accomplished with short wavelength UV light (254 and 365 nm) and/or staining with appropriate stains (anisaldehyde, orthophosphomolybdic acid). Purification were performed either *via* recrystallization, *via* preparative TLC; *via* standard flash chromatography (using silica gel of particle size 40−63 µm) or *via* a flash purification system (Biotage® Isolera™ One), unless specified otherwise. IR spectra were recorded on a Perkin Elmer Spectrum 65 FT-IR spectrometer with the absorption frequencies reported in wavenumber (cm^{-1}). Melting points were measured using capillaries in a melting point apparatus.

^{1}H NMR, ^{13}C NMR, ^{31}P NMR and ^{19}F NMR spectra were recorded on a Bruker® Avance™ 300, 400 or 600 MHz spectrometers in $CDCl_3$, DMSO-d_6, acetone-d_6, acetonitrile-d_3 or methanol-d_4 solution with internal solvent signal as reference. NMR data are reported as follows: chemical shift (ppm), multiplicity (s = singlet, d = doublet, t = triplet, q = quartet, quint = quintet, dd = doublet of doublets, ddd = doublet of doublet of doublets, td = triplet of doublets, qd = quartet of doublets, m = multiplet, br. s. = broad singlet), and coupling constants (Hz) and number of protons (for ^{1}H NMR).

High-Resolution Mass Spectrometry (HRMS) measurements were recorder either on a Bruker MicrOTOF-Q II™ or Q-TOF maXis™ spectrometer using an electrospray ionization (ESI) or an atmospheric-pressure chemical ionization (APCI).

Chapter I: Access to the isoquinoline scaffold *via* a Ag-catalyzed tandem hydroarylation/cycloisomerization

Sonogashira cross-coupling reaction

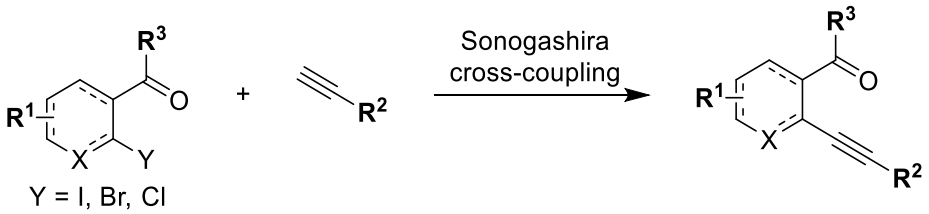

General procedure:

To an oven dried sealable glass vial were added CuI (1 mol%) and $PdCl_2(PPh_3)_2$ (2 mol%) to a solution of a halide derivative (1 eq.) in triethylamine (0.25 M). The solution was degassed with an inert gas for a few minutes before adding the alkyne (1.2 eq.). The vials were sealed with 20mm crimp caps with silicone/PTFE septum and stirred at room temperature (20-25°C) when using iodinated derivatives or at 50°C when using brominated derivatives. The reaction was monitored by TLC until completion and quenched by addition of distilled water and the pH was brought to neutrality by adding a saturated solution of ammonium chloride. The mixture was extracted with ethyl acetate, the combined organic phases were washed with brine, dried over Na_2SO_4, filtrated and concentrated under reduced pressure. The crude mixture was purified on a silica gel column chromatography, eluting with a cyclohexane/ethyl acetate mixture to afford the desired product.

2-(phenylethynyl)benzaldehyde **70**

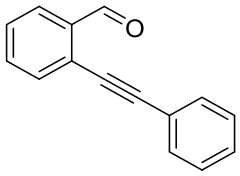

Formula: $C_{15}H_{10}O$

Mol. Weight: 206.24 g.mol^{-1}

Aspect: brown oil

R_f: 0.46 (cyclohexane:EA, 9:1)

Yield: 98%

^{1}H NMR (400 MHz, Chloroform-d): δ 10.66 (s, 1H), 7.96 (d, J = 7.7 Hz, 1H), 7.71 – 7.53 (m, 4H), 7.51 – 7.34 (m, 4H).

Spectral data were consistent with data reported in the literature.[233]

5-fluoro-2-(phenylethynyl)benzaldehyde **71**

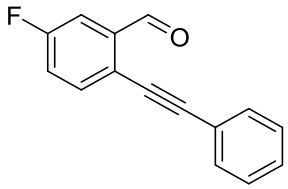

Formula: $C_{15}H_9FO$

Mol. Weight: 224,06 g.mol^{-1}

Aspect: yellow solid

R_f: 0.5 (cyclohexane:EA, 9:1)

Yield: 72%

^{1}H NMR (400 MHz, Chloroform-d): δ 10.60 (s, 1H), 7.69 – 7.59 (m, 2H), 7.56 (m, 2H), 7.43 – 7.36 (m, 3H), 7.30 (m, 1H).

Spectral data were consistent with data reported in the literature.[234]

5-chloro-2-(phenylethynyl)benzaldehyde **72**

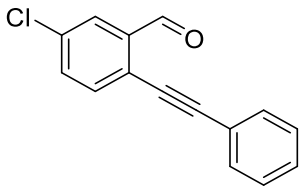

Formula: $C_{15}H_9ClO$

Mol. Weight: 240.69 g.mol^{-1}

Aspect: yellow solid

R_f: 0.44 (cyclohexane:EA, 9:1)

Yield: 78%

^{1}H NMR (400 MHz, Chloroform-d): δ 10.58 (s, 1H), 7.91 (d, J = 2.4 Hz, 1H), 7.53-7.60 (m, 4H), 7.39-7.40 (m, 3H).

[233] G. Dyker, W. Stirner, G. Henkel, *European Journal of Organic Chemistry* **2000**, *2000*, 1433–1441.
[234] P. C. Too, S. Chiba, *Chem. Commun.* **2012**, *48*, 7634–7636.

Spectral data were consistent with data reported in the literature.[235]

5-methoxy-2-(phenylethynyl)benzaldehyde **73**

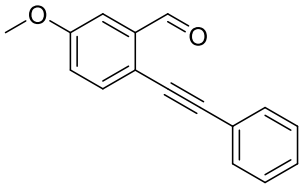

Formula: $C_{16}H_{12}O_2$

Mol. Weight: 236.27 g.mol^{-1}

Aspect: brown oil

R_f: 0.35 (cyclohexane:EA, 9:1)

Yield: Quant.

^{1}H NMR (400 MHz, Chloroform-d): δ 10.64 (d, J = 2.1 Hz, 1H), 7.57 (dd, J = 7.8, 2.5 Hz, 3H), 7.47 – 7.35 (m, 4H), 7.14 (dd, J = 8.6, 2.7 Hz, 1H), 3.87 (d, J = 2.2 Hz, 3H).
Spectral data were consistent with data reported in the literature.[236]

3,4,5-trimethoxy-2-(phenylethynyl)benzaldehyde **74**

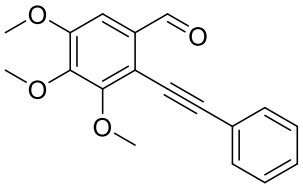

Formula: $C_{18}H_{16}O_4$

Mol. Weight: 296.32 g.mol^{-1}

Aspect: brown oil

R_f: 0.2 (cyclohexane:EA, 9:1)

Yield: Quant.

^{1}H NMR (400 MHz, Chloroform-d): δ 10.51 (s, 1H), 7.61 – 7.44 (m, 2H), 7.35 (dd, J = 4.9, 1.9 Hz, 3H), 7.26 (s, 1H), 4.02 (s, 3H), 3.96 (s, 3H), 3.91 (s, 4H).

Spectral data were consistent with data reported in the literature.[237]

2-(phenylethynyl)nicotinaldehyde **75**

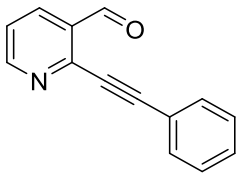

Formula: $C_{14}H_9NO$

Mol. Weight: 207.23 g.mol^{-1}

Aspect: brown oil

R_f: 0.12 (Cyclohexane)

Yield: 60%

[235] J. H. Park, S. V. Bhilare, S. W. Youn, *Org. Lett.* **2011**, *13*, 2228–2231.
[236] J. H. Park, S. V. Bhilare, S. W. Youn, *Org. Lett.* **2011**, *13*, 2228–2231.
[237] G. Lu, C. Cai, B. H. Lipshutz, *Green Chem.* **2012**, *15*, 105–109.

^{1}H NMR (400 MHz, Chloroform-d): δ 10.68 (s, 1H), 8.83 (d, J = 4.6 Hz, 1H), 8.23 (d, J = 7.9 Hz, 1H), 7.66 (d, J = 6.7 Hz, 2H), 7.42 (m, 4H).

Spectral data were consistent with data reported in the literature.[238]

2-((4-methoxyphenyl)ethynyl)benzaldehyde **76**

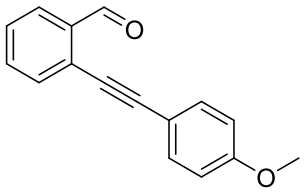

Formula: $C_{16}H_{12}O_2$

Mol. Weight: 236.27 g.mol^{-1}

Aspect: yellow solid

R_f: 0.38 (cyclohexane:EA, 9:1)

Yield: 88%

^{1}H NMR (400 MHz, Chloroform-d): δ 10.63 (s, 1H), 7.91 (d, J = 7.7 Hz, 1H), 7.64 (d, J = 7.6 Hz, 1H), 7.59 (dd, J = 7.6 Hz, 7.3 Hz, 1H), 7.53 (d, J = 8.8 Hz, 2H), 7.45 (dd, J = 7.7 Hz, 7.6 S-6 Hz, 1H), 6.93 (d, J = 8.8 Hz, 2H), 3.84 (s, 3H).

Spectral data were consistent with data reported in the literature.[234]

2-((2,5-dimethylphenyl)ethynyl)benzaldehyde **77**

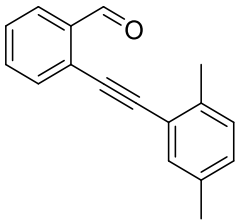

Formula: $C_{17}H_{14}O$

Mol. Weight: 234.30 g.mol^{-1}

Aspect: yellow oil

R_f: 0.21 (cyclohexane)

Yield: Quant.

^{1}H NMR (300 MHz, Chloroform-d): δ 10.68 (d, J = 0.8 Hz, 1H), 7.96 (ddd, J = 7.8, 1.5, 0.6 Hz, 1H), 7.69 – 7.55 (m, 2H), 7.45 (dddd, J = 7.9, 7.2, 1.5, 0.8 Hz, 1H), 7.39 – 7.34 (m, 1H), 7.18 – 7.07 (m, 2H), 2.49 (s, 3H), 2.33 (s, 3H).

^{13}C NMR (101 MHz, Chloroform-d): δ 191.94, 137.44, 135.76, 135.42, 133.95, 133.40, 132.70, 130.18, 129.69, 128.57, 127.35, 122.01, 110.07, 95.80, 88.47, 20.88, 20.53.

[238] G. Shore, M. Tsimerman, M. G. Organ, *Beilstein J. Org. Chem.* **2009**, *5*, 35.

2-((4-(trifluoromethyl)phenyl)ethynyl)benzaldehyde **78**

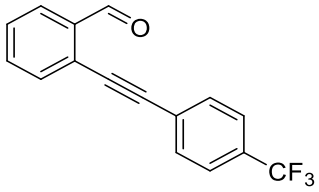

Formula: $C_{16}H_9F_3O$

Mol. Weight: 274.24 g.mol^{-1}

Aspect: brown solid

R_f: 0.56 (cyclohexane:EA, 9:1)

Yield: 74%

^{1}H NMR (400 MHz, Chloroform-d): δ 10.63 (s, 1H), 7.98 (d, J = 7.4 Hz, 1H), 7.69-7.59 (m, 6H), 7.51 (t, J =7.4 Hz, 1H).

Spectral data were consistent with data reported in the literature.[54]

2-((3-nitrophenyl)ethynyl)benzaldehyde **79**

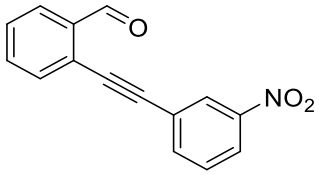

Formula: $C_{15}H_9NO_3$

Mol. Weight: 251.24 g.mol^{-1}

Aspect: yellow solid

R_f: 0.19 (cyclohexane:EA, 9:1)

Yield: quant.

^{1}H NMR (400 MHz, Chloroform-d): δ 10.61 (s, 1 H), 8.39-8.43 (m, 1 H), 8.21-8.27 (m, 1 H), 7.95-8.01 (m, 1 H), 7.84-7.90 (m, 1 H), 7.49-7.72 (m, 4 H).

Spectral data were consistent with data reported in the literature.[239]

2-(thiophen-2-ylethynyl)benzaldehyde **80**

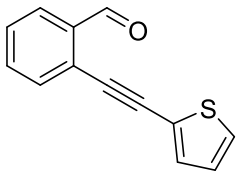

Formula: $C_{13}H_8OS$

Mol. Weight: 212.27 g.mol^{-1}

Aspect: brown solid

R_f: 0.59 (cyclohexane:EA, 9:1)

Yield: 69%

^{1}H NMR (400 MHz, Chloroform-d): δ 10.59 (d, J = 0.8 Hz, 1H), 7.97-7.94 (m, 1H), 7.65-7.56 (m, 2H), 7.49-7.43 (m, 1H), 7.38-7.35 (m, 2H), 7.05 (dd, J = 5.1, 3.7 Hz, 1H).

[239] J. Bucher, T. Stößer, M. Rudolph, F. Rominger, A. S. K. Hashmi, *Angewandte Chemie International Edition* **2015**, *54*, 1666–1670.

Spectral data were consistent with data reported in the literature.[240]

2-(cyclohex-1-en-1-ylethynyl)benzaldehyde **81**

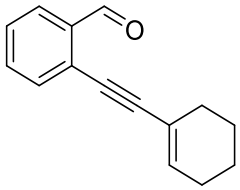

Formula: $C_{15}H_{14}O$

Mol. Weight: 210.28 $g.mol^{-1}$

Aspect: brown oil

R_f: 0.54 (cyclohexane:EA, 7:3)

Yield: 99%

^{1}H NMR (400 MHz, Chloroform-d): δ 10.55 (s, 1H), 7.90 (d, J = 8.0 Hz, 1H), 7.54–7.51 (m, 2H), 7.41–7.37 (m, 1H), 6.32–6.29 (m, 1H), 2.27–2.23 (m, 2H), 2.20–2.16 (m, 2H), 1.74–1.61 (m, 4H).

Spectral data were consistent with data reported in the literature.[241]

2-(oct-1-yn-1-yl)benzaldehyde **82**

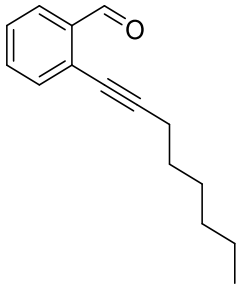

Formula: $C_{15}H_{18}O$

Mol. Weight: 214.31 $g.mol^{-1}$

Aspect: brown oil

R_f: 0.77 (cyclohexane:EA, 9:1)

Yield: 69%

^{1}H NMR (300 MHz, Chloroform-d): δ 10.54 (s, 1H), 7.88 (d, J = 7.7 Hz, 1H), 7.54 – 7.47 (m, 2H), 7.42 – 7.33 (m, 1H), 2.48 (t, J = 7.0 Hz, 2H), 1.64 (m, 2H), 1.54 – 1.40 (m, 2H), 1.33 (m, 4H), 0.96 – 0.85 (m, 3H).

Spectral data were consistent with data reported in the literature. [242]

[240] V. Claus, L. Molinari, S. Büllmann, J. Thusek, M. Rudolph, F. Rominger, A. S. K. Hashmi, *Chemistry – A European Journal* **2019**, *25*, 9385–9389.
[241] T. Yamada, K. Park, T. Tachikawa, A. Fujii, M. Rudolph, A. S. K. Hashmi, H. Sajiki, *Org. Lett.* **2020**, *22*, 1883–1888.
[242] V. Claus, L. Molinari, S. Büllmann, J. Thusek, M. Rudolph, F. Rominger, A. S. K. Hashmi, *Chemistry – A European Journal* **2019**, *25*, 9385–9389.

2-(3-hydroxy-3-methylbut-1-yn-1-yl)benzaldehyde **83**

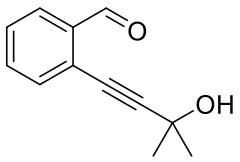

Formula: $C_{12}H_{12}O_2$

Mol. Weight: 188.23 g.mol^{-1}

Aspect: brown oil

R_f: 0.61 (cyclohexane:EA, 7:3)

Yield: 89%

^{1}H NMR (300 MHz, Chloroform-d): δ 10.49 (s, 1H), 7.89 (d, J = 7.7 Hz, 1H), 7.58 – 7.36 (m, 3H), 1.65 (s, 6H).

Spectral data were consistent with data reported in the literature.[243]

2-((trimethylsilyl)ethynyl)benzaldehyde **84**

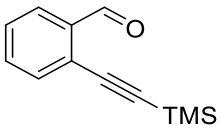

Formula: $C_{12}H_{14}OSi$

Mol. Weight: 202.33 g.mol^{-1}

Aspect: brown oil

R_f: 0.7 (cyclohexane:EA, 9:1)

Yield: 78%

^{1}H NMR (300 MHz, Chloroform-d): δ 10.56 (s, 1H), 7.91 (d, J = 7.8, 1.4, 0.7 Hz, 1H), 7.61 – 7.49 (m, 2H), 7.43 (m, 1H), 0.28 (s, 9H).

Spectral data were consistent with data reported in the literature.[244]

[243] K. R. Roesch, R. C. Larock, *J. Org. Chem.* **2002**, *67*, 86–94.

[244] S. K. Pagire, P. Kreitmeier, O. Reiser, *Angewandte Chemie International Edition* **2017**, *56*, 10928–10932.

Imine formation

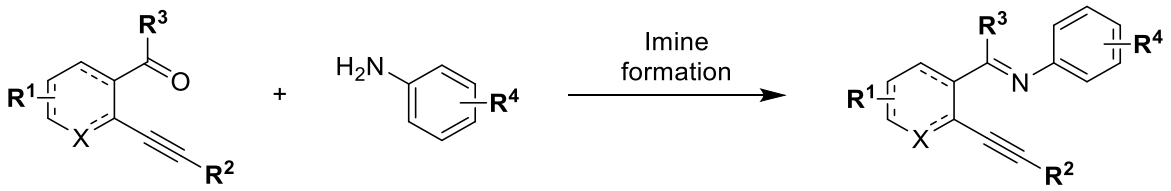

General procedure:

Protocol A: An oven dried re-sealable tube was charged with a mixture of aldehyde derivative (1 eq.), imine derivative (1 eq.) and 3 Å molecular sieves (100 mg), in CH_2Cl_2 (0.5 M). The tube was capped with a rubber septum and the mixture was stirred at room temperature. After completion of the reaction check by TLC, the resulting suspension was filtered and the solvent was removed under reduced pressure. Purification of the residue on silica gel column chromatography eluting with a cyclohexane/ethyl acetate mixture gave the desired product.

Protocol B: An oven dried re-sealable tube was charged with a mixture of aldehyde derivative (1 eq.), imine derivative (3 eq.), 3 Å molecular sieves (100 mg) and acetic acid (0.1 eq.), in CH_2Cl_2 (0.5 M). The tube was capped with a rubber septum and the mixture was stirred at room temperature. After completion of the reaction check by TLC, the resulting suspension was filtered and the solvent was removed under reduced pressure. Purification of the residue on silica gel column chromatography eluting with a cyclohexane/ethyl acetate mixture gave the desired product.

Note: Due to the slight acidity of silica, some imine hydrolysis was observed. To overcome this, neutralization of silica using a 1% solution of triethylamine in cyclohexane was performed prior to purification.

N-(4-methoxyphenyl)-1-(2-(phenylethynyl)phenyl)methanimine

85 (Protocol A)

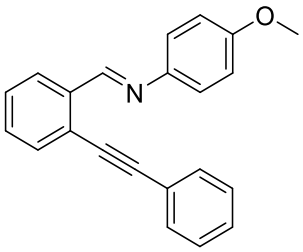

Formula: $C_{22}H_{17}NO$

Mol. Weight: 311.38 g.mol^{-1}

Aspect: orange solid

R_f: 0.39 (cyclohexane:EA, 9:1)

Yield: 97%

^{1}H NMR (400 MHz, DMSO-d_6): δ 9.06 (s, 1H), 8.16-8.19 (m, 1H), 7.71-7.68 (m, 1H), 7.59-7.64 (m, 2H), 7.58-7.53 (m, 2H), 7.49-7.44 (m, 3H), 7.34 (d, J = 8.7 Hz, 2H), 7.02 (d, J = 8.7 Hz, 2H), 3.79 (s, 3H).

Spectral data were consistent with data reported in the literature.[245]

1-(5-fluoro-2-(phenylethynyl)phenyl)-N-(4-methoxyphenyl)methanimine

86 (Protocol A)

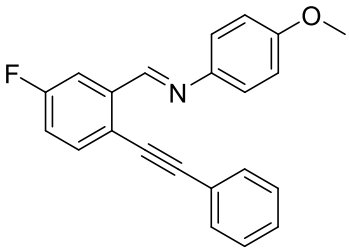

Formula: $C_{22}H_{16}FNO$

Mol. Weight: 329.37 g.mol^{-1}

Aspect: yellow solid

R_f: 0.68 (cyclohexane:EA, 8:2)

Yield: 86%

^{1}H NMR (300 MHz, Chloroform-d): δ 9.08 (d, J = 2.0 Hz, 1H), 7.97 (dd, J = 9.6, 2.3 Hz, 1H), 7.61 – 7.51 (m, 3H), 7.41 – 7.35 (m, 3H), 7.32 (d, J = 8.7 Hz, 2H), 7.14 (td, J = 8.4, 2.4 Hz, 1H), 6.96 (d, J = 8.7 Hz, 2H), 3.85 (s, 3H).

Spectral data were consistent with data reported in the literature.[65]

[245] T. Y. Chaudhari, Urvashi, S. K. Ginotra, P. Yadav, G. Kumar, V. Tandon, *Org. Biomol. Chem.* **2016**, *14*, 9896–9906.

1-(5-chloro-2-(phenylethynyl)phenyl)-N-(4-methoxyphenyl)methanimine

87 (Protocol B)

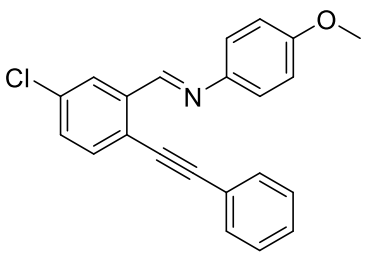

Formula: $C_{22}H_{16}ClNO$

Mol. Weight: 345.83 $g.mol^{-1}$

Aspect: yellow solid

R_f: 0.61 (cyclohexane:EA, 9:1)

Yield: 86%

^{1}H NMR (400 MHz, Acetone-d): δ 9.11 (s, 1H), 8.21 (s, 1H), 7.69 – 7.59 (m, 3H), 7.54 (d, J = 9.1 Hz, 1H), 7.47 – 7.43 (m, 3H), 7.39 (d, J = 8.1 Hz, 2H), 7.00 (d, J = 8.1 Hz, 2H), 3.83 (s, 3H).

^{13}C NMR (101 MHz, Acetone-d): δ 160.1, 154.7, 144.9, 139.6, 135.3, 135.1, 132.4, 131.4, 130.0, 129.6, 126.7, 123.9, 123.6, 123.3, 115.4, 97.0, 85.9, 55.8.

IR (neat): 3063, 2999, 2925, 2853, 2545, 2214, 1881, 1727, 1697, 1618, 1598, 1578, 1552, 1504, 1463, 1442, 1407, 1362 cm^{-1}.

mp: 68-70°C.

HR-MS (ESI+): m/z calculated for $C_{22}H_{16}NOClNa$ 368.0818 obtained 368.0818.

4-methoxy-N-(5-methoxy-2-(phenylethynyl)benzylidene)aniline

88 (Protocol B)

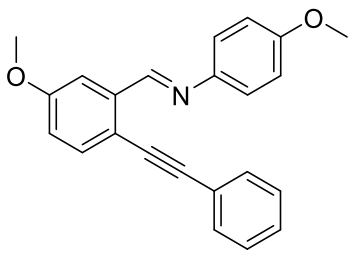

Formula: $C_{23}H_{19}NO_2$

Mol. Weight: 345.83 $g.mol^{-1}$

Aspect: yellow solid

R_f: 0.44 (cyclohexane:EA, 9:1)

Yield: 74%

^{1}H NMR (300 MHz, Chloroform-d): δ 9.14 (s, 1H), 7.81 (s, 1H), 7.6 – 7.5 (m, 3H), 7.40 – 7.31 (m, 5H), 7.06 – 6.94 (m, 3H), 3.92 (s, 3H), 3.85 (s, 3H).

Spectral data were consistent with data reported in the literature.[65]

N-(4-methoxyphenyl)-1-(3,4,5-trimethoxy-2-(phenylethynyl)phenyl)methanimine

89 (Protocol B)

Formula: $C_{25}H_{23}NO_4$

Mol. Weight: 401.46 $g.mol^{-1}$

Aspect: yellow solid

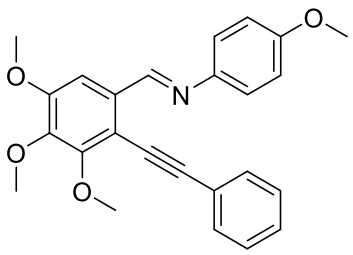

R_f: 0.2 (cyclohexane:EA, 9:1)

Yield: 74%

^{1}H NMR (300 MHz, Chloroform-d): δ 9.07 (s, 1H), 7.63 (s, 1H), 7.58 – 7.52 (m, 2H), 7.38 – 7.34 (m, 3H), 7.30 (d, J = 8.1 Hz, 2H), 7.13 (d, J = 8.1 Hz, 2H), 4.06 (s, 3H), 4 (s, 3H), 3.97 (s, 3H), 3.83 (s, 3H).

^{13}C NMR (101 MHz, Chloroform-d): δ 158.5, 156.3, 154.5, 154.1, 144.9, 144.7, 133.3, 131.4, 128.5, 128.5, 123.3, 122.4, 114.5, 113.3, 104.6, 98.3, 82.4, 61.5, 61.3, 56.2, 55.5.

IR (neat): 2998, 2935, 2884, 2210, 1732, 1619, 1579, 1505, 1494, 1485, 1464, 1409, 1370, 1338 cm^{-1}.

mp: 106-108°C.

HR-MS (ESI+): m/z calculated for $C_{25}H_{23}NO_4Na$ 424.1525 obtained 424.1526.

N-(4-methoxyphenyl)-1-(2-(phenylethynyl)pyridin-3-yl)methanimine

90 (Protocol A)

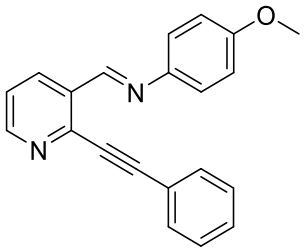

Formula: $C_{21}H_{16}N_2O$

Mol. Weight: 312.37 $g.mol^{-1}$

Aspect: brown solid

R_f: 0.12 (cyclohexane:EA, 9:1)

Yield: 60%

^{1}H NMR (300 MHz, Chloroform-d): δ 9.09 (s, 1H), 8.67 (d, J = 4.6 Hz, 1H), 8.53 (d, J = 8.0 Hz, 1H), 7.65 – 7.58 (m, 2H), 7.43 – 7.34 (m, 4H), 7.36 (d, 8.2 Hz, 4H), 7.36 (d, 8.2 Hz, 4H), 3.83 (s, 3H).

Spectral data were consistent with data reported in the literature.[65]

N-(4-methoxyphenyl)-1-(2-((4-methoxyphenyl)ethynyl)phenyl)methanimine

91 (Protocol B)

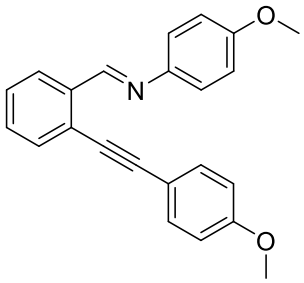

Formula: $C_{23}H_{19}NO_2$

Mol. Weight: 341.41 $g.mol^{-1}$

Aspect: orange oil

R_f: 0.31 (cyclohexane:EA, 9:1)

Yield: 49%

^{1}H NMR (300 MHz, Chloroform-d): δ 9.14 (s, 1H), 8.29 – 8.24 (m, 1H), 7.61 – 7.56 (m, 1H), 7.49 (d, J = 8.3 Hz, 2H), 7.44 – 7.39 (m, 2H), 7.31 (d, J = 8.5 Hz, 2H), 6.96 (d, J = 8.4 Hz, 2H), 6.90 (d, J = 8.4 Hz, 2H), 3.84 (d, J = 2.1 Hz, 6H).

Spectral data were consistent with data reported in the literature.[65]

1-(2-((2,5-dimethylphenyl)ethynyl)phenyl)-N-(4-methoxyphenyl)methanimine **92 (Protocol B)**

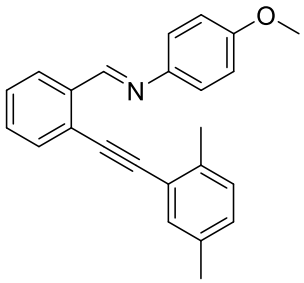

Formula: $C_{24}H_{21}NO$

Mol. Weight: 339.44 g.mol^{-1}

Aspect: yellow solid

R_f: 0.47 (cyclohexane:EA, 9:1)

Yield: 71%

^{1}H NMR (400 MHz, Chloroform-d): δ 9.23 (s, 1H), 8.34 – 8.27 (m, 1H), 7.67 – 7.60 (m, 1H), 7.48 – 7.42 (m, 2H), 7.39 (s, 1H), 7.35 (d, J = 8.7 Hz, 2H), 7.20 – 7.04 (m, 2H), 6.98 (d, J = 8.7 Hz, 2H), 3.86 (s, 3H), 2.52 (s, 3H), 2.36 (s, 3H).

^{13}C NMR (75 MHz, Chloroform-d): δ 158.6, 156.9, 145, 137.1, 136.9, 135.3, 132.7, 132.5, 130.6, 129.7, 129.6, 128.6, 126.4, 125.3, 122.6, 122.5, 114.5, 94.7, 90.1, 55.5, 20.8, 20.6.

IR (neat): 2922, 2835, 2206, 1697, 1619, 1600, 1578, 1504, 1462, 1441, 1362, 1298, 1245 cm^{-1}.

mp: 57-59°C.

HR-MS (ESI+): m/z calculated for $C_{24}H_{21}NONa$ 362.1521 obtained 362.1526.

N-(4-methoxyphenyl)-1-(2-((4-(trifluoromethyl)phenyl)ethynyl)phenyl)methanimine **93 (Protocol B)**

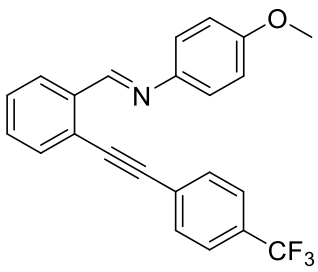

Formula: $C_{23}H_{16}F_3NO$

Mol. Weight: 379.38 g.mol^{-1}

Aspect: yellow solid

R_f: 0.53 (cyclohexane:EA, 9:1)

Yield: 15%

^{1}H NMR (400 MHz, Chloroform-d): δ 9.07 (s, 1H), 8.26 (d, J = 7.4 Hz, 1H), 7.63-7.58 (m, 5H), 7.44-7.41 (m, 2H), 7.29 (d, J = 8.6 Hz, 2H), 6.94 (d, J = 8.9 Hz, 2H), 3.81 (s, 3H).

Spectral data were consistent with data reported in the literature.[65]

N-(4-methoxyphenyl)-1-(2-(thiophen-2-ylethynyl)phenyl)methanimine

94 (Protocol B)

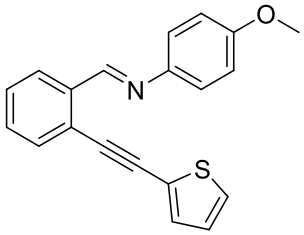

Formula: $C_{20}H_{15}NOS$

Mol. Weight: 317.41 g.mol^{-1}

Aspect: yellow solid

R_f: 0.45 (cyclohexane:EA, 9:1)

Yield: 41%

^{1}H NMR (300 MHz, Chloroform-d): δ 9.08 (s, 1H), 8.34 – 8.20 (m, 1H), 7.66 – 7.53 (m, 1H), 7.43 (dd, J = 5.8, 3.5 Hz, 2H), 7.37 – 7.28 (m, 4H), 7.09 – 7.00 (m, 1H), 6.96 (d, J = 8.8 Hz, 2H), 3.85 (s, 3H).

^{13}C NMR (75 MHz, Chloroform-d): δ 158.7, 156.6, 144.9, 137.0, 132.5, 132.3, 130.6, 129.0, 127.9, 127.4, 126.5, 125.6, 124.5, 122.6, 114.6, 90.4, 88.6, 55.6.

IR (neat): 3063, 2997, 2927, 2834, 2543, 2200, 2047, 1932, 1726, 1697, 1619, 1600, 1578, 1503, 1463, 1440, 1422, 1363 cm^{-1}.

mp: 65-67°C.

HR-MS (ESI+): m/z calculated for $C_{20}H_{16}NOS$ 318.0953 obtained 318.0943.

1-(2-(cyclohex-1-en-1-ylethynyl)phenyl)-N-(4-methoxyphenyl)methanimine

95 (Protocol B)

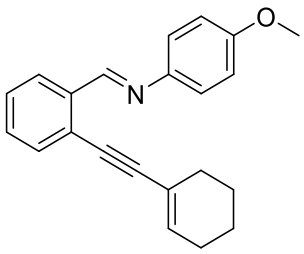

Formula: $C_{22}H_{21}NO$

Mol. Weight: 315.42 g.mol^{-1}

Aspect: orange oil

R_f: 0.57 (cyclohexane:EA, 7:3)

Yield: 81%

^{1}H NMR (300 MHz, Chloroform-d): δ 9.08 (s, 1H), 8.29 – 8.22 (m, 1H), 7.53 – 7.47 (m, 1H), 7.40 – 7.34 (m, 2H), 7.31 (d, J = 8.8 Hz, 2H), 6.96 (d, J = 8.8 Hz, 2H), 6.30 – 6.25 (m, 1H), 3.82 (s, 3H), 2.31 – 2.13 (m, 4H), 1.75 – 1.59 (m, 4H).

^{13}C NMR (101 MHz, Chloroform-d): δ 158.4, 156.8, 145.0, 136.7, 135.8, 132.4, 130.4, 128.1, 126.2, 125.4, 122.4, 120.6, 114.4, 97.4, 84.0, 55.4, 29.2, 25.8, 22.3, 21.5.

IR (neat): 3061, 3024, 2996, 2926, 2856, 2834, 2197, 2055, 1999, 1936, 1871, 1738, 1698, 1619, 1600, 1578, 1504, 1474, 1463, 1440, 1362 cm^{-1}.

HR-MS (ESI+): m/z calculated for $C_{22}H_{22}NO$ 316.1701 obtained 316.1699.

N-(4-chlorophenyl)-1-(2-(phenylethynyl)phenyl)methanimine

96 (Protocol A)

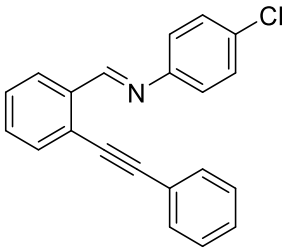

Formula: $C_{21}H_{14}ClN$

Mol. Weight: 315.80 $g.mol^{-1}$

Aspect: yellow solid

R_f: 0.48 (cyclohexane:EA, 95:5)

Yield: 75%

^{1}H NMR (300 MHz, DMSO-d_6) δ 9.02 (s, 1H), 8.18 (d, J = 7.3 Hz, 1H), 7.70-7.74 (m, 4H), 7.49 (d, J = 8.6 Hz, 2H), 7.48-7.43 (m, 3H), 7.34 (d, J = 8.6 Hz, 2H).

Spectral data were consistent with data reported in the literature.[246]

1-(2-(phenylethynyl)phenyl)-N-(3-(trifluoromethyl)phenyl)methanimine

97 (Protocol A)

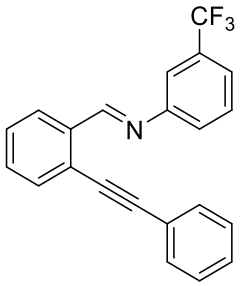

Formula: $C_{22}H_{14}F_3N$

Mol. Weight: 349.36 $g.mol^{-1}$

Aspect: orange solid

R_f: 0.12 (cyclohexane:EA, 95:5)

Yield: 75%

^{1}H NMR (400 MHz, Chloroform-d): δ 9.13 (s, 1H), 8.28 (d, J = 8.6 Hz, 1H), 7.64 (d, J = 8.6 Hz, 1H), 7.57-7.51 (m, 5H), 7.50 – 7.46 (m, 2H), 7.45 – 7.41 (m, 1H), 7.40 – 7.35 (m, 3H).

^{13}C NMR (75 MHz, Chloroform-d): δ 160.6, 152.8, 136.3, 132.8, 131.8 (q, J = 32.4 Hz), 131.7, 131.5, 129.9, 129, 128.9, 128.7, 126.8, 125.6, 124.4, 124.1 (q, J = 272.5 Hz), 122.8 (q, J = 3.8 Hz), 122.7, 118.2 (q, J = 3.8 Hz), 96, 86.2.

^{19}F NMR (376 MHz, Chloroform-d): δ -62.63.

IR (neat): 3063, 2916, 2215, 1714, 1626, 1599, 1589, 1492, 1442, 1324 cm^{-1}.

mp: 55-57°C.

HR-MS (ESI+): m/z calculated for $C_{22}H_{14}NF_3Na$ 372.0976 obtained 372.0972.

[246] T. Y. Chaudhari, Urvashi, S. K. Ginotra, P. Yadav, G. Kumar, V. Tandon, *Org. Biomol. Chem.* **2016**, *14*, 9896–9906.

1-(2-(phenylethynyl)phenyl)-N-(2,3,4-trifluorophenyl)methanimine

98 (Protocol A)

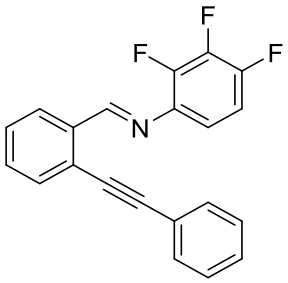

Formula: $C_{21}H_{12}F_3N$

Mol. Weight: 335.33 $g.mol^{-1}$

Aspect: yellow solid

R_f: 0.42 (cyclohexane:EA, 95:5)

Yield: 80%

^{1}H NMR (400 MHz, Chloroform-d): δ 9.16 (s, 1H), 8.29 (d, J = 7.6 Hz, 1H), 7.63 (d, J = 7.3 Hz, 1H), 7.57 – 7.51 (m, 2H), 7.51 – 7.42 (m, 2H), 7.42 – 7.33 (m, 3H), 7.05 – 6.9 (m, 2H).

^{13}C NMR (101 MHz, Chloroform-d): δ 162.1 (dd, J = 3.2, 1.7 Hz), 149.2 (ddd, J = 248.5, 10.4, 2.3 Hz), 144.8 (ddd, J = 253.4, 10.6, 3.4 Hz), 140.6 (dt, J = 251, 14 Hz), 137.5 (dd, J = 7.8, 3.8 Hz), 136.1, 132.8, 131.6, 131.6, 128.9, 128.8, 128.5, 126.8, 125.5, 122.6, 115.5 (ddd, J = 7.5, 3.5, 1.5 Hz), 111.6 (dd, J = 18.0, 4.2 Hz), 95.8, 85.9.

^{19}F NMR (376 MHz, Chloroform-d): δ -137.62 (d, J = 18.8 Hz), -146.21 (d, J = 19.2 Hz), -159.06 (t, J = 19.8 Hz).

IR (neat): 3464, 3057, 3031, 2970, 2923, 2853, 2210, 1943, 1738, 1610, 1591, 1505, 1494, 1371 cm^{-1}.

mp: 93-95°C.

HR-MS (ESI+): m/z calculated for $C_{21}H_{12}NF_3Na$ 358.0820 obtained 358.0814.

Spectral data were consistent with data reported in the literature.

N-benzyl-1-(2-(phenylethynyl)phenyl)methanimine

99 (Protocol B)

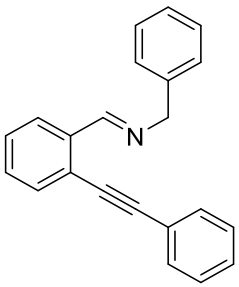

Formula: $C_{27}H_{17}N$

Mol. Weight: 295.39 $g.mol^{-1}$

Aspect: yellow solid

R_f: 0.35 (cyclohexane:EA, 95:5)

Yield: 77%

^{1}H NMR (400 MHz, Chloroform-d): δ 8.99 (s, 1H), 8.14 (d, J = 7.3 Hz, 1H), 7.57-7.28 (m, 13 H), 4.90 (s, 2H).

Spectral data were consistent with data reported in the literature.[65]

Tandem cycloisomerization/hydroarylation reaction

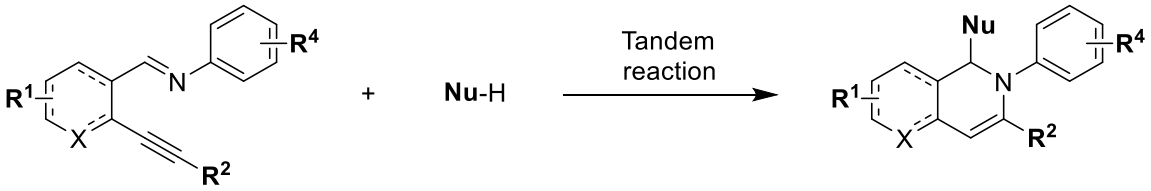

General procedure:

An oven dried re-sealable tube was charged with a mixture of ortho-alkynylbenzaldimine (1 eq), nucleophile (5 eq.), AgOTf (5 mol%) and acetic acid (1.1 eq.), in acetonitrile (0.08 M). The tube was capped with a rubber septum, evacuated and backfilled with nitrogen. The reaction mixture was stirred at room temperature overnight. After completion of the reaction check by TLC, the crude reaction mixture was immediately filtered on a short celite column to eliminate the catalyst. The filtrate was concentrated and purification of the residue by silica gel column chromatography eluting with cyclohexane/ethyl acetate mixture gave the desired product.

2-(4-methoxyphenyl)-1-(1-methyl-1H-indol-3-yl)-3-phenyl-1,2-dihydroisoquinoline **101**

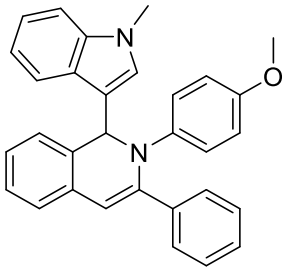

Formula: $C_{31}H_{26}N_2O$

Mol. Weight: 442.56 g.mol^{-1}

Aspect: ochre solid

R_f: 0.34 (cyclohexane:EA, 9:1);

Yield: 79%

^{1}H NMR (400 MHz, DMSO-d^6): δ 8.01 (d, J = 7.3 Hz, 1H), 7.47 (d, J = 7.1 Hz, 2H), 7.36 (d, J = 7.6 Hz, 2H), 7.30 – 7.07 (m, 8H), 7.09 (d, J = 7.2 Hz, 2H), 6.74 (d, J = 7.2 Hz, 2H), 6.72 (s, 1H), 6.61 (s, 1H), 6.34 (s, 1H), 3.62 (s, 6H)

^{13}C NMR (101 MHz, DMSO-d^6): δ 154.4, 141.5, 140.6, 137.6, 136.9, 131.8, 131.6, 128.3, 127.8, 127.7, 127.2, 126.4, 126.0, 125.7, 124.4, 123.1, 121.2, 119.4, 118.9, 116.5, 114.5, 114.2, 111.8, 109.9, 61.3, 55.1, 32.3.

IR (neat): 3048, 2922, 2853, 1712, 1607, 1558, 1505, 1488, 1463, 1452, 1372, 1330, 1291, 1242 cm^{-1}.

mp: 159-161°C.

HR-MS (ESI+): m/z calculated for $C_{31}H_{25}N_2ONa$ 465.1943 obtained 465.1931.

3,3'-((2-(phenylethynyl)phenyl)methylene)bis(1-methyl-1H-indole) **102**

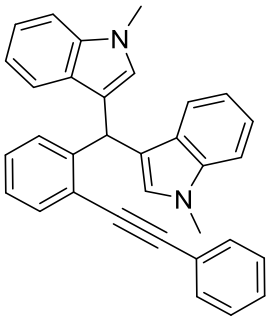

Formula: $C_{33}H_{26}N_2$

Mol. Weight: 450.59 g.mol^{-1}

Aspect: white solid

R_f: 0.23 (cyclohexane:EA, 9:1)

^{1}H NMR (400 MHz, DMSO-d$_6$): δ 7.57 (dd, J = 8.5, 1.5 Hz, 1H), 7.30-7.39 (m, 11H), 7.25-7.29 (qd, J = 8.5, 2.0 Hz, 1H), 7.12 (td, J = 7.5, 1.0 Hz, 2H), 6.91 (t, J = 7.0 Hz, 2H), 6.83 (s, 2H), 6.44 (s, 1H), 3.70 (s, 6H).

Spectral data were consistent with data reported in the literature.[247]

[247] G. Dyker, D. Hildebrandt, J. Liu, K. Merz, *Angewandte Chemie International Edition* **2003**, *42*, 4399–4402.

7-fluoro-2-(4-methoxyphenyl)-1-(1-methyl-1H-indol-3-yl)-3-phenyl-1,2-dihydroisoquinoline **103**

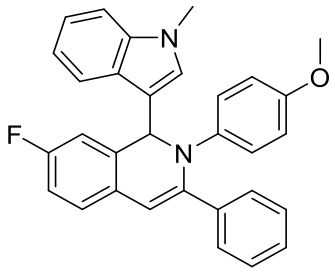

Formula: $C_{31}H_{25}FN_2O$

Mol. Weight: 460.55 g.mol^{-1}

Aspect: ochre solid

R_f: 0.39 (cyclohexane:EA, 9:1)

Yield: 77%

^{1}H NMR (400 MHz, Chloroform-d): δ 8.16 – 8.08 (m, 1H), 7.54 – 7.47 (m, 2H), 7.25 (h, J = 4.7, 3.8 Hz, 4H), 7.16 (dd, J = 9.8, 7.0 Hz, 3H), 7.09 – 7.01 (m, 2H), 7.00 – 6.86 (m, 2H), 6.73 – 6.64 (m, 2H), 6.61 (d, J = 8.3 Hz, 2H), 6.27 (s, 1H), 3.67 (s, 3H), 3.58 (s, 3H).

^{13}C NMR (101 MHz, Chloroform-d): δ 161.7 (d, J = 245.4 Hz), 155.1, 141.6 (d, J = 2.3 Hz), 141.1, 138.0, 137.3, 133.9 (d, J = 6.4 Hz), 128.5 (d, J = 2.8 Hz), 128.4, 127.9, 127.9, 127.8, 126.1, 125.8 (d, J = 7.9 Hz), 123.8, 121.8, 119.5 (d, J = 11.6 Hz), 116.8, 114.3, 114.2, 114.1, 113.0 (d, J = 21.8 Hz), 110.4, 109.7, 61.9, 55.5, 32.8.

^{19}F NMR (376 MHz, Chloroform-d): δ -115.62.

IR (neat): 3052, 2925, 2953, 1712, 1660, 1607, 1566, 1539, 1506, 1492, 1464, 1447, 1423, 1371, 1331, 1273, 1242 cm^{-1}.

mp: 158-160°C.

HR-MS (ESI+): m/z calculated for $C_{31}H_{24}N_2OFNa$ 483.1849 obtained 483.1850.

7-chloro-2-(4-methoxyphenyl)-1-(1-methyl-1H-indol-3-yl)-3-phenyl-1,2-dihydroisoquinoline **104**

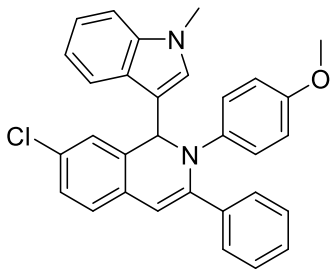

Formula: $C_{11}H_{25}ClN_2O$

Mol. Weight: 477.00 g.mol^{-1}

Aspect: ochre solid

R_f: 0.27 (cyclohexane:EA, 9:1)

Yield: 44%

^{1}H NMR (400 MHz, Chloroform-d): δ 8.19 – 8.10 (m, 1H), 7.57 – 7.48 (m, 2H), 7.35 – 7.16 (m, 9H), 7.07 (d, J = 8.2 Hz, 2H), 6.72 (d, J = 8.2 Hz, 2H), 6.66 (s, 1H), 6.61 (s, 1H), 6.30 (s, 1H), 3.73 (s, 3H), 3.66 (s, 3H).

^{13}C NMR (101 MHz, Chloroform-d): δ 154.8, 141.8, 140.5, 137.4, 137.0, 133.4, 130.9, 130.3, 128.5, 128.1, 127.9, 127.4, 127.2, 126.1, 125.9, 125.7, 123.4, 121.5, 119.5, 119.2, 116.1, 114.3, 110.8, 110.1, 60.8, 55.2, 32.5.

IR (neat): 3059, 2925, 2853, 1720, 1609, 1552, 1506, 1479, 1464, 1446, 1371, 1292, 1242 cm^{-1}.

mp: 163-165°C.

HR-MS (ESI+): m/z calculated for $C_{31}H_{26}ClN_2O$ 477.1728 obtained 477.1718.

7-methoxy-2-(4-methoxyphenyl)-1-(1-methyl-1H-indol-3-yl)-3-phenyl-1,2-dihydroisoquinoline **105**

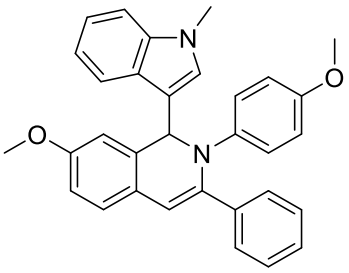

Formula: $C_{32}H_{28}N_2O_2$

Mol. Weight: 472.59 $g.mol^{-1}$

Aspect: yellow solid

R_f: 0.5 (cyclohexane:EA, 7:3)

Yield: 12% (23% at 50°C)

^{1}H NMR (400 MHz, Chloroform-d): δ 8.17 (s, 1H), 7.51 (s, 2H), 7.31 – 7.12 (m, 7H), 7.07 (d, J = 8.4 Hz, 2H), 6.84 (d, J = 9.0 Hz, 1H), 6.78 – 6.66 (m, 3H), 6.63 (s, 1H), 6.58 (s, 1H), 6.26 (s, 1H), 3.77 (s, 3H), 3.69 (s, 3H), 3.60 (s, 3H).

^{13}C NMR (101 MHz, Chloroform-d): δ 158.7, 154.8, 141.5, 140.1, 138.4, 137.3, 133.8, 128.3, 128.1, 127.6, 127.5, 126.4, 125.7, 125.6, 123.5, 121.6, 119.5, 119.4, 117.1, 114.2, 113.2, 111.6, 111.5, 109.6, 62.2, 55.5, 55.4, 32.8.

IR (neat): 3054, 2925, 2852, 1712, 1607, 1559, 1506, 1463, 1446, 1423, 1371, 1319, 1285, 1243 cm^{-1}.

mp: 164-166°C.

HR-MS (APCI): m/z calculated for $C_{32}H_{28}N_2O_2Na$ 495.2048 obtained 495.2028.

5,6,7-trimethoxy-2-(4-methoxyphenyl)-1-(1-methyl-1H-indol-3-yl)-3-phenyl-1,2-dihydroisoquinoline **106**

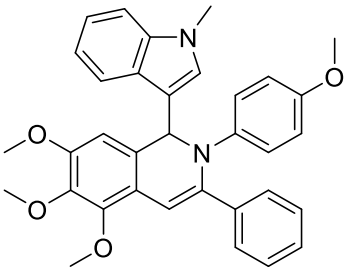

Formula: $C_{34}H_{32}N_2O_4$

Mol. Weight: 532.64 $g.mol^{-1}$

Aspect: ochre solid

R_f: 0.46 (cyclohexane:EA, 7:3)

Yield: 41% (at 50°C)

^{1}H NMR (400 MHz, Chloroform-d): δ 8.13 (d, J = 5.4 Hz, 1H), 7.51 (d, J = 7.3 Hz, 2H), 7.26 (s, 3H), 7.16 (q, J = 8.0, 7.3 Hz, 3H), 7.06 (d, J = 8.5 Hz, 2H), 6.83 (s, 1H), 6.70 (d, J = 8.5 Hz, 2H), 6.62 (s, 1H), 6.54 (s, 1H), 6.21 (s, 1H), 4.04 (s, 3H), 3.91 (s, 3H), 3.80 (s, 3H), 3.69 (s, 3H), 3.62 (s, 3H).

^{13}C NMR (101 MHz, Chloroform-d): δ 154.8, 152.4, 148.5, 141.4, 141.4, 141.1, 140.1, 138.4, 137.3, 128.3, 128.2, 128.1, 127.6, 127.5, 126.3, 123.4, 121.6, 119.4, 119.4, 117.1, 114.2, 109.7, 106.6, 105.5, 61.8, 61.6, 61.1, 56.1, 55.5, 32.9.

IR (neat): 3053, 2926, 2853, 1729, 1712, 1595, 1561, 1505, 1486, 1459, 1409, 1370, 1328, 1299 cm^{-1}.

mp: 68-70°C.

HR-MS (APCI): m/z calculated for $C_{34}H_{33}N_2O_4$ 533.2435 obtained 533.2430.

6-(4-methoxyphenyl)-5-(1-methyl-1H-indol-3-yl)-7-phenyl-5,6-dihydro-1,6-naphthyridine

107

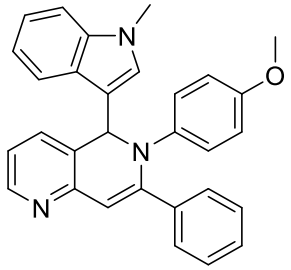

Formula: $C_{30}H_{25}N_3O$

Mol. Weight: 443.55 $g.mol^{-1}$

Aspect: yellow solid

R_f: 0.16 (cyclohexane:EA, 7:3)

Yield: 83%

^{1}H NMR (400 MHz, DMSO-d_6): δ 8.39 (d, J = 4.0 Hz, 1H), 7.99 (d, J = 7.8 Hz, 1H), 7.66 (d, J = 7.3 Hz, 1H), 7.49 (d, J = 6.6 Hz, 2H), 7.39 (d, J = 8.1 Hz, 1H), 7.29 – 7.07 (m, 6H), 6.97 (d, J = 8.8 Hz, 2H), 6.87 (s, 1H), 6.74 (d, J = 8.8 Hz, 2H), 6.64 (s, 1H), 6.44 (s, 1H), 3.65 (s, 3H), 3.62 (s, 3H).

^{13}C NMR (101 MHz, DMSO-d_6): δ 154.9, 150.6, 148.1, 145.8, 140.2, 137.1, 136.9, 133.3, 128.4, 127.7, 127.4, 126.2, 125.3, 123.9, 121.4, 121.1, 119.3, 119.1, 116.3, 114.1, 110.9, 110.0, 79.2, 61.2, 55.1, 32.4.

IR (neat): 3055, 2925, 2852, 1711, 1602, 1575, 1557, 1507, 1461, 1437, 1424, 1372, 1243 cm^{-1}.

mp: 168-170°C.

HR-MS (ESI+): m/z calculated for $C_{30}H_{26}N_3O$ 444.2070 obtained 444.2072.

2,3-bis(4-methoxyphenyl)-1-(1-methyl-1H-indol-3-yl)-1,2-dihydroisoquinoline

108

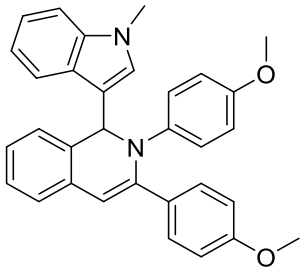

Formula: $C_{32}H_{28}N_2O_2$

Mol. Weight: 472.59 $g.mol^{-1}$

Aspect: ochre solid

R_f: 0.2 (cyclohexane:EA, 9:1)

Yield: 75%

^{1}H NMR (400 MHz, Acetone-d_6): δ 8.18 – 8.12 (m, 1H), 7.47 (d, J = 8.8 Hz, 2H), 7.35 – 7.32 (m, 1H), 7.31 (t, J = 1.4 Hz, 1H), 7.25 (dq, J = 5.9, 1.5 Hz, 2H), 7.19 – 7.13 (m, 3H), 7.08 (d, J = 9.0 Hz, 2H),

6.72 (dd, J = 8.9, 4.4 Hz, 4H), 6.66 (s, 1H), 6.61 (d, J = 0.9 Hz, 1H), 6.35 (s, 1H), 3.70 (s, 3H), 3.66 (s, 3H), 3.63 (s, 3H).

^{13}C NMR (101 MHz, Acetone-d_6): δ 160.4, 155.9, 142.6, 142.2, 138.3, 133.6, 132.7, 131.4, 129.7, 128.8, 128.0, 127.3, 126.8, 126.7, 125.0, 124.5, 122.1, 120.4, 119.8, 117.9, 114.8, 114.4, 111.3, 110.5, 63.0, 55.5, 55.4, 32.7.

IR (neat): 3050, 2954, 2925, 2854, 1714, 1606, 1577, 1559, 1505, 1483, 1463, 1451, 1441, 1424, 1371, 1328, 1289, 1242 cm^{-1}.

mp: 44-46°C.

HR-MS (APCI): m/z calculated for $C_{32}H_{29}N_2O_2$ 473.2224 obtained 473.2214.

3-(2,5-dimethylphenyl)-2-(4-methoxyphenyl)-1-(1-methyl-1H-indol-3-yl)-1,2-dihydroisoquinoline **109**

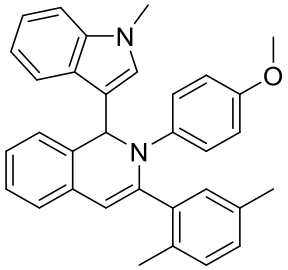

Formula: $C_{33}H_{30}N_2O$

Mol. Weight: 470.62 $g.mol^{-1}$

Aspect: ochre solid

R_f: 0.49 (cyclohexane:EA, 9:1)

Yield: 16%

^{1}H NMR (400 MHz, Chloroform-d): δ 8.01 (d, J = 7.8 Hz, 1H), 7.67 (s, 2H), 7.41 – 7.19 (m, 4H), 7.13 (s, 1H), 7.05 (s, 1H), 6.98 (d, J = 8.8 Hz, 2H), 6.91 (s, 1H), 6.85 (s, 2H), 6.62 (d, J = 8.9 Hz, 2H), 6.26 (s, 1H), 6.14 (s, 1H), 3.67 (s, 3H), 3.65 (s, 3H), 2.15 (s, 6H).

This compound is too unstable to get a proper ^{13}C NMR spectrum.

2-(4-methoxyphenyl)-1-(1-methyl-1H-indol-3-yl)-3-(thiophen-2-yl)-1,2-dihydroisoquinoline **110**

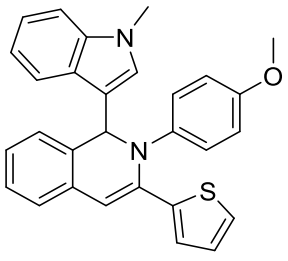

Formula: $C_{29}H_{24}N_2OS$

Mol. Weight: 448.58 $g.mol^{-1}$

Aspect: yellow solid

R_f: 0.3 (cyclohexane:EA, 9:1)

Yield: 59%

^{1}H NMR (400 MHz, DMSO-d_6):) δ 8.03 (d, J = 7.8 Hz, 1H), 7.35 (d, J = 7.8 Hz, 2H), 7.31 (d, J = 5.2 Hz, 1H), 7.29 – 7.24 (m, 2H), 7.20 (d, J = 7.1 Hz, 1H), 7.18 – 7.12 (m, 2H), 7.07 (d, J = 9.1 Hz, 3H), 6.89 – 6.86 (m, 1H), 6.79 (d, J = 7.2 Hz, 3H), 6.47 (s, 1H), 6.24 (s, 1H), 3.65 (s, 3H), 3.59 (s, 3H).

^{13}C NMR (101 MHz, DMSO-d_6): δ 154.8, 142.2, 140.6, 137.0, 135.5, 131.7, 131.3, 127.8, 127.4, 127.3, 126.4, 126.2, 126.2, 125.9, 125.4, 124.4, 123.2, 121.2, 119.7, 118.7, 115.9, 114.3, 111.3, 109.8, 61.9, 55.1, 32.3.

IR (neat): 3065, 2926, 2854, 1713, 1604, 1560, 1530, 1505, 1482, 1464, 1440, 1425, 1372, 1351, 1331, 1289, 1243 cm^{-1}.

mp: 39-41°C.

HR-MS (ESI+): m/z calculated for $C_{29}H_{24}N_2OSNa$ 471.1507 obtained 471.1500.

3-(cyclohex-1-en-1-yl)-2-(4-methoxyphenyl)-1-(1-methyl-1H-indol-3-yl)-1,2-dihydroisoquinoline **111**

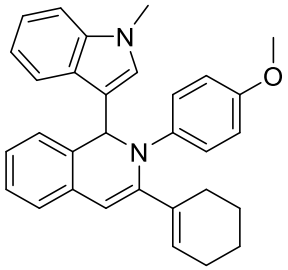

Formula: $C_{31}H_{30}N_2O$

Mol. Weight: 446.59 $g.mol^{-1}$

Aspect: ochre solid

R_f: 0.4 (cyclohexane:EA, 9:1)

Yield: 24%

^{1}H NMR (400 MHz, Chloroform-d): δ 8.19 (d, J = 7.9 Hz, 1H), 7.42 – 7.29 (m, 5H), 7.25 (m, 4H), 6.93 (d, J = 8.9 Hz, 2H), 6.64 (s, 1H), 6.49 (s, 1H), 6.32 (s, 1H), 6.28 (brs, 1H), 3.91 (s, 3H), 3.75 (s, 3H), 2.35 – 2.25 (m, 1H), 2.23 – 2.07 (m, 3H), 1.71 – 1.55 (m, 4H).

^{13}C NMR (101 MHz, Chloroform-d): δ 154.8, 144.3, 142.3, 137.4, 134.1, 132.6, 131.7, 129.5, 128.1, 127.1, 126.5, 126.1, 125.8, 124.3, 123.0, 121.5, 119.9, 119.1, 117.4, 114.0, 109.5, 109.1, 62.2, 55.6, 32.8, 26.7, 25.9, 22.8, 22.2.

IR (neat): 2928, 2832, 1711, 1601, 1557, 1505, 1483, 1464, 1371, 1241 cm^{-1}.

mp: 91-93°C.

HR-MS (APCI): m/z calculated for $C_{31}H_{31}N_2O$ 447.2431 obtained 447.2425.

2-(4-chlorophenyl)-1-(1-methyl-1H-indol-3-yl)-3-phenyl-1,2-dihydroisoquinoline **112**

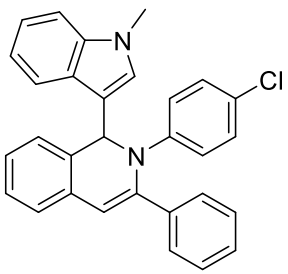

Formula: $C_{30}H_{23}ClN_2$

Mol. Weight: 446.98 $g.mol^{-1}$

Aspect: ochre solid

R_f: 0.5 (petroleum ether:EA, 9:1)

Yield: 76%

^{1}H NMR (400 MHz, Chloroform-d): δ 8.14 – 8.07 (m, 1H), 7.50 (dd, J = 7.7, 2.0 Hz, 2H), 7.36 – 7.18 (m, 10H), 7.13 – 7.03 (m, 4H), 6.70 (s, 1H), 6.59 (s, 1H), 6.40 (s, 1H), 3.59 (s, 3H).

^{13}C NMR (101 MHz, Chloroform-d): δ 146.0, 141.1, 137.7, 137.3, 132.6, 131.9, 128.8, 128.5, 128.1, 128.0, 127.6, 127.5, 126.8, 126.7, 126.1, 126.0, 124.8, 123.0, 121.8, 119.5, 119.3, 116.7, 113.1, 109.7, 61.5, 32.8.

IR (neat): 3057, 2923, 2852, 1660, 1625, 1613, 1557, 1532, 1488, 1453, 1419, 1392, 1371, 1341, 1318 cm^{-1}.

mp: 65-67°C.

HR-MS (ESI+): m/z calculated for $C_{30}H_{22}N_2ClNa$ 469.1447 obtained 469.1429.

1-(1-methyl-1H-indol-3-yl)-3-phenyl-2-(3-(trifluoromethyl)phenyl)-1,2-dihydroisoquinoline **113**

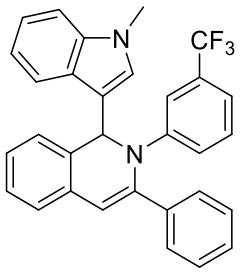

Formula: $C_{31}H_{23}F_3N_2$

Mol. Weight: 480.53 g.mol^{-1}

Aspect: brown solid

R_f: 0.31 (cyclohexane:EA, 9:1)

Yield: 68%

^{1}H NMR (400 MHz, Chloroform-d): δ 8.11 – 8.05 (m, 1H), 7.50 – 7.43 (m, 2H), 7.38 – 7.32 (m, 2H), 7.29 – 7.25 (m, 4H), 7.24 – 7.17 (m, 7H), 7.07 (d, J = 6.2 Hz, 1H), 6.72 (s, 1H), 6.59 (s, 1H), 6.45 (s, 1H), 3.61 (s, 3H).

^{13}C NMR (101 MHz, Chloroform-d): δ 147.7, 140.8, 137.5, 137.3, 132.9, 131.7, 131.1 (q, J = 32.0 Hz), 129.2, 128.6, 128.2, 128.1, 127.6, 127.5, 126.9, 126.1, 126.0, 125.0, 124.5, 124.1 (q, J = 272.0 Hz), 121.9, 119.6, 119.2, 118.1 (q, J = 3.8 Hz), 117.9 (q, J = 3.7 Hz), 116.5, 113.8, 109.8, 61.1, 32.9.

^{19}F NMR (376 MHz, Chloroform-d): δ -62.77;

IR (neat): 2953, 2923, 2854, 1735, 1654, 1607, 1492, 1453, 1372, 1329, 1248 cm^{-1}.

mp: 184-186°C;

HR-MS (APCI): m/z calculated for $C_{31}H_{24}F_3N_2$ 481.1886 obtained 481.1889.

1-(1-methyl-1H-indol-3-yl)-3-phenyl-2-(2,3,4-trifluorophenyl)-1,2-dihydroisoquinoline **114**

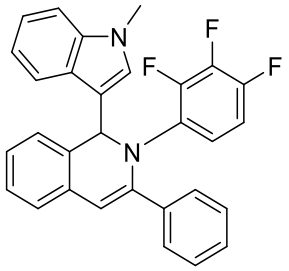

Formula: $C_{30}H_{21}F_3N_2$

Mol. Weight: 466.51 g.mol^{-1}

Aspect: ochre solid

R_f: 0.33 (cyclohexane:EA, 9:1)

Yield: 62%

^{1}H NMR (400 MHz, Chloroform-d): δ 8.08 – 8.01 (m, 1H), 7.61 – 7.53 (m, 2H), 7.38 – 7.28 (m, 2H), 7.28 – 7.15 (m, 8H), 6.80 (s, 1H), 6.68 (s, 1H), 6.64 – 6.56 (m, 2H), 6.16 (s, 1H), 3.61 (s, 3H).

^{13}C NMR (101 MHz, Chloroform-d): δ 147.64 (ddd, J = 247.0, 10.5, 2.3 Hz), 146.06 (ddd, J = 251.0, 10.9, 3.6 Hz), 141.76, 139.42 (dd, J = 16.0, 14.5 Hz), 137.14, 136.96, 132.74 (dd, J = 7.7, 3.4 Hz), 132.53, 131.98, 128.52, 128.42, 128.05, 127.60, 127.49, 127.10, 126.38, 126.14, 125.04, 121.60, 119.97, 119.91, 119.38, 116.25, 113.42, 110.97 (dd, J = 17.7, 3.9 Hz), 109.44, 61.33, 32.80.

^{19}F NMR (282 MHz, Chloroform-d): δ -139.96 (dd, J = 21.0, 3.6 Hz), -141.36 (dd, J = 20.2, 3.7 Hz), -158.82 (t, J = 20.6 Hz).

IR (neat): 3057, 2923, 2853, 1708, 1606, 1562, 1504, 1491, 1422, 1361, 1264, 1220 cm^{-1}.

m.p.: 65-67°C.

HR-MS (ESI+): m/z calculated for $C_{30}H_{22}F_3N_2$ 467.1730 obtained 467.1710.

1-(1-benzyl-1H-indol-3-yl)-2-(4-methoxyphenyl)-3-phenyl-1,2-dihydroisoquinoline **115**

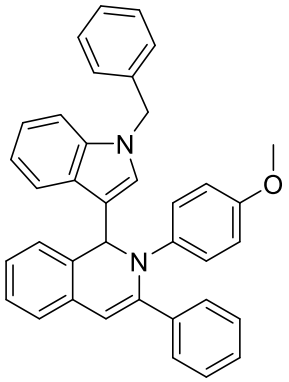

Formula: $C_{37}H_{30}N_2O$

Mol. Weight: 518.66 g.mol^{-1}

Aspect: dark oil

R_f: 0.45 (petroleum ether:EA, 9:1)

Yield: 63%

^{1}H NMR (400 MHz, Chloroform-d): δ 8.14 – 8.06 (m, 1H), 7.53 – 7.40 (m, 2H), 7.32 – 7.09 (m, 13H), 7.08 – 6.98 (m, 2H), 6.95 (dd, J = 6.6, 2.9 Hz, 2H), 6.78 (s, 1H), 6.71 – 6.62 (m, 2H), 6.58 (s, 1H), 6.32 (s, 1H), 5.15 (s, 2H), 3.68 (s, 3H).

^{13}C NMR (101 MHz, Chloroform-d): δ 154.9, 142.1, 141.2, 138.3, 137.6, 136.8, 132.2, 131.9, 128.7, 128.3, 127.8, 127.8, 127.6, 127.5, 127.3, 126.6, 126.5, 126.4, 126.1, 124.5, 123.8, 121.8, 119.7, 119.6, 118.1, 114.1, 111.4, 110.2, 62.1, 55.5, 50.1.

IR (neat): 3058, 2923, 2853, 1726, 1671, 1623, 1606, 1559, 1506, 1464, 1453, 1384, 1357, 1336, 1301, 1244 cm^{-1}.

HR-MS (APCI): m/z calculated for $C_{37}H_{31}N_2O$ 519.2431 obtained 519.2428.

2-(4-methoxyphenyl)-3-phenyl-1-(1,2,5-trimethyl-1H-pyrrol-3-yl)-1,2-dihydroisoquinoline **116**

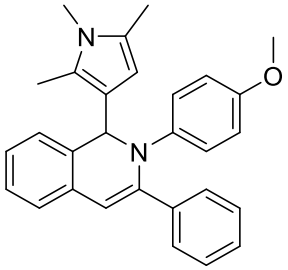

Formula: $C_{29}H_{28}N_2O$

Mol. Weight: 420.56 $g.mol^{-1}$

Aspect: brown solid

R_f: 0.38 (cyclohexane:EA, 9:1)

Yield: 68%

^{1}H NMR (400 MHz, Chloroform-d): δ 7.50 (d, J = 6.6 Hz, 2H), 7.18 (m, 5H), 7.07 (t, J = 7.9 Hz, 1H), 6.99 (d, J = 7.4 Hz, 1H), 6.86 (d, J = 8.9 Hz, 2H), 6.61 (d, J = 8.9 Hz, 2H), 6.42 (s, 1H), 5.85 (s, 1H), 5.81 (s, 1H), 3.66 (s, 3H), 3.35 (s, 3H), 2.41 (s, 3H), 2.05 (s, 3H).

^{13}C NMR (101 MHz, Chloroform-d): δ 154.7, 142.6, 141.9, 138.7, 133.6, 131.8, 128.2, 128.0, 127.5, 127.3, 126.8, 126.3, 125.6, 124.2, 123.8, 123.0, 121.4, 113.8, 110.0, 104.6, 62.3, 55.5, 30.2, 12.7, 11.0.

IR (neat): 3060, 2923, 2854, 1710, 1652, 1600, 1558, 1506, 1492, 1452, 1398, 1361, 1243 cm^{-1}.

mp: 78-80°C.

HR-MS (ESI+): m/z calculated for $C_{29}H_{29}N_2O$ 421.2274 obtained 421.2267.

2-(4-methoxyphenyl)-1-(1-methyl-1H-pyrrol-2-yl)-3-phenyl-1,2-dihydroisoquinoline **117**

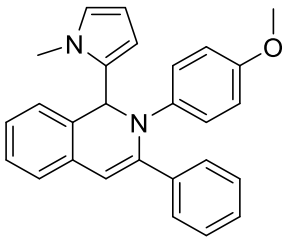

Formula: $C_{27}H_{24}N_2O$

Mol. Weight: 392.50 $g.mol^{-1}$

Aspect: ochre solid

R_f: 0.24 (petroleum ether:EA, 9:1)

Yield: 47% (69% at 50°C)

^{1}H NMR (400 MHz, Chloroform-d): δ 7.52 (d, J = 7.9 Hz, 2H), 7.19 (m, 6H), 7.05 (d, J = 7.4 Hz, 1H), 6.97 (d, J = 8.9 Hz, 2H), 6.70 – 6.62 (m, 3H), 6.61 – 6.56 (m, 1H), 5.98 (s, 1H), 5.93 – 5.87 (m, 1H), 5.65 – 5.57 (m, 1H), 3.99 (s, 3H), 3.67 (s, 3H).

^{13}C NMR (101 MHz, Chloroform-d): δ 155.5, 142.1, 141.2, 137.9, 133.4, 132.8, 130.4, 128.4, 127.9, 127.6, 127.4, 126.6, 126.4, 124.6, 124.3, 123.4, 114.2, 112.0, 110.0, 106.5, 62.4, 55.4, 35.3.

IR (neat): 3059, 2927, 1710, 1609, 1560, 1507, 1491, 1452, 1405, 1366, 1301, 1244 cm^{-1}.

mp: 62-64°C.

HR-MS (APCI): m/z calculated for $C_{27}H_{25}N_2O$ 393.1961 obtained 393.1956.

2-(4-methoxyphenyl)-1-(3-methyl-1H-indol-2-yl)-3-phenyl-1,2-dihydroisoquinoline

118

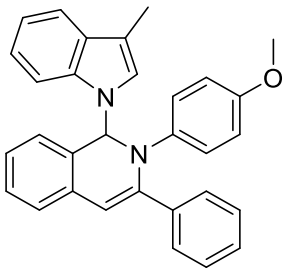

Formula: $C_{31}H_{26}N_2O$

Mol. Weight: 442.56 $g.mol^{-1}$

Aspect: brown solid

R_f: 0.15 (cyclohexane:EA, 9:1)

Yield: quant.

^{1}H NMR (400 MHz, Chloroform-d): δ 7.78 (d, J = 8.2 Hz, 1H), 7.61 (d, J = 7.8 Hz, 1H), 7.44 – 7.29 (m, 5H), 7.20 (td, J = 8.0, 6.8, 3.5 Hz, 6H), 7.11 (td, J = 7.4, 1.5 Hz, 1H), 6.98 – 6.94 (m, 1H), 6.87 – 6.81 (m, 2H), 6.62 (d, J = 8.9 Hz, 2H), 6.48 (s, 1H), 3.67 (s, 3H), 2.28 – 2.17 (m, 3H).

^{13}C NMR (101 MHz, Chloroform-d): δ 156.2, 142.6, 140.5, 137.8, 134.5, 131.4, 129.1, 128.6, 128.4, 128.2, 128, 127.9, 126.6, 126.3, 125.8, 124.8, 123.3, 123.3, 122.1, 119.4, 119.2, 114.1, 112.6, 109.5, 107.4, 72.9, 55.4, 9.9.

IR (neat): 3055, 2924, 2854, 1709, 1682, 1605, 1561, 1508, 1492, 1454, 1387, 1347, 1296, 1247 cm^{-1}.

mp: 52-54°C.

HR-MS (APCI): m/z calculated for $C_{31}H_{27}N_2O$ 443.2118 obtained 443.2104.

Precipitation of the isoquinolinium ion

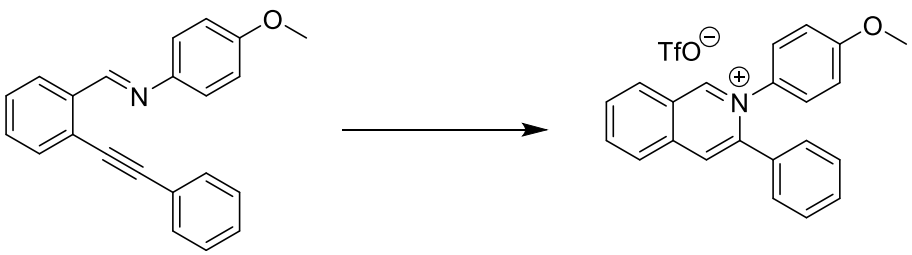

General procedure:

To an oven dried 10 mL round bottom flask were added the imine derivative (0.16 mmol, 1 eq.) and AgOTf (1 eq.) in dichloromethane (2 mL). The solution was degassed with an inert gas for a few minutes before being stirred at room temperature for 4 hours. Then, 1.5 eq. of TfOH was added through the septum, affording a precipitate which was recrystallized from a mixture of hexane and ethanol. A crystalline solid was filtered on a Büchner and rinsed with hexane.

2-(4-methoxyphenyl)-3-phenylisoquinolin-2-ium trifluoromethanesulfonate

135

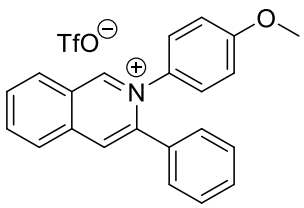

Formula: $C_{23}H_{18}F_3NO_4S$

Mol. Weight: 461.46 $g.mol^{-1}$

Aspect: white crystals

^{1}H NMR (400 MHz, Chloroform-d): δ 9.88 (s, 1H), 8.60 (d, J = 8.4 Hz, 1H), 8.30 (s, 1H), 8.20 – 8.10 (m, 2H), 7.91 (ddd, J = 8.3, 6.6, 1.5 Hz, 1H), 7.42 – 7.27 (m, 7H), 6.85 (d, J = 8.9 Hz, 2H), 3.76 (s, 3H).

^{13}C NMR (101 MHz, Chloroform-d): δ 160.95, 152.30, 146.21, 138.63, 138.19, 134.51, 132.26, 131.66, 131.62, 130.20, 130.08, 128.95, 127.90, 127.57, 127.23, 127.15, 114.97, 55.78.

Chapter III: Visible-Light catalyzed hydroamination using phosphonohydrazones as novel NCR precursors

Synthesis of phosphonohydrazines

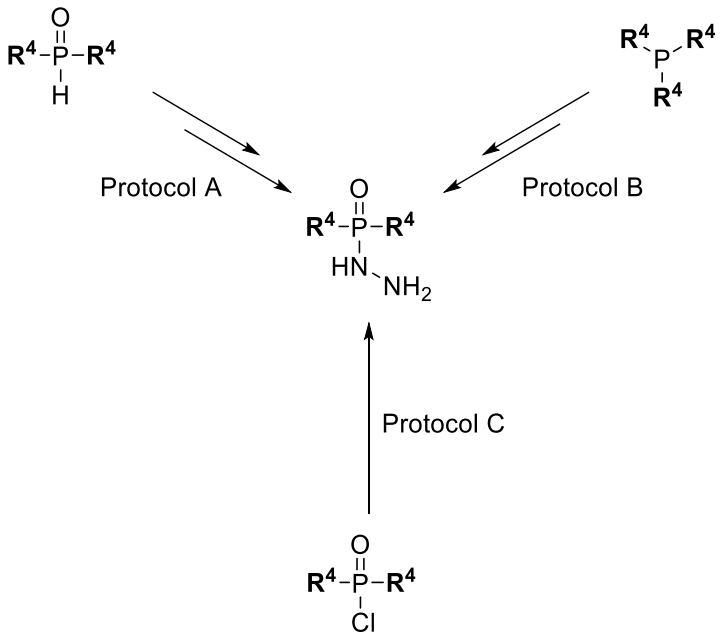

General procedure:

Protocol A: Hydrazine hydrate (1 eq.) was added dropwise at 20°C with efficient stirring to a mixture of CCl_4/CH_2Cl_2 (5:3, 0.625M), K_2CO_3 (1.5 eq.), and benzyltriethylammonium chloride (1 mol%). After 15 min, a solution of dialkylphosphite in CH_2Cl_2 was added slowly with external cooling if necessary. Stirring was continued for 4h at room temperature. The mixture was filtered, washed with CH_2Cl_2, and evaporated, affording the desired product without further purification.

Protocol B: To an ice-cooled solution of trialkylphosphite (1 eq.) in THF (2.7 M) was added a mixture of water (1 eq.) in THF under an inert atmosphere. The solution was stirred overnight at room temperature or reflux. The resulting dialkylphosphite was isolated after evaporation of THF and distillation and was engaged in protocol A.

Protocol C: Hydrazine monohydrate (3 eq.) was added dropwise into a solution of diarylphosphinic chloride (1 eq.) in THF (0.2 M) under an inert atmosphere, at 0°C. The mixture was stirred at 0°C for 30 min. After completion of the reaction, the solvent was evaporated and the residue was extracted with CH_2Cl_2 and the combined organic layer was washed with water, brine and dried over Na_2SO_4, affording the desired product.

Diethyl hydrazineylphosphonate **212 (Protocol A)**

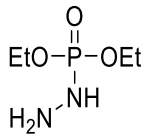

Formula: $C_4H_{13}N_2O_3P$

Mol. Weight: 168.13 g.mol^{-1}

Aspect: colorless oil

R_f: (cyclohexane:EA, 7:3)

Yield: quant.

^{1}H NMR (400 MHz, Chloroform-d): δ 4.45 (s, 1H), 4.18 – 4.03 (m, 287H), 3.25 (s, 168H), 1.34 (tdd, J = 7.1, 1.6, 0.8 Hz, 6H).

Spectral data were consistent with data reported in the literature.[248]

Dibenzyl hydrazineylphosphonate **262 (Protocol A)**

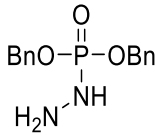

Formula: $C_{14}H_{17}N_2O_3P$

Mol. Weight: 292.27 g.mol^{-1}

Aspect: colorless oil

R_f: 0.13 (cyclohexane:EA, 7:3)

Yield: quant.

^{1}H NMR (400 MHz, Chloroform-d): δ 7.42 – 7.31 (m, 10H), 5.08 (d, J = 8.3 Hz, 2H), 2.94 (s, 3H).

Spectral data were consistent with data reported in the literature.[249]

Dimethyl hydrazineylphosphonate **263 (Protocol B)**

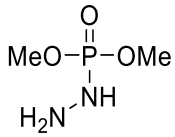

Formula: $C_2H_9N_2O_3P$

Mol. Weight: 140.08 g.mol^{-1}

Aspect: white solid

R_f: 0.28 (methanol:EA, 1:9)

Yield: 84%

^{1}H NMR (300 MHz, Chloroform-d): δ 3.80 (s, 6H).

Spectral data were consistent with data reported in the literature.[250]

[248] J. Verner, M. Potacek, *Molecules* **2006**, *11*, 34–42.
[249] R. Klement, K. O. Knollmüller, *Chemische Berichte* **1960**, *93*, 834–843.
[250] U. Felcht, M. Regitz, *Justus Liebigs Annalen der Chemie* **1977**, *1977*, 1309–1320.

P,P-diphenylphosphinic hydrazide **264 (Protocol C)**

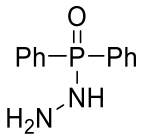

Formula: $C_{12}H_{13}N_2OP$

Mol. Weight: 232.22 $g.mol^{-1}$

Aspect: white solid

R_f:

Yield: 84%

^{1}H NMR (400 MHz, Chloroform-d): δ 7.97 – 7.86 (m, 4H), 7.58 – 7.41 (m, 6H).

Spectral data were consistent with data reported in the literature.[251]

[251] M. Balti, K. Dridi, M. Lotfi El Efrit, *HETEROCYCLES* **2014**, *89*, 1483.

Sonogashira cross-coupling reaction

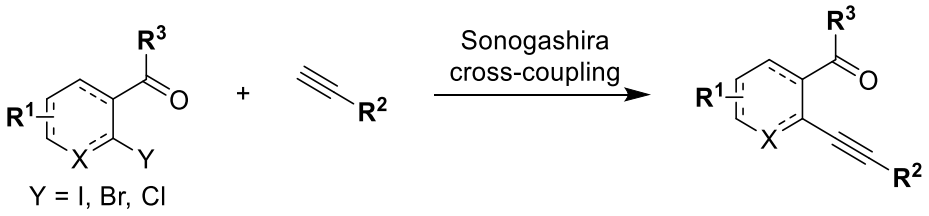

General procedure:

To an oven dried sealable glass vial were added CuI (1 mol%) and $PdCl_2(PPh_3)_2$ (2 mol%) to a solution of a halide derivative (1 eq.) in triethylamine (0.25 M). The solution was degassed with an inert gas for a few minutes before adding the alkyne (1.2 eq.). The vials were sealed with 20mm crimp caps with silicone/PTFE septum and stirred at room temperature (20-25°C) when using iodinated derivatives or at 50°C when using brominated derivatives. The reaction was monitored by TLC until completion and quenched by addition of distilled water and the pH was brought to neutrality by adding a saturated solution of ammonium chloride. The mixture was extracted with ethyl acetate, the combined organic phases were washed with brine, dried over Na_2SO_4, filtrated and concentrated under reduced pressure. The crude mixture was purified on a silica gel column chromatography, eluting with a cyclohexane/ethyl acetate mixture to afford the desired product.

7-(phenylethynyl)-2,3-dihydro-[1,4]dioxino[2,3-g]quinoline-8-carbaldehyde **265**

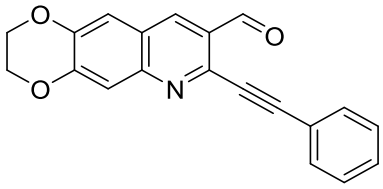

Formula: $C_{20}H_{13}NO_3$

Mol. Weight: 315.33 g.mol^{-1}

Aspect: yellow solid

R_f: 0.45 (cyclohexane:EA, 6:4)

Yield: 53%

We observed a rapid degradation of this compound so it was directly engaged in the following step.

2-(phenylethynyl)benzofuran-3-carbaldehyde **266**

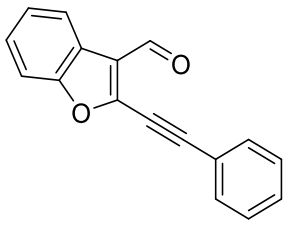

Formula: $C_{17}H_{10}O_2$

Mol. Weight: 246.27 g.mol^{-1}

Aspect: yellow solid

R_f: 0.58 (cyclohexane:EA, 9:1)

Yield: 51%

^{1}H NMR (400 MHz, Chloroform-d): δ 10.37 (s, 1H), 8.20 (dd, J = 7.7, 1.5 Hz, 1H), 7.65 (dd, J = 7.9, 1.6 Hz, 2H), 7.55 – 7.49 (m, 1H), 7.49 – 7.38 (m, 5H).

Spectral data were consistent with data reported in the literature.[252]

1-methyl-2-(phenylethynyl)-1H-indole-3-carbaldehyde **267**

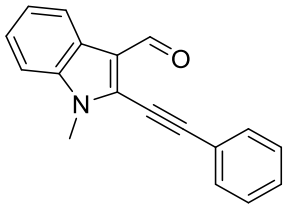

Formula: $C_{18}H_{13}NO$

Mol. Weight: 259.31 g.mol^{-1}

Aspect: beige solid

R_f: 0.29 (Cyclohexane:EA, 9:1)

Yield: 95%

^{1}H NMR (400 MHz, Chloroform-d): δ 10.28 (s, 1H), 8.36 – 8.30 (m, 1H), 7.63 (dd, J = 7.5, 2.2 Hz, 2H), 7.47 – 7.40 (m, 3H), 7.38 – 7.30 (m, 3H), 3.90 (s, 3H).

Spectral data were consistent with data reported in the literature.[252]

[252] M. Tiano, P. Belmont, *J. Org. Chem.* **2008**, *73*, 4101–4109.

2-((3,4,5-trimethoxyphenyl)ethynyl)benzaldehyde **268**

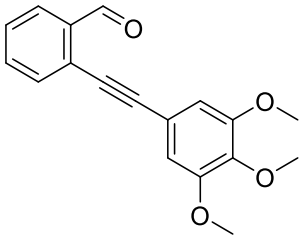

Formula: $C_{18}H_{16}O_4$

Mol. Weight: 296.32 $g.mol^{-1}$

Aspect: yellow solid

R_f: 0.56 (cyclohexane:EA, 7:3)

Yield: 60%

^{1}H NMR (400 MHz, Chloroform-d): δ 10.65 (s, 1H), 7.95 (d, J = 7.8Hz, 1H), 7.66-7.57 (m, 2H), 7.46 (t, J = 7.1 Hz, 1H), 6.80 (s, 2H), 3.90 (s, 9H).

Spectral data were consistent with data reported in the literature.[54]

2-(p-tolylethynyl)benzaldehyde **269**

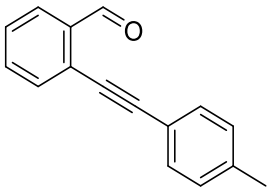

Formula: $C_{16}H_{12}O$

Mol. Weight: 220.27 $g.mol^{-1}$

Aspect: yellow solid

R_f: 0.64 (cyclohexane:EA, 9:1)

Yield: 81%

^{1}H NMR (400 MHz, Chloroform-d): δ 10.66 (s, 1H), 7.94 (d, J = 7.8 Hz, 1H), 7.64-7.55 (m, 2H), 7.48-7.44 (m, 3H), 7.20 (d, J = 8.2 Hz, 2H), 2.39 (s, 3H).

Spectral data were consistent with data reported in the literature.[48]

2-((4-fluorophenyl)ethynyl)benzaldehyde **270**

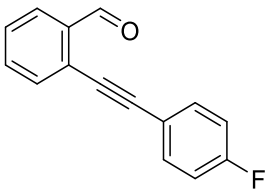

Formula: $C_{15}H_9FO$

Mol. Weight: 224.23 $g.mol^{-1}$

Aspect: yellow solid

R_f: 0.60 (cyclohexane:EA, 9:1)

Yield: 90%

^{1}H NMR (400 MHz, Chloroform-d): δ 10.62 (s, 1H), 7.94 (dd, J = 7.6, 0.9 Hz, 1H), 7.65-7.43 (m, 5H), 7.08 (td, J = 8.7, 2.9 Hz, 2H).

Spectral data were consistent with data reported in the literature.[48]

4-((2-formylphenyl)ethynyl)benzonitrile **271**

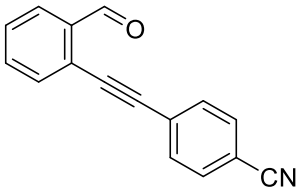

Formula: $C_{16}H_9NO$

Mol. Weight: 231.25 g.mol^{-1}

Aspect: yellow solid

R_f: 0.18 (cyclohexane:EA, 95:5)

Yield: Quant.

^{1}H NMR (400 MHz, Chloroform-d): δ 10.59 (d, J = 0.8 Hz, 1H), 7.97 (ddd, J = 7.8, 1.3, 0.5 Hz, 1H), 7.65-7.69 (m, 5H), 7.63 (dt, J = 7.3, 1.4 Hz, 1H), 7.53 (m, 1H).

Spectral data were consistent with data reported in the literature.[253]

2-((2-bromophenyl)ethynyl)benzaldehyde **272**

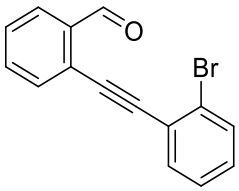

Formula: $C_{15}H_9BrO$

Mol. Weight: 285.14 g.mol^{-1}

Aspect: yellow solid

R_f: 0.50 (cyclohexane:acetone, 95:5)

Yield: 77%

^{1}H NMR (400 MHz, Chloroform-d): δ 7.21 (ddd, J = 1.7, 7.6, 7.9 Hz, 1H), 7.31 (ddd, J = 1.1, 7.6, 7.7 Hz, 1H), 7.45 (m, 1H), 7.55-7.62 (m, 3H), 7.67 (d, J = 7.8 Hz, 2H), 7.95 (d, J = 7.8 Hz, 1H), 10.74 (s, 1H).

Spectral data were consistent with data reported in the literature.[254]

2-(cyclopropylethynyl)benzaldehyde **273**

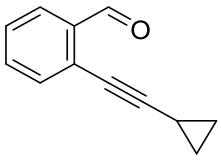

Formula: $C_{12}H_{10}O$

Mol. Weight: 170.21 g.mol^{-1}

Aspect: yellow oil

R_f: 0.91 (cyclohexane:EA, 3:7)

Yield: 67% (made by Dr. Gaëlle Mariaule)

^{1}H NMR (400 MHz, Chloroform-d): δ 10.29 (s, 1H), 7.26 (s, 1H), 6.85 (s, 1H), 6.03 (s, 2H), 1.47 (m, 1H), 0.87 (m, 4H).

Spectral data were consistent with data reported in the literature.[234]

[253] R. P. Kaiser, J. Mosinger, I. Císařová, M. Kotora, *Org. Biomol. Chem.* **2017**, *15*, 6913–6920.
[254] D. P. Iwaniuk, C. Wolf, *Organic Letters* **2011**, *13*, 2602–2605.

5-fluoro-2-((3,4,5-trimethoxyphenyl)ethynyl)benzaldehyde **274**

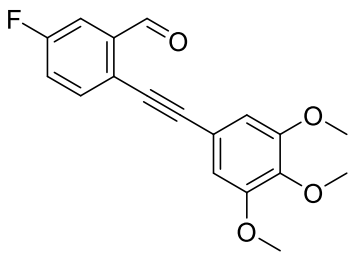

Formula: $C_{18}H_{15}FO_4$

Mol. Weight: 314.31 g.mol^{-1}

Aspect: yellow solid

R_f: 0.25 (cyclohexane:EA, 9:1)

Yield: 66%

^{1}H NMR (400 MHz, Chloroform-d): δ 10.60 (d, J = 3.2 Hz, 1H), 7.73 – 7.57 (m, 2H), 7.34 – 7.23 (m, 1H), 6.78 (s, 2H), 3.89 (d, J = 2.7 Hz, 9H).

Spectral data were consistent with data reported in the literature.[54]

2-(pyridin-2-ylethynyl)quinoline-3-carbaldehyde **275**

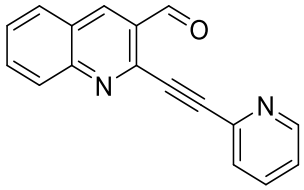

Formula: $C_{17}H_{10}N_2O$

Mol. Weight: 258.28 g.mol^{-1}

Aspect: brown solid

R_f: 0.8 (EA)

Yield: 78%

^{1}H NMR (400 MHz, Chloroform-d): δ 10.86 (s, 1H), 8.79 (s, 1H), 8.72 – 8.70 (m, 1H), 8.22 – 8.19 (m, 1H), 8.01 – 7.99 (m, 1H), 7.93 – 7.87 (m, 1H), 7.79 – 7.76 (m, 1H), 7.70 – 7.65 (m, 1H), 7.39-7.35 (m, 2H).

Spectral data were consistent with data reported in the literature.[255]

2-(3-methoxyprop-1-yn-1-yl)nicotinaldehyde **276**

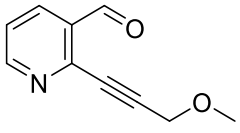

Formula: $C_{10}H_9NO_2$

Mol. Weight: 175.19 g.mol^{-1}

Aspect: beige solid

R_f: 0.3 (cyclohexane:EA, 6:4)

Yield: 80% (made by Dr. Gaëlle Mariaule)

[255] P. Belmont, T. Belhadj, *Org. Lett.* **2005**, *7*, 1793–1795.

^{1}H NMR (400 MHz, Chloroform-d): δ 10.53 (s, 1H), 8.78 (dd, J = 1.8, 4.8 Hz, 1H), 8.18 (dd, J = 1.8, 8.0 Hz, 1H), 7.41 (dd, J = 4.8, 8.0 Hz, 1H), 4.42 (s, 2H), 3.48 (s, 3H).

Spectral data were consistent with data reported in the literature.[256]

6-(3-methoxyprop-1-yn-1-yl)benzo[d][1,3]dioxole-5-carbaldehyde **277**

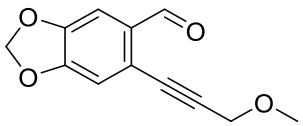

Formula: $C_{12}H_{10}O_4$

Mol. Weight: 218.21 g.mol^{-1}

Aspect: brown solid

R_f: 0.15 (cyclohexane:EA, 9:1)

Yield: 85% (made by Dr. Gaëlle Mariaule)

^{1}H NMR (400 MHz, Chloroform-d): δ 10.36 (s, 1H), 7.32 (s, 1H), 6.94 (s, 1H), 6.08 (s, 2H), 4.36 (s, 2H), 3.46 (s, 3H).

Spectral data were consistent with data reported in the literature.[257]

2-(3-methoxyprop-1-yn-1-yl)quinoline-3-carbaldehyde **278**

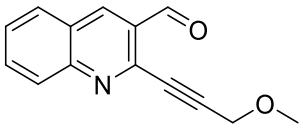

Formula: $C_{14}H_{11}NO_2$

Mol. Weight: 225.25 g.mol^{-1}

Aspect: brown solid

R_f: 0.69 (cyclohexane:EA, 3:7)

Yield: quant.

^{1}H NMR (400 MHz, Chloroform-d): δ 10.66 (s, 1H), 8.71 (s, 1H), 8.12 (d, J = 8.7 Hz, 1H), 7.94 (dd, J = 1.1, 8.3 Hz, 1 H), 7.85 (ddd, J = 1.5, 6.8, 8.3 Hz, 1H), 7.62 (ddd, J = 1.1, 6.8, 7.9 Hz, 1H), 4.47 (s, 2H), 3.51 ppm (s, 3H).

Spectral data were consistent with data reported in the literature.[46]

---

[256] A. Dore, B. Asproni, A. Scampuddu, G. A. Pinna, C. T. Christoffersen, M. Langgård, J. Kehler, *European Journal of Medicinal Chemistry* **2014**, *84*, 181–193.

[257] G. A. Kraus, J. Beasley, *Tetrahedron Letters* **2013**, *54*, 5597–5599.

1-(2-(phenylethynyl)phenyl)ethan-1-one **279**

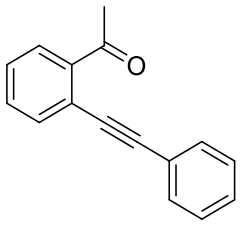

Formula: $C_{16}H_{12}O$

Mol. Weight: 220.27 g.mol^{-1}

Aspect: yellow oil

R_f: 0.42 (cyclohexane:EA, 95:5)

Yield: 38%

^{1}H NMR (400 MHz, Chloroform-d): δ 7.74 (d, J = 8.0 Hz, 1H), 7.61 (d, J = 7.6 Hz, 1H), 7.55-7.53 (m, 2H), 7.46-7.42 (m, 1H), 7.38-7.34 (m, 4H), 2.77 (s, 3H).

Spectral data were consistent with data reported in the literature.[258]

Phenyl(2-(phenylethynyl)phenyl)methanone **280**

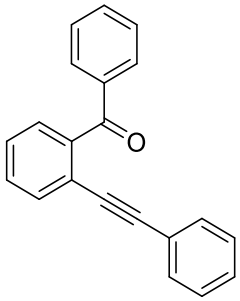

Formula: $C_{21}H_{14}O$

Mol. Weight: 282.34 g.mol^{-1}

Aspect: white solid

R_f: 0.55 (cyclohexane:EA, 95:5)

Yield: 38%

^{1}H NMR (400 MHz, Chloroform-d): δ 7.89-7.87 (m, 2H), 7.62-7.41 (m, 7H), 7.24-7.16 (m, 3H), 7.05-7.03 (m, 2H).

Spectral data were consistent with data reported in the literature.[258]

[258] T. Miao, Z.-Y. Tian, Y.-M. He, F. Chen, Y. Chen, Z.-X. Yu, Q.-H. Fan, *Angewandte Chemie International Edition* **2017**, *56*, 4135–4139.

Heck cross-coupling reaction

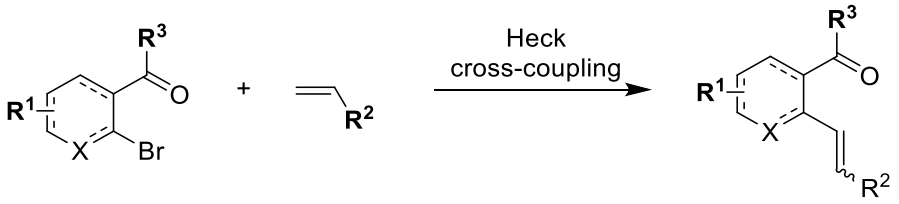

General procedure:

To an oven dried sealable glass vial were added $Pd(OAc)_2$ (10 mol%) and K_3PO_4 (1.5 eq.) to a solution of a halide derivative (1 eq.) in DMA (0.5 M). The solution was degassed with an inert gas for a few minutes before adding the alkene (10 eq.). The vials were sealed with 20mm crimp caps with silicone/PTFE septum and stirred at 120°C. The reaction was monitored by TLC until completion and quenched by addition of distilled water. The mixture was extracted with ethyl acetate, the combined organic phases were washed with brine, dried over Na_2SO_4, filtrated and concentrated under reduced pressure. The crude mixture was purified on a silica gel column chromatography, eluting with a cyclohexane/ethyl acetate mixture to afford the desired product.

2-styrylbenzaldehyde **281**

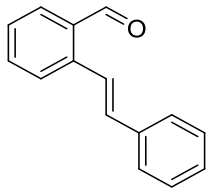

Formula: $C_{15}H_{12}O$

Mol. Weight: 208.26 $g.mol^{-1}$

Aspect: yellow oil

R_f: 0.41 (cyclohexane:EA, 9:1)

Yield: 88%

^{1}H NMR (400 MHz, Chloroform-d): δ 10.15 (s, 1H), 7.97 (d, J = 16.5 Hz, 1H), 7.17-7.70 (m, 9H), 6.92 (d, J = 16.5 Hz, 1H).

Spectral data were consistent with data reported in the literature.[259]

[259] W. Zhang, F. Ning, L. Váradi, D. E. Hibbs, J. A. Platts, M. Nyerges, R. J. Anderson, P. W. Groundwater, *Tetrahedron* **2014**, *70*, 3621–3629.

Synthesis of phosphonohydrazones

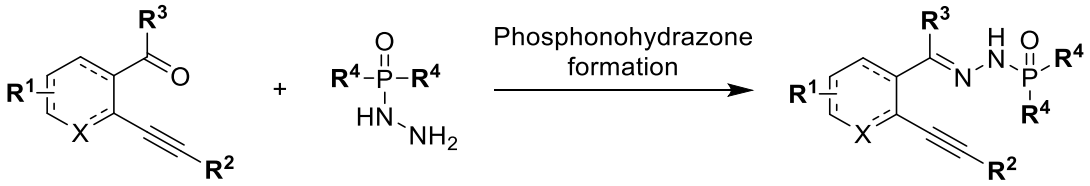

General procedure:

To an oven dried sealable glass vial were added an aldehyde or ketone derivative (1 eq.), phosphonohydrazine (1.1 eq) and MeOH (0.8 M). The vials were sealed with 20mm crimp caps with silicone/PTFE septum and stirred overnight at 20°C. After completion of the reaction checked by TLC, the reaction medium was filtered using a Büchner funnel if precipitation of the phosphonohydrazone occurred. The product was dried under vacuum, characterized and used without any further purification. If precipitation did not occur, the crude mixture was concentrated and purification of the residue by silica gel column chromatography eluting with a cyclohexane/ethyl acetate mixture gave the desired product.

Diethyl (2-(2-(phenylethynyl)benzylidene)hydrazineyl)phosphonate **282**

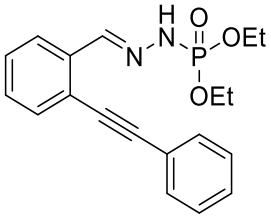

Formula: $C_{19}H_{21}N_2O_3P$

Mol. Weight: 356.36 $g.mol^{-1}$

Aspect: white solid

R_f: 0.29 (Cyclohexane:EA, 5:5)

Yield: 70%

^{1}H NMR (400 MHz, Chloroform-d): δ 8.38 (s, 1H), 8.00 – 7.95 (m, 1H), 7.61 – 7.55 (m, 2H), 7.55 – 7.47 (m, 1H), 7.38 (dd, J = 5.1, 1.8 Hz, 3H), 7.35 – 7.30 (m, 2H), 4.21 (dd, J = 15.6, 8.4 Hz, 4H), 1.36 (t, J = 7.4 Hz, 6H).

^{13}C NMR (101 MHz, Chloroform-d): δ 143.59 (d, J = 19.4 Hz), 135.57, 132.34, 131.83, 129.03, 128.71, 128.55, 128.52, 125.02, 123.04, 122.62, 95.10, 86.53, 63.54, 63.49, 16.33, 16.26.

^{31}P NMR (162 MHz, Chloroform-d): δ 0.81.

HR-MS (ESI-): m/z calculated for $C_{19}H_{20}N_2O_3P$ 355.1212 obtained 355.1219.

Diethyl (2-(5-methoxy-2-(phenylethynyl)benzylidene)hydrazineyl)phosphonate **283**

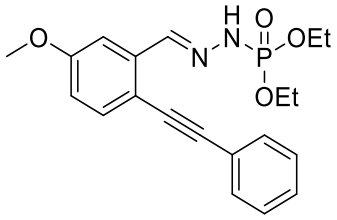

Formula: $C_{20}H_{23}N_2O_4P$

Mol. Weight: 386.39 $g.mol^{-1}$

Aspect: white solid

R_f: 0.33 (Cyclohexane:EA, 3:7)

Yield: 55%

^{1}H NMR (300 MHz, Chloroform-d): δ 8.82 (d, J = 28.7 Hz, 1H), 8.52 (s, 1H), 7.69 – 7.58 (m, 2H), 7.52 – 7.41 (m, 2H), 7.36 (d, J = 5.9 Hz, 3H), 6.87 (dd, J = 8.6, 2.7 Hz, 1H), 4.19 (ddp, J = 11.3, 7.1, 4.2 Hz, 4H), 3.85 (s, 3H), 1.34 (t, J = 7.1 Hz, 6H).

^{13}C NMR (75 MHz, Chloroform-d): δ 159.69, 143.65 (d, J = 19.5 Hz), 137.12, 133.67, 131.63, 128.43, 128.31, 123.37, 116.31, 115.33, 108.69, 93.74, 86.56, 63.45 (d, J = 5.4 Hz), 55.55, 16.27 (d, J = 6.9 Hz).

^{31}P NMR (121 MHz, Chloroform-d): δ 2.01.

HR-MS (ESI+): m/z calculated for $C_{20}H_{23}N_2O_4NaP$ 409.1293 obtained 409.1310.

Diethyl-(2-(5-chloro-2-(phenylethynyl)benzylidene)hydrazineyl)phosphonate **284**

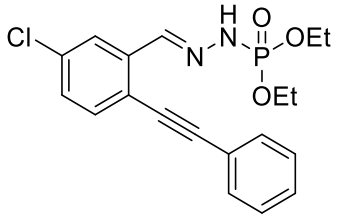

Formula: $C_{19}H_{20}ClN_2O_3P$

Mol. Weight: 390.80 $g.mol^{-1}$

Aspect: white solid

R_f: 0.28 (Cyclohexane:EA, 3:7)

Yield: 84%

^{1}H NMR (300 MHz, Chloroform-d) δ 8.59 (d, J = 28.8 Hz, 1H), 8.44 (s, 1H), 7.96 (d, J = 1.6 Hz, 1H), 7.64 (d, J = 3.4 Hz, 1H), 7.45 (d, J = 8.3 Hz, 1H), 7.40 – 7.34 (m, 3H), 7.29 – 7.23 (m, 1H), 4.27 – 4.11 (m, 4H), 1.35 (t, J = 7.0 Hz, 6H).

^{13}C NMR (75 MHz, Chloroform-d) δ 142.35 (d, J = 19.5 Hz), 137.07, 134.78, 133.48, 131.83, 129.17, 128.94, 128.57, 124.88, 122.73, 120.99, 95.92, 85.58, 63.63 (d, J = 5.5 Hz), 16.30 (d, J = 6.9 Hz).

^{31}P NMR (121 MHz, Chloroform-d) δ 1.46.

HR-MS (ESI+): m/z calculated for $C_{19}H_{21}ClN_2O_3P$ 391.0973 obtained 391.0967.

Diethyl-(2-(5-bromo-2-(phenylethynyl)benzylidene)hydrazineyl)phosphonate **285**

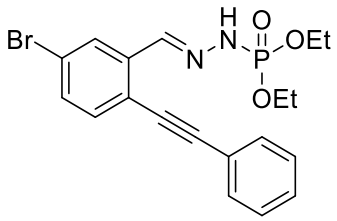

Formula: $C_{19}H_{20}BrN_2O_3P$

Mol. Weight: 435.26 $g.mol^{-1}$

Aspect: white solid

R_f: 0.39 (Cyclohexane:EA, 3:7)

Yield: 88%

^{1}H NMR (400 MHz, Chloroform-d) δ 8.39 (s, 1H), 8.28 (d, J = 28.6 Hz, 1H), 8.11 (s, 1H), 7.64 – 7.56 (m, 2H), 7.45 – 7.32 (m, 4H), 4.19 (dt, J = 14.3, 7.1 Hz, 4H), 1.36 (t, J = 7.1 Hz, 6H).

^{13}C NMR (101 MHz, Chloroform-d) δ 142.27, 137.13, 133.63, 132.08, 131.80, 129.00, 128.60, 127.88, 123.02, 122.70, 121.44, 96.12, 85.64, 63.67 (d, J = 5.4 Hz), 16.31 (d, J = 6.9 Hz).

^{31}P NMR (162 MHz, Chloroform-d) δ 1.21.

HR-MS (ESI+): m/z calculated for $C_{19}H_{21}BrN_2O_3P$ 435.0473 obtained 435.0469.

Diethyl (2-(3,4,5-trimethoxy-2-(phenylethynyl)benzylidene)hydrazineyl)-phosphonate **286**

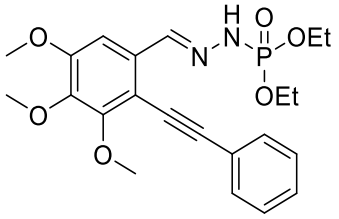

Formula: $C_{22}H_{27}N_2O_6P$

Mol. Weight: 446.44 g.mol^{-1}

Aspect: yellow solid

R_f: 0.31 (Cyclohexane:EA, 3:7)

Yield: 89%

^{1}H NMR (300 MHz, Chloroform-d): δ 9.03 (d, J = 29.1 Hz, 1H), 8.51 (s, 1H), 7.66 (d, J = 7.2 Hz, 2H), 7.34 (d, J = 6.4 Hz, 3H), 7.28 (s, 1H), 4.16 (tt, J = 11.1, 5.7 Hz, 4H), 4.00 (s, 3H), 3.89 (s, 6H), 1.32 (t, J = 7.0 Hz, 6H).

^{13}C NMR (75 MHz, Chloroform-d): δ 154.30, 154.00, 143.46 (d, J = 19.9 Hz), 143.20, 132.03, 131.57, 128.32, 128.29, 123.39, 111.08, 103.06, 97.96, 82.38, 63.24 (d, J = 5.7 Hz), 61.44, 61.23, 56.13, 16.20 (d, J = 7.3 Hz).

^{31}P NMR (121 MHz, Chloroform-d): δ 1.37.

HR-MS (ESI-): m/z calculated for $C_{22}H_{26}N_2O_6P$ 445.1529 obtained 445.1527.

Diethyl (2-((7-(phenylethynyl)-2,3-dihydro-[1,4]dioxino[2,3-g]quinolin-8-yl)methylene)hydrazineyl)phosphonate **287**

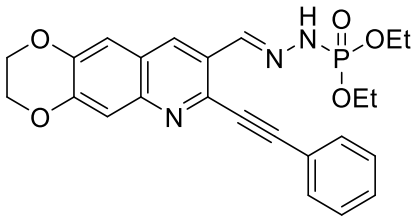

Formula: $C_{24}H_{24}N_3O_5P$

Mol. Weight: 465.45 g.mol^{-1}

Aspect: brown solid

R_f: 0.57 (EA)

Yield: 34%

^{1}H NMR (400 MHz, Chloroform-d): δ 8.52 (m, 2H), 7.77 (d, J = 4.0 Hz, 2H), 7.56 (s, 1H), 7.40 (d, J = 3.8 Hz, 3H), 7.23 (s, 1H), 4.39 (s, 4H), 4.22 (h, J = 6.9 Hz, 4H), 1.37 (t, J = 7.0 Hz, 6H).

^{13}C NMR (101 MHz, Chloroform-d): δ 148.46, 145.62, 132.51, 132.28, 132.18, 132.07, 132.05, 129.53, 129.53, 128.69, 128.56, 127.26, 123.63, 122.00, 112.29, 77.37, 64.59, 64.49, 63.61 (d, J = 5.2 Hz), 16.33 (d, J = 6.9 Hz).

^{31}P NMR (162 MHz, Chloroform-d): δ 1.75.

HR-MS (ESI+): m/z calculated for $C_{24}H_{25}N_3O_5P$ 466.1526 obtained 466.1527.

Diethyl (2-((2-(phenylethynyl)benzofuran-3-yl)methylene)hydrazineyl)-phosphonate **288**

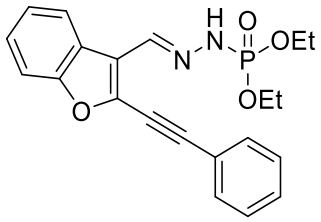

Formula: $C_{21}H_{21}N_2O_4P$

Mol. Weight: 396.38 g.mol^{-1}

Aspect: yellow solid

R_f: 0.38 (Cyclohexane:EA, 3:7)

Yield: 49%

^{1}H NMR (300 MHz, Chloroform-d): δ 8.58 (d, J = 27.8 Hz, 1H), 8.29 – 8.14 (m, 2H), 7.74 – 7.58 (m, 2H), 7.39 (dp, J = 23.2, 7.7 Hz, 6H), 4.26 (h, J = 7.1 Hz, 4H), 1.38 (t, J = 7.1 Hz, 6H).

^{13}C NMR (75 MHz, Chloroform-d): δ 154.92, 139.29, 138.39 (d, J = 20.2 Hz), 131.83, 129.63, 128.69, 126.65, 124.86, 124.10, 123.24, 121.58, 121.35, 111.22, 100.42, 78.28, 63.58 (d, J = 5.5 Hz), 16.38 (d, J = 6.9 Hz).

^{31}P NMR (121 MHz, Chloroform-d): δ 1.85.

HR-MS (ESI-): m/z calculated for $C_{21}H_{20}N_2O_4P$ 395.1161 obtained 395.1173.

Diethyl (2-((1-methyl-2-(phenylethynyl)-1H-indol-3-yl)methylene)hydrazineyl)-phosphonate **289**

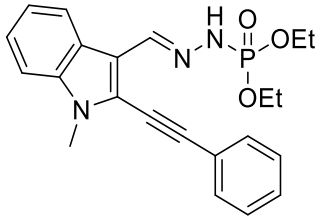

Formula: $C_{22}H_{24}N_3O_3P$

Mol. Weight: 409.43 g.mol^{-1}

Aspect: yellow solid

R_f: 0.45 (Cyclohexane:EA, 3:7)

Yield: 38%

^{1}H NMR (400 MHz, Chloroform-d): δ 8.34 (s, 1H), 8.31 (d, J = 7.9 Hz, 1H), 7.97 (d, J = 27.3 Hz, 1H), 7.66 (dd, J = 6.4, 3.0 Hz, 2H), 7.42 (dd, J = 5.0, 1.7 Hz, 3H), 7.38 – 7.19 (m, 3H), 4.27 (dq, J = 14.0, 7.1 Hz, 4H), 3.85 (s, 3H), 1.38 (t, J = 7.0 Hz, 6H).

^{13}C NMR (101 MHz, Chloroform-d): δ 141.12 (d, J = 20.2 Hz), 137.84, 131.62, 129.13, 128.64, 124.42, 124.34, 124.15, 122.85, 122.22, 121.55, 116.31, 109.38, 100.48, 78.93, 63.35 (d, J = 5.5 Hz), 30.96, 16.34 (d, J = 6.9 Hz).

^{31}P NMR (121 MHz, Chloroform-d): δ 1.89.

HR-MS (ESI-): m/z calculated for $C_{22}H_{23}N_3O_3P$ 408.1477 obtained 408.1480.

Diethyl (2-(2-((4-methoxyphenyl)ethynyl)benzylidene)hydrazineyl)phosphonate **290**

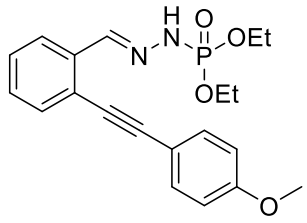

Formula: $C_{20}H_{23}N_2O_4P$

Mol. Weight: 386.39 $g.mol^{-1}$

Aspect: white solid

R_f: 0.1 (Cyclohexane:EA, 7:3)

Yield: 73%

^{1}H NMR (300 MHz, Chloroform-d): δ 8.49 (d, J = 3.1 Hz, 1H), 7.97 (dd, J = 5.9, 3.6 Hz, 1H), 7.58 (dd, J = 8.6, 1.7 Hz, 2H), 7.49 (dd, J = 5.9, 3.5 Hz, 1H), 7.39 – 7.24 (m, 2H), 6.90 (d, J = 8.5 Hz, 2H), 4.29 – 4.12 (m, 4H), 3.84 (s, 3H), 1.35 (t, J = 7.1 Hz, 6H).

^{13}C NMR (75 MHz, Chloroform-d): δ 160.01, 143.73 (d, J = 19.2 Hz), 135.22, 133.31, 132.14, 129.04, 128.20, 124.97, 123.01, 115.10, 114.16, 95.21, 85.27, 63.52 (d, J = 5.5 Hz), 55.45, 16.30 (d, J = 6.9 Hz).

^{31}P NMR (121 MHz, Chloroform-d): δ 0.70.

HR-MS (ESI-): m/z calculated for $C_{20}H_{22}N_2O_4P$ 385.1317 obtained 385.1324.

Diethyl (2-(2-((3,4,5-trimethoxyphenyl)ethynyl)benzylidene)hydrazineyl)-phosphonate **291**

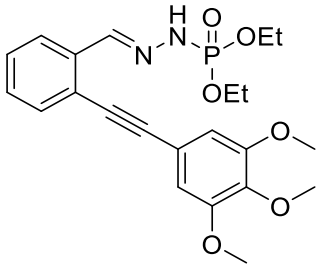

Formula: $C_{22}H_{27}N_2O_6P$

Mol. Weight: 446.44 $g.mol^{-1}$

Aspect: yellow solid

R_f: 0.05 (Cyclohexane:EA, 7:3)

Yield: 83%

^{1}H NMR (400 MHz, Chloroform-d): δ 8.36 (s, 1H), 8.01 – 7.96 (m, 1H), 7.55 – 7.51 (m, 1H), 7.35 – 7.31 (m, 2H), 6.79 (s, 2H), 4.30 – 4.13 (m, 4H), 3.91 (s, 6H), 3.89 (s, 3H), 1.36 (td, J = 7.1, 1.0 Hz, 6H).

^{13}C NMR (75 MHz, Chloroform-d): δ 153.34, 153.34, 143.31 (d, J = 18.2 Hz), 135.06, 132.61, 129.27, 128.65, 125.19, 122.55, 117.90, 108.92, 95.06, 85.48, 63.72 (d, J = 5.5 Hz), 61.16, 56.42, 16.30 (d, J = 7.0 Hz).

^{31}P NMR (162 MHz, Chloroform-d): δ 0.66.

HR-MS (ESI-): m/z calculated for $C_{22}H_{26}N_2O_6P$ 445.1529 obtained 445.1550.

Diethyl (2-(2-(p-tolylethynyl)benzylidene)hydrazineyl)phosphonate **292**

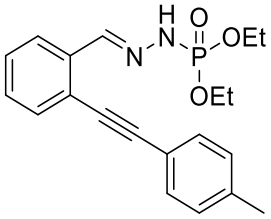

Formula: $C_{20}H_{23}N_2O_3P$

Mol. Weight: 370.39 g.mol^{-1}

Aspect: white solid

R_f: 0.53 (Cyclohexane:EA, 3:7)

Yield: 51%

^{1}H NMR (400 MHz, Chloroform-d): δ 8.90 (d, J = 29.2 Hz, 1H), 8.56 (s, 1H), 8.04 – 7.92 (m, 1H), 7.56 (d, J = 7.8 Hz, 2H), 7.50 (dd, J = 6.2, 2.8 Hz, 1H), 7.35 – 7.26 (m, 2H), 7.18 (d, J = 7.7 Hz, 2H), 4.20 (pt, J = 7.4, 4.0 Hz, 4H), 2.38 (s, 3H), 1.34 (t, J = 7.1 Hz, 6H).

^{13}C NMR (101 MHz, Chloroform-d): δ 143.73 (d, J = 19.7 Hz), 138.76, 135.51, 132.17, 131.71, 129.19, 128.89, 128.26, 124.87, 122.80, 119.94, 95.30, 85.89, 63.38 (d, J = 5.6 Hz), 21.62, 16.22 (d, J = 7.1 Hz).

^{31}P NMR (162 MHz, Chloroform-d): δ 2.16.

HR-MS (ESI+): m/z calculated for $C_{20}H_{24}N_2O_3P$ 371.1519 obtained 371.1520.

Diethyl (2-(2-((4-fluorophenyl)ethynyl)benzylidene)hydrazineyl) phosphonate **293**

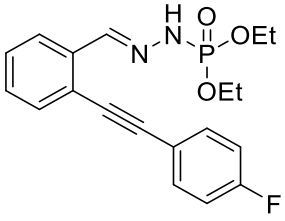

Formula: $C_{19}H_2FN_2O_3P$

Mol. Weight: 374.35 g.mol^{-1}

Aspect: yellow solid

R_f: 0.29 (Cyclohexane:EA, 5:5)

Yield: 57%

^{1}H NMR (300 MHz, Chloroform-d): δ 8.95 (d, J = 29.1 Hz, 1H), 8.55 (s, 1H), 8.03 – 7.94 (m, 1H), 7.67 (ddd, J = 8.9, 5.3, 1.4 Hz, 2H), 7.55 – 7.45 (m, 1H), 7.37 – 7.27 (m, 2H), 7.07 (td, J = 8.7, 1.4 Hz, 2H), 4.20 (dqd, J = 10.3, 7.2, 3.8 Hz, 4H), 1.34 (td, J = 7.1, 1.1 Hz, 6H).

^{13}C NMR (75 MHz, Chloroform-d): δ 162.82 (d, J = 249.9 Hz), 143.70 (d, J = 19.6 Hz), 135.60, 133.90, 133.79, 132.16, 128.79 (d, J = 33.6 Hz), 124.93, 122.46, 119.17 (d, J = 3.5 Hz), 115.77 (d, J = 22.1 Hz), 94.08, 86.26, 63.54 (d, J = 5.5 Hz), 16.28 (d, J = 7.0 Hz).

^{31}P NMR (162 MHz, Chloroform-d): δ 1.57.

^{19}F NMR (282 MHz, Chloroform-d): δ -110.45.

HR-MS (ESI+): m/z calculated for $C_{19}H_{20}N_2O_3FNaP$ 397.1093 obtained 397.1091.

Diethyl-(2-(2-((4-cyanophenyl)ethynyl)benzylidene)hydrazineyl) phosphonate **294**

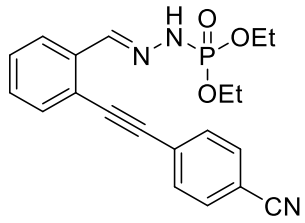

Formula: $C_{20}H_{20}N_3O_3P$

Mol. Weight: 381.37 g.mol^{-1}

Aspect: yellow solid

R_f: 0.38 (Cyclohexane:EA, 3:7)

Yield: 66%

^{1}H NMR (400 MHz, Chloroform-d) δ 9.47 (d, J = 29.5 Hz, 1H), 8.59 (s, 1H), 8.00 (d, J = 7.6 Hz, 1H), 7.82 (d, J = 8.4 Hz, 2H), 7.65 (d, J = 8.4 Hz, 2H), 7.56 – 7.47 (m, 1H), 7.40 – 7.29 (m, 3H), 4.27 – 4.13 (m, 6H), 1.34 (t, J = 7.1 Hz, 7H).

^{13}C NMR (101 MHz, Chloroform-d) δ 143.37 (d, J = 20.1 Hz), 136.15, 132.37, 132.31, 132.05, 129.36, 128.99, 127.98, 124.84, 121.43, 118.64, 111.66, 93.38, 90.86, 63.57 (d, J = 5.6 Hz), 16.25 (d, J = 6.9 Hz).

^{31}P NMR (162 MHz, Chloroform-d) δ 2.06.

HR-MS (ESI+): m/z calculated for $C_{20}H_{21}N_3O_3P$ 382.1315 obtained 382.1315.

Diethyl (2-(2-((2-bromophenyl)ethynyl)benzylidene)hydrazineyl)phosphonate **295**

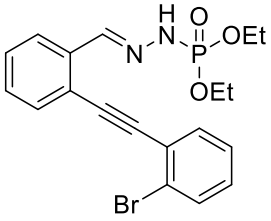

Formula: $C_{19}H_{20}BrN_2O_3P$

Mol. Weight: 435.26 g.mol^{-1}

Aspect: white solid

R_f: 0.38 (Cyclohexane:EA, 3:7)

Yield: 73%

^{1}H NMR (400 MHz, Chloroform-d): δ 8.40 (d, J = 11.9 Hz, 1H), 8.00 – 7.92 (m, 1H), 7.49 (dd, J = 6.1, 1.7 Hz, 1H), 7.44 – 7.38 (m, 1H), 7.36 – 7.27 (m, 3H), 7.03 (t, J = 5.0 Hz, 1H), 4.28 – 4.11 (m, 4H), 1.40 – 1.29 (m, 6H).

^{13}C NMR (101 MHz, Chloroform-d): δ 143.30 (dd, J = 18.9, 5.8 Hz), 135.35 (d, J = 9.4 Hz), 132.62 (d, J = 5.9 Hz), 132.19 (d, J = 2.9 Hz), 129.05 (d, J = 4.4 Hz), 128.69 (d, J = 2.0 Hz), 127.78 (d, J = 2.3 Hz), 127.33, 125.12 (d, J = 3.0 Hz), 122.88 (d, J = 2.4 Hz), 122.23, 90.24, 88.21, 63.54 (dd, J = 5.5, 3.7 Hz), 16.28 (d, J = 6.9 Hz).

^{31}P NMR (162 MHz, Chloroform-d): δ 1.41.

HR-MS (ESI+): m/z calculated for $C_{19}H_{20}N_2O_3NaPBr$ 457.0293 obtained 457.0287.

Diethyl (2-(2-(thiophen-2-ylethynyl)benzylidene)hydrazineyl)phosphonate **296**

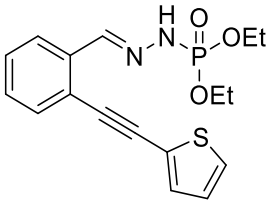

Formula: $C_{17}H_{19}N_2O_3PS$

Mol. Weight: 362.38 g.mol^{-1}

Aspect: white solid

R_f: 0.41 (Cyclohexane:EA, 3:7)

Yield: 44%

^{1}H NMR (400 MHz, Chloroform-d): δ 8.40 (d, J = 11.9 Hz, 1H), 8.00 – 7.92 (m, 1H), 7.49 (dd, J = 6.1, 1.7 Hz, 1H), 7.44 – 7.38 (m, 1H), 7.36 – 7.27 (m, 3H), 7.03 (t, J = 5.0 Hz, 1H), 4.28 – 4.11 (m, 4H), 1.40 – 1.29 (m, 6H).

^{13}C NMR (101 MHz, Chloroform-d): δ 143.30 (d, J = 18.9 Hz), 135.35, 132.62, 132.19, 129.05, 128.69, 127.78, 127.33, 125.12, 122.88, 122.23, 90.24, 88.21, 63.54 (d, J = 5.5), 16.28 (d, J = 6.9 Hz).

^{31}P NMR (162 MHz, Chloroform-d): δ 1.41.

HR-MS (ESI-): m/z calculated for $C_{17}H_{18}N_2O_3PS$ 361.0776 obtained 361.0777.

Diethyl (2-(2-((trimethylsilyl)ethynyl)benzylidene)hydrazineyl)phosphonate **297**

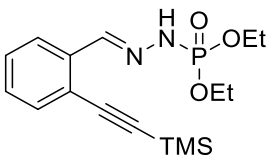

Formula: $C_{16}H_{25}N_2O_3PSi$

Mol. Weight: 352.45 g.mol^{-1}

Aspect: brown solid

R_f: 0.59 (Cyclohexane:EA, 3:7)

Yield: 96%

^{1}H NMR (300 MHz, Chloroform-d): δ 8.77 (d, J = 28.9 Hz, 1H), 8.36 (s, 1H), 7.92 (dd, J = 7.8, 1.3 Hz, 1H), 7.45 – 7.37 (m, 1H), 7.31 – 7.14 (m, 2H), 4.29 – 4.04 (m, 4H), 1.33 (td, J = 7.1, 0.9 Hz, 6H), 0.27 (s, 9H).

^{13}C NMR (75 MHz, Chloroform-d): δ 143.15 (d, J = 19.7 Hz), 135.94, 132.66, 128.68, 128.62, 124.68, 122.26, 101.85, 100.15, 63.26 (d, J = 5.5 Hz), 16.20 (d, J = 7.0 Hz), -0.06.

^{31}P NMR (121 MHz, Chloroform-d): δ 1.79.

HR-MS (ESI+): m/z calculated for $C_{16}H_{24}N_2O_3PSi$ 351.1294 obtained 351.1304.

Diethyl (2-(2-(cyclohex-1-en-1-ylethynyl)benzylidene)hydrazineyl)phosphonate **298**

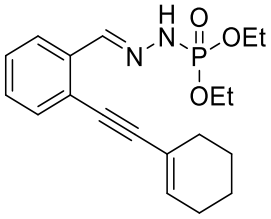

Formula: $C_{19}H_{25}N_2O_3P$

Mol. Weight: 360.39 $g.mol^{-1}$

Aspect: yellow solid

R_f: 0.59 (Cyclohexane:EA, 3:7)

Yield: 69%

^{1}H NMR (400 MHz, Chloroform-d): δ 8.29 (s, 1H), 7.97 – 7.88 (m, 1H), 7.63 (d, J = 28.0 Hz, 1H), 7.43 – 7.36 (m, 1H), 7.27 – 7.23 (m, 2H), 6.28 (tt, J = 3.9, 1.8 Hz, 1H), 4.26 – 4.13 (m, 4H), 2.29 – 2.23 (m, 2H), 2.21 – 2.14 (m, 2H), 1.76 – 1.59 (m, 4H), 1.36 (td, J = 7.1, 1.0 Hz, 6H).

^{13}C NMR (75 MHz, Chloroform-d): δ 143.68 (d, J = 19.6 Hz), 135.89, 135.17, 132.10, 128.87, 127.94, 124.79, 123.12, 120.64, 97.01, 83.81, 63.36 (d, J = 5.6 Hz), 29.16, 25.87, 22.38, 21.58, 16.25 (d, J = 7.0 Hz).

^{31}P NMR (162 MHz, Chloroform-d): δ 1.21.

HR-MS (ESI+): m/z calculated for $C_{19}H_{25}N_2NaO_3P$ 383.1495 obtained 383.1489.

Diethyl (2-(2-(cyclopropylethynyl)benzylidene)hydrazineyl)phosphonate **299**

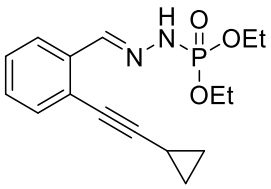

Formula: $C_{16}H_{21}N_2O_3P$

Mol. Weight: 320.33 $g.mol^{-1}$

Aspect: white solid

R_f: 0.36 (Cyclohexane:EA, 3:7)

Yield: 83%

^{1}H NMR (400 MHz, Chloroform-d): δ 8.57 – 8.12 (m, 2H), 7.94 – 7.83 (m, 1H), 7.38 – 7.31 (m, 1H), 7.25 – 7.16 (m, 2H), 4.29 – 4.10 (m, 4H), 1.49 (p, J = 6.7 Hz, 1H), 1.36 (t, J = 7.1 Hz, 6H), 0.89 (d, J = 6.9 Hz, 4H).

^{13}C NMR (101 MHz, Chloroform-d): δ 143.76 (d, J = 19.3 Hz), 135.44, 132.42, 128.85, 127.66, 124.81, 123.35, 99.39, 72.86, 63.38, 16.28 (d, J = 6.9 Hz), 8.86, 0.42.

^{31}P NMR (162 MHz, Chloroform-d): δ 1.70.

HR-MS (ESI+): m/z calculated for $C_{14}H_{21}N_3O_4P$ 326.1264 obtained 326.1258.

diethyl-(2-(2-(oct-1-yn-1-yl)benzylidene)hydrazineyl)phosphonate **300**

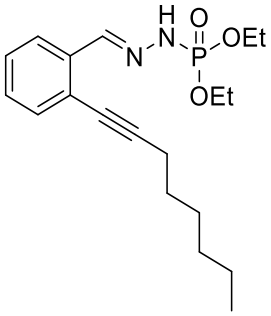

Formula: $C_{19}H_{29}N_2O_3P$

Mol. Weight: 364.43 $g.mol^{-1}$

Aspect: brown solid

R_f: 0.11 (Cyclohexane:EA, 3:7)

Yield: 61%

^{1}H NMR (400 MHz, Chloroform-d) δ 8.33 (s, 1H), 8.04 (d, J = 28.2 Hz, 1H), 7.92 – 7.84 (m, 1H), 7.40 – 7.30 (m, 1H), 7.26 – 7.19 (m, 2H), 4.27 – 4.08 (m, 4H), 2.45 (t, J = 7.2 Hz, 2H), 1.64 (p, J = 7.2 Hz, 2H), 1.45 (dqd, J = 12.5, 6.9, 5.9, 4.1 Hz, 2H), 1.37 – 1.28 (m, 10H), 0.96 – 0.86 (m, 3H).

^{13}C NMR (75 MHz, Chloroform-d) δ 143.76 (d, J = 19.3 Hz), 135.25, 132.43, 128.90, 127.72, 124.85, 123.48, 96.41, 77.65, 63.40 (d, J = 5.5 Hz), 31.39, 28.80 (d, J = 4.4 Hz), 22.66, 19.68, 16.29, 16.20, 14.15.

^{31}P NMR (162 MHz, Chloroform-d) δ 1.59.

HR-MS (ESI+): m/z calculated for $C_{19}H_{29}N_2O_3NaP$ 387.1814 obtained 387.1804.

Diethyl (2-(5-fluoro-2-((3,4,5-trimethoxyphenyl)ethynyl)benzylidene)-hydrazineyl)phosphonate **301**

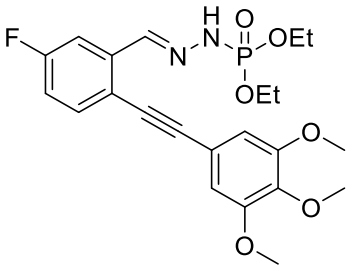

Formula: $C_{22}H_{26}FN_2O_6P$

Mol. Weight: 464.43 $g.mol^{-1}$

Aspect: white solid

R_f: 0.32 (Cyclohexane:EA, 3:7)

Yield: 84%

^{1}H NMR (400 MHz, Chloroform-d) δ 8.57 – 8.12 (m, 2H), 7.94 – 7.83 (m, 1H), 7.38 – 7.31 (m, 1H), 7.25 – 7.16 (m, 2H), 4.29 – 4.10 (m, 4H), 1.49 (p, J = 6.7 Hz, 1H), 1.36 (t, J = 7.1 Hz, 6H), 0.89 (d, J = 6.9 Hz, 4H).

^{31}P NMR (162 MHz, Chloroform-d) δ 1.70.

^{13}C NMR (101 MHz, Chloroform-d) δ 143.76 (d, J = 19.3 Hz), 135.44, 132.42, 128.85, 127.66, 124.81, 123.35, 99.39, 72.86, 63.38, 16.28 (d, J = 6.9 Hz), 8.86, 0.42.

HR-MS (ESI+): m/z calculated for $C_{14}H_{21}N_3O_4P$ 326.1264 obtained 326.1258.

Diethyl (2-((2-(pyridin-2-ylethynyl)quinolin-3-yl)methylene)hydrazineyl)-phosphonate

302

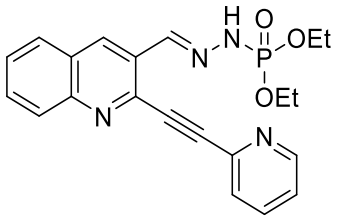

Formula: $C_{21}H_{21}N_4O_3P$

Mol. Weight: 408.40 g.mol^{-1}

Aspect: yellow solid

R_f: 0.2 (EA)

Yield: 72%

^{1}H NMR (300 MHz, Chloroform-d): δ 8.76 (s, 1H), 8.66 (d, J = 4.7 Hz, 1H), 8.64 (s, 1H), 8.07 (q, J = 11.4, 9.9 Hz, 2H), 7.86 (d, J = 8.1 Hz, 1H), 7.79 – 7.69 (m, 3H), 7.56 (t, J = 7.5 Hz, 1H), 7.38 – 7.30 (m, 1H), 4.31 – 4.16 (m, 4H), 1.38 (t, J = 7.1 Hz, 6H).

^{13}C NMR (75 MHz, Chloroform-d): δ 150.08, 148.15, 142.19, 141.28 (d, J = 20.3 Hz), 141.16, 136.32, 132.03, 130.58, 129.15, 129.11, 128.23, 128.14, 127.90, 127.36, 123.74, 92.32, 85.80, 63.43 (d, J = 5.4 Hz), 16.21 (d, J = 6.9 Hz).

^{31}P NMR (121 MHz, Chloroform-d): δ 1.29.

HR-MS (ESI+): m/z calculated for $C_{19}H_{25}N_2NaO_3P$ 383.1495 obtained 383.1489.

Diethyl (2-((2-(3-methoxyprop-1-yn-1-yl)pyridin-3-yl)methylene)hydrazineyl)-phosphonate

303

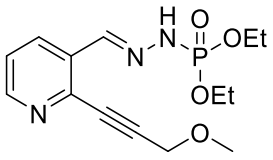

Formula: $C_{14}H_{20}N_3O_4P$

Mol. Weight: 325.30 g.mol^{-1}

Aspect: yellow solid

R_f: 0.08 (Cyclohexane:EA, 3:7)

Yield: 75%

^{1}H NMR (300 MHz, Chloroform-d): δ 8.55 (d, J = 4.5 Hz, 1H), 8.27 (d, J = 8.3 Hz, 1H), 8.22 (s, 1H), 7.54 (d, J = 28.9 Hz, 1H), 7.32 – 7.27 (m, 1H), 4.41 (s, 2H), 4.29 – 4.09 (m, 4H), 3.49 (s, 3H), 1.37 (t, J = 7.1 Hz, 6H).

^{13}C NMR (101 MHz, Chloroform-d): δ 150.19, 140.98 (d, J = 19.8 Hz), 140.82, 132.65, 132.38, 123.37, 90.53, 82.96, 63.53 (d, J = 5.4 Hz), 60.25, 58.06, 16.21 (d, J = 6.9 Hz).

^{31}P NMR (121 MHz, Chloroform-d): δ 0.47.

HR-MS (ESI+): m/z calculated for $C_{14}H_{21}N_3O_4P$ 326.1264 obtained 326.1258.

Diethyl (2-((6-(3-methoxyprop-1-yn-1-yl)benzo[d][1,3]dioxol-5-yl)methylene)hydrazineyl)phosphonate **304**

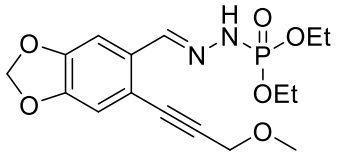

Formula: $C_{16}H_{21}N_2O_6P$

Mol. Weight: 368.33 g.mol^{-1}

Aspect: white solid

R_f: 0.2 (Cyclohexane:EA, 3:7)

Yield: 83%

^{1}H NMR (400 MHz, Chloroform-d): δ 8.23 (s, 1H), 8.06 (d, J = 28.0 Hz, 1H), 7.36 (s, 1H), 6.82 (s, 1H), 5.96 (s, 2H), 4.33 (s, 2H), 4.24 – 4.09 (m, 4H), 3.44 (s, 3H), 1.34 (t, J = 7.1 Hz, 6H).

^{13}C NMR (101 MHz, Chloroform-d): δ 148.69, 148.43, 143.12 (d, J = 19.4 Hz), 131.52, 116.09, 111.50, 104.52, 101.78, 89.37, 83.41, 63.44 (d, J = 5.6 Hz), 60.49, 57.91, 16.25 (d, J = 6.9 Hz).

^{31}P NMR (162 MHz, Chloroform-d): δ 1.66.

HR-MS (ESI+): m/z calculated for $C_{16}H_{22}N_2O_6P$ 369.1216 obtained 369.1224.

Diethyl-(2-((2-(3-methoxyprop-1-yn-1-yl)quinolin-3-yl)methylene)hydrazineyl)phosphonate **305**

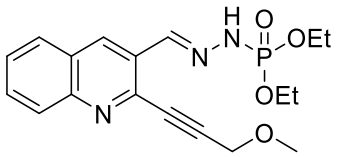

Formula: $C_{18}H_{22}N_3O_4P$

Mol. Weight: 375.36 g.mol^{-1}

Aspect: yellow solid

R_f: 0.09 (Cyclohexane:EA, 3:7)

Yield: 69%

^{1}H NMR (400 MHz, Chloroform-d) δ 8.89 (d, J = 28.7 Hz, 1H), 8.66 (s, 1H), 8.48 (s, 1H), 8.00 (d, J = 8.5 Hz, 1H), 7.79 (d, J = 8.1 Hz, 1H), 7.66 (t, J = 7.4 Hz, 1H), 7.49 (t, J = 7.4 Hz, 1H), 4.43 (s, 2H), 4.21 (q, J = 7.4 Hz, 4H), 3.50 (s, 3H), 1.37 (t, J = 7.0 Hz, 6H).

^{13}C NMR (101 MHz, Chloroform-d) δ 148.08, 141.40, 141.36 (d, J = 19.8 Hz), 132.13, 130.59, 129.05, 128.78, 128.21, 127.77, 127.29, 90.26, 83.59, 63.50 (d, J = 5.4 Hz), 60.33, 58.20, 16.24 (d, J = 6.8 Hz).

^{31}P NMR (162 MHz, Chloroform-d) δ 1.56.

HR-MS (ESI+): m/z calculated for $C_{18}H_{23}N_3O_4P$ 376.1426 obtained 376.1425.

Diethyl (2-(1-(2-(phenylethynyl)phenyl)ethylidene)hydrazineyl)phosphonate **306**

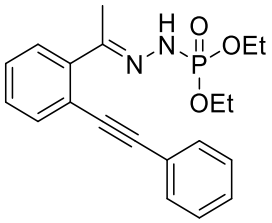

Formula: $C_{20}H_{23}N_2O_3P$

Mol. Weight: 370.39 g.mol^{-1}

Aspect: green oil

R_f: 0.24 (Cyclohexane:EA, 3:7)

Yield: 38%

This product has been obtained as a mixture of inseparable Z/E isomers.

^{1}H NMR (400 MHz, Dimethyl sulfoxide-d_6): δ 8.57 (d, J = 25.3 Hz, 1H), 7.66 (dd, J = 7.5, 1.6 Hz, 0H), 7.61 – 7.55 (m, 1H), 7.55 – 7.46 (m, 3H), 7.42 (tt, J = 6.8, 3.1 Hz, 6H), 7.39 – 7.34 (m, 1H), 7.27 (dd, J = 7.4, 1.6 Hz, 0H), 7.14 (d, J = 26.5 Hz, 0H), 4.09 – 3.96 (m, 4H), 3.96 – 3.83 (m, 1H), 2.30 (s, 3H), 2.20 (s, 1H), 1.18 (t, J = 7.1 Hz, 5H), 1.14 – 1.00 (m, 1H).

^{13}C NMR (75 MHz, Dimethyl sulfoxide-d_6): δ 150.47 (d, J = 19.2 Hz), 149.38 (d, J = 18.7 Hz), 143.02, 137.93, 132.47, 132.43, 131.27, 131.17, 129.66, 129.14, 129.01, 128.93, 128.78, 128.76, 128.26, 127.40, 122.29, 122.05, 120.25, 120.02, 93.18, 92.22, 88.34, 87.10, 62.26 (d, J = 5.5 Hz), 62.10 (d, J = 5.5 Hz), 24.07, 17.16, 16.01 (d, J = 6.4 Hz), 15.86.

^{31}P NMR (121 MHz, Dimethyl sulfoxide-d_6): δ 3.46, 2.68.

HR-MS (ESI-): m/z calculated for $C_{20}H_{22}N_2O_3P$ 369.1368 obtained 369.1372.

Diethyl (2-(phenyl(2-(phenylethynyl)phenyl)methylene)hydrazineyl)phosphonate **307**

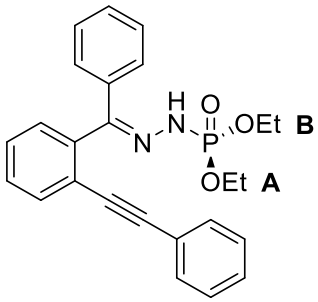

Formula: $C_{25}H_{25}N_2O_3P$

Mol. Weight: 432.46 g.mol^{-1}

Aspect: green solid

R_f: 0.32 (Cyclohexane:EA, 9:1)

Yield: 38%

In this compound, ethoxy chains A and B are not equivalent.

^{1}H NMR (400 MHz, Methanol-d_4): δ 7.82 – 7.67 (m, 1H), 7.63 – 7.55 (m, 2H), 7.52 (dd, J = 6.7, 3.0 Hz, 2H), 7.37 – 7.32 (m, 3H), 7.32 – 7.28 (m, 2H), 7.28 – 7.22 (m, 2H), 7.19 – 7.11 (m, 2H), 4.18 (pd, J = 7.1, 3.4 Hz, 2H), 4.04 (pt, J = 7.3, 3.5 Hz, 2H), 1.31 (t, J = 7.0 Hz, 3H), 1.08 (t, J = 7.1 Hz, 3H).

^{13}C NMR (151 MHz, Methanol-d_4): δ 152.71 (d, J = 18.3 Hz), 138.28, 136.24, 133.91, 132.46, 131.03, 130.66, 130.22, 130.08, 129.80, 129.43, 129.39, 127.76, 124.07, 123.78, 94.27, 87.69,

65.14 (d, J = 6.0 Hz, CH2 A), 64.88 (d, J = 5.8 Hz, CH2 B), 16.48 (d, J = 6.7 Hz, CH3 A), 16.32 (d, J = 6.9 Hz, CH3 B).

^{31}P NMR (162 MHz, Methanol-d$_4$): δ 2.05.

HR-MS (ESI+): m/z calculated for $C_{25}H_{25}N_2O_3NaP$ 455.1501 obtained 455.1488.

---

diethyl-(2-(1-(2-(phenylethynyl)quinolin-3-yl)ethylidene)hydrazineyl)phosphonate

308

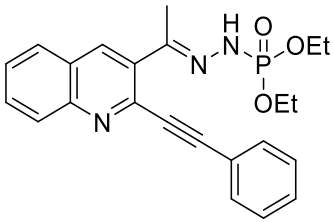

Formula: $C_{23}H_{24}N_3O_3P$

Mol. Weight: 421.44 g.mol^{-1}

Aspect: brown solid

R$_f$: 0.32 (Cyclohexane:EA, 3:7)

Yield: 69%

^{1}H NMR (300 MHz, Chloroform-d) δ 8.10 – 8.03 (m, 1H), 7.92 (s, 1H), 7.77 – 7.67 (m, 2H), 7.55 – 7.50 (m, 3H), 7.33 – 7.24 (m, 3H), 6.56 (d, J = 27.2 Hz, 1H), 4.12 – 3.79 (m, 4H), 2.42 – 2.32 (m, 6H), 1.22 (dt, J = 13.1, 6.1 Hz, 6H).

^{31}P NMR (121 MHz, Chloroform-d) δ 2.00.

^{13}C NMR (75 MHz, Deuterium Oxide) δ 148.27 (d, J = 17.9 Hz), 147.98, 140.39, 135.01, 132.07, 131.85, 130.95, 129.50, 129.07, 128.36, 127.85, 127.56, 126.49, 121.42, 92.78, 86.86, 63.13 (d, J = 5.6 Hz), 24.23, 15.98 (d, J = 6.7 Hz).

HR-MS (ESI+): m/z calculated for $C_{23}H_{24}N_3O_3NaP$ 444.1453 obtained 444.1433.

Diethyl (2-((E)-2-((E)-styryl)benzylidene)hydrazineyl)phosphonate

309

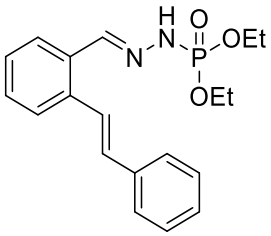

Formula: $C_{19}H_{23}N_2O_3P$

Mol. Weight: 358.38 g.mol^{-1}

Aspect: white solid

R$_f$: 0.43 (Cyclohexane:EA, 3:7)

Yield: 84%

^{1}H NMR (400 MHz, Chloroform-d): δ 8.52 (d, J = 28.3 Hz, 1H), 8.25 (s, 1H), 7.79 – 7.67 (m, 2H), 7.58 (dd, J = 18.5, 7.7 Hz, 3H), 7.41 – 7.32 (m, 3H), 7.29 (d, J = 7.4 Hz, 1H), 6.97 (d, J = 16.1 Hz, 1H), 4.26 – 4.12 (m, 4H), 1.32 (t, J = 7.1 Hz, 6H).

^{13}C NMR (101 MHz, Chloroform-d): δ 144.19 (d, J = 19.6 Hz), 137.51, 136.56, 131.79, 131.77, 129.25, 128.73, 127.90, 127.84, 127.60, 126.83, 126.75, 126.35, 63.50 (d, J = 5.9 Hz), 16.23 (d, J = 7.0 Hz).

^{31}P NMR (162 MHz, Chloroform-d): δ 1.97.

HR-MS (ESI+): m/z calculated for $C_{19}H_{23}N_2NaO_3P$ 381.1338 obtained 381.1336.

Dimethyl (2-(2-(phenylethynyl)benzylidene)hydrazineyl)phosphonate **310**

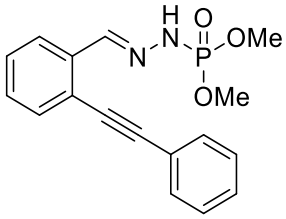

Formula: $C_{17}H_{17}N_2O_3P$

Mol. Weight: 328.31 g.mol^{-1}

Aspect: brown solid

R_f: 0.35 (Cyclohexane:EA, 3:7)

Yield: 35%

^{1}H NMR (300 MHz, Chloroform-d): δ 8.89 (d, J = 29.5 Hz, 1H), 8.59 (s, 1H), 8.03 – 7.96 (m, 1H), 7.73 – 7.65 (m, 2H), 7.53 (dd, J = 6.4, 2.6 Hz, 1H), 7.41 – 7.36 (m, 3H), 7.35 – 7.27 (m, 2H), 3.83 (d, J = 11.3 Hz, 6H).

^{13}C NMR (75 MHz, Chloroform-d): δ 144.30 (d, J = 19.8 Hz), 135.42, 132.24, 131.81, 129.10, 128.69, 128.50, 128.44, 125.01, 123.03, 122.66, 95.14, 86.50, 53.96 (d, J = 6.1 Hz).

^{31}P NMR (121 MHz, Chloroform-d): δ 3.73.

HR-MS (ESI+): m/z calculated for $C_{17}H_{17}N_2NaO_3P$ 351.0869 obtained 351.0859.

Dibenzyl (2-(2-(phenylethynyl)benzylidene)hydrazineyl)phosphonate **311**

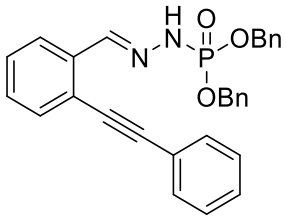

Formula: $C_{29}H_{25}N_2O_3P$

Mol. Weight: 480.50 g.mol^{-1}

Aspect: colorless crystals

R_f: 0.76 (EA)

Yield: 66%

^{1}H NMR (400 MHz, Chloroform-d): δ 9.48 (d, J = 29.7 Hz, 1H), 8.67 (s, 1H), 8.01 (dd, J = 5.9, 3.4 Hz, 1H), 7.77 (dd, J = 6.7, 3.0 Hz, 2H), 7.61 (dd, J = 5.8, 3.3 Hz, 1H), 7.49 – 7.42 (m, 4H), 7.40 – 7.27 (m, 11H), 5.26 (d, J = 7.8 Hz, 4H).

^{13}C NMR (101 MHz, Chloroform-d): δ 144.16 (d, J = 20.2 Hz), 136.01 (d, J = 7.3 Hz), 135.59, 132.12, 131.79, 128.92, 128.54, 128.45, 128.39, 128.37, 128.31, 127.98, 124.84, 122.98, 122.64, 95.23, 86.57, 68.89 (d, J = 5.3 Hz).

^{31}P NMR (121 MHz, Chloroform-d): δ 1.45.

HR-MS (ESI+): m/z calculated for $C_{29}H_{26}N_2O_3P$ 481.1676 obtained 481.1667.

P,P-diphenyl-N'-(2-(phenylethynyl)benzylidene)phosphinic hydrazide **312**

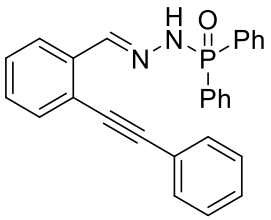

Formula: $C_{27}H_{21}N_2OP$

Mol. Weight: 420.45 g.mol^{-1}

Aspect: white solid

R_f: 0.41 (Cyclohexane:EA, 3:7)

Yield: 85%

^{1}H NMR (400 MHz, Chloroform-d): δ 8.49 (s, 1H), 7.95 – 7.87 (m, 4H), 7.76 (dd, J = 7.8, 1.6 Hz, 1H), 7.57 – 7.49 (m, 4H), 7.45 (qd, J = 8.0, 7.3, 2.5 Hz, 5H), 7.30 (dd, J = 6.2, 1.5 Hz, 3H), 7.25 – 7.17 (m, 2H), 2.00 (s, 1H).

^{13}C NMR (101 MHz, Chloroform-d): δ 143.93 (d, J = 16.3 Hz), 135.41, 132.46 (d, J = 9.9 Hz), 132.38, 132.29, 132.26, 131.73, 131.25 (d, J = 129.5 Hz), 128.94, 128.63, 128.59 (d, J = 12.3 Hz), 128.51, 125.32, 123.00, 122.39, 94.77, 86.62.

^{31}P NMR (121 MHz, Chloroform-d): δ 23.31.

HR-MS (ESI+): m/z calculated for $C_{27}H_{21}N_2ONaP$ 443.1289 obtained 443.1282.

Diethyl-(2-(2-cyanobenzylidene)hydrazineyl)phosphonate **336**

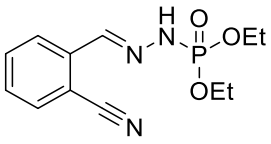

Formula: $C_{12}H_{16}N_3O_3P$

Mol. Weight: 281.25 g.mol^{-1}

Aspect: yellow solid

R_f: 0.12 (Cyclohexane:EA, 5:5)

Yield: 81%

^{1}H NMR (300 MHz, Chloroform-d) δ 8.14 (s, 1H), 8.01 (d, J = 8.0 Hz, 1H), 7.93 (d, J = 28.2 Hz, 1H), 7.65 (d, J = 7.2 Hz, 1H), 7.58 (t, J = 7.6 Hz, 1H), 7.42 (t, J = 7.6 Hz, 1H), 4.23 (h, J = 7.1 Hz, 4H), 1.38 (t, J = 7.1 Hz, 6H).

^{13}C NMR (75 MHz, Chloroform-d) δ 140.33 (d, J = 19.1 Hz), 137.27, 133.08, 132.94, 129.39, 126.34, 117.27, 111.01, 63.89 (d, J = 5.6 Hz), 16.32 (d, J = 6.9 Hz).

^{31}P NMR (121 MHz, Chloroform-d) δ 0.37.

HR-MS (ESI+): m/z calculated for $C_{12}H_{16}N_3O_3NaP$ 304.0827 obtained 304.0833.

Diethyl-(2-((4'-hydroxy-[1,1'-biphenyl]-2-yl)methylene)hydrazineyl)phosphonate

337

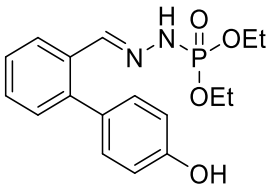

Formula: $C_{17}H_{21}N_2O_4P$

Mol. Weight: 348.34 $g.mol^{-1}$

Aspect: brown solid

R_f: 0.22 (Cyclohexane:EA, 3:7)

Yield: 68%

^{1}H NMR (300 MHz, Chloroform-d) δ 8.00 (d, J = 6.8 Hz, 1H), 7.74 (s, 1H), 7.34 (dd, J = 16.0, 8.3 Hz, 3H), 7.13 (d, J = 8.3 Hz, 2H), 6.92 (d, J = 8.4 Hz, 2H), 4.28 – 4.14 (m, 4H), 1.38 (t, J = 7.1 Hz, 6H).

^{13}C NMR (75 MHz, Chloroform-d) δ 156.52, 144.69 (d, J = 19.2 Hz), 141.98, 131.41, 131.08, 130.42, 129.48, 127.28, 125.88, 115.50, 63.99 (d, J = 6.0 Hz), 16.30 (d, J = 6.9 Hz).

HR-MS (ESI+): m/z calculated for $C_{17}H_{22}N_2O_4P$ 349.1317 obtained 349.1307.

Visible-light catalyzed synthesis of phthalazines

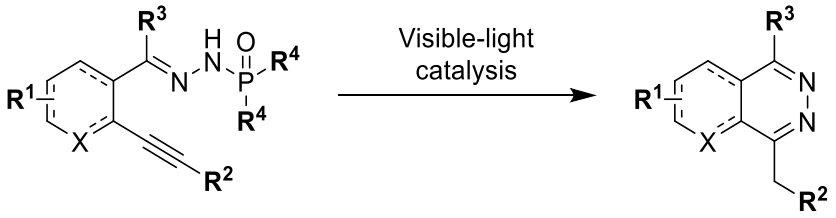

General procedure:

To an oven dried sealable glass vial were added phosphonohydrazone (0.3 mmol, 1 eq.), sodium *tert*-butoxide (0.9 mmol, 3 eq.), tris(2,2'-bipyridine)ruthenium(II) hexafluorophosphate (0.0075 mmol, 2.5 mol%) and MeOH (1 mL, 0.3 M). The vials were sealed with 20mm crimp caps with silicone/PTFE septum and stirred for 16 hours under visible-light irradiation. After completion of the reaction checked by TLC, the resulting suspension was filtered through a pad of celite eluting with ethyl acetate. The crude filtrate was concentrated and purification of the residue by silica gel column chromatography eluting with a cyclohexane/ethyl acetate mixture gave the desired product.

1-benzylphthalazine **314**

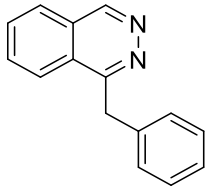

Formula: $C_{15}H_{12}N_2$

Mol. Weight: 220.28 g.mol^{-1}

Aspect: brown oil

R_f: 0.18 (Cyclohexane:EA, 3:7)

Yield: 58%

^{1}H NMR (300 MHz, Dimethyl sulfoxide-d_6): δ 9.59 (s, 1H), 8.37 – 8.23 (m, 1H), 8.20 – 8.10 (m, 1H), 8.04 – 7.92 (m, 2H), 7.25 (ddd, J = 28.9, 20.6, 7.4 Hz, 5H), 4.70 (s, 2H).

^{13}C NMR (75 MHz, Chloroform-d): δ 158.83, 150.73, 138.70, 132.96, 132.49, 128.63, 128.54, 127.12, 126.40, 126.35, 124.79, 124.58, 38.62.

HR-MS (ESI+): m/z calculated for $C_{15}H_{12}N_2Na$ 243.0898 obtained 243.0898.

1-benzyl-6-methoxyphthalazine **315**

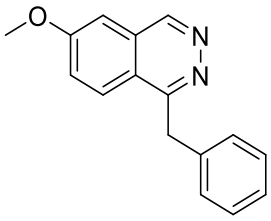

Formula: $C_{16}H_{14}N_2O$

Mol. Weight: 250.30 g.mol^{-1}

Aspect: brown oil

R_f: 0. (Cyclohexane:EA, 3:7)

Yield: 77%

^{1}H NMR (400 MHz, Chloroform-d): δ 9.36 (s, 1H), 7.94 (d, J = 9.1 Hz, 1H), 7.36 (dd, J = 9.1, 2.5 Hz, 1H), 7.28 (d, J = 7.2 Hz, 2H), 7.23 (t, J = 7.5 Hz, 2H), 7.15 (dd, J = 7.3, 4.9 Hz, 2H), 4.66 (s, 2H), 3.93 (s, 3H).

^{13}C NMR (101 MHz, Chloroform-d): δ 161.97, 158.35, 150.63, 138.57, 129.26, 128.73, 128.66, 126.73, 126.66, 124.66, 121.28, 104.87, 55.86, 40.05.

HR-MS (ESI+): m/z calculated for $C_{16}H_{14}N_2ONa$ 273.1004 obtained 273.1014.

1-benzyl-6-chlorophthalazine **316**

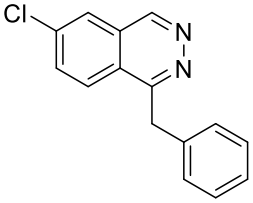

Formula: $C_{15}H_{11}ClN_2$

Mol. Weight: 254.72 g.mol^{-1}

Aspect: yellow solid

R_f: 0.36 (Cyclohexane:EA, 3:7)

Yield: 51%

^{1}H NMR (400 MHz, Chloroform-d) δ 9.38 (s, 1H), 7.99 (d, J = 8.8 Hz, 1H), 7.92 – 7.87 (m, 1H), 7.71 (dd, J = 8.8, 1.8 Hz, 1H), 7.26 (q, J = 7.5 Hz, 4H), 7.18 (t, J = 6.9 Hz, 1H), 4.71 (s, 2H).

^{13}C NMR (101 MHz, Chloroform-d) δ 158.83, 149.99, 138.16, 138.09, 133.55, 128.88, 128.67, 127.90, 126.90, 126.73, 125.99, 124.11, 40.19.

HR-MS (ESI+): m/z calculated for $C_{15}H_{12}ClN_2$ 255.0684 obtained 255.0685.

1-benzyl-6-bromophthalazine **317**

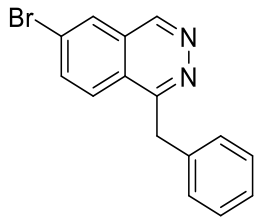

Formula: $C_{15}H_{11}BrN_2$

Mol. Weight: 299.17 g.mol^{-1}

Aspect: yellow solid

R_f: 0.65 (Cyclohexane:EA, 4:6)

Yield: 41%

^{1}H NMR (300 MHz, Chloroform-d) δ 9.32 (s, 1H), 8.03 (dd, J = 1.8, 0.6 Hz, 1H), 7.86 (dt, J = 8.8, 0.7 Hz, 1H), 7.80 (ddd, J = 8.8, 1.9, 1.1 Hz, 1H), 7.27 – 7.11 (m, 5H), 4.66 (s, 2H).

^{13}C NMR (75 MHz, Chloroform-d) δ 158.99, 149.80, 138.06, 136.20, 129.34, 128.89, 128.67, 128.13, 126.92, 126.64, 126.55, 124.33, 40.15.

HR-MS (ESI+): m/z calculated for $C_{15}H_{12}BrN_2$ 299.0178 obtained 299.0176.

1-benzyl-6,7,8-trimethoxyphthalazine **318**

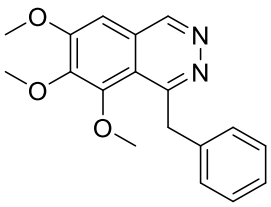

Formula: $C_{18}H_{18}N_2O_3$

Mol. Weight: 310.35 g.mol^{-1}

Aspect: white solid

R_f: 0.17 (Cyclohexane:EA, 3:7)

Yield: 35%

^{1}H NMR (400 MHz, Acetone-d_6): δ 9.31 (s, 1H), 7.39 (s, 1H), 7.27 – 7.09 (m, 5H), 4.81 (s, 2H), 4.06 (s, 3H), 3.90 (s, 3H), 3.78 (s, 3H).

^{13}C NMR (101 MHz, Acetone-d_6): δ 158.76, 156.55, 150.04, 149.78, 146.87, 141.39, 129.23, 128.96, 126.61, 126.30, 117.40, 103.05, 61.72, 61.21, 56.76, 42.86.

HR-MS (ESI+): m/z calculated for $C_{18}H_{18}N_2O_3Na$ 333.1215 obtained 333.1213.

7-benzyl-2,3-dihydro-[1,4]dioxino[2,3-g]pyridazino[4,5-b]quinoline **319**

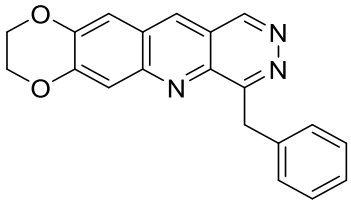

Formula: $C_{20}H_{15}N_3O_2$

Mol. Weight: 329.36 g.mol^{-1}

Aspect: yellow solid

R_f: 0.47 (CH_2Cl_2:MeOH, 9:1)

Yield: 42%

^{1}H NMR (300 MHz, Chloroform-d): δ 9.42 (s, 1H), 8.49 (s, 1H), 7.77 (s, 1H), 7.69 – 7.61 (m, 2H), 7.38 (s, 1H), 7.27 – 7.20 (m, 2H), 7.13 (dd, J = 8.4, 6.3 Hz, 1H), 4.95 (s, 2H), 4.54 – 4.40 (m, 4H).

^{13}C NMR (75 MHz, Chloroform-d): δ 162.19, 150.93, 150.76, 149.65, 146.90, 139.51, 139.00, 132.97, 129.95, 128.34, 126.48, 126.38, 118.69, 114.16, 111.34, 64.69, 64.53, 38.11.

HR-MS (ESI+): m/z calculated for $C_{20}H_{16}N_3O_2$ 330.1237 obtained 330.1233.

4-benzylbenzofuro[2,3-d]pyridazine **320**

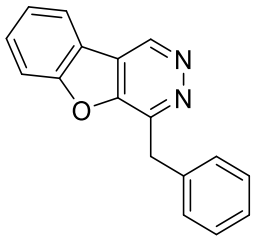

Formula: $C_{17}H_{12}N_2O$

Mol. Weight: 260.30 g.mol^{-1}

Aspect: yellow solid

R_f: 0.66 (EA:MeOH, 9:1)

Yield: 76%

^{1}H NMR (600 MHz, Chloroform-d): δ 9.78 (s, 1H), 8.09 (d, J = 7.7 Hz, 1H), 7.74 (d, J = 8.4 Hz, 1H), 7.69 (t, J = 8.2 Hz, 1H), 7.51 (dd, J = 13.6, 7.2 Hz, 3H), 7.29 (t, J = 7.6 Hz, 2H), 7.21 (t, J = 7.4 Hz, 1H), 4.72 (s, 2H).

^{13}C NMR (151 MHz, Chloroform-d): δ 156.31, 153.13, 150.45, 144.30, 137.15, 131.03, 129.34, 128.82, 127.05, 125.06, 122.88, 122.64, 120.02, 113.08, 37.87.

HR-MS (ESI+): m/z calculated for $C_{17}H_{12}N_2ONa$ 283.0847 obtained 283.0838.

4-benzyl-5-methyl-5H-pyridazino[4,5-b]indole **321**

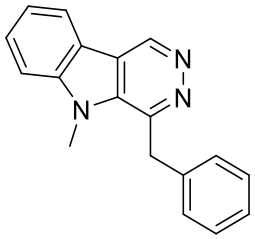

Formula: $C_{18}H_{15}N_3$

Mol. Weight: 273.34 g.mol^{-1}

Aspect: yellow solid

R_f: 0.19 (Cyclohexane:EA, 3:7)

Yield: 92%

^{1}H NMR (300 MHz, Chloroform-d): δ 9.69 (s, 1H), 8.15 (d, J = 7.9 Hz, 1H), 7.61 (t, J = 7.8 Hz, 1H), 7.39 (dd, J = 16.5, 8.3 Hz, 2H), 7.22 (m, 3H), 7.11 (d, J = 7.4 Hz, 2H), 4.90 (s, 2H), 3.85 (s, 3H).

^{13}C NMR (75 MHz, Chloroform-d): δ 147.08, 143.44, 141.17, 138.90, 135.95, 129.02, 128.94, 128.23, 126.77, 121.70, 121.49, 119.83, 119.59, 110.18, 40.30, 31.94.

HR-MS (ESI+): m/z calculated for $C_{18}H_{16}N_3$ 274.1344 obtained 274.1334.

1-(4-methoxybenzyl)phthalazine **322**

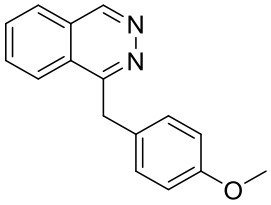

Formula: $C_{16}H_{14}N_2O$

Mol. Weight: 250.30 g.mol^{-1}

Aspect: orange solid

R_f: 0.12 (Cyclohexane:EA, 3:7)

Yield: 62%

^{1}H NMR (400 MHz, Chloroform-d): δ 9.46 (s, 1H), 8.15 – 8.04 (m, 1H), 7.95 (dd, J = 6.3, 2.5 Hz, 1H), 7.88 – 7.79 (m, 2H), 7.24 (d, J = 8.7 Hz, 2H), 6.80 (d, J = 8.7 Hz, 2H), 4.69 (s, 2H), 3.73 (s, 3H).

^{13}C NMR (101 MHz, Chloroform-d): δ 159.53, 158.50, 150.96, 132.83, 132.30, 130.61, 130.34, 129.78, 127.23, 126.00, 124.94, 114.26, 55.35, 39.22.

HR-MS (ESI+): m/z calculated for $C_{16}H_{14}N_2ONa$ 273.1004 obtained 273.0973.

1-(3,4,5-trimethoxybenzyl)phthalazine **323**

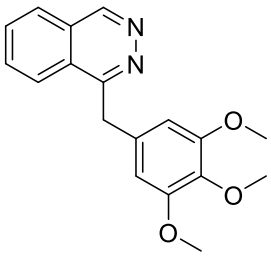

Formula: $C_{18}H_{18}N_2O_3$

Mol. Weight: 310.35 g.mol^{-1}

Aspect: yellow solid

R_f: 0. (Cyclohexane:EA, 3:7)

Yield: 70%

^{1}H NMR (400 MHz, Chloroform-d): δ 9.44 (s, 1H), 8.16 – 8.01 (m, 1H), 7.93 (m, 1H), 7.88 – 7.76 (m, 2H), 6.52 (s, 2H), 4.64 (s, 2H), 3.74 (s, 3H), 3.74 (s, 6H).

^{13}C NMR (101 MHz, Chloroform-d): δ 171.17, 159.00, 153.40, 150.98, 136.82, 133.89, 132.80, 132.32, 127.15, 125.92, 124.67, 105.88, 60.82, 56.20, 40.24.

HR-MS (ESI+): m/z calculated for $C_{18}H_{18}N_2O_3Na$ 333.1215 obtained 333.1200.

1-(4-methylbenzyl)phthalazine **324**

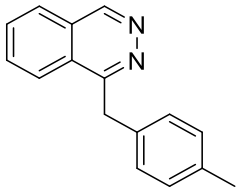

Formula: $C_{16}H_{14}N_2$

Mol. Weight: 234.30 g.mol^{-1}

Aspect: white solid

R_f: 0. (Cyclohexane:EA, 3:7)

Yield: 47%

^{1}H NMR (300 MHz, Chloroform-d): δ 9.44 (s, 1H), 8.15 – 8.01 (m, 1H), 7.96 – 7.87 (m, 1H), 7.82 (td, J = 7.2, 2.8 Hz, 2H), 7.21 (d, J = 7.9 Hz, 2H), 7.06 (d, J = 7.9 Hz, 2H), 4.69 (s, 2H), 2.26 (s, 3H).

^{13}C NMR (151 MHz, Chloroform-d): δ 159.44, 150.91, 136.36, 135.15, 132.86, 132.30, 129.48, 128.61, 127.18, 127.14, 125.98, 124.90, 39.62, 21.07.

HR-MS (ESI+): m/z calculated for $C_{16}H_{15}N_2$ 235.1230 obtained 235.1228.

1-(4-fluorobenzyl)phthalazine **325**

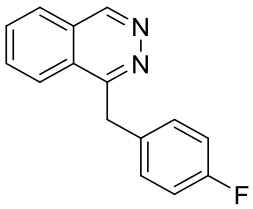

Formula: $C_{15}H_{11}FN_2$

Mol. Weight: 238.27 g.mol^{-1}

Aspect: white solid

R_f: 0.23 (Cyclohexane:EA, 3:7)

Yield: 65%

^{1}H NMR (300 MHz, Chloroform-d): δ 9.49 (s, 1H), 8.12 – 8.04 (m, 1H), 7.99 (dd, J = 5.8, 2.9 Hz, 1H), 7.94 – 7.84 (m, 3H), 7.29 (dt, J = 8.3, 4.3 Hz, 2H), 6.94 (t, J = 8.7 Hz, 2H), 4.73 (s, 2H).

^{13}C NMR (75 MHz, Chloroform-d): δ 161.83 (d, J = 245.3 Hz), 159.19, 151.00, 133.76 (d, J = 3.3 Hz), 133.14, 132.61, 130.27 (d, J = 8.0 Hz), 127.44, 127.20, 125.96, 124.74, 115.72 (d, J = 21.4 Hz), 39.07.

^{19}F NMR (376 MHz, Chloroform-d): δ -116.07.

HR-MS (ESI+): m/z calculated for $C_{15}H_{11}N_2NaF$ 261.0804 obtained 261.0799.

4-(phthalazin-1-ylmethyl)benzonitrile **326**

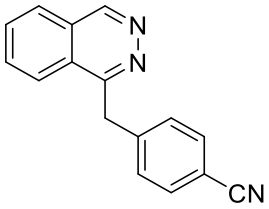

Formula: $C_{16}H_{11}N_3$

Mol. Weight: 245.29 g.mol^{-1}

Aspect: amorphous solid

R_f: 0.14 (Cyclohexane:EA, 3:7)

Yield: 44%

^{1}H NMR (300 MHz, Chloroform-d) δ 9.47 (s, 1H), 8.03 – 7.94 (m, 3H), 7.92 – 7.80 (m, 3H), 7.54 (d, J = 8.2 Hz, 2H), 7.42 (d, J = 8.2 Hz, 2H), 4.77 (s, 2H).

^{13}C NMR (75 MHz, Chloroform-d) δ 157.98, 151.19, 143.69, 133.06, 132.55, 129.58, 127.36, 126.99, 125.63, 124.07, 118.78, 110.74, 39.85.

HR-MS (ESI+): m/z calculated for $C_{16}H_{12}N_3$ 246.1026 obtained 246.1030.

1-(2-bromobenzyl)phthalazine **327**

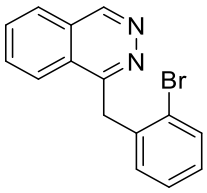

Formula: $C_{15}H_{11}BrN_2$

Mol. Weight: 299.17 g.mol^{-1}

Aspect: yellow oil

R_f: 0.19 (Cyclohexane:EA, 3:7)

Yield: 49%

^{1}H NMR (400 MHz, Chloroform-d): δ 9.55 (s, 1H), 8.02 (t, J = 7.0 Hz, 2H), 7.87 (t, J = 6.2 Hz, 2H), 7.60 (d, J = 7.6 Hz, 1H), 7.12 – 7.03 (m, 2H), 7.01 – 6.95 (m, 1H), 4.86 (s, 2H).

^{13}C NMR (101 MHz, Chloroform-d): δ 158.98, 150.95, 137.63, 133.36, 132.97, 132.66, 130.63, 128.49, 127.74, 127.42, 127.02, 126.14, 124.76, 124.30, 39.44.

HR-MS (ESI+): m/z calculated for $C_{15}H_{11}N_2NaBr$ 321.0003 obtained 321.0019.

1-(thiophen-2-ylmethyl)phthalazine **328**

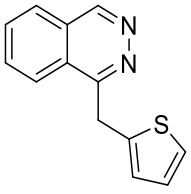

Formula: $C_{13}H_{10}N_2S$

Mol. Weight: 226.30 g.mol^{-1}

Aspect: brown oil

R_f: 0.29 (Cyclohexane:EA, 3:7)

Yield: 23%

^{1}H NMR (400 MHz, Chloroform-d): δ 9.46 (s, 1H), 8.16 (dd, J = 6.2, 3.3 Hz, 1H), 7.96 (dt, J = 6.0, 2.8 Hz, 1H), 7.87 (dt, J = 6.1, 3.5 Hz, 2H), 7.12 (dd, J = 4.2, 2.3 Hz, 1H), 6.93 – 6.83 (m, 2H), 4.91 (d, J = 2.4 Hz, 3H).

^{13}C NMR (75 MHz, Chloroform-d): δ 158.50, 151.16, 140.49, 132.91, 132.43, 127.23, 127.12, 127.12, 126.08, 125.70, 124.59, 124.55, 34.52.

HR-MS (ESI+): m/z calculated for $C_{13}H_{11}N_2S$ 227.0643 obtained 227.0643.

1-methylphthalazine **329**

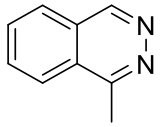

Formula: $C_9H_8N_2$

Mol. Weight: 144.18 g.mol^{-1}

Aspect: brown oil

R_f: 0.09 (Cyclohexane:EA, 3:7)

Yield: 70%

^{1}H NMR (400 MHz, Chloroform-d): δ 9.47 (s, 1H), 8.14 (dd, J = 6.7, 2.3 Hz, 1H), 8.04 – 7.93 (m, 3H), 3.07 (s, 3H).

^{13}C NMR (101 MHz, Chloroform-d): δ 157.93, 150.71, 133.24, 133.00, 127.30, 126.59, 126.55, 124.76, 19.53.

HR-MS (ESI+): m/z calculated for $C_9H_8N_2Na$ 167.0585 obtained 167.0576.

1-(cyclohex-1-en-1-ylmethyl)phthalazine **330**

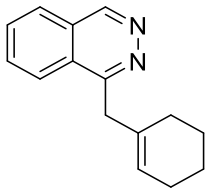

Formula: $C_{15}H_{16}N_2$

Mol. Weight: 224.31 g.mol^{-1}

Aspect: brown oil

R_f: 0.19 (Cyclohexane:EA, 3:7)

Yield: 26%

^{1}H NMR (400 MHz, Chloroform-d): δ 9.45 (s, 1H), 8.24 – 8.14 (m, 1H), 8.00 – 7.94 (m, 1H), 7.93 – 7.85 (m, 2H), 5.43 (dt, J = 3.6, 1.9 Hz, 1H), 4.05 (s, 2H), 2.01 – 1.93 (m, 4H), 1.61 – 1.54 (m, 2H), 1.53 – 1.47 (m, 2H).

^{13}C NMR (151 MHz, Chloroform-d): δ 159.18, 150.75, 135.29, 132.76, 132.45, 127.15, 126.87, 126.56, 125.00, 124.78, 42.17, 28.73, 25.41, 22.85, 22.23.

HR-MS (ESI+): m/z calculated for $C_{15}H_{17}N_2$ 225.1392 obtained 225.1391.

8-(2-methoxyethyl)pyrido[2,3-d]pyridazine **331**

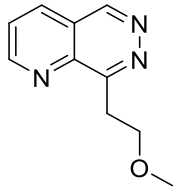

Formula: $C_{10}H_{11}N_3O$

Mol. Weight: 189.22 g.mol^{-1}

Aspect: brown oil

R_f: 0.28 (EA:MeOH, 9:1)

Yield: 95%

^{1}H NMR (400 MHz, Chloroform-d): δ 9.48 (s, 1H), 9.25 (dd, J = 4.3, 1.7 Hz, 1H), 8.26 (dd, J = 8.2, 1.7 Hz, 1H), 7.80 (dd, J = 8.2, 4.3 Hz, 1H), 4.04 (t, J = 6.8 Hz, 2H), 3.86 (t, J = 6.8 Hz, 2H), 3.37 (s, 3H).

^{13}C NMR (101 MHz, Chloroform-d): δ 161.22, 155.85, 150.39, 141.61, 134.59, 127.13, 121.84, 71.40, 58.74, 31.75.

HR-MS (ESI+): m/z calculated for $C_{10}H_{11}N_3ONa$ 212.0800 obtained 212.0793.

5-(2-methoxyethyl)-[1,3]dioxolo[4,5-g]phthalazine **332**

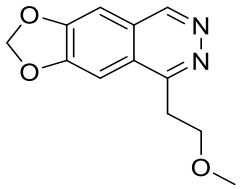

Formula: $C_{12}H_{12}N_2O_3$

Mol. Weight: 232.24 g.mol^{-1}

Aspect: yellow solid

R_f: 0.41 (EA:MeOH, 9:1)

Yield: 72%

^{1}H NMR (400 MHz, Chloroform-d): δ 9.18 (s, 1H), 7.39 (s, 1H), 7.14 (s, 1H), 6.17 (s, 2H), 3.94 (t, J = 6.9 Hz, 2H), 3.48 (t, J = 6.9 Hz, 2H), 3.36 (s, 3H).

^{13}C NMR (101 MHz, Chloroform-d): δ 157.08, 152.25, 151.69, 149.31, 125.00, 124.58, 102.97, 102.48, 101.21, 71.59, 58.97, 33.68.

HR-MS (ESI+): m/z calculated for $C_{12}H_{12}N_2O_3Na$ 255.0746 obtained 255.0737.

1-benzyl-4-methylphthalazine **333**

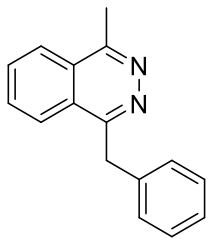

Formula: $C_{16}H_{14}N_2$

Mol. Weight: 234.30 g.mol^{-1}

Aspect: green solid

R_f: 0.47 (Cyclohexane:Acetone, 5:5)

Yield: 17%

^{1}H NMR (400 MHz, Chloroform-d): δ 8.06 (ddd, J = 7.8, 4.5, 1.3 Hz, 2H), 7.87 – 7.73 (m, 2H), 7.32 (d, J = 7.6 Hz, 2H), 7.28 – 7.22 (m, 2H), 7.17 (td, J = 6.9, 3.2 Hz, 1H), 4.70 (s, 2H), 3.00 (s, 3H).

^{13}C NMR (101 MHz, Chloroform-d): δ 158.22, 156.93, 138.71, 132.10, 131.93, 128.76, 128,76, 126.80, 126.68, 125.62, 125.38, 125.14, 40.08, 19.92.

HR-MS (ESI+): m/z calculated for $C_{16}H_{15}N_2$ 235.1230 obtained 235.1225.

1-benzyl-4-phenylphthalazine **334**

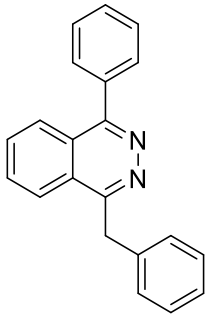

Formula: $C_{21}H_{16}N_2$

Mol. Weight: 296.37 g.mol^{-1}

Aspect: brown solid

R_f: 0.69 (Cyclohexane:EA, 3:7)

Yield: 34%

^{1}H NMR (300 MHz, Chloroform-d): δ 8.15 (d, J = 7.5 Hz, 1H), 8.07 (d, J = 8.2 Hz, 1H), 7.85 – 7.72 (m, 4H), 7.56 (d, J = 4.7 Hz, 3H), 7.40 (d, J = 7.6 Hz, 2H), 7.33 – 7.25 (m, 2H), 7.20 (t, J = 7.4 Hz, 1H), 4.81 (s, 2H).

^{13}C NMR (75 MHz, Chloroform-d): δ 159.64, 158.22, 138.52, 136.32, 132.19, 132.04, 130.30, 129.45, 128.87, 128.82, 128.64, 127.14, 126.79, 126.36, 126.00, 125.18, 40.12.

HR-MS (ESI+): m/z calculated for $C_{21}H_{16}N_2Na$ 319.1211 obtained 319.1213.

4-benzyl-1-methylpyridazino[4,5-b]quinoline **335**

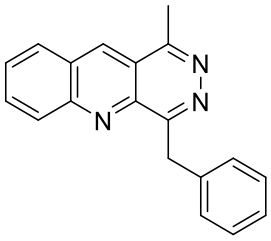

Formula: $C_{19}H_{15}N_3$

Mol. Weight: 285.35 g.mol^{-1}

Aspect: ochre solid

R_f: 0.35 (Cyclohexane:EA, 3:7)

Yield: 50%

^{1}H NMR (400 MHz, Chloroform-d) δ 8.93 (s, 1H), 8.40 (d, J = 8.8 Hz, 1H), 8.10 (d, J = 8.5 Hz, 1H), 7.97 (ddd, J = 8.5, 6.7, 1.4 Hz, 1H), 7.73 (dd, J = 8.3, 6.9 Hz, 1H), 7.70 – 7.63 (m, 2H), 7.23 (dd, J = 8.4, 6.9 Hz, 2H), 7.17 – 7.09 (m, 1H), 4.98 (s, 2H), 3.07 (s, 3H).

HR-MS (ESI+): m/z calculated for $C_{19}H_{16}N_3$ 286.1344 obtained 286.1357.

We observed a rapid degradation of this compound so no ^{13}C NMR could be undertaken.

6-methoxy-1-(3,4,5-trimethoxybenzyl)phthalazine **342**

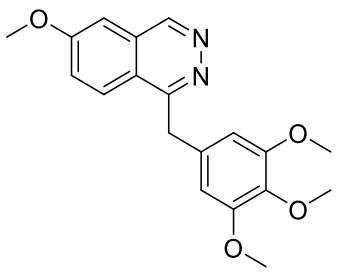

Formula: $C_{19}H_{20}N_2O_4$

Mol. Weight: 340.38 $g.mol^{-1}$

Aspect: white solid

R_f: 0.12 (EA)

Yield: 56%

^{1}H NMR (400 MHz, Chloroform-d) δ 9.37 (s, 1H), 7.98 (d, J = 9.0 Hz, 1H), 7.39 (d, J = 8.7 Hz, 1H), 7.16 (s, 1H), 6.50 (s, 2H), 4.58 (s, 2H), 3.93 (s, 3H), 3.74 (d, J = 3.6 Hz, 9H).

^{13}C NMR (75 MHz, Chloroform-d) δ 162.45, 153.46, 150.71, 136.83, 133.92, 126.89, 125.10, 121.39, 108.65, 105.85, 105.17, 60.89, 56.27, 56.01, 39.99.

HR-MS (ESI+): m/z calculated for $C_{19}H_{21}N_2O_4$ 341.1496 obtained 341.1497.

1-benzyl-6-ethoxyphthalazine **347**

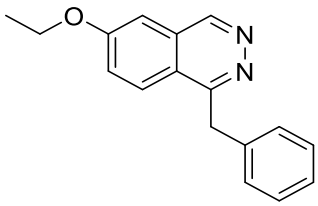

Formula: $C_{17}H_{16}N_2O$

Mol. Weight: 264.33 $g.mol^{-1}$

Aspect: white solid

R_f: 0.27 (Cyclohexane:EA, 3:7)

Yield: 22%

^{1}H NMR (300 MHz, Chloroform-d) δ 9.38 (s, 1H), 7.97 (d, J = 9.1 Hz, 1H), 7.38 (dd, J = 9.1, 2.5 Hz, 1H), 7.33 – 7.27 (m, 3H), 7.26 – 7.22 (m, 1H), 7.21 – 7.13 (m, 2H), 4.70 (s, 2H), 4.18 (q, J = 7.0 Hz, 2H).

^{13}C NMR (75 MHz, Chloroform-d) δ 161.49, 158.32, 150.60, 138.40, 129.37, 128.73, 128.65, 126.78, 126.68, 125.07, 121.18, 105.46, 64.32, 39.86, 14.58.

HR-MS (ESI+): m/z calculated for $C_{17}H_{16}N_2O$ 295.1000 obtained 295.1006.

Diethyl (1-benzylphthalazin-2(1H)-yl)phosphonate **374**

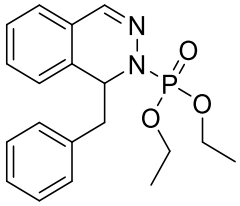

Formula: $C_{19}H_{23}N_2O_3P$

Mol. Weight: 358.38 $g.mol^{-1}$

Aspect: brown oil

R_f: 0.47 (Cyclohexane:EA, 5:5)

Yield: 40%

^{1}H NMR (400 MHz, Chloroform-d): δ 7.69 (s, 1H), 7.32 – 7.27 (m, 1H), 7.20 (dd, J = 7.6, 1.4 Hz, 1H), 7.18 – 7.11 (m, 4H), 6.94 – 6.80 (m, 2H), 6.39 (d, J = 7.6 Hz, 1H), 5.26 (ddd, J = 9.6, 5.1, 2.5 Hz, 1H), 4.31 – 4.17 (m, J = 7.2 Hz, 2H), 4.12 – 4.00 (m, 1H), 3.99 – 3.85 (m, 1H), 3.01 (dd, J = 12.8, 5.1 Hz, 1H), 2.92 (dd, J = 12.8, 9.6 Hz, 1H), 1.41 (td, J = 7.1, 1.0 Hz, 3H), 1.25 (td, J = 7.0, 1.0 Hz, 3H).

^{13}C NMR (101 MHz, Chloroform-d): δ 143.02 (d, J = 12.6 Hz), 136.47, 131.73 (d, J = 6.5 Hz), 130.61, 130.15, 128.17, 128.05, 126.90 (d, J = 1.4 Hz), 126.58, 125.13, 123.76, 64.03 (d, J = 6.3 Hz), 63.28 (d, J = 5.7 Hz), 55.87 (d, J = 8.7 Hz), 41.69, 16.41 (d, J = 7.1 Hz), 16.06 (d, J = 7.0 Hz).

^{31}P NMR (162 MHz, Chloroform-d): δ 1.67.

HR-MS (ESI+): m/z calculated for $C_{19}H_{23}N_2NaO_3P$ 381.1338 obtained 381.1345.

Diethyl methyl phosphate **375**

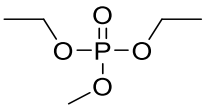

Formula: $C_{15}H_{13}O_4P$

Mol. Weight: 168.13 $g.mol^{-1}$

Aspect: brown oil

^{1}H NMR (300 MHz, Chloroform-d) δ 4.12 (p, J = 7.4 Hz, 4H), 3.76 (d, J = 11.2 Hz, 3H), 1.35 (t, J = 6.9 Hz, 6H).

Spectral data were consistent with data reported in the literature.[260]

[260] J. Dhineshkumar, K. R. Prabhu, *Org. Lett.* **2013**, *15*, 6062–6065.

1-(phenyl(phenylthio)methyl)phthalazine **378**

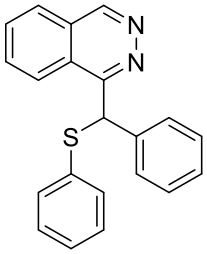

Formula: $C_{21}H_{16}N_2S$

Mol. Weight: 328.43 $g.mol^{-1}$

Aspect: brown oil

R_f: 0.63 (Cyclohexane:EA, 3:7)

Yield: 18%

^{1}H NMR (300 MHz, Chloroform-d): δ 9.49 (s, 1H), 8.08 (d, J = 7.9 Hz, 1H), 8.00 – 7.94 (m, 1H), 7.82 (pd, J = 7.0, 1.5 Hz, 2H), 7.46 – 7.40 (m, 2H), 7.34 (dd, J = 6.6, 2.9 Hz, 2H), 7.23 (q, J = 4.6, 4.1 Hz, 6H), 6.22 (s, 1H).

^{13}C NMR (75 MHz, Chloroform-d): δ 159.47, 150.92, 139.26, 134.82, 133.58, 133.51, 133.11, 132.74, 129.08, 129.04, 128.74, 128.44, 128.01, 127.86, 125.26, 124.78, 56.63.

HR-MS (ESI+): m/z calculated for $C_{21}H_{17}N_2S$ 329.1107 obtained 329.1096.

Chapter IV: Visible-Light catalyzed cascade of hydroamination and Smiles rearrangement using phosphonohydrazones as novel NCR precursor

Attempt to induce a radical 1,4-aryl migration

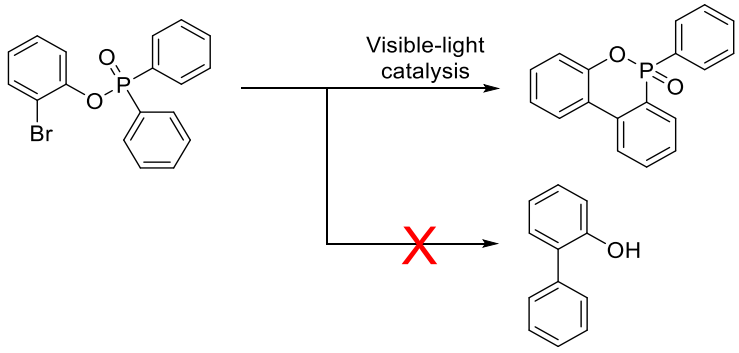

To an oven dried sealable glass vial were added 2-bromophenyl diphenylphosphinate (0.15 mmol, 1 eq.), triethylamine (2 eq.), $Ir(ppy)_3$ (0.003 mmol, 2 mol%) and DMSO (2 mL). The vials were sealed with 20mm crimp caps with silicone/PTFE septum and 12h under visible-light irradiation (Blue LED, 18 W). After completion of the reaction checked by TLC, the resulting suspension was filtered through a pad of celite eluting with ethyl acetate. The crude filtrate was concentrated and purification of the residue by silica gel column chromatography eluting with a cyclohexane/ethyl acetate mixture gave the desired product.

6-phenyldibenzo[c,e][1,2]oxaphosphinine 6-oxide **616**

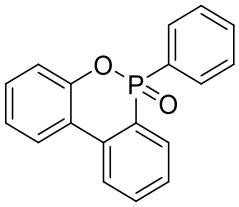

Formula: $C_{18}H_{13}O_2P$

Mol. Weight: 292.27 $g.mol^{-1}$

Aspect: white solid

R_f: 0.37 (Cyclohexane:EA, 5:5)

Yield: 25%

^{1}H NMR (400 MHz, Chloroform-d): δ 8.08 – 8.02 (m, 1H), 8.00 (dd, J = 7.9, 1.7 Hz, 1H), 7.87 – 7.79 (m, 2H), 7.69 (ddt, J = 8.4, 7.4, 1.3 Hz, 1H), 7.64 – 7.55 (m, 2H), 7.51 – 7.35 (m, 4H), 7.31 – 7.23 (m, 2H).

Spectral data were consistent with data reported in the literature.[261]

[261] G. Revol, T. McCallum, M. Morin, F. Gagosz, L. Barriault, *Angew. Chem. Int. Ed.* **2013**, *52*, 13342–13345.

Synthesis of dissymmetric phosphonohydrazine

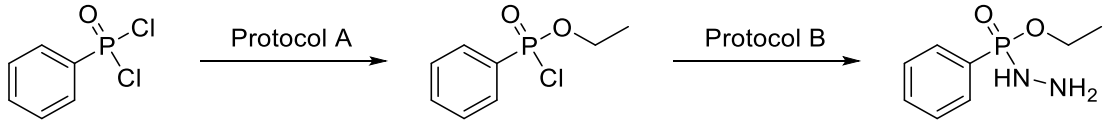

General procedure:

Protocol A: A solution of dry ethanol (1 eq.) and triethylamine (1.5 eq.) in anhydrous THF (0.85 M) was added dropwise to a stirred solution of phenylphosphonic dichloride (1 eq.) in anhydrous THF (0.85 M). The reaction mixture was kept in an ice bath. A white precipitate of triethylammonium chloride appeared instantaneously. When the reaction was over, the precipitate was filtered off. The filtrate, containing $C_6H_5P(O)(Cl)OCH_2CH_3$, was used without further treatment because attempts to distill the product resulted in polymerization.

Protocol B: Hydrazine monohydrate (3 eq.) was added dropwise into a solution of diarylphosphinic chloride (1 eq.) in THF (0.2 M) under an inert atmosphere, at 0°C. The mixture was stirred at 0°C for 30 min. After completion of the reaction, the solvent was evaporated and the residue was extracted with CH_2Cl_2 and the combined organic layer was washed with water, brine and dried over Na_2SO_4, affording the desired product.

Ethyl hydrazineyl(phenyl)phosphinate **622**

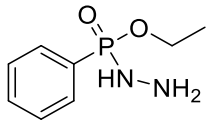

Formula: $C_8H_{13}N_2O_2P$

Mol. Weight: 200.18 $g.mol^{-1}$

Aspect: white solid

R_f: 0.2 (cyclohexane:EA, 3:7)

Yield: 25%

^{1}H NMR (400 MHz, Chloroform-d): δ = 10.54 (s, 1H), 7.88 (d, J = 7.8 Hz, 1H), 7.51-7.47 (m, 2H), 7.40-7.34 (m, 1H), 1.35 (s, 9H).

Spectral data were consistent with data reported in the literature.[262]

[262] J. Rahil, P. Haake, *J. Am. Chem. Soc.* **1981**, *103*, 1723–1734.

Synthesis of phosphonohydrazines

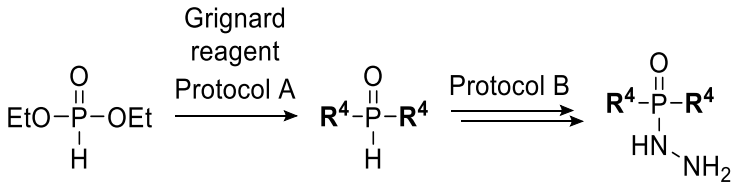

General procedure:

Protocol A: A round-bottom flask equipped with an addition funnel was evacuated/Ar filled (3X), then charged with the appropriate Grignard reagent in THF (3.3 eq.), and the solution cooled to 0°C under Ar. A solution of diethylphosphite (1 eq.) in THF (3 M) was then added dropwise over 15 minutes. The mixture was aged 15 minutes at 0°C, then the bath was removed, and the mixture stirred two hours at ambient temperature, then cooled again to 0°C. 0.1 M HCl was then added dropwise over 20 minutes (25 mL for 10 mmol of SM), then diethyl ether was added (25 mL for 10 mmol of SM), and the mixture agitated well for 5 minutes. The upper organic phase was decanted from the gel and saved. To the remaining gel was added CH_2Cl_2, and the mixture agitated well for 5 minutes. The resultant mixture was then filtered through a Celite pad, washing the pad with CH_2Cl_2. The filtrate phases were separated, and the organic phase combined with the first organic phase, dried over Na_2SO_4, and the solvents removed in vacuo. The residue was either azeotroped with hexane, causing a precipitate to form which was recrystallized from boiling hexane or purified over silica gel.

Protocol B: Hydrazine hydrate (1 eq.) was added dropwise at 20°C with efficient stirring to a mixture of CCl_4/CH_2Cl_2 (5:3, 0.625M), K_2CO_3 (1.5 eq.), and benzyltriethylammonium chloride (1 mol%).After 15 min, a solution of dialkylphosphite in CH_2Cl_2 was added slowly with external cooling if necessary. Stirring was continued for 4h at room temperature. The mixture was filtered, washed with CH_2Cl_2, and evaporated, affording the desired product without further purification.

P,P-di-p-tolylphosphinic hydrazide **629**

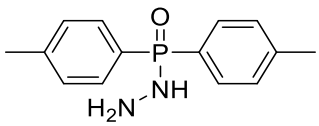

Formula: $C_{14}H_{17}N_2OP$

Mol. Weight: 260.28 $g.mol^{-1}$

Aspect: white solid

R_f: 0.09 (cyclohexane:EA, 3:7)

Yield: quant.

^{1}H NMR (400 MHz, Chloroform-d): δ 7.72 (dd, J = 11.6, 7.7 Hz, 4H), 7.21 (dd, J = 8.0, 3.0 Hz, 4H), 4.85 (s, 1H), 3.65 (s, 2H), 2.33 (s, 6H).

Spectral data were consistent with data reported in the literature.[263]

P,P-di-o-tolylphosphinic hydrazide **630**

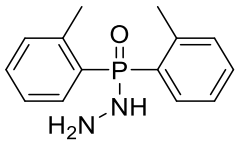

Formula: $C_{14}H_{17}N_2OP$

Mol. Weight: 260.28 $g.mol^{-1}$

Aspect: white solid

R_f: 0.18 (EA)

Yield: 64%

^{1}H NMR (400 MHz, Chloroform-d): δ 7.63 (dd, J = 13.3, 7.6 Hz, 2H), 7.29 (td, J = 7.4, 1.3 Hz, 2H), 7.11 (tt, J = 7.5, 3.7 Hz, 4H), 5.27 (d, J = 21.3 Hz, 1H), 4.05 (s, 2H), 2.34 (s, 6H).

^{13}C NMR (101 MHz, Chloroform-d): δ 142.37 (d, J = 9.9 Hz), 133.16 (d, J = 10.3 Hz), 131.90 (d, J = 2.6 Hz), 131.59 (d, J = 11.7 Hz), 129.03 (d, J = 122.4 Hz), 125.34 (d, J = 12.4 Hz), 21.38 (d, J = 3.9 Hz).

^{31}P NMR (162 MHz, Chloroform-d): δ 30.11.

P,P-bis(3,4,5-trimethoxyphenyl)phosphinic hydrazide **631**

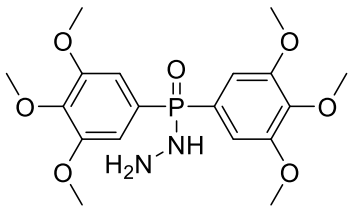

Formula: $C_{18}H_{25}N_2O_7P$

Mol. Weight: 412.38 $g.mol^{-1}$

Aspect: white solid

R_f: 0.03 (EA)

Yield: 86%

[263] M. El-Deek, E. El-Sawi, M. Mohamed, *J. Chem. Eng. Data* **1981**, *26*, 340–342.

^{1}H NMR (300 MHz, Chloroform-d): δ 7.17 – 6.97 (m, 4H), 3.84 (s, 18H).

We observed a rapid degradation of this compound so it was directly engaged in the following step.

P,P-bis(benzo[d][1,3]dioxol-5-yl)phosphinic hydrazide **632**

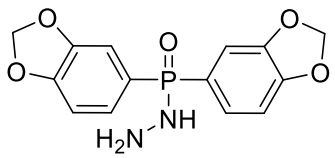

Formula: $C_{14}H_{13}N_2O_5P$

Mol. Weight: 320.24 g.mol^{-1}

Aspect: white solid

R_f: 0.03 (EA)

Yield: quant.

^{1}H NMR (300 MHz, Chloroform-d): δ 7.43 (dd, J = 13.1, 8.5 Hz, 2H), 7.25 (d, J = 4.5 Hz, 2H), 6.89 (dd, J = 7.9, 2.7 Hz, 2H), 6.01 (s, 4H), 4.56 (s, 1H), 2.08 (s, 2H).

We observed a rapid degradation of this compound so it was directly engaged in the following step.

P,P-bis(4-chlorophenyl)phosphinic hydrazide **633**

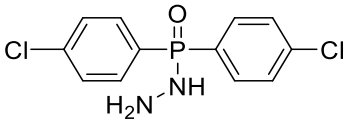

Formula: $C_{12}H_{11}Cl_2N_2OP$

Mol. Weight: 301.11 g.mol^{-1}

Aspect: white solid

R_f: 0.16 (cyclohexane:EA, 3:7)

Yield: quant.

^{1}H NMR (300 MHz, Chloroform-d): δ 7.77 (d, J = 8.5 Hz, 2H), 7.43 (d, J = 8.5 Hz, 2H), 3.36 (s, 3H).

Spectral data were consistent with data reported in the literature.[264]

[264] *Journal of general chemistry of the USSR* **1973**, *43*, 2186–2187.

P,P-bis(4-fluorophenyl)phosphinic hydrazide **634**

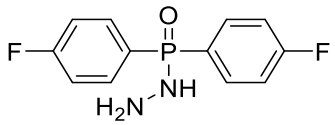

Formula: $C_{12}H_{11}F_2N_2OP$

Mol. Weight: 268.20 $g.mol^{-1}$

Aspect: white solid

R_f: 0.18 (cyclohexane:EA, 3:7)

Yield: 76%

^{1}H NMR (300 MHz, Chloroform-d): δ 7.89 (ddd, J = 11.3, 8.7, 5.7 Hz, 4H), 7.17 (td, J = 8.7, 2.5 Hz, 4H), 3.48 (s, 1H), 2.03 (s, 2H).

^{13}C NMR (75 MHz, Chloroform-d): δ 165.37 (dd, J = 254.0, 3.4 Hz), 134.74 (dd, J = 10.6, 8.9 Hz), 126.36 (dd, J = 133.0, 3.4 Hz), 116.20 (dd, J = 21.4, 13.6 Hz).

^{31}P NMR (121 MHz, Chloroform-d): δ 24.59.

^{19}F NMR (282 MHz, Chloroform-d): δ -105.89.

Sonogashira cross-coupling reaction

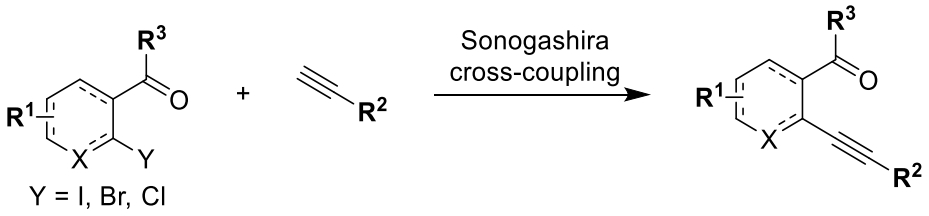

General procedure:

To an oven dried sealable glass vial were added CuI (1 mol%) and $PdCl_2(PPh_3)_2$ (2 mol%) to a solution of a halide derivative (1 eq.) in triethylamine (0.25 M). The solution was degassed with an inert gas for a few minutes before adding the alkyne (1.2 eq.). The vials were sealed with 20mm crimp caps with silicone/PTFE septum and stirred at room temperature (20-25°C) when using iodinated derivatives or at 50°C when using brominated derivatives. The reaction was monitored by TLC until completion and quenched by addition of distilled water and the pH was brought to neutrality by adding a saturated solution of ammonium chloride. The mixture was extracted with ethyl acetate, the combined organic phases were washed with brine, dried over Na_2SO_4, filtrated and concentrated under reduced pressure. The crude mixture was purified on a silica gel column chromatography, eluting with a cyclohexane/ethyl acetate mixture to afford the desired product.

2-(phenylethynyl)quinoline-3-carbaldehyde **635**

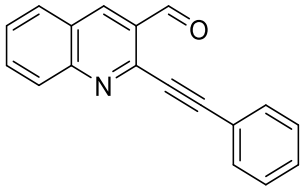

Formula: $C_{18}H_{11}NO$

Mol. Weight: 257.29 g.mol^{-1}

Aspect: brown solid

R_f: 0.53 (cyclohexane:EA, 7:3)

Yield: 55%

^{1}H NMR (400 MHz, Chloroform-d): δ 10.82 (s, 1H), 8.76 (s, 1H), 8.18 (d, J = 8.5 Hz, 1H), 7.98 (d, J = 8.1 Hz, 1H), 7.88 (t, J = 7.7 Hz, 1H), 7.71 (d, J = 5.3 Hz, 2H), 7.64 (t, J = 7.5 Hz, 1H), 7.48 – 7.39 (m, 3H).

Spectral data were consistent with data reported in the literature.[49]

2-(3,3-dimethylbut-1-yn-1-yl)benzaldehyde **636**

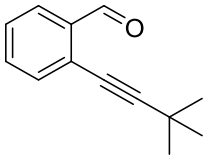

Formula: $C_{13}H_{14}O$

Mol. Weight: 186.25 g.mol^{-1}

Aspect: colorless oil

R_f: 0.53 (cyclohexane:EA, 95:5)

Yield: 93%

^{1}H NMR (400 MHz, Chloroform-d): δ = 10.54 (s, 1H), 7.88 (d, J = 7.8 Hz, 1H), 7.51-7.47 (m, 2H), 7.40-7.34 (m, 1H), 1.35 (s, 9H).

Spectral data were consistent with data reported in the literature.[265]

2-((6-methoxynaphthalen-2-yl)ethynyl)benzaldehyde **637**

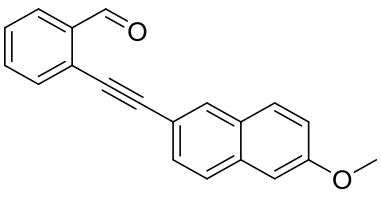

Formula: $C_{20}H_{14}O_2$

Mol. Weight: 286.33 g.mol^{-1}

Aspect: brown solid

R_f: 0.43 (cyclohexane:EA, 9:1)

Yield: Quant.

[265] A. S. K. Hashmi, M. Bührle, R. Salathé, J. W. Bats, *Advanced Synthesis & Catalysis* **2008**, *350*, 2059–2064.

^{1}H NMR (400 MHz, Chloroform-d): δ 10.68 (s, 1H), 7.96 (s, 1H), 7.93 (d, J = 7.1 Hz, 1H), 7.68 (d, J = 9.2 Hz, 2H), 7.62 (d, J = 7.7 Hz, 1H), 7.55–7.50 (m, 2H), 7.41–7.37 (m, 1H), 7.15 (dd, J = 8.9, 2.5 Hz, 1H), 7.07 (s, 1H), 3.88 (s, 3H).

Spectral data were consistent with data reported in the literature.[266]

2-(dibenzo[b,d]thiophen-2-ylethynyl)benzaldehyde

638

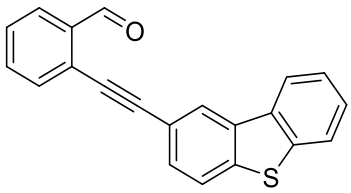

Formula: $C_{21}H_{12}OS$

Mol. Weight: 312.39 g.mol^{-1}

Aspect: yellow solid

R_f: 0.53 (cyclohexane:EA, 9:1)

Yield: 81%

We observed a rapid degradation of this compound so it was directly engaged in the following step.

5-fluoro-2-(3-methoxyprop-1-yn-1-yl)benzaldehyde

639

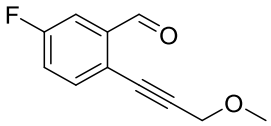

Formula: $C_{11}H_9FO_2$

Mol. Weight: 192.19 g.mol^{-1}

Aspect: white solid

R_f: 0.35 (cyclohexane:EA, 9:1)

Yield: 84%

^{1}H NMR (400 MHz, Chloroform-d): δ 10.47 (s, 1H), 7.60-7.55 (m, 2H), 7.26 (td, J = 8.5, 2.8 Hz, 1H), 4.37 (s, 2H), 3.46 (s, 3H).

Spectral data were consistent with data reported in the literature.[48]

---

[266] K. M. Saini, R. K. Saunthwal, Sushmita, A. K. Verma, *Chemistry – A European Journal* **2020**, *26*, 1017–1021.

Synthesis of phosphonohydrazones

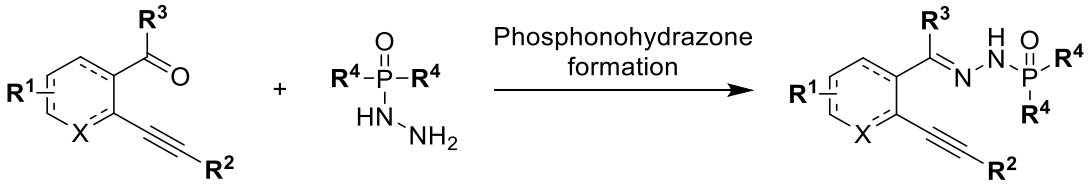

General procedure:

To an oven dried sealable glass vial were added an aldehyde or ketone derivative (1 eq.), phosphonohydrazine (1.1 eq) and MeOH (0.8 M). The vials were sealed with 20mm crimp caps with silicone/PTFE septum and stirred overnight at 20°C. After completion of the reaction checked by TLC, the reaction medium was filtered using a Büchner funnel if precipitation of the phosphonohydrazone occurred. The product was dried under vacuum, characterized and used without any further purification. If precipitation did not occur, the crude mixture was concentrated and purification of the residue by silica gel column chromatography eluting with a cyclohexane/ethyl acetate mixture gave the desired product.

N'-(5-fluoro-2-(phenylethynyl)benzylidene)-P,P-diphenylphosphinic hydrazide

640

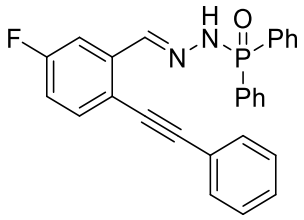

Formula: $C_{27}H_{20}FN_2OP$

Mol. Weight: 438.44 g.mol^{-1}

Aspect: white solid

R_f: 0.42 (Cyclohexane:EA, 3:7)

Yield: 87%

^{1}H NMR (400 MHz, Chloroform-d): δ 8.44 (s, 1H), 8.17 (s, 1H), 7.89 (dd, J = 12.4, 8.1 Hz, 4H), 7.54 (dd, J = 15.3, 7.2 Hz, 4H), 7.48 – 7.36 (m, 6H), 7.30 (d, J = 5.3 Hz, 3H), 6.94 (td, J = 8.4, 2.7 Hz, 1H).

^{13}C NMR (101 MHz, Chloroform-d): δ 162.42 (d, J = 249.2 Hz), 143.41 (d, J = 15.2 Hz), 137.88 (d, J = 8.6 Hz), 134.27 (d, J = 8.4 Hz), 132.62 (d, J = 2.9 Hz), 132.47 (d, J = 10.1 Hz), 131.87, 129.98 (d, J = 133.2 Hz), 128.71 (d, J = 13.2 Hz), 128.69, 128.54, 122.86, 118.70 (d, J = 3.1 Hz), 116.58 (d, J = 23.0 Hz), 111.63 (d, J = 23.7 Hz), 94.60 (d, J = 1.5 Hz), 85.60.

^{31}P NMR (162 MHz, Chloroform-d): δ 24.71.

HR-MS (ESI+): m/z calculated for $C_{27}H_{20}FN_2OP$ 439.1370 obtained 439.1369.

N'-(5-chloro-2-(phenylethynyl)benzylidene)-P,P-diphenylphosphinic hydrazide

641

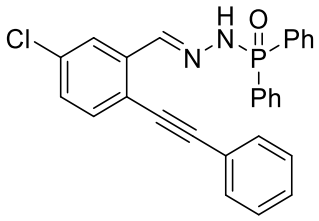

Formula: $C_{27}H_{20}ClN_2OP$

Mol. Weight: 454.89 g.mol^{-1}

Aspect: white solid

R_f: 0.61 (Cyclohexane:EA, 3:7)

Yield: 91%

^{1}H NMR (300 MHz, Chloroform-d): δ 8.43 (s, 1H), 8.05 (d, J = 18.6 Hz, 1H), 7.88 (dd, J = 12.3, 7.2 Hz, 4H), 7.69 (d, J = 1.7 Hz, 1H), 7.53 (t, J = 6.4 Hz, 4H), 7.44 (td, J = 7.4, 3.3 Hz, 4H), 7.38 (d, J = 8.4 Hz, 1H), 7.30 (d, J = 7.0 Hz, 3H), 7.18 (dd, J = 8.3, 2.0 Hz, 1H).

^{13}C NMR (75 MHz, Chloroform-d): δ 142.73 (d, J = 16.3 Hz), 136.93, 134.68, 133.52, 132.43 (d, J = 9.9 Hz), 132.40 (d, J = 2.8 Hz), 131.77, 131.01 (d, J = 129.4 Hz), 129.06, 128.85, 128.65 (d, J = 13.2 Hz), 128.56, 125.09, 122.72, 120.75, 95.58, 85.64.

^{31}P NMR (121 MHz, Chloroform-d): δ 24.34.

HR-MS (ESI+): m/z calculated for $C_{27}H_{21}ClN_2OP$ 455.1075 obtained 455.1071.

N'-(5-bromo-2-(phenylethynyl)benzylidene)-P,P-diphenylphosphinic hydrazide **642**

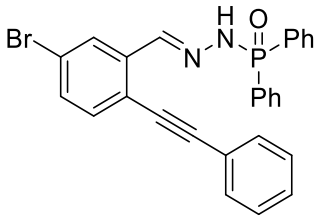

Formula: $C_{27}H_{20}BrN_2OP$

Mol. Weight: 499.35 g.mol^{-1}

Aspect: white solid

R_f: 0.45 (Cyclohexane:EA, 3:7)

Yield: 74%

^{1}H NMR (300 MHz, Chloroform-d): δ 8.39 (s, 1H), 7.93 – 7.80 (m, 6H), 7.57 – 7.51 (m, 4H), 7.48 – 7.42 (m, 4H), 7.37 – 7.28 (m, 5H).

^{13}C NMR (75 MHz, Chloroform-d): δ 142.64 (d, J = 16.1 Hz), 136.97, 133.65, 132.46 (d, J = 2.8 Hz), 132.45 (d, J = 9.9 Hz), 131.97, 131.75, 130.91 (d, J = 129.5 Hz), 128.91, 128.68 (d, J = 13.0 Hz), 128.58, 128.11, 122.96, 122.69, 121.19, 95.77, 85.69.

^{31}P NMR (121 MHz, Chloroform-d): δ 24.08.

HR-MS (ESI+): m/z calculated for $C_{27}H_{21}BrN_2OP$ 499.0569 obtained 499.0565.

P,P-diphenyl-N'-(3,4,5-trimethoxy-2-(phenylethynyl)benzylidene)phosphinic hydrazide **643**

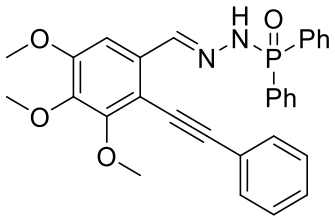

Formula: $C_{30}H_{27}N_2O_4P$

Mol. Weight: 510.53 g.mol^{-1}

Aspect: white solid

R_f: 0.34 (Cyclohexane:EA, 3:7)

Yield: 96%

^{1}H NMR (300 MHz, Chloroform-d): δ 8.56 (d, J = 19.1 Hz, 1H), 8.48 (s, 1H), 7.85 (dd, J = 12.2, 7.9 Hz, 4H), 7.60 – 7.52 (m, 2H), 7.46 (t, J = 7.3 Hz, 2H), 7.36 (dt, J = 10.0,

^{13}C NMR (101 MHz, Chloroform-d): δ 154.17, 153.70, 143.57 (d, J = 16.6 Hz), 142.88, 132.42 (d, J = 9.8 Hz), 132.03 (d, J = 1.5 Hz), 132.00, 131.49, 131.14 d, J = 129.7 Hz), 128.36 (d, J = 13.0 Hz), 128.35, 128.21, 123.42, 110.52, 103.27, 97.42, 82.71, 61.30, 61.12, 55.74.

^{31}P NMR (121 MHz, Chloroform-d): δ 24.13.

HR-MS (ESI+): m/z calculated for $C_{30}H_{27}N_2O_4P$ 511.1781 obtained 511.1771.

P,P-diphenyl-N'-((2-(phenylethynyl)quinolin-3-yl)methylene)phosphinic hydrazide **644**

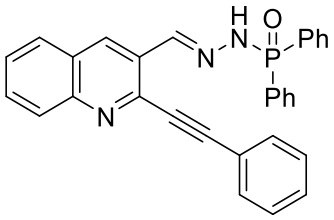

Formula: $C_{30}H_{22}N_3OP$

Mol. Weight: 471.50 g.mol^{-1}

Aspect: white solid

R_f: 0.48 (Cyclohexane:EA, 3:7)

Yield: 76%

^{1}H NMR (400 MHz, Chloroform-d): δ 8.73 (d, J = 20.6 Hz, 1H), 8.70 (s, 1H), 8.40 (s, 1H), 7.98 (d, J = 8.4 Hz, 1H), 7.95 – 7.86 (m, 4H), 7.69 (dd, J = 8.3, 1.3 Hz, 2H), 7.65 – 7.57 (m, 2H), 7.50 (ddd, J = 7.6, 6.4, 1.4 Hz, 2H), 7.42 (qd, J = 8.2, 7.3, 2.2 Hz, 5H), 7.36 – 7.31 (m, 1H), 7.29 – 7.24 (m, 2H).

^{13}C NMR (101 MHz, Chloroform-d): δ 147.59, 142.14 (d, J = 16.9 Hz), 141.57, 132.57, 132.48, 132.45 (d, J = 9.9 Hz), 132.34 (d, J = 2.7 Hz), 130.96 (d, J = 130.1 Hz), 130.71, 129.52, 128.81, 128.63 (d, J = 13.0 Hz), 128.50, 128.50, 128.30, 127.63, 127.05, 121.78, 94.90, 86.40.

^{31}P NMR (162 MHz, Chloroform-d): δ 24.14.

HR-MS (ESI+): m/z calculated for $C_{30}H_{23}N_3OP$ 472.1573 obtained 472.1572.

P,P-diphenyl-N'-((2-(phenylethynyl)benzofuran-3-yl)methylene)phosphinic hydrazide **645**

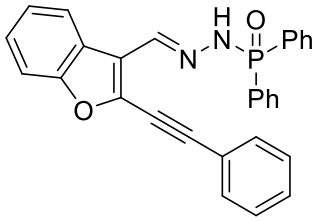

Formula: $C_{29}H_{21}N_2O_2P$

Mol. Weight: 460.47 g.mol^{-1}

Aspect: yellow solid

R_f: 0.31 (Cyclohexane:EA, 3:7)

Yield: 71%

^{1}H NMR (300 MHz, Chloroform-d): δ 8.88 (s, 1H), 8.35 (s, 1H), 7.92 (dd, J = 12.1, 7.5 Hz, 4H), 7.69 – 7.57 (m, 2H), 7.50 (t, J = 7.2 Hz, 2H), 7.45 – 7.29 (m, 8H), 7.24 (s, 2H), 7.06 – 6.88 (m, 1H).

^{13}C NMR (75 MHz, Chloroform-d): δ 154.49, 139.53 (d, J = 18.1 Hz), 138.85, 132.54 (d, J = 9.7 Hz), 132.24 (d, J = 2.6 Hz), 131.80, 130.52 (d, J = 133.8 Hz), 129.39, 128.65, 128.65, 128.47, 126.20, 124.39, 123.49 (d, J = 16.3 Hz), 121.82, 121.39, 110.59, 99.85, 78.43.

^{31}P NMR (121 MHz, Chloroform-d): δ 24.98.

HR-MS (ESI+): m/z calculated for $C_{29}H_{21}N_2O_2P$ 461.1413 obtained 461.1409.

N'-((1-methyl-2-(phenylethynyl)-1H-indol-3-yl)methylene)-P,P-diphenylphosphinic hydrazide **646**

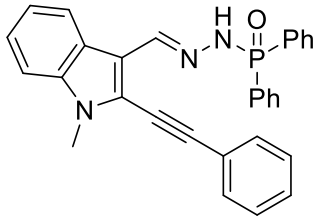

Formula: $C_{30}H_{24}N_3OP$

Mol. Weight: 473.52 g.mol^{-1}

Aspect: white solid

R_f: 0.38 (Cyclohexane:EA, 3:7)

Yield: 92%

^{1}H NMR (300 MHz, Chloroform-d): δ 8.39 (d, J = 1.6 Hz, 1H), 8.16 (d, J = 14.1 Hz, 1H), 8.01 – 7.89 (m, 4H), 7.60 (dd, J = 6.5, 3.0 Hz, 3H), 7.53 – 7.45 (m, 2H), 7.42 – 7.32 (m, 7H), 7.19 (t, J = 7.1 Hz, 1H), 7.07 (d, J = 8.2 Hz, 1H), 6.89 (t, J = 7.1 Hz, 1H), 3.55 (s, 3H).

^{13}C NMR (75 MHz, Chloroform-d): δ 142.07 (d, J = 17.2 Hz), 137.44, 132.58 (d, J = 9.6 Hz), 131.87 (d, J = 2.6 Hz), 131.63, 131.46 (d, J = 130.9 Hz), 128.92, 128.61, 128.39 (d, J = 12.8 Hz), 124.05, 123.85, 123.68, 123.29, 122.53, 121.01, 116.43, 108.64, 99.80, 79.16, 30.60.

^{31}P NMR (121 MHz, Chloroform-d): δ 24.37.

HR-MS (ESI+): m/z calculated for $C_{30}H_{24}N_3OP$ 474.1730 obtained 474.1727.

P,P-diphenyl-N'-(2-(p-tolylethynyl)benzylidene)phosphinic hydrazide **647**

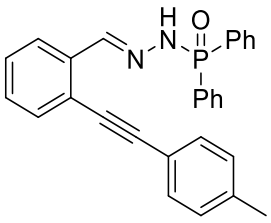

Formula: $C_{28}H_{23}N_2OP$

Mol. Weight: 434.48 g.mol^{-1}

Aspect: white solid

R_f: 0.45 (Cyclohexane:EA, 3:7)

Yield: 93%

^{1}H NMR (400 MHz, Chloroform-d): δ 8.51 (s, 1H), 7.94 (dd, J = 12.4, 7.3 Hz, 4H), 7.76 (d, J = 7.7 Hz, 1H), 7.56 – 7.40 (m, 9H), 7.30 – 7.18 (m, 2H), 7.13 (d, J = 7.8 Hz, 2H), 2.37 (s, 3H).

^{13}C NMR (101 MHz, Chloroform-d): δ 144.19 (d, J = 16.5 Hz), 138.81, 135.31, 132.49 (d, J = 10.0 Hz), 132.35, 132.32 (d, J = 1.5 Hz), 131.69, 130.90 (d, J = 128.8 Hz), 129.28, 128.93, 128.58 (d, J = 13.1 Hz), 128.29, 125.28, 122.70, 119.92, 95.10, 85.97, 21.65.

^{31}P NMR (162 MHz, Chloroform-d): δ 24.31.

HR-MS (ESI+): m/z calculated for $C_{28}H_{24}N_2OP$ 435.1621 obtained 435.1622.

N'-(2-((4-fluorophenyl)ethynyl)benzylidene)-P,P-diphenylphosphinic hydrazide

648

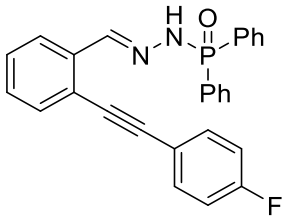

Formula: $C_{27}H_{20}FN_2OP$

Mol. Weight: 438.44 g.mol^{-1}

Aspect: white solid

R_f: 0.5 (Cyclohexane:EA, 3:7)

Yield: quant.

^{1}H NMR (400 MHz, Chloroform-d): δ 8.49 (s, 1H), 7.94 – 7.87 (m, 5H), 7.75 (d, J = 7.3 Hz, 1H), 7.58 – 7.50 (m, 4H), 7.47 – 7.42 (m, 5H), 7.26 – 7.19 (m, 2H), 6.99 (td, J = 8.7, 1.9 Hz, 2H).

^{13}C NMR (101 MHz, Chloroform-d): δ 162.79 (d, J = 250.1 Hz), 144.09 (d, J = 16.9 Hz), 135.45, 133.78 (d, J = 8.4 Hz), 132.48, 132.47 (d, J = 10.0 Hz), 132.37, 130.85 (d, J = 133.5 Hz), 129.01, 128.70, 128.57, 125.33, 122.35, 119.11 (d, J = 3.5 Hz), 115.81 (d, J = 22.1 Hz), 93.84, 86.28.

^{31}P NMR (162 MHz, Chloroform-d): δ 24.79.

^{19}F NMR (376 MHz, Chloroform-d): δ -110.41 – -110.54 (m).

HR-MS (ESI+): m/z calculated for $C_{27}H_{20}FN_2OP$ 439.1370 obtained 439.1368.

N'-(2-((4-cyanophenyl)ethynyl)benzylidene)-P,P-diphenylphosphinic hydrazide

649

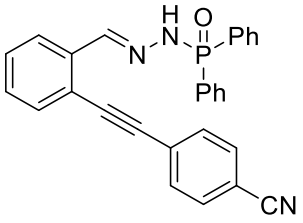

Formula: $C_{28}H_{20}N_3OP$

Mol. Weight: 445.46 g.mol^{-1}

Aspect: beige solid

R_f: 0.29 (Cyclohexane:EA, 3:7)

Yield: 76%

^{1}H NMR (400 MHz, Chloroform-d): δ 8.68 (d, J = 18.4 Hz, 1H), 8.58 (s, 1H), 7.90 – 7.81 (m, 4H), 7.77 – 7.71 (m, 1H), 7.63 (d, J = 8.3 Hz, 2H), 7.56 – 7.49 (m, 2H), 7.43 (m, 7H), 7.28 – 7.21 (m, 2H).

^{13}C NMR (101 MHz, Chloroform-d): δ 143.46 (d, J = 16.7 Hz), 136.05, 132.43, 132.41, 132.36 (d, J = 2.7 Hz), 132.28, 132.15 (d, J = 12.1 Hz), 131.20 (d, J = 128.6 Hz), 129.33, 128.91, 128.49, 127.91, 125.23, 121.21, 118.63, 111.55, 93.06, 91.01.

^{31}P NMR (162 MHz, Chloroform-d): δ 25.59.

HR-MS (ESI+): m/z calculated for $C_{28}H_{21}N_3OP$ 446.1417 obtained 446.1416.

P,P-diphenyl-N'-(2-((trimethylsilyl)ethynyl)benzylidene)phosphinic hydrazide **650**

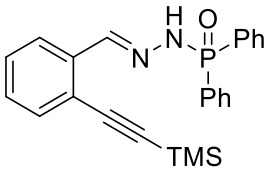

Formula: $C_{24}H_{25}N_2OPSi$

Mol. Weight: 416.54 $g.mol^{-1}$

Aspect: beige solid

R_f: 0.36 (Cyclohexane:EA, 3:7)

Yield: 44%

^{1}H NMR (400 MHz, Chloroform-d): δ 8.36 (s, 1H), 7.91 (dd, J = 12.3, 7.0 Hz, 4H), 7.78 (d, J = 18.3 Hz, 1H), 7.73 – 7.67 (m, 1H), 7.46 (ddt, J = 15.7, 12.3, 7.4 Hz, 7H), 7.24 – 7.14 (m, 2H), 0.24 (s, 9H).

^{13}C NMR (101 MHz, Chloroform-d): δ 143.49 (d, J = 16.5 Hz), 135.61, 132.79, 132.43 (d, J = 9.9 Hz), 132.24 (d, J = 2.8 Hz), 131.28 (d, J = 129.2 Hz), 128.75, 128.66, 128.50 (d, J = 13.0 Hz), 125.10, 122.15, 102.07, 100.11, 0.07.

^{31}P NMR (162 MHz, Chloroform-d): δ 24.42.

HR-MS (ESI+): m/z calculated for $C_{24}H_{26}N_2OPSi$ 417.1547 obtained 417.1547

N'-(2-(3,3-dimethylbut-1-yn-1-yl)benzylidene)-P,P-diphenylphosphinic hydrazide **651**

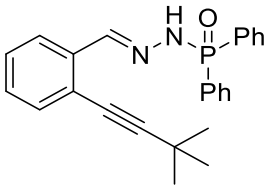

Formula: $C_{25}H_{25}N_2OP$

Mol. Weight: 400.46 $g.mol^{-1}$

Aspect: white solid

R_f: 0.5 (Cyclohexane:EA, 3:7)

Yield: 70%

^{1}H NMR (400 MHz, Chloroform-d): δ 8.35 (d, J = 16.4 Hz, 1H), 7.96 – 7.86 (m, 4H), 7.73 – 7.66 (m, 1H), 7.58 – 7.40 (m, 7H), 7.35 – 7.30 (m, 1H), 7.16 (m, 2H), 1.31 (s, 9H).

^{13}C NMR (101 MHz, Chloroform-d): δ 144.01 (d, J = 16.4 Hz), 135.05, 132.44 (d, J = 10.0 Hz), 132.37, 132.21 (d, J = 2.9 Hz), 129.71 (d, J = 123.7 Hz), 128.76, 128.50 (d, J = 13.0 Hz), 127.66, 125.04, 123.22, 104.24, 76.27, 31.08, 28.31.

^{31}P NMR (162 MHz, Chloroform-d): δ 24.51.

HR-MS (ESI+): m/z calculated for $C_{25}H_{26}N_2OP$ 401.1777 obtained 401.1771.

N'-(2-((3-nitrophenyl)ethynyl)benzylidene)-P,P-diphenylphosphinic hydrazide

652

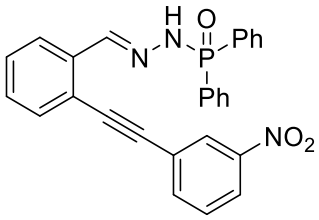

Formula: $C_{27}H_{20}N_3O_3P$

Mol. Weight: 465.45 g.mol^{-1}

Aspect: beige solid

R_f: 0.77 (Cyclohexane:EA, 3:7)

Yield: 85%

^{1}H NMR (400 MHz, Chloroform-d): δ 8.53 (s, 1H), 8.33 (s, 1H), 8.22 (d, J = 18.8 Hz, 1H), 8.12 (d, J = 8.3 Hz, 1H), 7.88 (dd, J = 12.4, 6.9 Hz, 5H), 7.80 – 7.72 (m, 1H), 7.56 – 7.36 (m, 8H), 7.30 – 7.21 (m, 2H).

^{13}C NMR (101 MHz, Chloroform-d): δ 148.14, 143.47 (d, J = 16.3 Hz), 137.65, 135.85, 132.58, 132.40 (d, J = 9.9 Hz), 132.30, 131.11 (d, J = 129.4 Hz), 129.52, 129.27, 128.99, 128.58 (d, J = 13.0 Hz), 126.28, 125.41, 124.83, 123.16, 121.15, 92.07, 89.18.

^{31}P NMR (162 MHz, Chloroform-d): δ 24.41.

HR-MS (ESI+): m/z calculated for $C_{27}H_{21}FN_3O_3P$ 466.1315 obtained 466.1310.

N'-(2-((6-methoxynaphthalen-2-yl)ethynyl)benzylidene)-P,P-diphenylphosphinic hydrazide

653

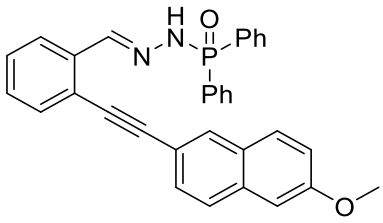

Formula: $C_{32}H_{25}N_2O_2P$

Mol. Weight: 500.54 g.mol^{-1}

Aspect: yellow solid

R_f: 0.41 (Cyclohexane:EA, 3:7)

Yield: 53%

^{1}H NMR (400 MHz, Chloroform-d): δ 8.49 (s, 1H), 8.00 – 7.87 (m, 5H), 7.79 (d, J = 7.4 Hz, 1H), 7.68 (dd, J = 8.7, 2.7 Hz, 2H), 7.56 – 7.43 (m, 8H), 7.31 – 7.18 (m, 3H), 7.17 – 7.08 (m, 2H), 3.93 (s, 3H).

^{13}C NMR (101 MHz, Chloroform-d): δ 158.58, 144.05 (d, J = 15.8 Hz), 135.14, 134.42, 132.52 (d, J = 9.9 Hz), 132.43 (d, J = 1.2 Hz), 132.38, 131.44, 131.09 (d, J = 129.8 Hz), 129.53, 129.13, 128.98, 128.98, 128.65 (d, J = 13.1 Hz), 128.47, 127.07, 125.46, 122.64, 119.68, 117.78, 105.93, 95.44, 86.21, 55.51.

^{31}P NMR (162 MHz, Chloroform-d): δ 23.48.

HR-MS (ESI+): m/z calculated for $C_{32}H_{26}N_2O_2P$ 501.1726 obtained 501.1729.

N'-(2-(dibenzo[b,d]thiophen-2-ylethynyl)benzylidene)-P,P-diphenylphosphinic hydrazide **654**

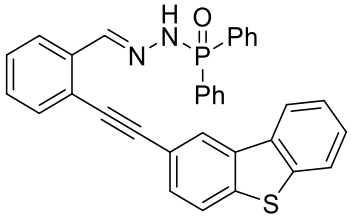

Formula: $C_{33}H_{23}N_2OPS$

Mol. Weight: 526.59 g.mol^{-1}

Aspect: white solid

R_f: 0.7 (Cyclohexane:EA, 3:7)

Yield: 96%

^{1}H NMR (400 MHz, Chloroform-d): δ 8.58 (s, 1H), 8.34 (s, 1H), 8.15 (d, J = 7.3 Hz, 1H), 7.96 – 7.86 (m, 5H), 7.83 (d, J = 7.6 Hz, 1H), 7.78 – 7.71 (m, 2H), 7.62 (d, J = 8.2 Hz, 1H), 7.53 – 7.36 (m, 9H), 7.29 – 7.15 (m, 2H).

^{13}C NMR (101 MHz, Chloroform-d): δ 143.99 (d, J = 16.0 Hz), 139.84, 139.73, 135.78, 135.42, 134.98, 132.47 (d, J = 9.9 Hz), 132.39, 132.27 (d, J = 2.8 Hz), 131.16 (d, J = 129.6 Hz), 129.86, 128.97, 128.55 (d, J = 13.0 Hz), 128.50, 127.26, 125.35, 124.90, 124.79, 122.88, 122,88, 122.40, 122.05, 119.01, 95.01, 86.60.

^{31}P NMR (162 MHz, Chloroform-d): δ 23.95.

HR-MS (ESI+): m/z calculated for $C_{33}H_{24}N_2OPS$ 527.1341 obtained 527.1337.

N'-(2-(pent-1-yn-1-yl)benzylidene)-P,P-diphenylphosphinic hydrazide **655**

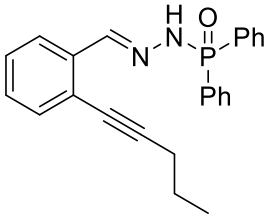

Formula: $C_{24}H_{23}N_2OP$

Mol. Weight: 386.43 g.mol^{-1}

Aspect: white solid

R_f: 0.45 (Cyclohexane:EA, 3:7)

Yield: 52%

^{1}H NMR (400 MHz, Chloroform-d): δ 8.33 (s, 1H), 7.93 (dd, J = 12.0, 7.7 Hz, 4H), 7.71 (d, J = 7.6 Hz, 1H), 7.54 (t, J = 6.6 Hz, 2H), 7.51 – 7.44 (m, 4H), 7.35 (d, J = 7.4 Hz, 1H), 7.18 (dd, J = 17.5, 8.2 Hz, 3H), 2.39 (t, J = 7.0 Hz, 2H), 1.63 (h, J = 7.1 Hz, 2H), 1.03 (t, J = 7.3 Hz, 3H).

^{13}C NMR (101 MHz, Chloroform-d): δ 144.32 (d, J = 16.0 Hz), 135.04, 132.49 (d, J = 9.9 Hz), 132.49, 132.33 (d, J = 3.0 Hz), 131.28 (d, J = 129.6 Hz), 128.97, 128.60 (d, J = 13.0 Hz), 127.78, 125.28, 123.37, 96.07, 77.98, 22.33, 21.69, 13.80.

^{31}P NMR (162 MHz, Chloroform-d): δ 23.41.

HR-MS (ESI+): m/z calculated for $C_{24}H_{24}N_2OP$ 387.1621 obtained 387.1621.

N'-(5-fluoro-2-(3-methoxyprop-1-yn-1-yl)benzylidene)-P,P-diphenylphosphinic hydrazide **656**

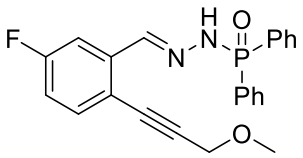

Formula: $C_{23}H_{20}FN_2O_2P$

Mol. Weight: 406.40 g.mol^{-1}

Aspect: beige solid

R_f: 0.32 (Cyclohexane:EA, 3:7)

Yield: 91%

^{1}H NMR (400 MHz, Chloroform-d): δ 8.58 (d, J = 19.4 Hz, 1H), 8.38 (s, 1H), 7.93 – 7.79 (m, 4H), 7.55 – 7.47 (m, 2H), 7.42 (td, J = 7.8, 3.2 Hz, 4H), 7.35 – 7.27 (m, 2H), 6.84 (td, J = 8.3, 2.7 Hz, 1H), 4.24 (s, 2H), 3.35 (s, 3H).

^{13}C NMR (101 MHz, Chloroform-d): δ 162.45 (d, J = 249.3 Hz), 142.94 (dd, J = 16.8, 2.6 Hz), 138.33 (d, J = 8.6 Hz), 134.43 (d, J = 8.5 Hz), 132.39 (d, J = 9.9 Hz), 132.29 (d, J = 2.8 Hz), 130.95 (d, J = 130.2 Hz), 128.56 (d, J = 13.0 Hz), 117.63 (d, J = 3.1 Hz), 116.24 (d, J = 23.0 Hz), 111.49 (d, J = 23.8 Hz), 89.94 (d, J = 1.6 Hz), 82.75, 60.43, 57.88.

^{31}P NMR (162 MHz, Chloroform-d): δ 23.90.

^{19}F NMR (376 MHz, Chloroform-d): δ -110.05.

HR-MS (ESI+): m/z calculated for $C_{23}H_{21}FN_2O_2P$ 407.1319 obtained 407.1318.

N'-(2-(phenylethynyl)benzylidene)-P,P-di-p-tolylphosphinic hydrazide **657**

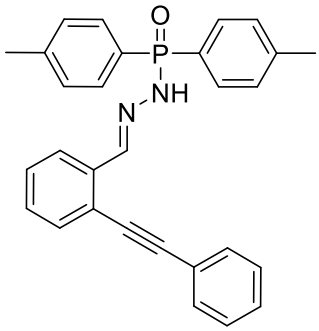

Formula: $C_{29}H_{25}N_2OP$

Mol. Weight: 448.51 g.mol^{-1}

Aspect: white solid

R_f: 0.43 (Cyclohexane:EA, 3:7)

Yield: 58%

^{1}H NMR (400 MHz, Chloroform-d): δ 8.48 (s, 1H), 7.78 (m, 6H), 7.55 (dd, J = 7.2, 2.0 Hz, 2H), 7.46 (d, J = 7.2 Hz, 1H), 7.29 (d, J = 6.1 Hz, 3H), 7.27 – 7.17 (m, 6H), 2.37 (s, 6H).

^{13}C NMR (101 MHz, Chloroform-d): δ 143.54 (d, J = 16.3 Hz), 142.61 (d, J = 2.8 Hz), 135.57, 132.43 (d, J = 10.3 Hz), 132.31, 131.71, 129.25 (d, J = 13.4 Hz), 128.77, 128.57, 128.46, 128.46, 128.24 (d, J = 131.8 Hz), 125.31, 123.02, 122.27, 94.70, 86.67, 21.73.

^{31}P NMR (162 MHz, Chloroform-d): δ 24.53.

HR-MS (ESI+): m/z calculated for $C_{29}H_{25}N_2OP$ 449.1777 obtained 449.1772.

N'-(2-(phenylethynyl)benzylidene)-P,P-di-o-tolylphosphinic hydrazide **658**

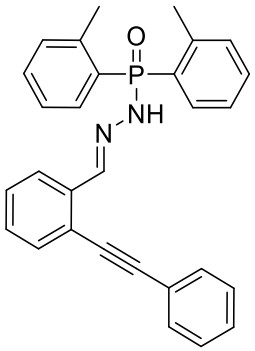

Formula: $C_{29}H_{25}N_2OP$

Mol. Weight: 448.51 $g.mol^{-1}$

Aspect: white solid

R_f: 0.63 (Cyclohexane:EA, 3:7)

Yield: 83%

^{1}H NMR (400 MHz, Chloroform-d): δ 8.58 (s, 1H), 8.45 (d, J = 20.4 Hz, 1H), 7.78 – 7.65 (m, 3H), 7.60 – 7.54 (m, 2H), 7.48 (dd, J = 7.6, 1.5 Hz, 1H), 7.40 (tt, J = 7.5, 1.5 Hz, 2H), 7.23 (dddd, J = 18.9, 11.5, 9.7, 4.3 Hz, 9H), 2.50 (d, J = 1.3 Hz, 6H).

^{13}C NMR (101 MHz, Chloroform-d): δ 142.65 (d, J = 9.9 Hz), 142.63 (d, J = 16.6 Hz), 135.86, 133.51 (d, J = 11.3 Hz), 132.35, 132.19 (d, J = 2.7 Hz), 131.75, 131.64 (d, J = 12.0 Hz), 130.15 (d, J = 124.4 Hz), 128.64, 128.53, 128.45, 128.41, 125.55 (d, J = 13.2 Hz), 125.06, 123.01, 122.25, 94.78, 86.68, 21.75 (d, J = 4.1 Hz).

^{31}P NMR (162 MHz, Chloroform-d): δ 29.60.

HR-MS (ESI+): m/z calculated for $C_{29}H_{25}N_2OP$ 449.1777 obtained 449.1774.

N'-(2-(phenylethynyl)benzylidene)-P,P-bis(3,4,5-trimethoxyphenyl)phosphinic hydrazide **659**

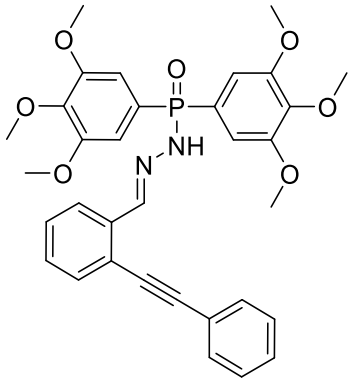

Formula: $C_{33}H_{33}N_2O_7P$

Mol. Weight: 600.61 $g.mol^{-1}$

Aspect: yellow solid

R_f: 0.13 (Cyclohexane:EA, 3:7)

Yield: 73%

^{1}H NMR (400 MHz, Chloroform-d): δ 8.65 (s, 1H), 8.49 (d, J = 16.5 Hz, 1H), 7.83 (d, J = 6.3 Hz, 1H), 7.61 – 7.43 (m, 3H), 7.30 – 7.04 (m, 9H), 3.86 (s, 6H), 3.75 (s, 12H).

^{13}C NMR (101 MHz, Chloroform-d): δ 153.21 (d, J = 18.8 Hz), 144.05 (d, J = 16.3 Hz), 141.32, 135.38, 132.42, 131.64, 129.02, 128.52 (d, J = 12.3 Hz), 128.41, 125.66 (d, J = 131.5 Hz), 124.79, 122.79, 122.34, 109.33, 109.19, 94.89, 86.47, 60.89, 56.27.

^{31}P NMR (162 MHz, Chloroform-d): δ 25.69.

HR-MS (ESI+): m/z calculated for $C_{33}H_{34}N_2O_7P$ 601.2098 obtained 601.2083.

P,P-bis(benzo[d][1,3]dioxol-5-yl)-N'-(2-(phenylethynyl)benzylidene)phosphinic hydrazide **660**

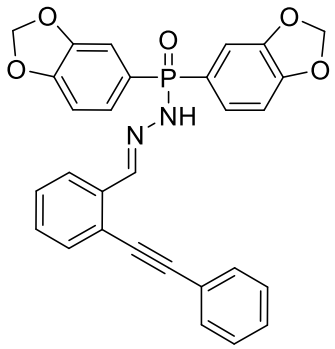

Formula: $C_{29}H_{21}N_2O_5P$

Mol. Weight: 508.47 g.mol^{-1}

Aspect: white solid

R_f: 0.57 (Cyclohexane:EA, 3:7)

Yield: 67%

^{1}H NMR (400 MHz, Chloroform-d): δ 8.42 (s, 1H), 7.90 – 7.72 (m, 1H), 7.61 – 7.53 (m, 2H), 7.49 (d, J = 8.5 Hz, 2H), 7.45 (d, J = 8.1 Hz, 1H), 7.39 – 7.23 (m, 8H), 6.88 (dd, J = 7.9, 2.3 Hz, 2H), 6.00 (d, J = 3.4 Hz, 4H).

^{13}C NMR (101 MHz, Chloroform-d): δ 150.92 (d, J = 3.0 Hz), 147.75 (d, J = 19.7 Hz), 143.89 (d, J = 16.8 Hz), 135.55, 132.24, 131.69, 128.70, 128.48, 128.38, 128,38, 127.88 (d, J = 10.9 Hz), 125.11, 124.51 (d, J = 135.3 Hz), 122.96, 122.23, 111.68 (d, J = 12.6 Hz), 108.58 (d, J = 16.3 Hz), 101.58, 94.68, 86.67.

^{31}P NMR (162 MHz, Chloroform-d): δ 24.53.

HR-MS (ESI+): m/z calculated for $C_{29}H_{22}N_2O_5P$ 509.1261 obtained 509.1264.

P,P-bis(4-chlorophenyl)-N'-(2-(phenylethynyl)benzylidene)phosphinic hydrazide **661**

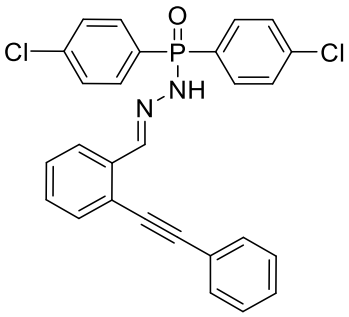

Formula: $C_{27}H_{19}Cl_2N_2OP$

Mol. Weight: 489.34 g.mol^{-1}

Aspect: white solid

R_f: 0.15 (Cyclohexane:EA, 3:7)

Yield: 80%

^{1}H NMR (400 MHz, Chloroform-d): δ 8.59 (d, J = 17.9 Hz, 1H), 8.58 (s, 1H), 7.75 (dd, J = 11.9, 8.4 Hz, 4H), 7.67 (d, J = 7.5 Hz, 1H), 7.58 – 7.51 (m, 2H), 7.49 – 7.43 (m, 1H), 7.36 (dd, J = 8.4, 2.5 Hz, 4H), 7.32 – 7.16 (m, 5H).

^{13}C NMR (101 MHz, Chloroform-d): δ 144.78 (d, J = 17.1 Hz), 139.02 (d, J = 3.5 Hz), 135.24, 133.73 (d, J = 10.8 Hz), 132.43, 131.74, 129.59 (d, J = 131.9 Hz), 129.09, 128.95 (d, J = 13.7 Hz), 128.67, 128.55, 128.48, 125.07, 122.98, 122.51, 94.86, 86.61.

^{31}P NMR (162 MHz, Chloroform-d): δ 23.41.

HR-MS (ESI+): m/z calculated for $C_{27}H_{20}Cl_2N_2OP$ 489.0685 obtained 489.0686.

P,P-bis(4-fluorophenyl)-N'-(2-(phenylethynyl)benzylidene)phosphinic hydrazide **662**

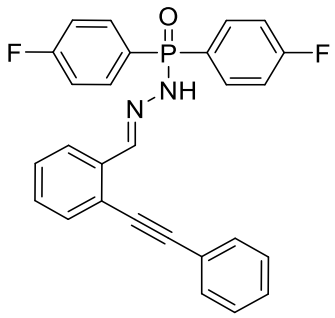

Formula: $C_{27}H_{19}F_2N_2OP$

Mol. Weight: 456.43 g.mol^{-1}

Aspect: beige solid

R_f: 0.53 (Cyclohexane:EA, 3:7)

Yield: 67%

^{1}H NMR (400 MHz, Chloroform-d): δ 8.44 (s, 1H), 7.86 (dddd, J = 11.3, 8.4, 5.1, 2.3 Hz, 4H), 7.70 (dd, J = 7.7, 1.7 Hz, 1H), 7.61 (d, J = 18.3 Hz, 1H), 7.54 – 7.49 (m, 2H), 7.46 (dd, J = 7.6, 1.6 Hz, 1H), 7.34 – 7.26 (m, 3H), 7.26 – 7.20 (m, 2H), 7.11 (td, J = 8.8, 2.5 Hz, 4H).

^{13}C NMR (101 MHz, Chloroform-d): δ 165.49 (dd, J = 254.0, 3.4 Hz), 144.46 (d, J = 16.4 Hz), 135.06, 135.01 (dd, J = 11.3, 8.9 Hz), 132.52, 131.72, 129.26, 128.79, 128.64, 128.57, 127.04 (dd, J = 134.0, 3.4 Hz), 125.27, 122.94, 122.55, 116.07 (dd, J = 21.5, 14.2 Hz), 94.88, 86.49.

^{31}P NMR (162 MHz, Chloroform-d): δ 22.39.

^{19}F NMR (376 MHz, Chloroform-d): δ -105.97.

HR-MS (ESI+): m/z calculated for $C_{27}H_{20}F_2N_2OP$ 457.1276 obtained 457.1271.

ethyl (E)-phenyl(2-(2-(phenylethynyl)benzylidene)hydrazineyl)phosphinate **663**

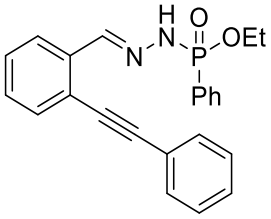

Formula: $C_{23}H_{21}N_2O_2P$

Mol. Weight: 388.41 $g.mol^{-1}$

Aspect: beige solid

R_f: 0.51 (Cyclohexane:EA, 3:7)

Yield: 44%

^{1}H NMR (400 MHz, Chloroform-d): δ 8.48 (s, 1H), 8.28 (d, J = 23.7 Hz, 1H), 8.03 – 7.90 (m, 3H), 7.63 – 7.55 (m, 2H), 7.51 (dd, J = 6.8, 1.8 Hz, 2H), 7.47 – 7.39 (m, 2H), 7.36 – 7.27 (m, 5H), 4.34 – 4.19 (m, 2H), 1.39 (t, J = 7.1 Hz, 3H).

^{13}C NMR (101 MHz, Chloroform-d): δ 143.06 (d, J = 17.5 Hz), 135.63, 132.40, 132.23 (d, J = 3.0 Hz), 131.80 (d, J = 9.7 Hz), 131.75, 131.04, 128.94, 128.69, 128.56, 128.51, 128.39 (d, J = 14.9 Hz), 124.92, 122.95, 122.53, 95.08, 86.50, 61.46 (d, J = 6.6 Hz), 16.48 (d, J = 6.6 Hz).

^{31}P NMR (162 MHz, Chloroform-d): δ 17.89.

HR-MS (ESI+): m/z calculated for $C_{23}H_{22}N_2O_2P$ 389.1413 obtained 389.1413.

Visible-light catalyzed synthesis of phthalazines

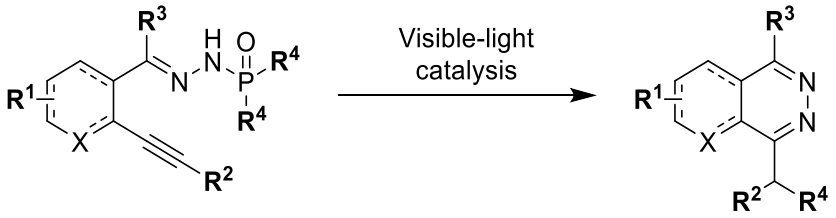

General procedure:

To an oven dried sealable glass vial were added phosphonohydrazone (0.15 mmol, 1 eq.), sodium hydroxide (0.225 mmol, 1.5 eq.), tris(2,2'-bipyridyl)dichlororuthenium(II) hexahydrate (0.00375 mmol, 2.5 mol%) and a mixture of EtOH (6 mL) and MeCN (2 mL). The vials were sealed with 20mm crimp caps with silicone/PTFE septum and 12h under visible-light irradiation (Blue LED, 18 W). After completion of the reaction checked by TLC, the resulting suspension was filtered through a pad of celite eluting with ethyl acetate. The crude filtrate was concentrated and purification of the residue by silica gel column chromatography eluting with a cyclohexane/ethyl acetate mixture gave the desired product.

1-benzhydrylphthalazine **664**

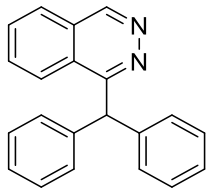

Formula: $C_{21}H_{16}N_2$

Mol. Weight: 296.37 $g.mol^{-1}$

Aspect: white solid

R_f: 0.65 (Cyclohexane:EA, 3:7)

Yield: 65%

^{1}H NMR (400 MHz, Chloroform-d): δ 9.47 (s, 1H), 8.17 (d, J = 7.5 Hz, 2H), 8.01 – 7.94 (m, 1H), 7.89 – 7.78 (m, 3H), 7.33 (d, J = 6.7 Hz, 11H), 7.28 – 7.23 (m, 2H), 6.44 (s, 1H).

^{13}C NMR (101 MHz, Chloroform-d): δ 160.70, 150.62, 141.61, 132.70, 131.96, 129.64, 128.60, 127.25, 127.06, 126.90, 125.95, 124.29, 54.29.

HR-MS (ESI+): m/z calculated for $C_{21}H_{16}N_2Na$ 319.1211 obtained 319.1212.

1-benzhydryl-6-fluorophthalazine **666**

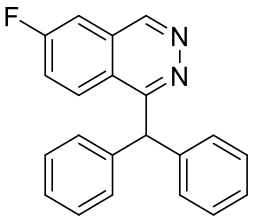

Formula: $C_{21}H_{15}FN_2$

Mol. Weight: 314.36 $g.mol^{-1}$

Aspect: yellow solid

R_f: 0.78 (Cyclohexane:EA, 3:7)

Yield: 50%

^{1}H NMR (400 MHz, Acetone-d_6): δ 9.56 (s, 1H), 8.51 (dd, J = 9.2, 5.1 Hz, 1H), 7.89 (dd, J = 8.5, 2.5 Hz, 1H), 7.77 (td, J = 9.0, 2.6 Hz, 1H), 7.37 (d, J = 7.6 Hz, 4H), 7.30 (t, J = 7.5 Hz, 4H), 7.22 (t, J = 7.2 Hz, 2H), 6.66 (s, 1H).

^{13}C NMR (101 MHz, Acetone-d_6): δ 164.40 (d, J = 253.3 Hz), 160.83 (d, J = 1.8 Hz), 150.99 (d, J = 4.4 Hz), 143.06, 130.47, 129.65 (d, J = 9.8 Hz), 129.11, 129.02, 127.44, 123.62 (d, J = 1.6 Hz), 123.21 (d, J = 24.9 Hz), 111.71 (d, J = 21.3 Hz), 54.08.

^{19}F NMR (376 MHz, Acetone-d_6): δ -106.10.

HR-MS (ESI+): m/z calculated for $C_{21}H_{16}N_2F$ 315.1298 obtained 315.1301.

1-benzhydryl-6-chlorophthalazine **667**

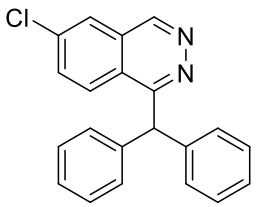

Formula: $C_{21}H_{15}ClN_2$

Mol. Weight: 330.82 $g.mol^{-1}$

Aspect: beige solid

R_f: 0.76 (Cyclohexane:EA, 3:7)

Yield: 50%

^{1}H NMR (400 MHz, Chloroform-d): δ 9.35 (s, 1H), 8.04 (d, J = 8.9 Hz, 1H), 7.89 (s, 1H), 7.70 (dd, J = 8.9, 1.9 Hz, 1H), 7.31 – 7.16 (m, 10H), 6.33 (s, 1H).

^{13}C NMR (101 MHz, Chloroform-d): δ 160.51, 149.68, 141.24, 138.07, 133.59, 129.58, 128.70, 127.93, 127.07, 126.40, 126.15, 124.19, 54.50.

HR-MS (ESI+): m/z calculated for $C_{21}H_{16}ClN_2$ 331.0997 obtained 331.0993.

1-benzhydryl-6-bromophthalazine **668**

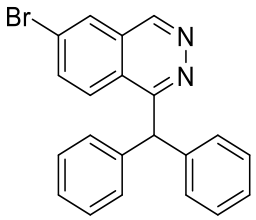

Formula: $C_{21}H_{15}BrN_2$

Mol. Weight: 375.27 $g.mol^{-1}$

Aspect: amorphous solid

R_f: 0.69 (Cyclohexane:EA, 3:7)

Yield: 11%

^{1}H NMR (400 MHz, Chloroform-d): δ 9.38 (s, 1H), 8.11 (d, J = 1.7 Hz, 1H), 7.98 (d, J = 8.9 Hz, 1H), 7.87 (dd, J = 8.9, 2.0 Hz, 1H), 7.37 – 7.34 (m, 2H), 7.31 – 7.29 (m, 3H), 7.29 – 7.27 (m, 5H), 6.35 (s, 1H).

^{13}C NMR (101 MHz, Chloroform-d): δ 160.70, 149.49, 141.43, 141.23, 136.26, 129.60, 128.74, 128.20, 127.11, 126.46, 126.35, 124.46, 54.52.

HR-MS (ESI+): m/z calculated for $C_{21}H_{16}BrN_2$ 375.0491 obtained 375.0489.

1-benzhydryl-6,7,8-trimethoxyphthalazine **669**

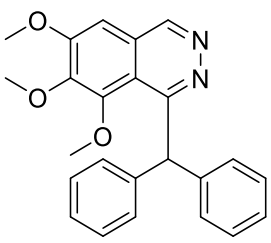

Formula: $C_{24}H_{22}N_2O_3$

Mol. Weight: 386.45 $g.mol^{-1}$

Aspect: yellow solid

R_f: 0.5 (EA)

Yield: 26%

^{1}H NMR (300 MHz, Acetone-d_6): δ 9.28 (s, 1H), 7.90 – 7.78 (m, 1H), 7.63 – 7.47 (m, 2H), 7.42 (s, 1H), 7.27 (s, 2H), 7.25 (s, 3H), 7.22 – 7.14 (m, 2H), 7.04 (s, 1H), 4.06 (s, 3H), 3.93 (s, 3H), 3.78 (s, 3H).

^{13}C NMR (101 MHz, Acetone-d_6): δ 149.26, 132.62, 132.59, 132.16, 132.06, 131.90, 130.54, 129.25, 129.13, 128.46, 126.57, 103.19, 61.86, 61.01, 56.53, 55.53.

HR-MS (ESI+): m/z calculated for $C_{24}H_{22}N_2O_3Na$ 409.1528 obtained 409.1517.

4-benzhydrylbenzofuro[2,3-d]pyridazine **670**

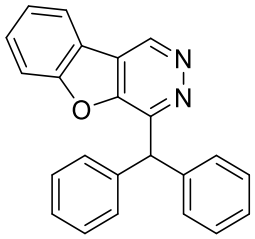

Formula: $C_{23}H_{16}N_2O$

Mol. Weight: 336.39 g.mol^{-1}

Aspect: beige solid

R_f: 0.77 (Cyclohexane:EA, 3:7)

Yield: 31%

^{1}H NMR (400 MHz, Chloroform-d): δ 9.79 (s, 1H), 8.08 (d, J = 7.8 Hz, 1H), 7.67 (d, J = 6.8 Hz, 2H), 7.49 (dd, J = 20.3, 7.0 Hz, 5H), 7.32 (t, J = 7.5 Hz, 4H), 7.28 – 7.22 (m, 2H), 6.39 (s, 1H).

^{13}C NMR (101 MHz, Chloroform-d): δ 156.16, 152.80, 152.27, 144.17, 140.69, 130.97, 129.52, 128.63, 127.13, 124.99, 122.93, 122.53, 120.08, 113.06, 52.84.

HR-MS (ESI+): m/z calculated for $C_{23}H_{16}N_2O$ 337.1335 obtained 337.1334.

4-benzhydryl-5-methyl-5H-pyridazino[4,5-b]indole **671**

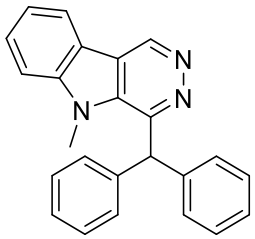

Formula: $C_{24}H_{19}N_3$

Mol. Weight: 349.44 g.mol^{-1}

Aspect: beige solid

R_f: 0.71 (Cyclohexane:EA, 3:7)

Yield: 37%

^{1}H NMR (400 MHz, Chloroform-d): δ 9.74 (s, 1H), 8.20 (d, J = 7.8 Hz, 1H), 7.67 (t, J = 7.6 Hz, 1H), 7.51 (d, J = 8.5 Hz, 1H), 7.44 (t, J = 7.5 Hz, 1H), 7.29 (m, 4H), 7.25 (m, 6H), 6.53 (s, 1H), 4.05 (s, 3H).

^{13}C NMR (101 MHz, Chloroform-d): δ 149.83, 142.28, 141.82, 141.63, 135.87, 129.87, 129.40, 128.74, 127.06, 122.18, 121.63, 120.30, 119.78, 110.46, 54.44, 32.88.

HR-MS (ESI+): m/z calculated for $C_{24}H_{19}N_3$ 350.1652 obtained 350.1651.

1-(phenyl(p-tolyl)methyl)phthalazine **672**

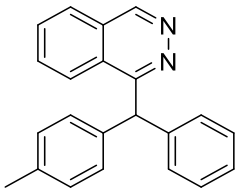

Formula: $C_{22}H_{18}N_2$

Mol. Weight: 310.40 g.mol^{-1}

Aspect: yellow solid

R_f: 0.69 (Cyclohexane:EA, 3:7)

Yield: 62%

^{1}H NMR (400 MHz, Chloroform-d): δ 9.48 (s, 1H), 8.15 (d, J = 8.9 Hz, 1H), 8.01 – 7.90 (m, 1H), 7.87 – 7.78 (m, 2H), 7.30 (d, J = 4.2 Hz, 4H), 7.20 (d, J = 7.9 Hz, 3H), 7.11 (d, J = 7.9 Hz, 2H), 6.38 (s, 1H), 2.30 (s, 3H).

^{13}C NMR (101 MHz, Chloroform-d): δ 160.82, 150.58, 141.82, 138.55, 136.48, 132.67, 131.92, 129.59, 129.48, 129.33, 128.55, 127.22, 127.02, 126.80, 125.93, 124.33, 53.91, 21.16

HR-MS (ESI+): m/z calculated for $C_{22}H_{18}N_2Na$ 333.1368 obtained 333.1365.

1-((4-fluorophenyl)(phenyl)methyl)phthalazine **673**

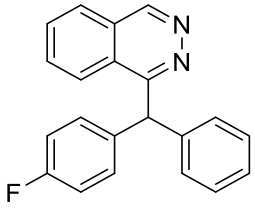

Formula: $C_{21}H_{15}FN_2$

Mol. Weight: 314.36 g.mol^{-1}

Aspect: yellow solid

R_f: 0.71 (Cyclohexane:EA, 3:7)

Yield: 49%

^{1}H NMR (300 MHz, Acetone-d_6): δ 9.54 (s, 1H), 8.42 – 8.33 (m, 1H), 8.22 – 8.10 (m, 1H), 8.01 – 7.88 (m, 2H), 7.47 – 7.35 (m, 4H), 7.30 (t, J = 7.3 Hz, 2H), 7.22 (t, J = 7.1 Hz, 1H), 7.14 – 7.00 (m, 2H), 6.69 (s, 1H).

^{13}C NMR (75 MHz, Acetone-d_6): δ 162.53 (d, J = 224.9 Hz), 160.80, 151.26, 143.16, 139.25 (d, J = 3.2 Hz), 133.62, 133.02, 132.32 (d, J = 8.0 Hz), 130.25, 129.23, 128.08, 127.74, 127.49, 126.18, 124.89, 115.57 (d, J = 21.4 Hz), 53.03.

^{19}F NMR (282 MHz, Acetone-d_6): δ -118.08 – -118.24 (m).

HR-MS (ESI+): m/z calculated for $C_{21}H_{16}N_2F$ 315.1298 obtained 315.1292.

1-(1-phenylbutyl)phthalazine **674**

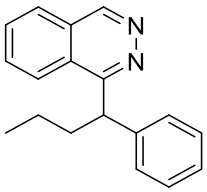

Formula: $C_{18}H_{18}N_2$

Mol. Weight: 262.36 $g.mol^{-1}$

Aspect: yellow solid

R_f: 0.47 (Cyclohexane:EA, 3:7)

Yield: 34%

^{1}H NMR (400 MHz, Chloroform-d): δ 9.42 (s, 1H), 8.23 – 8.08 (m, 1H), 7.90 (d, J = 4.1 Hz, 1H), 7.84 – 7.77 (m, 2H), 7.43 (d, J = 7.5 Hz, 2H), 7.25 (q, J = 7.8, 5.6 Hz, 2H), 7.15 (t, J = 7.5 Hz, 1H), 4.82 (t, J = 7.5 Hz, 1H), 2.60 (dq, J = 14.0, 6.9 Hz, 1H), 2.30 (tt, J = 13.6, 7.2 Hz, 1H), 1.48 – 1.31 (m, 2H), 0.96 (t, J = 7.4 Hz, 3H).

^{13}C NMR (101 MHz, Chloroform-d): δ 160.74, 150.58, 143.34, 132.54, 131.76, 128.70, 128.33, 127.24, 126.94, 126.72, 125.96, 124.03, 48.19, 37.80, 21.38, 14.26.

HR-MS (ESI+): m/z calculated for $C_{18}H_{19}N_2$ 263.1543 obtained 263.1546.

1-((6-methoxynaphthalen-2-yl)(phenyl)methyl)phthalazine **675**

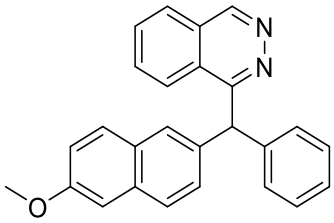

Formula: $C_{26}H_{20}N_2O$

Mol. Weight: 376.46 $g.mol^{-1}$

Aspect: amorphous solid

R_f: 0.61 (Cyclohexane:EA, 3:7)

Yield: 12%

^{1}H NMR (400 MHz, Chloroform-d): δ 9.45 (s, 1H), 8.18 (d, J = 8.1 Hz, 1H), 7.97 – 7.93 (m, 1H), 7.86 – 7.77 (m, 2H), 7.68 (d, J = 8.5 Hz, 1H), 7.59 (d, J = 7.5 Hz, 2H), 7.47 (dd, J = 8.5, 1.5 Hz, 1H), 7.37 – 7.24 (m, 5H), 7.09 (d, J = 7.7 Hz, 2H), 6.53 (s, 1H), 3.89 (s, 3H).

^{13}C NMR (101 MHz, Chloroform-d): δ 160.80, 157.80, 150.69, 141.68, 136.94, 133.64, 132.74, 131.98, 129.77, 129.55, 129.02, 128.62, 128.61, 127.90, 127.28, 127.19, 127.09, 126.94, 126.03, 124.37, 118.88, 105.75, 55.44, 54.27.

HR-MS (ESI+): m/z calculated for $C_{26}H_{21}N_2O$ 377.1648 obtained 377.1649.

1-(dibenzo[b,d]thiophen-2-yl(phenyl)methyl)phthalazine **676**

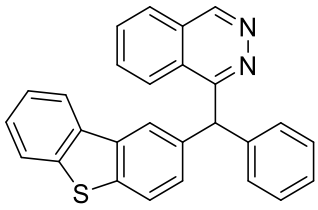

Formula: $C_{27}H_{18}N_2S$

Mol. Weight: 402.52 $g.mol^{-1}$

Aspect: yellow oil

R_f: 0.64 (Cyclohexane:EA, 3:7)

Yield: 44%

^{1}H NMR (400 MHz, Chloroform-d): δ 9.47 (s, 1H), 8.19 (d, J = 7.0 Hz, 1H), 8.08 (s, 1H), 8.04 – 7.94 (m, 2H), 7.90 – 7.75 (m, 4H), 7.49 – 7.25 (m, 8H), 6.60 (s, 1H).

^{13}C NMR (101 MHz, Chloroform-d): δ 160.72, 150.76, 141.65, 139.90, 138.15, 138.10, 135.94, 135.50, 132.83, 132.07, 129.67, 128.73, 128.69, 127.33, 127.08, 127.05, 126.81, 125.94, 124.35, 124.27, 122.98, 122.91, 122.53, 121.84, 54.25.

HR-MS (ESI+): m/z calculated for $C_{27}H_{19}N_2S$ 403.1263 obtained 403.1267.

1-(phenyl(p-tolyl)methyl)phthalazine **672'**

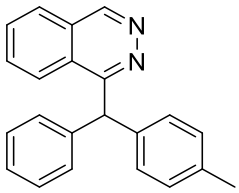

Formula: $C_{22}H_{18}N_2$

Mol. Weight: 310.40 $g.mol^{-1}$

Aspect: yellow solid

R_f: 0.69 (Cyclohexane:EA, 3:7)

Yield: 52%

^{1}H NMR (400 MHz, Chloroform-d): δ 9.48 (s, 1H), 8.15 (d, J = 8.9 Hz, 1H), 8.01 – 7.90 (m, 1H), 7.87 – 7.78 (m, 2H), 7.30 (d, J = 4.2 Hz, 4H), 7.20 (d, J = 7.9 Hz, 3H), 7.11 (d, J = 7.9 Hz, 2H), 6.38 (s, 1H), 2.30 (s, 3H).

^{13}C NMR (101 MHz, Chloroform-d): δ 160.82, 150.58, 141.82, 138.55, 136.48, 132.67, 131.92, 129.59, 129.48, 129.33, 128.55, 127.22, 127.02, 126.80, 125.93, 124.33, 53.91, 21.16

HR-MS (ESI+): m/z calculated for $C_{22}H_{18}N_2Na$ 333.1368 obtained 333.1365.

1-(phenyl(o-tolyl)methyl)phthalazine **677**

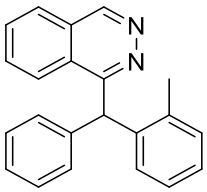

Formula: $C_{22}H_{18}N_2$

Mol. Weight: 310.40 $g.mol^{-1}$

Aspect: amorphous solid

R_f: 0.88 (Cyclohexane:EA, 3:7)

Yield: 32%

^{1}H NMR (300 MHz, Acetone-d_6) δ 9.53 (s, 1H), 8.26 – 8.11 (m, 2H), 7.99 – 7.87 (m, 2H), 7.31 (d, J = 4.3 Hz, 4H), 7.26 – 7.19 (m, 2H), 7.10 (dt, J = 23.2, 7.2 Hz, 2H), 6.87 (d, J = 7.5 Hz, 1H), 6.71 (s, 1H), 2.27 (s, 3H).

^{13}C NMR (75 MHz, Acetone-d_6) δ 161.26, 151.26, 142.04, 141.86, 136.91, 133.64, 132.95, 131.27, 130.98, 130.12, 129.03, 128.09, 127.72, 127.47, 127.39, 126.55, 126.26, 124.85, 51.33, 20.06.

HR-MS (ESI+): m/z calculated for $C_{22}H_{18}N_2$ 311.1543 obtained 311.1543.

1-(phenyl(3,4,5-trimethoxyphenyl)methyl)phthalazine **678**

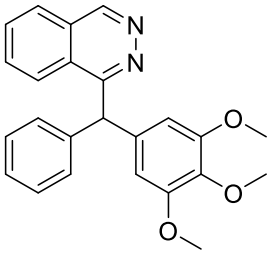

Formula: $C_{24}H_{22}N_2O_3$

Mol. Weight: 386.45 $g.mol^{-1}$

Aspect: yellow solid

R_f: 0.76 (EA)

Yield: 34%

^{1}H NMR (400 MHz, Chloroform-d): δ 9.49 (s, 1H), 8.17 (d, J = 8.7 Hz, 1H), 7.99 (dd, J = 5.8, 3.0 Hz, 1H), 7.92 – 7.81 (m, 2H), 7.30 (d, J = 4.2 Hz, 4H), 7.25 – 7.20 (m, 1H), 6.53 (s, 2H), 6.34 (s, 1H).

^{13}C NMR (101 MHz, Chloroform-d): δ 160.67, 153.25, 150.66, 141.46, 137.08, 136.87, 132.78, 132.05, 129.47, 128.59, 128.29, 127.28, 126.98, 125.93, 124.19, 106.88, 60.89, 56.15, 54.34.

HR-MS (ESI+): m/z calculated for $C_{24}H_{23}N_2O_3$ 387.1703 obtained 387.1703.

1-(benzo[d][1,3]dioxol-5-yl(phenyl)methyl)phthalazine **679**

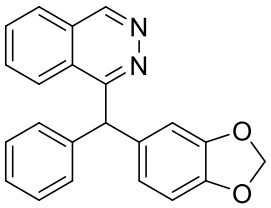

Formula: $C_{22}H_{16}F_2N_2O_2$

Mol. Weight: 340.38 $g.mol^{-1}$

Aspect: yellow oil

R_f: 0.52 (Cyclohexane:EA, 3:7)

Yield: 47%

^{1}H NMR (400 MHz, Chloroform-d): δ 9.42 (s, 1H), 8.14 – 8.06 (m, 1H), 7.96 – 7.89 (m, 1H), 7.86 – 7.75 (m, 2H), 7.28 – 7.23 (m, 4H), 7.20 (q, J = 4.5 Hz, 1H), 6.81 (d, J = 1.6 Hz, 1H), 6.73 – 6.68 (m, 2H), 6.29 (s, 1H), 5.88 (d, J = 3.3 Hz, 2H).

^{13}C NMR (101 MHz, Chloroform-d): δ 150.65, 147.93, 146.57, 141.70, 135.47, 132.80, 132.03, 129.49, 128.66, 127.32, 126.96, 126.96, 125.93, 124.26, 122.71, 122.71, 110.42, 108.23, 101.12, 53.86.

HR-MS (ESI+): m/z calculated for $C_{22}H_{17}N_2O_2$ 341.1285 obtained 341.1288.

1-((4-chlorophenyl)(phenyl)methyl)phthalazine **680**

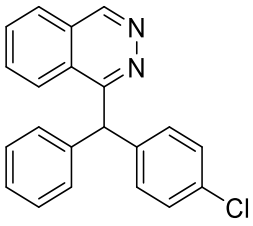

Formula: $C_{21}H_{15}ClN_2$

Mol. Weight: 330.82 $g.mol^{-1}$

Aspect: yellow solid

R_f: 0.56 (Cyclohexane:EA, 3:7)

Yield: 41%

^{1}H NMR (400 MHz, Chloroform-d): δ 9.45 (s, 1H), 8.10 (d, J = 7.8 Hz, 1H), 7.96 (d, J = 7.6 Hz, 1H), 7.85 (p, J = 7.1 Hz, 2H), 7.28 (t, J = 8.8 Hz, 9H), 6.36 (s, 1H).

^{13}C NMR (101 MHz, Chloroform-d): δ 160.29, 150.75, 141.23, 140.15, 132.86, 132.82, 132.13, 131.09, 129.47, 128.83, 128.71, 127.37, 127.19, 127.06, 125.85, 124.09, 53.58.

HR-MS (ESI+): m/z calculated for $C_{21}H_{16}ClN_2$ 331.0997 obtained 331.0994.

1-((4-fluorophenyl)(phenyl)methyl)phthalazine **673'**

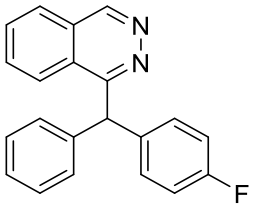

Formula: $C_{21}H_{15}FN_2$

Mol. Weight: 314.36 g.mol^{-1}

Aspect: yellow solid

R_f: 0.71 (Cyclohexane:EA, 3:7)

Yield: 42%

^{1}H NMR (400 MHz, Chloroform-d): δ 9.42 (s, 1H), 8.14 – 8.04 (m, 1H), 7.99 – 7.88 (m, 1H), 7.81 (tt, J = 7.2, 5.5 Hz, 2H), 7.29 – 7.18 (m, 7H), 6.96 (t, J = 8.7 Hz, 2H), 6.35 (s, 1H).

^{13}C NMR (101 MHz, Chloroform-d): δ 161.80 (d, J = 245.5 Hz), 160.48, 150.69, 141.52, 137.30 (d, J = 3.2 Hz), 132.82, 132.08, 131.26, 131.15, 129.42, 128.75, 127.32, 127.06, 125.81, 124.09, 115.36 (d, J = 21.2 Hz), 53.38

^{19}F NMR (376 MHz, Chloroform-d) δ -116.26.

HR-MS (ESI+): m/z calculated for $C_{21}H_{16}FN_2$ 315.1292 obtained 315.1294.

1-(3-nitrobenzyl)phthalazine **681**

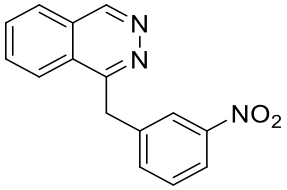

Formula: $C_{15}H_{11}N_3O_2$

Mol. Weight: 265.27 g.mol^{-1}

Aspect: amorphous solid

R_f: 0.49 (EA)

Yield: 79%

^{1}H NMR (400 MHz, Chloroform-d): δ 9.49 (d, J = 1.0 Hz, 1H), 8.22 (t, J = 2.1 Hz, 1H), 8.11 – 7.95 (m, 3H), 7.94 – 7.84 (m, 2H), 7.68 (ddd, J = 7.7, 1.9, 1.0 Hz, 1H), 7.44 (t, J = 7.9 Hz, 1H), 4.84 (s, 2H).

^{13}C NMR (101 MHz, Chloroform-d): δ 157.91, 151.25, 148.54, 140.24, 135.15, 133.13, 132.56, 129.77, 127.43, 127.06, 125.65, 124.03, 123.73, 122.10, 39.44.

HR-MS (ESI+): m/z calculated for $C_{15}H_{12}N_3O_2$ 266.0924 obtained 266.0923.

6-fluoro-1-(2-methoxyethyl)phthalazine **682**

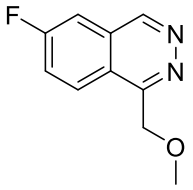

Formula: $C_{10}H_9FN_2O$

Mol. Weight: 192.19 g.mol^{-1}

Aspect: amorphous solid

R_f: 0.18 (Cyclohexane:EA, 3:7)

Yield: 72%

^{1}H NMR (400 MHz, Chloroform-d): δ 9.40 (s, 1H), 8.25 (dd, J = 9.1, 5.0 Hz, 1H), 7.65 (td, J = 8.8, 2.5 Hz, 1H), 7.55 (dd, J = 8.0, 2.4 Hz, 1H), 3.97 (t, J = 6.7 Hz, 2H), 3.61 (t, J = 6.7 Hz, 2H), 3.35 (s, 3H).

^{13}C NMR (101 MHz, Chloroform-d): δ 163.96 (d, J = 256.6 Hz), 158.10, 150.32, 128.78, 128.33 (d, J = 9.0 Hz), 123.64, 122.64 (d, J = 24.6 Hz), 110.69 (d, J = 21.0 Hz), 71.56, 59.01, 33.50.

^{19}F NMR (376 MHz, Chloroform-d): δ -103.16.

HR-MS (ESI+): m/z calculated for $C_{11}H_{12}FN_2O$ 207.0928 obtained 207.0931.

Ethyl diphenylphosphinate **683**

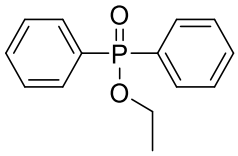

Formula: $C_{14}H_{15}O_2P$

Mol. Weight: 246.25 g.mol^{-1}

Aspect: oil

R_f: 0.59 (Cyclohexane:EA, 3:7)

^{1}H NMR (300 MHz, Chloroform-d): δ 7.80 (dd, J = 11.4, 7.5 Hz, 4H), 7.48 (dd, J = 14.3, 7.2 Hz, 4H), 4.19 – 3.96 (m, 2H), 1.35 (t, J = 6.8 Hz, 3H).

Spectral data were consistent with data reported in the literature.[267]

ethyl phenylphosphinate **684**

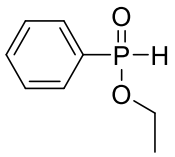

Formula: $C_8H_{11}O_2P$

Mol. Weight: 170.15 g.mol^{-1}

[267] E. Jablonkai, G. Keglevich, *Tetrahedron Letters* **2013**, *54*, 4185–4188.

Detected using LC-MS:

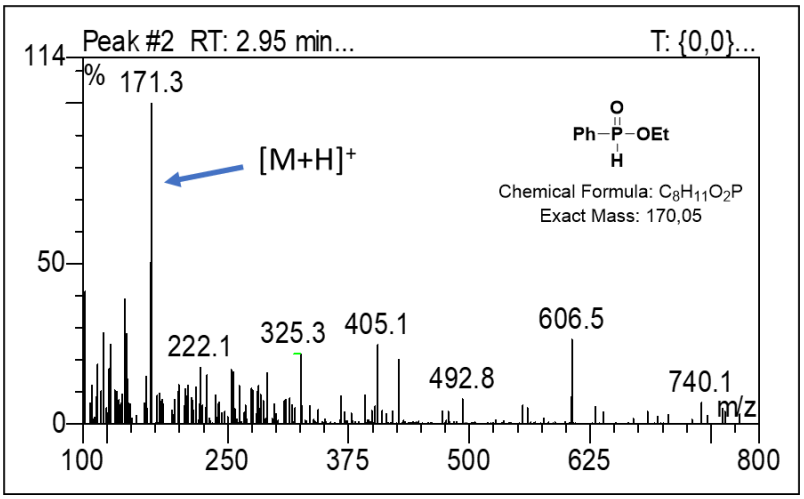

IV) Bibliography

[1] E. Vitaku, D. T. Smith, J. T. Njardarson, *J. Med. Chem.* **2014**, *57*, 10257–10274.

[2] J. F. Campos, S. Berteina-Raboin, *Catalysts* **2020**, *10*, 429.

[3] A. D. McNaught, A. Wilkinson, **1997**, DOI https://doi.org/10.1351/goldbook.H02798.

[4] A. F. Pozharskii, A. T. Soldatenkov, A. R. Katritzky, *Heterocycles in Life and Society: An Introduction to Heterocyclic Chemistry, Biochemistry and Applications*, John Wiley & Sons, Ltd, Chichester, UK, **2011**.

[5] M. Sainsbury, *Heterocyclic Chemistry*, Royal Society Of Chemistry, Cambridge, UK, **2001**.

[6] E. Campaigne, *J. Chem. Educ.* **1986**, *63*, 860.

[7] H. M. Staines, S. Krishna, Eds. , *Treatment and Prevention of Malaria*, Springer Basel, Basel, **2012**.

[8] P. B. Bloland, "Drug resistance in malaria," can be found under https://www.who.int/csr/resources/publications/drugresist/malaria.pdf, **n.d.**

[9] Y. Zhang, S. Chitale, N. Goyal, G. Li, Z. S. Han, S. Shen, S. Ma, N. Grinberg, H. Lee, B. Z. Lu, C. H. Senanayake, *J. Org. Chem.* **2012**, *77*, 690–695.

[10] D. N. Juurlink, **2020**, *192*, 4.

[11] T. Fiolet, A. Guihur, M. E. Rebeaud, M. Mulot, N. Peiffer-Smadja, Y. Mahamat-Saleh, *Clinical Microbiology and Infection* **2020**, *0*, DOI 10.1016/j.cmi.2020.08.022.

[12] D. N. Juurlink, **2020**, *192*, 4E. A. Meyerowitz, A. G. L. Vannier, M. G. N. Friesen, S. Schoenfeld, J. A. Gelfand, M. V. Callahan, A. Y. Kim, P. M. Reeves, M. C. Poznansky, *FASEB j.* **2020**, *34*, 6027–6037M. S. Cohen, *N Engl J Med* **2020**, NEJMe2020388D. R. Boulware, M. F. Pullen, A. S. Bangdiwala, K. A. Pastick, S. M. Lofgren, E. C. Okafor, C. P. Skipper, A. A. Nascene, M. R. Nicol, M. Abassi, N. W. Engen, M. P. Cheng, D. LaBar, S. A. Lother, L. J. MacKenzie, G. Drobot, N. Marten, R. Zarychanski, L. E. Kelly, I. S. Schwartz, E. G. McDonald, R. Rajasingham, T. C. Lee, K. H. Hullsiek, *N Engl J Med* **2020**, NEJMoa2016638.

[13] P. Zajdel, K. Marciniec, A. Maślankiewicz, G. Satała, B. Duszyńska, A. J. Bojarski, A. Partyka, M. Jastrzębska-Więsek, D. Wróbel, A. Wesołowska, M. Pawłowski, *Bioorganic & Medicinal Chemistry* **2012**, *20*, 1545–1556.

[14] A. Kubo, S. Nakahara, K. Inaba, Y. Kitahara, *Chem. Pharm. Bull.* **1986**, *34*, 4056–4068.

[15] J. Bedard, S. May, L. L'Heureux, T. Stamminger, A. Copsey, J. Drach, J. Huffman, L. Chan, H. Jin, R. F. Rando, *Antimicrob. Agents Chemother.* **2000**, *44*, 929–937.

[16] *Approaches to Design and Synthesis of Antiparasitic Drugs*, Elsevier, **1997**.

[17] M. M. Ghorab, M. S. Alsaid, M. S. Al-Dosari, F. A. Ragab, A. A. Al-Mishari, A. N. Almoqbil, *Acta Pharmaceutica* **2016**, *66*, 155–171.

[18] S. Hoogewerff, W. A. van Dorp, *Recl. Trav. Chim. Pays-Bas* **1885**, *4*, 125–129.

[19] Aug. Bischler, B. Napieralski, *Ber. Dtsch. Chem. Ges.* **1893**, *26*, 1903–1908.

[20] C. Pomeranz, *Monatshefte für Chemie und verwandte Teile anderer Wissenschaften* **1893**, *14*, 116–119P. Fritsch, *Ber. Dtsch. Chem. Ges.* **1893**, *26*, 419–422.

[21] A. Pictet, T. Spengler, *Ber. Dtsch. Chem. Ges.* **1911**, *44*, 2030–2036.

[22] A. Pictet, A. Gams, *Ber. Dtsch. Chem. Ges.* **1909**, *42*, 2943–2952.

[23] E. Schlittler, J. Müller, *Helvetica Chimica Acta* **1948**, *31*, 914–924.

[24] D. A. Widdowson, **n.d.**, 4.

[25] F. Maassarani, M. Pfeffer, G. Le Borgne, *J. Chem. Soc., Chem. Commun.* **1987**, 565.

[26] Guangzhong. Wu, A. L. Rheingold, S. J. Geib, R. F. Heck, *Organometallics* **1987**, *6*, 1941–1946G. Wu, S. J. Geib, A. L. Rheingold, R. F. Heck, *J. Org. Chem.* **1988**, *53*, 3238–3241.

[27] K. R. Roesch, R. C. Larock, *J. Org. Chem.* **1998**, *63*, 5306–5307.

[28] G. Dai, R. C. Larock, *Org. Lett.* **2001**, *3*, 4035–4038.

[29] G. Dai, R. C. Larock, *Org. Lett.* **2002**, *4*, 193–196.

[30] Q. Huang, R. C. Larock, *Tetrahedron Letters* **2002**, *43*, 3557–3560.

[31] W. Liu, X. Hong, B. Xu, *New York* **2013**, 13.

[32] H. Jiang, X. An, K. Tong, T. Zheng, Y. Zhang, S. Yu, *Angew. Chem. Int. Ed.* **2015**, *54*, 4055–4059.

[33] X.-D. An, S. Yu, *Org. Lett.* **2015**, *17*, 2692–2695.

[34] *Homogeneous Catalysis: Mechanisms and Industrial Applications*, John Wiley & Sons, Inc, Hoboken, NJ, **2014**.

[35] "Daily Metal Price: Free Metal Price Tables and Charts," can be found under https://www.dailymetalprice.com/, **n.d.**

[36] Z. Mazej, D. Kurzydłowski, W. Grochala, in *Photonic and Electronic Properties of Fluoride Materials* (Eds.: A. Tressaud, K. Poeppelmeier), Elsevier, Boston, **2016**, pp. 231–260S. Riedel, M. Kaupp, *Coordination Chemistry Reviews* **2009**, *253*, 606–624.

[37] R. Seaford, *Money and the Early Greek Mind: Homer, Philosophy, Tragedy*, Cambridge University Press, **2009**.

[38] A. C. Reardon, *Metallurgy for the Non-Metallurgist*, ASM International, Materials Park, Ohio, **2011**.

[39] T. Dai, Y.-Y. Huang, S. K. Sharma, J. T. Hashmi, D. B. Kurup, M. R. Hamblin, *PRI* **2010**, *5*, 124–151.

[40] C.-J. Li, X. Bi, "Silver Catalysis in Organic Synthesis, 2 Volume Set | Wiley," can be found under https://www.wiley.com/en-us/Silver+Catalysis+in+Organic+Synthesis%2C+2+Volume+Set-p-9783527342815, **n.d.**

[41] R. Hirsch, *Seizing the Light: A Social & Aesthetic History of Photography*, Routledge, Taylor & Francis Group, New York, **2017**.

[42] J.-M. Weibel, A. Blanc, P. Pale, *Chem. Rev.* **2008**, *108*, 3149–3173M. Álvarez-Corral, M. Muñoz-Dorado, I. Rodríguez-García, *Chem. Rev.* **2008**, *108*, 3174–3198Y. Yamamoto, *Chem. Rev.* **2008**, *108*, 3199–3222H. V. R. Dias, C. J. Lovely, *Chem. Rev.* **2008**, *108*, 3223–3238M. M. Díaz-Requejo, P. J. Pérez, *Chem. Rev.* **2008**, *108*, 3379–3394N. T. Patil, Y. Yamamoto, *Chemical Reviews* **2008**, *108*, 3395–3442.

[43] M. Naodovic, H. Yamamoto, *Chem. Rev.* **2008**, *108*, 3132–3148H. Pellissier, *Chem. Rev.* **2016**, *116*, 14868–14917.

[44] L. Ackermann, *Catalytic Hydroarylation of Carbon-Carbon Multiple Bonds*, Wiley-VCH Verlag GmbH & Co. KGaA, Weinheim, Germany, **2017**.

[45] A. Marinetti, H. Jullien, A. Voituriez, *Chem. Soc. Rev.* **2012**, *41*, 4884.

[46] T. Godet, C. Vaxelaire, C. Michel, A. Milet, P. Belmont, *Chemistry - A European Journal* **2007**, *13*, 5632–5641.

[47] E. Parker, N. Leconte, T. Godet, P. Belmont, *Chem. Commun.* **2011**, *47*, 343–345.

[48] G. Mariaule, G. Newsome, P. Y. Toullec, P. Belmont, V. Michelet, *Organic Letters* **2014**, *16*, 4570–4573.

[49] A. Bontemps, G. Mariaule, S. Desbène-Finck, P. Helissey, S. Giorgi-Renault, V. Michelet, P. Belmont, *Synthesis* **2016**, *48*, 2178–2190.

[50] G. S. Lewandos, D. K. Gregston, F. R. Nelson, *Journal of Organometallic Chemistry* **1976**, *118*, 363–374.

[51] X. Yao, C.-J. Li, *J. Org. Chem.* **2005**, *70*, 5752–5755.

[52] M. Fétizon, K. A. Parker, D.-S. Su, pp. 361-372, *Handbook of Reagents for Organic Synthesis, Oxidizing and Reducing Agents*, Wiley, Chichester, West Sussex, UK ; New York, **1999**.

[53] K. R. Roesch, R. C. Larock, *Org. Lett.* **1999**, *1*, 553–556*J. Org. Chem.* **2002**, *67*, 86–94.

[54] Q. Huang, J. A. Hunter, R. C. Larock, *The Journal of Organic Chemistry* **2002**, *67*, 3437–3444.

[55] N. Asao, S. Yudha S., T. Nogami, Y. Yamamoto, *Angewandte Chemie International Edition* **2005**, *44*, 5526–5528.

[56] S. Su, J. A. Porco, *Journal of the American Chemical Society* **2007**, *129*, 7744–7745.

[57] S. Ye, J. Wu, *Tetrahedron Letters* **2009**, *50*, 6273–6275.

[58] W. Sun, Q. Ding, X. Sun, R. Fan, J. Wu, *J. Comb. Chem.* **2007**, *9*, 690–694.

[59] H. Lou, S. Ye, J. Zhang, J. Wu, *Tetrahedron* **2011**, *67*, 2060–2065.

[60] Q. Ding, J. Wu, *Org. Lett.* **2007**, *9*, 4959–4962.

[61] X. Yu, J. Wu, *J. Comb. Chem.* **2010**, *12*, 238–244.

[62] X. Wang, G. Qiu, L. Zhang, J. Wu, *Tetrahedron Letters* **2014**, *55*, 962–964.

[63] M. Dell'Acqua, G. Abbiati, A. Arcadi, E. Rossi, *Organic & Biomolecular Chemistry* **2011**, *9*, 7836.

[64] C. Ye, Y. Li, H. Bao, *Advanced Synthesis & Catalysis* **2017**, *359*, 3720–3724.

[65] S. Obika, H. Kono, Y. Yasui, R. Yanada, Y. Takemoto, *The Journal of Organic Chemistry* **2007**, *72*, 4462–4468.

[66] W. M. Haynes, *CRC Handbook of Chemistry and Physics, 96th Edition*, CRC Press, **2015**.

[67] J. Ammer, C. Nolte, H. Mayr, *J. Am. Chem. Soc.* **2012**, *134*, 13902–13911H. Mayr, T. Bug, M. F. Gotta, N. Hering, B. Irrgang, B. Janker, B. Kempf, R. Loos, A. R. Ofial, G. Remennikov, H. Schimmel, *J. Am. Chem. Soc.* **2001**, *123*, 9500–9512T. A. Nigst, M. Westermaier, A. R. Ofial, H. Mayr, *European Journal of Organic Chemistry* **2008**, *2008*, 2369–2374S. Lakhdar, M. Westermaier, F. Terrier, R. Goumont, T. Boubaker, A. R. Ofial, H. Mayr, *The Journal of Organic Chemistry* **2006**, *71*, 9088–9095H. Mayr, A. R. Ofial, *Tetrahedron Letters* **1997**, *38*, 3503–3506M. Baidya, F. Brotzel, H. Mayr, *Org. Biomol. Chem.* **2010**, *8*, 1929.

[68] N. Asao, S. Yudha S., T. Nogami, Y. Yamamoto, *Angewandte Chemie International Edition* **2005**, *44*, 5526–5528.

[69] N. Asao, S. Yudha S., T. Nogami, Y. Yamamoto, *Angewandte Chemie International Edition* **2005**, *44*, 5526–5528S. Ye, J. Wu, *Tetrahedron Letters* **2009**, *50*, 6273–6275X. Yu, J. Wu, *J. Comb. Chem.* **2010**, *12*, 238–244.

[70] W. M. Haynes, *CRC Handbook of Chemistry and Physics, 96th Edition*, CRC Press, **2015**.

[71] G. Kidd, R. J. Goodfellow, *NMR and the Periodic Table*, Academic Press: London, **1978**.

[72] L. Lumata, M. E. Merritt, Z. Hashami, S. J. Ratnakar, Z. Kovacs, *Angew. Chem. Int. Ed.* **2012**, *51*, 525–527.

[73] U. Létinois-Halbes, P. Pale, S. Berger, *The Journal of Organic Chemistry* **2005**, *70*, 9185–9190.

[74] H. Gilman, J. M. Straley, *Recl. Trav. Chim. Pays-Bas* **1936**, *55*, 821–834.

[75] G. Koebrich, H. Froehlich, W. Drischel, *J. Organomet. Chem.* **1965**, *6*, 194–201.

[76] J. Davies, S. G. Booth, S. Essafi, R. A. W. Dryfe, D. Leonori, *Angew. Chem.* **2015**, *127*, 14223–14227.

[77] W. R. Bowman, S. L. Krintel, M. B. Schilling, *Org. Biomol. Chem.* **2004**, *2*, 585–592.

[78] D. H. Sliney, *Eye* **2016**, *30*, 222–229.

[79] C. Stephenson, T. Yoon, D. W. MacMillan, *Visible Light Photocatalysis in Organic Chemistry*, Wiley-VCH Verlag GmbH & Co. KGaA, **2018**.

[80] K. Teegardin, J. I. Day, J. Chan, J. Weaver, *Org. Process Res. Dev.* **2016**, *20*, 1156–1163L. Marzo, S. K. Pagire, O. Reiser, B. König, *Angew. Chem. Int. Ed.* **2018**, *57*, 10034–10072.

[81] R. J. Rapf, V. Vaida, *Phys. Chem. Chem. Phys.* **2016**, *18*, 20067–20084J. D. Haigh, *Living Rev. Sol. Phys.* **2007**, *4*, 2.

[82] T. Cardona, *Heliyon* **2018**, *4*, e00548.

[83] J. Priestley, **1790**, *3*, 126–128.

[84] H. Trommsdorff, *Annalen der Pharmacie* **1834**, *11*, 190–207.

[85] J. Šima, *Acta Chimica Slovaca* **2017**, *10*, 84–90.

[86] T. E. Thorpe, *Nature* **1922**, *109*, 245–246.

[87] A. Albini, M. Fagnoni, *ChemSusChem* **2008**, *1*, 63–66.

[88] G. Ciamician, *Science* **1912**, *36*, 385–394.

[89] A. Albini, M. Fagnoni, *Green Chem.* **2004**, *6*, 1.

[90] F. H. Burstall, *J. Chem. Soc.* **1936**, 173–175.

[91] S. Campagna, F. Puntoriero, F. Nastasi, G. Bergamini, V. Balzani, in *Photochemistry and Photophysics of Coordination Compounds I* (Eds.: V. Balzani, S. Campagna), Springer, Berlin, Heidelberg, **2007**, pp. 117–214.

[92] C. Stephenson, T. Yoon, D. W. MacMillan, *Visible Light Photocatalysis in Organic Chemistry*, Wiley-VCH Verlag GmbH & Co. KGaA, **2018**.

[93] C. Stephenson, T. Yoon, D. W. MacMillan, *Visible Light Photocatalysis in Organic Chemistry*, Wiley-VCH Verlag GmbH & Co. KGaA, **2018**.

[94] N. Hoffmann, *Eur. J. Org. Chem.* **2017**, *2017*, 1982–1992.

[95] A. J. Musacchio, L. Q. Nguyen, G. H. Beard, R. R. Knowles, *J. Am. Chem. Soc.* **2014**, *136*, 12217–12220.

[96] M. De Abreu, P. Belmont, E. Brachet, *European Journal of Organic Chemistry* **2020**, *2020*, 1327–1378.

[97] C. K. Prier, D. W. C. MacMillan, in *Visible Light Photocatalysis in Organic Chemistry*, John Wiley & Sons, Ltd, **2018**, pp. 299–333.

[98] F. Strieth-Kalthoff, M. J. James, M. Teders, L. Pitzer, F. Glorius, *Chem. Soc. Rev.* **2018**, *47*, 7190–7202.

[99] E. Brachet, T. Ghosh, I. Ghosh, B. König, *Chem. Sci.* **2015**, *6*, 987–992.

[100] G. E. M. Crisenza, D. Mazzarella, P. Melchiorre, *J. Am. Chem. Soc.* **2020**, *142*, 5461–5476.

[101] G. Nocera, A. Young, F. Palumbo, K. J. Emery, G. Coulthard, T. McGuire, T. Tuttle, J. A. Murphy, *J. Am. Chem. Soc.* **2018**, *140*, 9751–9757.

[102] M. D. Kärkäs, *ACS Catalysis* **2017**, *7*, 4999–5022.

[103] M. D. Kärkäs, *ACS Catalysis* **2017**, *7*, 4999–5022X.-Y. Yu, Q.-Q. Zhao, J. Chen, W.-J. Xiao, J.-R. Chen, *Acc. Chem. Res.* **2020**, *53*, 1066–1083.

[104] U. Lüning, P. S. Skell, *Tetrahedron* **1985**, *41*, 4289–4302.

[105] H. Kim, T. Kim, D. G. Lee, S. W. Roh, C. Lee, *Chem. Commun.* **2014**, *50*, 9273–9276.

[106] L. J. Allen, P. J. Cabrera, M. Lee, M. S. Sanford, *J. Am. Chem. Soc.* **2014**, *136*, 5607–5610.

[107] T. W. Greulich, C. G. Daniliuc, A. Studer, *Org. Lett.* **2015**, *17*, 254–257.

[108] Q. Qin, S. Yu, *Org. Lett.* **2014**, *16*, 3504–3507.

[109] Q. Qin, D. Ren, S. Yu, *Org. Biomol. Chem.* **2015**, *13*, 10295–10298.

[110] K. Tong, X. Liu, Y. Zhang, S. Yu, *Chemistry - A European Journal* **2016**, *22*, 15669–15673.

[111] E. Brachet, L. Marzo, M. Selkti, B. König, P. Belmont, *Chem. Sci.* **2016**, *7*, 5002–5006.

[112] X.-Q. Hu, J.-R. Chen, Q. Wei, F.-L. Liu, Q.-H. Deng, A. M. Beauchemin, W.-J. Xiao, *Angewandte Chemie International Edition* **2014**, *53*, 12163–12167.

[113] X.-Q. Hu, X. Qi, J.-R. Chen, Q.-Q. Zhao, Q. Wei, Y. Lan, W.-J. Xiao, *Nat Commun* **2016**, *7*, 11188.

[114] J. Chen, H.-M. Guo, Q.-Q. Zhao, J.-R. Chen, W.-J. Xiao, *Chem. Commun.* **2018**, *54*, 6780–6783.

[115] M. D. Kärkäs, *ACS Catalysis* **2017**, *7*, 4999–5022X.-Y. Yu, Q.-Q. Zhao, J. Chen, W.-J. Xiao, J.-R. Chen, *Acc. Chem. Res.* **2020**, *53*, 1066–1083.

[116] L. Huang, M. Arndt, K. Gooßen, H. Heydt, L. J. Gooßen, *Chem. Rev.* **2015**, *115*, 2596–2697.

[117] J. Seayad, A. Tillack, C. G. Hartung, M. Beller, *Advanced Synthesis & Catalysis* **2002**, *344*, 795–813.

[118] "Ullmann's Encyclopedia of Industrial Chemistry, 40 Volume Set, 7th Edition | Wiley," can be found under https://www.wiley.com/en-us/Ullmann%27s+Encyclopedia+of+Industrial+Chemistry%2C+40+Volume+Set%2C+7th+Edition-p-9783527329434, **n.d.**

[119] M. F. Semmelhack, B. M. Trost, I. Fleming, Eds. , *Comprehensive Organic Synthesis: Selectivity, Strategy & Efficiency in Modern Organic Chemistry. Vol. 4: Additions to and Substitutions at C - C π-Bonds*, Pergamon Press, Oxford, **1993**.

[120] D. Steinborn, R. Taube, *Z. Chem.* **2010**, *26*, 349–359.

[121] J. Huo, G. He, W. Chen, X. Hu, Q. Deng, D. Chen, *BMC Chemistry* **2019**, *13*, 89.

[122] W. Hickinbottom, *J. Chem. Soc.* **1932**, 2646–2654.

[123] D. R. Coulson, *Tetrahedron Letters* **1971**, *12*, 429–430.

[124] T. Mikami, K. Narasaka, *Chemistry Letters* **2000**, 338–339.

[125] T. M. Nguyen, D. A. Nicewicz, *J. Am. Chem. Soc.* **2013**, *135*, 9588–9591.

[126] S. Fukuzumi, K. Ohkubo, *Chem. Sci.* **2013**, *4*, 561–574.

[127] T. M. Nguyen, N. Manohar, D. A. Nicewicz, *Angew. Chem. Int. Ed.* **2014**, *53*, 6198–6201.

[128] T. Taniguchi, A. Idota, S. Yokoyama, H. Ishibashi, *Tetrahedron Letters* **2011**, *52*, 4768–4770.

[129] W. Liu, X. Hong, B. Xu, *New York* **2013**, 13.

[130] Z. Ding, Q. Tan, M. Gao, B. Xu, *Org. Biomol. Chem.* **2015**, *13*, 4642–4646.

[131] C. Lan, Z. Tian, X. Liang, M. Gao, W. Liu, Y. An, W. Fu, G. Jiao, J. Xiao, B. Xu, *Advanced Synthesis & Catalysis* **2017**, *359*, 3735–3740.

[132] J. F. Lalor, F. L. Scott, *J. Chem. Soc.* **1969**, 1034–1043.

[133] M. El-Deek, E. El-Sawi, M. Mohamed, *J. Chem. Eng. Data* **1981**, *26*, 340–342.

[134] A. Koziara, K. Turski, A. Zwierzak, *Synthesis* **1986**, *4*, 298–301.

[135] W. S. Wadsworth, W. D. Emmons, *J. Org. Chem.* **1964**, *29*, 2816–2820.

[136] R. Marek, I. St'astna-Sedlackova, J. Tousek, J. Marek, M. Potacek, *Bulletin des Societes Chimiques Belges* **1997**, *106*, 645.

[137] S. Man, J.-P. Bouillon, M. Nečas, M. Potáček, *Tetrahedron Letters* **2004**, *45*, 9419–9421.

[138] F. Loiseau, C. Clavette, M. Raymond, J.-G. Roveda, A. Burrell, A. M. Beauchemin, *Chem. Commun.* **2011**, *47*, 562–564.

[139] D. G. Morris, B. W. Smith, R. J. Wood, **n.d.**, 2.

[140] G. Zhang, Q. Fan, Y. Zhao, C. Ding, *Eur. J. Org. Chem.* **2019**, *2019*, 5801–5806.

[141] F. R. Atherton, H. T. Openshaw, A. R. Todd, *J. Chem. Soc.* **1945**, 660–663.

[142] D. Jabli, K. Dridi, M. L. Efrit, *Phosphorus, Sulfur, and Silicon and the Related Elements* **2016**, *191*, 759–764.

[143] R. Boobalan, C. Chen, *Advanced Synthesis & Catalysis* **2013**, *355*, 3443–3450.

[144] E. Steininger, *Monatshefte für Chemie* **1966**, *97*, 383–390.

[145] G. Chen, X. Zhang, Z. Zeng, W. Peng, Q. Liang, J. Liu, *ChemistrySelect* **2017**, *2*, 1979–1982.

[146] S. K. Pawar, C.-D. Wang, S. Bhunia, A. M. Jadhav, R.-S. Liu, *Angew. Chem. Int. Ed.* **2013**, *52*, 7559–7563.

[147] PubChem, "Potassium phosphate," can be found under https://pubchem.ncbi.nlm.nih.gov/compound/62657, **n.d.**

[148] M. De Abreu, M. Selkti, P. Belmont, E. Brachet, *Advanced Synthesis & Catalysis* **2020**, *362*, 2216–2222.

[149] M. De Abreu, M. Selkti, P. Belmont, E. Brachet, *Adv. Synth. Catal.* **2020**, DOI 10.1002/adsc.202000382.

[150] G. Kachkovskyi, C. Faderl, O. Reiser, *Adv. Synth. Catal.* **2013**, *355*, 2240–2248.

[151] F. Gao, C. Yang, G.-L. Gao, L. Zheng, W. Xia, *Org. Lett.* **2015**, *17*, 3478–3481.

[152] G. R. Fulmer, A. J. M. Miller, N. H. Sherden, H. E. Gottlieb, A. Nudelman, B. M. Stoltz, J. E. Bercaw, K. I. Goldberg, *Organometallics* **2010**, *29*, 2176–2179.

[153] J. Su, Q. Chen, L. Lu, Y. Ma, G. H. L. Auyoung, R. Hua, *Tetrahedron* **2018**, *74*, 303–307.

[154] J. P. Barham, G. Coulthard, K. J. Emery, E. Doni, F. Cumine, G. Nocera, M. P. John, L. E. A. Berlouis, T. McGuire, T. Tuttle, J. A. Murphy, *J. Am. Chem. Soc.* **2016**, *138*, 7402–7410.

[155] G. Nocera, A. Young, F. Palumbo, K. J. Emery, G. Coulthard, T. McGuire, T. Tuttle, J. A. Murphy, *J. Am. Chem. Soc.* **2018**, *140*, 9751–9757.

[156] J. F. Bunnett, J. Kook. Kim, *J. Am. Chem. Soc.* **1970**, *92*, 7463–7464.

[157] R. A. Rossi, J. F. Guastavino, M. E. Budén, in *Arene Chemistry* (Ed.: J. Mortier), John Wiley & Sons, Inc, Hoboken, NJ, **2015**, pp. 243–268.

[158] T.-H. Ding, J.-P. Qu, Y.-B. Kang, *Org. Lett.* **2020**, DOI 10.1021/acs.orglett.0c00827.

[159] J. Dhineshkumar, K. R. Prabhu, *Org. Lett.* **2013**, *15*, 6062–6065.

[160] K. M. Pelzer, L. Cheng, L. A. Curtiss, *J. Phys. Chem. C* **2017**, *121*, 237–245.

[161] K. Kalyanasundaram, *Coordination Chemistry Reviews* **1982**, *46*, 159–244.

[162] X. Lang, J. Zhao, *Chemistry – An Asian Journal* **2018**, *13*, 599–613.

[163] M. A. Cismesia, T. P. Yoon, *Chem. Sci.* **2015**, *6*, 5426–5434.

[164] P. J. Guiry, C. P. Saunders, *Advanced Synthesis & Catalysis* **2004**, *346*, 497–537A. Pfaltz, I. Drury, William J., *ChemInform* **2004**, *35*, DOI 10.1002/chin.200436268P. Nareddy, L. Mantilli, L. Guénée, C. Mazet, *Angew. Chem. Int. Ed.* **2012**, *51*, 3826–3831M. P. Carroll, P. J. Guiry, *Chem. Soc. Rev.* **2014**, *43*, 819–833B. V. Rokade, P. J. Guiry, *ACS Catal.* **2018**, *8*, 624–643.

[165] J. P. Wolfe, Ed. , *Synthesis of Heterocycles via Metal-Catalyzed Reactions That Generate One or More Carbon-Heteroatom Bonds*, Springer Berlin Heidelberg, Berlin, Heidelberg, **2013**.

[166] R. Lira, J. P. Wolfe, *J. Am. Chem. Soc.* **2004**, *126*, 13906–13907.

[167] T. Shimada, I. Nakamura, Y. Yamamoto, *J. Am. Chem. Soc.* **2004**, *126*, 10546–10547.

[168] T. Piou, T. Rovis, *Nature* **2015**, *527*, 86–90.

[169] J. Liebig, *Ann. Pharm.* **1838**, *25*, 1–31.

[170] H. Wieland, *Ber. Dtsch. Chem. Ges.* **1911**, *44*, 2550–2556.

[171] S. Thompson, A. G. Coyne, P. C. Knipe, M. D. Smith, *Chem. Soc. Rev.* **2011**, *40*, 4217–4231C. W. Spangler, *Chem. Rev.* **1976**, *76*, 187–217E. A. Ilardi, C. E. Stivala, A. Zakarian, *Chem. Soc. Rev.* **2009**, *38*, 3133–3148.

[172] J. Liebig, *Ann. Pharm.* **1838**, *25*, 1–31.

[173] Z.-L. Song, C.-A. Fan, Y.-Q. Tu, *Chem. Rev.* **2011**, *111*, 7523–7556.

[174] A. Y. Favorskii, *Journal of the Russian Physical and Chemical Society* **1894**, *26*, 590.

[175] M. Tiffeneau, *Comptes rendus hebdomadaires des séances de l'Académie des sciences* **1903**, *137*, 989–991.

[176] R. Fittig, *Ann. Chem. Pharm.* **1860**, *114*, 54–63.

[177] A. Butlerow, *Justus Liebigs Ann. Chem. Pharm.* **1873**, *170*, 151–162.

[178] M. Tiffeneau, *Bull. Soc. Chim. Fr.* **1925**, *4*, 437.

[179] E. Beckmann, *Ber. Dtsch. Chem. Ges.* **1886**, *19*, 988–993.

[180] J. Tinge, M. Groothaert, H. op het Veld, J. Ritz, H. Fuchs, H. Kieczka, W. C. Moran, in *Ullmann's Encyclopedia of Industrial Chemistry*, Wiley-VCH Verlag GmbH & Co. KGaA, Weinheim, Germany, **2018**, pp. 1–31.

[181] A. Baeyer, V. Villiger, *Ber. Dtsch. Chem. Ges.* **1899**, *32*, 3625–3633.

[182] E. E. Smissman, J. P. Li, Z. H. Israili, *J. Org. Chem.* **1968**, *33*, 4231–4236.

[183] W. H. Urry, M. S. Kharasch, *J. Am. Chem. Soc.* **1944**, *66*, 1438–1440.

[184] A. Effio, D. Griller, K. U. Ingold, J. C. Scaiano, S. J. Sheng, *Journal of the American Chemical Society* **1980**, *102*, 6063–6068.

[185] R. Leardini, G. Zanardi, E. Foresti, P. Palmieri, **1989**, *111*, 7723–7732.

[186] A. Asensio, J. J. Dannenberg, *J. Org. Chem.* **2001**, *66*, 5996–5999.

[187] M. S. Alnajjar, J. A. Franz, *J. Am. Chem. Soc.* **1992**, *114*, 1052–1058.

[188] D. Griller, K. U. Ingold, *Acc. Chem. Res.* **1980**, *13*, 317–323.

[189] S. Kim, J. Y. Do, *J. Chem. Soc., Chem. Commun.* **1995**, 1607–16082.

[190] E. Bacqué, M. El Qacemi, S. Z. Zard, *Org. Lett.* **2005**, *7*, 3817–3820.

[191] B. Quiclet-Sire, S. Z. Zard, *Pure and Applied Chemistry* **2010**, *83*, 519–551.

[192] Y.-R. Chen, W.-L. Duan, *J. Am. Chem. Soc.* **2013**, *135*, 16754–16757.

[193] S. Winstein, R. Heck, S. Lapporte, R. Baird, *Experientia* **1956**, *12*, 138–141.

[194] D. H. Hey, T. M. Moynehan, *J. Chem. Soc.* **1959**, 1563–1572.

[195] M. D. Bachi, E. Bosch, D. Denenmark, D. Girsh, *J. Org. Chem.* **1992**, *57*, 6803–6810.

[196] J. W. Wilt, C. F. Dockus, *J. Am. Chem. Soc.* **1970**, *92*, 5813–5814.

[197] L. Giraud, E. Lacŏte, P. Renaud, *HCA* **1997**, *80*, 2148–2156.

[198] S. Guidotti, R. Leardini, D. Nanni, P. Pareschi, G. Zanardi, *Tetrahedron Letters* **1995**, *36*, 451–454.

[199] D. L. J. Clive, S. Kang, *Tetrahedron Letters* **2000**, *41*, 1315–1319.

[200] D. L. J. Clive, S. Kang, *J. Org. Chem.* **2001**, *66*, 6083–6091.

[201] H.-L. Huang, H. Yan, C. Yang, W. Xia, *Chem. Commun.* **2015**, *51*, 4910–4913.

[202] Y. Li, B. Liu, X.-H. Ouyang, R.-J. Song, J.-H. Li, *Org. Chem. Front.* **2015**, *11*, 1457–1467.

[203] S. Cai, Y. Tian, J. Zhang, Z. Liu, M. Lu, W. Weng, M. Huang, *Adv. Synth. Catal.* **2018**, *360*, 4084–4088.

[204] M. Lu, H. Qin, Z. Lin, M. Huang, W. Weng, S. Cai, *Org. Lett.* **2018**, *20*, 7611–7615.

[205] Q.-L. Wang, Z. Chen, C.-S. Zhou, B.-Q. Xiong, P.-L. Zhang, C.-A. Yang, Y. Liu, Q. Zhou, *Tetrahedron Letters* **2018**, *59*, 4551–4556.

[206] L. Zheng, C. Yang, Z. Xu, F. Gao, W. Xia, *J. Org. Chem.* **2015**, *80*, 5730–5736.

[207] Y. Li, B. Hu, W. Dong, X. Xie, J. Wan, Z. Zhang, *J. Org. Chem.* **2016**, *81*, 7036–7041.

[208] H. Huang, Y. Li, *J. Org. Chem.* **2017**, *82*, 4449–4457.

[209] X. Gao, C. Li, Y. Yuan, X. Xie, Z. Zhang, *Org. Biomol. Chem.* **2020**, *18*, 263–271.

[210] J. J. Douglas, H. Albright, M. J. Sevrin, K. P. Cole, C. R. J. Stephenson, *Angewandte Chemie International Edition* **2015**, *54*, 14898–14902.

[211] T. M. Monos, R. C. McAtee, C. R. J. Stephenson, *Science* **2018**, *361*, 1369–1373.

[212] W. Shu, A. Genoux, Z. Li, C. Nevado, *Angew. Chem. Int. Ed.* **2017**, *56*, 10521–10524.

[213] D. Alpers, K. P. Cole, C. R. J. Stephenson, *Angew. Chem. Int. Ed.* **2018**, *57*, 12167–12170.

[214] C. Faderl, S. Budde, G. Kachkovskyi, D. Rackl, O. Reiser, *J. Org. Chem.* **2018**, *83*, 12192–12206.

[215] J. Li, Z. Liu, S. Wu, Y. Chen, *Org. Lett.* **2019**, *21*, 2077–2080.

[216] S.-F. Wang, X.-P. Cao, Y. Li, *Angew. Chem. Int. Ed.* **2017**, *56*, 13809–13813.

[217] R. Ruzi, J. Ma, X. Yuan, W. Wang, S. Wang, M. Zhang, J. Dai, J. Xie, C. Zhu, *Chem. Eur. J.* **2019**, *25*, 12724–12729.

[218] Jose. C. Gonzalez-Gomez, N. P. Ramirez, T. Lana-Villarreal, P. Bonete, *Org. Biomol. Chem.* **2017**, *15*, 9680–9684.

[219] Z.-H. Xia, L. Dai, Z.-H. Gao, S. Ye, *Chem. Commun.* **2020**, *56*, 1525–1528.

[220] J. Cossy, J.-P. Pete, *Tetrahedron* **1981**, *37*, 2287–2296.

[221] M. Huynh, M. D. Abreu, P. Belmont, E. Brachet, *Chemistry – A European Journal* **2020**, DOI 10.1002/chem.202003507.

[222] R. Henriques, *Ber. Dtsch. Chem. Ges.* **1894**, *27*, 2993–3005.

[223] O. Hinsberg, *J. Prakt. Chem.* **1914**, *90*, 345–353*J. Prakt. Chem.* **1915**, *91*, 307–324*J. Prakt. Chem.* **1916**, *93*, 277–301.

[224] L. A. Warren, S. Smiles, *J. Chem. Soc.* **1930**, 1327–1331Arthur. A. Levy, Harry. C. Rains, S. Smiles, *Journal of the Chemical Society (Resumed)* **1931**, 3264–3269.

[225] W. E. Truce, E. M. Kreider, W. W. Brand, *Organic Reactions* **1970**, 99–215.

[226] A. Levi, L. A. Warren, S. Smiles, *Journal of the Chemical Society* **1933**, 1490–1493.

[227] W. E. Truce, W. J. Ray, O. L. Norman, D. B. Eickemeyer, *J. Am. Chem. Soc.* **1958**, *80*, 3625–3629.

[228] Y. Cheng, X. Gu, P. Li, *Org. Lett.* **2013**, *15*, 2664–2667.

[229] J. D. Nguyen, E. M. D'Amato, J. M. R. Narayanam, C. R. J. Stephenson, *Nature Chem* **2012**, *4*, 854–859.

[230] G. Revol, T. McCallum, M. Morin, F. Gagosz, L. Barriault, *Angew. Chem. Int. Ed.* **2013**, *52*, 13342–13345.

[231] J.-N. Volle, D. Filippini, C. Midrier, M. Sobecki, M. Drag, D. Virieux, J.-L. Pirat, *Synthesis* **2011**, *2011*, 2490–2494.

[232] J. Rahil, P. Haake, *J. Am. Chem. Soc.* **1981**, *103*, 1723–1734.

[233] G. Dyker, W. Stirner, G. Henkel, *European Journal of Organic Chemistry* **2000**, *2000*, 1433–1441.

[234] P. C. Too, S. Chiba, *Chem. Commun.* **2012**, *48*, 7634–7636.

[235] J. H. Park, S. V. Bhilare, S. W. Youn, *Org. Lett.* **2011**, *13*, 2228–2231.

[236] J. H. Park, S. V. Bhilare, S. W. Youn, *Org. Lett.* **2011**, *13*, 2228–2231.

[237] G. Lu, C. Cai, B. H. Lipshutz, *Green Chem.* **2012**, *15*, 105–109.

[238] G. Shore, M. Tsimerman, M. G. Organ, *Beilstein J. Org. Chem.* **2009**, *5*, 35.

[239] J. Bucher, T. Stößer, M. Rudolph, F. Rominger, A. S. K. Hashmi, *Angewandte Chemie International Edition* **2015**, *54*, 1666–1670.

[240] V. Claus, L. Molinari, S. Büllmann, J. Thusek, M. Rudolph, F. Rominger, A. S. K. Hashmi, *Chemistry – A European Journal* **2019**, *25*, 9385–9389.

[241] T. Yamada, K. Park, T. Tachikawa, A. Fujii, M. Rudolph, A. S. K. Hashmi, H. Sajiki, *Org. Lett.* **2020**, *22*, 1883–1888.

[242] V. Claus, L. Molinari, S. Büllmann, J. Thusek, M. Rudolph, F. Rominger, A. S. K. Hashmi, *Chemistry – A European Journal* **2019**, *25*, 9385–9389.

[243] K. R. Roesch, R. C. Larock, *J. Org. Chem.* **2002**, *67*, 86–94.

[244] S. K. Pagire, P. Kreitmeier, O. Reiser, *Angewandte Chemie International Edition* **2017**, *56*, 10928–10932.

[245] T. Y. Chaudhari, Urvashi, S. K. Ginotra, P. Yadav, G. Kumar, V. Tandon, *Org. Biomol. Chem.* **2016**, *14*, 9896–9906.

[246] T. Y. Chaudhari, Urvashi, S. K. Ginotra, P. Yadav, G. Kumar, V. Tandon, *Org. Biomol. Chem.* **2016**, *14*, 9896–9906.

[247] G. Dyker, D. Hildebrandt, J. Liu, K. Merz, *Angewandte Chemie International Edition* **2003**, *42*, 4399–4402.

[248] J. Verner, M. Potacek, *Molecules* **2006**, *11*, 34–42.

[249] R. Klement, K. O. Knollmüller, *Chemische Berichte* **1960**, *93*, 834–843.

[250] U. Felcht, M. Regitz, *Justus Liebigs Annalen der Chemie* **1977**, *1977*, 1309–1320.

[251] M. Balti, K. Dridi, M. Lotfi El Efrit, *HETEROCYCLES* **2014**, *89*, 1483.

[252] M. Tiano, P. Belmont, *J. Org. Chem.* **2008**, *73*, 4101–4109.

[253] R. P. Kaiser, J. Mosinger, I. Císařová, M. Kotora, *Org. Biomol. Chem.* **2017**, *15*, 6913–6920.

[254] D. P. Iwaniuk, C. Wolf, *Organic Letters* **2011**, *13*, 2602–2605.

[255] P. Belmont, T. Belhadj, *Org. Lett.* **2005**, *7*, 1793–1795.

[256] A. Dore, B. Asproni, A. Scampuddu, G. A. Pinna, C. T. Christoffersen, M. Langgård, J. Kehler, *European Journal of Medicinal Chemistry* **2014**, *84*, 181–193.

[257] G. A. Kraus, J. Beasley, *Tetrahedron Letters* **2013**, *54*, 5597–5599.

[258] T. Miao, Z.-Y. Tian, Y.-M. He, F. Chen, Y. Chen, Z.-X. Yu, Q.-H. Fan, *Angewandte Chemie International Edition* **2017**, *56*, 4135–4139.

[259] W. Zhang, F. Ning, L. Váradi, D. E. Hibbs, J. A. Platts, M. Nyerges, R. J. Anderson, P. W. Groundwater, *Tetrahedron* **2014**, *70*, 3621–3629.

[260] J. Dhineshkumar, K. R. Prabhu, *Org. Lett.* **2013**, *15*, 6062–6065.

[261] G. Revol, T. McCallum, M. Morin, F. Gagosz, L. Barriault, *Angew. Chem. Int. Ed.* **2013**, *52*, 13342–13345.

[262] J. Rahil, P. Haake, *J. Am. Chem. Soc.* **1981**, *103*, 1723–1734.

[263] M. El-Deek, E. El-Sawi, M. Mohamed, *J. Chem. Eng. Data* **1981**, *26*, 340–342.

[264] *Journal of general chemistry of the USSR* **1973**, *43*, 2186–2187.

[265] A. S. K. Hashmi, M. Bührle, R. Salathé, J. W. Bats, *Advanced Synthesis & Catalysis* **2008**, *350*, 2059–2064.

[266] K. M. Saini, R. K. Saunthwal, Sushmita, A. K. Verma, *Chemistry – A European Journal* **2020**, *26*, 1017–1021.

[267] E. Jablonkai, G. Keglevich, *Tetrahedron Letters* **2013**, *54*, 4185–4188.

Résumé

Cette thèse est divisée en deux grandes parties ayant comme fil conducteur commun la synthèse d'hétérocycles azotés fonctionnalisés. La première partie concerne le développement d'une nouvelle méthodologie de synthèse de dérivés de 1,2-dihydroisoquinoléines via une catalyse tandem à l'argent en conditions douces. Cette dernière consiste, en 2 étapes successives, en une cycloisomérisation d'imines sur des alcynes catalysée par un sel d'argent, suivie d'une hydroarylation d'un composé hétérocyclique azoté sur l'intermédiaire isoquinoléinium. La seconde partie se concentre sur l'utilisation de la lumière visible en tant que source d'énergie, pour la synthèse de dérivés de phtalazines fonctionnalisées, grâce au développement d'une nouvelle famille de composés précurseurs de radicaux centrés sur l'azote appelée phosphonohydrazones. Les phosphonohydrazones peuvent être facilement oxydées en milieu basique par un photocatalyseur à base de ruthénium préalablement excité par la lumière visible permettant la formation d'un radical centré sur l'azote qui est l'intermédiaire clé de cette réaction. Une réactivité inattendue a été observée puisque la particule phosphorée est coupée lors de la réaction, sans étape supplémentaire requise, faisant de cette dernière un groupement auto-immolable. Enfin, une réactivité différente a été observée en fonction du type de groupement sur l'atome de phosphore. En effet, en substituant ce phosphore avec des chaînes ethoxylées, des dérivés de type benzylphtalazine sont obtenus tandis qu'en substituant le phosphore par des groupements aryles, une migration radicalaire 1,4 d'aryle s'opère, donnant lieu à la formation de dérivés de type benzhydrylphtalazine.

Mots-clés : photocatalyse, radicaux centrés sur l'azote, catalyse, photochimie, phtalazine, catalyse organométallique, argent, isoquinoléine

Abstract

This thesis is divided in two major axes having in common the synthesis of functionalized nitrogen-containing heterocycles. The first part tackles the development of a new synthetic methodology for the formation of 1,2-dihydroisoquinolines via a silver-catalyzed tandem reaction under mild conditions. The methodology consists, in two successive steps, in an imine cycloisomerization on an alkyne catalyzed by a silver salt, followed by a hydroarylation of a nitrogen-containing heterocycle on the isoquinolinium intermediate. The second part focuses on the use of visible-light as an energy source, for the synthesis of functionalized phthalazines, thanks to the development of a new family of nitrogen-centered radical precursors called phosphonohydrazones. The latter can be readily deprotonated and oxidized in a basic medium by an excited-state ruthenium-based photocatalyst previously irradiated by visible-light, allowing the formation of a nitrogen-centered radical: the key intermediate of the reaction. An unexpected reactivity was witnessed since the phosphorus-containing part is cleaved during the reaction, without any further necessary step, making it a self-immolative moiety. To finish, a different reactivity was observed depending on the substituents present on the phosphorus atom. Indeed, when substituting this phosphorus with ethoxy chains, benzylphthalazine derivatives are obtained whereas when substituting the phosphorus with aryl groups, a radical 1,4-aryl migration occurs, yielding benzhydrylphthalazine.

Key words: photocatalysis, nitrogen-centered radical, catalysis, photochemistry, phthalazine, organometallic catalysis, silver, isoquinoline